

Department of Medicine, Hematology
CENTRO DE INVESTIGACIÓN DEL CÁNCER – IBMCC



**VNiVERSiDAD
D SALAMANCA**

CAMPUS OF INTERNATIONAL EXCELLENCE

DOCTORAL DISSERTATION

**Unraveling the Biological Determinants of the Origin, Clonal Evolution
and Therapeutic Vulnerabilities of del(11q) Chronic Lymphocytic
Leukemia through Genome-Editing Approaches**

With the approval of the University of Salamanca, Department of Medicine, this thesis will be defended on 22nd July 2021, in the Lecture Hall, Centro de Investigación del Cáncer - IBMCC, Salamanca.

Supervisors:

Prof. Dr. Jesús M. Hernández Rivas

Dra. M. del Rocío Benito Sánchez

Dra. Ana E. Rodríguez Vicente

Miguel Quijada Álamo

2021



Esta tesis doctoral corresponde a la Modalidad de Compendio de Artículos, tres de los cuales han sido publicados en revistas internacionales de primer decil, y el cuarto acaba de ser aceptado para su publicación.

ARTÍCULO 1

Título: Next-generation sequencing and FISH studies reveal the appearance of gene mutations and chromosomal abnormalities in hematopoietic progenitors in chronic lymphocytic leukemia

Autores: Miguel Quijada-Álamo^{1*}, María Hernández-Sánchez^{1*}, Cristina Robledo¹, Jesús María Hernández-Sánchez¹, Rocío Benito¹, Adrián Montaña¹, Ana E Rodríguez-Vicente^{1,2}, Dalia Quwaider¹, Ana-África Martín¹, María García-Álvarez¹, María Jesús Vidal Manceñido³, Gonzalo Ferrer-Garrido⁴, María-Pilar Delgado-Beltrán⁴, Josefina Galende⁵, Juan-Nicolás Rodríguez⁶, Guillermo Martín-Núñez⁷, José-María Alonso⁸, Alfonso García de Coca⁹, José A. Queizán¹⁰, Magdalena Sierra¹¹, Carlos Aguilar¹², Alexander Kohlmann^{13,14}, José-Ángel Hernández¹⁵, Marcos González¹, Jesús-María Hernández Rivas¹

Afiliación de los autores: ¹Servicio de Hematología & IBSAL, IBMCC, CIC Universidad de Salamanca-CSIC, Hospital Universitario, Salamanca, Spain. ²Department of Molecular and Clinical Pharmacology, University of Liverpool, Liverpool, United Kingdom. ³Servicio de Hematología, Hospital Virgen Blanca, León, Spain. ⁴Servicio de Hematología, Hospital Miguel Servet, Zaragoza, Spain. ⁵Servicio de Hematología, Hospital del Bierzo, Ponferrada, León, Spain. ⁶Servicio de Hematología, Hospital Juan Ramón Jiménez, Huelva, Spain. ⁷Servicio de Hematología, Hospital Virgen del Puerto, Plasencia, Cáceres, Spain. ⁸Servicio de Hematología, Hospital Río Carrión, Palencia, Spain. ⁹Servicio de Hematología, Hospital Clínico, Valladolid, Spain. ¹⁰Servicio de Hematología, Hospital General de Segovia, Segovia, Spain. ¹¹Servicio de Hematología, Hospital Virgen de la Concha, Zamora, Spain. ¹²Servicio de Hematología, Hospital Santa Bárbara, Soria, Spain. ¹³MLL Munich, Germany. ¹⁴AstraZeneca, Personalized Healthcare and Biomarkers, Innovative Medicines, Cambridge, United Kingdom. ¹⁵Servicio de Hematología, Hospital Universitario Infanta Leonor, Universidad Complutense de Madrid, Madrid, Spain. *Equal contribution.

Estado del artículo: publicado en la revista **Journal of Hematology & Oncology**, 2017. doi: 10.1186/s13045-017-0450-y

ARTÍCULO 2

Título: CRISPR/Cas9-generated models uncover therapeutic vulnerabilities of del(11q) CLL cells to dual BCR and PARP inhibition

Autores: Miguel Quijada-Álamo^{1,2*}, María Hernández-Sánchez^{1,2,3,4*}, Verónica Alonso Pérez^{1,2}, Ana E Rodríguez-Vicente^{1,2}, Ignacio García-Tuñón^{1,2}, Marta Martín Izquierdo^{1,2}, Jesús María Hernández-Sánchez^{1,2}, Ana B Herrero^{1,2}, José María Bastida², Laura San Segundo^{1,2}, Michaela Gruber^{3,4,5,6}, Juan Luis García^{1,2}, Shanye Yin^{3,4}, Elisa ten Hacken^{3,4}, Rocío Benito^{1,2}, José Luis Ordóñez^{1,2}, Catherine J Wu^{3,4} and Jesús María Hernández-Rivas^{1,2,7}

Afiliación de los autores: ¹University of Salamanca, IBSAL, IBMCC, CSIC, Cancer Research Center, Salamanca, Spain. ²Department of Hematology, University Hospital of Salamanca, Salamanca, Spain. ³Department of Medical Oncology, Dana-Farber Cancer Institute, Boston, Massachusetts 02115, USA. ⁴Broad Institute of Harvard and MIT, Cambridge, Massachusetts 02142, USA. ⁵CeMM Research Center for Molecular Medicine, Vienna, Austria. ⁶Department of Internal Medicine I, Division of Hematology and Hemostaseology, Medical University of Vienna, Vienna, Austria. ⁷Department of Medicine, University of Salamanca, Salamanca, Spain. *Equal contribution.

Estado del artículo: publicado en la revista **Leukemia**, 2020. doi: 10.1038/s41375-020-0714-3

[ARTÍCULO 3](#)

Título: Dissecting the role of *TP53* alterations in del(11q) chronic lymphocytic leukemia

Autores: Miguel Quijada-Álamo^{1,2*}, Claudia Pérez-Carretero^{1,2*}, María Hernández-Sánchez^{1,2,3,4}, Ana-Eugenia Rodríguez-Vicente^{1,2}, Ana-Belén Herrero^{1,2}, Jesús-María Hernández-Sánchez^{1,2}, Marta Martín-Izquierdo^{1,2}, Sandra Santos-Mínguez^{1,2}, Mónica del Rey^{1,2}, Teresa González², Araceli Rubio-Martínez⁵, Alfonso García de Coca⁶, Julio Dávila-Valls⁷, José-Ángel Hernández-Rivas⁸, Helen Parker⁹, Jonathan C. Strefford⁹, Rocío Benito^{1,2}, José-Luis Ordóñez^{1,2} and Jesús-María Hernández-Rivas^{1,2,10}

Afiliación de los autores: ¹University of Salamanca, IBSAL, IBMCC, CSIC, Cancer Research Center, Salamanca, Spain. ²Department of Hematology, University Hospital of Salamanca, Salamanca, Spain. ³Department of Medical Oncology, Dana-Farber Cancer Institute, Boston, Massachusetts 02115, USA. ⁴Broad Institute of Harvard and MIT, Cambridge, Massachusetts 02142, USA. ⁵Department of Hematology, Hospital Miguel Servet, Zaragoza, Spain. ⁶Department of Hematology, Hospital Clínico de Valladolid, Valladolid, Spain. ⁷Department of Hematology, Hospital Nuestra Señora de Sonsoles, Ávila, Spain. ⁸Department of Hematology, Hospital Universitario Infanta Leonor. Universidad Complutense, Madrid,

Spain. ⁹Cancer Genomics, School of Cancer Sciences, Faculty of Medicine, University of Southampton, Southampton, UK. ¹⁰Department of Medicine, University of Salamanca, Salamanca, Spain. *Equal contribution

Estado del artículo: publicado en la revista **Clinical and Translational Medicine**, 2021. doi: 10.1002/ctm2.304

ARTÍCULO 4

Título: Biological significance of monoallelic and biallelic *BIRC3* loss in del(11q) chronic lymphocytic leukemia progression

Autores: Miguel Quijada-Álamo^{1,2}, María Hernández-Sánchez^{1,2,3,4}, Ana-Eugenia Rodríguez-Vicente^{1,2}, Claudia Pérez-Carretero^{1,2}, Alberto Rodríguez-Sánchez^{1,2}, Marta Martín-Izquierdo^{1,2}, Verónica Alonso-Pérez^{1,2}, Ignacio García-Tuñón^{1,2}, José María Bastida², María Jesús Vidal-Manceño⁵, Josefina Galende⁶, Carlos Aguilar⁷, José Antonio Queizán⁸, Isabel González-Gascón y Marín⁹, José-Ángel Hernández-Rivas⁹, Rocío Benito^{1,2}, José Luis Ordóñez^{1,2} and Jesús-María Hernández-Rivas^{1,2,10}

Afiliación de los autores: ¹University of Salamanca, IBSAL, IBMCC, CSIC, Cancer Research Center, Salamanca, Spain. ²Department of Hematology, University Hospital of Salamanca, Salamanca, Spain. ³Department of Medical Oncology, Dana-Farber Cancer Institute, Boston, Massachusetts 02115, USA. ⁴Broad Institute of Harvard and MIT, Cambridge, Massachusetts 02142, USA. ⁵Department of Hematology, Hospital Virgen Blanca, León, Spain. ⁶Department of Hematology, Hospital del Bierzo, Ponferrada, Spain. ⁷Department of Hematology, Hospital Santa Bárbara, Soria, Spain. ⁸Department of Hematology, Hospital General de Segovia, Segovia, Spain. ⁹Department of Hematology, Hospital Universitario Infanta Leonor. Universidad Complutense, Madrid, Spain. ¹⁰Department of Medicine, University of Salamanca, Salamanca, Spain.

Estado del artículo: aceptado en la revista **Blood Cancer Journal**, 2021. *In press*

D. **Jesús María Hernández Rivas**, Doctor en Medicina, Catedrático del Departamento de Medicina de la Universidad de Salamanca, Médico Adjunto del Servicio de Hematología del Hospital Clínico Universitario de Salamanca e Investigador del Centro de Investigación del Cáncer de Salamanca e Instituto de Investigación Biomédica de Salamanca,

D.^a **María del Rocío Benito Sánchez**, Doctora en Ciencias Biológicas por la Universidad de Salamanca e Investigadora del Centro de Investigación del Cáncer e Instituto de Investigación Biomédica de Salamanca,

D.^a **Ana Eugenia Rodríguez Vicente**, Doctora en Biociencias por la Universidad de Salamanca e Investigadora del Centro de Investigación del Cáncer e Instituto de Investigación Biomédica de Salamanca,

CERTIFICAN

Que D. **Miguel Quijada Álamo**, graduado en Biotecnología por la Universidad de Salamanca, ha realizado bajo nuestra dirección el trabajo de Tesis Doctoral titulado "*Unraveling the Biological Determinants of the Origin, Clonal Evolution and Therapeutic Vulnerabilities of del(11q) Chronic Lymphocytic Leukemia through Genome-Editing Approaches*", y que éste reúne, a nuestro juicio, las condiciones de originalidad y calidad científica requeridas para su presentación y defensa ante el tribunal correspondiente para optar al grado de Doctor, con mención "Doctor Internacional", por la Universidad de Salamanca.

La tesis doctoral ha sido escrita en inglés y, de acuerdo con la normativa de la Universidad de Salamanca para la obtención del título de Doctor, el doctorando presenta un resumen significativo en castellano de la misma.

Y para que así conste a los efectos oportunos, firmamos el presente certificado en Salamanca 16 de junio de 2021.

Fdo:

Prof. Dr. Jesús M. Hernández Rivas

Dra. M. del Rocío Benito Sánchez

Dra. Ana E. Rodríguez Vicente

This thesis was performed being Miguel Quijada Álamo fully supported by “Ayuda predoctoral de la Junta de Castilla y León”, Fondo Social Europeo (Orden del 10 de noviembre de 2016) (July 2017-February 2021) and by “Beca de Investigación de la Fundación Española de Hematología y Hemoterapia (FEHH) 2021” (March 2021-February 2023)

Acknowledgements:

- Fondo de Investigaciones Sanitarias (FIS) PI15/01471 and PI18/01500, Instituto de Salud Carlos III (ISCIII), European Regional Development Fund (ERDF) “Una manera de hacer Europa”.
 - Conserjería de Educación, Junta de Castilla y León (SA271P18).
 - Proyectos de Investigación del SACYL, Spain. GRS 2062/A/19, GRS 1847/A/18, GRS1653/A17.
 - “Fundación Memoria Don Samuel Solórzano Barruso” (FS/23-2018; FS/33-2020).
 - Red Temática de Investigación Cooperativa en Cáncer (RTICC) (RD12/0036/0069)
 - Centro de Investigación Biomédica en Red de Cáncer (CIBERONC CB16/12/00233)
 - SYNtherapy “Synthetic Lethality for Personalized Therapy-based Stratification In Acute Leukemia” (ERAPERMED2018-275); ISCIII (AC18/00093), co-funded by ERDF/ESF, “Investing in your future”.
 - Fundación Española de Hematología y Hemoterapia (FEHH)
 - European Hematology Association (EHA) – Research Mobility Grant 2020
-

Table of contents

LIST OF ABBREVIATIONS.....	5
INTRODUCTION.....	11
1. CHRONIC LYMPHOCYTIC LEUKEMIA – DISEASE OVERVIEW.....	13
1.1. Epidemiology.....	13
1.2. Etiology.....	13
1.3. Diagnosis.....	14
1.4. Risk stratification and response assessment.....	15
1.5. CLL therapy.....	16
1.5.1. Indication for treatment and response assessment.....	16
1.5.2. Therapeutic approaches and treatment algorithm.....	17
2. CLL GENETICS.....	18
2.1. Cellular origin of CLL.....	19
2.2. Genetic alterations in CLL.....	22
2.2.1. Chromosomal abnormalities.....	22
2.2.1.1. Del(11q).....	23
2.2.1.2. Del(13q).....	24
2.2.1.3. Del(17p).....	25
2.2.1.4. Trisomy 12.....	26
2.2.1.5. Other cytogenetic alterations.....	26
2.2.1.6. Complex karyotype.....	27
2.2.2. Somatic mutations.....	27
2.2.2.1. <i>ATM</i> mutations.....	28
2.2.2.2. <i>TP53</i> mutations.....	29
2.2.2.3. <i>BIRC3</i> mutations.....	30
2.2.2.4. <i>SF3B1</i> mutations.....	30
2.2.2.5. <i>NOTCH1</i> mutations.....	31
2.2.2.6. Other recurrent somatic mutations with prognostic impact.....	31
2.2.3. microRNAs.....	32
2.2.4. Epigenetics.....	32
2.3. Clonal evolution and growth kinetics of CLL.....	33
3. CLL BIOLOGY – TARGETING SIGNALING PATHWAYS.....	34

3.1. Molecular pathways in CLL.....	34
3.1.1. DNA damage response and cell cycle control.....	35
3.1.2. Apoptosis.....	37
3.1.3. BCR signaling and TLR signaling.....	38
3.1.4. NF-κB signaling.....	40
3.2. CLL microenvironment.....	42
3.3. Targeted therapy in CLL.....	44
3.3.1. BCR signaling inhibitors.....	44
3.3.2. BCL2 inhibitors.....	45
4. <i>IN VITRO, IN VIVO AND EX VIVO</i> MODELS FOR THE STUDY OF CLL	
BIOLOGY.....	46
4.1. <i>In vitro</i> CLL models.....	47
4.2. <i>In vivo</i> CLL models.....	48
4.3. <i>Ex vivo</i> CLL models.....	50
4.4. Genome-editing technologies for the generation of novel CLL models.....	51
HYPOTHESIS.....	56
AIMS.....	60
RESULTS.....	64
CHAPTER 1: Next-generation sequencing and FISH studies reveal the appearance of gene mutations and chromosomal abnormalities in hematopoietic progenitors in chronic lymphocytic leukemia.....	68
CHAPTER 2: CRISPR/Cas9-generated models uncover therapeutic vulnerabilities of del(11q) CLL cells to dual BCR and PARP inhibition.....	82
CHAPTER 3: Dissecting the role of <i>TP53</i> alterations in del(11q) chronic lymphocytic leukemia.....	99
CHAPTER 4: Biological significance of monoallelic and biallelic <i>BIRC3</i> loss in del(11q) chronic lymphocytic leukemia progression.....	119
GENERAL DISCUSSION.....	140
CONCLUDING REMARKS.....	155
RESUMEN EN CASTELLANO.....	161
REFERENCES.....	255

SUPPLEMENTARY APPENDIX.....	283
Supplementary Appendix – CHAPTER 1.....	285
Supplementary Appendix – CHAPTER 2.....	291
Supplementary Appendix – CHAPTER 3.....	311
Supplementary Appendix – CHAPTER 4.....	323
LIST OF TABLES AND FIGURES.....	339

LIST OF ABBREVIATIONS

14-3-3ζ	14-3-3 protein zeta	BCR	B cell receptor
α4β1	alpha 4 beta 1 integrin (VLA-4)	BER	Base excision repair
ACAT1	Acetyl-CoA acetyltransferase 1	BH	B-cell CLL/lymphoma 2 homology domain
ADAR	Adenosine deaminase RNA specific	BH3	B-cell CLL/lymphoma 2 homology domain 3
AKT	V-Akt murine thymoma viral oncogene homolog 1	BIM	B-cell CLL/lymphoma-2-like protein 11
allo-TPH	Allogeneic stem cell transplantation	BIRC2	Baculoviral inhibitor of apoptosis (IAP) repeat containing 2
amp	Amplification	BIRC3	Baculoviral inhibitor of apoptosis (IAP) repeat containing 3
APRIL	A proliferation inducing ligand (TNFSF13)	BM	Bone marrow
ARID1A	AT-rich interaction domain 1A	BMSC	Bone marrow stromal cell
ASXL1	Additional sex combs like 1, transcriptional regulator 1	bp	Base pair
ATM	Ataxia telangiectasia mutated	BR	Bendamustine + rituximab
ATR	Ataxia telangiectasia and Rad3- related protein	BRAF	V-Raf murine sarcoma viral oncogene homolog B
ATRX	Alpha thalassemia/mental retardation syndrome X-linked	BRCA1	Breast cancer type 1 susceptibility protein
β₂M	Beta-2 microglobulin	BRCA2	Breast cancer type 2 susceptibility protein
BAFF	B-cell activating factor (TNFSF13B)	BRCC3	BRCA1/BRCA2-containing complex subunit 3
BAFFR	B-cell activating factor receptor	BRD7	Bromodomain-containing protein 7
BAK	B-cell CLL/lymphoma-2 antagonist/killer 1	BTG1	B-cell translocation gene 1
BAX	B-cell CLL/lymphoma-2 associated X protein	BTK	Bruton's tyrosine kinase
BAZ2A	Bromodomain adjacent to zinc finger domain 2A	C-terminal	Carboxyl-terminal
BCL-B	B-cell CLL/lymphoma-2-like protein 10	CAR	Chimeric antigen receptor
BCL-w	B-cell CLL/lymphoma-2-like protein 2	CARD11	Caspase recruitment domain family member 11
BCL-xL	B-cell CLL/lymphoma-extra large	CBA	Chromosome banding analysis
BCL2	B-cell CLL/lymphoma-2	CCL19	C-C motif chemokine ligand 19
BCL2A1	B-cell CLL/lymphoma-2 related protein A1	CCL21	C-C motif chemokine ligand 21
BCL3	B-cell CLL/lymphoma 3	CCND2	Cyclin D2
BCL9	B-cell CLL/lymphoma 9	CCR7	C-C motif chemokine receptor 7
BCOR	B-cell CLL/lymphoma 6 corepressor	CD5	Cluster of differentiation 5
		CD10	Cluster of differentiation 10
		CD19	Cluster of differentiation 19
		CD20	Cluster of differentiation 20

CD23	Cluster of differentiation 23	CT	Computerized tomography
CD27	Cluster of differentiation 27	CXCL12	C-X-C motif chemokine ligand 12
CD31	Cluster of differentiation 31	CXCL13	C-X-C motif chemokine ligand 13
CD34	Cluster of differentiation 34	CXCR4	C-X-C motif chemokine receptor 4
CD38	Cluster of differentiation 38	CXCR5	C-X-C motif chemokine receptor 5
CD40	Cluster of differentiation 40	CUL5	Cullin 5
CD40L	Cluster of differentiation 40 ligand	DDR	DNA damage response
CD43	Cluster of differentiation 43	del	Deletion
CD45RA	Cluster of differentiation 45 isoform A	DLBCL	Diffuse large B-cell lymphoma
CD49d	Cluster of differentiation 49 family member D	DLEU7	Deleted in lymphocytic leukemia 7
CD79a	B-cell antigen receptor complex-associated protein alpha chain	DNA	Deoxyribonucleic acid
CD79b	B-cell antigen receptor complex-associated protein beta chain	DNA PK	DNA-dependent protein kinase
CD81	Cluster of differentiation 81	DSB	Double-strand break
CD90	Cluster of differentiation 90	DDX3X	DEAD-box helicase 3 X-linked
CD200	Cluster of differentiation 200	E2F1	E2 transcription factor 1
CDIPT	CDP-diacylglycerol--inositol 3-phosphatidyltransferase	EBV	Epstein-Barr virus
CDK4	Cyclin dependent kinase 4	EGR2	Early growth response 2
CDKN1B	Cyclin dependent kinase inhibitor 1B	ELF4	E74 like ETS transcription factor 4
CDKN2A/B	Cyclin dependent kinase inhibitor 2A/2B	EP300	E1A binding protein P300
CDR3	Complementary determining region 3	ERK	Extracellular signal-regulated kinase
CHD2	Chromodomain helicase DNA binding protein 2	EWSR1	Ewing sarcoma RNA binding protein 1
CHK1	Checkpoint kinase 1	EXPH5	Exophilin 5
CHK2	Checkpoint kinase 2	FBXW7	F-Box and WD repeat domain containing 7
CK	Complex karyotype	FAT1	Focal adhesion targeting atypical cadherin 1
CK1ε	Casein kinase 1 isoform epsilon	FCR	Fludarabine + cyclophosphamide + rituximab
CLL	Chronic lymphocytic leukemia	FDA	Food & drug administration
CLL-IPI	International prognostic index of CLL	FISH	Fluorescence <i>in situ</i> hybridization
CNA	Copy number alteration	FDX1	Ferredoxin 1
CpG-ODN	CpG oligodeoxynucleotides	FUBP1	Far upstream element binding protein 1
CREBBP	Cyclic AMP-responsive element-binding protein (CREB)-binding protein	FZD5	Frizzled class receptor 5
CRISPR	Clustered regularly interspaced short palindromic repeats	G1	Gap phase 1
crRNA	CRISPR RNA	G2	Gap phase 2
		GC	Germinal center

GEP	Gene expression profiling	IRAK2	Interleukin 1 receptor associated kinase 2
GLI1	Glioma-associated oncogene homolog 1	IRAK4	Interleukin 1 receptor associated kinase 4
GLI2	Glioma-associated oncogene homolog 2	IRF4	Interferon regulatory factor 4
GWAS	Genome-wide association studies	ITAM	Immunoreceptor tyrosine-based activation motif
H2AX	H2A histone family member X (H2AFX)	ITK	Interleukin 2-inducible T-cell kinase
HEV	High endothelial venules	ITPKB	Inositol-trisphosphate 3-kinase B
HIST1H1B	Histone cluster 1 H1 family member B	iwCLL	International workshop on CLL
HIST1H1E	Histone cluster 1 H1 family member E	KDEL2C3	Protein O-glucosyltransferase 3
HL	Hodgkin lymphoma	KLHL6	Kelch like family member 6
HR	Homologous recombination	KRAS	V-Ki-Ras2 Kirsten rat sarcoma 2 viral oncogene homolog
HRK	Harakiri, B-cell CLL/lymphoma-2 interacting protein	Ku70	X-Ray repair cross complementing 6 (XRCC6)
HS1	Hematopoietic cell-specific Lyn substrate 1	Ku80	X-Ray repair cross complementing 5 (XRCC5)
HSC	Hematopoietic stem cell	LCL	Lymphoblastoid cell line
IG	Immunoglobulin	LEF1	Lymphoid enhancer binding factor 1
IGHV	Immunoglobulin heavy chain variable region	LIG3	DNA ligase 3
IGLL5	Immunoglobulin lambda-like polypeptide 5	LIG4	DNA ligase 4
IgM	Immunoglobulin M	LTβR	Lymphotoxin β-73 receptor
IκB	Inhibitor of nuclear factor kappa B	LYN	V-Yes-1 Yamaguchi darcoma viral related oncogene homolog
IκBε	Inhibitor of nuclear factor kappa B epsilon	M-IGHV	Immunoglobulin heavy chain variable region mutated
IKK	Inhibitor of nuclear factor kappa B (IκB)-kinase	MAP2K1	Mitogen-activated protein kinase, kinase 1
IKKα	Inhibitor of nuclear factor kappa B (IκB)-kinase subunit alpha	MAPK	Mitogen-activated protein kinase
IKZF3	IKAROS family zinc finger 3	Mb	Megabase
IL-1R	Interleukin 1 receptor	MBL	Monoclonal B-cell lymphocytosis
IL-15	Interleukin 15	MCL1	Myeloid cell leukemia 1
IL-2	Interleukin 2	MDM2	Mouse double minute 2
IL-21	Interleukin 21	MDR	Minimal deleted region
IL-4	Interleukin 4	MGA	MYC-associated factor (MAX) gene-associated protein
Indel	Insertion/deletion	MED12	Mediator complex subunit 12
IRAK1	Interleukin 1 receptor associated kinase 1	miR-15a/16-1	microRNA 15a/16-1
		miR-29c	microRNA 29c
		miR-34a	microRNA 34a

miR-150	microRNA 150	PFS	Progression-free survival
miR-155	microRNA 155	PI3K	Phosphatidylinositol-4,5-bisphosphate 3-kinase
miRNA	microRNA	PI3Kδ	Phosphatidylinositol-4,5-bisphosphate 3-kinase catalytic subunit delta isoform
MMP	Mitochondrial membrane potential	PI3Kγ	Phosphatidylinositol-4,5-bisphosphate 3-kinase catalytic subunit gamma isoform
MPP	Multipotent progenitors	PKC	Protein kinase C
MRD	Minimal residual disease	PLCG2	Phospholipase C gamma 2
MRE11	Meiotic Recombination 11	POT1	Protection of telomeres 1
MRN	MRE11-RAD50-NBS1 complex	PP2A	Protein phosphatase 2
mTOR	Mammalian target of rapamycin	PPP2R1B	Protein phosphatase 2 scaffold subunit A beta
MYC	V-Myc avian myelocytomatosis viral oncogene homolog	Pro-B	B-cell progenitor
MYCN	MYC neuroblastoma derived homolog	PRKAB2	Protein kinase AMP-activated non-catalytic subunit beta 2
MYD88	Myeloid differentiation primary response 88	PTPN11	Protein tyrosine phosphatase non-receptor type 11
NBS1	Nibrin	PUMA	P53 up-regulated modulator of apoptosis
NF-κB	Nuclear factor of kappa B	R/R	Relapsed/refractory
NFκB1	Nuclear factor of kappa B subunit 1	RAB39	Ras-related protein Rab-39
NFκB2	Nuclear factor of kappa B subunit 2	RAD50	RAD50 homolog (<i>S. Cerevisiae</i>)
NFKBIE	Inhibitor of nuclear factor kappa B epsilon gene	RAD51	RAD51 homolog (RecA homolog, <i>E. Coli</i>) (<i>S. Cerevisiae</i>)
NGS	Next-generation sequencing	RANK	Receptor activator of nuclear factor kappa B
NHEJ	Non-homologous end joining	RB1	Retinoblastoma-associated protein 1
NIK	Nuclear factor of kappa B inducing kinase	RBPJ	Recombination signal binding protein for immunoglobulin kappa J region
NLC	Nurse-like cell	RDX	Radixin
NOTCH1	Notch receptor 1	REL	V-Rel avian reticuloendotheliosis viral oncogene homolog
NOXA	Phorbol-12-myristate-13-acetate-induced protein 1	RelA	V-Rel avian reticuloendotheliosis viral oncogene homolog A
NPAT	Nuclear protein of the ataxia telangiectasia mutated locus	RelB	V-Rel avian reticuloendotheliosis viral oncogene homolog B
NRAS	Neuroblastoma RAS viral (V-Ras) oncogene homolog	RING	Really interesting new gene
NSG	NOD-scid IL2R γ ^{-/-}	RNA	Ribonucleic acid
NXF1	Nuclear RNA export factor 1		
OS	Overall survival		
PAM	Protospacer adjacent motif		
PARP1	Poly(ADP-ribose) polymerase 1		
PAX5	Paired box 5		
PBMC	Peripheral blood mononuclear cell		
PCR	Polymerase chain reaction		

ROR1	Receptor tyrosine kinase like orphan receptor 1	TLR6	Toll-like receptor 6
RPA	Replication protein A	TLR9	Toll-like receptor 9
RPS15	Ribosomal protein S15	TNF	Tumor necrosis factor
RS	Richter's syndrome	TNFα	Tumor necrosis factor α
S	Synthesis phase	TNFAIP3	Tumor necrosis factor α induced protein 3
SAMHD1	SAM and HD domain containing deoxynucleoside triphosphate triphosphohydrolase 1	TNFR	Tumor necrosis factor receptor
sCD23	soluble CD23	TP53	Tumor protein P53
SETD1A	SET domain containing 1A, histone lysine methyltransferase	tracrRNA	Trans-activating CRISPR RNA
SETD2	SET domain containing 2, histone lysine methyltransferase	TRAF2	Tumor necrosis factor receptor associated factor 2
SF3B1	Splicing factor 3b subunit 1	TRAF3	Tumor necrosis factor receptor associated factor 3
sgRNA	Single-guide RNA	TTFT	Time to first treatment
SHM	Somatic hypermutation	U1	U1 small nuclear RNA
SHIP1	SH2 domain-containing inositol 5'-phosphatase 1	UM-IGHV	Immunoglobulin heavy chain variable region unmutated
SHIP2	SH2 domain-containing inositol 5'-phosphatase 2	USP7	Ubiquitin specific peptidase 7
SHP1	Protein tyrosine phosphatase non-receptor type 6	USP28	Ubiquitin specific peptidase 28
SMO	Smoothed, frizzled class receptor	UTR	Untranslated region
SNP	Single-nucleotide polymorphism	VCAM1	Vascular cell adhesion molecule 1
SNW1	SNW domain containing 1	WES	Whole-exome sequencing
SPEN	Spen family transcriptional repressor	WGS	Whole-genome sequencing
SSB	Single-strand break	WHO	World Health Organization
STAT3	Signal transducer and activator of transcription 3	Wnt	Wingless-type MMTV integration site family
SYK	Spleen associated tyrosine kinase	WNT5A	Wingless-type MMTV integration site family, member 5A
t	Translocation	WT	Wild-type
TALEN	Transcription activator-like effector nucleases	XPO1	Exportin 1
TCL1	T-cell leukemia/lymphoma 1	XPO4	Exportin 4
TCR	T-cell receptor	XRCC1	X-Ray repair cross complementing 1
TK	Thymidine kinase	XRCC4	X-Ray repair cross complementing 4
TLR2	Toll-like receptor 2	ZAP70	Zeta chain of T-cell receptor associated protein kinase 70
		ZMYM3	Zinc finger MYM-type containing 3
		ZNF	Zinc finger

INTRODUCTION

1. CHRONIC LYMPHOCYTIC LEUKEMIA – DISEASE OVERVIEW

Chronic lymphocytic leukemia (CLL), a recognized entity in the World Health Organization (WHO) 2017 classification of hematopoietic and lymphoid tumors¹, is a clonal B-cell lymphoproliferative disorder defined by the accumulation of small, mature, neoplastic lymphocytes in the blood, spleen, bone marrow and other lymphoid tissues^{2,3}.

1.1 Epidemiology

CLL is the most common form of leukemia in Europe and in the USA, with an age-adjusted incidence of 4.1/100,000 inhabitants. It accounts for more than 15,000 newly detected cancers and approximately 4,500 annual deaths are estimated in the USA⁴. The average incidence of CLL varies between people from different geographical regions. It is less common within African or Hispanic populations, and its incidence is remarkably lower within Asian individuals^{5,6}. The median age of diagnosis ranges from 70 to 72 years, with a male predominance (1.7:1) in all ethnic subgroups^{4,5}. The proportion of younger patients diagnosed with early stage CLL seems to increase due to more frequent blood testing nowadays. In addition, the demographic changes in society are likely to increase the prevalence and mortality of CLL in the upcoming decades^{4,7}.

1.2 Etiology

The disparities observed in the incidence of CLL between individuals from different geographical regions may indicate that CLL arise from a combination of genetic and environmental factors, however, the exact etiology of CLL remains elusive⁸. Although the vast majority of CLL cases occur sporadically, there is evidence of an inherited predisposition to this disease⁹. First-degree relatives of CLL patients have an 8.5-fold increased risk of developing the disease¹⁰. Moreover, the concordance of CLL is higher among monozygotic twins, when compared to dizygotic twins¹¹. Several genome-wide association studies (GWAS) have also identified single-nucleotide polymorphisms (SNPs) from multiple low-risk CLL susceptibility loci (i.e. 4q25/*LEF1*, 6p25.3/*IRF4*), which in total account for ~19% of familial risk of CLL¹²⁻²⁰.

In terms of environmental factors contributing to the development of CLL, data suggests that Agent Orange as well as exposure to insecticides might be a risk factor for CLL^{21,22}, whereas less evidence is found in relation to the contributing risk of ionizing radiation, viral infections or blood transfusions²³⁻²⁵.

1.3 Diagnosis

According to the latest version of the International Workshop on CLL (iwCLL) guidelines, the diagnosis of CLL is mainly determined by laboratory features, including blood count, differential counts, morphology and immunophenotyping²⁶. CLL is diagnosed when there is a presence of $\geq 5 \times 10^9/L$ clonal B-lymphocytes in the peripheral blood for at least 3 months. In terms of morphology, CLL cells are small, mature lymphocytes with a narrow border of cytoplasm and a dense nucleus lacking discernible nucleoli and having partially aggregated chromatin^{4,26}. The clonality of circulating B-lymphocytes needs to be confirmed by flow cytometry, being the **CLL immunophenotype** characterized by the abnormal expression of the T-cell antigen CD5 in combination with the expression of the B-cell antigens CD19, CD20 and CD23. In comparison to the normal B-cell counterpart, B-CLL cells express lower levels of surface immunoglobulin, CD20 and CD79b²⁶⁻²⁹. In addition, the expression of either kappa or lambda immunoglobulin light chains is restricted in each clone of leukemia cells²⁸. Recent harmonization efforts have confirmed that a panel of CD5, CD19, CD20, CD23, kappa and lambda is sufficient to determine CLL diagnosis³⁰. In borderline cases, other markers such as CD43, CD79b, CD81, CD200, CD10 or ROR1 may help to refine diagnosis³⁰.

The development of CLL is usually preceded by **monoclonal B-cell lymphocytosis (MBL)**, a premalignant state defined by the presence of less than $5 \times 10^9/L$ clonal B cells in the absence of lymphadenopathy, organomegaly (as defined by physical examination or CT scans) or cytopenias^{1,31}. The rate of progression from MBL to CLL ranges from 1% to 2% per year³². The 2017 revision of the WHO classification of lymphoid neoplasms differentiates between low-count MBL and high-count MBL, depending on the number of clonal B cells in the peripheral blood ($< 0.5 \times 10^9/L$ and $\geq 0.5 \times 10^9/L$, respectively). Low-count MBL is highly prevalent in elderly adults and the chance of progression to CLL is very limited, not requiring routine follow-up outside of standard medical care³³⁻³⁶. In contrast, high-count MBL requires routine follow-up and has similar phenotypic and genetic features as early-stage CLL^{36,37}.

At the other end of the spectrum, **CLL may undergo histologic transformation** into an aggressive B-cell lymphoma, being this process known as **Richter's Syndrome (RS)** and related to a very dismal clinical outcome³⁸. A lymph node biopsy is required to determine the diagnosis of CLL transformation into RS³⁹. The WHO classification of lymphoid

neoplasms recognizes two distinct pathologic variants of RS: diffuse large B-cell lymphoma (DLBCL) or Hodgkin Lymphoma (HL). The majority of DLBCL RS cases (~80%) are clonally related to the CLL clone, as determined by the analysis of the rearrangement of *IGHV-D-J* genes. On the other hand, only ~40-50% of HL RS cases are clonally related to the preceding CLL phase, being those clonally unrelated cases considered as *de novo* lymphomas arising in a CLL patient⁴⁰⁻⁴³. In the total CLL population, the incidence rate of RS is ~0.5% and ~0.05% per year of observation for the DLBCL and HL variants, respectively^{44,45}.

1.4 Risk stratification and prognostic markers

CLL is a disease with an extremely heterogeneous clinical course. The clinical manifestation can range from an indolent disease with no treatment requirement and a life expectancy similar to that of an age-matched healthy population, to an aggressive disease characterized by the urgent need of therapeutic intervention, refractoriness to standard treatment and short overall survival (OS)^{3,46}. In order to better classify patients in term of their individual clinical outcome, there are two **staging systems** that were proposed by **Rai**⁴⁷ and **Binet**⁴⁸ more than 40 years ago and are still used nowadays with minor modifications due to their overall simplicity, low-cost requirements, consistence and reliability for been applied by physicians worldwide²⁶. The revised version of Rai staging classifies patients into low, intermediate or high-risk subgroups based on lymphocytosis, anemia or thrombocytopenia, as well as clinical observations such as enlarged lymph nodes, splenomegaly or hepatomegaly. These parameters are also considered by the Binet staging system, which stratifies patients into three categories (A, B and C), and takes into consideration hemoglobin levels and platelet count^{47,48}. In the subsequent years, other easily measurable prognostic markers such as lymphocyte doubling time and bone marrow infiltration were implemented into the CLL risk assessment algorithm^{49,50}.

The recent advances in the research of CLL in the last few decades have enabled the characterization of an impressive amount of potential **biomarkers that provide prognostic information independently of the clinical stage**^{51,52}. These prognostic markers include serum markers (i.e. Beta-2 microglobulin (β_2M), thymidine kinase (TK), soluble CD23)⁵³⁻⁵⁸, genetic markers (i.e. immunoglobulin heavy chain variable region (IGHV) mutational status^{59,60}, B-cell receptor (BCR) immunoglobulin (IG) stereotypy^{61,62}, chromosomal abnormalities⁶³, karyotype complexity⁶⁴, somatic mutations⁶⁵⁻⁶⁸, non-coding alterations^{69,70}, epigenetic subtypes^{71,72}) and immunophenotypic markers (i.e. CD38, ZAP70, CD49d)^{59,73-76}.

Prognostic information about the most relevant biomarkers from each of these categories is depicted in **Table 1**, and detailed information about the prognostic impact of genetic markers will be addressed in *Section 2: CLL Genetics*. To reduce and simplify the great amount of prognostic markers into a few clinically relevant and accessible within hematologists worldwide, several prognostic scores such as the CLL International Prognostic Index (CLL-IPI), have been developed that combine both clinical and genetic information^{77–79}.

Table 1. Main prognostic biomarkers identified in CLL.

Marker	Status predictor for adverse prognosis	Ref.
Serum biomarkers		
β_2 M	> 3.5 mg/L	53,55
TK	> 7.0 U/L	53,56
sCD23	sCD23 doubling time < 1 year	57,58
Genetic biomarkers		
IGHV mutational status	Unmutated	59,60
BCR IG stereotypy	Subset #1, #2 and #8	61,80
FISH chromosomal abnormalities	17p deletion; 11q deletion	63
Karyotype complexity	Complex karyotype (≥ 3 abnormalities)	64
Somatic mutations	<i>TP53, ATM, SF3B1, NOTCH1, BIRC3, EGR2</i>	67,81–86
Non-coding mutations	<i>NOTCH1</i> non-coding mutation	66,69
miRNA expression	\uparrow miR-155, \downarrow miR-150, \downarrow miR-29c, \downarrow miR-34a	87–90
Epigenetic subtype	Naïve B-cell like CLLs	71,72
Immunophenotypic biomarkers		
CD38 expression	$\geq 30\%$ positive cells	59
ZAP70 expression	$\geq 20\%$ positive cells	73,74
CD49d expression	$\geq 30\%$ positive cells	75,76

β_2 M: beta-2 microglobulin; TK: thymidine kinase; sCD23: soluble CD23; IGHV: Immunoglobulin heavy chain variable region; BCR: B-cell receptor; IG: immunoglobulin; FISH: fluorescence *in situ* hybridization; miRNA: micro-RNA; \uparrow high expression; \downarrow low expression.

1.5 CLL Therapy

1.5.1 Indication for treatment and response assessment

Treatment of CLL should be initiated when patients present with progressive or symptomatic/active disease, as defined by a combination of biological or clinical parameters proposed by the iwCLL guidelines²⁶. Patients with asymptomatic disease do not require therapeutic intervention and should be monitored until there is evidence of disease progression⁴.

The criteria required for assessment of treatment response are also indicated in detail in the iwCLL guidelines, which mainly classify treatment response into the following categories: complete remission, partial remission, stable disease, progression and refractory disease²⁶. CLL patients that achieve complete responses can be further categorized based on the detection of minimal residual disease (MRD), a response-assessment marker that has gained crucial relevance in the last decade thanks to the development and improvement of multicolor flow cytometry, PCR or next-generation sequencing (NGS) techniques^{91,92}. Multiple clinical trials have demonstrated that therapies that are able to eradicate MRD (as defined by the presence of less than 1 CLL cell in 10,000 leukocytes) result in an improved long-term clinical outcome⁹³⁻⁹⁵.

1.5.2 Therapeutic approaches and treatment algorithm

The treatment of patients with CLL has come a long way since the first approval of chemotherapy-based regimes over 50 years ago. Chemotherapeutic agents employed for CLL management mainly included purine analogs (most commonly fludarabine) or alkylating agents such as chlorambucil, cyclophosphamide or bendamustine. In the early 2000s, combinations of chemotherapy with immunotherapy (mainly anti-CD20 antibodies such as rituximab) became the gold-standard for CLL treatment, being the combinations of **fludarabine, cyclophosphamide and rituximab (FCR)** or bendamustine plus rituximab (BR) the most prevalent treatment options for CLL patients. In the last decade, the deeper understanding of the biological processes underlying CLL pathogenesis has translated into the approval of drugs that target the signaling pathways that promote the growth and/or survival of CLL cells (alone or in combination with second-generation anti-CD20 antibodies such as ofatumumab or obinutuzumab). Specifically, **BCR signaling inhibitors** (the BTK inhibitors ibrutinib and acalabrutinib and the PI3K inhibitor idelalisib) and **BCL2 inhibitors** (venetoclax) are approved for the treatment of CLL nowadays^{2,4,96}. Although the advent of targeted therapies has revolutionized the CLL treatment scheme, allogeneic stem cell transplantation (allo-TPH) is a potentially curative approach for CLL patients and can be

considered in relapsed/refractory (R/R) patients to targeted agents, as well as in clonally-related RS patients responsive to chemotherapy^{97,98}. Other promising approaches under investigation include the use chimeric antigen receptor T (CAR-T) cells targeting CD19 in combination with ibrutinib or NK cells expressing anti-CD19 CAR⁹⁹⁻¹⁰¹.

In summary, the rapidly evolving treatment landscape over the past few years has shifted the treatment strategy from universal chemoimmunotherapy to a more individualized approach for CLL patients. The current therapeutic algorithm either for frontline or R/R CLL depends on multiple genetic, clinical and therapeutic factors, and is summarized in **Figure 1**.

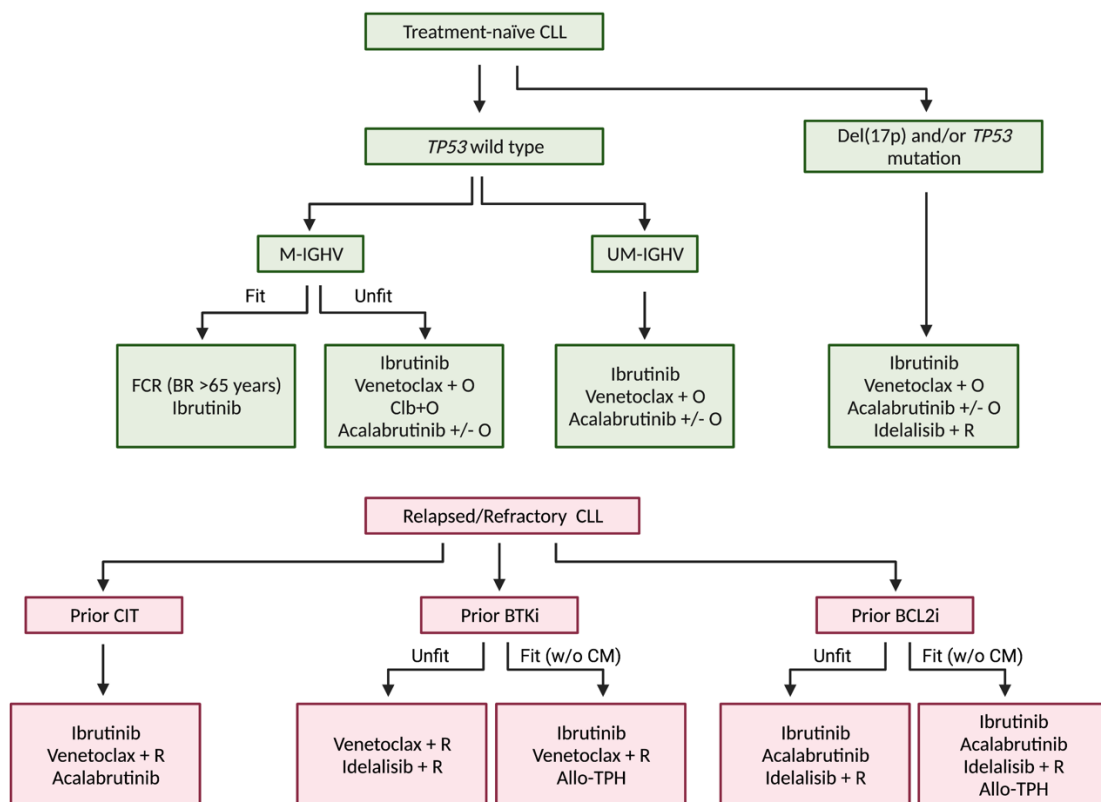


Figure 1. Treatment algorithm for treatment-naïve (green) and relapsed refractory (R/R) (red) CLL patients. FCR: fludarabine + cyclophosphamide + rituximab; BR: bendamustine + rituximab; O: obinutuzumab; Clb: chlorambucil; R: rituximab; CIT: chemoimmunotherapy; BTKi: BTK inhibitor; BCL2i: BCL2 inhibitor; CM: comorbidities; Allo-TPH: allogeneic stem cell transplantation.

2. CLL GENETICS

Emerging knowledge of CLL genetics has unveiled this leukemia as a highly heterogeneous entity, providing information about the distinct cell types from which this

malignancy can originate and the complex set of genetic lesions that are associated with its pathogenesis and prognosis.

2.1 Cellular origin of CLL

The identification of the cell of origin of CLL, as defined by the non-malignant cell from which the leukemic transformation originated, can be useful to determine which specific alteration(s) are the main drivers of the disease¹⁰². The increasing understanding of CLL biology over the years has provide evidence of several cell types compatible to be putative cells of origin. In particular, this has been possible by the extensive immunogenetic study of the CLL BCR IG¹⁰².

The IG molecule is an essential component of the multimeric BCR complex and defines a unique genetic identity that is present from the birth of every B-cell onwards, which is also applicable to B-CLL cells¹⁰³. In the late 1990s, reports began to emerge indicating a pronounced skewing of the IG usage in CLL¹⁰⁴. Specifically, CLL cells have been shown to preferentially use the VH1, VH3 and VH4 regions of the IGHV genes^{104,105}, and express a restricted BCR repertoire, including antibodies with quasi-identical complementary-determining region 3 (CDR3), alluding to antigen selection¹⁰⁶⁻¹⁰⁹. The fact that CLL cells present clonal IG rearrangements, alongside to the particular immunophenotype of these cells, has suggested that B-CLL cells are derived from a mature B cell that express low levels of B-cell markers (surface IG, CD19 and CD20) and are positive for expression of CD23, CD200 and CD5 antigens¹⁰². Specifically, the consistent expression of CD5 led to initial speculation that CLL might be derived from a B1 lineage of B cells that are involved in innate immunity^{110,111}. The subsequent discovery of a group of CLL patients harboring mutations in the IGHV genes (**M-IGHV**) indicated that CLL cells from these cases are derived from antigen-experienced B cells that have been gone through the process of somatic hypermutation in the germinal center (GC) of secondary lymphoid organs^{104,112}. On the other hand, there is another subgroup of CLL patients that do not harbor IGHV mutations (unmutated IGHV; **UM-IGHV**). In these patients, it remains unclear whether CLL cells are derived from pre-GC (naïve) B cells or GC-independent antigen-experienced B-cells^{60,104,112}. This hypothesis has both biological and clinical relevance, since both subgroups have different prognosis. Concretely, UM-IGHV patients, as defined by absent or very limited ($\geq 98\%$ germline identity) burden of SHM, present a more aggressive disease course, with a shorter time to first treatment (TTFT), poor responses to chemoimmunotherapy-based

regimes and reduced OS^{59,60}. In contrast, M-IGHV patients (< 98% germline identity) usually carry a more indolent disease and a remarkable benefit in TTFT and OS^{59,60}.

In the early 2000s, gene-expression profiling (GEP) analyses of CLL and normal human B cell subsets revealed that the transcriptomic profile of both UM-IGHV and M-IGHV cells was more similar to CD27⁺ memory B cells rather than CD5⁺ B cells, indicating that UM-IGHV cells originate from an antigen-experienced GC-independent CD27⁺ cell while M-IGHV derive from a post-GC CD27⁺ B cell^{113,114}. This hypothesis is supported by the finding that in ~40% CLL cases, unrelated patients can carry identical or almost identical BCR IGs, which have been grouped into > 200 sets of stereotyped receptors to date¹¹⁵⁻¹¹⁷, some of them with prognostic implications^{61,80,118-120}. Further GEP studies during the last decade led to the suggestion that M-IGHV CLL cells originate from a previously unrecognized CD27⁺CD5⁺ post-GC subset, whereas UM-IGHV cells resemble CD5⁺CD27⁻ naïve B cells¹²¹ (**Figure 2**). In this line, the methylation profile differs between M-IGHV and UM-IGHV CLL cells, and also resemble that of memory B cells and naïve B cells, respectively⁷¹. However, the possibility that CLL cells originate from a currently unknown non-malignant B cell subpopulation cannot be ruled out¹⁰².

Another controversial aspect of the cellular origin of CLL refers to the **maturation step where the first genetic and/or epigenetic alterations occur**. The recent implementation of large-scale sequencing techniques as well as the improvement of patient-derived xenograft transplantation has suggested that these events might occur in **CD34⁺ hematopoietic stem cells (HSCs)**¹²². In this context, xenotransplantation studies showed that purified HSCs (CD34⁺CD38⁻) from CLL patients, were able to engraft in immunodeficient mice, producing a higher number of polyclonal B cell progenitors (pro-B cells; CD34⁺CD19⁺) than those mice engrafted with HSCs from healthy donors¹²³, suggesting that differentiation of CLL-HSCs skews towards B cell lineage. In addition, CLL-HSCs xenotransplants, but not those mice injected with healthy donor HSCs, gave rise to clonal mature B cells with an immunophenotype CD5⁺CD23⁺ resembling that of MBL and CLL, presumably indicating the crucial role of the BCR signaling in CLL clonal selection¹²³. Consistent with the hypothesis of an existence of a “CLL-HSC” is the fact that in some patients that underwent allogeneic HSC transplantation, pre-malignant lymphoid cells were transmitted from the donor to the recipient and eventually led to CLL development^{122,124}. In addition, specific CLL-related gene mutations and chromosomal abnormalities have been found in CD34⁺ HSCs from CLL

patients^{125,126}, although the difficulty of isolation of pure HSCs without contamination by residual CLL cells remains a major challenge¹²⁷.

Finally, recent growing body of evidence indicate that hematopoietic clones with acquired gene mutations (clonal hematopoiesis) become common with advancing age and can lead to the development of blood cancers, including CLL^{128,129}. Some of these mutations can appear in genes related to CLL pathogenesis, in addition, the mutational landscape of low-count MBL, high-count MBL and early stage CLL is virtually undistinguishable, with CLL-related gene mutations appearing in all three stages, strengthening the notion that at least a fraction of CLL somatic mutations may occur before disease onset¹³⁰. Furthermore, CLL-related chromosomal abnormalities have also been recently found in elderly healthy individuals^{131,132}, reinforcing the hypothesis that the first genetic events might appear in HSCs of CLL patients.

In summary, the cell of origin of CLL has been a subject of continued debate over the years. The current suggested model (**Figure 2**) indicates that **M-IGHV CLL cells are likely to originate from post-GC CD5⁺CD27⁺ cells**, whereas **UM-IGHV CLL cells seem to originate from pre-GC CD5⁺CD27⁻ B cells**, which might arise from naïve B cells or a separated lineage of precursor B cells. In addition, the first genetic events leading to the development of CLL may occur in a previous maturational step involving self-renewing HSCs. However, further studies with the implementation of novel and more accurate techniques such as single-cell DNA and RNA sequencing would be required to fully validate these hypotheses.

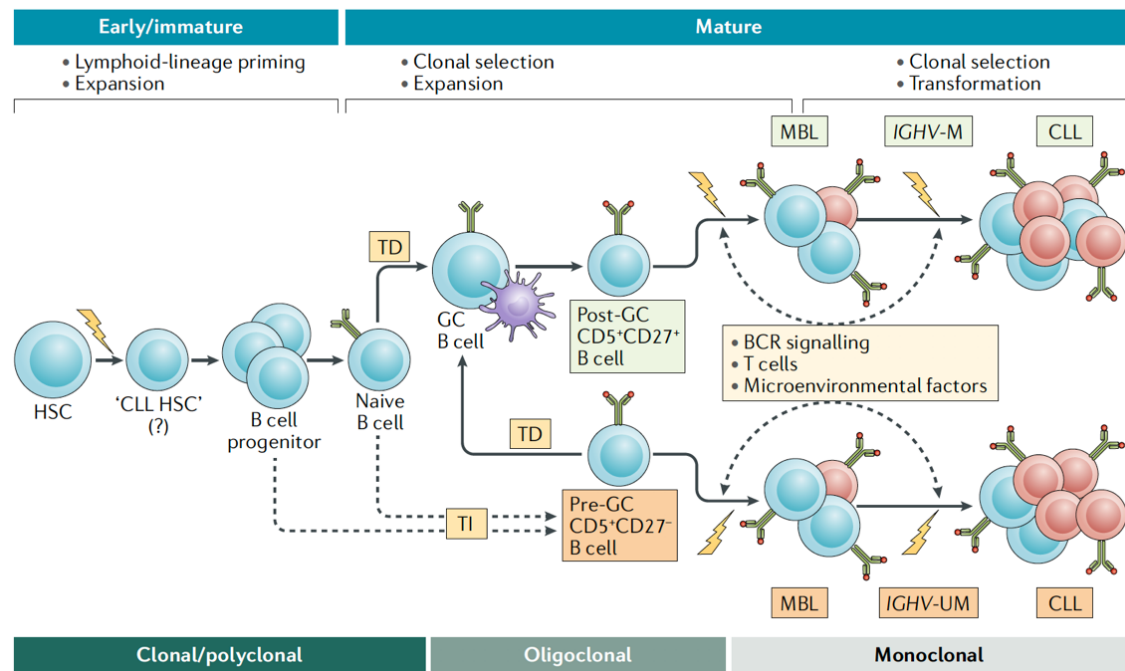


Figure 2. The cellular origin of CLL. Representative scheme of the proposed model for the cell of origin of CLL. The very first genetic events (lightning symbols) related to the pathogenesis of CLL have been suggested to occur in HSCs. These lesions might favor the polyclonal expansion of B cell progenitors and subsequent antigenic stimulation may lead to oligoclonal selection and expansion of mature B cells. Given that M-IGHV cells undergo SHM process, they are likely to derive from post-GC CD5⁺CD27⁺ cells. In contrast, UM-IGHV CLL cells might originate either from pre-GC CD5⁺CD27⁻ naive B cells or a separate lineage of B cell progenitors. Finally, the evolution of these predecessors to MBL and CLL might be orchestrated by additional genetic or epigenetic events, BCR signaling, T cell interaction or additional microenvironmental factors. TD: T-cell dependent; TI: T-cell independent. Dashed arrows indicate speculated pathways. (Taken from Bosch and Dalla-Favera. 2019)¹⁰².

2.2 Genetic alterations in CLL

The high prevalence of CLL and the vast availability of tumor cells in the peripheral blood of these patients has enabled the implementation of cutting-edge genomic techniques for the study of this disease over the years. This in-depth characterization has revealed an **extremely heterogeneous landscape of genomic alterations in this disease**, which reflect the highly variable clinical course observed between patients. Some of these genetic modifications have been shown to be a hallmark of CLL pathogenesis and prognosis, and include chromosomal abnormalities, somatic gene mutations, alterations in non-coding RNA or epigenetic dysregulation.

2.2.1 Chromosomal abnormalities

Since the late 1970s, numerous studies have implemented a wide range of cytogenetic techniques for the detection of chromosomal abnormalities in B-CLL cells: i.e. chromosome

banding analysis (CBA), fluorescence *in situ* hybridization (FISH), genomic arrays and more recently, high-throughput sequencing¹³³. These studies have shed light into the composition of the CLL genome, identifying a broad spectrum of cytogenetic alterations that can be found in up to 80% of CLL cases at diagnosis². Among them, the most prevalent are deletions of the long arm of chromosome 11 and 13, del(11q) and del(13q), respectively, deletion of the short arm of chromosome 17, del(17p), and trisomy of chromosome 12 (trisomy 12), displaying a known role in CLL prognosis and evolution^{63,134}. FISH analyses have become the gold-standard in clinical practice for the detection of CLL chromosomal abnormalities with prognostic significance, and FISH panels usually include probes targeting these four alterations. However, techniques such as genomic arrays or high-throughput sequencing have been shown to provide a more complete picture of the cytogenetic landscape of CLL, whereas CBA still remains as the preferential technique to determine the karyotype complexity of CLL patients¹³³.

2.2.1.1 Del(11q)

Deletion of chromosome 11q22.3 can be found in 12-20% of CLL cases at diagnosis^{63,134-136}. Patients harboring this alteration are usually younger than the typical CLL patient, with a median age of diagnosis of 59 years, and often present with a disease characterized by a bulky lymphadenopathy¹³⁷. This subgroup of CLLs frequently associates with poor prognostic features, such as UM-IGHV and ZAP70 positivity, and the clinical course of these patients is usually defined by a rapid disease progression, short TTFT and reduced OS in patients treated with chemotherapy-based regimes^{63,137-141}. In addition, it has been reported by our group and others that the clonal size of del(11q) has a prognostic impact^{142,143}.

The presence of del(11q) is exclusively monoallelic in CLL, and the size of this deletion is highly variable between patients¹⁴⁴⁻¹⁴⁶. The majority of the patients harbor a large del(11q), usually spanning more than 20 megabases (Mb) in size. In contrast, a small subgroup of del(11q) patients present a smaller deletion, although the biologic or prognostic significance of these differences is unknown¹⁴⁷. The implementation of high-resolution SNP arrays has revealed that the vast majority of del(11q) cases have a **common minimally deleted region (MDR)** of 2-3 Mb, encompassing the tumor suppressor gene *ATM*, among others¹⁴⁶⁻¹⁴⁹.

The biology underlying the progressive nature of del(11q) CLL cases is currently unknown. Traditionally, it has been considered that *ATM* deletion is the main responsible for the pathobiology of del(11q). This has been supported by the fact that **one third of**

del(11q) patients harbor deleterious *ATM* mutations in the remaining allele, having as a consequence a biallelic *ATM* loss and a complete *ATM* dysfunction^{82,150}. Given that **ATM** is a **central regulator of the DNA damage response (DDR)** signaling pathway, several reports have studied the role of del(11q) in chemotherapy response and genomic integrity, establishing that del(11q) CLL cells present an altered response to chemotherapy-based regimes and higher mean of copy number alterations (CNAs) representing genomic instability^{82,151–153}. In addition, other genes included within this deletion have been postulated to have a role in CLL progression. One of these genes is ***BIRC3***, a negative regulator of the nuclear factor kappa-light-chain-enhancer of activated B cell (NF-κB) signaling, which is deleted in ~80% of del(11q) cases and can also be biallelically affected through truncating mutations in the remaining allele^{85,154–156}. However, the biological significance of monoallelic and biallelic *BIRC3* deletion in CLL remains unexplored. Finally, the haploinsufficiency of other genes located in 11q22.3 (i.e. *RDX*, *FDX1*, *RAB39*, *CUL5*, *ACAT1*, *NPAT*, *KDELC2*, *EXPH5*, *MRE11*, *HA2XF*, *USP28* and *PPP2R1B*) might play a role in del(11q) pathogenesis, although to date there is only very circumstantial and limited data without further functional validation providing a link between the haploinsufficiency of some of these genes and the pathobiology of del(11q)^{147,152,157}.

2.2.1.2 Del(13q)

Deletion of 13q14 region is found in more than 50% of CLL cases at diagnosis and is the most common cytogenetic abnormality detected in CLL^{63,134–136,158}. The presence of this deletion defines a subset of patients associated with good prognostic characteristics, such as M-IGHV, longer TTFT and OS, especially in those cases harboring del(13q) as the sole cytogenetic abnormality^{63,135,159}.

This type of deletion displays substantial anatomic heterogeneity between patients, although the **MDR** usually comprises the microRNA (miRNA) cluster **miR-15a/16-1** as well as ***DLEU7*** and all the genes comprised in between^{160–164}. Large deletions of 13q14 can include the tumor suppressor *RB1*, which can aggravate the outcome of this subset of del(13q) CLL patients^{165–167}. In contrast to other recurrent chromosomal abnormalities in CLL, del(13q) biallelic losses can appear in ~30% of del(13q) CLL patients, although the clinical impact of this type of event is controversial^{159,167–169}.

At the biological level, it has been reported that the loss of miR-15a/16-1 results in dysregulation of cell cycle and apoptosis, both hallmarks of CLL biology². Specifically, these

miRNAs seem to modulate the expression of cyclin D2 and the anti-apoptotic protein BCL2^{170,171}. The role of this miRNA cluster in CLL pathogenesis has been confirmed *in vivo*, since conditional deletion of the murine locus equivalent to the human del(13q) MDR, as well as a larger common deleted region, recapitulate the different steps involved in evolution from MBL to CLL^{171,172}.

2.2.1.3 Del(17p)

Deletions of 17p13/*TP53* chromosomal region are found at different frequencies in CLL depending on the clinical stage of the disease, ranging from 4-12% at diagnosis up to 30% at relapse^{63,81,134,173-175}. **Del(17p)** has always been considered as the **highest risk chromosomal abnormality** in CLL, and patients harboring this alteration show the shortest progression-free survival (PFS) and OS among all cytogenetic subgroups^{63,134,176}. In addition, many studies have confirmed that del(17p) responds poorly to chemotherapy-based regimes¹⁷⁶⁻¹⁷⁸, and the presence of this deletion is also associated with transformation into RS^{179,180}. The clonal size of del(17p) has also been shown to have a prognostic impact^{134,181}, and the presence of del(17p) is usually associated with poor prognostic features such as CD38 positivity and UM-IGHV, although a subset of M-IGHV del(17p) patients with a more favorable outcome has also been reported¹⁸²⁻¹⁸⁴.

17p13 deletions are usually large in size (~18-22 Mb) and can be the consequence of various structural changes such as deletion itself, unbalanced translocations or isochromosomes¹⁸⁵. **Del(17p) invariably comprises the tumor suppressor *TP53*** within its deleted region¹⁵¹. In addition, *TP53* gene mutations in the remaining allele have been found in approximately 80% of del(17p) patients, indicating that biallelic dysfunction of this gene appears to be the main mechanism responsible for the pathobiology and prognostic implications of del(17p) CLL^{174,186-188}.

TP53 acts as a tumor suppressor gene that plays a key role in the intersection of several biological pathways such as **cell cycle, apoptosis and the DDR signaling**¹⁸⁹. In particular, apoptotic dysregulation underlies the poor responses of del(17p) CLLs to chemotherapy agents, especially purine analogs and alkylators, since these agents rely on a functional *TP53* protein for a correct apoptosis induction^{73,190}. Moreover, the role of *TP53* on the DDR signaling has been shown to profoundly impact the genomic integrity of CLL, being the presence of del(17p) associated with a high genomic complexity and multiple concurrent CNAs such as losses of 4p, 9p, 18p and 20p, or chromosome 8 alterations (either 8p deletion

or 8q gain)^{145,148,187,191}. This genetic complexity also seems to underlie transformation of del(17p) CLL cells into RS^{179,180,192}. Finally, providing the large size of 17p13 deletions in CLL, it is presumable that this type of lesion involves additional gene downregulations, although further research is needed to determine the biological impact of the loss of other genes within del(17p)¹⁸⁵.

2.2.1.4 Trisomy 12

Chromosomal gain of an entire copy of chromosome 12 appears in 12-18% of CLL cases at diagnosis^{63,134-136}. Trisomy 12 has always been considered as an **intermediate-risk** lesion in newly-diagnosed CLL, however, extensive research into this cytogenetic subgroup has unveiled trisomy 12 as a more complex and **heterogeneous clinical entity**^{63,193-196}. Trisomy 12 CLL cells are characterized for a distinct immunophenotype, showing atypical morphology, high expression of CD38 and CD49d, and loss of CD5 expression in some cases^{197,198}.

Given that the entire chromosome 12 is gained in this subset of CLL patients, it has been difficult to establish a main set of candidate genes responsible for the pathobiology of the disease. Nonetheless, overexpression of several chromosome 12 genes such as *MDM2*, *BAX*, *E2F1* or *CDK4* has been observed, suggesting a dysregulation in cell cycle, apoptotic and proliferation in this cytogenetic subgroup¹⁹⁹. Moreover, trisomy 12 patients present a **distinctive cytogenetic landscape** when compared to the rest of CLL subgroups, which is characterized by a high co-occurrence with additional trisomies (especially those on chromosome 18 and 19), 14q32 translocations and 14q deletions^{194,195,200-205}. Trisomy 12 CLL patients have also been shown to be highly enriched for mutations in genes implicated in Notch and MAPK-ERK signaling pathways, possibly indicating a role of these pathways in the progression of trisomy 12 cases^{193,196,206-209}.

2.2.1.5 Other cytogenetic alterations

In addition to the aforementioned chromosomal abnormalities, other recurrent CNAs have been observed in 1-5% of CLL cases. Among these, deletions of 3p, 6p, 6q, 8p, 9p, 10q, 14q, 18p and 20p, as well as gains of 2p, 8q, trisomy 18 and trisomy 19 have been consistently reported in CLL^{145,151,153,191,210,211}. The minimal deleted or amplified region of some of these lesions include genes involved in signaling pathways important for CLL pathogenesis, i.e. *CDKN2A/B* in 9p deletion^{153,210}, *TRAF3* in 14q deletion²¹², *XPO1*, *MYCN* and *REL* in 2p

amplification^{213,214} or *MYC* in 8q amplification²¹¹. Nevertheless, the biological and clinical implications from most of these CNAs have not been elucidated to date.

Apart from deletions, amplifications or gains of entire chromosomes, other cytogenetic events such as translocations can be observed at lower frequencies in CLL. The main translocations observed are those involving 14q32/*IGH*. This event usually has recurrent translocation partners such as *BCL2* -t(14;18)- or *BCL3* -t(14;19)-, although other non-recurrent partners have also been described²¹⁵. Other translocations found in CLL can involve 8q24/*MYC* or 13q14^{215,216}, and the prognostic impact of the presence of some of these translocations in CLL has been addressed in several studies^{203,216–219}.

2.2.1.6 Complex karyotype

Complex karyotype (CK) is generally defined as the finding of ≥ 3 numerical and/or structural abnormalities in one or more clones, although some studies define CK as a finding of 5 or more aberrations^{64,215,220–222}. In recent years, the presence of genomic complexity has attracted great interest in the CLL community, in light of reports suggesting that CK, besides representing an independent prognostic marker^{222–225}, may also constitute a predictive marker for refractoriness, not only to chemoimmunotherapy-based regimes^{226,227}, but also novel targeted agents, independent of *TP53* abnormalities^{228–232}. One particular exemption to the CK-associated poor-prognostic impact is constituted by a subgroup of trisomy 12 patients that harbor additional trisomies in chromosomes 18 and 19, which shows excellent clinical outcomes, even better than those of non-CK CLL patients^{64,194}.

Although the presence of karyotype complexity has an impact in CLL prognosis, evolution and treatment response²³³, the biological mechanisms underlying the effects of CK in these aspects of the disease remain far from being understood. It has been established however, that the presence of CK may be favored by a defective DDR signaling and incorrect maintenance of genomic integrity²³⁴. This is further supported by the fact that the presence of CK is enriched in CLL patients harboring del(11q)/*ATM* and/or del(17p)/*TP53* abnormalities^{64,153,191}.

2.2.2 Somatic mutations

The advent of NGS and the application of whole-exome sequencing (WES) and whole-genome sequencing (WGS) techniques has enabled the discovery of recurrent somatic mutations in a wide variety of driver genes, as well as refined algorithms for the detection

CNAs through sequencing data, transforming our understanding of the genetic heterogeneity of CLL^{65,66,83,235-240}. Overall, WES and WGS studies of approximately 1000 CLL specimens have revealed the presence of 0.6-0.9 mutations per Mb and an average of 15.3-26.7 somatic mutations per patient, indicating a low mutational load in comparison to other lymphoid or solid tumors^{65,66,241}. In particular, seminal studies by Landau *et al.*⁶⁵ and Puente *et al.*⁶⁶ have provided the largest sequenced collections to date, revealing a **vast genetic heterogeneity** in CLL, with few driver genes mutated in 10-15% of cases, and a **large number of candidate driver genes mutated at frequencies lower than 10% of cases (Figure 3)**. These studies have highlighted not only a high intertumoral genetic heterogeneity of CLL, but also have addressed the study of CLL intratumoral heterogeneity.

Among driver genes found to be recurrently mutated in CLL, some of them have been shown to impact the prognosis and treatment response of CLL. In the following sections, mutations in the most frequently mutated genes in CLL as well as their clinical implications will be described.

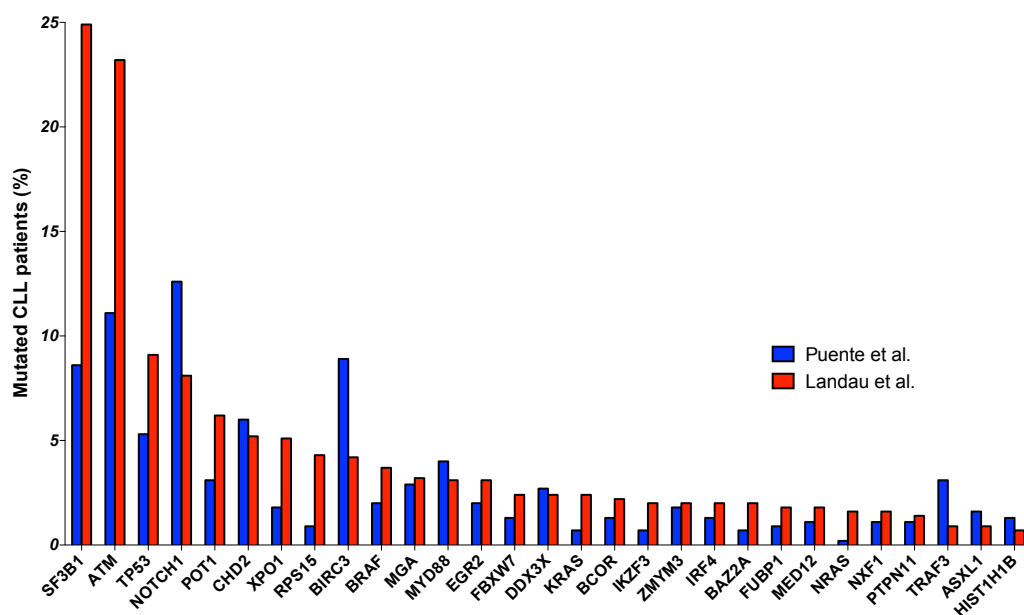


Figure 3. Recurrently mutated CLL driver genes identified in Landau *et al.*⁶⁵ and Puente *et al.*⁶⁶ Adapted from Rodríguez-Vicente AE *et al.* 2016²⁴¹

2.2.2.1 ATM mutations

ATM mutations can be found in 10-20% of CLL patients at diagnosis or prior to treatment^{65,66,242,243}. *ATM* mutations can be either missense substitutions, in-frame or out-of-

frame insertions/deletions (indels) or nonsense, frameshift or splice-site mutations, giving as a consequence a dysfunctional or truncated ATM protein¹⁴⁷. In addition, these type of mutations can occur throughout the entire coding region of the *ATM* gene, with no hotspot regions identified to date¹⁴⁷. As indicated in the previous section (2.2.1 *Chromosomal abnormalities*), *ATM* is located on the chromosomal band 11q22.3, and is located in the MDR of virtually all del(11q) CLL patients, resulting in a monoallelic *ATM* loss¹⁴⁷⁻¹⁴⁹. Indeed, ***ATM* mutations are highly enriched in cases harboring del(11q)** -approximately one third of del(11q) patients harbor *ATM* mutations in the remaining allele-, having as a consequence a complete biallelic dysfunction of the ATM protein^{82,146,150}. Although a high proportion of *ATM* mutations are somatic, germline heterozygous *ATM* mutations can also be found in CLL patients, which has been suggested to influence a rapid disease progression through *ATM* loss of the remaining allele^{242,244,245}.

In terms of clinical significance, ***ATM* mutations seem to have an impact when they lead to a complete loss of ATM function**. This has been especially observed in del(11q) patients, being the presence of biallelic *ATM* lesions related to a shorter PFS and OS than *ATM* wild-type (WT) or del(11q) patients without additional *ATM* defects, similar to that of *TP53*-altered patients^{82,146,150,246}. In contrast, monoallelic *ATM* mutations do not seem to confer a dismal prognosis in CLL^{65,150,247}, although they have been associated with shorter TTFT in some cohorts^{66,68}.

2.2.2.2 *TP53* mutations

Mutations in *TP53* are present in 5-10% CLL at diagnosis or prior treatment, and its incidence is further increased in R/R patients (~ 40%)^{65,66,81,174,176,248}. In addition, the presence of ***TP53* mutations in del(17p) CLL patients raises up to 80% of cases**, indicating a crucial role of biallelic *TP53* dysfunction in the pathogenesis of the disease^{174,186,187}. Albeit less frequent, *TP53* mutations can be also accompanied by a copy-number neutral loss of heterozygosity of the second *TP53* allele, leading to biallelic *TP53* dysfunction as well^{65,66,151}. *TP53* somatic variants include missense mutations, indels, nonsense mutations or splice-site mutations, leading to a gain-of-function phenotype in the case of missense substitutions, or a *TP53* loss-of-function in the rest of the variants^{188,249}. Although *TP53* mutations have been found throughout the entire coding region in CLL, they are heavily concentrated in exons 4-8, which correspond to the DNA binding domain of the *TP53* protein¹⁸⁸.

Alongside with del(17p), ***TP53* mutations are nowadays one of the strongest prognostic and predictive markers in CLL.** They are associated with a markedly short TTFT and OS, as well as impaired response to chemoimmunotherapy-based regimes^{65,66,81,174,176,248}. Both monoallelic and biallelic *TP53* defects are associated with unfavorable outcomes, although several studies have reported a more detrimental effect of biallelic *TP53* loss in comparison to monoallelic lesions^{81,150,186,187}. *TP53* mutations also seem to impact the outcome of CLL patients regardless of their clonal size in some cohorts^{68,250}, although further research needs to be performed in this area since other studies have not found a clinical impact of subclonal (variant allele frequency < 10-12%) *TP53* mutations^{156,187}. Interestingly, a very recent study indicates that *TP53* subclonal mutations only impact the outcome of UM-IGHV patients that have not received targeted therapy²⁵¹. Finally, recent evidence suggest that *TP53* lesions may also have a detrimental impact in the context of novel targeted agents^{231,252,253}.

2.2.2.3 *BIRC3* mutations

BIRC3 is mutated in 2.5-10% of CLL cases at diagnosis or prior to treatment^{65-67,85}. *BIRC3* mutations are usually frameshift or nonsense mutations affecting exons 6-9, which result in a premature truncation of the C-terminal RING domain of the *BIRC3* protein, resulting in a loss-of-function of the E3 ubiquitin ligase activity of this domain^{85,155}. In a lesser extent, frameshift and missense mutations have been found in other *BIRC3* coding exons as well⁶⁶. *BIRC3* mutations often associate with del(11q) in CLL (~10% of del(11q) cases), and given that *BIRC3* is located in chromosome 11q22.2 and is monoallelically lost in approximately 80% of del(11q) patients, the presence of a mutation in the remaining allele leads to a biallelic *BIRC3* disruption, resulting in a complete functional loss of *BIRC3* activity^{66,85,146,154,156}.

Recent studies have demonstrated that biallelic *BIRC3* inactivation is an independent prognostic marker for TTFT and OS in CLL^{66,154,156}. However, the prognostic significance of monoallelic *BIRC3* mutations remains uncertain, since some studies have found *BIRC3* mutations to have a clinical impact^{66,85,155,254} whereas others have not^{65,68,156,247}. Moreover, *BIRC3* mutations are enriched in chemoimmunotherapy R/R patients, conferring reduced PFS and OS in some fludarabine-treated cohorts^{85,155}, although the mechanistic insights by which *BIRC3* mutations could contribute to fludarabine resistance have not been elucidated.

2.2.2.4 *SF3B1* mutations

SF3B1 encodes for the splicing factor subunit 3b, one of the components of the multi-protein splicing machinery. *SF3B1* is one of the most recurrently mutated genes in CLL, with a mutational incidence ranging from 10% in newly diagnosed patients to nearly 20% in patients in need for treatment^{65,66,236,238,255}. *SF3B1* mutations in CLL are exclusively missense substitutions in hotspot regions belonging to the HEAT repeats, leading to a gain-of-function phenotype^{236,238,256,257}. Indeed, over 50% of *SF3B1* mutations in CLL correspond to a single aminoacid substitution, namely K700E^{236,238,258}. Mutations in *SF3B1* usually associate with del(11q) and UM-IGHV, and have been shown to impact TTFT and OS in several CLL cohorts^{65,67,238,256,258–260}.

2.2.2.5 *NOTCH1* mutations

NOTCH1 mutations can be found in 8-12% of CLL patients at diagnosis or prior to treatment^{65–67,83,235,258,259,261}, with a higher incidence in chemoimmunotherapy R/R and RS patients^{84,153,180,235,261}. This gene encodes for a protein that plays a role as the central activator of the Notch signaling pathway²⁶². *NOTCH1* mutations in CLL are mostly frameshift or nonsense events affecting exon 34, which correspond to the protein C-terminal PEST domain^{83,84,235,258,261}. More recent data have also revealed the presence of non-coding mutations in the 3'UTR region of *NOTCH1*, sharing the same functional consequence as “canonical” *NOTCH1* mutations⁶⁶. *NOTCH1* mutations strongly associate with trisomy 12 and UM-IGHV, and its presence is related to a shorter TTFT and OS in some cohorts^{84,206,207,235,258,260,261,263,264}. In addition, CLL patients harboring *NOTCH1* mutations do not favor from treatment with anti-CD20 antibodies in the context of chemoimmunotherapy^{176,265}.

2.2.2.6 Other recurrent somatic mutations with prognostic impact

NGS studies in several CLL cohorts worldwide have addressed whether the presence of other recurrently mutated driver genes (**Figure 3**) has a clinical impact in CLL. Among these, mutations in *EGR2*, *RPS15*, *NFKBIE*, *SETD2*, *POT1* and genes belonging to the MAPK-ERK signaling pathway (i.e. *BRAF*, *KRAS*, *NRAS*) are mostly associated with UM-IGHV and have been postulated to worsen the outcome of CLL patients^{86,117,126,156,196,208,227,239,266,267}, although larger harmonization efforts from multiple CLL cohorts would be required in order to fully validate these mutations as putative and independent prognostic markers in CLL. In

contrast, hotspot mutations in *MYD88* are associated with favorable biological factors such as M-IGHV and isolated del(13q), and may contribute to a longer OS^{67,247,268,269}.

2.2.3 microRNA expression

Apart from the presence of chromosomal aberrations or somatic mutations in coding regions, CLL is also characterized for an aberrant expression of miRNAs, which are non-coding RNAs that participate in post-transcriptional regulation of gene expression through direct targeting of UTR regions^{270,271}. Indeed, CLL was the first human disease that was found to be associated to miRNA dysregulation, highlighting the role of miR-15a/16-1 in the MDR of del(13q) patients¹⁶⁰. Since then, numerous miRNAs have been found to have a role in CLL biology, being the attention especially focused on those that are differentially expressed in subgroups with distinctive clinical and/or biological features^{272,273}. For instance, miR-34a is downregulated in del(17p)/*TP53* mutated patients and is involved in DDR signaling, cell cycle arrest and apoptosis^{89,274,275}, whereas miR-155 is upregulated in del(11q) patients and acts as a BCR signaling enhancer^{87,274}. In addition, differential expression of certain miRNAs such as miR-155, miR-150, miR-29c or miR-34a has an impact in the clinical outcome in CLL patients^{87,89,90,275,276}.

2.2.4 Epigenetics

Epigenetics describes heritable phenotypic changes in a chromosome or its associated histones that affect transcriptional activity but do not involve changes in the DNA sequence. This dysregulation in the transcriptional control can be caused by aberrant DNA methylation and/or histone modifications and is one of the hallmarks of cancer cells²⁷⁷. DNA methylation studies have revealed that **CLL displays global hypomethylation** in genes and enhancer regions, combined with local hypermethylation in single-gene promoters^{71,277}. In addition, the CLL epigenome remains highly stable since the MBL state throughout the rest of the disease course, as well as in relation to therapy, reflecting the epigenome of the cell of origin^{71,278,279}. Indeed, methylation signatures have been able to classify CLL patients into three clinically relevant epigenetic subgroups that correlate with IGHV mutational status and patient outcome: memory-like CLL (mainly M-IGHV, good prognosis), intermediate CLL (mixed between M-IGHV and UM-IGHV, intermediate prognosis) and naïve-like CLL (mainly UM-IGHV, poor prognosis)^{71,72}. Furthermore, high levels of intra-sample

methylation heterogeneity have been observed in CLL and correlate with high-risk genetic lesions, clonal evolution and adverse prognosis^{280,281}.

Recent efforts have also deepened into other aspects of the CLL epigenome by integrating DNA methylome, histone modification maps, chromatin accessibility, three-dimensional chromatin architecture, as well as transcriptomic and genomic data, revealing that although most genetic abnormalities are not associated with consistent epigenetic profiles, trisomy 12 and *MYD88* mutated patients show distinct chromatin configurations²⁸².

2.3 Clonal evolution and growth kinetics of CLL

Clonal evolution is characterized by the acquisition of genetic lesions during the lifetime of a tumor cell and it was first documented in CLL by CBA and FISH studies in the 2000s. However, it was not until the later development of WES and WGS techniques when a more comprehensive picture of clonal evolution throughout the disease course was characterized^{65,237,283–286}.

Sequential sampling of peripheral blood collected at different time points of CLL patients helped to describe the clonal dynamic patterns of the disease. These patterns include: **linear evolution**, defined as the persistence of a founder clone with further acquisition of novel mutations, **branching evolution**, defined as the parallel evolution of competitive clones, or **convergent evolution**, defined as the acquisition of more than 1 mutation in the same gene. In addition, some CLL patients lack clonal evolution during the course of the disease^{287–289}. Large clonal shifts have been usually observed between pre-treatment and relapsed samples while stable subclonal composition has been shown to be more prevalent within untreated CLL patients with stable disease^{65,237,290}, being the evolution from stable to active disease characterized by the acquisition of novel lesions²⁹¹. In terms of specific alterations, WGS and WES data consistently infers that *del(13q)*, trisomy 12 and *MYD88* mutations are clonal events occurring early in the disease course, whereas *ATM*, *TP53* or *BIRC3* mutations are mostly subclonal^{65,237}.

The growth dynamics of CLL cells is also heterogenous, some patients exhibit a **logistic growth** behavior in which the clone stabilizes overtime, whereas some others show an **exponential growth** pattern²⁹². Those patients with exponential growth are characterized by a higher number of driver mutations and have a higher rate of clonal evolution after therapy²⁹². In addition, it is well established that concurrent driver alterations usually coexist

within the same CLL clone, and the coexistence of driver alterations is not random, since large-scale WGS and WES have revealed specific patterns of co-occurrence or mutual exclusivity between CLL genetic lesions (i.e. co-occurrence of del(11q)/*ATM* and *SF3B1* mutations or mutual exclusivity within del(13q) and trisomy 12)^{65,66}. Indeed, recent efforts have demonstrated the development of CLL in mice harboring combined deletion of *ATM* and *SF3B1* mutation, but not on those carrying each single abnormality²⁹³. Nevertheless, extensive research needs to be performed in this field in order to unveil the biological determinants by which cooperation of specific abnormalities lead to exponential CLL growth and disease progression.

3. CLL BIOLOGY – TARGETING SIGNALING PATHWAYS

3.1 Molecular pathways in CLL

Recurrent genetic lesions in CLL tend to cluster within specific biological pathways critical for CLL pathogenesis and evolution^{65,66}. For example, both *ATM* and *TP53* alterations share a common function in the DDR signaling and cell cycle checkpoints, whereas the pathways activated downstream BCR signaling such as the MAPK-ERK or NF- κ B pathways can be affected by multiple alterations potentially resulting in the same functional consequence^{196,208,294–298}. In addition, Notch signaling is not only affected by coding and non-coding mutations in *NOTCH1*, but also alterations in genes encoding for positive (i.e. *MED12*) or negative (i.e. *FBXW7*, *SPEN*, *RBPJ*, *SNW1*) regulators of NOTCH1 activity^{66,153,299,300}. Other relevant molecular pathways in CLL frequently altered by genetic lesions are RNA (i.e. *SF3B1*, *U1*, *XPO1*) and ribosomal processing (i.e. *RPS15*)^{257,301–303}, as well as chromatin modification (i.e. *CHD2*, *STED2*, *HIST1H1B*, *HISTH1E*)^{65,66,267,304,305}. **Table 2** summarizes the most recurrently altered drivers identified in CLL, grouped according to the biological pathway in which they are involved. Understanding the biology resulting from the genetic heterogeneity of CLL has become essential in order to develop novel targeted therapies for the personalized treatment of the disease. In addition, it has been recently reported that the number of signaling pathways altered by driver mutations has an impact in the disease outcome and can be used as a biomarker in prognostic models of CLL²⁵⁴.

Table 2. Biological processes affected by recurrent genetic lesions in CLL drivers.

Biological Pathway	Genes altered in CLL*
DNA damage response & cell cycle control	<i>ATM, TP53, POT1, MIR-15A/16-1, SAMHD1, CHK1, CHK2, ATRX, CCND2, CDKN1B, CDKN2A/B, BRCC3, ELF4</i>
Apoptosis	<i>TP53, MIR-15A/16-1, BCL2</i>
BCR signaling	<i>EGR2, IKZF3, BCOR, IGLL5, KLHL6, PAX5, IRF4, ITPKB, CARD11</i>
MAPK-ERK signaling	<i>HRAS, NRAS, BRAF, PTPN11, MAP2K1</i>
TLR signaling	<i>MYD88, TLR2, TLR6, IRAK1, IRAK2, IRAK4</i>
NF-κB signaling	<i>BIRC3, BIRC2, NFKBIE, TRAF3, TRAF2, NFKB2, REL, TNFAIP3</i>
Notch signaling	<i>NOTCH1, FBXW7, MED12, SPEN, RBPJ, SNW1</i>
RNA and ribosomal processing	<i>SF3B1, XPO1, U1, RPS15, DDX3X, NXF1, XPO4, FUBP1, EWSR1</i>
Chromatin modification	<i>CHD2, ZMYM3, SETD2, HIST1H1B, HIST1H1E, ASXL1, ARD1A, BAZ2A, SETD1A, CREBBP</i>
Wnt signaling	<i>MED12, FAT1, BCL9, BRD7, FZD5</i>
Hedgehog signaling	<i>SMO, GLI1, GLI2, BCOR, MED12, CREBBP, EP300</i>
MYC signaling	<i>FBXW7, MGA, MYC, FUBP1, PTPN11</i>

*Genes affected by either recurrent CNAs and/or somatic mutations are included in the table. Bold labels: driver genes altered by somatic mutations and/or CNAs in more than 5% of CLL patients at diagnosis or prior treatment; alterations in the rest of the indicated genes are found in < 5% of CLL patients (frequencies can vary between untreated early stage, untreated advanced stage or R/R CLL cohorts). Note that genes may be involved in more than one pathway^{65,66,307,83,153,203,236,237,268,301,306}.

3.1.1 DNA damage response and cell cycle control

DNA double strand breaks (DSBs) or single strand breaks (SSBs) represent some of the most toxic DNA lesions, which, if unrepaired, lead to cell death and trigger genomic instability³⁰⁸. The DDR signaling process is initiated with the recognition of such lesions and often results in the activation of cell cycle checkpoints to arrest cell cycle progression³⁰⁹. The DNA damage checkpoint network is composed of DNA damage sensors, signal transducers and multiple effector pathways, and its central components are the protein kinases ATM, ATR and DNA PK. These kinases have multiple substrates, for example, CHK2 and TP53 for ATM, or CHK1 for ATR, which orchestrate arrest in G1, S or G2 cell cycle phases, as well as DNA repair and cell death (**Figure 4**)³¹⁰.

During G1 and G2 cell cycle checkpoints, **DSBs** can be repaired by two major pathways: **non-homologous end joining (NHEJ)** or **homologous recombination (HR)**. NHEJ does not depend on an intact DNA template for repair, and is primarily used in the G1 phase of the cell cycle when a sister chromatid is not available as a template³¹¹. In brief, NHEJ relies on

the catalytic activity of the protein kinase DNA PK, which is recruited to the DSB site through interaction with the non-catalytic subunits Ku70 and Ku80 (**Figure 4**)^{308,312}. Then, DNA PK in coordination with other proteins such as XRCC4 and Lig4 are able to promote re-ligation of the DSB ends in an error-prone process, since random nucleotide insertions or deletions are produced during re-ligation^{308,312}. On the other hand, HR is an error-free DSB repair mechanism that requires the presence of an intact DNA template for repair, being its use therefore restricted to late S and G2 cell cycle phases³¹¹. During HR, immediately following the occurrence of a DSB, the MRN complex (consisting on MRE11, RAD50 and NBS1 proteins) is recruited to the lesion site. In parallel, ATM is activated and recruited to the lesion through interaction with NBS1, subsequently phosphorylating histone H2AX on Ser-139 (γ H2AX), which serves as an assembly platform for the MRN complex itself and other DNA damage repair complexes^{147,313,314}. ATM and the MRN complex, in coordination with the BRCA1 complex, regulate the HR-required process of DSB resection, creating a single-stranded 3' DNA overhang, which is engaged and coated by RPA. Subsequently, the RPA coat is replaced by RAD51 in a multi-protein dependent process that includes ATM, BRCA1 and BRCA2 among others. Finally, RAD51 exerts a key role by mediating homology search and sister chromatid invasion, leading to the repair of the lesion (**Figure 4**)^{308,315}.

The ATR/CHK1 axis is activated in response to various types of **SSBs**. These lesions are mainly repaired by the **base excision repair (BER) pathway**, which requires the action of PARP1, LIG3 and XRCC1 (**Figure 4**)^{315,316}. Although the BER components are not affected by genetic abnormalities in CLL and rarely in other cancers, this pathway represents an attractive target for therapeutic approaches based on the concept of **synthetic lethality**, which is defined by a situation where the defect in either one of two genes has little impact on a cell but a combination of both defects results in cell death^{317,318}. In this context, PARP1 inhibition impairs BER, leading to the accumulation of DNA lesions that are subsequently repaired through HR-mediated DNA repair. If HR is unavailable, PARP1 inhibitor-induced DNA damage accumulates and ultimately results in cell death. This paradigm was first observed in *BRCA1* and *BRCA2* mutated cancers, which ultimately led to the clinical development and approval of PARP inhibitors in some HR-deficient solid tumors³¹⁹⁻³²¹.

In CLL, the **DDR signaling and cell cycle control** are dysregulated mostly due to **del(11q)/ATM** mutations or **del(17p)/TP53** mutations. Dysfunction of any of these genes results in the loss of the G1 or G2 cell cycle checkpoints as well as defective HR repair,

allowing CLL cells to enter mitosis with unrepaired DNA damage and favoring genomic instability^{294–296}. To a lesser extent, mutations in *ATRX*, *CHK1* and *CHK2* have also been found in CLL and possibly contribute to a similar outcome on the DDR signaling and cell cycle control^{65,66}. In addition, loss-of-function mutations in the telomere protector *POT1* have been identified in approximately 5% of CLL patients and also result in an increased number of structural aberrations³²². Finally, alterations in cyclin genes critical for cell cycle progression such as *CCND2* and *CDKN2A/B* have also been found in CLL, being the latter related to CLL transformation into RS (Figure 4)^{66,153,179}.

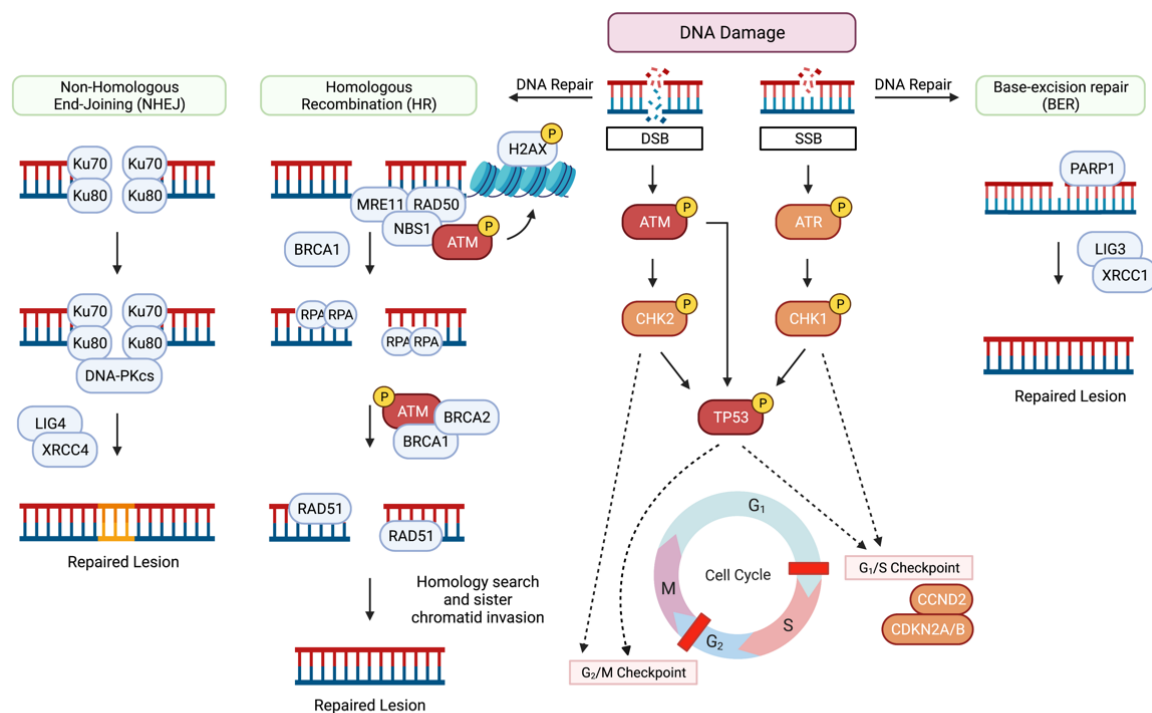


Figure 4. DDR signaling and cell cycle in CLL. Schematic overview of the proteins involved in cell cycle checkpoints activation, DDR signaling and DNA repair pathways upon the induction of DNA damage in the form of DSB or SSB. Proteins codified by recurrently altered genes in CLL (either by mutation or chromosomal deletion/gain) are highlighted in red (> 5% of patients) or orange (< 5% of patients). Proteins represented in blue are unaffected by recurrent genetic lesions in CLL.

3.1.2 Apoptosis

Evasion of apoptosis or programmed cell death is one of the hallmarks of cancer cells³²³. Apoptosis can be triggered via two main pathways activated by extracellular or intracellular stimuli. The **extrinsic apoptotic pathway** is initiated upon ligation of TNF α family members to TNF family receptors on the cell surface, which triggers the assembly of a death inducing signaling complex and activation of initiator caspase-8. The **intrinsic pathway** is initiated

upon DNA damage or cellular stress, which alter the balance of pro- and anti-apoptotic proteins and result in the loss of mitochondrial membrane potential (MMP), release of cytochrome c, assembly of the apoptosome complex and activation of the initiator caspase-9, eventually leading to cell death³²⁴. Changes in MMP are tightly regulated by protein members of the **BCL2 family**, consisting in a group of proteins that share BCL2 homology domains (BH). These proteins are subclassified in three groups depending on its function: anti-apoptotic (i.e. BCL2, BCL-xL, MCL1, BCL-w, BCL2A1, BCL-B), pro-apoptotic multidomain (BAK and BAX) or pro-apoptotic BH3-only (i.e. BIM, NOXA, PUMA, HRK)³²⁵. Apoptosis is triggered when pro-apoptotic multidomain proteins BAX and BAK are activated and oligomerize, which facilitate pore formation of the mitochondrial membrane and MMP loss. BAX and BAK are activated by BH3-only pro-apoptotic proteins, whereas the function of anti-apoptotic proteins is to sequester BH3-only proteins as well as pro-apoptotic multidomain proteins in order to keep BAX and BAK inactivated and prevent its oligomerization³²⁶.

Apoptosis is widely dysregulated in CLL and other hematological malignancies, driving survival, clonal evolution and resistance to therapy³²⁷. For instance, as indicated earlier, loss of miR-15a/16-1 through del(13q) in CLL leads to BCL2 overexpression, preventing cell death of CLL cells^{170,171}. In addition, *TP53* is also involved in direct apoptosis induction in response to DNA damage through up-regulation of pro-apoptotic proteins such as PUMA, NOXA and BAX³²⁸, which makes del(17p)/*TP53* mutated patients highly resistant to chemotherapy-based regimes^{65,190}. Finally, mutations in *BCL2* itself have also been described in a few percentage of treatment-naïve CLL cases and are likely to contribute to apoptosis dysregulation as well^{66,203}.

3.1.3 BCR signaling and TLR signaling

The BCR is a multimeric complex composed by the antigen-specific surface IG and the Ig- α (CD79A) and Ig- β (CD79B) heterodimer. Antigen binding to the surface IG induces activation of upstream kinases SYK and LYN, which phosphorylate immunoreceptor tyrosine-based activation motifs (ITAMs) in CD79A and CD79B, triggering **downstream BCR signaling** by phosphorylation of other upstream kinases such as BTK or PI3K, as well as HS1-mediated activation of the cytoskeleton (**Figure 5**)³²⁹⁻³³¹. BTK phosphorylation leads to subsequent phosphorylation of downstream kinases such as PLC γ 2, and activates diverse pathways such as calcium, NF- κ B, MAPK-ERK, or protein kinase C (PKC) signaling,

whereas PI3K phosphorylation activates the PI3K/AKT/mTOR signaling axis. This convergence of signaling pathway activation ultimately leads to increased nuclear transcriptional activity that results in increased **migration, proliferation and survival** (Figure 5)^{2,329,331}. In addition, the BCR signaling is tightly controlled by the activation of the phosphatases SHP1, SHIP1 and SHIP2, as well as receptors CD5 and CD22, that act as negative regulators of the BCR signaling response (Figure 5)³²⁹.

A functional BCR is required for the survival of mature B cells and is maintained in most mature B cell malignancies, including CLL². Although the components of this pathway have not been found to be recurrently mutated in CLL, many genes involved in the transcriptional activity or signaling pathways downstream the BCR are recurrently mutated in CLL. In particular, mutations in genes involved in **MAPK-ERK signaling** (i.e. *BRAF*, *KRAS*, *NRAS*) are frequent in CLL, ultimately leading to cell cycle dysregulation and uncontrolled proliferation^{196,208}. In addition, mutations in the transcription factor *IZKF3* have been recently reported to enhance BCR signaling and drive CLL development³³². Other genes indirectly related to this pathway recurrently mutated in CLL are *EGR2*, *BCOR*, *KLHL6*, *PAX5*, *IRF4* and those involved in the **NF- κ B signaling** (see below)^{65,66}.

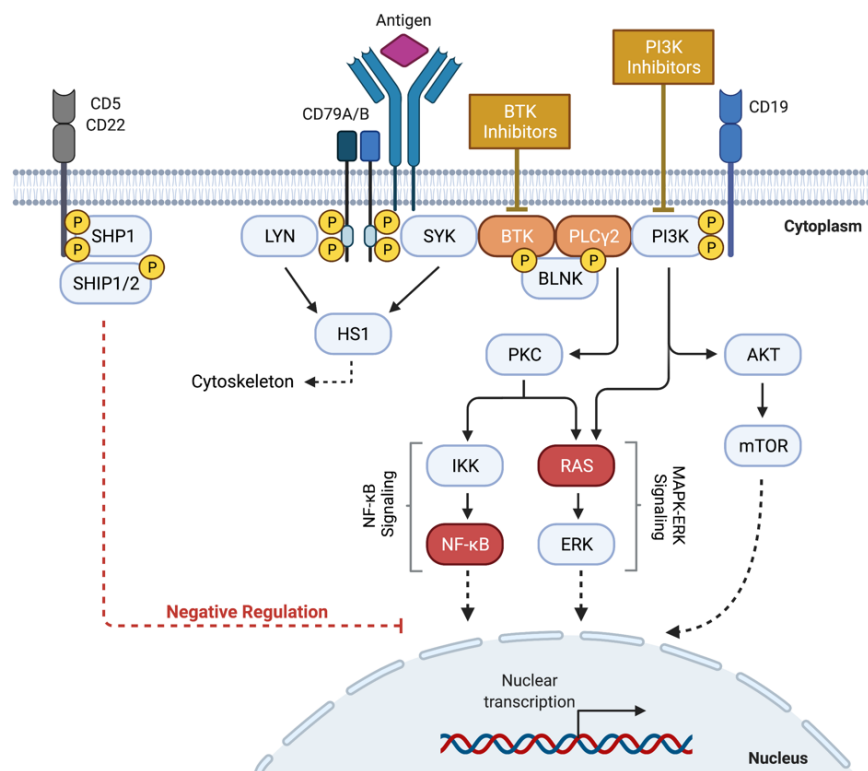


Figure 5. The BCR signaling pathway in CLL. Representation of the events occurring downstream the BCR upon antigen recognition. BTK and PI3K inhibitors can suppress BCR signaling and represent a group of

highly effective novel targeted agents for the treatment of CLL (see 3.3.1 section: *BCR Signaling inhibitors*). Proteins codified by recurrently altered genes in CLL (either by mutation or chromosomal deletion/gain) are highlighted in red (> 5% of patients) or orange (< 5% of patients). Note that multiple genes of the MAPK-ERK or NF- κ B signaling pathways are recurrently altered in CLL at a global frequency of > 5%. A detailed overview of the NF- κ B signaling in CLL can be found in Figure 6. Also note that *BTK* and *PLCG2* only emerge in patients under treatment with BTK inhibitors, and are not present in CLL at diagnosis³³³. Proteins represented in blue are unaffected by recurrent genetic lesions in CLL.

Moreover, other receptors such as those belonging to the **Toll-like receptor (TLR) family** can fuel B cell proliferation and survival by activating downstream signaling pathways such as NF- κ B and STAT3^{298,334}. Some of the genes belonging to the TLR signaling are also recurrently mutated in CLL, being the most prominent example *MYD88*, and adaptor of the TLR signaling that acts as a signal transducer to activate canonical NF- κ B signaling²⁶⁸. Mutations in other genes belonging to this pathway are less frequent in CLL (< 1%), and include those in *TLR2*, *TLR6*, *IRAK1*, *IRAK2* and *IRAK4*^{65,66,83,268}.

3.1.4 NF- κ B signaling

The NF- κ B signaling is a key player in CLL pathogenesis, maintenance and evolution, and is composed of two main pathways, the canonical and the non-canonical signaling²⁹⁸.

The **canonical NF- κ B pathway** is the most extensively studied among the two in CLL, and is mainly triggered by downstream signaling activation coming from cell surface receptors such as the BCR, TLRs, TNF receptors (TNFR) or interleukin-1 receptors (IL-1R)³³⁵. Ligand-receptor interaction activates the I κ B-kinase (IKK) complex, leading to phosphorylation and subsequent proteasomal degradation of the inhibitors of NF- κ B proteins (I κ Bs), a family of proteins that sequester the NF- κ B transcription factors and keep them inactive in the cytoplasm. Upon I κ B degradation, NF- κ B transcription factors are released and translocate into the nucleus to activate transcription of NF- κ B target genes (**Figure 6**)²⁹⁸. The NF- κ B transcription factors that play a role in the canonical signaling are p65 (RelA), p105/p50 (NF κ B1) and c-Rel (Rel), and translocate into the nucleus in the form of various combinations of homo- or heterodimers with distinct patterns of transcriptional activity³³⁶.

The **non-canonical NF- κ B pathway** is initiated by TNF signals engaging other B-cell receptors such as B-cell activation factor receptor (BAFFR), CD40, lymphotoxin β -73 receptor (LT β R) or receptor activator for NF- κ B (RANK)³³⁵. In the absence of a stimulus, this pathway is kept inactive by the action of a multi-protein regulatory complex composed by TRAF2,

TRAF3, BIRC2 and BIRC3, which triggers continuous ubiquitination and proteasomal degradation of the NF- κ B-inducing kinase (NIK)³³⁷. Upon receptor stimulation, this regulatory complex is recruited to the active receptor complex and NIK is stabilized in the cytoplasm, promoting IKK α activation which in turn phosphorylates the inactive form of the NF- κ B transcription factor NF κ B2 (p100), leading to the proteasomal degradation of its C-terminus and the translocation of p52 into the nucleus in the form of homo- or heterodimers with RelB to initiate NF- κ B-dependent transcription (**Figure 6**)³³⁸.

Overall, the NF- κ B signaling is enhanced in CLL cells in comparison to its normal B-cell counterparts. This increased activity can be the result of constitutive BCR, TLR or Notch signaling activation, fueled either by genetic abnormalities within components of these pathways or by the microenvironmental interactions of the CLL cells within the lymph node niche²⁹⁸. In addition, recurrent genetic alterations have been found in some of the NF- κ B pathways proteins. Regarding the canonical signaling, truncating mutations of *NFKBIE*, encoding for I κ B ϵ , have been reported in advanced-stage CLL patients²⁶⁶. Alterations in other genes involved in the canonical signaling are losses of 6q23/*TNFAIP3* or gains in 2p16/*REL*^{213,339}. Intriguingly, albeit less studied in CLL, recurrent abnormalities are most frequent in genes encoding for proteins involved in the non-canonical signaling. Truncating mutations in *BIRC3* lead to NIK cytoplasmic stabilization and constitutive pathway activation^{85,155}, although it remains unclear how monoallelic *BIRC3* deletion in del(11q) patients contribute to CLL biology and whether non-canonical signaling plays a role in CLL progression. Other recurrently mutated drivers belonging to the non-canonical signaling are *TRAF2* and *TRAF3*^{65,66}, whereas *BIRC2* is frequently deleted in del(11q) cases³⁴⁰. In addition, *TRAF3* has also been found to be deleted through chromosomal loss of 14q32²¹² and *NFKB2* is consistently truncated in CLL patients harboring 10q24 losses⁶⁶.

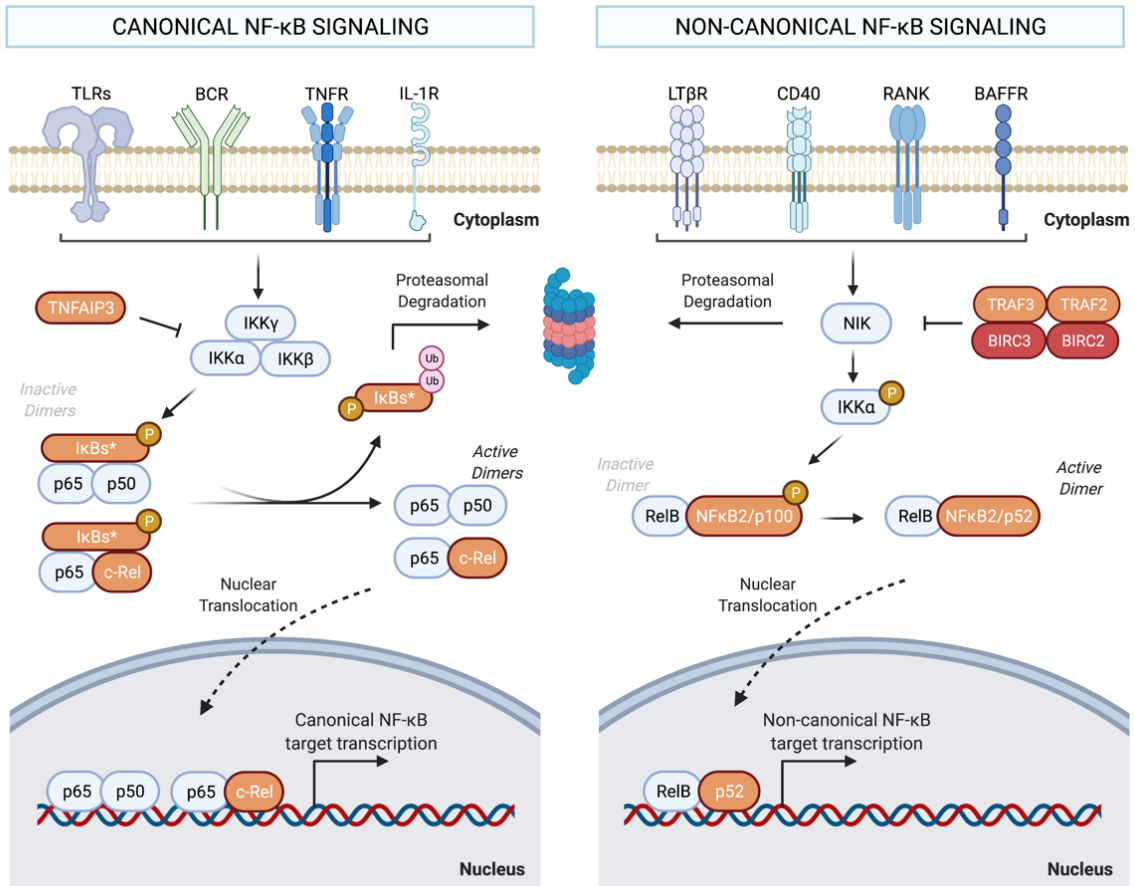


Figure 6. The NF- κ B signaling pathway in CLL. Schematic overview of the canonical and non-canonical NF- κ B pathways in CLL. Proteins codified by recurrently altered genes in CLL (either by mutation or chromosomal deletion/gain) are highlighted in red (> 5% of patients) or orange (< 5% of patients). *Note that family of I κ B proteins is composed by several members (i.e. I κ B α , I κ B β , I κ B ϵ) and only I κ B ϵ , codified by the *NFKBIE* gene, is affected by recurrent mutations in CLL. Proteins represented in blue are unaffected by recurrent genetic lesions in CLL.

3.2 CLL microenvironment

CLL cells are highly dependent on signals coming from the microenvironment for proliferation and survival. CLL cells follow chemokine gradients into lymph nodes, the preferential site for CLL cell proliferation. In the lymph node, CLL cells form “proliferation centers”, where leukemic cells contact with non-malignant stromal cells, nurse-like cells (NLCs), T cells and endothelial cells among others (**Figure 7**)². The interactions between CLL cells and this complex microenvironment are mediated by a network of cell surface ligands, adhesion molecules, chemokines, cytokines, and their respective receptors.

NLCs are cells of monocytic origin critical for the CLL microenvironment. They induce chemotaxis and promote survival of CLL cells through secretion of chemokines CXCL12 and CXCL13 (ligands of CXCR4 and CXCR5, respectively, in CLL cells), and expression of TNF

family ligands such as BAFF or APRIL, sustaining the BCR and NF- κ B signaling of CLL cells³⁴¹⁻³⁴⁴. In addition, they secrete WNT5A, the ligand of transmembrane receptor ROR1, activating non-canonical Wnt signaling which in turn promotes CLL proliferation and migration (**Figure 7**)^{345,346}. NLCs also express CD31, the ligand of CD38 receptor usually expressed in high-risk CLLs³⁴⁷.

T cells promote survival of CLL cells mainly through CD40L/CD40 ligation, which subsequently activates NF- κ B signaling of CLL cells^{329,348}. In addition, T cells secrete cytokines such as IL-4, which can upregulate the expression of the surface IG in CLL cells, potentially facilitating the interaction of the BCR with (auto)antigens³⁴⁹. **Stromal cells** are “feeder” layers of normal hematopoietic progenitors that protect CLL cells from spontaneous and drug-induced apoptosis. Chemotaxis of CLL towards stromal cells involves the CXCR4/CXCL12 axis and they contribute to CLL survival through the interaction between VCAM1 and α 4 β 1 integrin (**Figure 7**)^{350,351}. Finally, **endothelial cells** from high endothelial venules (HEV) play an important role in the migration of CLL to the lymph nodes through the secretion of CCL19 and CCL21, ligands of CCR7 in CLL cells³⁵².

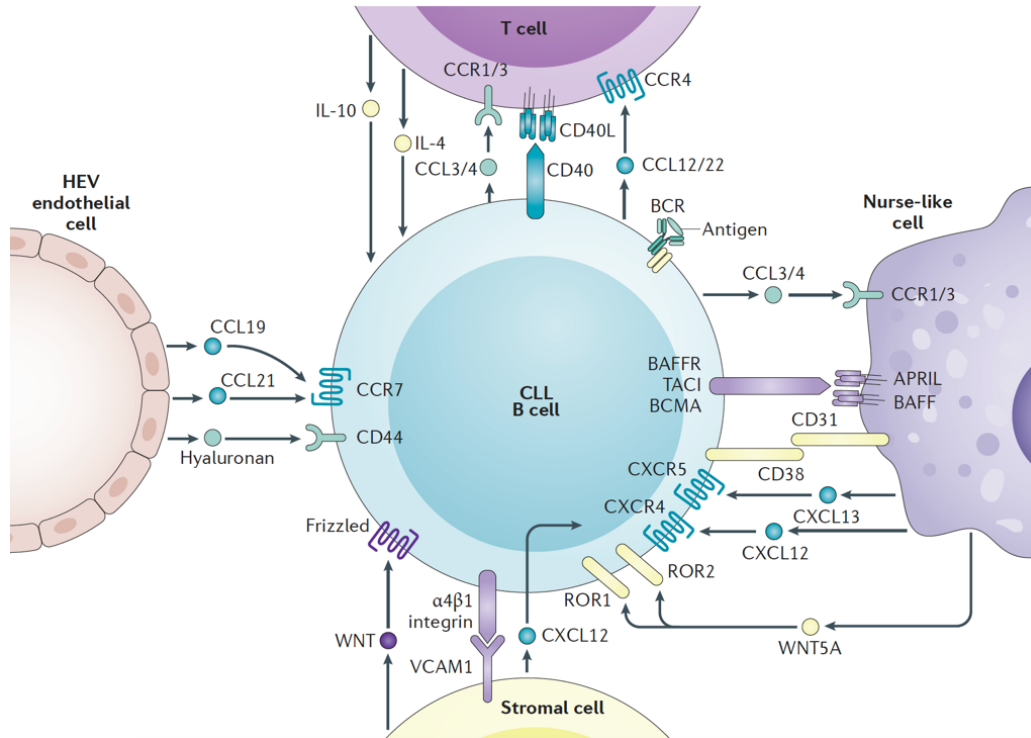


Figure 7. The CLL microenvironment. Representative scheme of the contact of CLL with the microenvironment in the lymph node proliferation centers. The specific interactions between receptors and ligands from each individual cell type are described throughout the main text. (Taken from Kipps TJ *et al.*²)

3.3 Targeted therapy in CLL

Treatment of CLL has profoundly changed in the last decade. The thorough study of the biological processes underlying CLL pathogenesis has made possible to displace chemotherapy-based regimes in favor of novel targeted agents such as BCR signaling inhibitors or BCL2 inhibitors in the majority of CLL patients nowadays, highlighting the importance of understanding the genetics and the biology of the disease in order to progress towards targeted and personalized medicine.

3.3.1 BCR signaling inhibitors

The deep understanding about the critical role of the BCR signaling for the survival of CLL cells led to the development of inhibitors targeting the BCR-related kinases BTK and PI3K in the early 2010s³⁵³⁻³⁵⁵. Subsequent clinical trials demonstrated a biological response characterized by rapid shrinkage of enlarged lymph nodes accompanied by CLL cell egression into the peripheral blood and transient lymphocytosis, which clinically translated into high response rates and durable remissions^{356,357}.

The first BTK inhibitor included in the CLL treatment algorithm was **ibrutinib**, a **first-in-class, orally available, irreversible BTK inhibitor** that was initially approved for R/R CLL patients back in 2014, and is nowadays broadly used for CLL patients both in the frontline and R/R settings^{356,358-360}. Its mechanism of action relies on a covalent bond with a conserved cysteine residue (Cys481) in the active site of BTK, inhibiting thereby downstream BCR signaling and impairing CLL survival, proliferation, migration and microenvironmental interactions (**Figure 5**)^{354,361,362}. In addition to its on-target effects, ibrutinib has been shown to exert additional effects in other cellular pathways or even an immunomodulatory action on T cells by inhibiting ITK, a central regulator of the T cell receptor (TCR) signaling^{363,364}. Since ibrutinib approval, **second-generation BTK inhibitors** have been subsequently developed and, in particular, acalabrutinib is already approved by the US Food and Drug Administration (FDA) for treatment-naïve and R/R CLL^{365,366}. **Acalabrutinib** is a more selective, irreversible BTK inhibitor that also targets Cys481 residue, and its high selectivity seems to result in fewer off-target adverse events than ibrutinib³⁶⁷. Other second-generation BTK inhibitors under advanced stages of clinical development are zanubrutinib and tirabrutinib, also irreversible, high-selective BTK inhibitors that bind covalently to Cys481^{368,369}. In addition, **third-generation reversible BTK inhibitors** such as

pirtobrutinib (LOXO-305) or ARQ-531 are in early clinical development for ibrutinib- or acalabrutinib-resistant R/R CLL patients^{370–372}.

PI3K inhibitors also represent a promising option for the inhibition of the BCR-mediated signal in CLL. **Idelalisib** is an oral, reversible inhibitor of the the PI3K catalytic subunit- δ isoform that blocks downstream signaling of this kinase, resulting in decreased AKT phosphorylation and mTOR activity (**Figure 5**), disrupting interactions between CLL cells and the microenvironment^{355,373}. Idelalisib is currently approved for R/R CLL patients, although its use is limited due the better safety profile of ibrutinib or acalabrutinib^{357,366}. Other next-generation PI3K inhibitors under clinical investigation are duvelisib (dual PI3K γ/δ inhibitor) and umbralisib (dual PI3K δ /CK1 ϵ inhibitor). In particular, duvelisib is already granted by the FDA for the treatment of R/R CLL patients after at least 2 prior lines of therapy^{374–376}.

Although the use of BCR signaling inhibitors has enabled the achievement of durable and deep remissions, the development of novel **mechanisms of resistance** to these drugs has been increasingly reported and is becoming a therapeutic challenge in CLL, urging the need for the development of novel treatment strategies or combinatorial therapies. Ibrutinib and acalabrutinib resistance is associated with **BTK and PLCG2 mutations**, which are found in approximately 80% CLL patients with acquired resistance to these inhibitors^{333,377,378}. BTK mutations mostly appear at the ibrutinib binding site, being the most common C481S mutation, which prevents the binding of ibrutinib to the BTK binding site, resulting in a loss of inhibition of BTK binding activity^{333,379}. *PLCG2* mutations (R665W, L845F and S707Y) are potentially gain-of-function lesions that promote BCR-mediated signaling independent of BTK inhibition^{333,380,381}. Other proposed mechanisms of resistance include clonal evolution, del(8p) or mutations in downstream regulators of BTK such as *ITPKB* or *CDIPT*^{288,377,382}. In addition, CK and del(17p)/*TP53* mutations have been postulated as predictive markers for inferior outcome in CLL patients treated with ibrutinib^{228,231,383}. In contrast, del(11q) has been proposed as a predictive marker for favorable response in treatment-naïve patients, but it is associated with inferior PFS in R/R patients treated with ibrutinib^{231,384–386}, however, the biological insights underlying this duality are currently unknown. Mechanisms of resistance to PI3K inhibitors have been less studied to date, although recent evidence point out to activating mutations in MAPK-ERK signaling genes downstream the BCR³⁸⁷.

3.3.2 BCL2 inhibitors

BH3 mimetics are small molecules capable of binding to and antagonizing anti-apoptotic BCL2 family members (i.e. BCL2, BCL-xL or MCL1). Specifically, BH3-mimetic compounds bind to the anti-apoptotic proteins by virtue of its structural similarity to the BH3 domains of the BH3-only proteins (such as BIM or NOXA), displacing them and inducing apoptosis through BAX and BAK oligomerization³⁸⁸. The only BH3-mimetic molecule currently approved for CLL treatment is **venetoclax, an orally available, highly selective BCL2 inhibitor**. Mechanistically, venetoclax binds to BCL2, displacing the BH3-only pro-apoptotic protein BIM and resulting in potent apoptosis induction independent of TP53³⁸⁹⁻³⁹¹. Venetoclax was first approved for R/R CLL, where it showed high response rates in terms of PFS and OS across all CLL subgroups³⁹¹⁻³⁹³, and is now approved in combination with anti-CD20 antibodies in the treatment-naïve setting as well^{394,395}.

Acquired resistance to venetoclax can also occur in a subset of patients and is an emerging therapeutic challenge in CLL. Similar to BTK inhibitors, the first and most common **mechanism of resistance** to venetoclax identified in CLL is the acquisition of a **point mutation in BCL2 (G101V)** which dramatically reduces the binding affinity of venetoclax to BCL2^{396,397}. Since the discovery of this point mutation, other missense substitutions within the same region of *BCL2* have been discovered, resulting in reduced binding as well³⁹⁸⁻⁴⁰⁰. In addition, up-regulation of alternative anti-apoptotic proteins has been described as mechanisms of acquired resistance. In particular, *MCL1* amplification or *BCL-xL* overexpression have been found in venetoclax-resistant CLL patients^{396,401}. Other proposed mechanisms of resistance point to homozygous *CKNA2A/B* deletions, *BTG1* mutations or high oxidative phosphorylation levels through *PRKAB2* amplification^{401,402}. Finally, less is known about which recurrent CLL genetic lesions can predict response to venetoclax-based regimes, although recent data from two clinical trials indicate that *del(17p)/TP53* mutations remain as adverse prognostic factors^{253,403}.

4. IN VITRO, IN VIVO AND EX VIVO MODELS FOR THE STUDY OF CLL BIOLOGY

The vast genetic heterogeneity and the diverse dysfunction of cancer-related cellular pathways underlying CLL clinical response highlights the need to characterize the individual and combined effects of specific CLL-related genetic lesions in the biology of the disease in order to make tailored treatment decisions. Traditionally, the biological significance of CLL driver alterations or dysregulated biological pathways has been studied

through a combination of *in vitro*, *in vivo* or *ex vivo* approaches, each of them with inherent advantages and pitfalls.

4.1 *In vitro* CLL models

Cultures of CLL-derived lymphoblastoid cell lines (LCLs) have been the cornerstone for the study of the biological and molecular features of CLL *in vitro*. These models are useful to interrogate gene function, regulation, protein interactions and response to CLL therapeutic agents. Unlike primary CLL cells, CLL cell lines present proliferative capacity in the absence of the tumor microenvironment and do not undergo spontaneous apoptosis, making them easy to grow in culture, transfect with expression vectors and engraft into immunodeficient mice^{404,405}.

However, the **number of CLL cell lines accurately reflecting the heterogeneity of the disease is very limited**⁴⁰⁴. To date, only a handful of immortalized CLL cell lines are available for research, and this panel of cell lines does not include models covering all the main cytogenetic backgrounds of the disease. For instance, there are available cell lines harboring del(13q), trisomy 12 or del(17p) (**Table 3**), but **there are no authenticated del(11q) models** in order to study the haploinsufficiency of the genes located within this deletion or the biological determinants underlying this cytogenetic alteration⁴⁰⁴. In addition, some of these cell lines present a triploid or tetraploid karyotype, which is not representative of the common CLL karyotypic background⁴⁰⁴. In terms of somatic mutations, some of these cell lines have been subjected to targeted sequencing or WES and only a few mutations in putative CLL drivers have been identified, hindering the study of the functional consequences of the majority of CLL driver mutations. Indeed, mutations in some of the most recurrently mutated CLL drivers such as *ATM*, *SF3B1* or *NOTCH1* have not been identified in any of the cell lines analyzed. **Table 3** recapitulates the characteristics of the currently available CLL cell lines in terms of immunophenotypic, IGHV mutation, karyotype, FISH and CLL driver mutation status.

The resistance of primary CLL cells to viral transformation by Epstein-Barr virus (EBV) has been cited as a major reason for the lack of immortalized cell lines which accurately reflect the heterogeneity of the disease^{405,406}. Indeed, the utility of CLL cell lines as a surrogate model of primary CLL cells has been questioned primarily due to the effect of EBV-transformation, since CLL cell lines do not recapitulate the pro-survival CLL-microenvironment interactions and EBV-transformation itself might dysregulate critical

biological pathways involved in CLL pathogenesis^{404,407}. Nevertheless, gene expression profiling studies have revealed that most of the differences in gene expression levels between LCLs and primary B cells are of small magnitude, and that LCLs can often recapitulate the naturally occurring gene expression variation in primary B cells⁴⁰⁷.

Table 3. Characteristics of currently available, authenticated patient-derived CLL cell lines for research (Adapted from Lanemo-Myhrinder *et al.*⁴⁰⁴).

Cell line	Patient age/sex/Binet/Rai	Immuno-phenotype ¹	IGHV	Karyotype/ FISH ²	Driver mutations ³	Available at	Ref.
MEC1	62/Male/Rai II	IgM, κ CD5-/CD19 ⁺	M	Diploid ⁴ / Del(17p), -12	<i>TP53</i> ^{MUT} <i>BIRC3</i> ^{DEL}	DSMZ	408
MEC2	62/Male/Rai II	IgM, κ CD5-/CD19 ⁺	M	Triploid ⁴ / Del(17p), -12	<i>TP53</i> ^{MUT}	DSMZ	408
HG3	70/Male/Rai II	IgM, λ CD5 ⁺ /CD19 ⁺	UM	Diploid/ Del(13q)	None	DSMZ	409
PGA1	Male	IgG, λ CD5 ^{dim} /CD19 ⁺	M	Diploid/ +12, del(13q)	<i>KRAS</i> ^{MUT}	DSMZ	410
OSU-CLL	Male	IgM, κ CD5 ⁺ /CD19 ⁺	M	Diploid/ +12, +19	None	OSU	405
I83-E95	75/Male/Binet A	IgM, λ CD5 ⁺ /CD19 ⁺	M	Tetraploid/ +12, del(13q), del(17p)	NA	DSMZ	404
WaC3CD5⁺	Male/Rai I	IgM, κ CD5 ⁺ /CD19 ⁺	UM	Diploid/ Del(13q), del(17p)	NA	DSMZ	404
Wa-ose1	Male/Rai I	IgM, κ CD5-/CD19 ⁺	UM	Tetraploid	NA	DSMZ	404
232B4	Male/Rai 0	IgG, κ CD5-/CD19 ⁺	M	Tetraploid -17	NA	Li.U	404

¹Information about additional immunophenotypic markers can be found at www.dsmz.de or the references indicated in the table. ²Only recurrent CLL CNAs are indicated in the table, for a complete karyotype description please refer to www.dsmz.de or the references indicated in the table. ³NGS data from MEC1, HG3 and PGA1 has been obtained in our laboratory using a custom-designed panel for the analysis of 54 CLL-related drivers⁴¹¹. WES data is also available for MEC1, HG3 and PGA1 cell lines⁴¹². Only *TP53* mutational status is known for MEC2 cells. OSU-CLL was only analyzed for hotspot mutations in *NOTCH1*, *TP53*, *MYD88*, *KLHL6*, *XPO1*, *SF3B1*, *BRAF* and *BTK* genes⁴⁰⁵. ⁴MEC1 and MEC2 cells display a near diploid or triploid karyotype, respectively, with 10% of polyploidy (www.dsmz.de). M: mutated; UM: unmutated; NA: not available; DSMZ: German Collection of Microorganisms and Cell Cultures; OSU: Ohio State University; Li.U: Linköping University.

4.2 *In vivo* CLL models

Mouse models that recapitulate hematological malignancies are useful tools for elucidation of the pathogenic mechanisms underlying disease biology and progression, as well as for the development of preclinical studies. In CLL, two main approaches have been undertaken to model and study the disease in an *in vivo* setting: murine xenotransplantation models or genetically-engineered mouse models^{413,414}.

Xenotransplantation models in CLL have been attempted using either CLL cell lines or primary CLL cells. Most of CLL cell lines have been shown to engraft either subcutaneously or intravenously only in highly immunodeficient recipients such as NOD-scid IL2R $\gamma^{-/-}$ (NSG) or Rag2 $^{-/-}$ $\gamma_c^{-/-}$ mice, characterized by the lack of B, T and NK cells^{405,413,415-417}. Xenotransplantation of CLL cell lines into these models is easily reproducible, and cells are able to spread fast and systemically recapitulating aggressive human CLL. However, proliferation of cell lines is induced by EBV transformation and not by the CLL-microenvironment interactions, impeding the study of this critical aspect of CLL biology^{413,415}. On the other hand, several efforts in the last decade have made possible to establish **patient-derived CLL xenografts**. These models use also highly immunodeficient mice such as NSG and are based in the intravenous infusion of CLL peripheral blood mononuclear cells (PBMCs), usually in the presence of autologous T cells, previously activated either *in vitro* or *in vivo*^{413,418-421}. Patient-derived xenografts are useful for the study evaluation of drug effects in CLL cells as well as the tissue microenvironment, overcoming some limitations of xenotransplantation of CLL cell lines. However, there are differences between methodologies across different research groups that need to be standardized for these models to become widely available for CLL research⁴¹⁸⁻⁴²⁴. Notably, recent patient-derived RS xenografts have also been developed and have been proved to be useful for the study of novel therapeutic approaches in CLL transformation⁴²⁵⁻⁴²⁷.

CLL genetically-engineered mouse models have been generated either mimicking deregulated gene expression or CLL-related genetic abnormalities. The most widely utilized is the transgenic TCL1 mouse model which expresses the human *TCL1* gene and mimic the development of aggressive CLL⁴²⁸. Other transgenic mice models include the *BCL2* \times *Traf2dn* double transgenic mouse, *APRIL* transgenic mouse or *ROR1* transgenic mouse^{414,429-431}. All these models are quite useful for preclinical testing and the interrogation of several aspects of the disease pathogenesis, although disadvantages include a delayed time to disease onset (usually of more than one year) and absence of human microenvironmental accessory cells.

Moreover, they do not recapitulate the genetic heterogeneity of CLL^{414,420}. In terms of mouse models emulating recurrent CLL abnormalities, several efforts established CLL-like models by B cell-restricted deletion of the mouse locus of *mir-15a/16-1* or the mouse 14qC3 common or minimal deleted region, all of them emulating del(13q) of human CLL^{171,172}. In addition, exciting recent approaches have established novel models by combining B cell-restricted murine *Sf3b1* mutation and *Atm* deletion²⁹³ or *Ikzf3* mutation³³². Nevertheless, extensive research would be required in order to generate mouse models covering the main genetic abnormalities of the heterogeneous CLL genetic landscape. Furthermore, modeling of large CNAs remains a challenge, not only for technical reasons, but also for notorious differences in gene distribution between the mouse and human chromosomes⁴³².

4.3 *Ex vivo* CLL models

As discussed in previous sections, it is well known that CLL cells are highly dependent on the tumor microenvironment for survival, and leukemic cells undergo spontaneous apoptosis when cultured *in vitro*. For these reasons, *ex vivo* CLL culture techniques have focused on modelling microenvironmental interactions through co-culture systems with accessory cells or conditioned media to replicate microenvironmental induced signaling⁴²⁰.

The most relevant co-culture systems studied to date in CLL for *ex vivo* cultures are those based on either bone marrow stromal cells (BMSCs) or NLCs. **CLL-BMSCs co-cultures** can be done with patient-derived BMSCs, murine stromal cell lines (i.e. M210B4, SUM4, KUSA-H1) or human stromal cell lines (HS5 or StromaNKTert)^{433,434}. These type of co-cultures have demonstrated efficacy in maintaining CLL cells in culture for weeks, and preventing CLL cells to undergo spontaneous or drug-induced apoptosis by upregulation of anti-apoptotic proteins or activation of pro-survival signaling pathways such as PI3K or NF- κ B^{420,433-435}. Additionally, **CLL-NLCs co-cultures** are established from patient-derived NLCs and mimic the CLL microenvironment by activation of the BCR and NF- κ B signaling, and upregulation of anti-apoptotic proteins, providing long-term survival and proliferation for CLL cells^{341,343,344}.

Microenvironmental-induced signaling can be also reproduced using **soluble factors** that ligate surface receptors of CLL cells, triggering pro-survival downstream signaling activation. In particular, ligation of the BCR using anti-IgM mimics downstream BCR signaling and NF- κ B activation, resulting in decreased spontaneous apoptosis and increased proliferation, especially in UM-IGHV cases⁴³⁶⁻⁴³⁸. Moreover, activation of TLR signaling

using the TLR9 ligand CpG-ODN is widely used for *ex vivo* CLL cultures and also results in NF- κ B activation and pro-survival cytokine production^{439,440}. CD40 stimulation via CD40L is another widespread method that mimics the microenvironmental interaction between CLL cells and T-cells^{348,420}.

Co-culture systems and soluble factors can also be combined for the *ex vivo* culture of CLL cells. Some of the best approaches to induce CLL cell proliferation and reduction of spontaneous apoptosis include CLL co-culture with HS5 stromal cells in the presence of CpG-ODN and IL-2 or IL-15, or CLL co-culture with CD40L-expressing fibroblasts supplemented with IL-4 or IL-21⁴⁴¹⁻⁴⁴⁴. In summary, *ex vivo* CLL cultures represent an adequate option to study CLL-microenvironmental interactions as well as CLL drug response in the context of the tumor microenvironment. Nevertheless, inter-patient genetic heterogeneity might not be well recapitulated if large cohorts of primary CLL cells are not used. Besides, genetic and mechanistic studies in primary CLL cells are hampered by the difficulty of transfection or transduction of these cells^{445,446}.

4.4 Genome-editing technologies for the generation of novel CLL models

As stated throughout the previous sections, the dynamic development of high-throughput sequencing technologies has uncovered a vast number of genetic abnormalities in CLL at chromosomal level, gene level, expression level or even in non-coding regions of the CLL genome^{65,66}. The biological function of some of these lesions is beginning to be understood partly as the result of the parallel development and improvement of *in vitro*, *in vivo* and *ex vivo* CLL models^{404,413,414,420}. However, CLL, as well as the majority of cancer types, arises and progresses due to complex interaction of multiple disease drivers, and new models are required to assess the contribution of individual or combined genetic lesions to cellular fitness, their preferential co-occurrences or mutual exclusivity mechanisms and how the resultant dysregulation of biological pathways impacts clonal evolution or treatment response.

The recent advances in genome-engineering technologies have opened a broad range of new possibilities to model diseases *in vitro* and *in vivo*. In particular, **genome-editing systems** provide an excellent tool for precise genome modification to mimic cancer-related driver alterations and interrogate their functional impact. The first genome-editing techniques implemented in cancer modelling included zinc-finger nucleases (ZNFs) and transcription activator-like effector nucleases (TALENs), although their widespread

adoption has been limited due to technical complexity and cost^{447,448}. However, the recent introduction of the **Clustered Regularly Interspaced Short Palindromic Repeats (CRISPR)/Cas9 technology** has dramatically changed the landscape of genome engineering by addressing many of the limitations from earlier methods, transforming our ability to rapidly interrogate the role of somatic mutations or chromosomal abnormalities *in vitro*, *in vivo* and *ex vivo*^{449–452}.

The CRISPR/Cas9 system is derived from a prokaryotic adaptive immune system and is mainly composed of two biological components: the **RNA-guided DNA endonuclease Cas9 and a chimeric single-guide RNA (sgRNA)**. The sgRNA molecule is composed of a CRISPR RNA (crRNA) sequence, complementary to the target region of interest, and a trans-activating crRNA (tracrRNA) component, which binds to the nuclease Cas9 and directs it to the genomic region of interest by base pairing (**Figure 8**). The only requirement defining the target sequence is that it must be adjacent to a protospacer adjacent motif (PAM), which consists of either a NGG trinucleotide for *S. pyogenes*-derived Cas9, which is the one of most commonly used nucleases for CRISPR-based editing^{449,453}. Therefore, by just combining the expression of the protein Cas9 and a 20 pb sgRNA sequence complementary to a target DNA sequence, high efficient cleavage of the target genome region can be achieved, leading to the formation of DSBs, which will be repaired by either NHEJ or HR (**Figure 8**)⁴⁵³ (See Introduction 3.1.1 section *DNA damage response and cell cycle control*). NHEJ-mediated repair frequently leads to the introduction of small indels that can result in disruptive frameshift mutations and the generation of premature stop codons, which can be useful to emulate loss-of-function driver mutations. On the other hand, in the presence of an exogenous donor DNA template, DSBs can be repaired through HR, which can be used for precise DNA modifications such as missense substitutions resulting in a gain-of-function phenotype, or correction of existent mutations (**Figure 8**)^{449,453}.

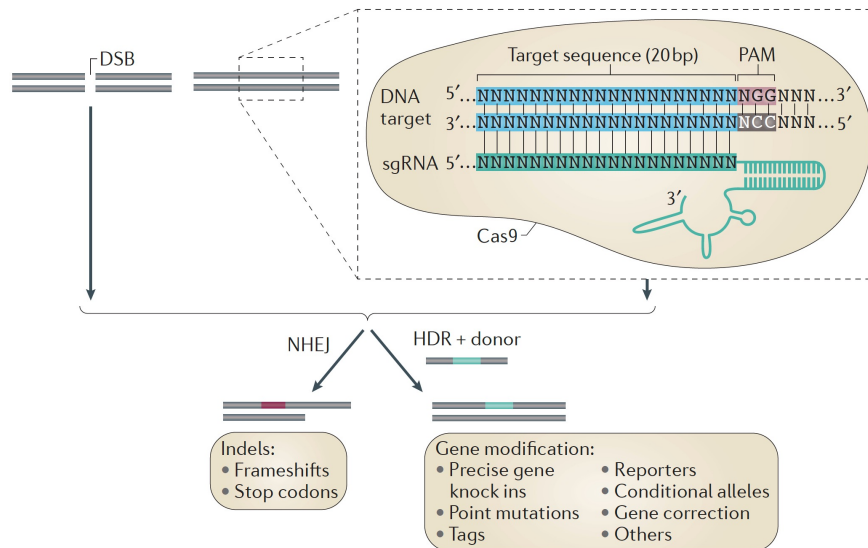


Figure 8. CRISPR/Cas9 system components and applications. Representative scheme of the components required for CRISPR/Cas9-genome editing. The nuclease Cas9 is directed towards a genomic region of interest (blue), adjacent to a trinucleotide PAM sequence (red) essential for site recognition, by complementary binding to the sgRNA molecule (green). Cas9 nuclease activity results in a formation of a DSB within nucleotides 17-18 of the target sequence, which will be subsequently repaired through NHEJ, leading to the formation of indels, or precise sequence modification via homology-directed repair (HDR) in the presence of a donor DNA template (Taken from Sánchez-Rivera FJ & Jacks T. 2015)⁴⁵³.

The high simplicity and versatility of this genome-editing system has resulted in an **impressive range of potential applications to model cancer biology**, most of which have been successfully carried out in cell culture systems or animal models⁴⁵³. Apart from the rapid and precise engineering of both loss-of-function or gain-of-function mutations in an isogenic context, as well as correction of point mutations, the CRISPR/Cas9 system can be used to trigger **chromosomal rearrangements**. This can be achieved by the induction of two DSBs simultaneously in different chromosomes leading to the induction of a translocation, or by induction of two distant DSBs within the same chromosome, which can lead to either chromosomal inversion or deletion^{454–457}. Other CRISPR/Cas9 applications useful for cancer biology research are the generation of endogenous conditional alleles for the development of mouse models, or the tagging of endogenous alleles with fluorescent reporters or synthetic tags, all of these been achieved by HR-mediated repair of the Cas9-induced DSB^{453,458}. Moreover, this system can be used to interrogate the function of non-coding DNA elements such as enhancers or promoters^{459,460}. In addition, the facility to **multiplex** the CRISPR/Cas9 offers the opportunity to investigate **synthetic lethal interactions** between genes or even the implementation of high-throughput genetic screens to identify novel genes involved in various cellular processes, or unknown genes involved in either resistance or susceptibility

to certain drugs^{453,461}. Variations of the CRISPR/Cas9 system can also be used to repress or activate gene expression, induce chromatin modifications or edit RNA sequences⁴⁶²⁻⁴⁶⁴. At last, this system could also potentially be used for clinical application. Indeed there are several clinical trials exploring the possibilities of either correcting gene mutations or targeting cancer-related genes⁴⁶⁵.

Contemporary to the development of this PhD research, some studies have implemented the CRISPR/Cas9 technology to understand the function of CLL-related driver mutations such as *NOTCH1*, *TP53*, *FBXW7* or *RPS15* in CLL cell lines *in vitro*^{299,303,416,466}. Other studies have also applied this technology to elucidate the contribution of certain proteins such as 14-3-3 ζ or ADAR in Wnt signaling or RNA editing processes, respectively^{467,468}. In addition, high-throughput CRISPR screens have been performed to uncover unknown mechanisms of resistance to venetoclax⁴⁰¹ and attempts for multiplexed CRISPR/Cas9-mediated edition for the generation of mouse models harboring CLL driver mutations have recently been described⁴⁶⁹. Nevertheless, the versatility of the CRISPR/Cas9 offers many additional, yet unexplored, opportunities for the progress in our understanding of CLL. This system can be exploited to model not only gene mutations with unknown biological significance, but also chromosomal abnormalities that play a critical role in CLL pathogenesis. In addition, it can address unsolved questions about the process of clonal evolution and how chromosomal lesions and gene mutations cooperate to drive CLL progression and response to treatment. Finally, the CRISPR/Cas9 system can be applied to uncover therapeutic vulnerabilities based on synthetic lethal combinations between different driver genetic lesions, helping make progress towards the implementation novel treatment strategies for personalized medicine in CLL.

HYPOTHESIS

Recent breakthroughs in the study of chronic lymphocytic leukemia (CLL) genomics have highlighted this disease as an extremely heterogeneous entity at the genetic level, characterized by the presence of a large number of recurrent chromosomal abnormalities and gene mutations that ultimately reflect the highly variable clinical course observed between patients. High-throughput sequencing efforts have also revealed the presence of intra-clonal heterogeneity within CLL cells, defining preferential patterns of co-occurrence or mutual exclusivity between certain genetic alterations. Understanding the timing of appearance and the contribution of each of these lesions into the biology of CLL is essential to determine how the interaction between multiple disease drivers leads to clonal evolution, CLL progression and influences treatment responses.

Expansion of malignant CLL clones is believed to originate from pre- or post-germinal center experienced B cells, depending on the immunoglobulin gene somatic hypermutation status. However, the specific moment during hematopoiesis where the first oncogenic CLL-related events occur is a current matter of debate. Several reports have suggested that some CLL driver mutations may appear at previous maturational levels or even in hematopoietic stem cells (HSCs). Nevertheless, further investigation is required to assess whether mutations in specific genes appear preferentially at the HSC level and therefore are likely to contribute to CLL origin, or which lesions appear at later steps of the maturation process where they will be likely to contribute to CLL expansion and maintenance rather than origin itself. Furthermore, within the plethora of genetic abnormalities occurring in CLL cells, only the appearance of particular gene mutations has been interrogated at the HSC level, whereas the presence of certain chromosomal abnormalities such as del(11q) has not been addressed, leaving unsolved questions about the role of these alterations in CLL initiation.

Monoallelic del(11q) defines a high-risk subgroup of CLL patients characterized by the presence of bulky lymphadenopathy, rapid disease progression and reduced survival. The size of this deletion is variable and it can encompass hundreds of genes, being specifically *ATM* and *BIRC3* suggested to have a role in CLL pathogenesis, since loss-of-function mutations of *ATM* or *BIRC3* preferentially occur in del(11q) cases. This complete dysfunction of *ATM* or *BIRC3* proteins has been shown to aggravate the outcome of del(11q) patients. However, the biological determinants by which the co-occurrence of these abnormalities drives CLL progression, clonal evolution and therapy response are largely unexplored. In addition, other concomitant genetic abnormalities have also been described in del(11q)

patients, although their role in the prognosis of this specific subgroup of CLLs has not been established.

The study of the biological implications of del(11q) as well as associated mutations in *ATM* or *BIRC3* has been hampered by the lack of cell lines harboring this specific chromosomal lesion or mouse models able to recapitulate the biology of del(11q), added to the difficulty of manipulating primary CLL cells *ex vivo*. Understanding the role of these lesions in the biology of the disease has become more relevant than ever with the introduction of targeted agents into the CLL treatment landscape, not only to determine which subgroups of patients might benefit from current therapies, but also to explore novel tailored therapeutic approaches based on synthetic lethal interactions. The recent introduction of the CRISPR/Cas9 system for genome editing has transformed our ability to interrogate the function of driver mutations and chromosomal abnormalities, both *in vitro* and *in vivo*, and its application in CLL research open exciting new horizons to help elucidate how different genetic lesions interact to drive disease pathogenesis and evolution.

We believe that the CRISPR/Cas9 system can be used to successfully establish *in vitro* and *in vivo* CLL models recapitulating the biology of del(11q) as well as concurrent mutations in *ATM*, *BIRC3* or other genes. These models, in combination with *ex vivo* primary CLL cultures from genetically-matched patients, will help us understand the specific contribution of each of these genetic backgrounds into critical aspects of CLL biology and treatment response. In addition, the parallel implementation of high-throughput sequencing techniques to study the genetic landscape of del(11q) CLL patients as well as CLL-HSCs, could unveil other genetic lesions with prognostic relevance in this high-risk subgroup of CLL patients, as well as the contribution of del(11q) and other driver lesions to the origin of the disease. Therefore, the integration of genomic analysis and CRISPR/Cas9-generated models might be useful to decipher the role of del(11q) and its concurrent alterations in many aspects of the disease: from initiation to progression and clonal evolution, helping the evaluation of tailored treatment for CLL patients belonging to this cytogenetic subgroup based on their inherent genetic characteristics.

AIMS

General aim

To gain insight into the biological determinants underlying del(11q) CLL initiation, progression and clonal evolution, as well as to explore novel therapeutic vulnerabilities that can be clinically exploitable in CLL patients harboring these alterations, through a combination of high-throughput sequencing techniques, *in vitro* CRISPR/Cas9-edited models, *in vivo* xenograft models and primary CLL *ex vivo* cultures.

Specific aims

1. To analyze the presence of gene mutations and chromosomal abnormalities in CD34⁺ HSCs from CLL patients to infer the stage of the B cell maturation process where these alterations appear as well as their contribution to CLL initiation.
2. To determine the mutational landscape of del(11q) CLL patients to identify preferential patterns of co-occurrence or mutual exclusivity with clinical relevance.
3. To generate novel isogenic CLL models that recapitulate the biology of del(11q) and/or associated loss-of-function mutations in *ATM*, *TP53* or *BIRC3* through CRISPR/Cas9-based gene-editing.
4. To evaluate the functional consequences of monoallelic and biallelic *ATM* loss in del(11q) CLL in the DNA damage response signaling and to assess specific therapeutic vulnerabilities of this subgroup of patients based on synthetic lethality.
5. To characterize the biological impact of concurrent monoallelic and biallelic *ATM* and *TP53* lesions in del(11q) CLL cells *in vitro* and *in vivo*, as well as the implications of these genetic backgrounds in treatment response.
6. To elucidate the biological significance of *BIRC3* loss through del(11q) and/or *BIRC3* mutations in the NF- κ B signaling and apoptosis dysregulation, as well as its contribution to CLL progression, response to therapy and clonal evolution.

RESULTS

This section includes the experimental work performed on this thesis, including Material and Methods, Results and Discussion. This section has been divided into four chapters:

Chapter 1. M Quijada-Álamo, M Hernández-Sánchez, C Robledo, JM Hernández-Sánchez, R Benito, A Montaña, AE Rodríguez-Vicente, D Quwaider, AA Martín, M García-Álvarez, MJ Vidal-Manceño, G Ferrer-Garrido, MP Delgado-Beltrán, J Galende, JN Rodríguez, G Martín-Núñez, JM Alonso, A García de Coca, JA Queizán, M Sierra, C Aguilar, A Kohlmann, JA Hernández, M González, JM Hernández Rivas. **Next-generation sequencing and FISH studies reveal the appearance of gene mutations and chromosomal abnormalities in hematopoietic progenitors in chronic lymphocytic leukemia.** *Journal of Hematology & Oncology*. 2017 Apr 11;10(1):83. doi: 10.1186/s13045-017-0450-y. PMID: 28399885

Chapter 2. M Quijada-Álamo, M Hernández-Sánchez, V Alonso-Pérez, AE Rodríguez-Vicente, I García-Tuñón, M Martín-Izquierdo, JM Hernández-Sánchez, AB Herrero, JM Bastida, L San Segundo, M Gruber, JL García, S Yin, E ten Hacken, R Benito, JL Ordóñez, CJ Wu, JM Hernández-Rivas. **CRISPR/Cas9-generated models uncover therapeutic vulnerabilities of del(11q) CLL cells to dual BCR and PARP inhibition.** *Leukemia*. 2020 Jun;34(6):1599-1612. doi: 10.1038/s41375-020-0714-3. PMID: 31974435

Chapter 3. M Quijada-Álamo, C Pérez-Carretero, M Hernández-Sánchez, AE Rodríguez-Vicente, AB Herrero, JM Hernández-Sánchez, M Martín-Izquierdo, S Santos-Mínguez, M del Rey, T González, A Rubio-Martínez, A García de Coca, J Dávila-Valls, JA Hernández-Rivas, H Parker, JC Strefford, R Benito, JL Ordóñez, JM Hernández-Rivas. **Dissecting the role of TP53 alterations in del(11q) chronic lymphocytic leukemia.** *Clinical and Translational Medicine*. 2021 Feb;11(2):e304. doi: 10.1002/ctm2.304. PMID: 33634999

Chapter 4. M Quijada-Álamo, M Hernández-Sánchez, AE Rodríguez-Vicente, C Pérez-Carretero, A Rodríguez-Sánchez, M Martín-Izquierdo, V Alonso-Pérez, I García-Tuñón, JM Bastida, MJ Vidal-Manceño, J Galende, C Aguilar, JA Queizán, I González-Gascón y Marín, JA Hernández-Rivas, R Benito¹, JL Ordóñez, JM Hernández-Rivas. **Biological significance of monoallelic and biallelic BIRC3 loss in del(11q) chronic lymphocytic leukemia progression.** *Blood Cancer Journal*. 2021. In press

All of them have been developed to accomplish the general aim of this work and give the title to this doctoral dissertation: “Unraveling the Biological Determinants of the Origin, Clonal Evolution and Therapeutic Vulnerabilities of del(11q) Chronic Lymphocytic Leukemia through Genome-Editing Approaches”.

A General Discussion, with additional data and which comprises all research, is addressed in a separate section of this thesis.

In addition, the supplementary material corresponding to each of the chapters indicated above is collected at the end of the thesis.

CHAPTER 1

Next-generation sequencing and FISH studies reveal the appearance of gene mutations and chromosomal abnormalities in hematopoietic progenitors in chronic lymphocytic leukemia

Miguel Quijada-Álamo^{1*}, María Hernández-Sánchez^{1*}, Cristina Robledo¹, Jesús María Hernández-Sánchez¹, Rocío Benito¹, Adrián Montaña¹, Ana E Rodríguez-Vicente^{1,2}, Dalia Quwaider¹, Ana-África Martín¹, María García-Álvarez¹, María Jesús Vidal Manceño³, Gonzalo Ferrer-Garrido⁴, María-Pilar Delgado-Beltrán⁴, Josefina Galende⁵, Juan-Nicolás Rodríguez⁶, Guillermo Martín-Núñez⁷, José-María Alonso⁸, Alfonso García de Coca⁹, José A. Queizán¹⁰, Magdalena Sierra¹¹, Carlos Aguilar¹², Alexander Kohlmann^{13,14}, José-Ángel Hernández¹⁵, Marcos González¹, Jesús-María Hernández Rivas¹

¹Servicio de Hematología & IBSAL, IBMCC, CIC Universidad de Salamanca-CSIC, Hospital Universitario, Salamanca, Spain.

²Department of Molecular and Clinical Pharmacology, University of Liverpool, Liverpool, United Kingdom. ³Servicio de Hematología, Hospital Virgen Blanca, León, Spain. ⁴Servicio de Hematología, Hospital Miguel Servet, Zaragoza, Spain. ⁵Servicio de Hematología, Hospital del Bierzo, Ponferrada, León, Spain. ⁶Servicio de Hematología, Hospital Juan Ramón Jiménez, Huelva, Spain. ⁷Servicio de Hematología, Hospital Virgen del Puerto, Plasencia, Cáceres, Spain. ⁸Servicio de Hematología, Hospital Río Carrión, Palencia, Spain. ⁹Servicio de Hematología, Hospital Clínico, Valladolid, Spain. ¹⁰Servicio de Hematología, Hospital General de Segovia, Segovia, Spain. ¹¹Servicio de Hematología, Hospital Virgen de la Concha, Zamora, Spain. ¹²Servicio de Hematología, Hospital Santa Bárbara, Soria, Spain. ¹³MLL Munich, Germany. ¹⁴AstraZeneca, Personalized Healthcare and Biomarkers, Innovative Medicines, Cambridge, United Kingdom. ¹⁵Servicio de Hematología, Hospital Universitario Infanta Leonor, Universidad Complutense de Madrid, Madrid, Spain. *Equal contribution.

Journal of Hematology & Oncology. 2017 Apr 11;10(1):83. doi: 10.1186/s13045-017-0450-y. PMID: 28399885

RESEARCH

Open Access



Next-generation sequencing and FISH studies reveal the appearance of gene mutations and chromosomal abnormalities in hematopoietic progenitors in chronic lymphocytic leukemia

Miguel Quijada-Álamo^{1†}, María Hernández-Sánchez^{1†}, Cristina Robledo¹, Jesús-María Hernández-Sánchez¹, Rocío Benito¹, Adrián Montaña¹, Ana E. Rodríguez-Vicente^{1,2}, Dalia Quwaider¹, Ana-África Martín¹, María García-Álvarez¹, María Jesús Vidal-Manceño³, Gonzalo Ferrer-Garrido⁴, María-Pilar Delgado-Beltrán⁴, Josefina Galende⁵, Juan-Nicolás Rodríguez⁶, Guillermo Martín-Núñez⁷, José-María Alonso⁸, Alfonso García de Coca⁹, José A. Queizán¹⁰, Magdalena Sierra¹¹, Carlos Aguilar¹², Alexander Kohlmann^{13,14}, José-Ángel Hernández¹⁵, Marcos González¹ and Jesús-María Hernández-Rivas^{1,16*}

Abstract

Background: Chronic lymphocytic leukemia (CLL) is a highly genetically heterogeneous disease. Although CLL has been traditionally considered as a mature B cell leukemia, few independent studies have shown that the genetic alterations may appear in CD34+ hematopoietic progenitors. However, the presence of both chromosomal aberrations and gene mutations in CD34+ cells from the same patients has not been explored.

Methods: Amplicon-based deep next-generation sequencing (NGS) studies were carried out in magnetically activated-cell-sorting separated CD19+ mature B lymphocytes and CD34+ hematopoietic progenitors ($n = 56$) to study the mutational status of *TP53*, *NOTCH1*, *SF3B1*, *FBXW7*, *MYD88*, and *XPO1* genes. In addition, ultra-deep NGS was performed in a subset of seven patients to determine the presence of mutations in flow-sorted CD34+CD19- early hematopoietic progenitors. Fluorescence in situ hybridization (FISH) studies were performed in the CD34+ cells from nine patients of the cohort to examine the presence of cytogenetic abnormalities.

(Continued on next page)

* Correspondence: jmhr@usal.es

†Equal contributors

¹Servicio de Hematología & IBSAL, IBMCC, CIC Universidad de Salamanca-CSIC, Hospital Universitario, Salamanca, Spain

¹⁶IBMCC, CIC Universidad de Salamanca-CSIC, Hospital Universitario de Salamanca, Paseo de San Vicente s/n, 37007 Salamanca, Spain

Full list of author information is available at the end of the article



© The Author(s). 2017 **Open Access** This article is distributed under the terms of the Creative Commons Attribution 4.0 International License (<http://creativecommons.org/licenses/by/4.0/>), which permits unrestricted use, distribution, and reproduction in any medium, provided you give appropriate credit to the original author(s) and the source, provide a link to the Creative Commons license, and indicate if changes were made. The Creative Commons Public Domain Dedication waiver (<http://creativecommons.org/publicdomain/zero/1.0/>) applies to the data made available in this article, unless otherwise stated.

(Continued from previous page)

Results: NGS studies revealed a total of 28 mutations in 24 CLL patients. Interestingly, 15 of them also showed the same mutations in their corresponding whole population of CD34+ progenitors. The majority of *NOTCH1* (7/9) and *XPO1* (4/4) mutations presented a similar mutational burden in both cell fractions; by contrast, mutations of *TP53* (2/2), *FBXW7* (2/2), and *SF3B1* (3/4) showed lower mutational allele frequencies, or even none, in the CD34+ cells compared with the CD19+ population. Ultra-deep NGS confirmed the presence of *FBXW7*, *MYD88*, *NOTCH1*, and *XPO1* mutations in the subpopulation of CD34+CD19- early hematopoietic progenitors (6/7). Furthermore, FISH studies showed the presence of 11q and 13q deletions (2/2 and 3/5, respectively) in CD34+ progenitors but the absence of *IGH* cytogenetic alterations (0/2) in the CD34+ cells. Combining all the results from NGS and FISH, a model of the appearance and expansion of genetic alterations in CLL was derived, suggesting that most of the genetic events appear on the hematopoietic progenitors, although these mutations could induce the beginning of tumoral cell expansion at different stage of B cell differentiation.

Conclusions: Our study showed the presence of both gene mutations and chromosomal abnormalities in early hematopoietic progenitor cells from CLL patients.

Keywords: Chronic lymphocytic leukemia, Next-generation sequencing, Hematopoietic progenitors, Mutation, FISH, Chromosomal abnormality

Background

Chronic lymphocytic leukemia (CLL) is characterized by the clonal proliferation and accumulation of neoplastic B lymphocytes in the blood, bone marrow, lymph nodes, and spleen [1, 2]. Immunophenotype analysis of CLL cells shows expression of CD5 T cell antigen as well as CD19, CD20, and CD23 B cell surface antigens [3]. In molecular terms, CLL is defined by the presence of chromosomal abnormalities (11q-, +12, 13q-, 17p-) that play an important role in CLL prognosis [4]. The mutational status of the immunoglobulin heavy chain (*IGHV*) is also considered a prognostic marker in CLL [5, 6]. Recently, the development of next-generation sequencing (NGS) techniques has enabled mutations to be identified in novel target genes in CLL [7, 8], and mutations in some drivers such as *NOTCH1*, *SF3B1*, *TP53*, and *MYD88* genes have been shown to have a prognostic impact in CLL patients [9–11].

The cellular origin of this disease remains controversial [12–14]. Recent studies have reported that CLL pathogenesis may start at a previous maturational cell stage, or even in hematopoietic stem cells (HSCs). Fluorescence in situ hybridization (FISH) studies showed that +12 and 13q- abnormalities are present in CD34+CD19- cells, suggesting that these common chromosomal abnormalities could appear in HSCs [15, 16]. Interestingly, xenotransplantation studies reported that HSCs from CLL patients were able to reproduce the CLL phenotype in murine models [17]. In addition, CLL mutations may appear in HSCs, supporting the idea that CLL pathogenic events occur at an early stage of the hematopoietic process [18].

Taking the previous studies in this field into account, it is well known that chromosomal abnormalities as well as gene mutations are important events in CLL

pathogenesis [19]. However, it is still not clear which genetic events are related with the origin of the disease and when these alterations occur and have a functional impact inducing tumoral cell expansion during B cell differentiation. For these reasons, in this study, chromosomal abnormalities and gene mutations in hematopoietic progenitors were analyzed, showing that the whole population of CD34+ progenitors, even at the level of CD34+CD19-, are already affected at genetic level in CLL patients. In particular, mutations of *FBXW7*, *MYD88*, *NOTCH1*, and *XPO1* as well as 11q and 13q deletions were detected in CD34+ progenitors. By contrast, the origin of *TP53* and *SF3B1* mutations and *IGH* alterations could take place at a later maturational stage. Apart from B lymphocytes, some of these genetic alterations were also observed in other mature cell fractions (T lymphocytes and monocytes) derived from HSCs. Integrating all these results, a pattern of appearance and expansion of these genetic events during B-CLL cell differentiation was suggested.

Methods

Patients

Samples were collected from the bone marrow (BM) of 56 CLL patients. CLL was diagnosed according to the World Health Organization (WHO) classification [20] and the National Cancer Institute (NCI) Working Group criteria [21]. A complete immunophenotypic analysis of all cases was carried out by flow cytometry. The main biological features of the CLL patients are summarized in Additional file 1: Table S1.

Cell isolation and DNA extraction

Total CD34+ progenitor cells and CD19+ B cells were separately isolated from BM samples of CLL patients

using magnetically activated cell sorting (MACS) CD34 and CD19 MicroBeads (Miltenyi Biotec, Bergisch Gladbach, Germany), respectively, according to the manufacturer's instructions. The workflow followed consisted of three steps: first, the isolation of the whole population of CD34+ cells (including CD34+CD19- early progenitors and CD34+CD19+ pro-B cells) from the total BM mononuclear cells, followed by the selection of CD19+ cells from the CD34 negative cell fraction resultant from the first step. Cell purities were determined by flow cytometry, being greater than 90 and 98% for each CD34+ and CD19+ cell fractions, respectively.

In addition, fluorescence-activated cell sorting (FACS) (BD Biosciences, San Jose, CA, USA) was carried out in order to sort the specific subpopulation of CD34+CD19- cells as well as other mature cells such as CD19+ B lymphocytes, CD3+ T lymphocytes, and CD14+ monocytes, from peripheral blood (PB) samples in a second time point of the disease of seven CLL patients. Samples were stained with FITC anti-CD14 (Beckman Coulter), phycoerythrin (PE) anti-CD3 (Becton Dickinson), PE-Cy7 anti-CD19 (Immunostep S.L.), PerCP-Cy5.5 anti-CD45 (BioLegend), and allophycocyanin (APC) anti-CD34 (Becton Dickinson). Purities were greater than 98% in all cell fractions (Additional file 1: Figure S1).

Genomic DNA was extracted from the different cell populations by column-based purification (AllPrep DNA/RNA Mini Kit, Qiagen, Hilden, Germany) following the manufacturer's instructions.

Next-generation sequencing

NGS was performed in CD19+ B lymphocytes from all 56 CLL patients. Amplicon-based NGS was carried out on a GS Junior platform (454 Life Sciences, Branford, CT, USA) using the 454 Titanium Amplicon system (Roche Applied Science, Penzberg, Germany) [22] to investigate the mutational status of *TP53* (exons 4–11), *NOTCH1* (exons 33–34), *SF3B1* (exons 10–16), *FBXW7* (exons 8–12), *MYD88* (exons 4–5), and *XPO1* (exons 14–15) in CD19+ cells. The mutations identified in CD19+ cells were further analyzed in the corresponding whole population of CD34+ progenitors in order to determine whether the same mutations were present in an earlier step than B mature cells. Primer information, PCR conditions, and oligonucleotide design used in previous studies were adopted [23, 24]. The oligonucleotide was designed as part of the work of the IRON-II network. Sequencing data were obtained and analyzed using the GS Data Analysis Software package (Roche Applied Science, Penzberg, Germany) and the Sequence Pilot software for genetic analysis (JSI Medical Systems, Ettenheim, Germany). Mutations detected in more than 2% of bidirectional reads per amplicon in CD19+ cells and in more than 10% in CD34+ cells were accepted

taking into account sequencing coverage (median 980 reads; coverage range 304–9387-fold) [25, 26] and MACS purities from each cell population (98% for CD19+ and 90% for CD34+ cells).

Ultra-deep NGS

To define if the mutations appeared in the specific subpopulation of CD34+CD19- cells and other mature populations derived from the hematopoietic progenitors, mutated target regions were sequenced by ultra-deep NGS, using an Illumina platform, in flow-sorted CD34+CD19-, CD19+, CD3+, and CD14+ cell populations from seven CLL patients. NGS analysis was performed on MiSeq (Illumina, San Diego, CA, USA) using genomic DNA from peripheral blood flow-sorted CD19+ B lymphocytes, CD34+CD19- early progenitors, CD3+ T lymphocytes, and CD14+ monocytes. DNA was amplified using REPLI-g Mini Kit (Qiagen, Hilden, Germany). Target PCRs were performed using exon-specific primers (Additional file 1: Table S2). The experimental design and reaction conditions followed the manufacturer's recommendations. Briefly, PCR products were purified with High Pure PCR Product Purification Kit (Roche Diagnostics, Mannheim, Germany) and quantified using Qubit dsDNA HS Assay Kit (Life Technologies, Waltham, MA, USA). The purified amplicons were pooled to a total amount of 50 ng. The indexed paired-end library was prepared with NEBNext Ultra II DNA Library Prep kit for Illumina (NEW ENGLAND BioLabs) and sequenced using MiSeq (median coverage 4399 reads; range 1491–8614-fold). In order to verify the accuracy of the variant allele frequency (VAF), non-amplified DNA was sequenced in all cases with available material, finding no differences comparing to the VAFs obtained with a previous step of whole-genome amplification.

In-house pipeline was performed to analyze sequencing data. Sequencing reads were aligned to the reference genome GRCh37/hg19 using BWA-0.7 [27]. The alignments were refined with tools of the GATK-3.5 suite [28], and the variants were called according to GATK Best Practice recommendations [29, 30]. Finally, ANNOVAR was used for annotations and prediction of functional consequences [31].

The variant detection was set at 2% taking into account the sequencing coverage and the purities from all sorted cell fractions (more than 98%). Mutations detected at low frequencies (< 15%) by ultra-deep NGS were also validated using 454 Titanium Amplicon System (Roche Applied Science, Penzberg, Germany) (median 1712 reads; coverage range 1277–2638-fold) [23, 24].

Fluorescence in situ hybridization

Interphase FISH was carried out in B cells from 56 BM samples using commercially available probes: 11q22/

ATM, 12p11.1-q11 (alpha satellite), 13q14, 14q32/*IGH*, and 17p13/*TP53* (Vysis/Abbott Co, Abbott Park, IL, USA). Dual-color FISH using differently labeled control and test probes was implemented following the methods previously described [32]. FISH was also performed in the CD34+ cells of a group of nine CLL patients to assess the presence of the cytogenetic alterations identified in the corresponding CD19+ cell fraction. Samples were placed in a Cytospin cytocentrifuge (Thermo Scientific, Waltham, MA, USA) to concentrate the low number of cells. Signal screening was performed in at least 200 cells with well-delineated fluorescence spots. According to our cut-off standards, a score $\geq 10\%$ was considered positive in all cases.

Statistical analysis

Statistical analyses were performed using IBM SPSS for Windows, Version 22.0 (IBM Corp., Armonk, NY, USA). Time to first therapy (TFT) and overall survival (OS) were analyzed on the date of the initial FISH study. Only leukemia-related deaths were considered when analyzing OS. The chi-square test was used to assess associations between categorical variables; continuous variables were analyzed with the Mann-Whitney *U* test. Variables significantly associated with TFT and OS were identified by the Kaplan-Meier method, and the curves of each group were compared with the log-rank test. Results were considered statistically significant for values of $p < 0.05$.

Results

Mutations of driver genes are already present in hematopoietic progenitor cells of CLL patients

Sequencing studies revealed a total of 28 mutations in 24 of the 56 (42.9%) CLL patients. Most of these patients (20/24; 83.3%) showed a single mutation in the analyzed genes, and four of them had two mutations in different genes (ID-34, ID-49, ID-50, and ID-53) (Table 1). The most frequently mutated gene was *NOTCH1* (23.2%), followed by *XPO1* (8.9%), *SF3B1* (7.1%), *FBXW7* (5.4%), *TP53* (3.6%), and *MYD88* (1.8%) (Fig. 1). All of them have been previously reported as mutations in the COSMIC database (<http://cancer.sanger.ac.uk/cosmic>). All patients with mutations in *NOTCH1* carried the same alteration (p.P2514Rfs*4), while *XPO1* mutations corresponded to a previously reported gain-of-function mutation (p.E571K) in all cases. In addition, all *SF3B1*, *FBXW7*, *TP53*, and *MYD88* mutations analyzed were missense mutations.

In order to assess whether the mutations identified in CD19+ cells were also present in a previous step during B cell differentiation, the mutated target regions were analyzed by NGS in the total CD34+ cells. Strikingly, 15/24 patients (62.5%) showed the same mutations in their corresponding CD34+ cells (Table 1). The allele

frequencies of mutations observed in a higher percentage than 10% of both CD19+ and CD34+ cell populations were compared calculating a CD19/CD34 ratio based on the percentage of mutated cells from each cell population. The cut-off CD19/CD34 ratio of 2.5 revealed two different mutational patterns between both cell fractions: “maintained” (ratio < 2.5) and “decreased” (ratio ≥ 2.5). Specifically, most of the mutations in *NOTCH1* (7/9) and *XPO1* (4/4) presented a similar mutational burden in both CD19+ and CD34+ cell fractions (Table 1; Fig. 2a). By contrast, alterations in *TP53* (2/2), *FBXW7* (2/2), and *SF3B1* (3/4) showed a clearly lower percentage or even an absence in the CD34+ cells with respect to the corresponding mature B lymphocytes (Table 1; Fig. 2b).

In a further step to assess if the mutations observed in the whole population of CD34+ progenitor cells appeared in the subpopulation of CD34+CD19- early hematopoietic progenitors, ultra-deep NGS was performed. Flow-sorted CD34+CD19- cells in a second time point from PB of a subset of patients were sequenced, confirming that six out of seven mutations—validated on the B lymphocytes from this time point—were also detected in the hematopoietic progenitor cells (Table 2). Particularly, *MYD88*, *NOTCH1*, *XPO1*, and *FBXW7* mutations were observed in CD34+CD19- cells. On the other hand, *SF3B1* mutation was not observed in the CD34+CD19- cells from patient ID-50. Apart from this, this patient, who was treated before the second time point, did not show *FBXW7* mutation in its B lymphocytes.

Distinctive pattern of distribution of CLL driver mutations along hematopoietic lineages

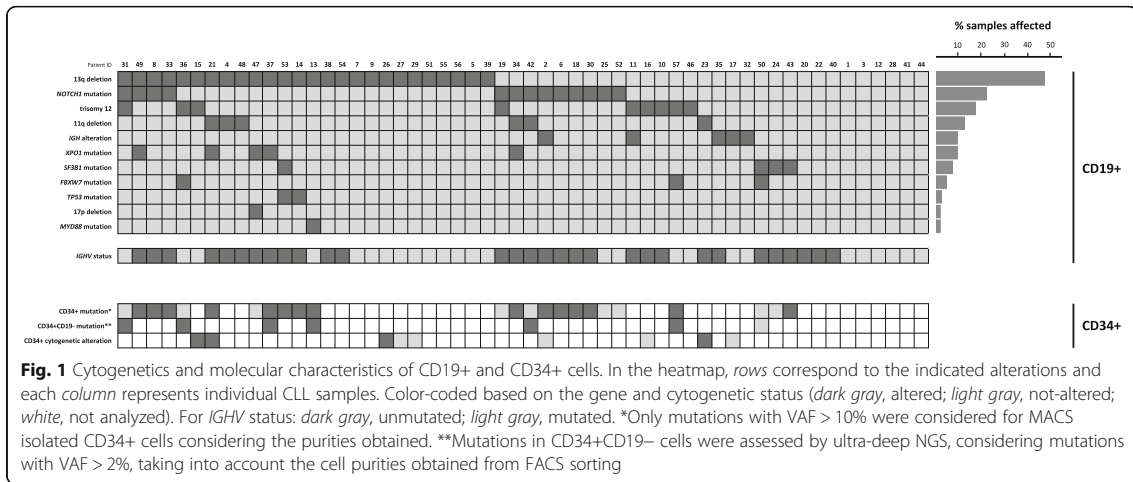
Ultra-deep NGS revealed that gene mutations can be also present in other mature cells derived from hematopoietic stem cells. Thus, the same mutations detected in CD19+ B lymphocytes as well as in their corresponding CD34+CD19- progenitors were also detected in a very low percentage of CD3+ cells and in CD14+ cells in some CLL patients (Table 2). Specifically, ID-13 and ID-36 patients, who harbored *MYD88* and *FBXW7* mutations, respectively, also presented these mutations in both CD3+ and CD14+ cell populations. Moreover, ID-57 (*FBXW7* mutated) showed the mutation on its monocytes whereas ID-37 (*XPO1* mutated) carried the same alteration on the T lymphocytes.

Interestingly, when the allele frequencies from all cell populations were compared, different patterns could be observed. First, *MYD88* and *NOTCH1* mutations (ID-13 and ID-42) appeared in $> 10\%$ of CD34+CD19- cells. In case of *XPO1* and *FBXW7*, their mutations also appeared in CD34+CD19- cells but in a relatively low percentage ($< 5\%$). In addition, *NOTCH1* mutations only appeared on the hematopoietic progenitors and the mature B lymphocytes whereas *FBXW7* and *MYD88* mutations

Table 1 Mutations in CD19+ and CD34+ cell populations identified in 56 CLL patients

ID	IGHV mutation status	Mutated gene	Exon	cDNA change	AA change	COSMIC ID	Mutational load CD19+ (%)	Presence in CD34+ cells*	Mutational load CD34+ (%)	CD19/CD34 ratio	Mutational pattern
2	Unmutated	NOTCH1	34	c.7541_7542delCT	p.P2514Rfs*4	COSM12774	51.0	Yes	31.0	1.6	Maintained
6	Unmutated	NOTCH1	34	c.7541_7542delCT	p.P2514Rfs*4	COSM12774	50.0	Yes	58.0	0.9	Maintained
8	Unmutated	NOTCH1	34	c.7541_7542delCT	p.P2514Rfs*4	COSM12774	97.5	Yes	79.5	1.2	Maintained
13	Mutated	MYD88	4	c.695T>C	p.M232T	COSM85942	34.0	Yes	22.5	1.5	Maintained
14	Unmutated	TP53	5	c.523C>G	p.R175G	COSM10870	87.5	Yes	12.0	7.3	Decreased
18	Unmutated	NOTCH1	34	c.7541_7542delCT	p.P2514Rfs*4	COSM12774	36.5	Yes	13.5	2.7	Decreased
19	Unmutated	NOTCH1	34	c.7541_7542delCT	p.P2514Rfs*4	COSM12774	10.0	No	< 10	-	-
24	Unmutated	SF3B1	16	c.2225G>A	p.G742D	COSM145923	24.0	No	< 10	> 2.5	Decreased
21	Unmutated	XPO1	15	c.1711G>A	p.E571K	COSM96797	39.5	Yes	31.0	1.3	Maintained
25	Mutated	NOTCH1	34	c.7541_7542delCT	p.P2514Rfs*4	COSM12774	3.0	No	< 10	-	-
30	Unmutated	NOTCH1	34	c.7541_7542delCT	p.P2514Rfs*4	COSM12774	57.0	Yes	24.0	2.4	Maintained
31	Mutated	NOTCH1	34	c.7541_7542delCT	p.P2514Rfs*4	COSM12774	4.5	No	< 10	-	-
33	Unmutated	NOTCH1	34	c.7541_7542delCT	p.P2514Rfs*4	COSM12774	41.0	Yes	40.5	1.0	Maintained
34	Unmutated	NOTCH1	34	c.7541_7542delCT	p.P2514Rfs*4	COSM12774	50.0	Yes	51.5	0.9	Maintained
34	Unmutated	XPO1	15	c.1711G>A	p.E571K	COSM96797	24.5	Yes	24.5	1.0	Maintained
36	Mutated	FBXW7	9	c.1394G>T	p.R465L	COSM33762	39.0	No	< 10	> 2.5	Decreased
37	Unmutated	XPO1	15	c.1711G>A	p.E571K	COSM96797	50.5	Yes	38.5	1.3	Maintained
42	Unmutated	NOTCH1	34	c.7541_7542delCT	p.P2514Rfs*4	COSM12774	5.0	No	< 10	-	-
43	Unmutated	SF3B1	15	c.2110A>T	p.I704F	COSM132954	47.5	Yes	45.0	1.1	Maintained
47	Unmutated	XPO1	15	c.1711G>A	p.E571K	COSM96797	2.5	No	< 10	-	-
49	Unmutated	NOTCH1	34	c.7541_7542delCT	p.P2514Rfs*4	COSM12774	55.0	Yes	56.0	0.9	Maintained
49	Unmutated	XPO1	15	c.1711G>A	p.E571K	COSM96797	42.5	Yes	31.5	1.4	Maintained
50	Unmutated	FBXW7	9	c.1268G>T	p.G423V	COSM1052095	8.0	No	< 10	-	-
50	Unmutated	SF3B1	14	c.1874G>A	p.R625H	COSM255276	21.0	No	< 10	> 2.5	Decreased
52	Mutated	NOTCH1	34	c.7541_7542delCT	p.P2514Rfs*4	COSM12774	16.0	No	< 10	> 2.5	Decreased
53	Unmutated	SF3B1	14	c.1996A>G	p.K666E	COSM110694	43.0	Yes	14.0	3.1	Decreased
53	Unmutated	TP53	7	c.734G>A	p.G245D	COSM43606	41.5	Yes	16.5	2.5	Decreased
57	Mutated	FBXW7	9	c.1394G>A	p.R465H	COSM22965	41.5	Yes	13.0	3.2	Decreased

*Only cases with > 10% CD34+ cells mutated were considered providing the purity for this cell fraction was higher than 90% in all the cases



seemed to appear in all the sequenced cell fractions, affecting even myeloid lineage and T lymphoid lineage. On the other hand, patient ID-50 did not present its *SF3B1* mutation in the CD34+CD19- nor the T lymphocytes and monocytes (Table 2).

All these mutations detected at low frequencies (< 15%) in CD34+CD19-, CD3+, and CD14+ cells were also validated by 454 sequencing when material was available (Additional file 1: Table S3).

Several cytogenetic abnormalities are detected in a previous developmental stage of the mature B lymphocytes of CLL patients

FISH studies revealed a total of 39/56 (69.6%) CLL patients with cytogenetic abnormalities in B lymphocytes. Specifically, 13q deletion was the most common aberration in our cohort (46.3%), followed by trisomy 12 (17%), 11q deletion (11.3%), *IGH* alterations (9.3%), and 17p deletion (1.9%) (Additional file 1: Table S1).

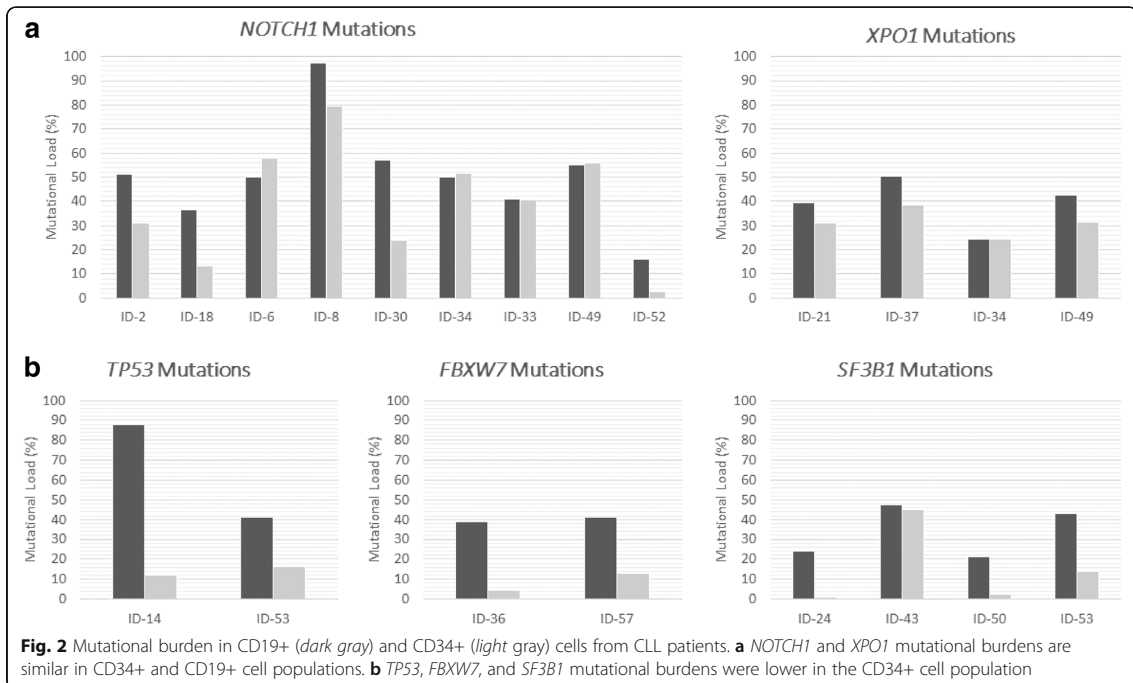


Table 2 Mutations in CD19+, CD34+CD19-, CD3+ and CD14+ PB cell populations identified by ultra-deep NGS

Patient ID	IGHV mutation status	Mutated gene	AA change	Time point 1; bone marrow		Time point 2: peripheral blood			
				%mut CD19	%mut CD34	%mut CD19+	%mut CD34+CD19-	%mut CD3+	%mut CD14+
13	Mutated	MYD88	p.M232T	36	22	23.1	12.2	2.6	7.7
31	Mutated	NOTCH1	p.P2514Rfs*4	4	< 10	15.3	2.1	0	0
36	Mutated	FBXW7	p.R465L	39	< 10	3.2	3.0	2.7	3.6
37	Unmutated	XPO1	p.E571K	51	38	53.0	3.0	3.0	0.4
42	Unmutated	NOTCH1	p.P2514Rfs*4	5.25	< 10	33.0	12.9	0	0.6
50	Unmutated	SF3B1	p.R625H	21	< 10	15.0	1.0	0.1	0.1
50	Unmutated	FBXW7	p.G423V	8	< 10	0	0	0	0
57	Mutated	FBXW7	p.R465H	42	13	46.5	2.4	0.8	2.6

The cut-off set for the second time point was 2% (bold) provided that our FACS purities were higher than 98% in all cases for all cell populations

To assess if the chromosomal abnormalities were also present in a previous step of the B cell differentiation, FISH analyses were performed in the whole population of CD34+ cells of a subset of patients ($n = 9$) (Fig. 1). Interestingly, these analyses revealed that five of nine CLL patients with cytogenetic alterations in mature B lymphocytes showed the same chromosomal aberration in the CD34+ cells, although at a lower percentage than in CD19+ cells (Table 3). Specifically, both CLL patients with 11q- and three of five patients with 13q- showed the same cytogenetic alteration in the corresponding CD34+ cells. By contrast, IGH abnormalities identified by FISH in two CLL patients (ID-02 and ID-17) were not identified in their corresponding CD34+ cells. Apart from these alterations, the only CLL patient with +12, whose CD34+ cells were analyzed by FISH, did not have this trisomy in their corresponding progenitor cells.

Patients with multiple genetic alterations show a hierarchy in the appearance of these events

The combination of NGS and FISH data revealed that two patients presented both mutations and chromosomal abnormalities (Table 3). The first case (ID-02) had an IGH alteration and a NOTCH1 mutation in the CD19+ cells. However, FISH studies and NGS analysis of CD34+ progenitors revealed that the NOTCH1 mutation was the only genetic event. The second case (ID-21) showed two chromosomal abnormalities (11q- and 13q-) and an XPO1 mutation. These three alterations were also observed in the CD34+ cells, although 11q- and 13q- were present in a higher percentage of cells (72 and 49%) than the XPO1 variant (30%).

Four cases showed a co-occurrence of mutations in two different genes. Thus, two patients (ID-34 and ID-49) carried mutations in NOTCH1 and XPO1, present in both CD19+ and CD34+ cell fractions, with NOTCH1

Table 3 FISH analysis in CD34+ cell populations of nine patients

Patient ID	IGHV mutation status	FISH results				NGS results		
		Cytogenetic alteration	Altered CD19+ cells (%)	Presence in CD34+ cells	Altered CD34+ cells (%)	Mutated gene	Mutational load CD19+ (%)	Mutational load CD34+ (%)
2	Unmutated	IGH alt	80	No	-	NOTCH1	51	31
15	Mutated	13q-	65	Yes	25	-	-	-
16	Unmutated	+12	22	No	-	-	-	-
17	Mutated	IGH alt	54	No	-	-	-	-
21	Unmutated	11q-	64	Yes	49	XPO1	39.5	31
21		13q-	93	Yes	72			
23	Unmutated	11q-	79	Yes	36	-	-	-
26	Mutated	13q-	67	Yes	46.5	-	-	-
27	Mutated	13q-	86	No	-	-	-	-
29	Mutated	13q-	25	No	-	-	-	-

always being the dominant clone with respect to *XPO1* (52 vs. 25%; 55 vs. 31%). The patient ID-50 harbored mutations in *SF3B1* and *FBXW7*, which occurred at a much lower or null percentage in the CD34+ progenitors (21 vs. 2.5%; 8 vs. 0%). Finally, patient ID-53 had mutations in *SF3B1* and *TP53* in a low percentage of CD34+ cells compared with that in CD19+ B lymphocytes (43 vs. 14%; 41.5 vs. 16.5%).

Clinical and biological correlations with genetic alterations in CD34+ cells in CLL patients

The clinical impact of the presence of mutations in the whole population of CD34+ cells was explored. The presence of mutations in the whole CD34+ cell population was associated with an unmutated *IGHV* status ($p = 0.003$) and high levels of serum β_2 microglobulin ($p = 0.011$) (Additional file 1: Table S4). Interestingly, patients with mutations in their CD34+ progenitors also showed shorter OS ($p = 0.01$) (Additional file 1: Figure S2A) than patients without mutations in this cell fraction. In addition, patients harboring mutations in *NOTCH1*, *SF3B1*, and *TP53* in their hematopoietic progenitors presented a shorter TFT ($p = 0.028$) (Additional file 1: Figure S2B). Moreover, comparing the two mutational patterns identified in the CD34+ cells fraction, the mutations maintained on the CD34+ progenitors were significantly associated with the absence of trisomy 12 in the B lymphocytes ($p = 0.014$) (Additional file 1: Table S5).

Comparing the mutational burden in the CD34+ fraction between BM samples collected before and after treatment revealed no significant differences ($p = 0.605$). Four patients who received treatment before the extraction of the BM relapsed. Interestingly, all of them showed mutations in the CD34+ progenitors with a similar mutational burden as the corresponding CD19+ B lymphocytes (Additional file 1: Table S6).

Discussion

Our data provide evidence of the presence of mutations and chromosomal abnormalities in early hematopoietic progenitors in BM samples of CLL patients. These results shed light on the cell of origin of CLL in a previous developmental stage to mature B cells, demonstrating CLL patients can also show genetic events in the CD34+ hematopoietic progenitors. These results are consistent with the findings of two recent studies [17, 18]. MACS isolation was performed on the whole population of CD34+ cells including CD34+CD19+ pro-B cells. A previous study has reported that the pro-B cell population is larger in the bone marrow of CLL patients than in healthy donors (mean range of 18% pro-B cells in the total bone marrow CD34+ cell count, exceeding 30% in some cases) [17]. This suggests that the patients who presented a mutational burden of < 30% in the CD34+

cell population may only harbor the mutation in CD34+CD19+ pro-B cells, rather than in the early hematopoietic progenitors. It is of particular note that 10 out of 15 patients with mutations in the whole population of CD34+ cells had mutational rates of > 30%, suggesting that these mutations not only appear in the pro-B cells, but also at earlier maturational stages of B cell differentiation (CD34+CD19- progenitors). In order to assess this hypothesis, we could perform ultra-deep NGS studies of flow-sorted CD34+CD19- cells using PB samples in a small subset of patients within the main cohort, detecting that all the mutations, except to one, were already present in this cellular fraction. Therefore, these results confirmed that mutations on CLL driver genes could occur in early hematopoietic progenitor cells of these patients. In particular, our sequencing results suggest that mutations in *NOTCH1*, *MYD88*, *FBXW7*, and *XPO1* may appear in CD34+CD19- cells whereas *TP53* and *SF3B1* mutations could appear in a later stage of B cell differentiation. As far as we are concerned, these results were demonstrated for the first time in fresh hematopoietic progenitor cells without having been cultured.

As these driver mutations have been detected in early hematopoietic progenitors of some CLL patients, we hypothesized that these alterations can affect hematopoietic lineages other than B cells. As it was previously reported, some mutations in well-known CLL drivers can also appear on a low percentage in other mature cell fractions as CD3+ T lymphocytes and/or CD14+ monocytes [18].

In order to determine the stage of B cell differentiation in which these mutations induced an expansion of the tumoral cell population, first, the mutational burdens in CD19+ mature B lymphocytes and CD34+ progenitors were compared. Since the mutational burden in CD34+ cells with *NOTCH1* mutations was as high as that observed in CD19+ cells in most of the cases, it could be hypothesized that mutations in this gene induced an expansion of the CLL hematopoietic progenitors. Indeed, ultra-deep NGS studies confirmed this in patient ID-42 who had *NOTCH1* mutation in more than 10% of CD34+CD19- cells. Moreover, every *XPO1* mutation observed in our cohort was present in the CD34+ progenitors and the mutational burden remained similar in both cellular fractions. However, the percentage of *XPO1* mutations in the CD34+ cells exceeded 30% in very few cases, suggesting that these mutations could be enriched at an intermediate B cell stage as CD34+CD19+ pro-B cells. On the other hand, the mutational burdens of *TP53*, *SF3B1*, and *FBXW7* were considerably lower in the CD34+ cell population. Although *SF3B1* mutation was not detected in CD34+CD19- cells, suggesting it as a late event in B-CLL differentiation, one out of four *SF3B1* mutated patients (ID-43) carried a mutation in a

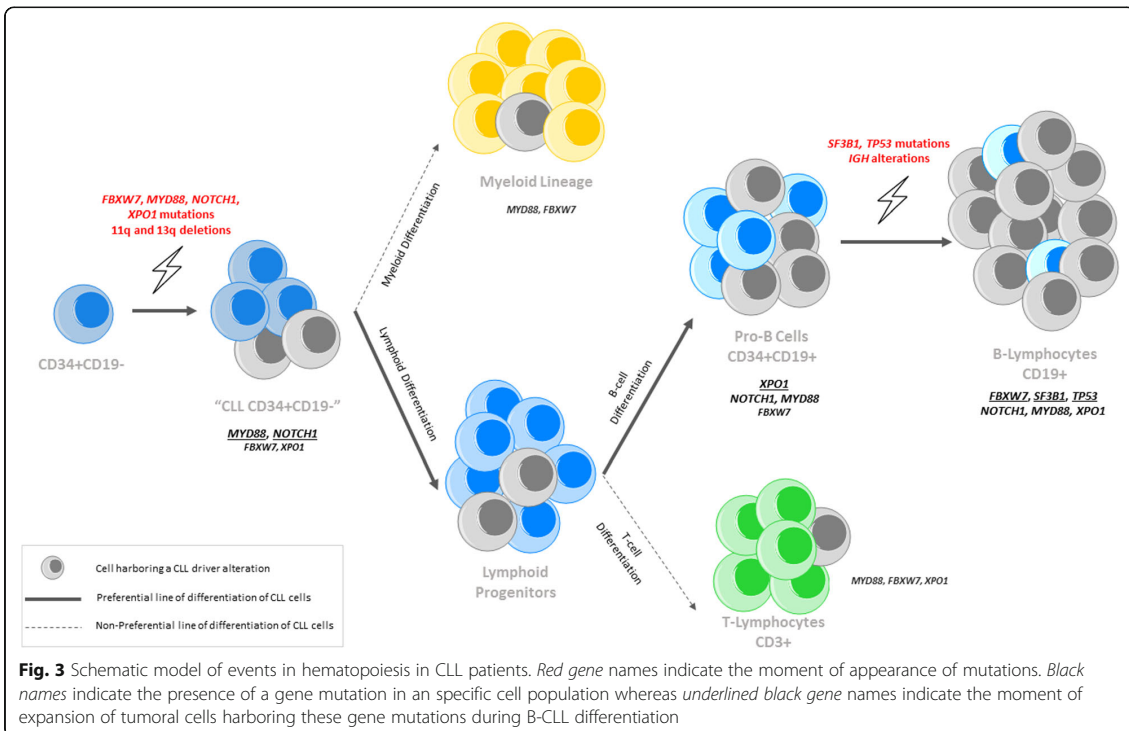
high percentage of the whole population of CD34+ progenitors, similar to results from a previous study [18]. Besides this, alterations in this gene have been also reported in CD34+ cells of patients with myeloid malignancies [33]. Therefore, it should be essential to study larger cohorts of CLL patients in order to determine what type of *SF3B1* mutations occur in HSCs of CLL patients and functional studies to assess the differences between “CLL-HSCs *SF3B1* mutated” and “MDS-HSCs *SF3B1* mutated.”

Focusing on the presence of cytogenetic abnormalities in CD34+ cell populations in our cohort, 11q- and 13q- appeared in the CD34+ progenitors at high percentages, as reported previously [15, 16], supporting the hypothesis that these chromosomal aberrations could be an early event in CLL [8]. By contrast, *IGH* alterations were not present in any of the CD34+ hematopoietic progenitors. Previous case report studies have yielded similar results [34, 35], suggesting that *IGH* alterations occur in an advanced stage of the lymphocyte maturation process.

The analysis of patients with more than one genetic alteration allowed us to define a hierarchy of the appearance of these genetic events. When *IGH* alterations and the *NOTCH1* mutation are present in the same patient (ID-02), it is clear that the *NOTCH1* mutation is an earlier step than the *IGH* alteration during B cell differentiation. Moreover, when 11q-, 13q-, and *XPO1* mutations

are present in the same patient (ID-21), they all appear in the CD34+ progenitors. However, 11q- and 13q- are certainly present at a higher allele frequency than the mutational load of *XPO1*, suggesting that cells with 11q- and 13q- were expanded in an earlier stage than the *XPO1* mutation in the pathogenesis of the disease [8]. Specifically, the dominant clone in the two cases with a double mutation in *NOTCH1* and *XPO1* (ID-34 and ID-49) was always *NOTCH1* rather than *XPO1*. Therefore, since *XPO1* is still present in a small part of the CD34+CD19- cell population and greatly enriched on the total CD34+ fraction, we may consider that cells carrying *XPO1* mutations are expanded in an intermediate event of B-CLL differentiation, given the previous possible events such as 13q- and 11q- abnormalities or *MYD88* and *NOTCH1* mutations. Taking into account all these results, a model of the appearance of genetic events during the hematopoiesis in CLL has been suggested (Fig. 3). However, as some of these genetic alterations were observed in few cases, it would be interesting to sequence all cell fractions in larger cohorts of patients.

The prognostic impact of gene mutations and chromosomal abnormalities in CLL has been well characterized in several studies of large cohorts of patients [4, 9, 23, 36]. *TP53*, *NOTCH1*, and *SF3B1* are described as poor prognostic mutations [10, 37–40]. The prognostic impact of the presence of mutations in CD34+ cells from CLL patients



has been assessed for the first time in this study, showing that CLL patients harboring mutations in the hematopoietic progenitors showed worse prognosis. It is essential to achieve a better understanding of these results since only six genes were analyzed in our study, whereas a CLL exome exhibits an average of 20 mutations [8, 10]. Therefore, further studies analyzing the whole exome in larger cohorts should be performed in order to accurately define their impact. In addition, conventional CLL therapies may not be able to eradicate or reduce the malignant CD34+ CLL clone and may be responsible for the relapse of patients bearing mutations in these cells. Given that these therapies seem not to have a clear effect on CD34+ CLL cells, allogeneic stem cell transplantation could be an option for overcoming the challenges that may arise from CD34+ cell treatment [41].

Conclusions

Our data show that recurrent CLL chromosomal abnormalities and gene mutations are present not only in mature B lymphocytes but also in hematopoietic progenitors. Although CLL is a clonal mature B cell disease, our results provide strong evidence that CLL may originate in the early stages of hematopoiesis. Both chromosomal alterations and point mutations are highly relevant to the disease pathogenesis, with a clinical impact as soon as they appear. To the best of our knowledge, our study is the first to analyze both genetic events in different cellular fractions of the same patients by NGS and FISH. It provides us with a broader understanding of CLL initiation and development, opening up possibilities for future therapies.

Additional file

Additional file 1: Table S1. Clinico-biological characteristics from CLL patients. **Table S2.** Illumina Primer Design. **Table S3.** Validation of mutations detected at low frequency by ultra-deep NGS in flow-sorted cell fractions using 454 sequencing. **Table S4.** Patients' characteristics regarding the presence of mutations in CD34+ progenitors. **Table S5.** Patients' characteristics regarding the mutational burden maintenance or decrease in CD34+ progenitors. **Table S6.** Treatments prior bone marrow extraction of 4 CLL patients who relapsed and correlation with the CD19+ and CD34+ mutational status. **Figure S1.** Representation of the purity analysis of FACS sorted cell populations. **Figure S2.** Kaplan-Meier analysis of overall survival (A) and time to first therapy (B) in patients with mutations in their CD34+ progenitors. (DOCX 200 kb)

Abbreviations

BM: Bone marrow; CLL: Chronic lymphocytic leukemia; FACS: Fluorescence-activated cell sorting; FISH: Fluorescence in situ hybridization; HSC: Hematopoietic stem cell; IGHV: Immunoglobulin heavy chain gene; MACS: Magnetically activated cell sorting; NGS: Next-generation sequencing; OS: Overall survival; PB: Peripheral blood; TFT: Time to first therapy; VAF: Variant allele frequency

Acknowledgements

We thank Irene Rodríguez, Sara González, Teresa Prieto, M^o Ángeles Ramos, Almudena Martín, Ana Díaz, Ana Simón, María del Pozo, Isabel M. Isidro,

Vanesa Gutiérrez, Sandra Pujante, and Sandra Santos from the Centro de Investigación del Cáncer, Salamanca, Spain, for their technical assistance.

Funding

This work was partially supported by grants from the Spanish Fondo de Investigaciones Sanitarias PI12/00281, PI15/01471, Instituto de Salud Carlos III (ISCIII), European Regional Development Fund (ERDF) "Una manera de hacer Europa," Consejería de Educación, Junta de Castilla y León (SA085U16), Proyectos de Investigación del SACYL, Spain: GRS 1172/A/15, BIO/SA10/14, GRS 1343/A/16, and Fundación Española de Hematología y Hemoterapia (FEHH) and by a grant (RD12/0036/0069) from the Red Temática de Investigación Cooperativa en Cáncer (RTICC), Instituto de Salud Carlos III (ISCIII), Spanish Ministry of Economy and Competitiveness & European Regional Development Fund (ERDF) "Una manera de hacer Europa" (Innocampus; CEI-2010-1-0010), Fundación "Memoria Don Samuel Solórzano Barruso" 2016, and the European Union Seventh Framework Programme [FP7/2007–2013] under Grant Agreement no. 306242-NGS-PTL. MHS is fully supported by an "Ayuda predoctoral de la Junta de Castilla y León" by the Fondo Social Europeo (JCYL-EDU/346/2013 PhD scholarship). Oligonucleotide primer plates for amplicon deep-sequencing were provided by Roche Diagnostics, Penzberg, Germany, as part of the IRON-II study.

Availability of data and materials

The datasets analyzed during the current study are available from the corresponding author on reasonable request.

Authors' contributions

MQA and MHS designed and performed the research and statistical analyses, analyzed the data, and wrote the paper. CR and RB performed the next-generation sequencing studies and analyzed the data. AERV designed the study and performed the cell isolation. JMHS and DQ performed the cell isolation and FISH studies. AM proceeded the samples and performed the sequencing studies. AAM, MJVM, GFG, MPDB, JG, JNR, GMN, JMA, AGC, JAQ, MS, and CA provided the patients' data. JAH provided the patients' data and critically reviewed the manuscript. MGA performed the IGHV mutational status analysis. AK designed the sequencing studies. MG designed the IGHV mutational status analysis and critically reviewed the manuscript. JAH critically reviewed the manuscript. JMHR designed and performed the research and corrected and approved the final version of the manuscript. All the authors approved the final version of manuscript.

Competing interests

The authors declare that they have no competing interests.

Consent for publication

Not applicable.

Ethics approval and consent to participate

The present study was approved by the local ethics committee (*Comité Ético de Investigación Clínica, Hospital Universitario de Salamanca*). Written informed consent was obtained from all participants before they entered the study.

Publisher's Note

Springer Nature remains neutral with regard to jurisdictional claims in published maps and institutional affiliations.

Author details

¹Servicio de Hematología & IBSAL, IBMCC, CIC Universidad de Salamanca-CSIC, Hospital Universitario, Salamanca, Spain. ²Department of Molecular and Clinical Pharmacology, University of Liverpool, Liverpool, UK. ³Servicio de Hematología, Hospital Virgen Blanca, León, Spain. ⁴Servicio de Hematología, Hospital Miguel Servet, Zaragoza, Spain. ⁵Servicio de Hematología, Hospital del Bierzo, Ponferrada, León, Spain. ⁶Servicio de Hematología, Hospital Juan Ramón Jiménez, Huelva, Spain. ⁷Servicio de Hematología, Hospital Virgen del Puerto, Plasencia, Cáceres, Spain. ⁸Servicio de Hematología, Hospital Río Carrión, Palencia, Spain. ⁹Servicio de Hematología, Hospital Clínico, Valladolid, Spain. ¹⁰Servicio de Hematología, Hospital General de Segovia, Segovia, Spain. ¹¹Servicio de Hematología, Hospital Virgen de la Concha, Zamora, Spain. ¹²Servicio de Hematología, Hospital Santa Bárbara, Soria, Spain. ¹³MLL Munich, Munich, Germany. ¹⁴AstraZeneca, Personalized Healthcare and Biomarkers, Innovative

Medicines, Cambridge, UK. ¹⁵Servicio de Hematología, Hospital Universitario Infanta Leonor, Universidad Complutense de Madrid, Madrid, Spain. ¹⁶IBMCC, CIC Universidad de Salamanca-CSIC, Hospital Universitario de Salamanca, Paseo de San Vicente s/n, 37007 Salamanca, Spain.

Received: 28 January 2017 Accepted: 24 March 2017

Published online: 11 April 2017

References

- Chiorazzi N, Rai KR, Ferrarini M. Chronic lymphocytic leukemia. *N Engl J Med*. 2005;352(8):804–15.
- Rozman C, Montserrat E. Chronic lymphocytic leukemia. *N Engl J Med*. 1995; 333(16):1052–7.
- Hallek M, Cheson BD, Catovsky D, Caligaris-Cappio F, Dighiero G, Dohner H, et al. Guidelines for the diagnosis and treatment of chronic lymphocytic leukemia: a report from the International Workshop on Chronic Lymphocytic Leukemia updating the National Cancer Institute-Working Group 1996 guidelines. *Blood*. 2008;111(12):5446–56.
- Dohner H, Stilgenbauer S, Benner A, Leupolt E, Krober A, Bullinger L, et al. Genomic aberrations and survival in chronic lymphocytic leukemia. *N Engl J Med*. 2000;343(26):1910–6.
- Hamblin TJ, Davis Z, Gardiner A, Oscier DG, Stevenson FK. Unmutated Ig V(H) genes are associated with a more aggressive form of chronic lymphocytic leukemia. *Blood*. 1999;94(6):1848–54.
- Naylor M, Capra JD. Mutational status of Ig V(H) genes provides clinically valuable information in B-cell chronic lymphocytic leukemia. *Blood*. 1999;94(6):1837–9.
- Puente XS, Pinyol M, Quesada V, Conde L, Ordóñez GR, Villamor N, et al. Whole-genome sequencing identifies recurrent mutations in chronic lymphocytic leukaemia. *Nature*. 2011;475(7354):101–5.
- Landau DA, Tausch E, Taylor-Weiner AN, Stewart C, Reiter JG, Bahlo J, et al. Mutations driving CLL and their evolution in progression and relapse. *Nature*. 2015;526(7574):525–30.
- Baliakas P, Hadzidimitriou A, Sutton LA, Rossi D, Minga E, Villamor N, et al. Recurrent mutations refine prognosis in chronic lymphocytic leukemia. *Leukemia*. 2015;29(2):329–36.
- Quesada V, Conde L, Villamor N, Ordóñez GR, Jares P, Bassaganyas L, et al. Exome sequencing identifies recurrent mutations of the splicing factor SF3B1 gene in chronic lymphocytic leukemia. *Nat Genet*. 2012;44(1):47–52.
- Young E, Noerenberg D, Mansouri L, Ljungstrom V, Frick M, Sutton LA, et al. EGR2 mutations define a new clinically aggressive subgroup of chronic lymphocytic leukemia. *Leukemia*. 2017.
- Caligaris-Cappio F, Gobbi M, Boffill M, Janossy G. Infrequent normal B lymphocytes express features of B-chronic lymphocytic leukemia. *J Exp Med*. 1982;155(2):623–8.
- Caligaris-Cappio F. B-chronic lymphocytic leukemia: a malignancy of anti-self B cells. *Blood*. 1996;87(7):2615–20.
- Seifert M, Sellmann L, Bloehdorn J, Wein F, Stilgenbauer S, Durig J, et al. Cellular origin and pathophysiology of chronic lymphocytic leukemia. *J Exp Med*. 2012;209(12):2183–98.
- Gahn B, Schafer C, Neef J, Troff C, Feuring-Buske M, Hiddemann W, et al. Detection of trisomy 12 and Rb-deletion in CD34+ cells of patients with B-cell chronic lymphocytic leukemia. *Blood*. 1997;89(12):4275–81.
- Gahn B, Wendenburg B, Troff C, Neef J, Grove D, Haferlach T, et al. Analysis of progenitor cell involvement in B-CLL by simultaneous immunophenotypic and genotypic analysis at the single cell level. *Br J Haematol*. 1999;105(4):955–9.
- Kikushige Y, Ishikawa F, Miyamoto T, Shima T, Urata S, Yoshimoto G, et al. Self-renewing hematopoietic stem cell is the primary target in pathogenesis of human chronic lymphocytic leukemia. *Cancer Cell*. 2011;20(2):246–59.
- Damm F, Mylonas E, Cosson A, Yoshida K, Della Valle V, Mouly E, et al. Acquired initiating mutations in early hematopoietic cells of CLL patients. *Cancer Discov*. 2014;4(9):1088–101.
- Fabbri G, Dalla-Favera R. The molecular pathogenesis of chronic lymphocytic leukaemia. *Nat Rev Cancer*. 2016;16(3):145–62.
- Harris NL, Jaffe ES, Diebold J, Flandrin G, Muller-Hermelink HK, Vardiman J, et al. World Health Organization classification of neoplastic diseases of the hematopoietic and lymphoid tissues: report of the Clinical Advisory Committee meeting-Airlie House, Virginia, November 1997. *J Clin Oncol*. 1999;17(12):3835–49.
- Binet JL, Caligaris-Cappio F, Catovsky D, Cheson B, Davis T, Dighiero G, et al. Perspectives on the use of new diagnostic tools in the treatment of chronic lymphocytic leukemia. *Blood*. 2006;107(3):859–61.
- Margulies M, Egholm M, Altman WE, Attiya S, Bader JS, Benben LA, et al. Genome sequencing in microfabricated high-density picolitre reactors. *Nature*. 2005;437(7057):376–80.
- Jeromin S, Weissmann S, Haferlach C, Dicker F, Bayer K, Grossmann V, et al. SF3B1 mutations correlated to cytogenetics and mutations in NOTCH1, FBXW7, MYD88, XPO1 and TP53 in 1160 untreated CLL patients. *Leukemia*. 2014;28(1):108–17.
- Hernandez JA, Hernandez-Sanchez M, Rodriguez-Vicente AE, Grossmann V, Collado R, Heras C, et al. A low frequency of losses in 11q chromosome is associated with better outcome and lower rate of genomic mutations in patients with chronic lymphocytic leukemia. *PLoS One*. 2015;10(11), e0143073.
- Forero-Castro M, Robledo C, Lumbreras E, Benito R, Hernandez-Sanchez JM, Hernandez-Sanchez M, et al. The presence of genomic imbalances is associated with poor outcome in patients with burkitt lymphoma treated with dose-intensive chemotherapy including rituximab. *Br J Haematol*. 2016; 172(3):428–38.
- Grossmann V, Roller A, Klein HU, Weissmann S, Kern W, Haferlach C, et al. Robustness of amplicon deep sequencing underlines its utility in clinical applications. *J Mol Diagn*. 2013;15(4):473–84.
- Li H, Durbin R. Fast and accurate long-read alignment with Burrows-Wheeler transform. *Bioinformatics*. 2010;26(5):589–95.
- McKenna A, Hanna M, Banks E, Sivachenko A, Cibulskis K, Kernytzky A, et al. The Genome Analysis Toolkit: a MapReduce framework for analyzing next-generation DNA sequencing data. *Genome Res*. 2010;20(9):1297–303.
- DePristo MA, Banks E, Poplin R, Garimella KV, Maguire JR, Hartl C, et al. A framework for variation discovery and genotyping using next-generation DNA sequencing data. *Nat Genet*. 2011;43(5):491–8.
- Van der Auwera GA, Carneiro MO, Hartl C, Poplin R, Del Angel G, Levy-Moonshine A, et al. From FastQ data to high confidence variant calls: the Genome Analysis Toolkit best practices pipeline. *Curr Protoc Bioinformatics*. 2013;43(11 10):1–33.
- Wang K, Li M, Hakonarson H. ANNOVAR: functional annotation of genetic variants from high-throughput sequencing data. *Nucleic Acids Res*. 2010; 38(16):e164.
- Gonzalez MB, Hernandez JM, Garcia JL, Lumbreras E, Castellanos M, Hernandez JM, et al. The value of fluorescence in situ hybridization for the detection of 11q in multiple myeloma. *Haematologica*. 2004;89(10):1213–8.
- Mian SA, Rouault-Pierre K, Smith AE, Seidl T, Pizzitola I, Kizilers A, et al. SF3B1 mutant MDS-initiating cells may arise from the haematopoietic stem cell compartment. *Nat Commun*. 2015;6:10004.
- Gottardi M, Gattei V, Degan M, Bomben R, Zucchetto A, Tecchio C, et al. Concomitant chronic lymphocytic leukemia and acute myeloid leukemia: evidence of simultaneous expansion of two independent clones. *Leuk Lymphoma*. 2006;47(5):885–9.
- Mitterbauer G, Schwarzmeier J, Mitterbauer M, Jaeger U, Fritsch G, Schwarzwinger I. Myelodysplastic syndrome/acute myeloid leukemia supervening previously untreated chronic B-lymphocytic leukemia: demonstration of the concomitant presence of two different malignant clones by immunologic and molecular analysis. *Ann Hematol*. 1997;74(4):193–7.
- Rossi D, Rasi S, Spina V, Brusca G, Monti S, Ciardullo C, et al. Integrated mutational and cytogenetic analysis identifies new prognostic subgroups in chronic lymphocytic leukemia. *Blood*. 2013;121(8):1403–12.
- Zenz T, Krober A, Scherer K, Habe S, Buhler A, Benner A, et al. Monoallelic TP53 inactivation is associated with poor prognosis in chronic lymphocytic leukemia: results from a detailed genetic characterization with long-term follow-up. *Blood*. 2008;112(8):3322–9.
- Rossi D, Rasi S, Fabbri G, Spina V, Fangazio M, Forconi F, et al. Mutations of NOTCH1 are an independent predictor of survival in chronic lymphocytic leukemia. *Blood*. 2012;119(2):521–9.
- Cortese D, Sutton LA, Cahill N, Smedby KE, Geisler C, Gunnarsson R, et al. On the way towards a 'CLL prognostic index': focus on TP53, BIRC3, SF3B1, NOTCH1 and MYD88 in a population-based cohort. *Leukemia*. 2014;28(3):710–3.
- Weissmann S, Roller A, Jeromin S, Hernandez M, Abaigar M, Hernandez-Rivas JM, et al. Prognostic impact and landscape of NOTCH1 mutations in chronic lymphocytic leukemia (CLL): a study on 852 patients. *Leukemia*. 2013;27(12):2393–6.
- Dreger P, Dohner H, Ritgen M, Bottcher S, Busch R, Dietrich S, et al. Allogeneic stem cell transplantation provides durable disease control in poor-risk chronic lymphocytic leukemia: long-term clinical and MRD results of the German CLL Study Group CLL3X trial. *Blood*. 2010;116(14):2438–47.

CHAPTER 2

CRISPR/Cas9-generated models uncover therapeutic vulnerabilities of del(11q) CLL cells to dual BCR and PARP inhibition

Miguel Quijada-Álamo^{1,2*}, María Hernández-Sánchez^{1,2,3,4*}, Verónica Alonso Pérez^{1,2}, Ana E Rodríguez-Vicente^{1,2}, Ignacio García-Tuñón^{1,2}, Marta Martín Izquierdo^{1,2}, Jesús María Hernández-Sánchez^{1,2}, Ana B Herrero^{1,2}, José María Bastida², Laura San Segundo^{1,2}, Michaela Gruber^{3,4,5,6}, Juan Luis García^{1,2}, Shanye Yin^{3,4}, Elisa ten Hacken^{3,4}, Rocío Benito^{1,2}, José Luis Ordóñez^{1,2}, Catherine J Wu^{3,4} and Jesús María Hernández-Rivas^{1,2,7}

¹University of Salamanca, IBSAL, IBMCC, CSIC, Cancer Research Center, Salamanca, Spain. ²Department of Hematology, University Hospital of Salamanca, Salamanca, Spain. ³Department of Medical Oncology, Dana-Farber Cancer Institute, Boston, Massachusetts 02115, USA. ⁴Broad Institute of Harvard and MIT, Cambridge, Massachusetts 02142, USA. ⁵CeMM Research Center for Molecular Medicine, Vienna, Austria. ⁶Department of Internal Medicine I, Division of Hematology and Hemostaseology, Medical University of Vienna, Vienna, Austria. ⁷Department of Medicine, University of Salamanca, Salamanca, Spain. *Equal contribution.

Leukemia. 2020 Jun;34(6):1599-1612. doi: 10.1038/s41375-020-0714-3.

PMID: 31974435



Chronic lymphocytic leukemia

CRISPR/Cas9-generated models uncover therapeutic vulnerabilities of del(11q) CLL cells to dual BCR and PARP inhibition

Miguel Quijada-Álamo^{1,2} · María Hernández-Sánchez^{1,2,3,4} · Verónica Alonso-Pérez^{1,2} · Ana E. Rodríguez-Vicente^{1,2} · Ignacio García-Tuñón^{1,2} · Marta Martín-Izquierdo^{1,2} · Jesús María Hernández-Sánchez^{1,2} · Ana B. Herrero^{1,2} · José María Bastida² · Laura San Segundo^{1,2} · Michaela Gruber^{3,4,5,6} · Juan Luis García^{1,2} · Shanye Yin^{3,4} · Elisa ten Hacken^{3,4} · Rocío Benito^{1,2} · José Luis Ordóñez^{1,2} · Catherine J. Wu^{3,4} · Jesús María Hernández-Rivas^{1,2,7}

Received: 18 October 2019 / Revised: 10 December 2019 / Accepted: 14 January 2020
© The Author(s) 2020. This article is published with open access

Abstract

The deletion of 11q (del(11q)) invariably comprises *ATM* gene in chronic lymphocytic leukemia (CLL). Concomitant mutations in this gene in the remaining allele have been identified in 1/3 of CLL cases harboring del(11q), being the biallelic loss of *ATM* associated with adverse prognosis. Although the introduction of targeted BCR inhibition has significantly favored the outcomes of del(11q) patients, responses of patients harboring *ATM* functional loss through biallelic inactivation are unexplored, and the development of resistances to targeted therapies have been increasingly reported, urging the need to explore novel therapeutic approaches. Here, we generated isogenic CLL cell lines harboring del(11q) and *ATM* mutations through CRISPR/Cas9-based gene-editing. With these models, we uncovered a novel therapeutic vulnerability of del(11q)/*ATM*-mutated cells to dual BCR and PARP inhibition. *Ex vivo* studies in the presence of stromal stimulation on 38 CLL primary samples confirmed a synergistic action of the combination of olaparib and ibrutinib in del(11q)/*ATM*-mutated CLL patients. In addition, we showed that ibrutinib produced a homologous recombination repair impairment through RAD51 dysregulation, finding a synergistic link of both drugs in the DNA damage repair pathway. Our data provide a preclinical rationale for the use of this combination in CLL patients with this high-risk cytogenetic abnormality.

These authors contributed equally: Miguel Quijada-Álamo, María Hernández-Sánchez

These authors jointly supervised this work: Catherine J. Wu, Jesús María Hernández-Rivas

Supplementary information The online version of this article (<https://doi.org/10.1038/s41375-020-0714-3>) contains supplementary material, which is available to authorized users.

✉ José Luis Ordóñez
jlog@usal.es

✉ Catherine J. Wu
cwu@partners.org

✉ Jesús María Hernández-Rivas
jmhr@usal.es

¹ University of Salamanca, IBSAL, IBMCC, CSIC, Cancer Research Center, Salamanca, Spain

² Department of Hematology, University Hospital of Salamanca,

Introduction

Deletion of chromosome 11q22.3 (del(11q)) can be found in up to 20% of chronic lymphocytic leukemia (CLL) patients at diagnosis and is associated with poor outcome [1–3]. Although the size of this deletion is variable [4–6], *ATM* is consistently deleted in most cases [6–8]. This gene, which plays a central role in double-strand break (DSB) signaling and repair [9], is mutated in 10–20% of CLL cases

Salamanca, Spain

³ Department of Medical Oncology, Dana-Farber Cancer Institute, Boston, MA 02115, USA

⁴ Broad Institute of Harvard and MIT, Cambridge, MA 02142, USA

⁵ CeMM Research Center for Molecular Medicine, Vienna, Austria

⁶ Department of Internal Medicine I, Division of Hematology and Hemostaseology, Medical University of Vienna, Vienna, Austria

⁷ Department of Medicine, University of Salamanca, Salamanca, Spain

at diagnosis [10–13]. One-third of CLL patients with del(11q) carry *ATM* mutations in the remaining allele, resulting in complete loss-of-function of the ATM protein [14] and significantly reducing the survival of these patients [15].

Novel agents targeting BCL2 and BCR signaling pathways have revolutionized the treatment landscape in CLL [16]. Specifically, it has been recently reported that treatment-naïve del(11q) CLL patients show durable responses upon first-line ibrutinib treatment [17] and an integrated analysis of long-term follow-up data from three randomized trials of ibrutinib in CLL revealed that ibrutinib-treated patients with del(11q) had a significantly longer progression-free survival than ibrutinib-treated patients without del(11q) [18]. However, responses to ibrutinib of high-risk patients harboring ATM functional loss through biallelic inactivation have not been explored yet. In addition, survival outcomes are inferior for relapsed/refractory CLL patients, including those with del(11q) [19], and resistance to BTK inhibitors is becoming an increasing therapeutic challenge [20–24]. For these reasons, novel combinatorial therapies need to be explored in CLL patients.

One of the major impediments to the study of CLL biology has been the lack of cellular models faithfully representing the key genetic events of this disease, such as del(11q). While some studies have interrogated the biological impact of diverse individual CLL-associated genetic alterations [25–29], very few have analyzed the effects of concurrently expressed mutations in CLL [30]. Recently, Clustered Regularly Interspaced Short Palindromic Repeats (CRISPR)/Cas9 technology has allowed the efficient generation of mutations and chromosomal alterations in human cell lines and animal models, opening new approaches for modeling human diseases [31–34]. These new capabilities provide fresh opportunities to generate cell lines to mimic the concurrence of genetic alterations and to study specific therapeutic options.

In the present study, we used the CRISPR/Cas9 technology to generate stable isogenic CLL-derived cell lines harboring del(11q) and/or *ATM* mutations. The loss of *ATM* by del(11q) and gene mutation led to a defective double-strand break (DSB) signaling resulting in increased genomic instability and hypersensitivity to the PARP inhibitor olaparib in vitro, in vivo and ex vivo. Furthermore, we showed that ibrutinib synergizes with PARP inhibition triggering synthetic lethality and significantly improving the effects of BCR inhibition as monotherapy in del(11q) cell lines and primary CLL cells. In addition, we demonstrated that the synergy mechanism between both is associated with the effect of ibrutinib in interfering with the homologous recombination repair through RAD51 downregulation. Our studies suggest that CRISPR/Cas9-generated models may provide powerful tools to study the effects of individual or

combined CLL genetic alterations on cellular processes and treatment response.

Methods

Study approval

The ex vivo study was conducted in accordance of the Declaration of Helsinki and prior approval by the Bioethics Committee from our institution. Written informed consent was obtained from all patients. Animal studies were conducted in accordance with the Spanish and European Union guidelines for animal experimentation (RD53/2013, Directive-2010/63/UE, respectively) and received prior approval from the Bioethics Committee of our institution.

Primary CLL samples

Peripheral blood mononuclear cells (PBMCs) from 38 CLL patients were isolated using Ficoll-Paque Plus density gradient media (GE Healthcare, Life Sciences) and viably cryopreserved in liquid nitrogen until the time of analysis. A complete immunophenotypic analysis of all cases was carried out by flow cytometry. The main biological features of the CLL patients used in the study are summarized in Supplementary Table S1. Only CLL samples with CD19+/CD5+ purities greater than 85% were included.

Next-generation sequencing (NGS)

NGS results from the primary samples used in the ex vivo experiments are detailed in Supplementary Tables S2 and S3. Full details in Supplementary Information.

CRISPR/Cas9-mediated mutagenesis in CLL cell lines

HG3 and MEC1 cell lines (which harbor del(13q) and del(17p), respectively) were transduced with lentiviral particles containing plasmids for the constitutive Cas9 expression (LentiCas9-Blast, Addgene_#52692).

SgRNAs were designed using the online CRISPR design tool (<http://crispr.mit.edu/>) to target *ATM*. The selection of the sgRNAs was based on choosing those of highest efficiency to target the gene of interest and with the lowest predicted off-targets effects. For the generation of del(11q) on the HG3 cell line, two sgRNAs were designed targeting two ~17 Mb distal regions on chromosome 11 (11q22.1 and 11q23.3, respectively). In addition, a sgRNA designed not to target the human genome was used as a negative control. Sequences of the selected sgRNAs are detailed in Supplementary Table S4. SgRNAs targeting 11q23.3 were cloned into pLKO5.sgRNA.EFS.GFP (Addgene_#57822) and

sgRNAs targeting *ATM* and 11q22.1 into pLKO5.sgRNA.EFS.tRFP (Addgene_#57823). Negative control sgRNA was cloned in both vectors. Cloning was carried out as previously described [35] and lentiviral transduction, nucleofection of 11q-targeting sgRNAs and clone screening are detailed below. At least three different clones harboring loss-of-function mutations were chosen for each CRISPR-generated cell line to perform further functional studies. To mitigate against the possible biases due to off-targets effects of the sgRNAs, clones were generated using two different sgRNAs per gene.

Ex vivo experiments

Primary CLL ex vivo experiments were carried out in the presence of HS-5 bone marrow stromal cells as previously described [36]. Briefly, HS-5 stromal cells were seeded 24 h prior to the ex vivo study at a concentration of 1.5×10^4 cells/mL. On the following day, primary CLL cells were viably unfrozen and resuspended in RPMI 1640 medium (Life Technologies) supplemented with 10% FBS, 1% penicillin/streptomycin and 1.5 μ g/mL CpG ODN (Sigma-Aldrich) plus 50 ng/mL IL-2 (PeproTech) and subsequently seeded onto the HS-5 cell layer at a co-culture ratio of 100:1 (1.5×10^6 CLL cells /mL) to stimulate proliferation of CLL cells [37].

Cells were γ -irradiated (2 Gy) 24 h after co-culture for γ H2AX experiments. In the cell viability experiments, CLL cells in the co-culture condition were treated with the indicated drug doses on each experiment. After 120 h, CLL cells were detached from the stromal cell layer and viability was measured by CellTiter-Glo Luminescent Assay (Promega) and normalized with cells with no drug treatment.

Statistics

Statistical significance was determined using GraphPad Prism software v6 (GraphPad Software). Data are summarized as the mean \pm standard deviation (SD). Otherwise specified three independent clones per condition were used in the functional studies. Student's *t* test, Mann–Whitney, ANOVA or Kruskal–Wallis tests were used to determine statistical significance. *P* values lower than 0.05 were considered as statistically significant.

Supplemental methods

Supplemental Methods section include detailed protocols of cell lines and culture conditions, NGS, lentiviral production, cell transduction and nucleofection, PCR, FISH, flow cytometry, western blot, viability and apoptosis analyses, immunofluorescence, comet assay, transwell migration

assay, homologous recombination (HR) activity assay and in vivo experiments.

Results

Generation of del(11q) and *ATM*-deficient isogenic CLL-derived cell lines using the CRISPR/Cas9 system

To address the biological implications of del(11q) and/or *ATM* mutations in CLL, HG3 and MEC1 CLL-derived cell lines were selected. Both are diploid for chromosome 11 and have wild-type (WT) *ATM* gene. Both cell lines were transduced with lentivirus expressing a constitutive Cas9 protein, generating HG3-Cas9 and MEC1-Cas9 cell lines with a Cas9 activity greater than 80% (Supplementary Fig. S1a, b).

For the generation of del(11q), HG3-Cas9 cells were nucleofected with two sgRNAs targeting specific regions on chromosome 11q22.1 (sgRNA-A) and 11q23.3 (sgRNA-B), respectively. After single-cell sorting of GFP + RFP + cells, clones were screened by PCR for the presence of a fusion region between 11q22.1 and 11q23.3 (Fig. 1a). Monoallelic del(11q) was present in 100% of the cells of the selected clone as validated by FISH (Fig. 1b), thereby establishing an isogenic HG3-del(11q) cell line. Truncating mutations of *ATM* were introduced on the remaining WT allele of HG3-del(11q) cells (Fig. 1a). Single-cell FACS-sorted clones were sequenced and the absence of *ATM* functional protein was assessed by western blot (Fig. 1c). In total, we generated three different clones of HG3-del(11q) and HG3-del(11q) *ATM*^{KO} conditions. A similar approach was used to generate single-cell clones with single *ATM* mutations in MEC1 and HG3 cell lines, validating the loss of *ATM* in three clones per condition (Fig. 1c; Supplementary Fig. S2a, b).

Del(11q) *ATM*^{KO} cells show impaired double-strand breaks signaling, leading to DNA damage accumulation

ATM is known to phosphorylate histone H2AX in response to DSBs, promoting DSB repair [9]. To test how the CRISPR/Cas9-engineered CLL cells respond to DSBs, γ H2AX foci formation was investigated in the presence or absence of exposure to γ -irradiation (IR). By immunofluorescence, the number of foci was markedly lower in HG3-del(11q) clones than in HG3^{WT} cells following IR exposure ($P = 0.004$; Fig. 2a). In addition, biallelic inactivation of *ATM* dramatically reduced the number of foci formed after IR (Fig. 2a). These results were corroborated in HG3 and MEC1 *ATM*^{KO} cells (Supplementary Fig. S3a, b) as well as in del(11q)/*ATM*-mutated primary CLL cells (Fig. 2b).

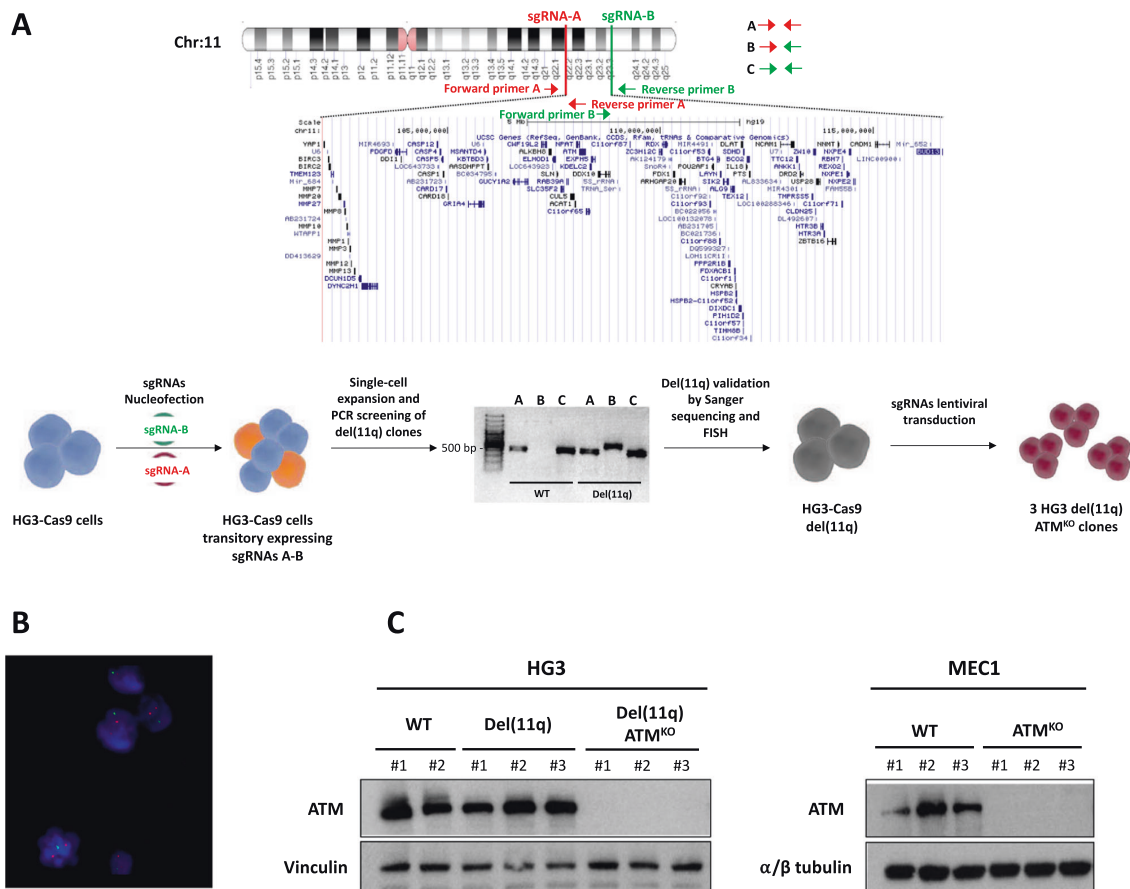


Fig. 1 Generation of 11q deletion and *ATM* mutations in CLL cell lines using the CRISPR/Cas9 system. **a** Upper panel presents the design of the generation of 11q deletion in HG3 cells and the genes contained within the two sgRNA-targeting sites (sgRNA-A in red, sgRNA-B in green). PCR primers used for detection of the deletion are indicated by arrows. Lower panel shows a diagram with the steps for the generation of an HG3-del(11q) cell line. Single-cell sorted clones transitory expressing sgRNAs A and B were screened for the presence of del(11q) by PCR reactions A, B and C, using two pairs of primers flanking upstream and downstream sgRNAs cut sites on chromosome 11. Only del(11q)-positive clones showed amplification using the

forward primer A (11q22.1) and the reverse primer B (11q23.3) (indicated as “PCR B”), as a result of a fusion product between both cut sites A and B. HG3-del(11q) isogenic cell line was subsequently used for the generation of *ATM* mutations on the remaining wild-type allele of HG3-del(11q) cells. In total, $n = 3$ HG3-del(11q) *ATM*^{KO} clones were generated. **b** FISH analysis of HG3-del(11q) cell line. Green signals correspond to 11q22/*ATM* probe and the control red signals correspond to 17p13/*TP53* probe. **c** Western blot analyses of HG3-del(11q) and MEC1 edited single-cell clones with *ATM* mutations ($n = 3$ clones per condition).

Since del(11q) cells displayed impaired DNA damage signaling, neutral comet assays were performed to elucidate whether these cells presented DSB accumulation after γ -irradiation. Notably, all the HG3 clones harboring del(11q) showed DNA damage accumulation 3 h after IR whereas HG3^{WT} cells were able to repair the DSBs (Fig. 2c). Furthermore, comet analyses revealed that the tail moment was higher in HG3 cells with biallelic inactivation of *ATM* than HG3-del(11q) cells with the remaining *ATM*^{WT} allele ($P < 0.0001$; Fig. 2c).

CRISPR/Cas9-engineered del(11q)/*ATM*^{KO} CLL cells show high sensitivity to PARP inhibition in vitro and in vivo

Considering that del(11q) and *ATM* mutations lead to defective DNA repair, we hypothesized that these cells could be hypersensitive to other drugs that also interfere the DNA repair pathways, such as PARP inhibitors [38]. To analyze this, HG3 clones were treated with olaparib. Of note, clones with biallelic inactivation of *ATM* due to del

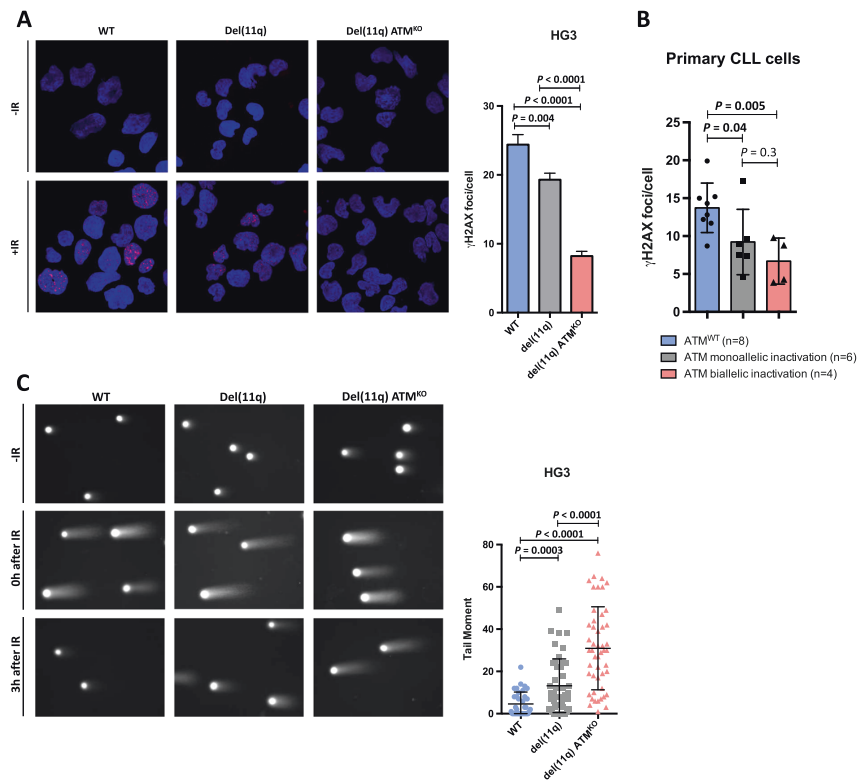


Fig. 2 Evaluation of double-strand breaks signaling and repair in del(11q)/ATM-deficient CLL cells. **a** Left panel: representative images of γ H2AX foci formation (red) in HG3^{WT}, HG3-del(11q) and HG3-del(11q) ATM^{KO} clones. Upper panel shows non-irradiated (-IR) HG3 cells and lower panel represents HG3 clones 1 h after 2 Gy irradiation (+IR). Right panel: quantification of the number of γ H2AX foci per cell 1 h after irradiation. Data are represented as the mean values \pm SD of three independent experiments. At least 75 cells per experiment were counted. **b** Quantification of the number of γ H2AX foci per cell 1 h after irradiation in primary CLL samples stimulated to proliferate for 24 h before IR (2 Gy). Groups are stratified based on ATM^{WT} (n = 8) ATM monoallelic (n = 6) or biallelic (n = 4)

defects in CLL samples. At least 75 cells per patient were counted. Primary samples used in this experiment are detailed in Supplementary Table 1. **c** Left panel: representative images of the neutral comet assay experiment in HG3^{WT}, HG3-del(11q) and HG3-del(11q) ATM^{KO} clones. Upper images show non-irradiated HG3 comets, middle panel represents comets right after 40 Gy irradiation and lower images present comets 3 h after 40 Gy irradiation, when HG3^{WT} were able to repair the IR-generated DNA damage. Right panel: tail moment quantification of neutral comet assays in HG3^{WT}, HG3-del(11q) and HG3-del(11q) ATM^{KO} clones 3 h after 40 Gy irradiation. Data represent the mean values \pm SD of at least 50 comets analyzed per condition in three independent experiments.

(11q) and mutation on the other allele showed incipient sensitivity 72 h after treatment (Supplementary Fig. S4a). In addition, proliferation assays confirmed that del(11q) ATM^{KO} cells could not proliferate after olaparib treatment even after prolonged exposure (Fig. 3a). These results were also confirmed in MEC1 ATM^{KO} clones (Supplementary Fig. S4b).

To investigate the in vivo impact of olaparib treatment, HG3^{WT} (n = 10) and HG3-del(11q) ATM^{KO} (n = 10) xenografts were generated in NSG mice. Olaparib or vehicle treatment started one week after cell injection (vehicle n = 4; olaparib n = 6) and hCD45 + GFP + populations in the peripheral blood were monitored twice weekly. By FACS analysis, slower leukemic progression was observed in the del(11q) ATM^{KO} mice treated with olaparib (P =

0.004, at day 16 post-injection) whereas no differences were found between vehicle or olaparib treated WT xenografts (Supplementary Fig. S4c). Finally, overall survival was assessed at the end of the experiment, showing a significantly longer survival of del(11q) ATM^{KO} xenografts treated with olaparib as compared with control (P < 0.01) (Fig. 3b).

Ibrutinib has a synergistic effect with olaparib in vitro, enhancing its cytotoxic effects in del(11q) CLL cells

To test whether the CRISPR/Cas9-engineered CLL cell lines could be used as models to pre-clinically test new therapeutic approaches, and given the promising effects of

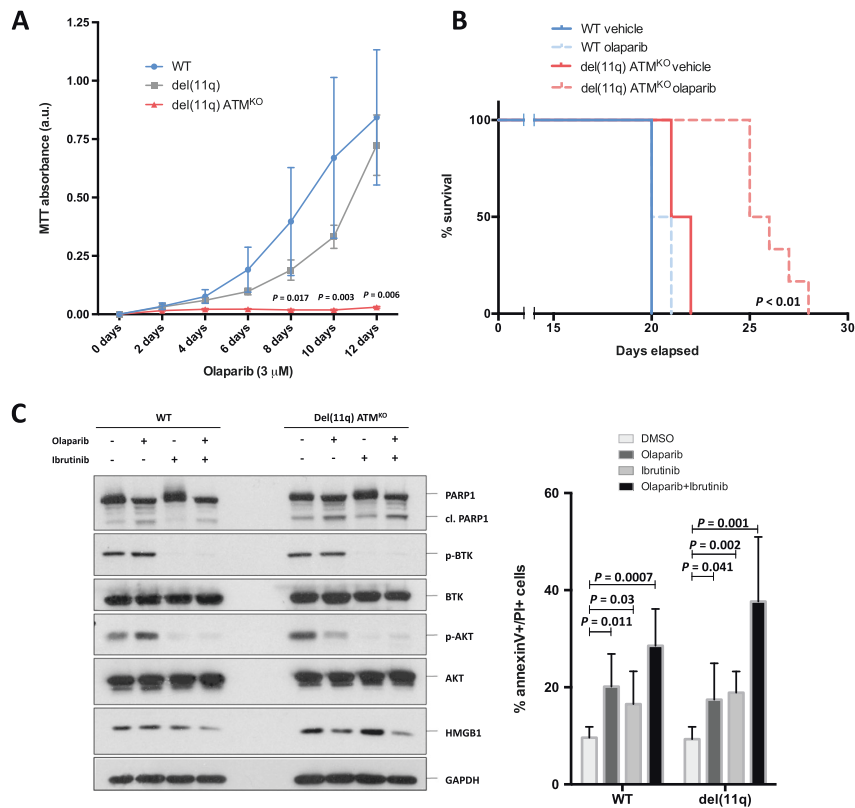


Fig. 3 Olaparib effects in CRISPR/Cas9-edited del(11q) cells **in vitro**, **in vivo** and **in combination with ibrutinib**. **a** HG3-edited clones were treated with 3 μ M olaparib and cell viability was assessed by MTT every 2 days up to 12 days. Proliferation rates are presented as MTT absorbance units, and data are shown as mean \pm SD. *P* values indicate differences between HG3^{WT} and HG3-del(11q) *ATM*^{KO} clones. **b** Kaplan–Meier overall survival curve of HG3^{WT} ($n = 10$) and HG3-del(11q) *ATM*^{KO} ($n = 10$) xenografted mice treated with olaparib ($n = 6$) or vehicle ($n = 4$). The reported *P* value was calculated by

Log-rank test. **c** Left panel: immunoblot analysis of whole-cell lysates of HG3^{WT} and HG3-del(11q) *ATM*^{KO} cells exposed to 5 μ M olaparib and ibrutinib, either alone or in combination, after 48 h. Right panel: cytotoxicity studies by annexin V/PI staining of HG3^{WT} and HG3-del(11q) cells treated with 5 μ M olaparib and ibrutinib for 48 h. Cytotoxicity is measured as the percentage of PI + and annexin V + cells. Data are summarized as the mean \pm SD of four independent experiments.

olaparib on del(11q)/*ATM*-mutated CLL cells, synergy experiments were performed to test whether PARP inhibition could be combined with other drugs employed in CLL therapy. Strikingly, BCR inhibition by ibrutinib potentiated the effects of olaparib in cell viability in all the HG3-del(11q) and HG3-del(11q) *ATM*^{KO} CRISPR/Cas9-generated clones and MEC1 cells (Supplementary Fig. S5a, b). Furthermore, olaparib also synergized with the alkylating agent bendamustine in all HG3-edited cell lines (Supplementary Fig. S5a). Responses of these isogenic HG3 cells to ibrutinib and bendamustine in monotherapy are depicted in Supplementary Fig. S5c.

We next focused on the combination of olaparib and ibrutinib due to its potential therapeutic application in del(11q)/*ATM*-mutated-relapsed/refractory CLL patients. As expected, the combination of these drugs induced

PARP cleavage added to p-BTK and downstream p-AKT inhibition (Fig. 3c, left panel). In addition, ibrutinib synergistically enhanced olaparib cytotoxicity, leading to an incremented cell death, mostly by necrosis, as shown by annexin V and PI staining (Fig. 3c, right panel; Supplementary Fig. S5d, e). Moreover, necrosis-dependent HMGB1 release [39] was studied in response to the drugs alone or in combination, finding a marked reduction of HMGB1 levels in HG3^{WT} and HG3-del(11q) *ATM*^{KO} cells exposed to the combination of olaparib and ibrutinib (Fig. 3c). Furthermore, we tested whether this combination affected the CCL19-mediated migration by chemotaxis assays, revealing that the drug combination at non-cytotoxic doses significantly reduced migration of CLL cell lines towards CCL19 (Supplementary Fig. S5f).

Dual BCR and PARP inhibition is highly effective in del(11q)/ATM-mutated primary CLL samples in the presence of stromal stimulation

In order to validate whether these del(11q)/ATM-mutated CRISPR/Cas9 models could be used as a predictive pre-clinical tool for the study of novel therapeutic approaches, we examined the effects of the combination of olaparib and ibrutinib *ex vivo* in primary cells from a cohort of 38 CLL samples (non-del(11q) $n = 23$; del(11q) $n = 15$). Given that olaparib exerts its action during G2/M cell cycle phase, CLL primary cells were stimulated to proliferate in the presence of stromal cells, CpG and IL-2 [37]. Consistently, the combination of olaparib and ibrutinib in stimulated primary CLL cells was synergistic, and more effective in those cases with del(11q) (Fig. 4a). The tested drug doses did not affect the viability of the HS-5 stromal cells used in the co-culture with CLL cells (Supplemental Fig. S6a). Furthermore, stratifying these samples by ATM monoallelic or biallelic inactivation, we observed that CLL cells harboring ATM biallelic inactivation were even more sensitive to dual BCR and PARP inhibition (Fig. 4b).

Next, we sought to determine if other traditional prognostic factors would predict response to the combination of BCR and PARP inhibition. Regarding FISH cytogenetic alterations, we found that only del(11q) patients, and not del(13q), trisomy 12 or normal karyotype patients, had significantly higher *ex vivo* sensitivity to the drug combination (Fig. 4c). In addition, by stratifying the cohort regarding IGHV mutational status, we detected an improved response of IGHV unmutated patients when compared with those IGHV mutated (Fig. 4c), in line with previous results showing a higher sensitivity of unmutated CLLs to ibrutinib [40]. In order to evaluate which genetic marker could have a greater influence on drug response, we compared IGHV unmutated/ATM^{WT} group versus cases with ATM biallelic inactivation, showing that CLL patients with biallelic loss of ATM were more sensitive to the drug combination (Supplemental Fig. S6b). In addition, we dissected the response to dual BCR and PARP inhibition based on the mutational status of known CLL driver genes, demonstrating that only patients harboring ATM mutations significantly correlated with a greater sensitivity to the drug combination (Fig. 4c). Interestingly, SF3B1 mutations, which also play a role on the DNA damage response [30, 41], showed a trend towards higher sensitivity to the combination as well. On the other hand, TP53, NOTCH1 or XPO1 mutations did not have an influence on the response to the combination of olaparib and ibrutinib (Fig. 4c).

BCR inhibition impairs homologous recombination repair through RAD51 downregulation

Considering that olaparib and ibrutinib exert its action through different pathways, we hypothesized that the synergistic effects of this combination could be due to an off-target effect of ibrutinib in DNA damage repair. To determine if BTK inhibition affected the assembly of DNA repair foci on CLL cells, we investigated whether HG3^{WT} and HG3-del(11q) ATM^{KO} cells were able to recruit RAD51 to DSBs after γ -irradiation in the presence of ibrutinib. Surprisingly, the formation of RAD51 foci 6 h after IR was significantly reduced in CLL cells treated with ibrutinib or the combination than in untreated cells (Fig. 5a, left panel). In addition, ibrutinib treatment reduced the protein levels of RAD51 in these clones (Supplementary Fig. S7a). Similar results were obtained in MEC1 cells treated with ibrutinib (Supplementary Fig. S7b). We further investigated these findings through the analysis of transcriptomic RNA-seq data of serial samples of CLL patients treated with ibrutinib [23], confirming that RAD51 RNA levels are significantly reduced in CLL patients after 1 month and 6 months of ibrutinib therapy (Fig. 5a, right panel).

Moreover, we determined whether this RAD51 downregulation after ibrutinib exposure could be related to the downstream PI3K/AKT/mTOR signaling modulation of BTK inhibition. To this extent, we first used the pan-specific PI3K inhibitor copanlisib in the CRISPR/Cas9-generated cells, showing that PI3K inhibition also reduced the recruitment of RAD51 to DSB lesions (Supplementary Fig. S7c), presenting synergistic effects with olaparib in stimulated primary CLL cells (Fig. 5b, left panel) and CLL cell lines (Supplementary Fig. S7d). In addition, the selective PI3K δ inhibitor idelalisib also showed synergism with olaparib in primary CLL cells (Fig. 5b, middle panel). In line with these results, the RAD51 inhibitor B02 also synergized with olaparib in stimulated CLL primary samples (Fig. 5b, right panel) and HG3^{WT} and HG3-del(11q) ATM^{KO} CRISPR/Cas9-edited cells (Supplementary Fig. S7d).

We next examined whether ibrutinib-mediated downregulation of RAD51 could reduce the homologous recombination (HR) repair activity of HG3 cells. Thus, we used an HR-reporter plasmid [42, 43] where GFP expression is restored upon HR repair (Fig. 5c). Consistently, ibrutinib treatment reduced the HR repair activity of HG3 cells at 1 and 2.5 μ M concentrations (Fig. 5c).

Ibrutinib enhances olaparib and bendamustine-dependent accumulation of DSBs in del(11q) cells

Taking into account these results, it could be suggested that the mechanism of synergy of olaparib and ibrutinib in del

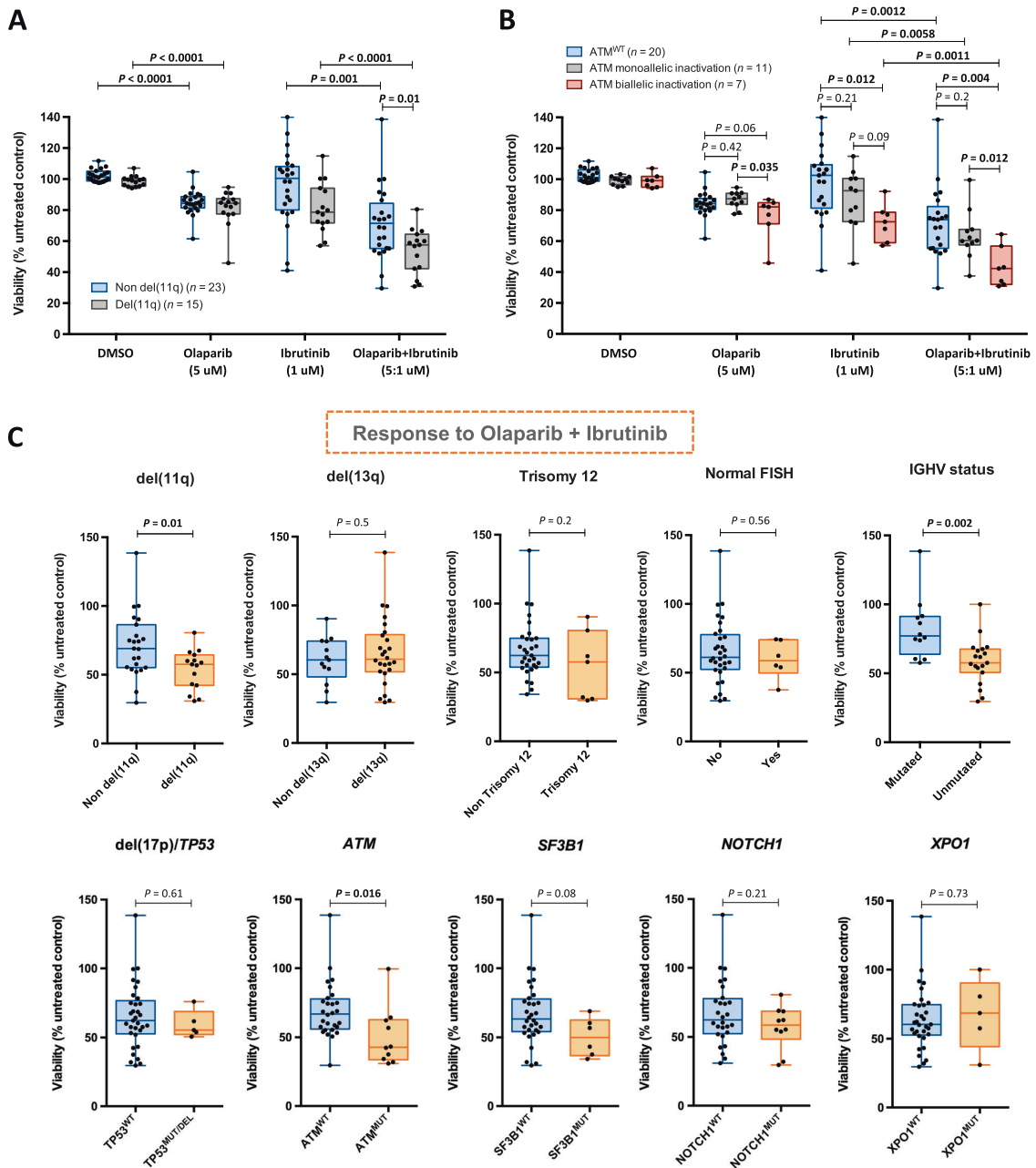
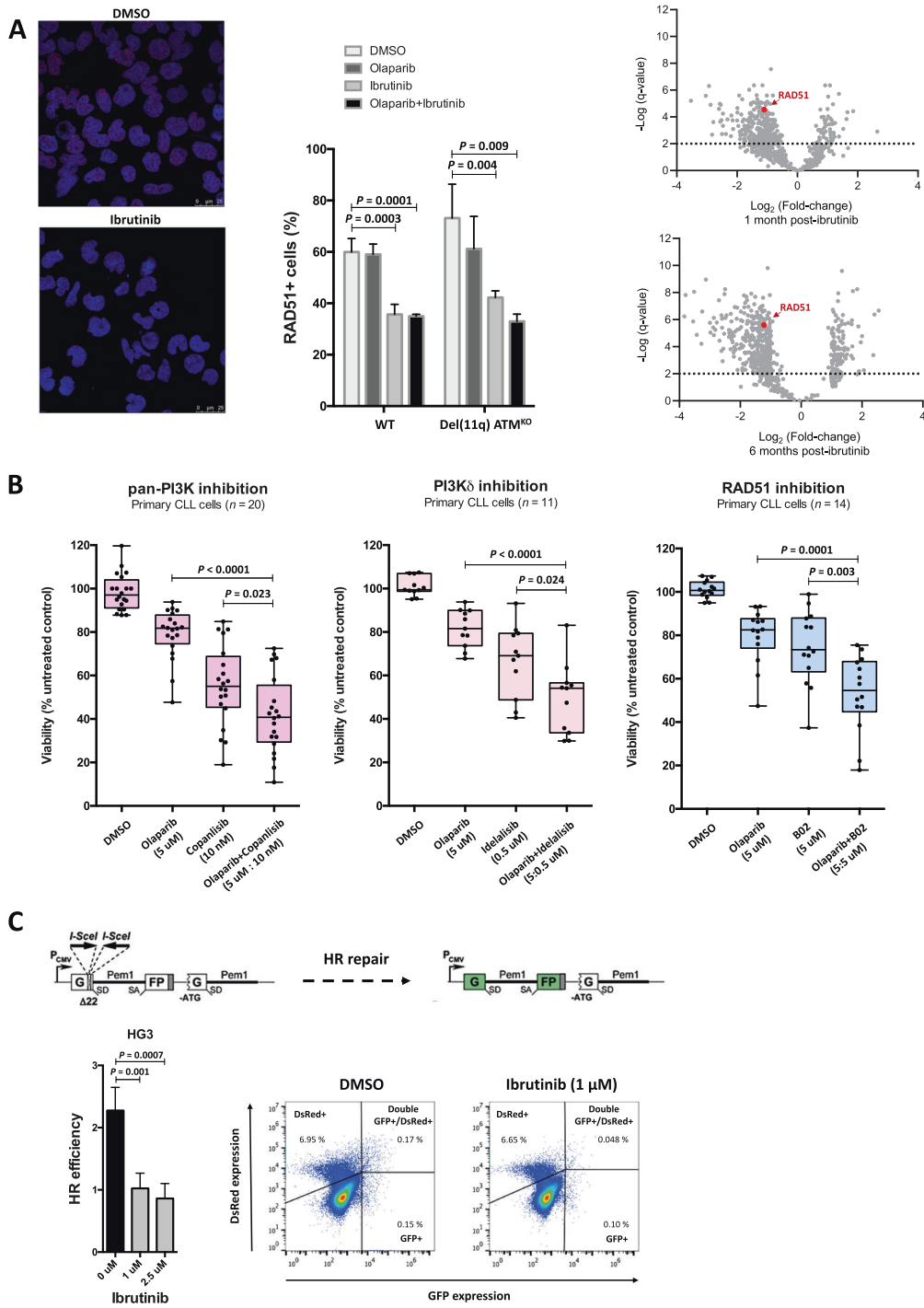


Fig. 4 Response to dual BCR and PARP inhibition of 38 CLL primary samples in the presence of stromal stimulation. **a**, **b** Primary CLL cells were seeded in co-culture with HS-5 bone marrow stromal cells, 1.5 μ g/mL CpG and 50 ng/mL IL-2 and treated with olaparib (5 μ M), ibrutinib (1 μ M) or the combination of both for 5 days. Normalized surviving fraction is expressed relative to untreated cells. Data are presented as the mean \pm SD of del(11q) (n = 15) vs. non del(11q) (n = 23) (**a**) or ATM^{WT} (n = 20); ATM monoallelic defective

(n = 11) and ATM biallelic defective (n = 7) CLL cases (**b**). **c** Response of primary CLL cells (n = 38) to the combination of olaparib (5 μ M) and ibrutinib (1 μ M) based on cytogenetics, IGHV mutational status and mutations in known CLL driver genes. Cells were seeded in co-culture with HS-5 bone marrow stromal cells, 1.5 μ g/mL CpG and 50 ng/mL IL-2 and treated with the drug combination for 5 days.



(11q) cells could be explained, at least in part, by synthetic lethality. Therefore, the addition of a DNA damage-inducing agent should increase the cytotoxicity of this combination

due to large amounts of unrepaired DSBs. Interestingly, the addition of bendamustine to olaparib and ibrutinib synergistically reduced viability in all the HG3-del(11q) and

Fig. 5 Effects of ibrutinib in RAD51-mediated HR repair in CLL. **a** Left panel: representative images and quantification of the number RAD51-positive cells 6 h after irradiation (2 Gy) in HG3^{WT} and HG3-del(11q) *ATM*^{KO} clones. Cells were pretreated for 24 h with 5 μ M olaparib, 1 μ M ibrutinib or the drug combination. Data are represented as the mean values \pm SD of three independent experiments. Cells were scored RAD51+ when five or more foci were formed. At least 100 cells per experiment were counted. Right panel: volcano plots of transcripts changes comparing 1- (top) and 6-month (bottom) post-ibrutinib initiation vs. pretreated longitudinal samples in 14 CLL patients. *RAD51* expression is significantly downregulated in samples after 1 month and 6 months of ibrutinib therapy. Log₂ of fold-changes (treatment vs. control) are shown in *x* axis and statistical significance ($-\log_{10}$ of *q* value) is shown in *y* axis. RNA-seq data were previously generated in Landau et al. [23]. **b** Primary CLL cells were seeded in co-culture with HS-5 bone marrow stromal cells, 1.5 μ g/mL CpG and 50 ng/mL IL-2 and treated with the indicated drugs and doses for 5 days. Normalized surviving fraction is expressed relative to untreated cells. Data are presented as the mean \pm SD. **c** Upper panel displays a representation of the HR-reporter plasmid adapted from Seluanov et al. [43]. Lower-left panel represents the HR repair efficiency as calculated by dividing the number of GFP+ cells of the totality of positive-transfected DsRed+ cells. Data represent mean \pm SD of three independent experiments. Right panel displays representative plots of the HR efficiency of HG3 treated with DMSO or ibrutinib (1 μ M).

MEC1 *ATM*^{KO} CRISPR/Cas9-edited clones (Fig. 6a; Supplementary Fig. S8a). In addition, the combination of the three of these drugs also resulted in decreased viability in a subset of stimulated CLL primary cells (Fig. 6b).

To validate that this reduction in cell viability was due to the accumulation of lethal DSBs, neutral comet assays were performed on HG3^{WT} and HG3-del(11q) *ATM*^{KO} cells after treatment with olaparib, ibrutinib and/or bendamustine. Remarkably, the triple combination of olaparib, ibrutinib and bendamustine led to larger amounts of unrepaired DSBs (Fig. 6c, Supplementary Fig. 8b). Of note, the dual combinations of olaparib + ibrutinib or ibrutinib + bendamustine induced higher levels of DNA damage than these drugs in monotherapy, supporting the aforementioned ibrutinib-mediated impairment of HR repair. In addition, HG3-del(11q) *ATM*^{KO} cells exhibited more DNA damage upon olaparib + ibrutinib and the triple combination than HG3^{WT} cells, providing further evidence of the selective hypersensitivity of del(11q)/*ATM*^{KO} CLL cells to PARP inhibitors in combination with ibrutinib.

Discussion

The advent of next-generation sequencing has made feasible to unveil CLL as a highly genetically heterogeneous disease [12, 13]. Specifically, del(11q) patients represent a heterogeneous group inclusive of individuals carrying bi-allelic inactivation of *ATM* [6, 14, 15]. The absence of cellular models harboring this deletion and the difficulty of collecting large cohorts of patients harboring all the possible combinations of del(11q) and/or *ATM* truncating mutations,

have left remaining questions about the biological effects and treatment response related to these genomic alterations. In this study, we explored the implementation of the CRISPR/Cas9 technology to generate in vitro CLL models carrying del(11q) and/or *ATM* mutations. In this fashion, we generated unique isogenic cell lines mimicking the *ATM*-related genomic heterogeneity seen in CLL patients.

Considering the genetic intratumoral heterogeneity underlying CLL patients, we have generated del(11q)/*ATM*-mutated models in two different cytogenetic backgrounds (del(13q) in HG3 and del(17p) in MEC1). In addition, multiple driver mutations can co-occur within the same tumoral clone, usually driving clonal expansion of CLL cells [44, 45]. Therefore, it is important to study how genetic alterations could synergistically act within the same tumor cell. To this extent, our CRISPR/Cas9 model is the first of its kind analyzing the biological impact of concurrent del(11q) and *ATM* mutations.

Our data show that these models faithfully represent the biology of *ATM* loss in the pathogenesis of CLL. In this way, the response of our CRISPR/Cas9-generated isogenic cell models to γ -irradiation was analyzed, showing that biallelic loss of *ATM* strongly impaired γ H2AX foci formation after irradiation [46], leading to the accumulation of unrepaired DSBs. Interestingly, del(11q) CLL cells also showed moderate levels of unrepaired DNA damage after irradiation and biallelic *ATM* inactivation lead to higher levels of unrepaired DNA damage. Of note, del(11q) CLL patients displayed a higher rate of genomic alterations than patients without del(11q) [47, 48]. Therefore, our results suggest that the presence of del(11q) together with *ATM* mutations may be able to increase the risk of developing secondary genetic abnormalities in CLL cells, contributing to the appearance of subclonal genomic alterations frequently observed in CLL patients during the disease course and associated with poor outcomes [12, 44, 49].

Ibrutinib-mediated BCR inhibition has transformed the treatment landscape of CLL. Despite its proved benefits, disease progression on ibrutinib is being increasingly reported and ibrutinib resistance has emerged as a therapeutic challenge [20–24]. In addition, complex karyotype, which is associated with del(11q) [50], has been associated with poor outcome in ibrutinib-treated patients [51]. Therefore, novel therapeutic approaches need to be explored in high-risk CLL patients. Some studies have shown the efficacy of PARP inhibitors in *ATM*-deficient cell lines and murine models, respectively, but not in isogenic del(11q) models or large cohorts of genetically-matched CLL samples [52, 53]. The application of PARP inhibition to our CLL models has highlighted the efficacy of this drug in del(11q) cells with biallelic inactivation of *ATM* in vitro, in vivo and ex vivo. Remarkably, olaparib was especially effective in CLL cells with complete dysfunctional *ATM*

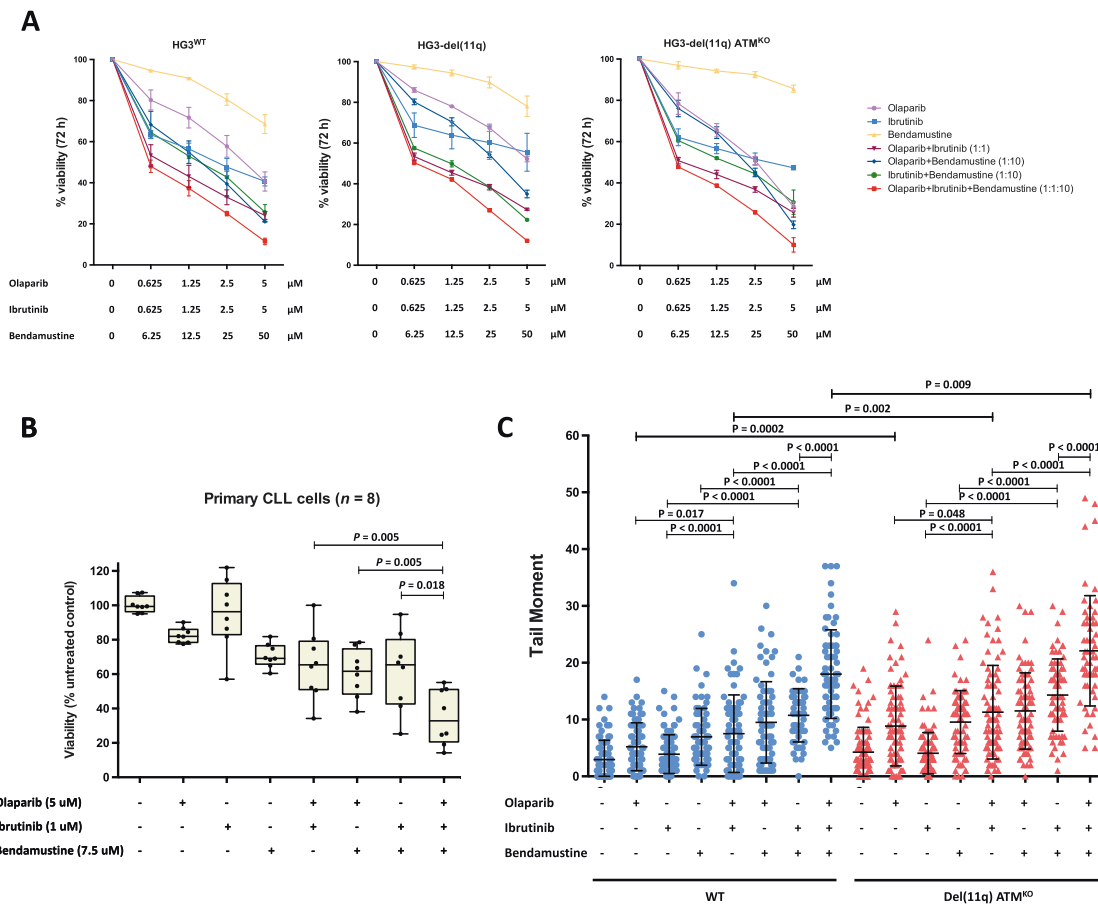


Fig. 6 Implications of BCR inhibition in HR-mediated DSBs repair in CRISPR/Cas9-edited clones and primary CLLs. **a** HG3^{WT}, HG3-del(11q) and HG3-del(11q) *ATM*^{KO} cells were treated with olaparib, ibrutinib and/or bendamustine and cell viability was assessed by MTT assay 72 h later. Surviving fraction is expressed relative to untreated controls and data are presented as the mean \pm SD of two independent experiments. **b** Primary CLL cells were seeded in co-culture with HS-5 bone marrow stromal cells, 1.5 μ g/mL CpG and 50 ng/mL IL-2 and

treated with the indicated doses of olaparib, ibrutinib and/or bendamustine for 5 days. Normalized surviving fraction is expressed relative to untreated cells. **c** Tail moment quantification of neutral comet assays in HG3^{WT} (blue) and HG3-del(11q) *ATM*^{KO} (red) clones 16 h after olaparib (5 μ M), ibrutinib (5 μ M) and/or bendamustine (50 μ M). Data are shown as the mean values \pm SD of at least 50 comets analyzed per condition in three independent experiments.

protein. Since CLL patients harboring biallelic inactivation of *ATM* represent a group with dismal outcome [6, 14, 15], olaparib could be a rational therapeutic alternative for this high-risk subgroup of CLL patients. Therefore, our CRISPR/Cas9-engineered CLL cell lines may be also suitable models to predict drug response of CLL-related genomic alterations.

Our work provides evidence of synergizing effects of PARP and BCR inhibition in isogenic CLL cell lines as well as in primary CLL cells combining olaparib and ibrutinib treatment. Since ibrutinib has been proven to be one of the most optimal therapeutic strategies for fludarabine-relapsed/refractory CLL patients [54], and olaparib is highly effective in del(11q)/*ATM*-mutated CLL cells, the combination of

both drugs could be effective for del(11q)-relapsed/refractory CLL patients. Furthermore, our study suggests that the synergy mechanism could be due to a PI3K signaling-dependent off-target effect of ibrutinib on HR repair through downregulation of RAD51, triggering synthetic lethality when combined with PARP inhibitors. Interestingly, combined PI3K and PARP inhibition have also provided more efficient responses in BRCA1-deficient breast cancer cells [55] and dual ATR and BCR inhibition has also been proven to be synergistic in *ATM*-defective CLL cells [56]. Moreover, it has been reported that BCR inhibitors could increase genomic instability in B cells [57] and transcriptomic data also support the evidence of RAD51 downregulation in CLL patients treated with ibrutinib (Fig. 5a) [23]. In fact, since the

addition of ibrutinib to bendamustine plus rituximab can significantly improve outcomes of CLL patients [58] and PARP inhibitors have been proven to be highly effective in HR-impaired breast and ovarian cancer patients [59, 60], relapsed/refractory del(11q)/*ATM*-mutated CLL patients may potentially benefit from this combinatorial strategy.

Altogether, our results highlight that the CRISPR/Cas9 system is an applicable technique for the generation of in vitro CLL models mimicking specific genomic alterations frequently observed in CLL patients. By using these models, we have delved into the knowledge on the effects of monoallelic del(11q) or biallelic *ATM* loss on the DNA damage response signaling in CLL. Furthermore, this work demonstrates that PARP inhibition in combination with ibrutinib may be explored as a therapeutic option for del(11q) CLL patients showing *ATM* biallelic inactivation.

Acknowledgements This work was supported by grants from the Spanish *Fondo de Investigaciones Sanitarias* PI15/01471, PI18/01500, *Instituto de Salud Carlos III* (ISCIII), European Regional Development Fund (ERDF) “Una manera de hacer Europa”, “Consejería de Educación, Junta de Castilla y León” (SA271P18), “Proyectos de Investigación del SACYL”, Spain GRS 1847/A/18, GRS1653/A17, “Fundación Memoria Don Samuel Solórzano Barruso” (FS/23-2018), by grants (RD12/0036/0069) from Red Temática de Investigación Cooperativa en Cáncer (RTICC), Centro de Investigación Biomédica en Red de Cáncer (CIBERONC CB16/12/00233) and SYNtherapy “Synthetic Lethality for Personalized Therapy-based Stratification In Acute Leukemia” (ERAPERMED2018-275); ISCIII (AC18/00093). MQÁ is fully supported by an “Ayuda predoctoral de la Junta de Castilla y León” by the Fondo Social Europeo (JCYL-EDU/529/2017 PhD scholarship); MHS was supported by a grant from FEHH/Janssen (“Sociedad Española de Hematología y Hemoterapia”) and now holds a Sara Borrell postdoctoral contract (CD19/00222) from *Instituto de Salud Carlos III* (ISCIII), co-funded by *Fondo Social Europeo* (FSE) “El Fondo Social Europeo invierte en tu futuro”; AERV is supported with a research grant by FEHH (“Fundación Española de Hematología y Hemoterapia”); MG is supported by a Marie Curie Action International Outgoing Fellowship (PIOF-2013-624924); EtH is a Special Fellow of the Leukemia and Lymphoma Society (LLS) and a Scholar of the American Society of Hematology (ASH) and JLO is supported by a grant from the University of Salamanca (“Contrato postdoctoral programa IP”). We thank Almudena Martín-Martín, Sara González, Irene Rodríguez, Teresa Prieto, M^a Ángeles Ramos, Filomena Corral, M^a Almudena Martín, Ana Díaz, Ana Simón, María del Pozo, Isabel M Isidro, Vanesa Gutiérrez, Sandra Pujante, M^a Ángeles Hernández, Sandra Santos and Cristina Miguel from the Cancer Research Center of Salamanca, Spain, for their technical support. We are grateful to Ángel Prieto, Ana I García and Sara Armenteros, María Luz Sánchez and María Carmen Macías from the Microscopy Unit, Cytometry Unit and Molecular Pathology Unit, respectively, from the Cancer Research Center of Salamanca for their technical assistance. We thank Javier Borrajo from the Service of NUCLEUS, University of Salamanca for his help with the irradiation experiments and Luis Muñoz and all the members from the Animal Experimentation Research Center from the University of Salamanca. We also thank Dr Gorbunova for the HR-reporter plasmid. We also want to thank Noelia Purroy and Romain Guièze from Wu’s lab (Dana-Farber Cancer Institute, Boston) for their helpful suggestions about ex vivo experiments and CRISPR/Cas9-edited models, respectively. We are deeply grateful to Teresa González, José Ramón González Porras, Josefina

Galende, José Antonio Queizán, Carlos Aguilar and María Jesús Vidal Manceñido for providing patient samples and clinical information.

Author contributions MQÁ designed the experiments, performed CRISPR/Cas9 generation of KO cell lines, carried out functional studies, analyzed the data and wrote the paper, MHS designed the experiments, contributed to interpret the results and wrote the paper, VAP performed CRISPR/Cas9 generation of KO cell lines and functional studies, AERV performed functional studies and together with IGT contributed to the experiment design and data analyses, MMI and JMHS performed NGS studies, ABH designed DNA damage and repair experiments and contributed to data analysis, JMB provided primary samples for the ex vivo studies, LSS contributed in the xenograft experiments, MG contributed to the CRISPR system design, JLG performed functional studies, SY performed RNA-seq data analysis, EtH and RB contributed to data analyses, interpretation of the results and critically reviewed the manuscript, JLO performed functional studies, xenograft experiments, contributed to data analyses and critically reviewed the manuscript, CJW and JMHR conceived the study, designed the experiments and wrote the manuscript. All authors discussed the results and revised the manuscript.

Compliance with ethical standards

Conflict of interest CJW is a co-founder of Neon Therapeutics, Inc and is a member of its scientific advisory board. The remaining authors declare no conflict of interest.

Publisher’s note Springer Nature remains neutral with regard to jurisdictional claims in published maps and institutional affiliations.

Open Access This article is licensed under a Creative Commons Attribution 4.0 International License, which permits use, sharing, adaptation, distribution and reproduction in any medium or format, as long as you give appropriate credit to the original author(s) and the source, provide a link to the Creative Commons license, and indicate if changes were made. The images or other third party material in this article are included in the article’s Creative Commons license, unless indicated otherwise in a credit line to the material. If material is not included in the article’s Creative Commons license and your intended use is not permitted by statutory regulation or exceeds the permitted use, you will need to obtain permission directly from the copyright holder. To view a copy of this license, visit <http://creativecommons.org/licenses/by/4.0/>.

References

1. Döhner H, Stilgenbauer S, James MR, Benner A, Weilguni T, Bentz M, et al. 11q deletions identify a new subset of B-cell chronic lymphocytic leukemia characterized by extensive nodal involvement and inferior prognosis. *Blood*. 1997;89:2516–22.
2. Neilson JR, Auer R, White D, Bienz N, Waters JJ, Whittaker JA, et al. Deletions at 11q identify a subset of patients with typical CLL who show consistent disease progression and reduced survival. *Leukemia*. 1997;11:1929–32.
3. Döhner H, Stilgenbauer S, Benner A, Leupolt E, Kröber A, Bullinger L, et al. Genomic aberrations and survival in chronic lymphocytic leukemia. *N. Engl J Med*. 2000;343:1910–6.
4. Stilgenbauer S, Liebisch P, James MR, Schröder M, Schlegelberger B, Fischer K, et al. Molecular cytogenetic delineation of a novel critical genomic region in chromosome bands 11q22.3-923.1 in lymphoproliferative disorders. *Proc Natl Acad Sci USA*. 1996;93:11837–41.

5. Gunnarsson R, Mansouri L, Isaksson A, Göransson H, Cahill N, Jansson M, et al. Array-based genomic screening at diagnosis and during follow-up in chronic lymphocytic leukemia. *Haematologica* 2011;96:1161–9.
6. Rose-Zerilli MJ, Forster J, Parker H, Parker A, Rodriguez AE, Chaplin T, et al. ATM mutation rather than BIRC3 deletion and/or mutation predicts reduced survival in 11q-deleted chronic lymphocytic leukemia: data from the UK LRF CLL4 trial. *Haematologica*. 2014;99:736–42.
7. Edelman J, Holzmann K, Miller F, Winkler D, Bühler A, Zenz T, et al. High-resolution genomic profiling of chronic lymphocytic leukemia reveals new recurrent genomic alterations. *Blood*. 2012;120:4783–94.
8. Stankovic T, Skowronska A. The role of *ATM* mutations and 11q deletions in disease progression in chronic lymphocytic leukemia. *Leuk Lymphoma*. 2014;55:1227–39.
9. Lavin MF. Ataxia-telangiectasia: from a rare disorder to a paradigm for cell signalling and cancer. *Nat Rev Mol Cell Biol*. 2008;9:759–69.
10. Choi M, Kipps T, Kurzrock R. ATM mutations in cancer: therapeutic implications. *Mol Cancer Ther*. 2016;15:1781–91.
11. Austen B, Powell JE, Alvi A, Edwards I, Hooper L, Starczynski J, et al. Mutations in the *ATM* gene lead to impaired overall and treatment-free survival that is independent of IGVH mutation status in patients with B-CLL. *Blood*. 2005;106:3175–82.
12. Landau DA, Tausch E, Taylor-Weiner AN, Stewart C, Reiter JG, Bahlo J, et al. Mutations driving CLL and their evolution in progression and relapse. *Nature*. 2015;526:525–30.
13. Puente XS, Beà S, Valdés-Mas R, Villamor N, Gutiérrez-Abril J, Martín-Subero JJ, et al. Non-coding recurrent mutations in chronic lymphocytic leukaemia. *Nature*. 2015;526:519–24.
14. Austen B, Skowronska A, Baker C, Powell JE, Gardiner A, Oscier D, et al. Mutation status of the residual *ATM* allele is an important determinant of the cellular response to chemotherapy and survival in patients with chronic lymphocytic leukemia containing an 11q deletion. *J Clin Oncol*. 2007;25:5448–57.
15. Skowronska A, Parker A, Ahmed G, Oldreive C, Davis Z, Richards S, et al. Biallelic *ATM* inactivation significantly reduces survival in patients treated on the United Kingdom Leukemia Research Fund Chronic Lymphocytic Leukemia 4 trial. *J Clin Oncol*. 2012;30:4524–32.
16. Brown JR, Porter DL, O'Brien SM. Novel treatments for chronic lymphocytic leukemia and moving forward. *Am Soc Clin Oncol Educ B*. 2014;34:e317–25.
17. Barr PM, Robak T, Owen C, Tedeschi A, Bairey O, Bartlett NL, et al. Sustained efficacy and detailed clinical follow-up of first-line ibrutinib treatment in older patients with chronic lymphocytic leukemia: extended phase 3 results from RESONATE-2. *Haematologica*. 2018;103:1502–10.
18. Kipps TJ, Fraser G, Coutre SE, Brown JR, Barrientos JC, Barr PM, et al. Long-term studies assessing outcomes of ibrutinib therapy in patients with del(11q) chronic lymphocytic leukemia. *Clin Lymphoma Myeloma Leuk*. 2019;19:715–22.
19. O'Brien S, Furman RR, Coutre S, Flinn IW, Burger JA, Blum K, et al. Single-agent ibrutinib in treatment-naïve and relapsed/refractory chronic lymphocytic leukemia: a 5-year experience. *Blood*. 2018;131:1910–9.
20. Woyach JA, Furman RR, Liu T-M, Ozer HG, Zapatka M, Ruppert AS, et al. Resistance mechanisms for the Bruton's tyrosine kinase inhibitor ibrutinib. *N Engl J Med*. 2014;370:2286–94.
21. Furman RR, Cheng S, Lu P, Setty M, Perez AR, Guo A, et al. Ibrutinib resistance in chronic lymphocytic leukemia. *N Engl J Med*. 2014;370:2352–4.
22. Burger JA, Landau DA, Taylor-Weiner A, Bozic I, Zhang H, Sarosiek K, et al. Clonal evolution in patients with chronic lymphocytic leukaemia developing resistance to BTK inhibition. *Nat Commun*. 2016;7:11589.
23. Landau DA, Sun C, Rosebrock D, Herman SEM, Fein J, Sivina M, et al. The evolutionary landscape of chronic lymphocytic leukemia treated with ibrutinib targeted therapy. *Nat Commun*. 2017;8:2185.
24. Ahn IE, Underbayev C, Albitar A, Herman SEM, Tian X, Maric I, et al. Clonal evolution leading to ibrutinib resistance in chronic lymphocytic leukemia. *Blood*. 2017;129:1469–79.
25. Rodríguez D, Bretones G, Quesada V, Villamor N, Arango JR, López-Guillermo A, et al. Mutations in *CHD2* cause defective association with active chromatin in chronic lymphocytic leukemia. *Blood*. 2015;126:195–202.
26. Zenz T, Häbe S, Denzel T, Mohr J, Winkler D, Bühler A, et al. Detailed analysis of p53 pathway defects in fludarabine-refractory chronic lymphocytic leukemia (CLL): dissecting the contribution of 17p deletion, TP53 mutation, p53-p21 dysfunction, and miR34a in a prospective clinical trial. *Blood*. 2009;114:2589–97.
27. Navrkalova V, Sebejova L, Zemanova J, Kminkova J, Kubesova B, Malcikova J, et al. ATM mutations uniformly lead to ATM dysfunction in chronic lymphocytic leukemia: application of functional test using doxorubicin. *Haematologica*. 2013;98:1124–31.
28. Arruga F, Gizdic B, Bologna C, Cignetto S, Buonincontri R, Serra S, et al. Mutations in *NOTCH1* PEST domain orchestrate CCL19-driven homing of chronic lymphocytic leukemia cells by modulating the tumor suppressor gene *DUSP22*. *Leukemia*. 2017;31:1882–93.
29. Close V, Close W, Kugler SJ, Reichenzeller M, Yosifov DY, Bloehdorn J, et al. *FBXW7* mutations reduce binding of *NOTCH1*, leading to cleaved *NOTCH1* accumulation and target gene activation in CLL. *Blood*. 2019;133:830–9.
30. Yin S, Gambe RG, Sun J, Martínez AZ, Cartun ZJ, Regis FFD, et al. A murine model of chronic lymphocytic leukemia based on B cell-restricted expression of *Sf3b1* mutation and *Atm* deletion. *Cancer Cell*. 2019;35:283–296.e5.
31. Cong L, Ran FA, Cox D, Lin S, Barretto R, Habib N, et al. Multiplex genome engineering using CRISPR/Cas systems. *Science*. 2013;339:819–23.
32. Hsu PD, Lander ES, Zhang F. Development and applications of CRISPR-Cas9 for genome engineering. *Cell*. 2014;157:1262–78.
33. Canver MC, Bauer DE, Dass A, Yien YY, Chung J, Masuda T, et al. Characterization of genomic deletion efficiency mediated by clustered regularly interspaced palindromic repeats (CRISPR)/Cas9 nuclease system in mammalian cells. *J Biol Chem*. 2014;289:21312–24.
34. Essletzbichler P, Konopka T, Santoro F, Chen D, Gapp BV, Kralovics R, et al. Megabase-scale deletion using CRISPR/Cas9 to generate a fully haploid human cell line. *Genome Res*. 2014;24:2059–65.
35. García-Tuñón I, Hernández-Sánchez M, Ordoñez JL, Alonso-Pérez V, Álamo-Quijada M, Benito R, et al. The CRISPR/Cas9 system efficiently reverts the tumorigenic ability of *BCR/ABL* in vitro and in a xenograft model of chronic myeloid leukemia. *Oncotarget*. 2017;8:26027–40.
36. Purroy N, Abrisqueta P, Carabia J, Carpio C, Calpe E, Palacio C, et al. Targeting the proliferative and chemoresistant compartment in chronic lymphocytic leukemia by inhibiting survivin protein. *Leukemia*. 2014;28:1993–2004.
37. Primo D, Scarfò L, Xochelli A, Mattsson M, Ranghetti P, Espinosa AB, et al. A novel ex vivo high-throughput assay reveals antiproliferative effects of idelalisib and ibrutinib in chronic lymphocytic leukemia. *Oncotarget*. 2018;9:26019–31.
38. Knittel G, Liedgens P, Reinhardt HC. Targeting *ATM*-deficient CLL through interference with DNA repair pathways. *Front Genet*. 2015;6:207.

39. Scaffidi P, Misteli T, Bianchi ME. Release of chromatin protein HMGB1 by necrotic cells triggers inflammation. *Nature*. 2002;418:191–5.
40. Guo A, Lu P, Galanina N, Nabhan C, Smith SM, Coleman M, et al. Heightened BTK-dependent cell proliferation in unmutated chronic lymphocytic leukemia confers increased sensitivity to ibrutinib. *Oncotarget*. 2016;7:4598–610.
41. te Raa GD, Derks IAM, Navrkalova V, Skowronska A, Moerland PD, van Laar J, et al. The impact of SF3B1 mutations in CLL on the DNA-damage response. *Leukemia*. 2015;29:1133–42.
42. Mao Z, Bozzella M, Seluanov A, Gorbunova V. Comparison of nonhomologous end joining and homologous recombination in human cells. *DNA Repair (Amst)*. 2008;7:1765–71.
43. Seluanov A, Mao Z, Gorbunova V. Analysis of DNA double-strand break (DSB) repair in mammalian cells. *J Vis Exp*. 2010; e2002.
44. Landau DA, Carter SL, Stojanov P, McKenna A, Stevenson K, Lawrence MS, et al. Evolution and impact of subclonal mutations in chronic lymphocytic leukemia. *Cell*. 2013;152:714–26.
45. Wang L, Fan J, Francis JM, Georghiou G, Hergert S, Li S, et al. Integrated single-cell genetic and transcriptional analysis suggests novel drivers of chronic lymphocytic leukemia. *Genome Res*. 2017;27:1300–11.
46. Burma S, Chen BP, Murphy M, Kurimasa A, Chen DJ. ATM phosphorylates histone H2AX in response to DNA double-strand breaks. *J Biol Chem*. 2001;276:42462–7.
47. Ouilllette P, Fossum S, Parkin B, Ding L, Bockenstedt P, Al-Zoubi A, et al. Aggressive chronic lymphocytic leukemia with elevated genomic complexity is associated with multiple gene defects in the response to DNA double-strand breaks. *Clin Cancer Res*. 2010;16:835–47.
48. Hernández JÁ, Hernández-Sánchez M, Rodríguez-Vicente AE, Grossmann V, Collado R, Heras C, et al. A low frequency of losses in 11q chromosome is associated with better outcome and lower rate of genomic mutations in patients with chronic lymphocytic leukemia. *PLoS ONE*. 2015;10:e0143073.
49. Bakhoun SF, Landau DA. Chromosomal instability as a driver of tumor heterogeneity and evolution. *Cold Spring Harb Perspect Med*. 2017;7:a029611.
50. Puiggros A, Collado R, Calasanz MJ, Ortega M, Ruiz-Xivillé N, Rivas-Delgado A, et al. Patients with chronic lymphocytic leukemia and complex karyotype show an adverse outcome even in absence of TP53/ATM FISH deletions. *Oncotarget*. 2017;8:54297–303.
51. Thompson PA, O'Brien SM, Wierda WG, Ferrajoli A, Stingo F, Smith SC, et al. Complex karyotype is a stronger predictor than del(17p) for an inferior outcome in relapsed or refractory chronic lymphocytic leukemia patients treated with ibrutinib-based regimens. *Cancer*. 2015;121:3612–21.
52. Weston VJ, Oldreive CE, Skowronska A, Oscier DG, Pratt G, Dyer MJS, et al. The PARP inhibitor olaparib induces significant killing of ATM-deficient lymphoid tumor cells in vitro and in vivo. *Blood*. 2010;116:4578–87.
53. Knittel G, Rehkämper T, Korovkina D, Liedgens P, Fritz C, Torgovnick A, et al. Two mouse models reveal an actionable PARP1 dependence in aggressive chronic lymphocytic leukemia. *Nat Commun*. 2017;8:153.
54. Byrd JC, Brown JR, O'Brien S, Barrientos JC, Kay NE, Reddy NM, et al. Ibrutinib versus Ofatumumab in previously treated chronic lymphoid leukemia. *N. Engl J Med*. 2014;371:213–23.
55. Juvekar A, Burga LN, Hu H, Lunsford EP, Ibrahim YH, Balmaña J, et al. Combining a PI3K inhibitor with a PARP inhibitor provides an effective therapy for BRCA1-related breast cancer. *Cancer Disco*. 2012;2:1048–63.
56. Kwok M, Davies N, Agathangelou A, Smith E, Oldreive C, Petermann E, et al. ATR inhibition induces synthetic lethality and overcomes chemoresistance in TP53- or ATM-defective chronic lymphocytic leukemia cells. *Blood*. 2016;127:582–95.
57. Compagno M, Wang Q, Pighi C, Cheong T-C, Meng F-L, Poggio T, et al. Phosphatidylinositol 3-kinase δ blockade increases genomic instability in B cells. *Nature*. 2017;542:489–93.
58. Chanan-Khan A, Cramer P, Demirkan F, Fraser G, Silva RS, Grosicki S, et al. Ibrutinib combined with bendamustine and rituximab compared with placebo, bendamustine, and rituximab for previously treated chronic lymphocytic leukaemia or small lymphocytic lymphoma (HELIOS): a randomised, double-blind, phase 3 study. *Lancet Oncol*. 2016;17:200–11.
59. Robson M, Im S-A, Senkus E, Xu B, Domchek SM, Masuda N, et al. Olaparib for metastatic breast cancer in patients with a germline *BRCA* mutation. *N. Engl J Med*. 2017;377:523–33.
60. Pujade-Lauraine E, Ledermann JA, Selle F, Gebski V, Penson RT, Oza AM, et al. Olaparib tablets as maintenance therapy in patients with platinum-sensitive, relapsed ovarian cancer and a *BRCA1/2* mutation (SOLO2/ENGOT-Ov21): a double-blind, randomised, placebo-controlled, phase 3 trial. *Lancet Oncol*. 2017;18:1274–84.

CHAPTER 3

Dissecting the role of *TP53* alterations in del(11q) chronic lymphocytic leukemia


Miguel Quijada-Álamo^{1,2*}, Claudia Pérez-Carretero^{1,2*}, María Hernández-Sánchez^{1,2,3,4}, Ana-Eugenia Rodríguez-Vicente^{1,2}, Ana-Belén Herrero^{1,2}, Jesús-María Hernández-Sánchez^{1,2}, Marta Martín-Izquierdo^{1,2}, Sandra Santos-Mínguez^{1,2}, Mónica del Rey^{1,2}, Teresa González², Araceli Rubio-Martínez⁵, Alfonso García de Coca⁶, Julio Dávila-Valls⁷, José-Ángel Hernández-Rivas⁸, Helen Parker⁹, Jonathan C. Strefford⁹, Rocío Benito^{1,2}, José-Luis Ordóñez^{1,2} and Jesús-María Hernández-Rivas^{1,2,10}

¹University of Salamanca, IBSAL, IBMCC, CSIC, Cancer Research Center, Salamanca, Spain. ²Department of Hematology, University Hospital of Salamanca, Salamanca, Spain. ³Department of Medical Oncology, Dana-Farber Cancer Institute, Boston, Massachusetts 02115, USA. ⁴Broad Institute of Harvard and MIT, Cambridge, Massachusetts 02142, USA. ⁵Department of Hematology, Hospital Miguel Servet, Zaragoza, Spain. ⁶Department of Hematology, Hospital Clínico de Valladolid, Valladolid, Spain. ⁷Department of Hematology, Hospital Nuestra Señora de Sonsoles, Ávila, Spain. ⁸Department of Hematology, Hospital Universitario Infanta Leonor. Universidad Complutense, Madrid, Spain. ⁹Cancer Genomics, School of Cancer Sciences, Faculty of Medicine, University of Southampton, Southampton, UK. ¹⁰Department of Medicine, University of Salamanca, Salamanca, Spain. *Equal contribution

**Clinical and Translational Medicine. 2021 Feb;11(2):e304. doi: 10.1002/ctm2.304.
PMID: 33634999**

RESEARCH ARTICLE

Dissecting the role of *TP53* alterations in del(11q) chronic lymphocytic leukemia

Miguel Quijada-Álamo^{1,2,#} | Claudia Pérez-Carretero^{1,2,#} |
 María Hernández-Sánchez^{1,2,3,4} | Ana-Eugenia Rodríguez-Vicente^{1,2} |
 Ana-Belén Herrero^{1,2} | Jesús-María Hernández-Sánchez^{1,2} |
 Marta Martín-Izquierdo^{1,2} | Sandra Santos-Mínguez^{1,2} | Mónica del Rey^{1,2} |
 Teresa González² | Araceli Rubio-Martínez⁵ | Alfonso García de Coca⁶ |
 Julio Dávila-Valls⁷ | José-Ángel Hernández-Rivas⁸ | Helen Parker⁹ |
 Jonathan C. Strefford⁹ | Rocío Benito^{1,2} | José-Luis Ordóñez^{1,2,#} |
 Jesús-María Hernández-Rivas^{1,2,10,#} 

¹ Cancer Research Center, University of Salamanca, IBSAL, IBMCC, CSIC, Salamanca, Spain² Department of Hematology, University Hospital of Salamanca, Salamanca, Spain³ Department of Medical Oncology, Dana-Farber Cancer Institute, Boston, Massachusetts, USA⁴ Broad Institute of Harvard and MIT, Cambridge, Massachusetts, USA⁵ Department of Hematology, Hospital Miguel Servet, Zaragoza, Spain⁶ Department of Hematology, Hospital Clínico de Valladolid, Valladolid, Spain⁷ Department of Hematology, Hospital Nuestra Señora de Sonsoles, Ávila, Spain⁸ Department of Hematology, Hospital Universitario Infanta Leonor, Universidad Complutense, Madrid, Spain⁹ School of Cancer Sciences, Faculty of Medicine, University of Southampton, Southampton, UK¹⁰ Department of Medicine, University of Salamanca, Salamanca, Spain**Correspondence**

José-Luis Ordóñez, Universidad de Salamanca, IBMCC, CIC, IBSAL, Centro de Investigación del Cáncer, Campus Miguel de Unamuno, s/n, Salamanca, Spain.
 Email: jlog@usal.es

Jesús-María Hernández-Rivas, IBMCC, CIC Universidad de Salamanca-CSIC, Hospital Universitario de Salamanca, Paseo de San Vicente s/n, 37007 Salamanca, Spain.

Abstract

Background: Several genetic alterations have been identified as driver events in chronic lymphocytic leukemia (CLL) pathogenesis and oncogenic evolution. Concurrent driver alterations usually coexist within the same tumoral clone, but how the cooperation of multiple genomic abnormalities contributes to disease progression remains poorly understood. Specifically, the biological and clinical consequences of concurrent high-risk alterations such as del(11q)/*ATM*-mutations and del(17p)/*TP53*-mutations have not been established.

Abbreviations: ATR, ataxia telangiectasia and Rad3 related; BCR, B cell receptor; CLL, chronic lymphocytic leukemia; CRISPR, clustered regularly interspaced short palindromic repeats; DDR, DNA damage response; FACS, fluorescence-activated cell sorting; FISH, fluorescence in situ hybridization; GFP, green fluorescent protein; iwCLL, international workshop on CLL; MACS, magnetically activated cell sorting; MTT, (3-(4,5-dimethylthiazol-2-yl)-2,5-diphenyltetrazolium bromide; NGS, next-generation sequencing; OS, overall survival; PBS, phosphate-buffered saline; WES, whole exome sequencing studies

This is an open access article under the terms of the [Creative Commons Attribution](https://creativecommons.org/licenses/by/4.0/) License, which permits use, distribution and reproduction in any medium, provided the original work is properly cited.

© 2021 The Authors. *Clinical and Translational Medicine* published by John Wiley & Sons Australia, Ltd on behalf of Shanghai Institute of Clinical Bioinformatics

Email: jmhr@usal.es

#These authors contributed equally to this work.

Funding information

Spanish Fondo de Investigaciones Sanitarias, Grant/Award Numbers: PI15/01471, PI18/01500); Fundación Memoria Don Samuel Solórzano Barruso, Grant/Award Number: RD12/0036/0069

Methods: We integrated next-generation sequencing (NGS) and clustered regularly interspaced short palindromic repeats (CRISPR)/Cas9 techniques to characterize the in vitro and in vivo effects of concurrent monoallelic or biallelic *ATM* and/or *TP53* alterations in CLL prognosis, clonal evolution, and therapy response.

Results: Targeted sequencing analysis of the co-occurrence of high-risk alterations in 271 CLLs revealed that biallelic inactivation of both *ATM* and *TP53* was mutually exclusive, whereas monoallelic del(11q) and *TP53* alterations significantly co-occurred in a subset of CLL patients with a highly adverse clinical outcome. We determined the biological effects of combined del(11q), *ATM* and/or *TP53* mutations in CRISPR/Cas9-edited CLL cell lines. Our results showed that the combination of monoallelic del(11q) and *TP53* mutations in CLL cells led to a clonal advantage in vitro and in in vivo clonal competition experiments, whereas CLL cells harboring biallelic *ATM* and *TP53* loss failed to compete in in vivo xenotransplants. Furthermore, we demonstrated that CLL cell lines harboring del(11q) and *TP53* mutations show only partial responses to B cell receptor signaling inhibitors, but may potentially benefit from ATR inhibition.

Conclusions: Our work highlights that combined monoallelic del(11q) and *TP53* alterations coordinately contribute to clonal advantage and shorter overall survival in CLL.

KEYWORDS

biomarkers, chromosomal abnormality, chronic lymphocytic leukemia, CRISPR/Cas9 system, next-generation sequencing, *TP53* gene

1 | BACKGROUND

Chronic lymphocytic leukemia (CLL) is a clonal B-cell malignancy characterized by an extremely variable clinical course.^{1,2} This variability is a result of the underlying biological heterogeneity, highlighted by the presence of genomic alterations that play an important role in disease prognosis.^{3–5} Monoallelic deletion of chromosome 11q22.3 (del(11q)) is present in 15–20% of CLL cases at diagnosis, and it is considered a high-risk cytogenetic alteration in CLL.^{3,6,7} The size of this deletion is variable, with a commonly minimal deleted region almost always encompassing the *ATM* gene.^{8–10} *ATM* has a key role in cell-cycle checkpoint activation and the DNA damage response (DDR) pathway.¹¹ Although the presence of this deletion is associated with poor outcomes,^{3,12} del(11q) CLL exhibits considerable clinical heterogeneity,¹³ suggesting that other concomitant genetic alterations may have a role in the prognosis of CLL patients from this high-risk subgroup.¹⁴ Indeed, it has been reported that monoallelic *ATM* deletion is not enough to cause a CLL-like disease in mice.¹⁵ Deleterious mutations in the remaining allele of *ATM* or gain-of-function *SF3BI* mutations in del(11q) patients have

been shown to drive CLL oncogenesis, being associated with a worse prognosis.^{15–19} Nevertheless, these mutations only account for 30% or 20% of del(11q) cases, respectively, leaving more than half of del(11q) patients with unknown second driver of the disease.

Another high-risk-associated cytogenetic feature in CLL is the deletion of chromosome 17p13.1 (del(17p)), which appears in 4–10% of CLL cases at diagnosis^{20,21} and in up to 40% of relapsing cases to chemoimmunotherapy.^{22,23} Del(17p) invariably comprises the tumor suppressor gene *TP53*, which is mutated in ~10% of CLL cases at diagnosis and plays a critical role in the DDR pathway, apoptosis and cell cycle.²⁴ In addition, *TP53* gene mutations in the remaining allele of del(17p) patients have been found in 80% of these cases,²⁵ indicating that biallelic dysfunction of this gene appears to be the main mechanism driving CLL progression and relapse in this subgroup CLL patients.^{20,26}

Some studies have reported that biallelic *ATM* abnormalities appear in low co-occurrence with *TP53* lesions, suggesting that the complete dysfunction of any of these proteins cannot coexist with the defect of the other.^{20,27} On the contrary, monoallelic del(11q) or *ATM* mutations

have been associated in some cases with monoallelic *TP53* defects, suggesting that monoallelic abnormalities in both of these genes may be co-selected during the disease evolution.^{20,28} However, these observations have only been made through FISH or next-generation sequencing (NGS) studies. There lacks further research investigating the biological effects of combined monoallelic or biallelic *ATM* and *TP53* alterations in CLL. Recent work by our group and others has implemented the clustered regularly interspaced short palindromic repeats (CRISPR)/Cas9 technology for the efficient generation of CLL driver gene mutations or chromosomal abnormalities in human cell lines and animal models,^{15,29–32} offering new opportunities to study the potential co-operative effects of concurrent genetic alterations in CLL as well as the biological basis of mutual exclusivity among CLL driver alterations.

In this study, we used targeted sequencing and CRISPR/Cas9 approaches to systematically characterize the biological effects of concurrent monoallelic or biallelic *ATM* and/or *TP53* lesions in CLL cells in relation to patient clinical outcome. We showed that *TP53* alterations are a robust prognostic marker for overall survival in monoallelic del(11q) patients, whereas biallelic inactivation of both of these genes occurs in a mutually exclusive way. We functionally validated these findings with isogenic CRISPR/Cas9 generated models of del(11q) together with *TP53* and/or *ATM* mutations, showing that CLL cell lines harboring biallelic loss of *ATM* and *TP53* present abnormal cell cycle and mitotic profiles, failing to engraft and compete in murine xenotransplants. These results offer a functional insight into the mutual exclusivity of these alterations in CLL. Conversely, *TP53* mutations conferred a clonal advantage of CLL cells with a monoallelic del(11q) background, being able to outgrow cells with single del(11q) in in vivo clonal competition experiments.

2 | METHODS

2.1 | Patients

This study was based on 271 well-characterized CLL cases, diagnosed according to the international workshop on CLL (iwCLL) guidelines, with clinical data and FISH information. Overall, this cohort was enriched in del(11q)/del(17p) cases in concordance to the main purpose of the study. Forty-seven patients harbored del(11q), and the rest of them ($n = 224$), designated as the control group, were representative of the entire CLL cohort in terms of demographic and clinical-biologic characteristics. At the time of analysis, 94% of patients were untreated

and 50% of them received treatment during follow-up. The median follow-up was 60 months (range 0–264 months), and the median time to first treatment (TFT) was 18.5 months (range 0–221 months). Clinical and biological characteristics of the 271 CLL patients are summarized in Table 1.

Samples and clinical data were collected from 16 Spanish institutions. This study was approved by the local ethical committee (Comité Ético de Investigación Clínica, Hospital Universitario de Salamanca). Written informed consent was obtained from all participants before they entered the study. In addition, 136 CLL patients (n del(11q) = 38) from an independent cohort were included for external validation.¹⁰

2.2 | NGS

Mutational analysis was performed in the whole cohort of CLL patients included in this study ($n = 271$). Genomic DNA was isolated from peripheral blood or bone marrow MACS-sorted CD19+ B-lymphocytes. The Agilent SureSelectQXT Target Enrichment system for Illumina Multiplexed Sequencing (Agilent Technologies, Santa Clara, CA, USA) was used to produce libraries of exonic regions from 54 CLL-related genes included in a custom-designed panel previously validated³³ (Table S1). Genomic DNA extracted from each sample was fragmented and used to construct a sequencing library with the SureSelectQXT Library Prep Kit following the manufacturer's instructions. Paired-end sequencing (151-bp reads) was run on the Illumina NextSeq instrument (Illumina, San Diego, CA, USA). Median coverage of target regions was 600 reads/base, with at least 100X in 97% of them. Data analysis and variant calling were performed using the bioinformatic pipelines described in the Supplementary Methods.

2.3 | CRISPR/Cas9-mediated mutagenesis in CLL cell lines

The constitutive Cas9 expression vector (LentiCas9-Blast, Addgene #52962) was used to generate HG3 cell lines stably expressing the protein Cas9. Lentiviral particles containing plasmid-expressing Cas9 and blasticidine resistance were transduced into each cell line and selected by blasticidine (20 μ g/ml) for 2 weeks.³⁴ Cas9 activity was tested using a previously reported system based on the pXPR-011 plasmid (Addgene #59702) which delivers green fluorescent protein (GFP) and RNA guide (sgRNA) targeting GFP.³⁵

SgRNAs were designed using the online CRISPR design tool (<http://crispr.mit.edu/>) to target *TP53* (exon 4) and/or *ATM* (exon 10). These exons were chosen

TABLE 1 Clinical and biological characteristics of CLL patients

	Non del(11q) (n = 224), %	del(11q) (n = 47), %	p value
Male	63.8	73.7	0.239
Age of diagnosis (median, range)	73 (38-97)	69 (43-97)	0.152
Binet stage B/C	24.0	41.3	0.016
<i>IGHV</i> unmutated	38.1	81.0	<0.001
CD38 positivity	25.3	44.8	0.034
Hepatomegaly	3.9	11.4	0.046
Splenomegaly	15.6	27.3	0.066
FISH cytogenetics			
Del(13q)	62.1	48.9	0.095
Trisomy 12	21.4	2.2	0.002
Del(17p)	7.6	25.5	0.0003
Next-generation sequencing			
Mutated gene	75.4	92.5	0.014
<i>ATM</i> ^{MUT}	4.9	34.0	<0.001
<i>NOTCH1</i> ^{MUT}	20.5	17.0	0.574
<i>SF3B1</i> ^{MUT}	10.3	17.0	0.19
<i>BIRC3</i> ^{MUT}	3.6	19.1	<0.001
<i>TP53</i> ^{MUT}	12.1	23.4	0.043
Monoallelic <i>TP53</i> alteration (% del(17p)/ % <i>TP53</i> ^{MUT})	10.3 (2.7/7.6)	14.9 (8.5/6.4)	0.413
Biallelic <i>TP53</i> alteration (del(17p) and <i>TP53</i> ^{MUT})	4.5	17.0	0.002

for editing in order to generate frameshift mutations that result in a complete deletion of the DNA Binding Domain of TP53 or the FAT and PIKK C-terminal domains of ATM,^{11,25} producing a protein disruption as a consequence. The selection of the sgRNAs was based on choosing those of highest efficiency to target the gene of interest and with the lowest predicted off-targets effects. In addition, a sgRNA designed not to target the human genome was used as a negative control. Sequences of the selected sgRNAs are detailed in Table S2. The procedure and sgRNAs used for the generation of del(11q) were previously described.³² SgRNAs targeting *TP53* were cloned into pLKO5.sgRNA.EFS.GFP (Addgene_#57822) or pLKO5.sgRNA.EFS.tRFP (Addgene_#57823), and sgRNAs targeting *ATM* into pLKO5.sgRNA.EFS.tRFP (Addgene_#57823). Negative control sgRNA was cloned in both vectors. Cloning, transduction, and clone screening are detailed in Supplementary Methods.

The presence of CRISPR/Cas9-mediated off-target indels was examined in each generated clone by analyzing the top #3 gene off-targets of each sgRNA designed using Sanger sequencing. The Off-Spotter online tool was used to predict the off-target regions for each sgRNA (<https://cm.jefferson.edu/Off-Spotter/>).³⁶ Off-target regions, number of mismatches and primers designed for sequencing are detailed in Table S3.

2.4 | In vivo clonal competition and survival experiments

Animal studies were conducted in accordance with the Spanish and European Union guidelines for animal experimentation (RD53/2013, Directive-2010/63/UE, respectively) and received prior approval from the Bioethics Committee of our institution.

For the in vivo clonal competition experiments, a total of 16 4- to 5-week-old female NSG mice were previously randomized and used for intravenous injection of pooled HG3^{WT} + HG3 *TP53*^{MUT} cells (1.25 × 10⁶ cells/mice; ratio 1:1; n = 8) and HG3-del(11q) + HG3-del(11q) *TP53*^{MUT} + HG3-del(11q) *ATM*^{MUT} *TP53*^{MUT} (1.25 × 10⁶ cells/mice; ratio 1:1:1; n = 8). Mice were sacrificed 7 and 14 days after cell injection (n = 4/condition each time point), and spleens and bone marrow were collected for engraftment and clonal evolution analysis. Red blood cells were lysed with erythrocyte lysis buffer, and the remaining cells were then washed twice in phosphate-buffered saline (PBS). Samples were subjected to FACS analysis on a FACSAria flow cytometer. Data were analyzed with FlowJo software based on GFP and/or RFP positivity: HG3^{WT} (GFP⁺RFP⁻), HG3 *TP53*^{MUT} (GFP⁻RFP⁺); HG3-del(11q) (GFP⁻RFP⁺), HG3-del(11q) *TP53*^{MUT} (GFP⁺RFP⁻), HG3-del(11q) *ATM*^{MUT} *TP53*^{MUT} (GFP⁺RFP⁺).

For the survival analysis, 1.25×10^6 cells of HG3^{WT}, HG3 *TP53*^{MUT}, HG3-del(11q), HG3-del(11q) *TP53*^{MUT}, and HG3-del(11q) *ATM*^{MUT} *TP53*^{MUT} clones were injected individually into NSG mice (n = 5/group). Peripheral blood was extracted at day 17 post-injection for the assessment of engraftment by flow cytometry. Mice were monitored daily during the experiment and euthanized by anesthesia overdose when they presented symptoms of severe disease.

2.5 | Statistics

Statistical analyses were performed using IBM SPSS for Windows, Version 23.0 (IBM Corp.) or GraphPad Prism software v6 (GraphPad Software). Data are summarized as the mean \pm standard deviation (SD). Student's *t*-test, Mann-Whitney, ANOVA, and Kruskal-Wallis tests were used to determine statistical significance. The chi-square test was used to assess associations between categorical variables. Variables significantly associated with OS were identified by the Kaplan-Meier method, and the curves of each group were compared with the log-rank test. *p* values lower than 0.05 were considered as statistically significant.

3 | RESULTS

3.1 | Monoallelic del(11q) can co-occur with *TP53* alterations while biallelic *ATM* and *TP53* alterations are mutually exclusive in CLL patients

A total of 271 patients were included in this study: 47 del(11q) cases and 224 non-del(11q). Mutational analyses showed that 93.6% (44/47) of del(11q) patients harbored a mutation in at least one of the 54 genes analyzed, whereas 75.4% (169/224) were mutated within the control group (*p* = 0.014) (Table 1). High mutational frequencies in *ATM* (34%), *TP53* (23.4%), *BIRC3* (19%), *SF3B1* (17%), and *NOTCH1* (17%) were observed in del(11q) patients (Figure 1A), being *ATM*, *BIRC3*, and *TP53* mutations significantly associated with del(11q) (*p* < 0.0001, *p* < 0.0001, *p* = 0.043, respectively) (Table 1).

TP53 alterations (deletions and/or mutations) were one of the most abundant genetic lesions in our del(11q) series (15/47, 31.9%), after *ATM* mutations (16/47, 34%) (Figure 1A). Within this subgroup, a total of 12 patients had del(17p), and eight of them exhibited a *TP53* mutation in the remaining allele (67%), therefore considered to have a biallelic *TP53* alteration. In addition, *TP53* mutations were detected in three del(11q) patients without del(17p). Regarding the type of the genetic mutations in patients with del(11q) and del(17p), we found that four of them were

frameshift, one encoded for a stop codon, and nine were missense mutations, while mutations in del(11q) patients without del(17p) were all missense substitutions (Table 2).

In addition to the mutational analysis, we also focused on the co-occurrence of del(11q)/*ATM* mutations and del(17p)/*TP53* mutations in CLL patients, according to the presence of monoallelic or biallelic alteration and the type of the genetic alteration: deletion or gene mutation. First, regarding only mutations, we detected a significantly low co-occurrence between *ATM* and *TP53* mutations (*p* < 0.0001). Second, considering also chromosomal deletions in the analysis, we found a significant lack of *ATM* mutations in patients with biallelic *TP53* alterations (deletion and mutation) (*p* = 0.002) as well as a complete absence of *TP53* mutations in patients with biallelic *ATM* inactivation (*p* = 0.0002) (Figure 1B). We also detected a mutual exclusivity between biallelic *TP53* and biallelic *ATM* alteration (*p* = 0.03). Conversely, we observed a statistically significant association between *TP53* alterations (del(17p) and/or *TP53* mutation) and monoallelic *ATM* loss by del(11q) (*p* = 0.0002) (Figure 1B). Altogether, these results indicate that del(11q) CLL cells may harbor additional *TP53* alterations as long as they have the remaining *ATM*^{WT} allele intact.

3.2 | CLL patients harboring combined del(11q) and *TP53* alterations exhibit a highly adverse outcome

We next analyzed whether mutations in the most frequently mutated genes in del(11q) patients had an impact on their survival. Notably, only *TP53* mutations were able to stratify del(11q) patients in terms of clinical impact: those patients with *TP53* mutations had shorter OS than the rest of del(11q) (median 15 vs 88 months, *p* < 0.0001) (Figure 1C; Table S4). In addition, no significant differences regarding OS were observed between del(11q) patients harboring mutations in the rest of the genes analyzed by targeted NGS (Table S4; Figure S1).

Given the clinical impact of *TP53* mutations in the OS of del(11q) patients, we performed a clinical analysis with respect to the number of alleles affected by *TP53* alterations. Regarding the entire CLL cohort, we observed that patients harboring a biallelic *TP53* inactivation showed a significantly shorter overall survival than those with monoallelic *TP53* alteration (median 19 vs 60 months, *p* = 0.016) (Figure S2A).

Within del(11q) cases, the median OS of patients with biallelic *TP53* alteration was significantly shorter than del(11q) *TP53*^{WT} patients (median 11 vs 88 months, *p* = 0.001) (Figure 1D). Besides, we detected differences between the median OS of del(11q) cases harboring

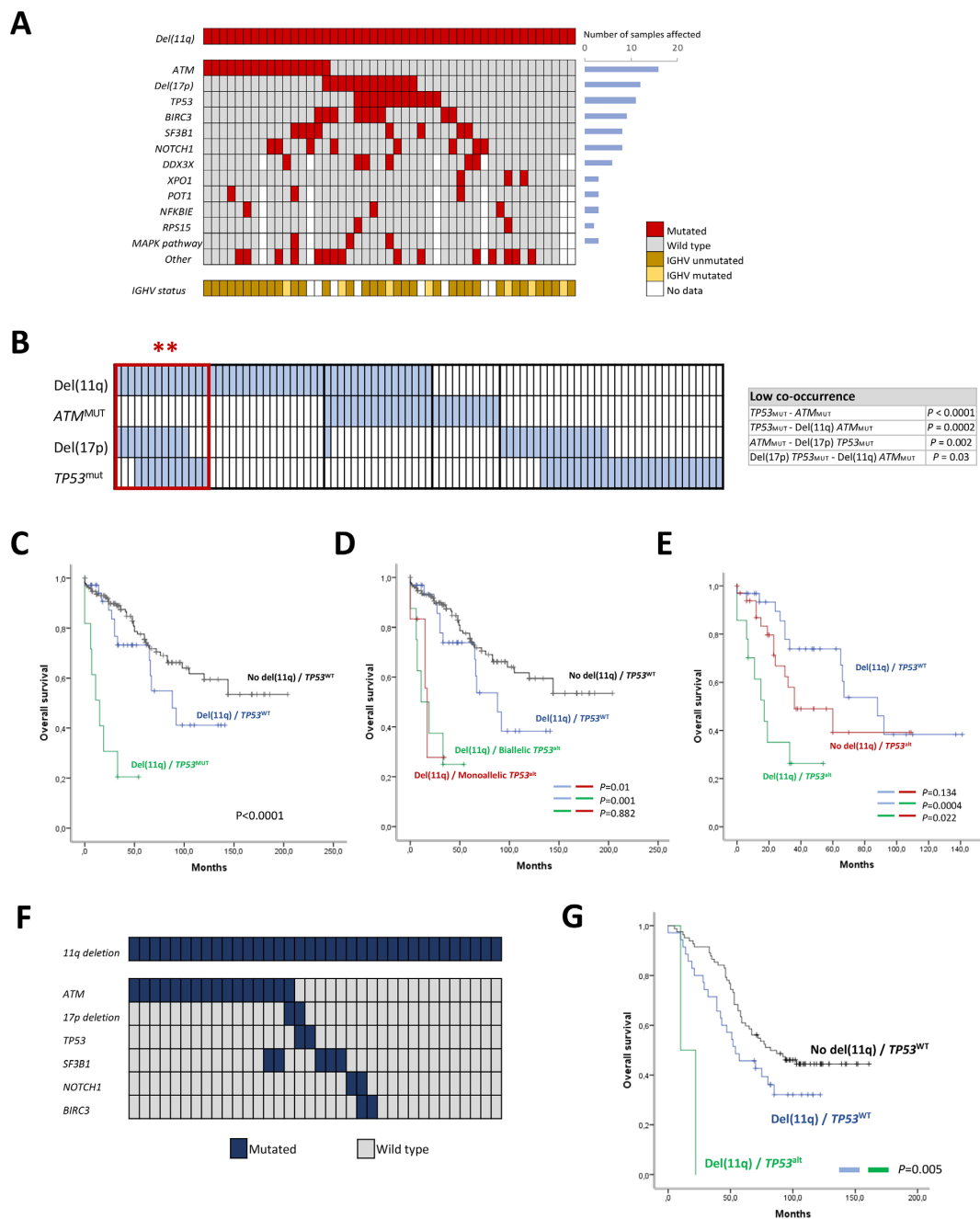


FIGURE 1 Mutational analysis and overall survival (OS) of del(11q) patients. (A) Mutational landscape of del(11q) patients; each column represents a patient and each row corresponds to a genetic alteration. Mutation or cytogenetic events are indicated in red, IGHV unmutated status in dark yellow, and IGHV mutated status in light yellow. White indicates missing data. (B) Significantly high and low co-occurrences of *ATM* and *TP53* alterations in CLL patients (chi-square test). Each column corresponds to one patient, and the presence of mutations or deletions is clustered according to the type of *ATM* and *TP53* alterations, shown in blue. Left red rectangle indicates the presence of high co-occurrence between monoallelic del(11q) and *TP53* alterations (** $p < 0.01$). Right table indicates the grades of low co-occurrences between the indicated conditions. (C) Impact of *TP53* mutations in the survival of del(11q) CLL patients. (D) OS of del(11q) patients according to the presence of monoallelic or biallelic *TP53* alterations (deletion and/or mutation). (E) Clinical impact of the presence of del(11q) in patients with *TP53* alterations (deletion and/or mutations). (F) Mutational analysis and (G) overall survival (OS) of del(11q) patients in the validation cohort from the UK LRF CLL4 trial

TABLE 2 TP53 alterations identified in del(11q) CLL patients

Patient ID	del(11q), % of cells	TP53 alterations (del/mut)	del(17p), % of cells	TP53 mutations, AA change (Transcript: NM_000546.5)	VAF, %	Other mutated genes
16	92	del/wt	86	–	–	ATM, BIRC3, ZMYM3, SETD2
17	50	del/wt	34	–	–	BIRC3, NOTCH1, CHD2, BCOR
18	20.5	del/wt	18	–	–	CHD2
19	90	del/wt	22	–	–	KRAS
20	15	del/mut	59	R273L; I332fs; M384fs	4.75; 3.09; 2.86	BIRC3, RPS15, DDX3X
21	62	del/mut	24	L330R	6.26	BIRC3, DDX3X
22	89	del/mut	87	P278R	98.96	BIRC3, NFKBIE
23	48.5	del/mut	38	R342X	15.33	BIRC3
24	62	del/mut	65	R273L; G105fs; P152L	33.96; 7.91; 3.77	SF3B1, MAP2K1, BRAF, DDX3X, FUBP1, ZC3H18
25	50	del/mut	25	R290H; Y163C	42.35; 11.92	NOTCH1, ZMYM3, ASXL1, FAT1
26	54	del/mut	51	I195T	20.72	–
27	46	del/mut	38	L130V; L93fs	21.9; 13.53	MGA
28	43	wt/mut	–	L145P	65.57	SF3B1, ARIDIA, ASXL1, MED12
29	10	wt/mut	–	Y234C	3.33	–
30	83	wt/mut	–	Y205D	7	–

Abbreviations: fs, frameshift mutation; VAF, variant allele frequency.

monoallelic *TP53* alterations by either del(17p) or somatic mutation and the rest of del(11q) patients (median 17 vs 88 months, $p = 0.01$) (Figure 1D). Interestingly, no differences in OS were observed between biallelic and monoallelic del(11q) *TP53*^{ALT} patients (median 11 vs 17 months, $p = 0.882$), suggesting that the highly negative clinical impact of this co-occurrence is independent of the number of alleles affected by *TP53* aberrations. In addition, patients with combined del(11q) and *TP53* abnormalities had a shorter TFT than those with only *TP53* alterations (median 7 vs 36 months, $p = 0.05$), while there were no significant differences with respect to the presence of sole del(11q) abnormality (median 7 vs 11 months, $p = 0.33$) (Figure S2B).

Furthermore, the presence of del(11q) also contributed to a shorter OS for patients with *TP53* alterations in our study (median 17 vs 36 months, $p = 0.022$), corroborating that the coexistence of both del(11q) and *TP53* alterations accounts for a marked poor outcome even in del(17p) cases (Figure 1E). These results were validated in cases from a previously published cohort from the UK LRF CLL4 trial (Figure 1F),¹⁰ where *TP53* alterations also accounted for

a reduced survival of del(11q) patients (median 10 vs 54 months, $p = 0.005$; Figure 1G).

3.3 | Concurrence of biallelic *ATM* and *TP53* alterations in CLL cells results in defective mitosis and the formation of abnormal multinucleated cells

Based on the sequencing results observed in our CLL cohort, we next prompted to address the biological implications of concurrent monoallelic or biallelic loss of *ATM* and *TP53* in del(11q) CLL cells. For this purpose, we used the HG3 CLL derived cell line, which is diploid for chromosomes 11 and 17 and also has wild-type *ATM* and *TP53* genes. HG3 parental cells were transduced to stably express Cas9 protein, and sgRNAs targeting chromosome 11q22.1/11q23.3 were introduced to generate an isogenic HG3 CLL cell line harboring del(11q) (HG3-del(11q)) of ~17 Mb size including *ATM* gene (Figures 2A and 2B).³² We then introduced sgRNAs targeting *ATM* and/or *TP53* genes in both wild-type HG3 cells (HG3^{WT}) and

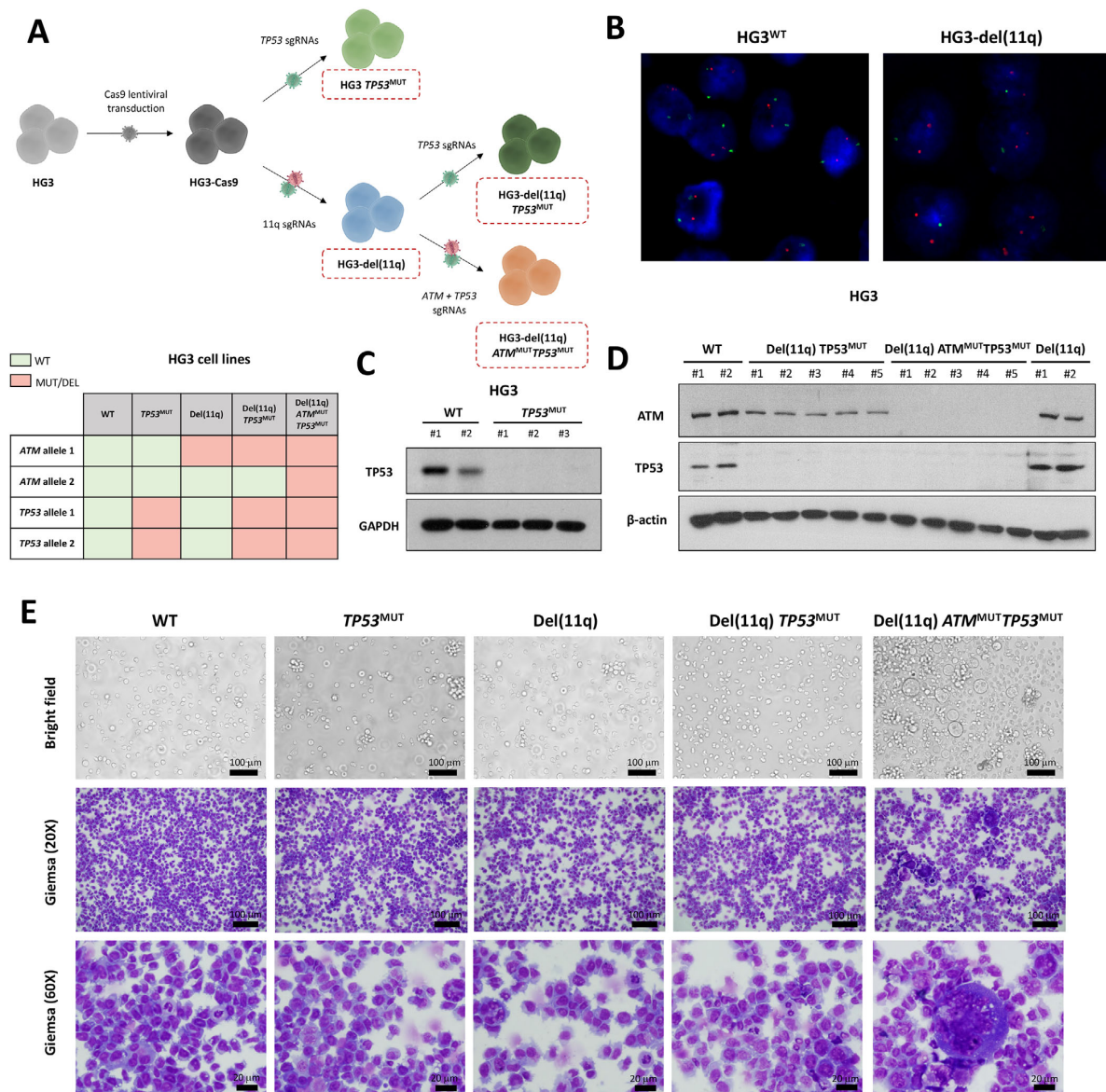


FIGURE 2 Generation of CRISPR/Cas9-edited CLL cell lines harboring del(11q), TP53 and/or ATM mutations and phenotypical analysis of edited cells. (A) Upper panel: experimental design for the introduction of del(11q), TP53 and/or ATM mutations in the HG3 CLL derived cell line using the CRISPR/Cas9 system. sgRNAs targeting 11q22.1 and 11q23.3 were nucleofected for transitory expression in HG3-Cas9 cells. Nucleofected single-cell sorted clones were screened for the presence of del(11q), and the presence of this deletion was validated by Sanger sequencing and FISH. The resulting HG3-del(11q) isogenic cell line, as well as parental HG3-Cas9 cells, was further transduced with sgRNAs targeting TP53 and/or ATM genes for the generation of truncating mutations. In total, 3 HG3^{WT}, 3 HG3 TP53^{MUT}, 3 HG3-del(11q), 5 HG3-del(11q) TP53^{MUT}, and 5 HG3-del(11q) ATM^{MUT} TP53^{MUT} clones were generated. Lower panel: number of alleles affected by mutations and deletions in the CRISPR/Cas9-generated cell lines. (B) Representative FISH images of HG3^{WT} and HG3-del(11q) cells. Green signals correspond to 11q22/ATM probe and the control red signals correspond to 17p13/TP53 probe. (C) Western blot analysis of isogenic HG3-edited clones with TP53 mutations. Upper panel shows TP53 protein expression of 2 HG3^{WT} clones and 3 HG3 TP53^{MUT} clones. Lower panel shows GAPDH, which was used as loading control. (D) Western blot analysis of HG3-edited single-cell clones. Upper and middle panels show ATM and TP53 expression, respectively, of 2 HG3^{WT} clones, 5 HG3-del(11q) TP53^{MUT} clones, 5 HG3-del(11q) TP53^{MUT} ATM^{MUT} clones, and 2 HG3-del(11q) clones. β -actin was used as loading control. (E) Bright field and Giemsa stained representative images of HG3-edited cell lines

HG3-del(11q) cells. Single-cell FACS sorted clones were expanded and screened for the presence of truncating mutations in *TP53* and *ATM*. In total, we generated 3–5 different single-cell clones of the following conditions: HG3^{WT}, HG3 *TP53*^{MUT} (biallelic *TP53* truncating mutation), HG3-del(11q) (monoallelic *ATM* loss), HG3-del(11q) *TP53*^{MUT} (monoallelic *ATM* loss / biallelic *TP53* truncating mutation), and HG3-del(11q) *ATM*^{MUT}*TP53*^{MUT} (biallelic *ATM* loss / biallelic *TP53* truncating mutation) (Figure 2A). The type of CRISPR/Cas9-mediated indels of *TP53* and/or *ATM* in each generated clone is specified in Table S5, and the functional absence of these proteins was validated by western blot (Figures 2C and 2D). In addition, no off-target indels were found in any of the HG3-edited clones (Table S5).

Phenotypical analyses of these edited cell lines revealed that HG3-del(11q) *ATM*^{MUT}*TP53*^{MUT} cells were markedly enlarged compared to the rest of the conditions (Figure 2E). Giemsa staining of these cell lines showed that these atypical cells had an irregular cytoplasm with the presence of degenerative vacuoles and were frequently multinucleated, suggesting a profound defect in mitosis. In fact, the mitotic index was found significantly lower in these cells than CLL cells without biallelic loss of *ATM* and *TP53* (Figure 2E; Table S6). 3-(4,5-dimethylthiazol-2-yl)-2,5-diphenyltetrazolium bromide (MTT) and growth assays corroborated impaired proliferation of these cells in comparison to HG3 *TP53*^{MUT} cells (Figures 3A and 3B). Besides, cell-cycle distribution analysis under basal conditions revealed the presence of increased G2/M and >4n events in HG3-del(11q) *ATM*^{MUT}*TP53*^{MUT} clones (Figures 3D and 3E). Interestingly, these differences in proliferation were not related to an apoptotic defect, since PARP1 and caspase-3 cleavage levels were similar between all cell lines (Figure 3C).

In order to determine how these CRISPR/Cas9-generated cell lines responded to double strand breaks induction, cells were irradiated (IR), and cell cycle profiles were analyzed by measuring the DNA content after staining with propidium iodide (PI) 24, 48, and 72 hours after irradiation (Figures 3D and 3E). As expected, we found that HG3^{WT} and HG3-del(11q) cells exhibited cell cycle arrest 24 hours post-IR, but after that time cells had repaired their lesions and escaped the G2 arrest. In addition, HG3 *TP53*^{MUT}, and HG3-del(11q) *TP53*^{MUT} cells showed a G2/M cell cycle arrest in accordance with *TP53*-defective cell-cycle phenotype,³⁷ which was also overcome 48 hours post-IR. Conversely, HG3-del(11q) *ATM*^{MUT}*TP53*^{MUT} cells exhibited a profound G2/M cell cycle arrest 24 hours post-IR, with an increase in the number of events >4n, revealing the existence of polyploid cells in accordance with the presence of enlarged multinucleated cells even in the absence of exogenous

DNA damage. The polyploid population (>4n), together with the persistence of G2/M arrest after irradiation (Figure 3E), further indicates the presence of mitotic defects in CLL cells harboring biallelic *ATM* and *TP53* defects.

3.4 | *TP53* mutations can co-exist with monoallelic del(11q), favoring in vivo clonal expansion of del(11q) CLL cells

Considering that *TP53* mutations or deletions were significantly enriched in the subset of monoallelic del(11q) CLL patients from our NGS analysis and significantly correlated with a worse prognosis, we next investigated the effects of the combination of these alterations in our CRISPR/Cas9-engineered cell lines. We first interrogated whether the introduction of these alterations had an impact on CLL cell growth in vitro. Viability and growth assays revealed that the introduction of *TP53* mutations in HG3^{WT} cells resulted in increased proliferation (Figures 3A and 3B). In addition, HG3-del(11q) *TP53*^{MUT} cells had higher in vitro growth rates than HG3-del(11q) cells. Notably, the introduction of an *ATM* truncating mutation in the remaining allele of these cell lines suppressed this proliferative advantage, since HG3-del(11q) *ATM*^{MUT}*TP53*^{MUT} cells growth rates were comparable to those of HG3-del(11q) cells (Figures 3A and 3B).

In order to evaluate how monoallelic or biallelic *ATM* and/or *TP53* lesions contributed to the clonal dynamics of CLL in an in vivo setting, GFP and/or RFP-tagged HG3^{WT} and HG3 *TP53*^{MUT} cells, as well as HG3-del(11q), HG3-del(11q) *TP53*^{MUT}, and HG3-del(11q) *ATM*^{MUT}*TP53*^{MUT} were mixed at a ratio 1:1 and injected into NSG mice (Figures 4A and 4B). Clonal evolution was assessed by quantifying the relative number of the different subclones in both the spleen and the bone marrow one and 2 weeks after cell injection. In the first subset of mice, clonal competition between HG3^{WT} and HG3 *TP53*^{MUT} cells was assessed, showing that *TP53*^{MUT} cells were able to rapidly outcompete WT cells in spleen (Figure 4A). Intriguingly, *TP53*^{MUT} cells had a preferential engraftment toward spleen than bone marrow of xenotransplanted mice, since HG3^{WT} cell counts were higher in the bone marrow 1 week after injection. However, *TP53*^{MUT} cells were able to progress at a higher growth rate in the bone marrow compartment in the following week (Figure 4A).

The second subset of mice was injected with HG3-del(11q), HG3-del(11q) *TP53*^{MUT}, and HG3-del(11q) *ATM*^{MUT}*TP53*^{MUT} cells. At day 7, a marked clonal advantage of HG3-del(11q) *TP53*^{MUT} cells over HG3-del(11q) in spleen was observed, being these differences even higher 14 days after injection (Figure 4B). Similar effects were observed in the bone marrow of these mice, being the

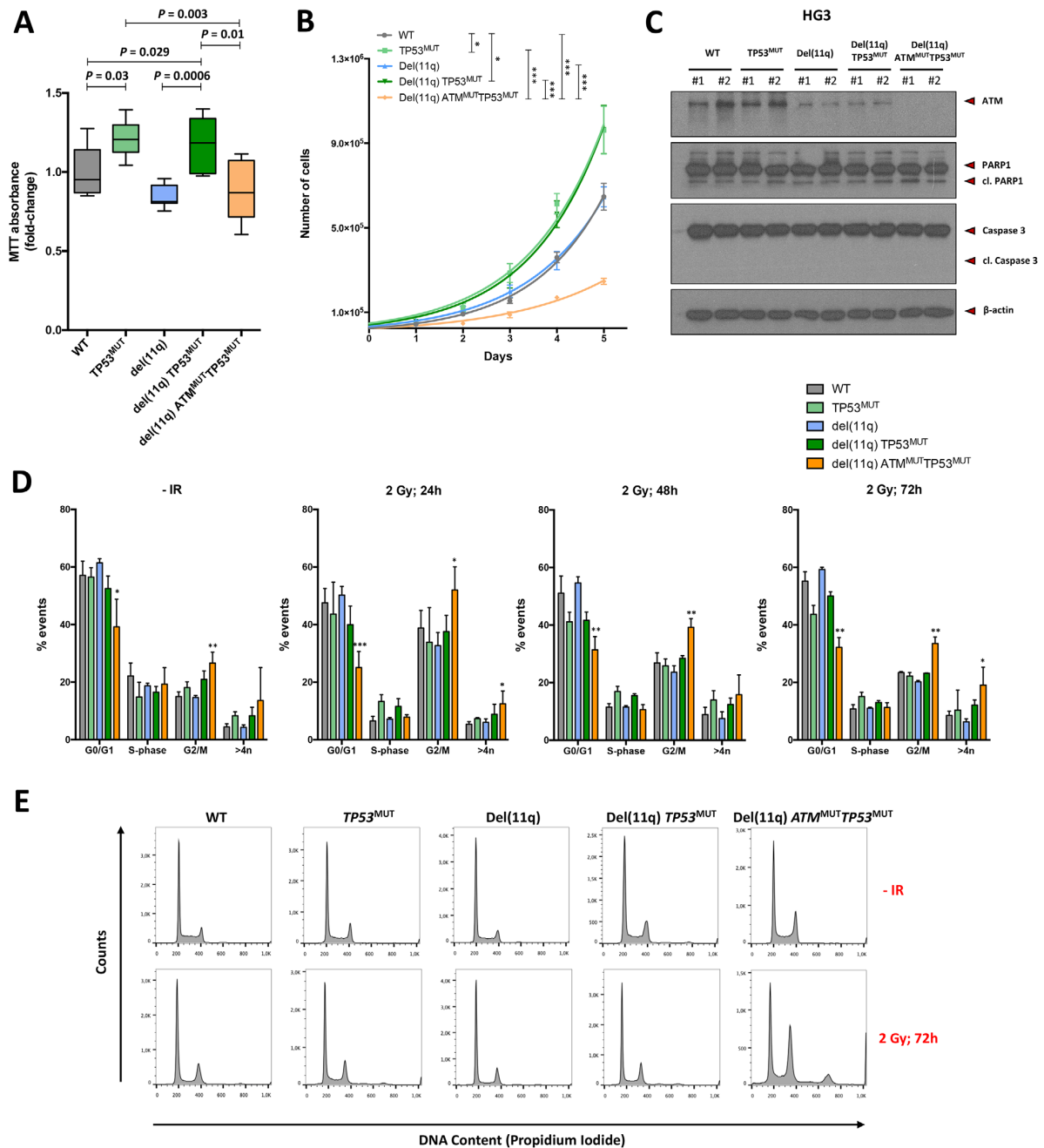


FIGURE 3 Effects of biallelic loss of *TP53* and *ATM* on viability, cell growth, apoptosis, and cell cycle control of CRISPR/Cas9-edited cell lines. (A) Effects of $del(11q)$, *TP53*, and/or *ATM* mutations on proliferation of HG3 cells after 72 hours. MTT absorbance values are normalized with the HG3^{WT} clones. Data are summarized as the mean \pm SD. (B) HG3-edited cell lines were seeded at a concentration of 3×10^4 cells/mL, and cell growth was assessed at five time points every 24 hours by Trypan Blue exclusion. Data were fitted in an exponential growth equation, and time point values are presented as the mean \pm SEM. (C) Representative immunoblot analyses of HG3^{WT}, HG3 $TP53^{MUT}$, HG3- $del(11q)$, HG3- $del(11q) TP53^{MUT}$, and HG3- $del(11q) ATM^{MUT} TP53^{MUT}$ whole cell lysates. ATM, PARP1, and Caspase-3 protein expression and/or cleavage were analyzed. β -actin was used as loading control. (D) Cell cycle phase distribution of HG3-edited cell lines upon exposure to irradiation at the indicated time points. Data represent the mean values \pm SD of at least three independent experiments. $p < 0.05$ (*), $p < 0.01$ (**). (E) Representative cell cycle profiles of CRISPR/Cas9-edited clones after 72 hours irradiation exposure (2 Gy). All the events placed right from the G2/M peak at 400 DNA content units were considered >4n population

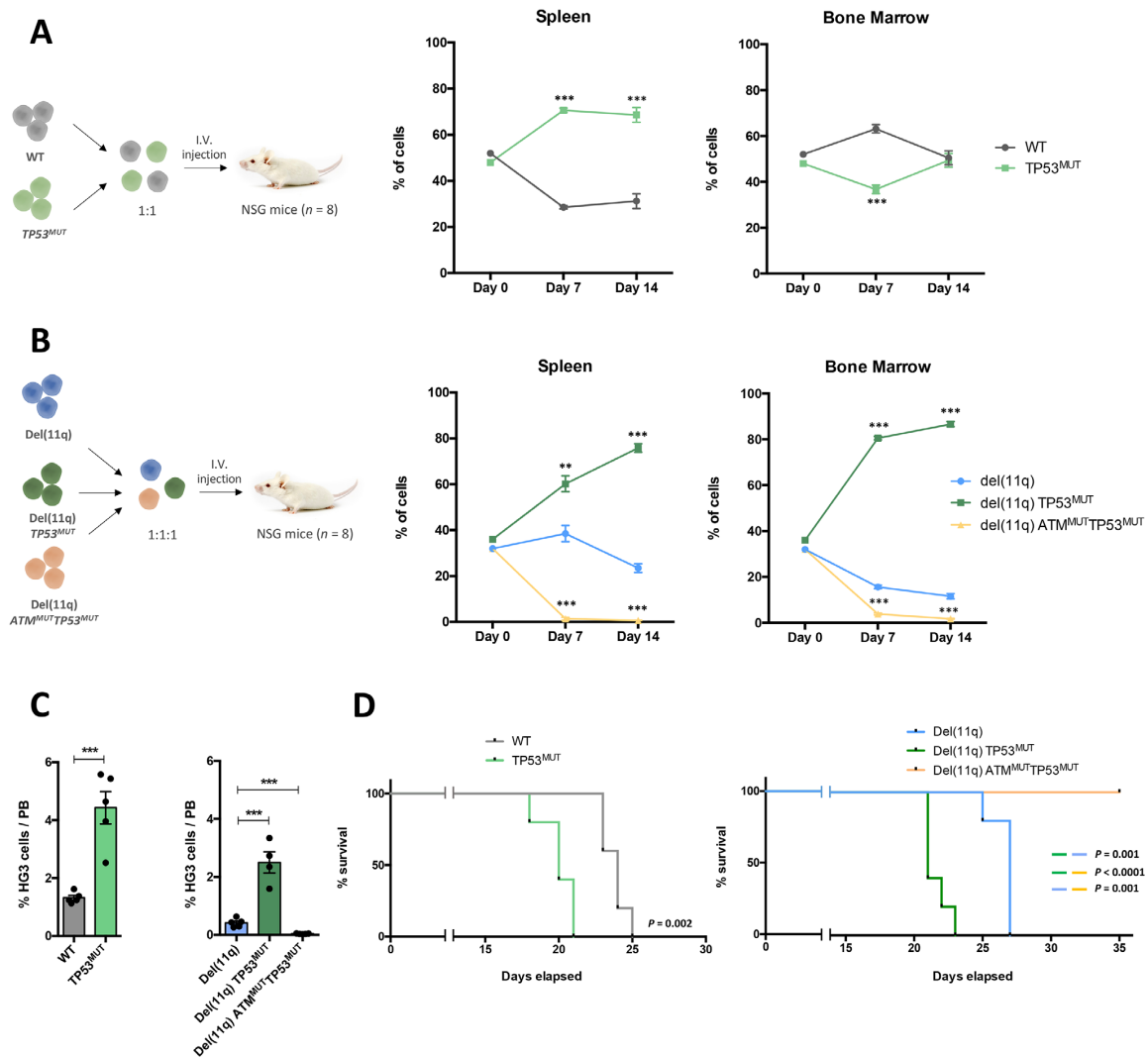


FIGURE 4 In vivo clonal competition analysis of xenotransplanted NSG mice. (A) HG3^{WT} GFP-tagged and HG3 TP53^{MUT} RFP-tagged cells were mixed at a ratio 1:1 and injected into NSG mice ($n = 8$). Spleen and bone marrow infiltration were assessed by flow cytometry 7 ($n = 4$) and 14 ($n = 4$) days post-injection. (B) HG3-del(11q) RFP-tagged, HG3-del(11q) TP53^{MUT} GFP-tagged, and HG3-del(11q) ATM^{MUT} TP53^{MUT} GFP, and RFP-tagged cells were mixed at a ratio 1:1:1 and injected into NSG mice ($n = 8$). Spleen and bone marrow infiltration were assessed by flow cytometry 7 ($n = 4$) and 14 ($n = 4$) days post-injection. Data are represented as the mean \pm SD. $p < 0.05$ (*), $p < 0.01$ (**), $p < 0.001$ (***). (C) Quantification of GFP+ and/or RFP+ cell populations in the peripheral blood of HG3^{WT} and HG3 TP53^{MUT} (left), and HG3-del(11q), HG3-del(11q) TP53^{MUT}, and HG3-del(11q) ATM^{MUT} TP53^{MUT} (right) xenografted mice 17 days after intravenous injection. Data are shown as mean \pm SEM. $p < 0.001$ (***). (D) Kaplan-Meier overall survival curve of HG3^{WT} ($n = 5$) and HG3 TP53^{MUT} ($n = 5$) xenografted mice (left panel) and HG3-del(11q) ($n = 5$), HG3-del(11q) TP53^{MUT} ($n = 5$), and HG3-del(11q) ATM^{MUT} TP53^{MUT} ($n = 5$) xenotransplants (right panel). The reported p value was calculated by using the Log-rank test

growth dynamics of HG3-del(11q) TP53^{MUT} cells four-fold faster than HG3-del(11q) cells. Interestingly, HG3-del(11q) ATM^{MUT} TP53^{MUT} cells failed to engraft and compete with HG3-del(11q) and HG3-del(11q) TP53^{MUT} cells, almost disappearing from both spleen and bone marrow 2 weeks after cell injection (Figure 4B).

In an additional experiment, HG3-edited clones were injected individually into NSG recipients ($n = 5$ /group) to investigate the effects of clonal expansion of each cell line in mice survival. To evaluate the engraftment capacity of each condition in the peripheral blood, mice were bled at day 17 post-injection, and blood cell counts were

analyzed by flow cytometry. In concordance with the results observed in the clonal competition experiments, HG3 $TP53^{MUT}$ and HG3-del(11q) $TP53^{MUT}$ xenotransplanted mice had higher percentage of leukemic cells than HG3^{WT} and HG3-del(11q) xenotransplants, respectively, whereas the percentage of leukemic cells in mice xenografted with HG3-del(11q) $ATM^{MUT}TP53^{MUT}$ was almost negligible (Figure 4C). These observations correlated with an impact in OS, having HG3 $TP53^{MUT}$ and HG3-del(11q) $TP53^{MUT}$ xenotransplants a significantly shorter OS than HG3^{WT} and HG3-del(11q) mice, respectively (Figure 4D). Moreover, HG3-del(11q) $ATM^{MUT}TP53^{MUT}$ xenotransplants had the longest survival of all groups, being still alive at the end of the experiment (day 35, Figure 4D). Altogether, these results are consistent with the poorer prognosis observed in del(11q) patients harboring $TP53$ alterations (Figure 1) and strongly reinforce the severe cell cycle defects in HG3-del(11q) $ATM^{MUT}TP53^{MUT}$ cells and therefore, the mutual exclusivity of biallelic ATM alterations and $TP53$ loss in CLL patients.

3.5 | Del(11q) $TP53^{MUT}$ CLL cells show incomplete responses to B cell receptor signaling inhibitors

Given that $TP53$ mutations seem to be a key determinant on disease progression for del(11q) CLL cells, we next evaluated drug responses of these isogenic CLL cell lines harboring high-risk alterations. To validate that our CRISPR/Cas9-generated cell lines could be used as models for treatment response, we tested the responses of all the cell lines to fludarabine since $TP53$ mutations are a well-known marker for fludarabine refractoriness.^{22,23} We confirmed that truncated $TP53$ was associated with fludarabine resistance independently of ATM status since HG3-del(11q) $TP53^{MUT}$, as well as HG3 $TP53^{MUT}$ and HG3-del(11q) $ATM^{MUT}TP53^{MUT}$ cells showed consistently higher IC_{50} values compared to HG3^{WT} cells 72 hours after fludarabine treatment (mean IC_{50} 8.8, 8.48, 8.58 vs 4.36 μ M, respectively) (Figures 5A and 5C). These results were also confirmed at longer fludarabine exposure times (Figures 5B and 5D).

Moreover, we tested responses of these cell lines to the novel targeted B cell receptor (BCR) signaling inhibitors such as ibrutinib and idelalisib, which were initially approved specifically for del(17p)/ $TP53$ -mutated CLL patients. Notably, HG3-del(11q) $TP53^{MUT}$ and HG3 $TP53^{MUT}$ cells showed a response to these drugs, although the IC_{50} values were still higher than the ones observed on the HG3^{WT} clones, especially in the case of idelalisib treatment (27.42 and 20.64 vs 1.78 μ M, respectively, 72 hours

after treatment) (Figures 5A, 5E, and 5G). HG3-del(11q) $TP53^{MUT}$ and HG3 $TP53^{MUT}$ cells also showed higher IC_{50} values than HG3^{WT} cells after a 120-hour exposure to these drugs (Figures 5B, 5F, and 5H).

Considering these results, we next prompted to assess whether this partial response of HG3-del(11q) $TP53^{MUT}$ cells to ibrutinib and idelalisib could be overcome with the use of novel preclinical therapies. Since AZD6738, an Ataxia Telangiectasia and Rad3 related (ATR) serine/threonine protein kinase inhibitor, has been shown to induce synthetic lethality on $TP53$ - or ATM -defective CLL cells,³⁸ we determined the response of our CRISPR/Cas9-edited cell lines to this inhibitor. We found that HG3-del(11q) $TP53^{MUT}$ cells were as sensitive to selective ATR inhibition as HG3^{WT} cells (Figures 5I and 5J), with a comparable 96-hour treatment IC_{50} value between both conditions (mean IC_{50} 0.55 vs 0.67 μ M).

4 | DISCUSSION

Although the biological and prognostic impact of some individual CLL-related alterations has been addressed in recent years,^{4,5,16,21,22,29–31} most of these alterations usually co-exist within the same tumoral clone, and how and which one of them cooperates with each other to drive leukemogenesis remains largely unknown. In this study, we explored the concurrence of monoallelic and biallelic del(11q)/ ATM and $TP53$ lesions by generating isogenic CRISPR/Cas9 in vitro models mimicking the genetic heterogeneity we observed in a high-risk cohort of del(11q) CLL patients. Using this approach, we were able to determine the biological basis of the concurrence or mutual exclusivity of $TP53$ alterations in del(11q) CLL.

Our targeted sequencing data of del(11q) CLL patients provide an understanding into the additional driver events accompanying this cytogenetic abnormality, highlighting that the vast majority of del(11q) patients harbor mutations in known CLL driver genes (Figure 1A), in contrast to what has been reported in del(13q) patients where 50% of them do not harbor any additional abnormalities.^{4,5} Specifically, mutations in ATM and $BIRC3$ in our study were significantly associated with the presence of del(11q), in accordance with previous studies showing that truncating mutations in these genes in del(11q) CLL patients result in a complete loss of functional ATM and $BIRC3$ proteins.^{5,10,16,39} In addition, we also detected the presence of $TP53$ lesions in a subset of del(11q) patients with a highly adverse clinical outcome. Indeed, $TP53$ alterations were the only marker associated with a worse OS within the subgroup of del(11q) patients. Furthermore, we were able to recapitulate this combination of events (del(11q) $TP53^{MUT}$) in in vitro CLL models using the CRISPR/Cas9 editing

A

72-hour treatment		FLUDARABINE		IBRUTINIB		IDELALISIB		AZD6738	
Alteration	IC ₅₀ ± SEM	P (vs WT)	IC ₅₀ ± SEM	P (vs WT)	IC ₅₀ ± SEM	P (vs WT)	IC ₅₀ ± SEM	P (vs WT)	
WT	4.36 ± 0.17	-	2.38 ± 0.11	-	1.78 ± 0.45	-	0.67 ± 0.01	-	
TP53 ^{MUT}	8.48 ± 1.33	0.037	5.36 ± 2.11	0.102	20.64 ± 15.98	0.042	0.6 ± 0.2	0.181	
Del(11q)	4.24 ± 0.19	0.663	4.74 ± 1.92	0.117	3.27 ± 0.49	0.086	0.97 ± 0.04	0.751	
Del(11q) TP53 ^{MUT}	8.8 ± 1.27	0.019	5.45 ± 0.7	0.002	27.42 ± 5.99	0.003	0.55 ± 0.06	0.405	
Del(11q) ATM ^{MUT} TP53 ^{MUT}	8.58 ± 0.23	0.006	4.76 ± 0.26	0.001	15.14 ± 6.82	0.066	0.43 ± 0.11	0.178	

B

120-hour treatment		FLUDARABINE		IBRUTINIB		IDELALISIB		AZD6738	
Alteration	IC ₅₀ ± SEM	P (vs WT)	IC ₅₀ ± SEM	P (vs WT)	IC ₅₀ ± SEM	P (vs WT)	IC ₅₀ ± SEM	P (vs WT)	
WT	3.05 ± 1.00	-	1.64 ± 0.14	-	0.15 ± 0.04	-	0.42 ± 0.03	-	
TP53 ^{MUT}	7.14 ± 0.71	0.011	2.57 ± 0.23	0.012	0.87 ± 0.26	0.035	0.53 ± 0.02	0.032	
Del(11q)	3.54 ± 0.22	0.241	2.14 ± 0.46	0.328	0.47 ± 0.11	0.037	0.44 ± 0.01	0.679	
Del(11q) TP53 ^{MUT}	7.31 ± 1.73	0.068	4.59 ± 1.10	0.037	1.81 ± 0.63	0.039	0.45 ± 0.06	0.622	
Del(11q) ATM ^{MUT} TP53 ^{MUT}	10.61 ± 0.89	0.001	6.08 ± 0.97	0.004	3.2 ± 1.24	0.049	0.25 ± 0.02	0.003	

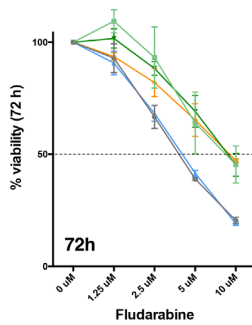
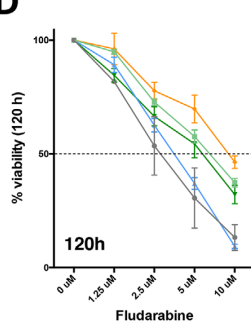
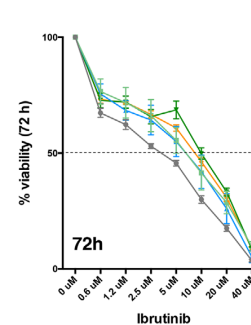
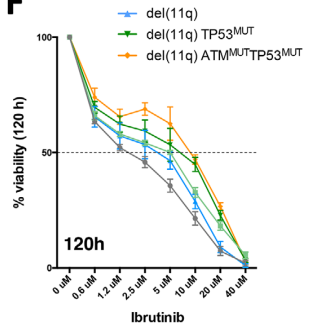
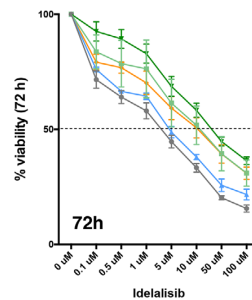
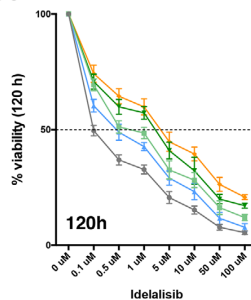
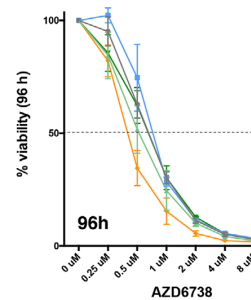
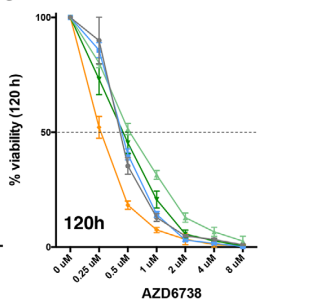
C**D****E****F****G****H****I****J**

FIGURE 5 Cell viability studies of HG3-edited clones in response to different drug treatments. (A and B) Tables indicating the IC₅₀ ± SEM values of each CRISPR/Cas9-edited HG3 cell line in response to fludarabine, ibrutinib, idelalisib or AZD6738, as well as the p-values of the comparison between HG3^{WT} IC₅₀ mean concentrations with the mean IC₅₀ values from the rest of the conditions. (C-J) HG3-edited clones were treated with escalating doses of fludarabine (C and D), ibrutinib (E and F), idelalisib (G and H), and AZD6738 (I and J), and cell viability was assessed by MTT assay after the indicated treatment times. Surviving fraction is expressed relative to untreated controls. Data are summarized as the mean ± SD of three independent experiments

system, showing that these cells have an *in vivo* clonal advantage over del(11q) cells without *TP53* alterations, offering a biological insight into the cooperation of these alterations in CLL progression and relapse. Taken together, our results suggest that the presence of *TP53* alterations in monoallelic del(11q) CLL patients may contribute to a negative predictive impact due to an increase competitive fitness of CLL clones harboring both of these alterations.

Large-scale whole exome sequencing studies (WES) have revealed that genetic alterations in CLL do not randomly occur, and patterns of co-occurrence or mutual exclusivity between these alterations have been suggested.^{4,5,40} However, the relationship between del(11q)/*ATM* and del(17p)/*TP53* lesions has not been well-established. Previous reports have suggested that alterations in both of these genes tend to be mutually

exclusive^{18,27} whereas others have reported the concurrence of these alterations within the same tumoral clone.^{20,28} In addition, WES studies from more than 1000 CLL samples were not able to identify any statistical evidence for a specific pattern of co-occurrence or mutual exclusivity of *ATM* and *TP53* genetic alterations in CLL.^{4,5} Our NGS and functional studies based on isogenic CRISPR/Cas9-generated models indicate that co-existence of these alterations within the same CLL clone robustly depends on the number of alleles affected by these events. We found that monoallelic del(11q) CLLs may harbor additional del(17p) and/or *TP53* mutations, whereas biallelic loss of *ATM* and *TP53* is virtually inexistent and therefore mutually exclusive in CLL patients. When we generated these scenarios in vitro, HG3 del(11q) *ATM*^{MUT}*TP53*^{MUT} cells showed abnormal phenotypic features such as mitotic impairment, leading to cell enlargement, polyploidy, and diminished proliferation capacity. Indeed, these cells failed to compete in vivo in xenotransplanted mice, being rapidly outcompeted by HG3-del(11q) or HG3-del(11q) *TP53*^{MUT} cells. Thus, CRISPR/Cas9-engineered CLL cell lines could be useful models not only to study the effects of individual or concurrent genetic abnormalities, but also to define the mechanisms underlying mutual exclusivity in order to find synthetic lethal interactions of clinical interest.

In the recent years, BCR kinase inhibitors such as ibrutinib and to a lesser extent idelalisib have revolutionized the treatment paradigm in CLL.⁴¹ Despite their proved benefits in comparison to previous chemotherapy-based regimes in high-risk cytogenetics patients, disease progression after treatment with these inhibitors has been increasingly reported.^{42–44} Our CRISPR/Cas9-edited isogenic models have highlighted that del(11q) *TP53*^{MUT} cell lines show only a partial response to ibrutinib or idelalisib, indicating that clones harboring these alterations might not be fully sensitive in a real-life setting under therapy with these inhibitors. Although further studies in additional CLL cell lines with different genetic backgrounds would be required to validate these findings, our results are in line with observations made in ex vivo studies and clinical trials where del(17p)/*TP53* mutations are still a marker for less sensitivity and shorter OS in ibrutinib treated patients.^{45,46} In the case of idelalisib, although the presence of del(17p)/*TP53* mutation did not show negative effects on clinical outcomes in a phase III trial of idelalisib in combination with rituximab,⁴⁷ overall responses of *TP53*-altered patients are still less frequent within this subgroup of patients.^{48,49} Altogether, our results suggest that these CRISPR/Cas9-edited CLL cell lines could be useful models to further predict treatment response of high risk del(11q) *TP53*^{MUT} CLL cells, providing a pre-clinical tool to explore novel therapeutic strategies such as ATR inhibitors in this subset of CLL cases.

In conclusion, this work addresses the biologic and prognostic implications of concurrent *TP53* alterations in del(11q) CLL. We show that mutations in *TP53* can appear in a subset of monoallelic del(11q) CLL cases, conferring clonal advantage in vivo, and therefore a dismal clinical impact in terms of OS in this subgroup of CLL patients. In addition, we also assess the biological basis of mutual exclusivity of biallelic *ATM* and *TP53* alterations in CLL, underscoring the importance of the number of alleles affected by these alterations in CLL, establishing novel pre-clinical models for the study of the biology and therapeutic response of concurrent genetic abnormalities in the disease.

ACKNOWLEDGMENTS

This work was supported by grants from the Spanish Fondo de Investigaciones Sanitarias (grant numbers: PI15/01471 and PI18/01500), Instituto de Salud Carlos III (ISCIII), European Regional Development Fund (ERDF) “Una manera de hacer Europa,” “Consejería de Educación, Junta de Castilla y León” (grant number: SA271P18), “Proyectos de Investigación del SACYL,” Spain GRS 1847/A/18, GRS1653/A17, “Fundación Memoria Don Samuel Solórzano Barruso” (FS/23-2018), by grants (grant number: RD12/0036/0069) from Red Temática de Investigación Cooperativa en Cáncer (RTICC), Centro de Investigación Biomédica en Red de Cáncer (CIBERONC CB16/12/00233) and SYNtherapy “Synthetic Lethality for Personalized Therapy-based Stratification In Acute Leukemia” (ERAPERMED2018-275); ISCIII (AC18/00093). MQÁ has been fully supported by an “Ayuda predoctoral de la Junta de Castilla y León” by the Fondo Social Europeo (JCYL-EDU/529/2017 PhD scholarship) and is now a recipient of a research grant by FEHH (“Fundación Española de Hematología y Hemoterapia”); CPC was supported by an “Ayuda predoctoral en Oncología” (AECC) and is a recipient of a PFIS grant (FI19/00191) from Instituto de Salud Carlos III; MHS was supported by a grant from FEHH/Janssen (“Sociedad Española de Hematología y Hemoterapia”) and now holds a Sara Borrell post-doctoral contract (CD19/00222) from the Instituto de Salud Carlos III (ISCIII). PFIS grant and Sara Borrell post-doctoral contract are co-funded by Fondo Social Europeo (FSE) “El Fondo Social Europeo invierte en tu futuro”; AERV is supported with a research grant by FEHH (“Fundación Española de Hematología y Hemoterapia”); JLO and RBS are supported by a grant from the University of Salamanca (“Contrato postdoctoral programa II” and “Contrato postdoctoral programa II 2020-21”, respectively). The authors gratefully acknowledge Professor Daniel Catovsky, the Chief Investigator of the UK LRF CLL4 trial, and all the patients and clinicians that contributed. The trial was funded by a core grant from Leukaemia and Lymphoma

Research, and subsequent molecular characterization was supported by Bloodwise (11052, 12036), the Kay Kendall Leukaemia Fund (873), and Cancer Research UK (C34999/A18087, ECMC C24563/A15581).

We thank Sara González, Cristina Miguel, Irene Rodríguez, Almudena Martín-Martín, Teresa Prieto, M^l Ángeles Ramos, Filomena Corral, M^l Almudena Martín, Ana Díaz, Ana Simón, María del Pozo, Isabel M Isidro, Vanesa Gutiérrez, Sandra Pujante and M^l Ángeles Hernández from the Cancer Research Center of Salamanca, Spain for their technical support. We are grateful to Ángel Prieto, Ana I García and Sara Armenteros, María Luz Sánchez and María Carmen Macías from the Microscopy Unit, Cytometry Unit and Molecular Pathology Unit, respectively, from the Cancer Research Center of Salamanca for their technical assistance. We are deeply grateful to Lucía Torío for her help in the functional studies. We thank Javier Borrajo from the Service of NUCLEUS, University of Salamanca for his help with the irradiation experiments and Luis Muñoz and all the members from the Animal Experimentation Research Center from the University of Salamanca.

CONFLICT OF INTEREST

The authors declare that there is no conflict of interest that could be perceived as prejudicing the impartiality of the research reported.

ETHICS COMMITTEE APPROVAL

The present study was approved by the local ethics committee (Comité Ético de Investigación Clínica, Hospital Universitario de Salamanca). Written informed consent was obtained from all participants before they entered the study.

AUTHOR CONTRIBUTIONS

Miguel Quijada-Álamo designed experiments, performed CRISPR/Cas9 generation of engineered CLL cell lines, carried out functional studies, analyzed the data, and wrote the paper. Claudia Pérez-Carretero designed experiments, performed sample selection, carried out NGS experiments, analyzed the data, and wrote the paper. María Hernández-Sánchez designed CRISPR/Cas9 experiments and together with Ana-Eugenia Rodríguez-Vicente contributed to NGS experiments, data analysis, and interpretation of the results. Ana-Belén Herrero designed DNA damage and repair experiments and contributed to data analysis. Jesús-María Hernández-Sánchez, Marta Martín-Izquierdo, and Sandra Santos-Mínguez performed NGS studies and data analysis. Mónica del Rey contributed in the revision experiments and analyses. Teresa González performed sample selection and provided clinical data. Araceli Rubio-Martínez, Alfonso García de Coca, Julio

Dávila-Valls, and José-Ángel Hernández-Rivas provided patient samples and clinical data. Helen Parker and Jonathan C. Strefford provided biological and clinical data from the validation cohort. Rocío Benito contributed to data analysis and interpretation of the results. José-Luis Ordóñez performed functional experiments and together with Jesús-María Hernández-Rivas conceived the study, designed the experiments, supervised the research, and critically reviewed the manuscript. All authors discussed the results and revised the manuscript.

DATA AVAILABILITY STATEMENT

The data that support the findings of this study are available from the corresponding author upon reasonable request.

ORCID

Jesús-María Hernández-Rivas  <https://orcid.org/0000-0002-9661-9371>

REFERENCES

- Chiorazzi N, Rai KR, Ferrarini M. Chronic lymphocytic leukemia. *N Engl J Med*. 2005;352(8):804–815.
- Hallek M, Cheson BD, Catovsky D, et al. iwCLL guidelines for diagnosis, indications for treatment, response assessment, and supportive management of CLL. *Blood*. 2018;131(25):2745–2760.
- Döhner H, Stilgenbauer S, Benner A, et al. Genomic aberrations and survival in chronic lymphocytic leukemia. *N Engl J Med*. 2000;343(26):1910–1916.
- Landau DA, Tausch E, Taylor-Weiner AN, et al. Mutations driving CLL and their evolution in progression and relapse. *Nature*. 2015;526(7574):525–530.
- Puente XS, Beà S, Valdés-Mas R, et al. Non-coding recurrent mutations in chronic lymphocytic leukaemia. *Nature*. 2015;526(7574):519–524.
- Döhner H, Stilgenbauer S, James MR, et al. 11q deletions identify a new subset of B-cell chronic lymphocytic leukemia characterized by extensive nodal involvement and inferior prognosis. *Blood*. 1997;89(7):2516–2522.
- Neilson JR, Auer R, White D, et al. Deletions at 11q identify a subset of patients with typical CLL who show consistent disease progression and reduced survival. *Leukemia*. 1997;11(11):1929–1932.
- Stilgenbauer S, Liebisch P, James MR, et al. Molecular cytogenetic delineation of a novel critical genomic region in chromosome bands 11q22.3-923.1 in lymphoproliferative disorders. *Proc Natl Acad Sci U S A*. 1996;93(21):11837–11841.
- Gunnarsson R, Mansouri L, Isaksson A, et al. Array-based genomic screening at diagnosis and during follow-up in chronic lymphocytic leukemia. *Haematologica*. 2011;96(8):1161–1169.
- Rose-Zerilli MJ, Forster J, Parker H, et al. ATM mutation rather than BIRC3 deletion and/or mutation predicts reduced survival in 11q-deleted chronic lymphocytic leukemia: data from the UK LRF CLL4 trial. *Haematologica*. 2014;99(4):736–742.
- Lavin MF. Ataxia-telangiectasia: from a rare disorder to a paradigm for cell signalling and cancer. *Nat Rev Mol Cell Biol*. 2008;9(10):759–769.

12. Van Dyke DL, Werner L, Rassenti LZ, et al. The Dohner fluorescence in situ hybridization prognostic classification of chronic lymphocytic leukaemia (CLL): the CLL research consortium experience. *Br J Haematol*. 2016;173(1):105–113.
13. Hernández JÁ, Hernández-Sánchez M, Rodríguez-Vicente AE, et al. A low frequency of losses in 11q chromosome is associated with better outcome and lower rate of genomic mutations in patients with chronic lymphocytic leukemia. *PLoS One*. 2015;10(11):e0143073.
14. Stankovic T, Skowronska A. The role of ATM mutations and 11q deletions in disease progression in chronic lymphocytic leukemia. *Leuk Lymphoma*. 2014;55(6):1227–1239.
15. Yin S, Gambe RG, Sun J, et al. A murine model of chronic lymphocytic leukemia based on B cell-restricted expression of Sf3b1 mutation and ATM deletion. *Cancer Cell*. 2019;35(2):283–296.
16. Austen B, Skowronska A, Baker C, et al. Mutation status of the residual ATM allele is an important determinant of the cellular response to chemotherapy and survival in patients with chronic lymphocytic leukemia containing an 11q deletion. *J Clin Oncol*. 2007;25(34):5448–5457.
17. Skowronska A, Parker A, Ahmed G, et al. Biallelic ATM inactivation significantly reduces survival in patients treated on the United Kingdom Leukemia Research Fund Chronic Lymphocytic Leukemia 4 trial. *J Clin Oncol*. 2012;30(36):4524–4532.
18. Baliakas P, Hadzidimitriou A, Sutton LA, et al. Recurrent mutations refine prognosis in chronic lymphocytic leukemia. *Leukemia*. 2015;29(2):329–336.
19. Lozano-Santos C, García-Vela JA, Pérez-Sanz N, et al. Biallelic ATM alterations detected at diagnosis identify a subset of treatment-naïve chronic lymphocytic leukemia patients with reduced overall survival similar to patients with p53 deletion. *Leuk Lymphoma*. 2017;58(4):859–865.
20. Malcikova J, Smardova J, Rocnova L, et al. Monoallelic and biallelic inactivation of TP53 gene in chronic lymphocytic leukemia: selection, impact on survival, and response to DNA damage. *Blood*. 2009;114(26):5307–5314.
21. Zenz T, Eichhorst B, Busch R, et al. TP53 mutation and survival in chronic lymphocytic leukemia. *J Clin Oncol*. 2010;28(29):4473–4479.
22. Zenz T, Häbe S, Denzel T, et al. Detailed analysis of p53 pathway defects in fludarabine-refractory chronic lymphocytic leukemia (CLL): dissecting the contribution of 17p deletion, TP53 mutation, p53-p21 dysfunction, and miR34a in a prospective clinical trial. *Blood*. 2009;114(13):2589–2597.
23. Stilgenbauer S, Schnaiter A, Paschka P, et al. Gene mutations and treatment outcome in chronic lymphocytic leukemia: results from the CLL8 trial. *Blood*. 2014;123(21):3247–3254.
24. Hafner A, Bulyk ML, Jambhekar A, Lahav G. The multiple mechanisms that regulate p53 activity and cell fate. *Nat Rev Mol Cell Biol*. 2019;20(4):199–210.
25. Campo E, Cymbalista F, Ghia P, et al. TP53 aberrations in chronic lymphocytic leukemia: an overview of the clinical implications of improved diagnostics. *Haematologica*. 2018;103(12):1956–1968.
26. Yu L, Kim HT, Kasar SN, et al. Survival of Del17p CLL depends on genomic complexity and somatic mutation. *Clin Cancer Res*. 2017;23(3):735–745.
27. Pettitt AR, Sherrington PD, Stewart G, Cawley JC, Malcolm R Taylor A, Stankovic T. p53 dysfunction in B-cell chronic lymphocytic leukemia: inactivation of ATM as an alternative to TP53 mutation. *Blood*. 2001;98(3):814–822.
28. Greipp PT, Smoley SA, Viswanatha DS, et al. Patients with chronic lymphocytic leukaemia and clonal deletion of both 17p13.1 and 11q22.3 have a very poor prognosis. *Br J Haematol*. 2013;163(3):326–333.
29. Arruga F, Gizdic B, Bologna C, et al. Mutations in NOTCH1 PEST domain orchestrate CCL19-driven homing of chronic lymphocytic leukemia cells by modulating the tumor suppressor gene DUSP22. *Leukemia*. 2017;31(9):1882–1893.
30. Bretones G, Álvarez MG, Arango JR, et al. Altered patterns of global protein synthesis and translational fidelity in RPS15-mutated chronic lymphocytic leukemia. *Blood*. 2018;132(22):2375–2388.
31. Close V, Close W, Kugler SJ, et al. FBXW7 mutations reduce binding of NOTCH1, leading to cleaved NOTCH1 accumulation and target gene activation in CLL. *Blood*. 2019;133(8):830–839.
32. Quijada-Álamo M, Hernández-Sánchez M, Alonso-Pérez V, et al. CRISPR/Cas9-generated models uncover therapeutic vulnerabilities of del(11q) CLL cells to dual BCR and PARP inhibition. *Leukemia*. 2020;34(6):1599–1612.
33. Hernández-Sánchez M, Rodríguez-Vicente AE, González-Gascón Y, Marín I, et al. DNA damage response-related alterations define the genetic background of patients with chronic lymphocytic leukemia and chromosomal gains. *Exp Hematol*. 2019;72:9–13.
34. Sanjana NE, Shalem O, Zhang F. Improved vectors and genome-wide libraries for CRISPR screening. *Nat Methods*. 2014;11(8):783–784.
35. Doench JG, Hartenian E, Graham DB, et al. Rational design of highly active sgRNAs for CRISPR-Cas9-mediated gene inactivation. *Nat Biotechnol*. 2014;32(12):1262–1267.
36. Pliatsika V, Rigoutsos I. “Off-Spotter”: very fast and exhaustive enumeration of genomic lookalikes for designing CRISPR/Cas guide RNAs. *Biol Direct*. 2015;10(1):4.
37. Strasser-Wozak EM, Hartmann BL, Geley S, et al. Irradiation induces G2/M cell cycle arrest and apoptosis in p53-deficient lymphoblastic leukemia cells without affecting Bcl-2 and Bax expression. *Cell Death Differ*. 1998;5(8):687–693.
38. Kwok M, Davies N, Agathangelou A, et al. ATR inhibition induces synthetic lethality and overcomes chemoresistance in TP53- or ATM-defective chronic lymphocytic leukemia cells. *Blood*. 2016;127(5):582–595.
39. Rossi D, Fangazio M, Rasi S, et al. Disruption of BIRC3 associates with fludarabine chemoresistance in TP53 wild-type chronic lymphocytic leukemia. *Blood*. 2012;119(12):2854–2862.
40. Lazarian G, Guièze R, Wu CJ. Clinical implications of novel genomic discoveries in chronic lymphocytic leukemia. *J Clin Oncol*. 2017;35(9):984–993.
41. Brown JR, Porter DL, O’Brien SM. Novel treatments for chronic lymphocytic leukemia and moving forward. *Am Soc Clin Oncol Educ B*. 2014;34:e317–e325.
42. Woyach JA, Furman RR, Liu T-M, et al. Resistance mechanisms for the Bruton’s tyrosine kinase inhibitor ibrutinib. *N Engl J Med*. 2014;370(24):2286–2294.
43. Furman RR, Cheng S, Lu P, et al. Ibrutinib resistance in chronic lymphocytic leukemia. *N Engl J Med*. 2014;370(24):2352–2354.

44. Ahn IE, Underbayev C, Albitar A, et al. Clonal evolution leading to ibrutinib resistance in chronic lymphocytic leukemia. *Blood*. 2017;129(11):1469–1479.
45. Amin NA, Balasubramanian S, Saiya-Cork K, Shedden K, Hu N, Malek SN. Cell-intrinsic determinants of ibrutinib-induced apoptosis in chronic lymphocytic leukemia. *Clin Cancer Res*. 2017;23(4):1049–1059.
46. O'Brien S, Furman RR, Coutre S, et al. Single-agent ibrutinib in treatment-naïve and relapsed/refractory chronic lymphocytic leukemia: a 5-year experience. *Blood*. 2018;131(17):1910–1919.
47. Sharman JP, Coutre SE, Furman RR, et al. Final results of a randomized, phase III study of rituximab with or without idelalisib followed by open-label idelalisib in patients with relapsed chronic lymphocytic leukemia. *J Clin Oncol*. 2019;37(16):1391–1402.
48. Zelenetz AD, Barrientos JC, Brown JR, et al. Idelalisib or placebo in combination with bendamustine and rituximab in patients with relapsed or refractory chronic lymphocytic leukaemia: interim results from a phase 3, randomised, double-blind, placebo-controlled trial. *Lancet Oncol*. 2017;18(3):297–311.
49. Jones JA, Robak T, Brown JR, et al. Efficacy and safety of idelalisib in combination with ofatumumab for previously treated chronic lymphocytic leukaemia: an open-label, randomised phase 3 trial. *Lancet Haematol*. 2017;4(3):e114–e126.

SUPPORTING INFORMATION

Additional supporting information may be found online in the Supporting Information section at the end of the article.

How to cite this article: Quijada-Álamo M, Pérez-Carretero C, Hernández-Sánchez M, et al. Dissecting the role of *TP53* alterations in del(11q) chronic lymphocytic leukemia. *Clin Transl Med*. 2021;11:e304. <https://doi.org/10.1002/ctm2.304>

CHAPTER 4

Biological significance of monoallelic and biallelic *BIRC3* loss in del(11q) chronic lymphocytic leukemia progression

Miguel Quijada-Álamo^{1,2}, María Hernández-Sánchez^{1,2,3,4}, Ana-Eugenia Rodríguez-Vicente^{1,2}, Claudia Pérez-Carretero^{1,2}, Alberto Rodríguez-Sánchez^{1,2}, Marta Martín-Izquierdo^{1,2}, Verónica Alonso-Pérez^{1,2}, Ignacio García-Tuñón^{1,2}, José María Bastida², María Jesús Vidal-Manceñido⁵, Josefina Galende⁶, Carlos Aguilar⁷, José Antonio Queizán⁸, Isabel González-Gascón y Marín⁹, José-Ángel Hernández-Rivas⁹, Rocío Benito^{1,2}, José Luis Ordóñez^{1,2} and Jesús-María Hernández-Rivas^{1,2,10}

¹University of Salamanca, IBSAL, IBMCC, CSIC, Cancer Research Center, Salamanca, Spain. ²Department of Hematology, University Hospital of Salamanca, Salamanca, Spain. ³Department of Medical Oncology, Dana-Farber Cancer Institute, Boston, Massachusetts 02115, USA. ⁴Broad Institute of Harvard and MIT, Cambridge, Massachusetts 02142, USA. ⁵Department of Hematology, Hospital Virgen Blanca, León, Spain. ⁶Department of Hematology, Hospital del Bierzo, Ponferrada, Spain. ⁷Department of Hematology, Hospital Santa Bárbara, Soria, Spain. ⁸Department of Hematology, Hospital General de Segovia, Segovia, Spain. ⁹Department of Hematology, Hospital Universitario Infanta Leonor. Universidad Complutense, Madrid, Spain. ¹⁰Department of Medicine, University of Salamanca, Salamanca, Spain.

Blood Cancer Journal. 2021. In press

Biological significance of monoallelic and biallelic *BIRC3* loss in del(11q) chronic lymphocytic leukemia progression

Miguel Quijada-Álamo^{1,2}, María Hernández-Sánchez^{1,2,3,4}, Ana-Eugenia Rodríguez-Vicente^{1,2}, Claudia Pérez-Carretero^{1,2}, Alberto Rodríguez-Sánchez^{1,2}, Marta Martín-Izquierdo^{1,2}, Verónica Alonso-Pérez^{1,2}, Ignacio García-Tuñón^{1,2}, José María Bastida², María Jesús Vidal-Manceño⁵, Josefina Galende⁶, Carlos Aguilar⁷, José Antonio Queizán⁸, Isabel González-Gascón y Marín⁹, José-Ángel Hernández-Rivas⁹, Rocío Benito^{1,2}, José Luis Ordóñez^{1,2*} and Jesús-María Hernández-Rivas^{1,2,10*}

¹University of Salamanca, IBSAL, IBMCC, CSIC, Cancer Research Center, Salamanca, Spain.

²Department of Hematology, University Hospital of Salamanca, Salamanca, Spain.

³Department of Medical Oncology, Dana-Farber Cancer Institute, Boston, Massachusetts 02115, USA.

⁴Broad Institute of Harvard and MIT, Cambridge, Massachusetts 02142, USA

⁵Department of Hematology, Hospital Virgen Blanca, León, Spain.

⁶Department of Hematology, Hospital del Bierzo, Ponferrada, Spain.

⁷Department of Hematology, Hospital Santa Bárbara, Soria, Spain.

⁸Department of Hematology, Hospital General de Segovia, Segovia, Spain.

⁹Department of Hematology, Hospital Universitario Infanta Leonor. Universidad Complutense, Madrid, Spain.

¹⁰Department of Medicine, University of Salamanca, Salamanca, Spain

*JLO and JMHR contributed equally to this work

BIRC3 is monoallelically deleted in up to 80% of chronic lymphocytic leukemia (CLL) cases harboring del(11q). In addition, truncating mutations in the remaining allele of this gene can lead to *BIRC3* biallelic inactivation, which has been shown to be a marker for reduced survival in CLL. Nevertheless, the biological mechanisms by which these lesions could contribute to del(11q) CLL pathogenesis and progression are partially unexplored. We implemented the CRISPR/Cas9-editing system to generate isogenic CLL cell lines harboring del(11q) and/or *BIRC3* mutations, modeling monoallelic and biallelic *BIRC3* loss. Our results reveal that monoallelic *BIRC3* deletion in del(11q) cells promotes non-canonical NF-κB signaling activation via RelB-p52 nuclear translocation, being these effects allelic dose-dependent and therefore further enhanced in del(11q) cells with biallelic *BIRC3* loss. Moreover, we demonstrate *ex vivo* in primary cells that del(11q) cases including *BIRC3* within their deleted region show evidence of non-canonical NF-κB activation which correlates with high BCL2 levels and enhanced sensitivity to venetoclax. Furthermore, our results show that *BIRC3* mutations in del(11q) cells promote clonal advantage *in vitro* and accelerate leukemic progression in an *in vivo* xenograft model. Altogether, this work highlights the biological bases underlying disease progression of del(11q) CLL patients harboring *BIRC3* deletion and mutation.

Key words: *BIRC3*, del(11q), chronic lymphocytic leukemia, NF-κB signaling, CRISPR/Cas9

INTRODUCTION

Chronic lymphocytic leukemia (CLL) patients harboring 11q22.3 deletion (del(11q)) are characterized by the presence of bulky lymphadenopathy, rapid disease progression and short time to first treatment (TTFT) and overall survival (OS) (1–4), even in early stage Binet A CLL cases (5). The size of this deletion is heterogeneous, it can cover a region greater than 20 Mb in most of the patients, involving the loss of over a hundred genes (6). The minimal deleted region almost always includes *ATM*, a putative CLL driver gene and one of the key components of the DNA damage response signaling (7, 8). Another gene that has been hypothesized to also contribute to the pathobiology of del(11q) is *BIRC3*, which is located in the chromosomal band 11q22.2 and is entirely deleted in approximately 80% of del(11q) cases (9). In addition, it has been shown that *BIRC3* disruption through truncating mutations occurs recurrently in CLL, ranging from frequencies of 3-5% in untreated cohorts to a two-fold higher incidence in relapsed/refractory CLL patients (10–13). Interestingly, *BIRC3* mutations can appear in the remaining allele of approximately 10% of del(11q) patients with *BIRC3* monoallelic loss, resulting in a biallelic *BIRC3* inactivation (10, 12, 14). Recent studies have shown that biallelic inactivation of *BIRC3* is an independent prognostic marker of inferior TTFT and OS in CLL (14, 15). However, the clinical significance of *BIRC3* monoallelic mutations or deletion remains uncertain. Some studies have provided evidence of the clinical impact of *BIRC3* monoallelic mutations whereas others have not (10, 12, 14, 16–20). Moreover, *BIRC3* mutations have also been found to be enriched in fludarabine relapsed/refractory CLL cases in some cohorts

(10, 18), although the mechanistic insights by which *BIRC3* mutations could contribute to fludarabine resistance have not been elucidated.

Biologically, *BIRC3* is known to have a role as a negative regulator of the non-canonical NF- κ B signaling (21). This pathway, alongside with the canonical NF- κ B signaling, plays a key role on CLL pathogenesis, evolution and therapy response (22). The non-canonical signaling is initiated by tumor necrosis factor (TNF) signals engaging B-cell activation factor receptor (BAFFR), CD40, lymphotoxin β -receptor (LT β R) or receptor activator for NF- κ B (RANK) among others. In the absence of a stimulus, this pathway is kept inactive by the *BIRC3*-mediated ubiquitination and proteasomal degradation of NF- κ B-inducing kinase (NIK). Upon receptor stimulation, *BIRC3* is recruited to the active receptor complex and NIK is stabilized in the cytoplasm, promoting IKK α activation which in turn phosphorylates p100, leading to the proteasomal degradation of its C-terminus and the translocation of p52-RelB heterodimers into the nucleus to initiate NF- κ B-dependent transcription (23). In CLL, *BIRC3* mutations usually result in the loss of the E3 ubiquitin ligase domain essential for NIK targeting for proteasomal degradation, constitutively activating the non-canonical NF- κ B signaling in a ligand-independent manner (10). Nevertheless, the most frequent *BIRC3* alteration in CLL is monoallelic deletion of the entire gene through del(11q), being the functional consequences of this type of *BIRC3* monoallelic loss unexplored. In addition, it is unclear how biallelic *BIRC3* defects through del(11q) and *BIRC3* mutation in the remaining allele could contribute to a NF- κ B-dependent acceleration of CLL progression.

The implementation of novel genomic editing technologies into the study of CLL has opened exciting possibilities to interrogate the functional effects of multiple driver genetic alterations as well as how some of these events cooperate to drive CLL progression and therapy response (24–27). In this study, we used the CRISPR/Cas9 system to generate isogenic CLL derived cell lines harboring del(11q) and/or *BIRC3* mutations in the remaining allele. We show that monoallelic *BIRC3* loss through del(11q) is enough to promote NIK-mediated non-canonical NF- κ B signaling via p52-RelB nuclear translocation. *Ex vivo* experiments in primary del(11q) CLL cases revealed that del(11q) patients encompassing *BIRC3* within the deleted region had higher NIK levels as well as p52-RelB activity, which correlated with BCL2 overexpression. In addition, *BIRC3* loss-of-function mutations in del(11q) cells resulted in a higher activation of the non-canonical NF- κ B signaling cascade, ultimately leading to increased clonal advantage *in vitro* and acceleration of leukemic progression in an *in vivo* xenograft model. Thus, our study provides novel biological insights about the role of *BIRC3* deletion and mutation in CLL evolution and progression.

METHODS

CRISPR/Cas9-mediated engineering of CLL cell lines

HG3 and MEC1 Cas9-expressing cell lines (HG3-Cas9 and MEC1-Cas9) were previously generated and tested for Cas9 activity (27). Single-guide RNAs (sgRNAs) targeting *BIRC3* (exons 2 or 7) were designed using the online CRISPR tool (<http://crispr.mit.edu/>), based on the predicted on-target efficiency and the lowest off-

target effects. In addition, a sgRNA designed not to target the human genome was used as a negative control. SgRNAs targeting *BIRC3* were cloned into pLKO5.sgRNA.EFS.GFP (Addgene_#57822) plasmids and control sgRNAs were cloned in pLKO5.sgRNA.EFS.tRFP (Addgene_#57823). Sequences of the selected sgRNAs are detailed in Supplementary Table S1. The procedures and sgRNAs used for the generation of del(11q) and *TP53* mutations in HG3 cells were previously described (27, 28). pLKO5 vectors carrying the desired sgRNAs were transduced into HG3-Cas9 and MEC1-Cas9 cells and single-cell flow-sorted clones were expanded and screened. At least three different clones harboring loss-of-function mutations were chosen for each CRISPR-generated cell line to perform functional studies.

Primary CLL samples

Viable cryopreserved peripheral blood mononuclear cells (PBMCs) from 22 CLL patients were used in the *ex vivo* studies. PBMCs were isolated by Ficoll-Paque Plus density gradient media (GE Healthcare, Life Sciences) and a complete immunophenotypic analysis was performed in all samples by flow cytometry. Only samples with a CD19+/CD5+ fraction greater than 85% were included in the study. Supplementary Table S2 summarizes the main biological characteristics of CLL patients. Research was conducted in accordance of the Declaration of Helsinki and prior approval by the Bioethics Committee from our institution. Written informed consent was obtained from all patients.

Next-generation sequencing (NGS) data from the primary CLLs used in the *ex vivo* experiments are detailed in Supplementary Table

S3 and Supplementary Fig. S1. A custom NGS panel was applied and analyzed as previously reported (27, 29). Full details about NGS procedure and analysis can be found in Supplementary Information.

NF- κ B family members activity ELISA

Canonical (p65/RelA, NF- κ B1 p50, c-Rel) and non-canonical (NF- κ B2 p52, RelB) NF- κ B activity of nuclear extracts of HG3 and MEC1 clones and lysates from primary CLL samples was measured using the NF- κ B Transcription Factor Assay Kit (Colorimetric) (Abcam, ab207216) following manufacturer's instructions. Briefly, an oligonucleotide containing the NF- κ B consensus site (5'-GGGACTTCC-3') has been immobilized onto a 96-well plate. Active NF- κ B subunits present on the nuclear extracts specifically bind this oligonucleotide and p65, p50, c-Rel, p52 or RelB subunits are recognized by using specific primary antibodies accessible only when NF- κ B is activated and bound to its target DNA.

***Ex vivo* co-culture conditions**

HS-5 stromal cells were seeded 24 hours prior to the *ex vivo* experiments at a concentration of 7.5×10^4 cells/well in a 6-well plate. On the following day, primary CLL cells were viably thawed and resuspended in RPMI 1640 medium (Life Technologies) supplemented with 10% FBS, 1% penicillin/streptomycin and 1.5 μ g/mL CpG ODN (Sigma-Aldrich) plus 50 ng/mL IL-2 (Peprotech) and subsequently seeded onto the HS-5 cell layer at a co-culture ratio of 100:1 (7.5×10^6 CLL cells/well) (30). CLL cells were carefully detached and lysed 24 hours after co-culture and proteins were subjected to NF- κ B activity assays and/or immunoblot. CpG stimulation was

chosen in order not to involve receptors directly implicated in non-canonical NF- κ B activation such as CD40 or BAFFR.

Xenograft experiments

Animal studies were conducted in accordance with the Spanish and European Union guidelines for animal experimentation (RD53/2013, Directive- 2010/63/UE, respectively) and received prior approval from the Bioethics Committee of our institution.

For intravenous xenograft experiments, 20 four-to-five-week-old female NSG mice were used for injection of HG3 cells harboring del(11q) and/or *BIRC3* mutations ($n=5$ /each group). 3×10^6 cells were resuspended in 100 μ L of RPMI media and injected into the tail vein of the mice. 14 days after cell injection, mice were culled and spleens were subjected to FACS and immunohistochemistry analyses. For FACS analysis, spleens were lysed with erythrocyte lysis buffer, and the remaining cells were then washed twice in PBS. Samples were stained with fluorophore-conjugated antibodies against mouse-CD45 (PerCP-Cy5.5, BD Biosciences) and human-CD45 (hCD45) (CF Blue, Immunostep). Data were obtained on a FACS Aria flow cytometer and analyzed with FlowJo software. Full details about subcutaneous xenografts in the Supplementary Information.

Statistics

Statistical analyses were carried out using GraphPad Prism software v6 (GraphPad Software). Otherwise specified, data are summarized as the mean \pm standard deviation (SD). Student's t test, Mann-Whitney, ANOVA or Kruskal-Wallis tests were used to determine statistical significance. *P* values lower than 0.05

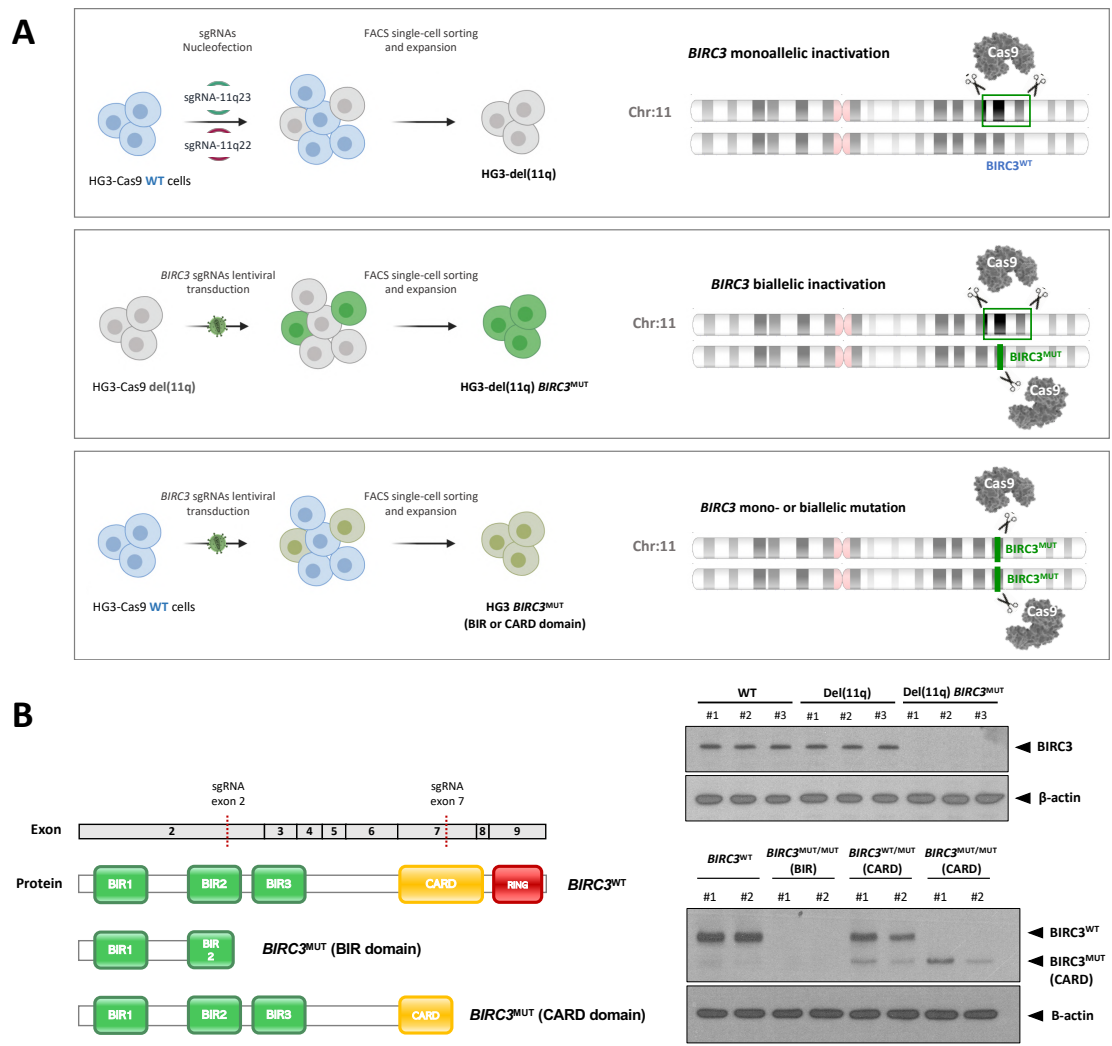


Figure 1. Generation of isogenic CRISPR/Cas9-edited CLL cell lines harboring del(11q) and/or *BIRC3* mutations. (A) Experimental design for the CRISPR/Cas9-mediated generation of *BIRC3*-related alterations in the Cas9-expressing HG3 CLL-derived cell line. Upper panel represents the design for monoallelic del(11q) (including monoallelic *BIRC3* loss) by the introduction of sgRNAs targeting 11q22.1 and 11q23.3. Middle panel displays the introduction of *BIRC3* mutations in HG3-del(11q) cells by the lentiviral transduction of a *BIRC3*-targeting sgRNA, generating HG3 cells with biallelic *BIRC3* loss through del(11q) and mutation in the remaining allele. Lower panel shows the steps required for the generation of *BIRC3* mutations (either in *BIRC3* exon 2 or exon 7) in HG3 cells without del(11q). The presence of del(11q) and/or *BIRC3* mutations was validated by FISH and Sanger sequencing, respectively. In total, at least three independent clones per condition were generated. (B) Left panel: *BIRC3* WT and mutant protein diagram indicating the protein domains and the corresponding exons of the *BIRC3* coding sequence included in each *BIRC3*^{MUT}-generated cell line. Right panel: *BIRC3* western blot analysis of HG3-edited single-cell clones. β -actin was used as loading control.

were considered as statistically significant. At least three independent clones per condition were used in the functional studies.

Supplementary Methods

Supplementary Methods section includes detailed protocols of cell lines, culture conditions, drugs and reagents, NGS, FISH, subcellular fractionation and western blot, viability, apoptosis and cell cycle analyses, *in*

in vitro clonal competition assays, subcutaneous *in vivo* xenografts and immunohistochemistry.

RESULTS

CRISPR/Cas9-mediated generation of isogenic CLL cell lines harboring del(11q) and/or *BIRC3* mutations

In order to understand how monoallelic or biallelic *BIRC3* loss contribute to the pathobiology of del(11q) CLL, we used the CRISPR/Cas9-editing technology to model these alterations in an *in vitro* system. For this purpose, we selected HG3 and MEC1 CLL derived cell lines. HG3 is diploid for chromosome 11 and has wild type (WT) *BIRC3* gene. sgRNAs targeting chromosomal bands 11q22.1 and 11q23.3 were introduced in Cas9-expressing HG3 cells, generating an isogenic HG3 CLL cell line harboring a ~17 Mb monoallelic del(11q) (HG3-del(11q)) encompassing *BIRC3* gene among others (27). sgRNAs specifically targeting *BIRC3* (exon 2) were then introduced in HG3-del(11q) cells in order to induce *BIRC3* truncating mutations (*BIRC3*^{MUT}) in the remaining WT allele, generating HG3-del(11q) *BIRC3*^{MUT} isogenic cell lines (Fig. 1a), mimicking the *BIRC3* biallelic loss through del(11q) and mutation observed in high-risk CLL patients. Furthermore, we also generated HG3 cell lines harboring only *BIRC3* mutation (HG3 *BIRC3*^{MUT}) following the same strategy (Fig. 1a). *BIRC3* mutations were generated in a monoallelic or a biallelic fashion either in *BIRC3* exon 2 or exon 7, having as a consequence the truncation of the BIR or CARD *BIRC3* protein domains, respectively (Fig. 1b, left panel), emulating the type of *BIRC3* mutations mainly detected in CLL (12, 16). *BIRC3* protein expression was evaluated by western blot in all the generated clones, showing that *BIRC3* levels

were absent in cells harboring truncating mutations in the exon 2 (BIR domain) or detecting a truncated form of *BIRC3* in those clones harboring exon 7 mutations (CARD domain) (Fig. 1b; right panel).

In parallel, we used the MEC1 cell line as a model to study the *BIRC3* allelic dose effects in CLL. Parental MEC1 cells harbor a monoallelic *BIRC3* deletion (MEC1 *BIRC3*^{DEL/WT}) as indicated by NGS copy number analysis (Supplementary Fig. S1). We also introduced sgRNAs targeting *BIRC3* (exon 2) following the previous approach, generating MEC1 cell lines harboring biallelic *BIRC3* loss through deletion and mutation (MEC1 *BIRC3*^{DEL/MUT}) (Supplementary Fig. S2).

***BIRC3* loss through del(11q) promotes p52-RelB nuclear translocation and activation of the non-canonical NF- κ B signaling downstream targets**

Considering the role of *BIRC3* in the NF- κ B signaling (21, 31), we assessed the impact of monoallelic and biallelic *BIRC3* loss through del(11q) and/or mutation in this pathway using our CRISPR/Cas9-engineered cell lines. We first analyzed the nuclear DNA-binding activity of the main NF- κ B transcription factors implicated in both the canonical and non-canonical pathway. Regarding the canonical signaling, we did not observe significant changes in the activity of p65 and c-Rel. However, HG3-del(11q) *BIRC3*^{MUT} cells showed a significant increase of p50 nuclear activity in comparison to HG3^{WT} cells (Fig. 2a). Conversely, monoallelic *BIRC3* loss in HG3-del(11q) cells resulted in a marked increase of p52 and RelB activity, being this effect further enhanced in HG3-del(11q) *BIRC3*^{MUT} cells (Fig. 2a). These results were also confirmed in HG3 in all *BIRC3*^{MUT} clones (Supplementary Fig. S3a), confirming that either truncating mutations in

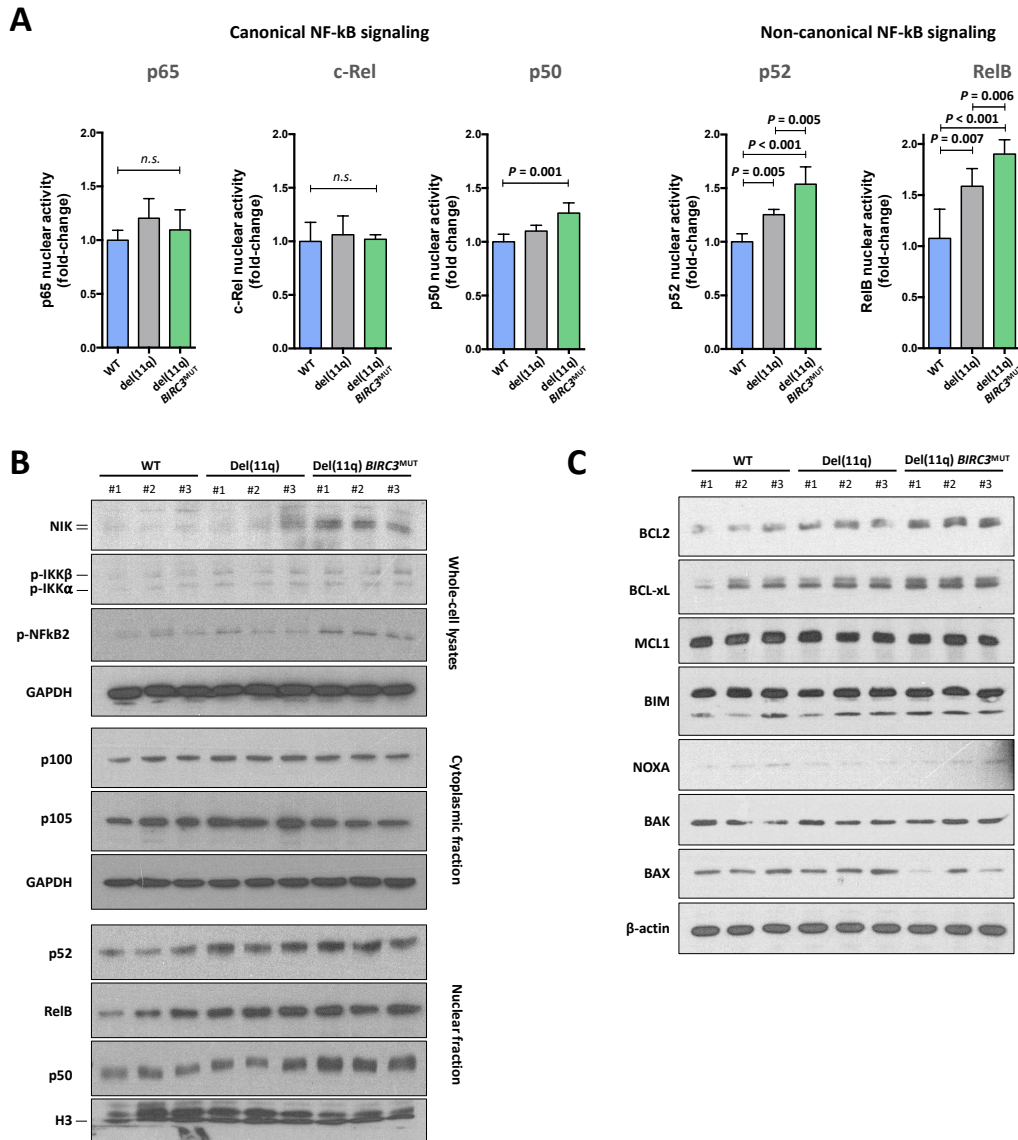


Figure 2. Evaluation of canonical and non-canonical NF-κB activity in del(11q)/BIRC3-deficient CRISPR/Cas9-engineered CLL cells. (A) ELISA measurement of relative NF-κB family transcription factor DNA-binding activity in nuclear extracts from HG3-edited clones. Left panel shows DNA-binding activity of NF-κB transcription factors involved in the canonical signaling (p65, c-Rel and p50). Right panel displays the DNA-binding activity of non-canonical NF-κB transcription factors (p52 and RelB). Data are represented as the mean ± SD. **(B)** Whole-cell, cytoplasmic and nuclear lysates of HG3-del(11q) clones analyzed by immunoblotting for NIK, p-IKKα/β, p-NF-κB2, NF-κB2 (p100/p52), NF-κB1 (p105/p50) and RelB proteins. GAPDH was used as loading control for whole-cell and cytoplasmic lysates and H3 was used as loading control for nuclear extracts. Relative quantification for each protein (mean of three clones per condition) is depicted in Supplementary Fig. 3b. **(C)** Whole-cell lysates from HG3^{WT}, HG3-del(11q) and HG3-del(11q) BIRC3^{MUT} analyzed by immunoblotting for BCL2 family members: BCL2, BCL-xL, MCL1, BIM, NOXA, BAK and BAX. β-actin was used as loading control. Relative quantification for each protein (mean of three clones per condition) is detailed in Supplementary Fig. 4a.

the BIR or CARD domains have the same functional consequence on the non-canonical

NF-κB signaling. Additional characterization of proteins involved in the non-canonical NF-κB

signaling by western blot revealed that monoallelic, and to a greater extent, biallelic *BIRC3* loss resulted NIK cellular stabilization and increased levels of phosphorylated IKK α/β and NF- κ B2, in line with a higher p52 and RelB accumulation in the nucleus (Fig. 2b; Supplementary Fig. S3b). Furthermore, we corroborated an increase of p50 nuclear levels in the nucleus of HG3-del(11q) *BIRC3*^{MUT} cells (Fig. 2b; Supplementary Fig. S3b).

To validate these results in an independent CLL cell line, NF- κ B activity as well as NIK and p52 levels were analyzed in MEC1 cells. As expected, MEC1 *BIRC3*^{DEL/MUT} clones likewise presented higher p52, RelB and p50 activity rates, NIK stabilization and accumulation of p52 in the nucleus than MEC1 *BIRC3*^{DEL/WT} cells (Supplementary Fig. S3c, d).

Given that activation of the non-canonical signaling has been shown to upregulate some anti-apoptotic proteins such as BCL2 and BCL-xL (32, 33), we next assessed the protein levels of such these targets in our CRISPR/Cas9-edited cell lines in order to determine the impact of monoallelic or biallelic *BIRC3* loss in the regulation of these proteins expression. Interestingly, HG3-del(11q) *BIRC3*^{MUT} CLL cell lines showed higher levels of BCL2 and BCL-xL, alongside to reduced levels of pro-apoptotic protein BAX, whereas no changes were observed regarding MCL1 or pro-apoptotic family members such as BIM, BAK and NOXA (Fig. 2c; Supplementary Fig. S4a). To test whether these increased levels of anti-apoptotic proteins were the result of *BIRC3*-mediated non-canonical signaling activation, cells were treated with a NIK small molecule inhibitor (NIK SMI1) (34), showing that NIK-dependent inhibition of p100/p52 processing translated into

downregulation of BCL2 and BCL-xL protein expression in HG3-del(11q) *BIRC3*^{MUT} cells (Supplemental Figure S4b).

***BIRC3*-deleted primary del(11q) CLL cells show enhanced non-canonical NF- κ B activity which correlates with high BCL2 levels**

In order to validate whether the results obtained in our CRISPR/Cas9-generated models could resemble the actual biology of *BIRC3*-deleted del(11q) CLL patients, we tested the DNA-binding activity of non-canonical NF- κ B transcription factors in a cohort of 22 CLL cases ($n = 11$ *BIRC3*^{WT}; $n = 11$ *BIRC3*-deleted through del(11q) or mutation) (Supplementary Table S2) in the absence or presence of stromal + CpG + IL-2 stimulation. Remarkably, stimulated *BIRC3*-deleted CLL cells showed higher p52 activity than *BIRC3*^{WT} cases (Fig. 3a; left panel), in line with the results observed in HG3-del(11q) cells. To a lesser extent, *BIRC3*-deleted cases also showed a trend of higher RelB activity than *BIRC3*^{WT} cells (Fig. 3a, left panel). In addition, focusing on the subgroup of patients harboring del(11q), we could observe a significant correlation between the percentage of *BIRC3*-deleted cells and p52 activity (Fig. 3a, right panel), further evidencing the NF- κ B-related effect of *BIRC3* monoallelic loss in del(11q) cases.

Next, we performed western blot analyses in a homogenous cohort of del(11q) samples including or not including *BIRC3* within the deleted region ($n = 4$, del(11q)/*BIRC3* deleted; $n = 3$, del(11q)/*BIRC3* undeleted). Interestingly, del(11q)/*BIRC3* deleted cases presented high levels of stabilized NIK, resulting in a marked NF- κ B2 p52 processing, which was virtually absent in del(11q)/*BIRC3* undeleted cases (Fig. 3b). Indeed, there was a clear correlation between

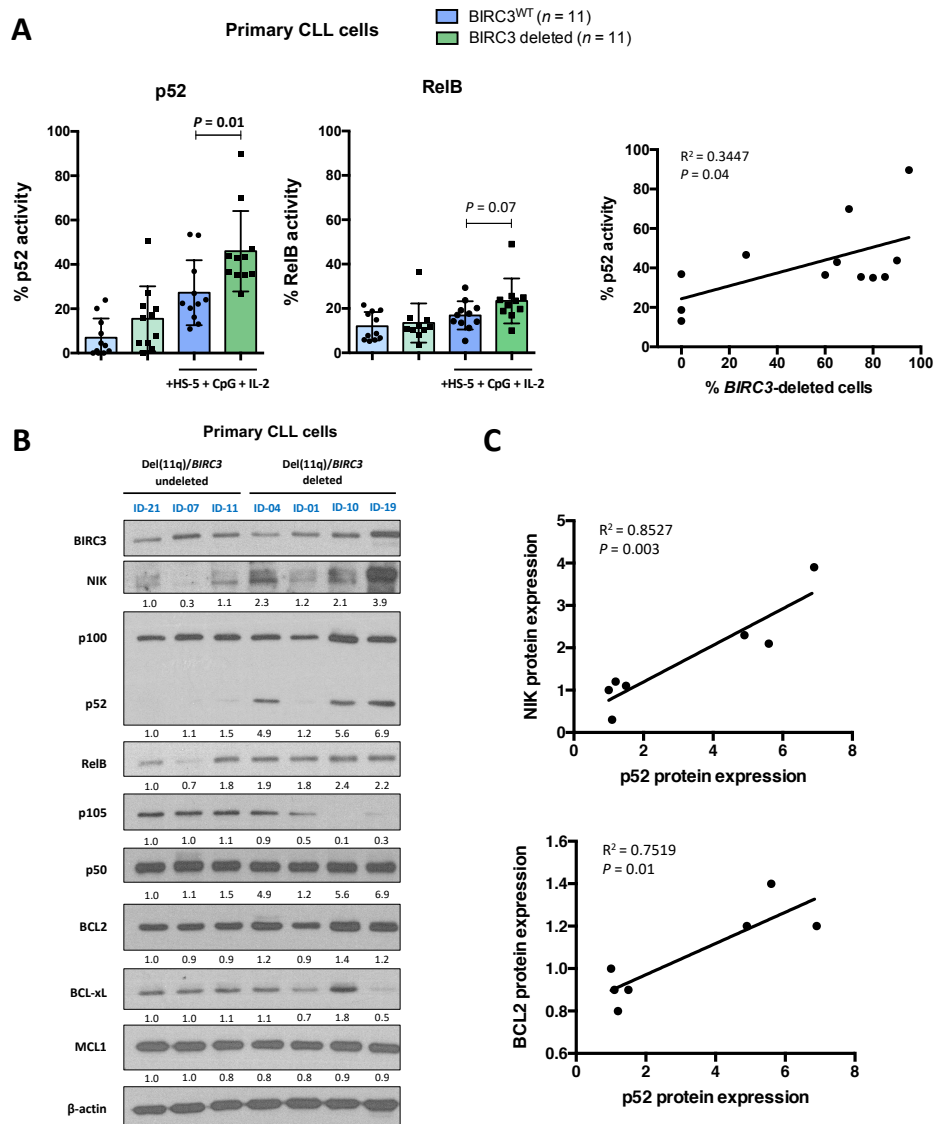


Figure 3. Effects of *BIRC3* loss in NF- κ B activity and *BCL2* levels of del(11q) primary CLL cells. (A) Left panel: ELISA measurement of relative NF- κ B2 p52 and RelB DNA-binding activity in cell lysates from *BIRC3*^{WT} (including both non-del(11q) or del(11q) without *BIRC3* loss) ($n = 11$) and *BIRC3*-deleted ($n = 11$) primary CLL samples stimulated to proliferate with HS-5 cells, 1.5 μ g/mL CpG and 50 ng/mL IL-2 or without stimulation. Proteins were extracted 24 hours after co-culture. Data are represented as the mean \pm SD. Right panel: correlation between the percentage of *BIRC3*-deleted cells in del(11q) patients (by integrating FISH and NGS data) and relative p52 activity taken from DNA-binding activity assays. Full details about cytogenetics and mutational status of the primary CLL cells used in the experiments are summarized in Supplementary Table S2. (B) Whole-cell lysates from stimulated CLL primary samples harboring del(11q) not involving *BIRC3* (del(11q)/*BIRC3*-undeleted) (ID-21, ID-07, ID-11) and del(11q) involving *BIRC3* (del(11q)/*BIRC3* deleted) (ID-04, ID-01, ID-10, ID-19) primary CLL samples were analyzed by immunoblotting for *BIRC3*, NIK, NF- κ B2 (p100/p52), RelB, NF- κ B1 (p105/p50), *BCL2*, *BCL-xL* and *MCL1* proteins. β -actin was used as loading control. (C) Correlation between p52 protein levels and NIK (left panel) or *BCL2* (right panel) protein levels from the patients analyzed by immunoblot.

NIK and p52 levels in these patients (Fig. 3c, upper panel). Of note, del(11q)/*BIRC3* deleted

cases also showed increased levels of RelB and a reduction of NF- κ B1 p105 precursor levels,

although we did not observe differences in p50 protein expression between these groups (Fig. 3b). In addition, among anti-apoptotic BCL2 family members, del(11q)/*BIRC3* deleted cases showed higher BCL2 protein expression than del(11q)/*BIRC3* undeleted cases (Fig. 3b), which correlated to the amount of p52 levels in these patients (Fig. 3c, lower panel).

Biallelic *BIRC3* loss confers sensitivity to BCL2 and BCL-xL inhibition *in vitro*

Considering the effects of *BIRC3* loss in the upregulation of some anti-apoptotic family members, we next evaluated the response of the isogenic CRISPR/Cas9 HG3 clones to selective BCL2, BCL-xL or MCL1 inhibition. BCL2 inhibition with venetoclax (ABT-199) highlighted a higher sensitivity of HG3-del(11q) *BIRC3*^{MUT} cells than HG3^{WT} cells (Fig. 4a), in line with the

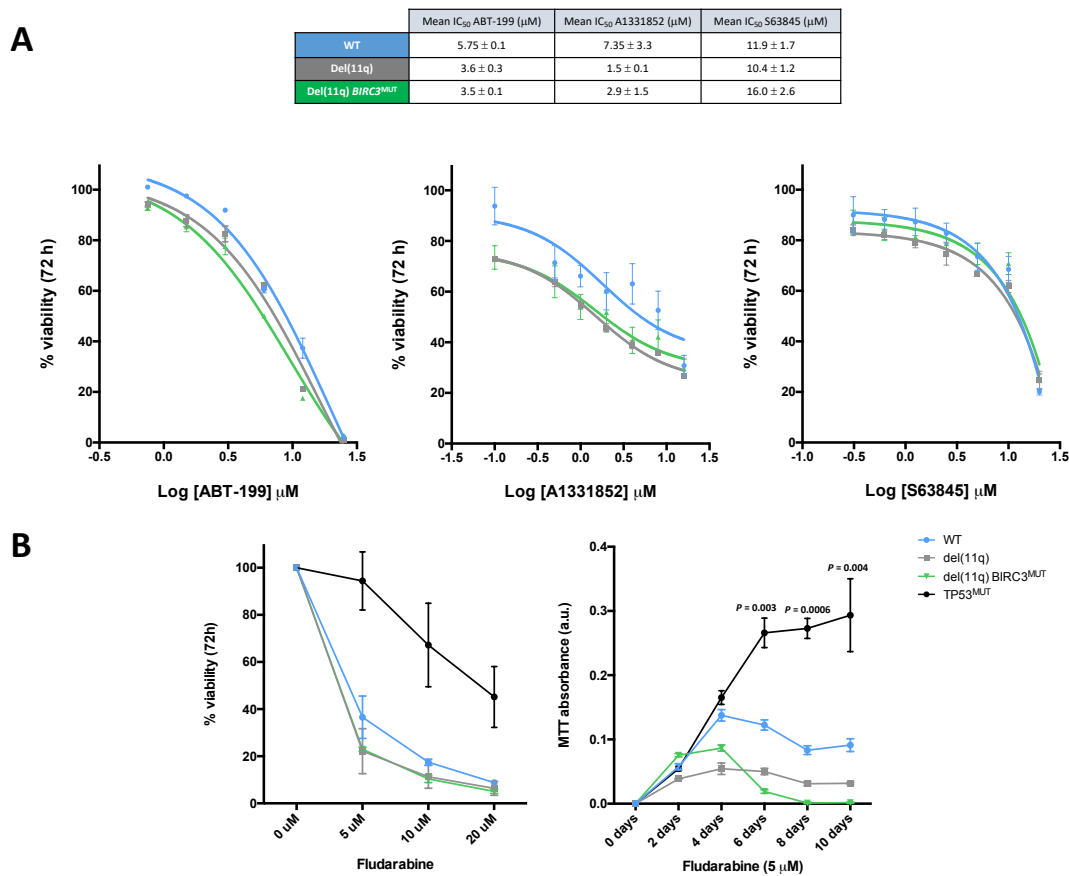


Figure 4. Cell viability studies of del(11q)/*BIRC3*-mutated cell lines in response to BCL2, BCL-xL, MCL1 inhibition or fludarabine treatment. (A) Dose-response curves of HG3^{WT}, HG3-del(11q) and HG3-del(11q) *BIRC3*^{MUT} clones treated with venetoclax (ABT-199; BCL2 inhibitor, left panel), A1331852 (BCL-xL inhibitor; middle panel) and S63845 (MCL1 inhibitor, right panel). Cell viability was assessed by MTT assay after 72 hours and surviving fraction is expressed relative to DMSO control. Data is summarized as mean ± SEM. **(B)** Left panel: HG3-edited clones were treated with escalating doses of fludarabine and cell viability was assessed by MTT assay after 72 hours. Surviving fraction is expressed relative to DMSO control. Data is summarized as the mean ± SD. Right panel: HG3-edited clones were treated with fludarabine at a concentration of 5 μM. Cell viability was assessed by MTT every 2 days up to 10 days. Proliferation rates are presented as MTT absorbance units, and data is shown as mean ± SD. *P*-values indicate differences between HG3^{WT} and HG3 *TP53*^{MUT} clones.

observed non-canonical NF- κ B-dependent BCL2 upregulation of these cell lines. In addition, HG3-del(11q) and HG3-del(11q) *BIRC3*^{MUT} cells were also more sensitive to BCL-xL inhibition by A1331852 than HG3^{WT} cells (Fig. 4a). Contrarily, monoallelic or biallelic *BIRC3* loss in HG3 cells did not seem to influence the response to MCL1 inhibition by S63845 (Fig. 4a), consistently with our observations regarding MCL1 protein levels. Furthermore, we also tested the response of these cell lines to the BTK inhibitor ibrutinib, showing that HG3-del(11q) *BIRC3*^{MUT} cells were slightly less sensitive in comparison to HG3^{WT} cells (Supplementary Fig. S5a).

Moreover, since *BIRC3* disruption in CLL patients has been associated with fludarabine refractoriness even in *TP53* wild-type CLLs (10), we tested HG3-del(11q) clones (with or without *BIRC3* disruption) for evidence of resistance to fludarabine treatment. HG3 *TP53*^{MUT} clones, also generated by CRISPR/Cas9, were used as positive controls for fludarabine resistance. Interestingly, after 72 hours of fludarabine treatment, only *TP53*^{MUT} clones presented marked resistance (by MTT assay) whereas HG3-del(11q) *BIRC3*^{MUT} clones showed the same sensitivity as HG3^{WT} cells (Fig. 4b, left panel). Longer drug exposures were also tested, and we found no significant resistance of *BIRC3* disrupted clones (Fig. 4b, right panel). Further support for fludarabine treatment-induced apoptosis in *BIRC3*-deficient clones was observed through the appearance of a sub-G₀ peak in cell cycle profiles and annexin studies (Supplementary Fig. S5b, c).

Biallelic *BIRC3* loss in del(11q) CLL cells favors clonal advantage *in vitro*

We next hypothesized that the effects of *BIRC3* loss in the NF- κ B signaling and apoptosis may have an impact on CLL evolution and progression. For this purpose, proliferation assays were performed to characterize the consequences of the CRISPR/Cas9-generated alterations in CLL expansion. We noted that HG3-del(11q) *BIRC3*^{MUT} cells showed enhanced viability and growth than HG3-del(11q) and HG3^{WT} cells (Fig. 5a, left panel; Supplementary Fig. S6a). In addition, cell cycle analyses of these clones revealed that HG3-del(11q) *BIRC3*^{MUT} cells had a higher proportion of cells transitioning through S-phase (Supplementary Fig. S6b) To test whether this effect on proliferation could be attributed to *BIRC3* loss, MTT and growth assays were carried out in HG3 *BIRC3*^{MUT} cells without del(11q), and these indeed confirmed the higher proliferation rates of *BIRC3*-deficient cells (Fig. 5a, right panel; Supplementary Fig. S6a). Moreover, HG3^{WT} cells treated with the BIRC2/BIRC3 inhibitor birinapant also displayed increased growth (Supplementary Fig. S6c) as well as MEC1 *BIRC3*^{DEL/MUT} cells in comparison to MEC1 *BIRC3*^{DEL/WT} (Supplementary Fig. S6d). We also determined that this enhanced proliferation rate was driven by enhanced BIRC3-mediated non-canonical NF- κ B signaling activation, since NIK inhibition by SMI1 was able to reduce viability of HG3-del(11q) and HG3-del(11q) *BIRC3*^{MUT} cells (Fig. 5b).

In order to evaluate how *BIRC3* deletion and/or mutation could contribute to the CLL clonal dynamics, we next carried out *in vitro* clonal competition experiments by mixing RFP- or GFP-tagged CRISPR/Cas9-edited cells at a ratio 1:1 and tracked clonal evolution overtime by flow cytometry. In the first experiment, clonal competition was assessed to investigate how

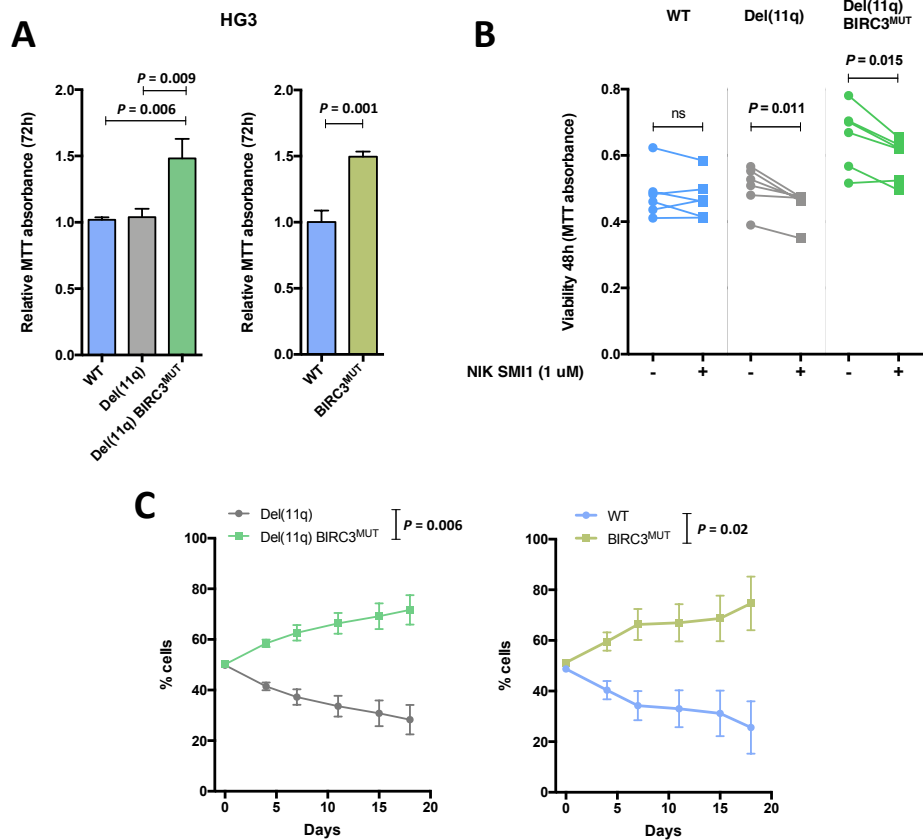


Figure 5. Effects of del(11q) and/or BIRC3 mutations in CLL cell lines proliferation and clonal evolution. (A) Analysis of del(11q) and/or BIRC3 mutations on proliferation of HG3 cells after 72 hours. MTT absorbance values are normalized with the HG3^{WT} clones. Data are summarized as the mean \pm SD. (B) Viability analysis of HG3^{WT}, HG3-del(11q) and HG3-del(11q) BIRC3^{MUT} cells treated with DMSO or 1 μ M NIK SMI1. Cell viability was assessed by MTT assay after 48 hours and data is represented as the absolute absorbance value for each independent clone. (C) HG3-del(11q) RFP-tagged and HG3-del(11q) BIRC3^{MUT} GFP-tagged cells (left panel), HG3^{WT} RFP-tagged and HG3 BIRC3^{MUT} GFP-tagged cells (right panel), were mixed at a ratio 1:1 and left in culture for the indicated days. Clonal evolution was assessed at the indicated time points by flow cytometry. Bars represent mean \pm SD.

BIRC3 mutation could confer a clonal advantage of del(11q) cells. Notably, HG3-del(11q) BIRC3^{MUT} cells progressively outgrew HG3-del(11q) cells overtime (Fig. 5c). In a second experiment, we evaluated the clonal competition between HG3^{WT} and HG3 BIRC3^{MUT} cells, showing that HG3 BIRC3^{MUT} cells were able to outcompete HG3^{WT} cells (Fig. 5c).

Biallelic BIRC3 loss in del(11q) CLL cells accelerates leukemic progression in *in vivo* xenografts

To confirm the effects of BIRC3 loss in a physiological context *in vivo*, we individually injected the monoallelic and biallelic BIRC3-deleted CRISPR/Cas9-edited cell lines intravenously into NSG mice, observing that mice xenografted with HG3 BIRC3^{MUT} and HG3-del(11q) BIRC3^{MUT} cells showed an increase of human CD45⁺ cells in spleen 14 days after

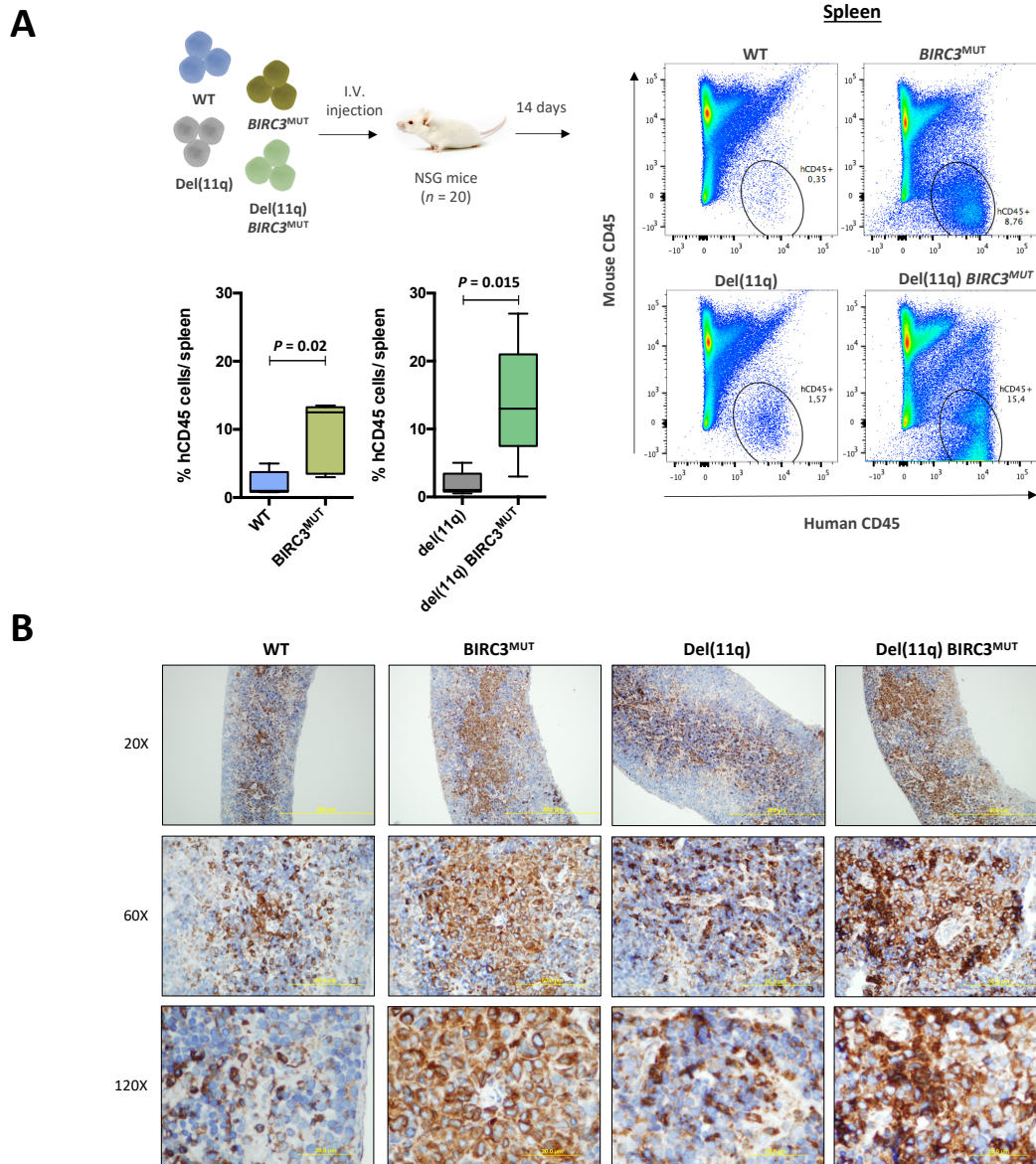


Figure 6. *In vivo* analysis of leukemic progression of del(11q)/*BIRC3*-mutated CRISPR/Cas9-edited clones. **(A)** Spleen infiltration of xenotransplanted HG3^{WT}, HG3 *BIRC3*^{MUT}, HG3-del(11q) and HG3-del(11q) *BIRC3*^{MUT} cell lines ($n = 5$ /per group) into NSG mice. Mice spleens were analyzed by FACS 14 days after cell injection and hCD45⁺ cells were monitored to evaluate the leukemic infiltration in each condition. **(B)** Immunohistochemical analysis of NF- κ B2 (p52) expression in spleens of HG3^{WT}, HG3 *BIRC3*^{MUT}, HG3-del(11q) and HG3-del(11q) *BIRC3*^{MUT} xenografted mice.

injection, compared to HG3^{WT} and HG3-del(11q) cells, respectively, by flow cytometry (Fig. 6a). By immunohistochemistry, spleens collected from HG3 *BIRC3*^{MUT} and HG3-del(11q) *BIRC3*^{MUT} intravenous xenografted cells propagating *in vivo*

also showed evidence of NF- κ B2 activation (Fig. 6b).

In addition, to validate this effect in the proliferation, HG3^{WT} and HG3 *BIRC3*^{MUT} cells were injected subcutaneously in the flank of NSG

mice and tumor growth was monitored for 17 days. HG3 *BIRC3*^{MUT} cells generated larger tumors than HG3^{WT} cells (Supplementary Fig. S7a). Besides, tumors collected from HG3 *BIRC3*^{MUT} engrafted mice showed higher levels of p52 expression than those from HG3^{WT} mice (Supplementary Fig. S7b).

DISCUSSION

Del(11q) is one of the most frequent cytogenetic abnormalities occurring in CLL patients (4, 35, 36), yet, the functional consequences of the haploinsufficiency of the vast majority of genes comprised within this region remains largely unknown. Here, we undertook a CRISPR/Cas9-based genome editing approach to characterize novel biological implications of monoallelic and biallelic *BIRC3* loss in del(11q) CLL. In this way, our work presents *in vitro*, *ex vivo* and *in vivo* evidence of how *BIRC3*-deletion and/or mutation in the remaining allele of del(11q) cells contributes to NF- κ B signaling activation, CLL progression and therapy response.

Our data indicate that monoallelic *BIRC3* deletion contributes to the pathobiology of del(11q) by a NIK-dependent triggering of the non-canonical NF- κ B signaling, resulting in enhanced p52-RelB nuclear translocation and activation (Supplementary Figure S8). This effect appears to be allelic dose-dependent, since biallelic *BIRC3* loss resulted in higher activation rates (Fig. 2). Our results obtained in isogenic CLL-derived cell lines provide a more comprehensive landscape of the role of each CLL *BIRC3*-related alterations in the non-canonical NF- κ B pathway, complementing previous findings hinted in a panel of lymphoid-related cell lines (18). In addition, we were also able to address the biological differences between

del(11q) CLL patients including or not *BIRC3* within their deleted region, showing that, in response to stromal stimulation and TLR ligation by CpG, del(11q)/*BIRC3*-deleted cases present marked levels of stabilized NIK and p52 activity. Indeed, further evidence of hyperactive non-canonical signaling was found in B-lymphocytes from mice lacking *clap1/clap2* (*Birc2/Birc3*) (37) and in B-cells treated with *BIRC2/BIRC3* inhibitors (21), as well as in our isogenic del(11q) CLL cell lines (Fig. 2). Furthermore, a previous report observed that CLL cells with low *BIRC3* mRNA expression presented activation of the canonical NF- κ B signaling in the presence of BAFF or CD40L stimulation (31). Interestingly, we did find partial evidence of canonical NF- κ B activation by increased nuclear p50 activity in HG3-del(11q) *BIRC3*^{MUT} cells, which has also been shown to contribute in the pathogenesis of E μ -TCL1 model of CLL (38). This enhanced p50 activity could be in line with the high phosphorylation levels of IKK β , a member of the I κ B-kinase (IKK) complex, implicated in canonical NF- κ B activation (39). Altogether, these results suggest that, in the presence of the CLL microenvironment, *BIRC3* loss displays a dual role on both canonical and non-canonical NF- κ B signaling activation.

The recent introduction of the selective BCL2 inhibitor venetoclax into the CLL treatment scheme has led to effective remissions for relapsed/refractory CLL patients, especially when combined with anti-CD20 antibodies (40, 41). Nevertheless, little is still known regarding which genetic alterations may predict for better venetoclax responses in CLL. We show that enhanced non-canonical NF- κ B activity in *BIRC3*-deleted cells results in BCL2 overexpression, making isogenic del(11q)

BIRC3^{MUT} cells more sensitive to venetoclax treatment. These observations are limited due to the use of CLL cell lines which do not display the same venetoclax sensitivity as primary CLL cells (42). However, we also observe a correlation between BCL2 levels and the percentage of *BIRC3*-deleted cells in del(11q) cases, as well as between p52 and BCL2 levels, suggesting that *BIRC3*-deleted cases may potentially benefit from venetoclax-based regimens. In fact, recent data from the CLL14 trial suggest that del(11q) or *BIRC3*^{MUT} patients significantly favor from venetoclax plus obinutuzumab in comparison to the chlorambucil plus obinutuzumab treatment arm (43). In addition, we show that NIK pharmacological inhibition can counteract *BIRC3*-mediated non-canonical NF-κB signaling and anti-apoptotic protein overexpression, making it an attractive candidate for combinatorial therapy with venetoclax (44). Contrarily, del(11q) *BIRC3*^{MUT} cells did not selectively benefit from ibrutinib treatment, in agreement with previous reports indicating that BTK inhibition does not suppress non-canonical NF-κB signaling activity (18, 45). Furthermore, we also assessed the treatment implications of *BIRC3* deletion and/or mutation in response to fludarabine, given that these alterations have been associated with fludarabine relapse in some, but not all, cohorts (10, 12, 18). Nonetheless, neither isogenic HG3-del(11q) *BIRC3*^{MUT} nor *BIRC3*^{MUT} cells show evidence of fludarabine resistance, whereas isogenic HG3 *TP53*^{MUT} cells present marked resistance in the same conditions (Fig. 4b). These results indicate that *BIRC3* alterations may not be enough to generate fludarabine resistance *per se*, as opposed to *TP53* alterations. Further investigation is required to decipher whether extrinsic factors

such as the CLL microenvironment as well as the concurrence with other genetic alterations would play a critical role in fludarabine resistance of *BIRC3* mutated CLL cells.

Although there is still controversy regarding clinical impact of *BIRC3* mutations, recent reports have highlighted the negative predictive impact on TTFT and OS of biallelic *BIRC3* loss through del(11q) and mutation in the remaining allele (14, 15). Our work biologically demonstrates that biallelic *BIRC3* loss promotes CLL proliferation, clonal evolution and progression *in vitro* and *in vivo*. These results are further supported by the notion that mice lacking *clap1/clap2* show an uncontrolled accumulation of B-cells *in vivo* (37). Interestingly, we did not observe enhanced proliferation of isogenic cell lines harboring monoallelic *BIRC3* loss, suggesting that *BIRC3* mutations may only have a clinical impact in patients with a previous del(11q) background. These data therefore reinforce the notion that biallelic *BIRC3* inactivation should be considered as a high-risk CLL entity.

In summary, this work displays a comprehensive biological analysis of the impact of monoallelic and biallelic *BIRC3* lesions in del(11q) CLL patients by combining *in vitro*, *ex vivo*, and xenograft models. We show that monoallelic *BIRC3* deletion activates NF-κB signaling in del(11q) CLL cells, contributing to the pathobiology of this high-risk cytogenetic alteration. We also demonstrate that *BIRC3* mutation in the remaining allele of del(11q) CLL cells confers clonal advantage which could account for the negative predictive impact of *BIRC3* biallelic inactivation in CLL. Moreover, cells harboring these alterations could be therapeutically targeted with BCL2 inhibitors.

Taken together, our results suggest that del(11q) CLL patients harboring *BIRC3* mutations should be considered as a CLL subgroup at a high risk of progression that might benefit from venetoclax-based therapies.

ACKNOWLEDGEMENTS

This work was supported by grants from the Spanish Fondo de Investigaciones Sanitarias PI15/01471, PI18/01500, Instituto de Salud Carlos III (ISCIII), European Regional Development Fund (ERDF) “Una manera de hacer Europa”, “Consejería de Educación, Junta de Castilla y León” (SA271P18), “Proyectos de Investigación del SACYL”, Spain GRS 2062/A/19, GRS 1847/A/18, GRS1653/A17, “Fundación Memoria Don Samuel Solórzano Barruso” (FS/23-2018), by grants (RD12/0036/0069) from Red Temática de Investigación Cooperativa en Cáncer (RTICC), Centro de Investigación Biomédica en Red de Cáncer (CIBERONC CB16/12/00233) and SYNtherapy “Synthetic Lethality for Personalized Therapy-based Stratification In Acute Leukemia” (ERAPERMED2018-275); ISCIII (AC18/00093), co-funded by ERDF/ESF, “Investing in your future”. MQÁ and AERV are supported with a research grant by FEHH (“Fundación Española de Hematología y Hemoterapia”); MHS holds a Sara Borrell post-doctoral contract (CD19/00222) from the Instituto de Salud Carlos III (ISCIII). CPC was supported by an “Ayuda predoctoral en Oncología” (AECC) and is a recipient of a PFIS grant (FI19/00191) from Instituto de Salud Carlos III; PFIS grant and Sara Borrell post-doctoral contract are co-funded by Fondo Social Europeo (FSE) “El Fondo Social Europeo invierte en tu futuro”; JLO and RBS are supported by a grant from the University of Salamanca (“Contrato postdoctoral programa II”). We thank Irene Rodríguez, Sandra Santos, Sara González, Cristina Miguel, Almudena Martín-Martín, Teresa Prieto, M^a Ángeles Ramos, Filomena Corral, M^a Almudena Martín, Ana Díaz, Ana Simón, María del Pozo, Isabel M Isidro, Vanesa Gutiérrez, Sandra Pujante and M^a Ángeles Hernández from the Cancer Research Center of Salamanca, Spain, for their technical support. We are grateful to Ángel Prieto, Ana I García and Sara Armenteros, María Luz Sánchez and María Carmen Macías from the Microscopy Unit, Cytometry Unit and

Molecular Pathology Unit, respectively, from the Cancer Research Center of Salamanca for their technical assistance. We thank Luis Muñoz and all the members from the Animal Experimentation Research Center from the University of Salamanca. The authors are grateful to C.J. Wu and E. ten Hacken (Dana-Farber Cancer Institute) for constructive and valuable discussion on this project.

AUTHOR CONTRIBUTIONS

M.Q.Á. designed the experiments, carried out functional studies, analyzed the data and wrote the paper. M.H.S. designed CRISPR/Cas9 experiments and together with A.E.R.V. performed data analysis and contributed to the interpretation of the results. C.P.C. and A.R.S. performed experiments and contributed to the interpretation of the results. M.M.I. performed NGS studies and data analysis. V.A.P. and I.G.T. contributed to the experiment design and interpretation of the results. J.M.B., M.J.V.M., J.G., C.A., J.A.Q., I.G.G.M. and J.A.H.R. provided patient samples and clinical data. R.B. contributed to data analyses and interpretation of the results. J.L.O. performed functional experiments and together with J.M.H.R. conceived the study, designed the experiments, supervised the research and critically reviewed the manuscript. All authors discussed the results and revised the manuscript.

CONFLICT OF INTEREST

The authors declare no potential conflicts of interest

REFERENCES

1. Döhner H, Stilgenbauer S, James MR, Benner A, Weilguni T, Bentz M, et al. 11q deletions identify a new subset of B-cell chronic lymphocytic leukemia characterized by extensive nodal involvement and inferior prognosis. *Blood*. 1997 Apr 1;89(7):2516–22.
2. Stilgenbauer S, Liebisch P, James MR, Schröder M, Schlegelberger B, Fischer K, et al. Molecular cytogenetic delineation of a novel critical genomic region in chromosome bands 11q22.3-923.1 in lymphoproliferative disorders. *Proc Natl Acad Sci U S A*. 1996 Oct 15;93(21):11837–41.
3. Neilson JR, Auer R, White D, Bienz N, Waters JJ, Whittaker JA, et al. Deletions at 11q identify a subset of patients with typical CLL who show consistent disease progression and reduced survival. *Leukemia*. 1997 Nov;11(11):1929–32.
4. Döhner H, Stilgenbauer S, Benner A, Leupolt E, Kröber A, Bullinger L, et al. Genomic aberrations and survival in chronic lymphocytic leukemia. *N Engl J Med*. 2000 Dec

- 28;343(26):1910–6.
5. Hoehstetter MA, Busch R, Eichhorst B, Bühler A, Winkler D, Bahlo J, et al. Prognostic model for newly diagnosed CLL patients in Binet stage A: results of the multicenter, prospective CLL1 trial of the German CLL study group. *Leukemia*. 2020 Apr 1;34(4):1038–51.
 6. Gunnarsson R, Mansouri L, Isaksson A, Göransson H, Cahill N, Jansson M, et al. Array-based genomic screening at diagnosis and during follow-up in chronic lymphocytic leukemia. *Haematologica*. 2011 Aug 1;96(8):1161–9.
 7. Austen B, Skowronska A, Baker C, Powell JE, Gardiner A, Oscier D, et al. Mutation status of the residual ATM allele is an important determinant of the cellular response to chemotherapy and survival in patients with chronic lymphocytic leukemia containing an 11q deletion. *J Clin Oncol*. 2007 Dec 1;25(34):5448–57.
 8. Stankovic T, Skowronska A. The role of *ATM* mutations and 11q deletions in disease progression in chronic lymphocytic leukemia. *Leuk Lymphoma*. 2014 Jun 12;55(6):1227–39.
 9. Rose-Zerilli MJ, Forster J, Parker H, Parker A, Rodriguez AE, Chaplin T, et al. *ATM* mutation rather than *BIRC3* deletion and/or mutation predicts reduced survival in 11q-deleted chronic lymphocytic leukemia: data from the UK LRF CLL4 trial. *Haematologica*. 2014 Apr 1;99(4):736–42.
 10. Rossi D, Fangazio M, Rasi S, Vaisitti T, Monti S, Cresta S, et al. Disruption of *BIRC3* associates with fludarabine chemorefractoriness in TP53 wild-type chronic lymphocytic leukemia. *Blood*. 2012 Mar 22;119(12):2854–62.
 11. Baliakas P, Hadzidimitriou A, Sutton LA, Rossi D, Minga E, Villamor N, et al. Recurrent mutations refine prognosis in chronic lymphocytic leukemia. *Leukemia*. 2015 Feb 7;29(2):329–36.
 12. Landau DA, Tausch E, Taylor-Weiner AN, Stewart C, Reiter JG, Bahlo J, et al. Mutations driving CLL and their evolution in progression and relapse. *Nature*. 2015 Oct 14;526(7574):525–30.
 13. Guièze R, Robbe P, Clifford R, De Guibert S, Pereira B, Timbs A, et al. Presence of multiple recurrent mutations confers poor trial outcome of relapsed/refractory CLL. *Blood*. 2015 Oct 29;126(18):2110–7.
 14. Blakemore SJ, Clifford R, Parker H, Antoniou P, Stec-Dziedzic E, Larrayoz M, et al. Clinical significance of TP53, *BIRC3*, *ATM* and *MAPK-ERK* genes in chronic lymphocytic leukaemia: data from the randomised UK LRF CLL4 trial. *Leukemia*. 2020;
 15. Raponi S, Del Giudice I, Ilari C, Cafforio L, Messina M, Cappelli L V., et al. Biallelic *BIRC3* inactivation in chronic lymphocytic leukaemia patients with 11q deletion identifies a subgroup with very aggressive disease. *Br J Haematol*. 2018 May 22;
 16. Puente XS, Beà S, Valdés-Mas R, Villamor N, Gutiérrez-Abril J, Martín-Subero JL, et al. Non-coding recurrent mutations in chronic lymphocytic leukaemia. *Nature*. 2015 Oct 22;526(7574):519–24.
 17. Nadeu F, Delgado J, Royo C, Baumann T, Stankovic T, Pinyol M, et al. Clinical impact of clonal and subclonal TP53, SF3B1, *BIRC3*, *NOTCH1*, and *ATM* mutations in chronic lymphocytic leukemia. *Blood*. 2016 Apr 28;127(17):2122–30.
 18. Diop F, Moia R, Favini C, Spaccarotella E, De Paoli L, Brusca A, et al. Biological and clinical implications of *BIRC3* mutations in chronic lymphocytic leukemia. *Haematologica*. 2020 Jan 31;105(2):448–56.
 19. Tausch E, Beck P, Schlenk RF, Jebaraj BJ, Dolnik A, Yosifov DY, et al. Prognostic and predictive role of gene mutations in chronic lymphocytic leukemia: results from the pivotal phase III study *COMPLEMENT1*. *Haematologica*. 2020 Jan 9;haematol.2019.229161.
 20. Brieghel C, da Cunha-Bang C, Yde CW, Schmidt AY, Kinalis S, Nadeu F, et al. The number of signaling pathways altered by driver mutations in chronic lymphocytic leukemia impacts disease outcome. *Clin Cancer Res*. 2020 Mar 15;26(6):1507–15.
 21. Zarnegar BJ, Wang Y, Mahoney DJ, Dempsey PW, Cheung HH, He J, et al. Noncanonical NF- κ B activation requires coordinated assembly of a regulatory complex of the adaptors *ciAP1*, *ciAP2*, *TRAF2* and *TRAF3* and the kinase *NIK*. *Nat Immunol*. 2008 Dec 9;9(12):1371–8.
 22. Mansouri L, Papakonstantinou N, Ntoufa S, Stamatopoulos K, Rosenquist R. NF- κ B activation in chronic lymphocytic leukemia: A point of convergence of external triggers and intrinsic lesions. *Semin Cancer Biol*. 2016 Aug;39:40–8.
 23. Sun S-C. The non-canonical NF- κ B pathway in immunity and inflammation. *Nat Rev Immunol*. 2017 Jun 5;17(9):545–58.
 24. Yin S, Gambe RG, Sun J, Martinez AZ, Cartun ZJ, Regis FFD, et al. A Murine Model of Chronic Lymphocytic Leukemia Based on B Cell-Restricted Expression of *Sf3b1* Mutation and *Atm* Deletion. *Cancer Cell*. 2019 Feb 11;35(2):283–296.e5.
 25. Arruga F, Gizdic B, Bologna C, Cignetto S, Buonincontri R, Serra S, et al. Mutations in *NOTCH1* PEST domain orchestrate CCL19-driven homing of chronic lymphocytic leukemia cells by modulating the tumor suppressor gene *DUSP22*. *Leukemia*. 2017 Sep;31(9):1882–93.
 26. Close V, Close W, Kugler SJ, Reichenzeller M, Yosifov DY, Bloehdorn J, et al. *FBXW7* mutations reduce binding of *NOTCH1*, leading to cleaved *NOTCH1* accumulation and target gene activation in CLL. *Blood*. 2019 Feb 21;133(8):830–9.
 27. Quijada-Álamo M, Hernández-Sánchez M, Alonso-Pérez V, Rodríguez-Vicente AE, García-Tuñón I, Martín-Izquierdo M, et al. CRISPR/Cas9-generated models uncover therapeutic vulnerabilities of del(11q) CLL cells to dual BCR and PARP inhibition. *Leukemia*. 2020 Jun 1;34(6):1599–612.

28. Quijada-Álamo M, Pérez-Carretero C, Hernández-Sánchez M, Rodríguez-Vicente A, Herrero A, Hernández-Sánchez J, et al. Dissecting the role of TP53 alterations in del(11q) chronic lymphocytic leukemia. *Clin Transl Med.* 2021 Feb;11(2).
29. Hernández-Sánchez M, Rodríguez-Vicente AE, González-Gascón Y, Marín I, Quijada-Álamo M, Hernández-Sánchez JM, Martín-Izquierdo M, et al. DNA damage response-related alterations define the genetic background of patients with chronic lymphocytic leukemia and chromosomal gains. *Exp Hematol.* 2019 Apr;72:9–13.
30. Purroy N, Abrisqueta P, Carabia J, Carpio C, Calpe E, Palacio C, et al. Targeting the proliferative and chemoresistant compartment in chronic lymphocytic leukemia by inhibiting survivin protein. *Leukemia.* 2014 Oct 12;28(10):1993–2004.
31. Asslaber D, Wacht N, Leisch M, Qi Y, Maeding N, Hufnagl C, et al. BIRC3 expression predicts CLL progression and defines treatment sensitivity via enhanced NF- κ B nuclear translocation. *Clin Cancer Res.* 2019;25(6):1901–12.
32. Viatour P, Bentires-Alj M, Chariot A, Deregowski V, de Leval L, Merville MP, et al. NF- κ B2/p100 induces Bcl-2 expression. *Leukemia.* 2003 Jul 1;17(7):1349–56.
33. Tromp JM, Tonino SH, Elias JA, Jaspers A, Luijckx DM, Kater AP, et al. Dichotomy in NF- κ B signaling and chemoresistance in immunoglobulin variable heavy-chain-mutated versus unmutated CLL cells upon CD40/TLR9 triggering. *Oncogene.* 2010 Sep 9;29(36):5071–82.
34. Brightbill HD, Suto E, Blaquiére N, Ramamoorthi N, Sujatha-Bhaskar S, Gogol EB, et al. NF- κ B inducing kinase is a therapeutic target for systemic lupus erythematosus. *Nat Commun.* 2018 Jan 12;9(1):1–14.
35. Van Dyke DL, Werner L, Rassenti LZ, Neuberg D, Ghia E, Heerema NA, et al. The Dohner fluorescence in situ hybridization prognostic classification of chronic lymphocytic leukaemia (CLL): the CLL Research Consortium experience. *Br J Haematol.* 2016 Apr;173(1):105–13.
36. Hernández JA, Hernández-Sánchez M, Rodríguez-Vicente AE, Grossmann V, Collado R, Heras C, et al. A Low Frequency of Losses in 11q Chromosome Is Associated with Better Outcome and Lower Rate of Genomic Mutations in Patients with Chronic Lymphocytic Leukemia. Gibson SB, editor. *PLoS One.* 2015 Dec 2;10(11):e0143073.
37. Gardam S, Turner VM, Anderton H, Limaye S, Basten A, Koentgen F, et al. Deletion of cIAP1 and cIAP2 in murine B lymphocytes constitutively activates cell survival pathways and inactivates the germinal center response. *Blood.* 2011 Apr 14;117(15):4041–51.
38. Chen TL, Tran M, Lakshmanan A, Harrington BK, Gupta N, Goettl VM, et al. NF- κ B p50 (nfb1) contributes to pathogenesis in the E μ -TCL1 mouse model of chronic lymphocytic leukemia. Vol. 130, *Blood.* American Society of Hematology; 2017. p. 376–9.
39. Gasparini C, Celeghini C, Monasta L, Zauli G. NF- κ B pathways in hematological malignancies. Vol. 71, *Cellular and Molecular Life Sciences.* Birkhauser Verlag AG; 2014. p. 2083–102.
40. Seymour JF, Kipps TJ, Eichhorst B, Hillmen P, D’Rozario J, Assouline S, et al. Venetoclax-rituximab in relapsed or refractory chronic lymphocytic leukemia. *N Engl J Med.* 2018 Mar 22;378(12):1107–20.
41. Kater AP, Seymour JF, Hillmen P, Eichhorst B, Langerak AW, Owen C, et al. Fixed duration of venetoclax-rituximab in relapsed/refractory chronic lymphocytic leukemia eradicates minimal residual disease and prolongs survival: Post-treatment follow-up of the Murano phase III study. *J Clin Oncol.* 2019 Feb 1;37(4):269–77.
42. Guièze R, Liu VM, Rosebrock D, Jourdain AA, Hernández-Sánchez M, Martínez Zurita A, et al. Mitochondrial Reprogramming Underlies Resistance to BCL-2 Inhibition in Lymphoid Malignancies. *Cancer Cell.* 2019 Oct 14;36(4):369–384.e13.
43. Tausch E, Schneider C, Robrecht S, Zhang C, Dolnik A, Bloehdorn J, et al. Prognostic and predictive impact of genetic markers in patients with CLL treated with obinutuzumab and venetoclax. *Blood.* 2020 Mar 23;
44. Haselager M, Thijssen R, West C, Young L, Van Kampen R, Willmore E, et al. Regulation of Bcl-XL by non-canonical NF- κ B in the context of CD40-induced drug resistance in CLL. *Cell Death Differ.* 2021;
45. Rahal R, Frick M, Romero R, Korn JM, Kridel R, Chan FC, et al. Pharmacological and genomic profiling identifies NF- κ B-targeted treatment strategies for mantle cell lymphoma. *Nat Med.* 2014;20(1):87–92.

GENERAL DISCUSSION

CLL is a highly genetically heterogeneous disease characterized by the presence of recurrent chromosomal abnormalities and gene mutations that modify diverse biological pathways, ultimately impacting the clinical course of patients suffering from this disease^{65,66}. Individual genetic lesions are not likely to be the only responsible for CLL pathogenesis, indeed, the vast majority of patients harbor different combinations of multiple alterations that coexist within the same tumoral clone²³⁷. These interactions between disease drivers have been postulated to contribute to cellular fitness, fueling disease evolution²⁹². Understanding the biological function of these abnormalities, both individually and combined, and their role in CLL initiation, progression and therapy response has become essential to assess patient prognosis and adopt therapeutic decisions, as well as to evaluate novel tailored therapeutic approaches based on the genetic profile of each patient.

It is well known that cancer is a clonal disease that arises from the accumulation of acquired abnormalities in an individual cell. However, **the cell of origin of many cancers, including CLL, is widely unknown**, and the exact initial lesion(s) that triggers the cascade of events leading to malignant transformation is yet to be identified. This question is relevant not only to determine what type of genetic events orchestrate the initiation of CLL, but also to understand which cell populations should be the target for therapeutic approaches. In the first study from this PhD research, this critical issue was addressed by analyzing the presence of somatic mutations and chromosomal abnormalities in CD34⁺ hematopoietic progenitors isolated from bone marrow aspirates of CLL patients (**Results Section – Chapter 1: Next-generation sequencing and FISH studies reveal the appearance of gene mutations and chromosomal abnormalities in hematopoietic progenitors in chronic lymphocytic leukemia**). This study was inspired by the previous findings from Kikushige *et al.*¹²³ and Damm *et al.*¹²⁶, which pointed out towards HSCs as the cell of origin of CLL where the first driver events occur. We initially confirmed that somatic mutations in well-known CLL driver genes such as *NOTCH1*, *XPO1* and *MYD88* can appear in the total CD34⁺ cell population from CLL patients, which include CD34⁺CD19⁻ HSCs as well as CD34⁺CD19⁺ pro-B cells that are already committed to B-cell lineage. Furthermore, we subsequently validated the presence of some of these mutations in FACS-sorted CD34⁺CD19⁻ HSCs (**Results Section – Chapter 1: Figure 1-2; Table 2**). Later studies have validated and expanded these observations, indicating that CLL driver mutations can appear in early HSCs and multi-potent progenitor cells (MPP), as defined by a Lin⁻CD34⁺CD38^{low}CD45RA⁻CD90⁺/CD90⁻ immunophenotype^{127,470}. Altogether, these

results clearly indicate that some **CLL driver lesions can appear in early steps of hematopoiesis**, tightening the net around the cell of origin of CLL.

Nevertheless, there are still limitations and further questions that should be acknowledged in this regard. First, our study and others are based on the analysis of small cohorts of CLL patients and a study restricted to few CLL driver genes, leaving unsolved questions about the complete genetic landscape of CLL-HSCs and which are the most prevalent mutations or biological pathways dysregulated at this maturational step. In addition, Marsilio *et al.*¹²⁷ showed that isolation of pure CD34⁺ cell fractions without contaminants from CD19⁺ mature B-CLL cells is a challenging process, and subsequent improvement of high-sensitivity MRD detection methods by flow cytometry or ultra-deep NGS may help the evaluation of the CLL-HSC genetic landscape in larger cohorts of patients with purer HSCs fractions. These questions could be further addressed thanks to the recent refinement of single-cell DNA and RNA sequencing strategies^{471–473}, which I believe could shed light into these aspects in the near future.

On the other hand, one of the strengths of our study was the evaluation not only of driver gene mutations, but also well-known chromosomal abnormalities in CD34⁺ cells, an issue that was not addressed in any of the other studies investigating this topic^{123,126,127,470}. Indeed, the four most recurrent cytogenetic abnormalities in CLL (del(11q), trisomy 12, del(13q) and del(17p)) are present in approximately 80% of the total of CLL cases⁶³, and WES analysis of the cancer cell fraction from > 500 patients have revealed that del(11q), del(13q) and trisomy 12 are mostly clonal lesions that are likely to appear early in the disease course⁶⁵. Our results further expand these observations, describing the presence of del(13q) and del(11q) in CD34⁺ cells from 3/5 and 2/2 patients, respectively, thus **confirming the early nature of these abnormalities and placing its appearance in CD34⁺ progenitors (Results Section – Chapter 1: Table 3)**. Two recent studies analyzed chromosomal mosaicism of > 300,000 elderly individuals and also described the presence del(13q) and del(11q), as well as trisomy 12 in age-related hematopoietic clones^{131,132}, suggesting that these chromosomal abnormalities are already present years before disease onset. This finding further reinforces the notion that these alterations may appear in CD34⁺ HSCs and presumably contribute to the origin of CLL. Intriguingly, these specific abnormalities are considerably more prevalent in European individuals when compared to Asian individuals, being the subjects harboring these

alterations at higher risk of developing CLL^{131,132}, which is consistent with the geographical incidence of CLL and the crucial role of these abnormalities in the initiation of the disease.

Taken together, these facts could suggest that the presence of genetic lesions in HSCs favor CLL initiation but it might not be sufficient to drive expansion of mature B-CLL clones, requiring from other **subclonal events** in order to gain cellular fitness and to contribute to disease progression^{65,126,292}. This could be the case of del(11q) as inferred from the results obtained in chapters second, third and fourth of this PhD thesis. First of all, in the study of mutational status of 54 CLL drivers genes in a cohort of 47 del(11q) CLL cases, we observed that the vast majority of them (93.6%) harbored alterations in at least one of these drivers (**Results Section – Chapter 3: Figure 1A**), indicating that del(11q) cases invariably present additional concurrent genetic alterations⁶⁵. Second, our CRISPR/Cas9-generated models biologically demonstrate that the presence of monoallelic del(11q) can favor genomic instability by impaired repair of DSBs, which could facilitate the subsequent acquisition of subclonal events (**Results Section – Chapter 2: Figure 2**). Indeed, del(11q) cases have been shown to present high levels of genomic instability in other independent cohorts^{151–153}. Third, we provide functional evidence about the synergistic role of additional *ATM*, *BIRC3* or *TP53* mutations in del(11q) CLL expansion and progression, in agreement with the subclonal and concurrent nature of these mutations in del(11q) CLL cells, especially those on *ATM* and *BIRC3*⁶⁵.

In the case of *ATM* (**Results Section – Chapter 2: CRISPR/Cas9-generated models uncover therapeutic vulnerabilities of del(11q) CLL cells to dual BCR and PARP inhibition**), we show that the loss of the second allele through truncating mutation leads to a profound dysregulation of the DDR resulting in higher genomic instability as determined by γ H2AX analysis and comet assays, respectively. Although we did not observe an *in vitro* proliferative advantage of HG3-del(11q) *ATM*^{MUT} cells in comparison to HG3-del(11q) cells, we did find a marked increase in the homing capacity of HG3-del(11q) *ATM*^{MUT} cells in the spleen of NSG mice when compared to HG3-del(11q) or HG3^{WT} cells (**Supplementary Appendix – Chapter 2: Appendix 2**). Certainly, recent studies analyzing the growth dynamics over time of untreated CLL cells revealed that *ATM* mutations usually arise in cases with progressive disease and are related to an exponential growth pattern^{292,474}. Albeit we could not analyze the mutational status of *ATM* in our cohort of CD34⁺ cells from CLL patients, Damm *et al.* analyzed the CD34⁺CD19⁻ fraction of 5 patients harboring *ATM* mutations in the mature

CD19⁺ B-CLL population, and interestingly, none of these patients presented *ATM* mutations in their CD34⁺CD19⁻ counterparts¹²⁶, further indicating that *ATM* mutations are subclonal events that appear late in CLL development and possibly contribute to clonal expansion when they co-occur with del(11q) through impaired DDR and increased genomic instability.

In relation to *BIRC3* (**Results Section – Chapter 4: Biological significance of monoallelic and biallelic *BIRC3* loss in del(11q) chronic lymphocytic leukemia progression**), our studies reveal that truncating mutations in the remaining allele of this gene in del(11q) cells constitutively activate non-canonical NF-κB signaling leading to upregulation of anti-apoptotic BCL2 family members, which translates into enhanced clonal advantage *in vitro* and *in vivo*. We also show that this promotion of the non-canonical NF-κB signaling is dependent on *BIRC3* allelic dosage, since monoallelic *BIRC3* loss through del(11q) boosts non-canonical NF-κB activity in a lesser extent than biallelic *BIRC3* loss (**Results Section – Chapter 4: Figure 2**). However, the non-canonical signaling activity of monoallelic del(11q) does not seem sufficient enough to drive clonal expansion of CLL cells in our *in vitro* model (**Results Section – Chapter 4: Figure 5 and 6**), which is consistent with the hypothesis that del(11q) cells need from other subclonal events, in this case truncating mutation of the remaining allele of *BIRC3*, to orchestrate CLL progression. In accordance, *BIRC3* mutations have always been found to be subclonal events in independent cohorts, and its presence in del(11q) cases confers a shorter TTFT^{65,154,156}. In addition, subclonal *BIRC3* mutations have been shown to increase their variant allele frequency in longitudinal samples from CLL patients and associate with the development of active disease^{291,474}. Even though none of the current studies analyzing CD34⁺ populations of CLL patients, including ours, have looked for *BIRC3* mutations in HSCs, they are not likely to appear until a later maturational step as it is observed in the case of *ATM* mutations, although further studies in larger cohorts of CD34⁺ samples would be required^{126,127,470}.

Moreover, the results from our NGS study of 47 del(11q) CLL cases prompted us to further interrogate the biological basis of concurrent *TP53* biallelic lesions in del(11q) CLL cells (**Results Section – Chapter 3: Dissecting the role of *TP53* alterations in del(11q) chronic lymphocytic leukemia**). In accordance to the reduced survival of del(11q) patients harboring additional *TP53* lesions in our cohort, we could demonstrate that *TP53* alterations contributed to enhanced cellular fitness and clonal advantage of del(11q) cells *in vitro* and *in vivo* (**Results Section – Chapter 3: Figure 3A-B, Figure 4**). The functional basis underlying

this aggressiveness may be related to a cooperative dysregulation of the DDR and loss of cell-cycle checkpoints, resulting in increased genomic instability as already observed in del(11q)/*ATM* and del(17p)/*TP53* mutated patients^{64,151–153}. Moreover, a recent report showed that CLL transformation into RS is primarily dictated by the accumulation of mutations in genes involved in the DDR signaling pathway¹⁹², providing further evidence about the impact of dysregulation of this pathway in CLL evolution. In consistence to the aforementioned scenarios for *ATM* and *BIRC3*, *TP53* mutations are usually subclonal in CLL and have been proposed as late events of the disease course^{65,237}. In the context of del(11q), our NGS results reveal that the variant allele frequency is predominantly lower for *TP53* mutations than del(11q) (**Results Section – Chapter 3: Table 2**), highlighting its subclonal nature in this specific subset of CLL patients. This is consistent with our findings in CD34⁺ cells, where we detected *TP53* mutations in a considerably lower proportion (borderline to our cut-off of 10%) than in their mature CD19⁺ counterparts (**Results Section – Chapter 1: Figure 2**).

Additional evidence supporting the hypothesis that del(11q) requires from other events to drive CLL pathogenesis has been recently addressed in mouse models²⁹³. Specifically, Yin *et al.* generated mouse models with B-cell restricted monoallelic *ATM* deletion and *SF3B1* gain-of-function mutation. Interestingly, *ATM* deletion alone was not sufficient to cause a CLL-like disease in mice, neither *SF3B1* mutation alone. However, mice harboring the combination of both *ATM* deletion and *SF3B1* mutation were able to develop a CLL-like disease characterized by increased genomic instability and dysregulation of multiple CLL-related biological pathways such as the BCR signaling²⁹³. This is consistent with the high co-occurrence observed between del(11q) and *SF3B1* mutations in CLL patients, which indeed accounts for a reduced TTFT⁶⁷. Furthermore, other significantly concurrent genetic events have been described in del(11q) CLL cases. For instance, amp(2p) is a recurrent abnormality in advanced-stage CLL and it is strongly associated with the presence of del(11q)^{65,475}. The common amplified region includes oncogenes such as *XPO1*, *REL* or *MYCN* and its biological role in CLL remains elusive⁴⁷⁶. Although further functional investigation is required, it could be presumable that del(11q) in combination with overexpression of any of these genes located in the common amplified region of 2p might drive CLL progression, evolution and therapy response.

Another interesting aspect highlighted by large-scale WES studies in CLL is the presence of **mutually exclusive genetic lesions**^{65,66}. This phenomenon has also been observed across multiple cancer types, and it is usually attributed to a redundant effect of different alterations in the same biological pathway, suggesting that the coexistence of two of these alterations does not provide an additional benefit to the cell^{477,478}. However, if that were the case, the co-occurrence of both alterations should not bring any negative consequences to the cell. Therefore, another potential explanation is that coexistence of two lesions may be harmful and causes cell cycle exit, senescence, or death^{478,479}. These scenarios have remained largely unexplored *in vitro* or *in vivo* even though the knowledge of this aspect of cancer biology might be useful in order to identify novel synthetic lethal interactions that may be therapeutically exploited. In CLL, mutual exclusivity is mainly observed between del(13q) and trisomy 12 or *SF3B1* mutations and trisomy 12, among other patterns^{65,66}, nevertheless, any of these interactions has been further functionally explored. In this regard, our *in vitro* and *in vivo* work shed light into the **mutual exclusive nature of biallelic *ATM* and *TP53* alterations** in CLL, underscoring the detrimental effect of the combination of these lesions in CLL proliferation and *in vivo* homing (**Results Section – Chapter 3: Figure 3A-B, Figure 4**). Interestingly, as mentioned earlier, the opposite effect was observed in those cells harboring monoallelic *ATM* deletion through del(11q) in combination with *TP53* alterations, highlighting that the number of alleles affected by these lesions is critical to determine a cooperative or detrimental function in CLL clonal fitness.

Importantly, to fully understand the biology underlying del(11q) in CLL, further investigation is indispensable to assess whether the **collective or individual haploinsufficiency of genes** (other than *ATM* or *BIRC3*) encompassed within this deletion play a role in the pathogenesis of the disease. Despite the lack of functional studies investigating this issue in CLL, it has been suggested that loss of *NPAT*, *CUL5* or *PPP2R1B* might result in dysregulation of apoptosis and cell cycle¹⁵⁷. Indeed, *NPAT* germline loss-of-function mutations have been identified as a risk factor for familial Hodgkin lymphoma⁴⁸⁰, whereas *CUL5* deficiency has been shown to promote small-cell lung cancer metastasis⁴⁸¹. *PPP2R1B* alterations have been found in lung and colon cancer⁴⁸². This gene encodes for a subunit of the protein phosphatase 2A (PP2A), a master regulator for diverse cellular functions such as cell cycle, mTOR signaling or MAPK-ERK signaling⁴⁸³. Interestingly, alternative splicing transcripts of *PPP2R1B* have been reported in CLL cases, resulting in reduced PP2A activity¹⁵⁷, and pharmacological activation of PP2A elicits apoptosis of CLL

cells via SHP1 activation, which results in dephosphorylation of the BCR signaling protein LYN⁴⁸⁴. Based on these data, it could be hypothesized that reduced PP2A activity through *PPP2R1B* loss in del(11q) might influence phosphorylation of BCR signaling proteins, and we are currently investigating this aspect as well as the implication of PP2A activity in ibrutinib response. Other genes within del(11q) that have been proposed to have a role in the pathogenesis of CLL are *MRE11* and *H2AFX*, both implicated in the DDR signaling¹⁵². In addition, the deubiquitinase *USP28* is usually deleted through del(11q), and it has been shown that reduced *USP28* expression results in activation of NOTCH1 signaling, suggesting that del(11q) might influence this pathway in CLL⁴⁸⁵.

In addition to the study of the biological role of del(11q) and associated mutations in CLL initiation, clonal evolution and progression, this PhD research work explored how these cells can be **therapeutically targeted by novel pre-clinical approaches**. In this regard, we mainly focused on synthetic lethal approaches based on the DDR signaling dysfunction and impaired HR-mediated DSB repair observed in del(11q) CLL cells harboring additional *ATM* mutations. We first hypothesized that these cells could be targeted with PARP inhibitors that inhibit BER-mediated SSB repair, in the same way it has been reported with *BRCA1* or *BRCA2* deficiency in breast cancer and other solid tumors³¹⁹⁻³²¹. In accordance, we observed that HG3-del(11q) *ATM*^{MUT} cells were hypersensitive to PARP inhibition with olaparib *in vitro* and *in vivo*, which is consistent with two previous reports on primary CLL cells and the TCL1 mouse model^{486,487}. Notably, our study on CRISPR/Cas9-generated isogenic models highlighted that *ATM* biallelic loss is required for this hypersensitivity, since HG3-del(11q) cells without *ATM* mutation in the remaining allele were able to proliferate after olaparib exposure (**Results Section – Chapter 2: Figure 3A**).

Furthermore, our data revealed that the combination of olaparib and the BTK inhibitor ibrutinib was synergistic and especially effective in CLL harboring biallelic *ATM* loss, which was subsequently validated in *ex vivo* cultures of del(11q) *ATM*^{MUT} patients in the presence of the microenvironmental stimulation, providing a novel off-target effect of BTK/PI3K inhibitors on the HR repair through RAD51 dysregulation (**Results Section – Chapter 2: Figure 3, 4 and 5**). This previously unappreciated effect of BCR signaling inhibitors in the HR repair process opens a new window of possibilities for synthetic lethal combinatorial strategies in HR-deficient CLL by combining BCR signaling inhibitors with chemotherapy and/or other drugs inhibiting DSB or SSB repair pathways. Indeed, we show that the

combination of ibrutinib with bendamustine is synergistic and results in a higher amount of unrepaired DSBs (**Results Section – Chapter 2: Figure 6**). Our results expand previous observations from other studies that also found evidence of synergism between these two drugs or between idelalisib and bendamustine^{488–490}. In addition, combinations between BCR signaling inhibitors and chemoimmunotherapy are also being currently explored in young CLL patients and have shown promising results in early trials, achieving deep and durable responses with undetectable MRD^{491–493}, although longer follow-up and cytogenetic and mutational status data would be required to determine whether del(11q) *ATM*^{MUT} patients would benefit from these approaches. Furthermore, other groups have also explored the field of synthetic lethality as a therapeutic strategy for del(11q)/*ATM* mutated or del(17p)/*TP53* mutated HR-defective CLL. Specifically, the ATR inhibitor AZD6738 showed remarkable responses in pre-clinical studies using *ex vivo* primary CLL cultures and *in vivo* patient-derived xenografts⁴⁹⁴. This study also showed a synergistic effect of ATR inhibition and ibrutinib, further reinforcing the use of BCR signaling inhibitors in combination with DNA damage repair inhibitors⁴⁹⁴. Notably, we also demonstrated that AZD6738 was effective in isogenic *in vitro* models harboring combined del(11q) and *TP53* alterations. Future experiments in these models and genetically-matched primary CLL cells are warranted to explore the combination AZD6738 and BCR signaling inhibitors for CLLs with this extremely high-risk genetic background. Finally, other promising therapeutic strategies interfering the DNA damage repair pathways for *ATM*-defective CLL include SSB repair inhibition by the DNA-PKcs inhibitors KU-0060648 or CC-115^{495,496}, whereas the use of CHK1 or USP7 inhibitors has been shown to be effective in *ATM*- or *TP53*-defective CLL cells^{497,498}. In agreement with our results, it would be presumable that combination therapies between these drugs and ibrutinib or other BCR signaling inhibitors may enhance the responses of each of these treatments, although further studies would be required to assess the pre-clinical efficacy of these combinations.

After analyzing tailored treatment strategies for del(11q) *ATM*^{MUT} CLLs, we also explored whether del(11q) cells harboring additional *BIRC3* mutations could be therapeutically targeted. Based on the results obtained regarding the biological function of *BIRC3* deletion and/or mutation *in vitro*, *in vivo* and *ex vivo*, we hypothesized that del(11q) *BIRC3*^{MUT} CLLs could be targeted by either inhibiting the non-canonical NF- κ B signaling pathway or by inhibiting the resultant overexpression of anti-apoptotic BCL2 and BCL-xL proteins. To disrupt the non-canonical signaling activation of these cells we used the NIK

inhibitor NIK SMI1, observing that it was capable of inhibiting the induced proliferation resultant of non-canonical constitutive signaling mediated by *BIRC3* loss (**Results Section – Chapter 4: Figure 5B**). These results are in agreement with a very recent report that showed that NIK inhibition with CW15337 abrogated CD40L-induced non-canonical NF- κ B signaling activation in primary CLL cells⁴⁹⁹. In addition, NIK inhibition has also been explored in other lymphoid malignancies such as multiple myeloma, where the non-canonical NF- κ B signaling is also hyperactive due to alterations in *BIRC3* and other components of the pathway^{500–502}. Nevertheless, neither our study nor the one from Haselager *et al.* showed a high cytotoxic activity of NIK inhibition alone in CLL cells⁴⁹⁹, suggesting that these inhibitors may be explored in combination with other agents. Indeed Haselager *et al.* showed that NIK inhibition enhances sensitivity of CLL cells to venetoclax⁴⁹⁹. In accordance, we also showed that del(11q) *BIRC3*^{MUT} cells were more sensitive to venetoclax or BCL-xL inhibition by A1331852 and a previous study also reported that low *BIRC3* expression predicts for enhanced venetoclax or navitoclax sensitivity, being the latter a dual BCL2/BCL-xL inhibitor³⁴⁰. Collectively, these results suggest that del(11q) *BIRC3*^{MUT} cells could be therapeutically targeted by counteracting anti-apoptotic protein expression using BCL2 or BCL-xL inhibitors, as well as abrogating constitutive non-canonical NF- κ B activation by using NIK inhibitors.

Our work also revealed that the presence of del(11q) and/or associated mutations in *ATM*, *BIRC3* or *TP53* might predict responses to current treatment strategies. For instance, del(11q) *ATM*^{MUT} CLL cells are more sensitive to ibrutinib *ex vivo* (**Results Section – Chapter 2: Figure 4**), whereas del(11q) *BIRC3*^{MUT} cells favor from venetoclax therapy (**Results Section – Chapter 4: Figure 4**). These observations challenge the traditional risk stratification model based on the hierarchy of FISH-detected cytogenetic alterations^{134,503}, where patients harboring del(11q) carry a dismal prognosis in terms of both PFS and OS. However, these models are based on data from the chemoimmunotherapy treatment era, and the dramatic changes that have taken place in the treatment algorithms of CLL in the last few years urge the **need to reevaluate the prognostic implications of some CLL genetic alterations** such as del(11q). In fact, the pooled analysis of three phase III clinical trials (RESONATE, RESONATE-2 and HELIOS) comparing ibrutinib versus chemotherapy or chemoimmunotherapy has demonstrated that del(11q) patients present a more favorable outcome than those patients harboring other cytogenetic alterations or those with a normal karyotype³⁸⁵. In addition, data from the extended analysis of the trial RESONATE-2 have

revealed that del(11q) cases treated frontline with ibrutinib show excellent and durable responses, demonstrating again a superior PFS of these patients in comparison to the rest of cytogenetic groups³⁸⁴. These clinical observations are in line with the results we have obtained in our *ex vivo* models, reinforcing their validity for prediction of treatment response. Our next research step focuses on characterizing the whole transcriptome, proteome and phospho-proteome of del(11q) CLL cells in order to understand the biological implications by which the presence of this cytogenetic abnormality increases sensitivity to BCR-mediated inhibition by ibrutinib.

Nevertheless, the promising results observed with ibrutinib treatment for frontline del(11q) CLL patients are in marked contrast to those obtained in trials when ibrutinib was administered in the chemotherapy R/R CLL population, where del(11q) emerges again as a poor prognostic marker both for PFS and OS^{231,386}. The inherent mechanism(s) underlying poor responses of del(11q) chemotherapy R/R patients to ibrutinib and this sharp contrast in comparison to del(11q) patients treated frontline are still unknown. One hypothesis could be related to the crucial role of del(11q) and *ATM* in the DDR signaling and HR repair. In this way, chemotherapy-induced DSBs in *ATM*-deficient CLL cells may not be satisfactorily repaired, thus increasing genomic instability in these clones and ultimately resulting in the appearance of CK, which is a bona-fide predictive marker of poor response to ibrutinib^{228,231}. These intriguing aspects are currently being addressed thanks to my PhD research collaboration abroad at Dr. Thomas J Kipps lab in the University of California, San Diego, last year. Early findings in serial del(11q) patients collected before and after treatment confirm that treatment with chemotherapy-based regimes increases the genomic complexity of del(11q) cases, whereas treatment with non-chemotherapy-based regimes do not. In addition, preliminary findings of long-term chemotherapy (i.e. bendamustine) exposure of our CRISPR/Cas9-generated models corroborate the acquisition of novel chromosomal abnormalities in HG3-del(11q) *ATM*^{MUT} cells, but not in those HG3^{WT} clones. Additional research is currently being performed in order to expand these data, and hopefully the resulting answers will help refine treatment decisions for del(11q) in the context of novel targeted therapies.

All in all, the advances made throughout this PhD research have been possible thanks to the combined implementation of NGS and the CRISPR/Cas9 genome-editing system to generate **novel *in vitro* del(11q) models**. This versatile technique is rapidly changing our

ability to interrogate the function of individual and concurrent genetic lesions in cancer, and its true explosion is yet to come for the study of CLL biology. What the immediate future holds relies on the generation of additional *in vitro* and *in vivo* models investigating the functional consequences of CLL driver alterations with unknown biological significance^{65,66}. This is especially important in a genetically heterogeneous disease like CLL, where a large fraction of driver alterations are present in a low percentage of patients, which would require impressively large and homogeneous cohorts of primary CLL cells to address genotype-specific biological functions. Moreover, the implementation of large-scale CRISPR screens will be essential in CLL therapy in order to help uncover which genes and biological pathways play a role in resistance to novel targeted agents as well as to identify and characterize essential genes in the CLL genome that can be targeted by synthetic lethal approaches^{401,461,504}. A qualitative leap that is yet to be achieved is the capacity of CRISPR/Cas9-mediated genome-editing of primary CLL cells. If accomplished, it will substantially help overcome the limitations associated to the use of CLL cell lines and mouse models, improving our understanding of CLL-related lesions in an *ex vivo* context in the presence of the microenvironment or *in vivo* in patient-derived xenografts. To be able to genetically manipulate primary CLL cells, it will be necessary to improve transfection or transduction methods in order to deliver the CRISPR/Cas9 system components. In this way, a very recent preprint describes a novel strategy of highly efficient retroviral transduction of primary CLL cells, unveiling previously unappreciated functions of *NOTCH1* mutations in CLL⁵⁰⁵. It would be of great interest to apply this method to retrovirally deliver the CRISPR/Cas9 components into primary CLL cells in order to investigate loss-of-function or gain-of-function CLL-related driver mutations, as well their concurrent effects in an *ex vivo* setting. Finally, genetic manipulation of primary B cells or CD34⁺ HSCs from healthy individuals are feasible strategies nowadays that have been applied for the study of other hematological malignancies, and their implementation to interrogate the role of CLL-related lesions could improve our understanding of disease initiation and progression^{451,506–509}.

In summary, this work has established novel CRISPR/Cas9-based models to understand the biological mechanisms governed by concurrent CLL-related driver lesions in disease initiation and progression, as well as to identify specific therapeutic vulnerabilities amenable for therapeutic interventions. The present research highlights the feasibility of genome-editing approaches for the study of the biology of CLL, laying the groundwork for future

investigations aiming to untangle the biological determinants underlying the genetic heterogeneity of CLL.

CONCLUDING REMARKS

1. Driver chromosomal abnormalities and gene mutations are present not only in mature B lymphocytes, but also in CD34⁺ hematopoietic progenitors of CLL patients. Specifically, del(11q) and del(13q), as well as mutations in *NOTCH1* and *MYD88* are early events in CLL hematopoiesis, whereas *IGH* alterations and *TP53*, *SF3B1* and *FBXW7* mutations emerge at later B-cell maturational steps.
2. The majority of del(11q) CLL patients present additional mutations in CLL driver genes. The mutational landscape of these patients is characterized by a high co-occurrence of mutations in *ATM*, *TP53* and *BIRC3*.
3. Isogenic CRISPR/Cas9-generated CLL models represent a novel and powerful tool to interrogate the effects of individual or concurrent CLL driver alterations in cellular processes and clonal evolution. Moreover, these models provide a novel pre-clinical platform for the study of genotype-specific therapeutic responses in CLL.
4. Monoallelic *ATM* loss through del(11q) results in impaired double strand break signaling and repair, leading to DNA damage accumulation, which is further enhanced when the remaining *ATM* allele is affected by loss-of-function mutations. CLL cells harboring biallelic *ATM* inactivation show *in vitro*, *in vivo* and *ex vivo* hypersensitivity to PARP inhibition with olaparib.
5. Dual BCR and PARP inhibition through the combination of ibrutinib and olaparib is synergistic in del(11q)/*ATM* mutated CLL cell lines and primary cells, overcoming the induction of proliferation from the stromal microenvironment. The mechanism of synergy of this combination relies in an off-target effect of ibrutinib in the homologous recombination repair, leading to RAD51 foci formation impairment in double strand break lesions and enhancing the lethal DNA damage accumulation of del(11q) CLL cells.
6. Biallelic *ATM* and *TP53* lesions are mutually exclusive in CLL patients. Mechanistically, the combination of both events leads to defective mitosis and impaired clonal fitness *in vitro*, added to deficient engraftment *in vivo*.
7. The combination of monoallelic del(11q) and *TP53* alterations defines an extremely high-risk subgroup of CLL patients with shorter overall survival than patients harboring these alterations individually. Del(11q) cooperates with *TP53* loss to drive clonal advantage *in vitro* and *in vivo*, as well as to alter *in vitro* responses to BCR and PI3K inhibitors.

8. *BIRC3* mutation and/or deletion through del(11q) in CLL cells activates non-canonical NF- κ B signaling through NIK cytoplasmic stabilization and RelB-p52 nuclear translocation and activation, resulting in BCL2 overexpression and defining a genotype-specific vulnerability to venetoclax. Moreover, BIRC3-dependent non-canonical NF- κ B signaling activation can be counteracted by pharmacological NIK inhibition using NIK SMI1.
9. *BIRC3* mutation in the remaining allele of del(11q) CLL cells further enhances non-canonical NF- κ B signaling activation, conferring clonal advantage *in vitro* and accelerating leukemic progression in an *in vivo* xenograft model, providing a biological explanation of the negative predictive impact of *BIRC3* biallelic inactivation in CLL patients.

Resumen en Castellano

Tesis Doctoral

Estudio de los determinantes biológicos implicados en el origen, evolución clonal y vulnerabilidades terapéuticas de la leucemia linfática crónica con del(11q) mediante herramientas de edición genética

Supervisores:

Prof. Dr. Jesús M. Hernández Rivas

Dra. M. del Rocío Benito Sánchez

Dra. Ana E. Rodríguez Vicente

Miguel Quijada Álamo

2021



INTRODUCCIÓN

1. LEUCEMIA LINFÁTICA CRÓNICA – CARACTERÍSTICAS GENERALES

La leucemia linfática crónica (LLC) es una entidad reconocida en la clasificación de neoplasias hematopoyéticas y linfoides de la Organización Mundial de la Salud (OMS) del año 2017¹. La LLC es una síndrome linfoproliferativo de células B clonales, caracterizado por la acumulación de linfocitos neoplásicos de aspecto pequeño y maduro, que se acumulan en la sangre, bazo, médula ósea y otros órganos linfoides^{2,3}.

1.1 Epidemiología

La LLC es la forma más frecuente de leucemia en Europa y Estados Unidos, con una incidencia de 4,1/100.000 casos. Esta neoplasia supone más de 15.000 nuevos diagnósticos de cáncer y más de 4,500 muertes anuales en Estados Unidos⁴. La incidencia de LLC varía entre sujetos de diferentes regiones geográficas. Es menos común en poblaciones africanas o hispanas, y su incidencia es marcadamente baja en individuos asiáticos^{5,6}. La mediana de edad al diagnóstico se encuentra entre los 70-72 años, con una predominancia en hombres en un ratio 1,7:1 en todos los subgrupos étnicos^{4,5}. La proporción de pacientes jóvenes diagnosticados con LLC de estadio temprano ha incrementado en los últimos años, posiblemente debido al incremento de los análisis de sangre en la rutina clínica. Además, es posible que los cambios demográficos en la sociedad actual se traduzcan en un incremento de la prevalencia y la mortalidad de la LLC en las próximas décadas^{4,7}.

1.2 Etiología

Las disparidades observadas en la incidencia de LLC en diferentes regiones geográficas apuntan a que la LLC podría surgir por una combinación de factores genéticos y ambientales, sin embargo, la etiología exacta de esta enfermedad no es conocida⁸. A pesar de que la gran mayoría de casos de LLC ocurren de forma esporádica, existen evidencias de predisposición hereditaria a padecer esta patología⁹. En primer lugar, los familiares de primer grado de pacientes con LLC tienen un riesgo 8,5 veces mayor de desarrollar esta enfermedad¹⁰. Además, la concordancia de LLC es mayor entre gemelos monocigóticos en comparación con gemelos dicigóticos¹¹. Numerosos estudios de asociación de genoma completo (GWAS; genome-wide association studies) han identificado polimorfismos de nucleótido único (SNPs; single-nucleotide polymorphisms) en múltiples loci de susceptibilidad de LLC (ej.

4q25/*LEF1*, 6p25.3/*IRF4*), que en total suponen aproximadamente el 19% del riesgo hereditario de LLC¹²⁻²⁰.

Respecto a factores ambientales que contribuyan al desarrollo de la LLC, ciertas evidencias sugieren que tanto el Agente Naranja como la exposición a insecticidas podrían considerarse factores de riesgo en LLC^{21,22}, mientras que no hay certeza de que la radiación ionizante, las infecciones virales o las transfusiones de sangre tengan una implicación en este aspecto²³⁻²⁵.

1.3 Diagnóstico

De acuerdo a la última versión de las guías del grupo internacional de LLC (iwCLL; International Workshop on CLL), el diagnóstico de la LLC se determina principalmente a través de test de laboratorio, como el recuento de leucocitos y linfocitos, morfología e inmunofenotipo²⁶. La LLC se diagnostica cuando hay una presencia de $\geq 5 \times 10^9/L$ linfocitos B clonales en sangre periférica durante al menos 3 meses. En términos morfológicos, las células de LLC se corresponden con linfocitos pequeños y maduros con un citoplasma reducido y un núcleo denso, con un nucléolo indiscernible y agregados parciales de cromatina^{4,26}. La clonalidad de los linfocitos B circulantes necesita ser confirmada por citometría de flujo, estando el **inmunofenotipo de la LLC** caracterizado por la expresión anormal del antígeno de célula T CD5 en combinación con los antígenos de célula B CD19, CD20 y CD23. En comparación con las células B sanas, los linfocitos B de LLC expresan menores niveles de inmunoglobulina de superficie, CD20 y CD79b²⁶⁻²⁹. Además, la expresión de las cadenas ligeras de inmunoglobulinas está restringida a kappa o lambda en cada clon leucémico²⁸. Recientes trabajos colaborativos de armonización han confirmado que un panel de CD5, CD19, CD20, CD23, kappa y lambda es suficiente para determinar el diagnóstico de LLC³⁰. En casos dudosos, otros marcadores como CD43, CD79b, CD81, CD200, CD10 o ROR1 podrían también ayudar a refinar el diagnóstico de la enfermedad³⁰.

El desarrollo de la LLC está normalmente precedido por **linfocitosis B monoclonal (LBM)**, una entidad pre-maligna definida por la presencia de menos de $5 \times 10^9/L$ células B clonales en ausencia de linfadenopatía, organomegalia (definida por examen físico o tomografía computarizada) o citopenias^{1,31}. El ratio de progresión de LBM a LLC es de un 1-2% por año³². La revisión del 2017 de la clasificación de la OMS para neoplasias linfoides diferencia entre LBM de bajo recuento y alto recuento, dependiendo del número de células B clonales en sangre periférica ($< 0.5 \times 10^9/L$ y $\geq 0.5 \times 10^9/L$, respectivamente). La LBM de bajo

recuento tiene una alta prevalencia en individuos de edad avanzada y su riesgo de progresión a LLC es muy limitado, por lo que no requiere de control clínico específico adicional al seguimiento rutinario³³⁻³⁶. Por el contrario, la LBM de alto recuento sí que requiere seguimiento específico y tiene un fenotipo y unas características genéticas similares a la LLC de estadio temprano^{36,37}.

En el extremo contrario, una LLC puede sufrir una **transformación histológica** en un linfoma agresivo de célula B, en un proceso conocido como **síndrome de Richter (RS; Richter's Syndrome)**, que está asociado con un pronóstico marcadamente desfavorable³⁸. Para el diagnóstico de transformación a RS se requiere una biopsia del ganglio linfático³⁹. La clasificación de la OMS de neoplasias linfoides reconoce dos variantes patológicas distintas de RS: linfoma difuso de células B grandes (DLBCL; diffuse large B cell lymphoma) o Linfoma Hodgkin (HL; Hodgkin lymphoma). La mayoría de los casos de DLBCL RS (~80%) están relacionados a nivel clonal con el clon iniciador de la LLC según los estudios de recombinación de los genes *IGHV-D-J*. Por el contrario, solamente el ~40-50% de los casos HL RR están relacionados clonalmente con el estadio precedente de LLC, siendo estos casos sin relación clonal considerados como linfomas *de novo* que surgen en el paciente de LLC⁴⁰⁻⁴³. En la totalidad de casos de LLC, la incidencia de transformación a RS es de ~0.5% y ~0.05% por año de observación para las variantes DLBCL y HL, respectivamente^{44,45}.

1.4 Grupos de riesgo y marcadores pronósticos

La LLC es una enfermedad con un curso clínico extremadamente heterogéneo. Las manifestaciones clínicas pueden variar desde formas indolentes de la enfermedad sin necesidad de tratamiento y expectativa de vida similar a la de la población sana, hasta una enfermedad agresiva caracterizada por la necesidad urgente de intervención terapéutica, refractariedad al tratamiento estándar y supervivencia global (OS; overall survival) reducida^{3,46}. Para la clasificación de los pacientes en base a sus características clínicas, existen dos **modelos de estratificación** propuestos por **Rai**⁴⁷ y **Binet**⁴⁸ hace más de 40 años, que se siguen usando a día de hoy con modificaciones menores debido principalmente a su simplicidad, requerimientos de bajo coste, consistencia y fiabilidad para ser usados por hematólogos en todo el mundo²⁶. La versión revisada de la clasificación Rai estratifica a los pacientes en riesgo bajo, intermedio o alto dependiendo de parámetros como linfocitosis, anemia o trombocitopenia, así como observaciones clínicas como agrandamiento de ganglios linfáticos, esplenomegalia o hepatomegalia. Estos parámetros están también recogidos en la

clasificación de Binet, que subdivide a los pacientes en tres categorías (A, B y C) y considera también los niveles de hemoglobina y el recuento de plaquetas^{47,48}. Tras la definición de estos sistemas, otros marcadores pronósticos de fácil acceso como el tiempo de doblaje linfocitario o la infiltración de médula ósea han sido implementados también en el algoritmo de estratificación de riesgo^{49,50}.

Los recientes avances en la investigación de la LLC en las últimas décadas han permitido la caracterización de una cantidad significativa de potenciales **biomarcadores que proporcionan información pronóstica independiente del estadio clínico**^{51,52}. Estos marcadores pronósticos incluyen proteínas a nivel de suero (ej. Beta-2 microglobulina (β_2M), timidina quinasa (TK), CD23 soluble)⁵³⁻⁵⁸, marcadores genéticos (ej. Estado mutacional de la región variable del gen de la cadena pesada de las inmunoglobulinas (IGHV)^{59,60}, estereotipos de la inmunoglobulina (IG) del receptor de célula B (BCR; B-cell receptor)^{61,62}, alteraciones cromosómicas⁶³, cariotipo complejo⁶⁴, mutaciones somáticas⁶⁵⁻⁶⁸, alteraciones en regiones no codificantes del genoma^{69,70}, subtipos epigenéticos^{71,72}) y marcadores inmunofenotípicos (ej. CD38, ZAP70, CD49d)^{59,73-76}. La información pronóstica de los biomarcadores más relevantes de cada una de estas categorías se encuentra reflejada en la **Tabla 1**, además, se proporcionará más información sobre el impacto pronóstico de los marcadores genéticos en la *Sección 2: Genética de la LLC*. Para reducir y simplificar la gran cantidad de marcadores pronósticos disponibles, en unos pocos con relevancia clínica probada y accesibles para hematólogos alrededor del mundo, se han creado índices pronósticos que combinan tanto información genética como clínica, como es el caso del CLL-IPI (CLL International Prognostic Index)⁷⁷⁻⁷⁹.

Tabla 1. Principales biomarcadores pronósticos identificados en LLC.

Marcador	Predictor de pronóstico adverso	Ref.
Biomarcadores serológicos		
β_2M	> 3.5 mg/L	53,55
TK	> 7.0 U/L	53,56
sCD23	sCD23 tiempo de doblaje < 1 año	57,58
Biomarcadores genéticos		
Estado mutacional IGHV	No mutado	59,60
Estereotipo BCR IG	Subset #1, #2 y #8	61,80

Alteraciones cromosómicas	Deleción de 17p; deleción de 11q	63
Cariotipo complejo	Cariotipo complejo (≥ 3 alteraciones)	64
Mutaciones somáticas	<i>TP53, ATM, SF3B1, NOTCH1, BIRC3, EGR2</i>	67,81-86
Mutaciones no-codificantes	<i>NOTCH1 3'UTR</i>	66,69
Expresión de miRNAs	\uparrow miR-155, \downarrow miR-150, \downarrow miR-29c, \downarrow miR-34a	87-90
Subtipos epigenéticos	"Naïve B-cell like" LLCs	71,72

Biomarcadores

inmunofenotípicos

Expresión de CD38	$\geq 30\%$ células positivas	59
Expresión de ZAP70	$\geq 20\%$ células positivas	73,74
Expresión de CD49d	$\geq 30\%$ células positivas	75,76

β_2M : beta-2 microglobulina; TK: timidina quinasa; sCD23: CD23 soluble; IGHV: región variable del gen de la cadena pesada de las inmunoglobulinas; BCR: receptor de célula B; IG: inmunoglobulina; FISH: hibridación fluorescente *in situ*; miRNA: micro-RNA; \uparrow alta expresión; \downarrow baja expresión.

1.5 Terapia de la LLC

1.5.1 Necesidad de tratamiento y evaluación de la respuesta

El tratamiento de la LLC debe ser iniciado en el momento en el que el paciente presente progresión o enfermedad activa o sintomática, definida por una combinación de parámetros clínicos y biológicos recogidos en las guías del iwCLL²⁶. Los pacientes con enfermedad asintomática no requieren de intervención terapéutica y deben ser monitorizados hasta que haya evidencia de progresión de la enfermedad⁴.

Los criterios de evaluación de respuesta al tratamiento están también recogidos en detalle en las guías del iwCLL, y clasifican principalmente la respuesta en las siguientes categorías: remisión completa, remisión parcial, enfermedad estable y enfermedad refractaria²⁶. Los pacientes de LLC que alcanzan remisión completa pueden ser subclasificados en base a la detección de enfermedad mínima residual (MRD; minimal residual disease), un marcador de respuesta que ha ganado amplia relevancia en la última década gracias al desarrollo y la mejora de técnicas como la citometría de flujo multicolor, PCR o la secuenciación masiva (NGS; next-generation sequencing)^{91,92}. Numerosos ensayos clínicos han demostrado que las terapias que son capaces de eliminar la MRD (definida como la presencia de menos de 1 célula de LLC por cada 10.000 leucocitos) dan lugar a un beneficio clínico a largo plazo⁹³⁻⁹⁵.

1.5.2 Aproximaciones terapéuticas y algoritmo de tratamiento

El tratamiento de los pacientes de LLC ha recorrido una larga trayectoria desde la primera aprobación de regímenes basados en quimioterapia hace más de 50 años. Los agentes quimioterapéuticos empleados para el tratamiento de la LLC principalmente incluyen fármacos análogos de las purinas (comúnmente fludarabina) o agentes alquilantes como el clorambucilo, la ciclofosfamida o la bendamustina. A principios de los años 2000, el uso de quimioterapia en combinación con inmunoterapia (principalmente en la forma de anticuerpos anti-CD20 como rituximab) se convirtió en el tratamiento de referencia en la LLC, siendo las combinaciones de **fludarabina, ciclofosfamida y rituximab (FCR)** o bendamustina y rituximab (BR) las opciones más ampliamente utilizadas. En la última década, el conocimiento en profundidad de los procesos biológicos causantes de la patogénesis de la LLC ha resultado en la aprobación de fármacos dirigidos que inhiben vías de señalización responsables del crecimiento y/o supervivencia de las células de LLC (solos o en combinación con anticuerpos anti-CD20 de segunda generación como ofatumumab o obinutuzumab). Específicamente, los **inhibidores de la señalización por BCR** (los inhibidores de BTK ibrutinib y acalabrutinib, así como el inhibidor de PI3K idelalisib) y los **inhibidores de BCL2** (venetoclax) han sido aprobados para el tratamiento de la LLC^{2,4,96}. A pesar de que la llegada de las terapias dirigidas ha supuesto una revolución en los esquemas del tratamiento de la LLC, el trasplante alogénico de progenitores hematopoyéticos es una estrategia terapéutica potencialmente curativa en la LLC y puede considerarse para aquellos pacientes refractarios o en recaída (R/R) a terapias dirigidas, así como en los casos de RS con relación clonal a la LLC precedente que responden a quimioterapia^{97,98}. Otra aproximación terapéutica prometedora que se encuentra en fase de investigación es la inmunoterapia CAR-T anti-CD19 en combinación con ibrutinib, así como el uso de células NK que expresan anti-CD19 CAR⁹⁹⁻¹⁰¹.

En resumen, la evolución constante del algoritmo de tratamiento de la LLC en los últimos años ha supuesto un cambio de paradigma, sustituyendo los regímenes basados en quimioterapia en favor de estrategias más individualizadas para los pacientes de LLC. El esquema de tratamiento actual tanto para LLC en primera línea como R/R depende de múltiples parámetros genéticos, clínicos y terapéuticos, y se encuentra resumido en la **Figura 1**.

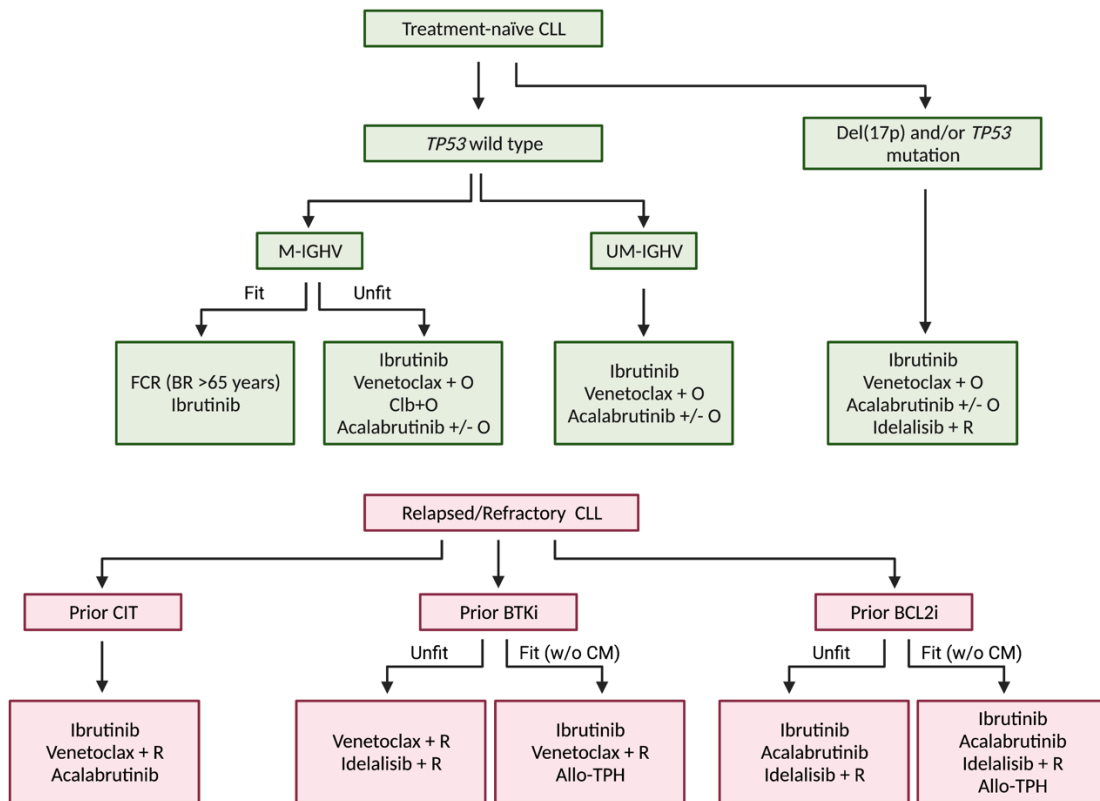


Figure 1. Algoritmo de tratamiento para pacientes de LLC en primera línea (verde) o en recaída o con enfermedad refractaria (R/R) (rojo). FCR: fludarabina + ciclofosfamida + rituximab; BR: bendamustina + rituximab; O: obinutuzumab; Clb: clorambucilo; R: rituximab; CIT: quimioinmunoterapia; BTKi: inhibidor de BTK; BCL2i: inhibidor de BCL2; CM: comorbilidades; Allo-TPH: trasplante alogénico de progenitores hematopoyéticos.

2. GENÉTICA DE LA LLC

El creciente conocimiento de la genética de la LLC en las últimas décadas ha permitido definir a este tipo de leucemia como una entidad altamente heterogénea, proporcionando información acerca de los distintos tipos celulares a partir de los cuales esta enfermedad se podría originar, así como el complejo conjunto de lesiones genéticas que están asociadas con su patogénesis y pronóstico.

2.1 Origen celular de la LLC

La identificación de la célula de origen de la LLC, definida como la célula no maligna a partir de la cual se inicia la transformación leucémica, puede ser útil para determinar qué alteración o alteraciones específicas son los principales “drivers” de la enfermedad¹⁰². El estudio biológico de la LLC en los últimos años ha proporcionado evidencia acerca de varios

tipos celulares compatibles como iniciadores de la enfermedad. Concretamente, esto ha sido posible gracias al análisis exhaustivo del BCR IG mediante técnicas de inmunogenética¹⁰².

La molécula de IG es un componente esencial del complejo multimérico que compone el BCR y define una identidad genética única que está presente desde el nacimiento de cada célula B a lo largo de su vida, lo que es aplicable también a aquellas células B de la LLC¹⁰³. A finales de la década de 1990, varias investigaciones empezaron a sugerir un sesgo en el uso de la IG en LLC¹⁰⁴. Específicamente, se demostró que las células de LLC usan preferente las regiones VH1, VH3 y VH4 de la familia de genes IGHV^{104,105}, y expresan un repertorio de BCRs restringido, incluyendo anticuerpos con una región determinante de complementariedad 3 (CDR3) casi idéntica, indicando la posibilidad de una selección antigénica¹⁰⁶⁻¹⁰⁹. El hecho de que las células de LLC presenten reordenamientos clonales de la molécula de IG, en paralelo al inmunofenotipo particular de estas células, sugería que las células de LLC derivan de un tipo de célula B madura que expresa bajos niveles de marcadores de célula B (IG de superficie, CD19 y CD20), y es positiva para la expresión de los antígenos CD23, CD200 y CD5¹⁰². Concretamente, la expresión de CD5 llevó a la especulación inicial de que la LLC podría derivar de células B B1 involucradas en inmunidad innata^{110,111}. El posterior descubrimiento de un grupo de pacientes de LLC que portaban mutaciones somáticas en los genes IGHV (**M-IGHV**) indicaba que las células de LLC de estos casos procedían de células B con experiencia antigénica, es decir, que habían sufrido el proceso de hipermutación somática (SHM; somatic hypermutation) en los centros germinales (GC; germinal center) de órganos linfoides secundarios^{104,112}. Por otro lado, hay otro grupo de pacientes que no porta mutaciones en IGHV (**UM-IGHV**). En estos casos, no está claro si este tipo de LLCs derivan de células B naïve (pre-GC) o de células B con experiencia antigénica independientes de los GC^{60,104,112}. Esta hipótesis tiene relevancia tanto a nivel biológico como clínico, ya que ambos subgrupos (M-IGHV y UM-IGHV) tienen implicaciones pronósticas. Particularmente, los pacientes UM-IGHV, definidos por la ausencia o carga limitada ($\geq 98\%$ identidad con la línea germinal) de SHM, presentan un curso clínico más agresivo, con un menor tiempo hasta el primer tratamiento (TTFT; time to first treatment), mala respuesta a regímenes basados en quimioinmunoterapia y OS reducida^{59,60}. Por el contrario, los pacientes M-IGHV ($< 98\%$ identidad con la línea germinal) normalmente presentan una enfermedad de carácter más indolente y tiempos de TTFT y OS más elevados^{59,60}.

A principios de los años 2000, el empleo de técnicas para el estudio del perfil de expresión génica (GEP; gene-expression profiling) en células B normales y células B de LLC reveló que el perfil transcriptómico tanto de los casos UM-IGHV como los M-IGHV es más similar al de las células B de memoria CD27⁺ que al de las células B CD5⁺, indicando que las células de LLC UM-IGHV se originan a partir de células B CD27⁺ con experiencia antigénica e independientes de los GC, mientras que las células M-IGHV derivan de células B CD27⁺ post-GC^{113,114}. Esta hipótesis es apoyada por el hecho de que en aproximadamente el 40% de los casos de LLC, pacientes no relacionados entre sí portan idénticos o casi idénticos BCR IGs, que han sido agrupados en > 200 subgrupos de “receptores estereotipados” hasta la fecha¹¹⁵⁻¹¹⁷, algunos de ellos con implicaciones pronósticas^{61,80,118-120}. Posteriores estudios adicionales de GEP han sugerido que las células M-IGHV derivan de una entidad B CD27⁺CD5⁺ post-GC previamente desconocida, mientras que los casos UM-IGHV se parecerían más a células B naïve CD5⁺CD27⁻¹²¹ (**Figura 2**). En concordancia, el perfil de metilación global es también diferente entre los casos M-IGHV y UM-IGHV, y se asemeja a las células B de memoria y a las células B naïve, respectivamente⁷¹. Sin embargo, la posibilidad de que las células de LLC deriven de un tipo de célula B no conocido hasta el momento tampoco puede ser descartada¹⁰².

Otro aspecto controvertido en relación al origen celular de la LLC hace referencia al **momento de la maduración en el que ocurre el primer evento genético o epigenético** que desencadena la enfermedad. La reciente implementación de técnicas de secuenciación del exoma y genoma, así como la mejora de los métodos de xenotrasplante de células humanas en ratón, han sugerido que estos eventos podrían ocurrir en **progenitores hematopoyéticos CD34⁺ (HSCs; hematopoietic stem cells)**¹²². En este contexto, estudios de xenotrasplante han mostrado que las células HSCs (CD34⁺CD38⁻) purificadas de muestras de médula ósea de pacientes de LLC son capaces de injertar en ratones inmunodeficientes, dando lugar a un número elevado de progenitores B policlonales (células pro-B; CD34⁺CD19⁺), en comparación con ratones trasplantados con HSCs de individuos sanos¹²³, sugiriendo que la diferenciación de las células HSCs de LLC está sesgada hacia el linaje de célula B. Además, los xenotrasplantes de células HSCs de LLC, pero no aquellos de HSCs de individuos sanos, dan lugar a células B clonales y maduras con un inmunofenotipo CD5⁺CD23⁺ similar al de la LBM y LLC, potencialmente indicando el rol crucial de la señalización del BCR en la selección clonal¹²³. En consistencia con la hipótesis de existencia de una célula HSC de LLC, existen evidencias de que en algunos pacientes que han sido sometidos a trasplante alogénico de

progenitores hematopoyéticos, se han transmitido células linfoides pre-neoplásicas del donante al receptor, que con el tiempo han dado lugar al desarrollo de una LLC^{122,124}. Adicionalmente, se ha reportado la presencia de mutaciones somáticas y alteraciones cromosómicas típicas de la LLC en CD34⁺ HSCs de pacientes de LLC^{125,126}, aunque la dificultad de separación de poblaciones HSC puras sin contaminación de células de LLC residuales sigue siendo un reto metodológico¹²⁷.

Finalmente, numerosos estudios recientes han indicado que existen clones hematopoyéticos con mutaciones génicas adquiridas (hematopoyesis clonal). Estos clones son más frecuentes en edades avanzadas y pueden conducir al desarrollo de neoplasias hematológicas, incluyendo la LLC^{128,129}. Algunas de estas mutaciones pueden aparecer en genes relacionados con la patogénesis de la LLC, además, el panorama mutacional de la LBM de bajo recuento, la LBM de alto recuento y la LLC de estadio temprano es prácticamente indistinguible, con mutaciones génicas que aparecen indistintamente en estas tres entidades, reforzando la hipótesis de que al menos una fracción de las alteraciones somáticas en la LLC ocurre previamente al desarrollo de la enfermedad¹³⁰. Además, recientemente se ha reportado la presencia de alteraciones cromosómicas típicas de la LLC en individuos sanos de edad avanzada^{131,132}, lo que podría concordar con la aparición del primer evento genético de la LLC en el estadio de maduración correspondiente a las HSCs.

En resumen, la célula de origen de la LLC ha sido objeto de continuo debate durante años. El modelo más aceptado a día de hoy (**Figura 2**) indica que es probable que las células de **LLC M-IGHV deriven de células B CD5⁺CD27⁺ post-GC**, mientras que las células de **LLC UM-IGHV parecen originarse a partir de células B CD5⁺CD27⁻ pre-GC**, que podrían surgir de células B naïve o a partir de un linaje alternativo de precursores de célula B. Además, el primer evento genético que conduce al desarrollo de la LLC podría ocurrir en un estadio de maduración temprano que afecte a células HSC con capacidad de autorrenovación. Sin embargo, futuros estudios que incorporen nuevas y precisas técnicas como la secuenciación de célula única de ADN y ARN serían necesarios para validar plenamente estas hipótesis.

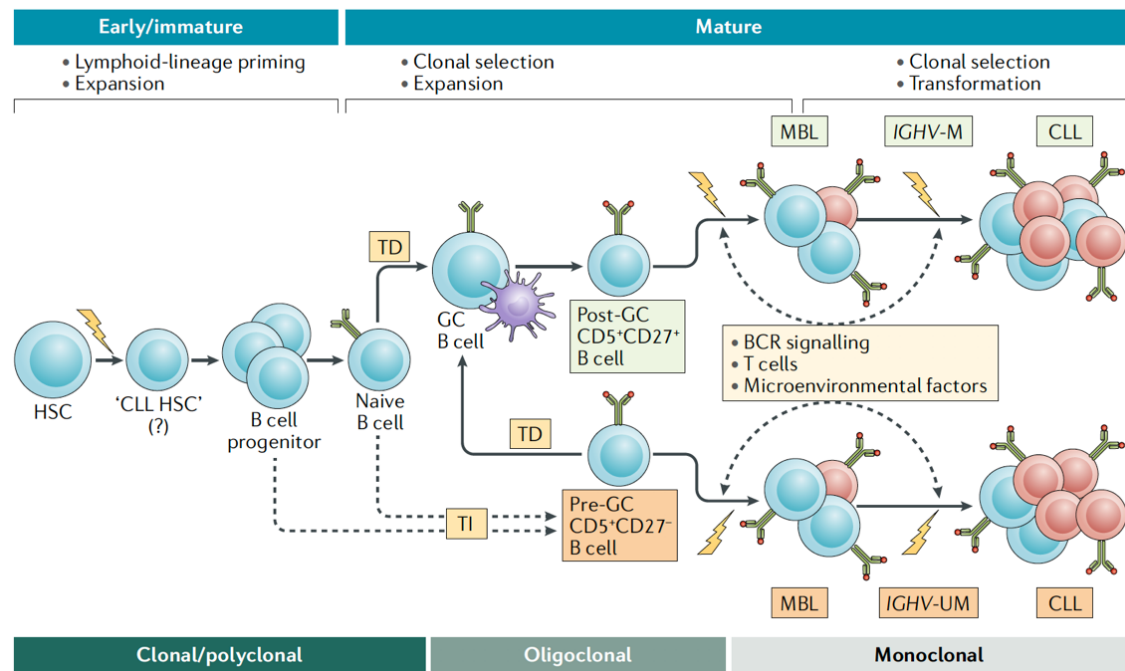


Figura 2. El origen celular de la LLC. Esquema representativo del modelo actual propuesto para el origen de la LLC. Se ha sugerido que el primer evento genético (símbolo del rayo) relacionado con la patogénesis de la enfermedad puede ocurrir en HSCs. Estas lesiones podrían favorecer la expansión de progenitores B policlonales y la subsecuente estimulación antigénica podría conducir a una selección oligoclonal y posterior expansión de células B maduras. Dado que las células M-IGHV sufren un proceso de SHM, es probable que deriven de células B CD5⁺CD27⁺ post-GC. Por el contrario, las células de LLC UM-IGHV podrían originarse o bien a partir de células B naïve CD5⁺CD27⁻ pre-GC, o bien a partir de un linaje alternativo de progenitores B. Finalmente, la evolución de estos predecesores a LBM y LLC podría estar orquestada por eventos genéticos o epigenéticos adicionales, señalización por BCR, interacciones con células T o interacciones con elementos del microambiente. TD: dependiente de célula T; TI: independiente de célula T. Las flechas con guiones indican posibles vías implicadas (Tomada de Bosch & Dalla-Favera. 2019)¹⁰².

2.2 Alteraciones genéticas en la LLC

La elevada prevalencia de LLC y la amplia disponibilidad de células tumorales en la sangre periférica de estos pacientes ha permitido la implementación de técnicas genómicas pioneras para el estudio de esta enfermedad a lo largo de los años. Esta profunda caracterización ha mostrado que el panorama de alteraciones genéticas de la LLC es extremadamente heterogéneo, lo que se traduce la gran variabilidad observada entre el curso clínico de diferentes pacientes. Algunas de estas alteraciones son una marca distintiva de la patogénesis y el pronóstico de la enfermedad, e incluyen alteraciones cromosómicas, mutaciones somáticas, alteraciones en ARN no codificante o desregulación epigenética.

2.2.1 Alteraciones cromosómicas

Desde finales de 1970, numerosos estudios han implementado un amplio abanico de técnicas citogenéticas para la detección de alteraciones cromosómicas en la LLC. Estas técnicas incluyen el cariotipo convencional o bandeo G (CBA; chromosome banding analysis), hibridación fluorescente *in situ* (FISH; fluorescence *in situ* hybridization), arrays genómicos, y más recientemente, secuenciación masiva¹³³. Estos estudios han aportado información acerca de la composición del genoma de la LLC, identificando una amplia variedad de alteraciones citogenéticas que pueden aparecer hasta en un 80% de los casos de LLC al diagnóstico². De todas ellas, las más frecuentes son las deleciones del brazo largo de los cromosomas 11 y 13, del(11q) y del(13q), respectivamente, la deleción del brazo corto del cromosoma 17, del(17p), y la trisomía del cromosoma 12 (trisomía 12). Estas cuatro alteraciones tienen además un papel destacado en el pronóstico y evolución de la LLC^{63,134}. El estudio de FISH se ha convertido en la técnica de referencia en la práctica clínica para la detección de alteraciones cromosómicas con relevancia pronóstica, y los paneles de FISH normalmente incluyen sondas que detectan estas cuatro alteraciones. Sin embargo, otras técnicas como los arrays genómicos y la secuenciación masiva han demostrado proporcionar un panorama citogenético más completo de los pacientes de LLC, mientras que el cariotipo convencional sigue siendo la técnica de referencia para la determinación de la complejidad genómica en la LLC¹³³.

2.2.1.1 Del(11q)

La deleción de la región cromosómica 11q22.3 aparece en un 12-20% de los casos de LLC al diagnóstico^{63,134-136}. Los pacientes portadores de esta alteración suelen ser más jóvenes que el paciente de LLC promedio, con una mediana de edad al diagnóstico de 59 años, y presentan una enfermedad caracterizada por linfadenopatías de gran volumen¹³⁷. Este subgrupo de LLCs normalmente se asocia con características de mal pronóstico, como UM-IGHV y positividad de ZAP70, y el curso clínico de estos pacientes está definido habitualmente por una rápida progresión de la enfermedad, TTFT corto y OS reducida en aquellos pacientes tratados con regímenes basados en quimioterapia^{63,137-141}. Además, nuestro grupo y otros han reportado previamente que el tamaño clonal de la del(11q) tiene un impacto pronóstico^{142,143}.

La presencia de del(11q) es exclusivamente monoalélica en la LLC, y el tamaño de esta deleción es altamente variable entre pacientes¹⁴⁴⁻¹⁴⁶. La mayoría de los casos suelen presentar una deleción larga que normalmente abarca un tamaño de más de 20 Mb. Por el contrario,

un pequeño porcentaje de pacientes con del(11q) presenta una deleción corta, aunque el significado biológico o pronóstico de estas diferencias se desconoce¹⁴⁷. La implementación de arrays de SNP de alta resolución ha revelado que la práctica totalidad de pacientes con del(11q) presentan una **región común delecionada (MDR; minimal deleted region)** de 2-3 Mb, que comprende al gen supresor de tumores *ATM*, entre otros¹⁴⁶⁻¹⁴⁹.

Se desconocen las causas biológicas subyacentes a la elevada tasa de progresión de los casos de LLC con del(11q). Tradicionalmente, se ha considerado que la deleción de *ATM* es la principal responsable de la patobiología de la del(11q). Esto además se apoya en el hecho de que **un tercio de los pacientes con del(11q) presentan mutaciones en el alelo restante de *ATM***, dando como consecuencia una pérdida bialélica de *ATM* y una completa pérdida de función de la proteína *ATM*^{82,150}. Dado que *ATM* es un **regulador central de la señalización en respuesta a daño en el ADN (DDR; DNA damage response)**, numerosos estudios han investigado el papel de la del(11q) en la respuesta a quimioterapia y en la integridad genómica, demostrando que las células de LLC con del(11q) presentan alteraciones en la respuesta a regímenes basados en quimioterapia y una media más elevada de alteraciones del número de copias (CNAs; copy-number alterations), lo que es indicativo de inestabilidad genética^{82,151-153}. Además, se ha propuesto que otros genes incluidos en esta deleción podrían tener un papel en la progresión de la LLC. Uno de estos genes es *BIRC3*, un regulador negativo de la ruta no canónica de NF- κ B (“nuclear factor kappa-light-chain-enhancer of activated B cell”), que aparece delecionado en ~80% de los casos con del(11q) y puede estar también afectado de forma bialélica como consecuencia de mutaciones truncadoras en el alelo restante^{85,154-156}. Sin embargo, la significancia biológica de la pérdida monoalélica o bialélica de *BIRC3* no ha sido explorada. Finalmente, la haploinsuficiencia de otros genes localizados en 11q22.3 (ej. *RDX*, *FDX1*, *RAB39*, *CUL5*, *ACAT1*, *NPAT*, *KDELC2*, *EXPH5*, *MRE11*, *HA2FX*, *USP28* y *PPP2R1B*) podría tener un papel en la patogénesis de la enfermedad, aunque hasta el momento solo hay evidencias circunstanciales y datos limitados sin validación a nivel funcional que relacionen la haploinsuficiencia de alguno de estos genes y la patobiología de la del(11q)^{147,152,157}.

2.2.1.2 Del(13q)

La deleción de la región cromosómica 13q14 está presente en más del 50% de los casos de LLC al diagnóstico y es la alteración citogenética más frecuente detectada en este tipo de leucemia^{63,134-136,158}. La presencia de esta deleción define un subgrupo de pacientes con

características de buen pronóstico, como M-IGHV y mayor TTFT y OS, especialmente en aquellos casos que portan del(13q) como alteración única^{63,135,159}.

Este tipo de delección muestra una heterogeneidad anatómica manifiesta, aunque la MDR normalmente comprende los miRNAs **miR-15a/16-1** así como **DLEU7**, y todos los genes comprendidos entre ambos¹⁶⁰⁻¹⁶⁴. Las delecciones más largas de 13q14 pueden incluir al gen supresor de tumores **RBI**, lo que empeora el pronóstico del subgrupo de pacientes con del(13q)¹⁶⁵⁻¹⁶⁷. Al contrario de lo que sucede con otras alteraciones citogenéticas recurrentes en la LLC, se pueden dar del(13q) bialélicas en un ~30% de los casos de este subgrupo, aunque no existe un consenso acerca del impacto clínico de este tipo de eventos^{159,167-169}.

A nivel biológico, se ha postulado que la pérdida de miR-15a/16-1 produce una desregulación del ciclo celular y la apoptosis². Específicamente, estos miRNAs modulan la expresión de la ciclina D2 y la proteína anti-apoptótica BCL2^{170,171}. El papel de este conjunto de miRNAs en la patogénesis de la LLC se ha confirmado *in vivo*, dado que la delección condicional del locus murino equivalente a la MDR de la del(13q), así como delecciones más grandes, son capaces de recapitular diferentes pasos de la evolución de LBM a LLC en modelos de ratón^{171,172}.

2.2.1.3 Del(17p)

Las delecciones de la región cromosómica 17p13/**TP53** se han reportado en diferentes frecuencias dependiendo del estadio clínico de la enfermedad, y oscilan desde un 4-12% al diagnóstico hasta más de un 30% en pacientes en recaída^{63,81,134,173-175}. La **Del(17p)** siempre se ha considerado como la **alteración citogenética de mayor riesgo** en LLC, y los pacientes portadores de esta delección muestran la supervivencia libre de progresión (PFS; progression-free survival) y la OS más corta dentro de todos los subgrupos citogenéticos^{63,134,176}. Además, numerosos estudios han demostrado que los pacientes con del(17p) no responden al tratamiento con regímenes basados en quimioterapia¹⁷⁶⁻¹⁷⁸, y la presencia de esta delección se ha asociado también con un mayor riesgo de transformación a RS^{179,180}. El tamaño clonal de la del(17p) también ha mostrado tener un impacto pronóstico^{134,181}, y la presencia de esta alteración se asocia normalmente con características de mal pronóstico como positividad de CD38 y UM-IGHV, aunque cabe destacar que el subgrupo de pacientes con M-IGHV y del(17p) puede presentar un pronóstico más favorable¹⁸²⁻¹⁸⁴.

Las deleciones de 17p13 son normalmente de tamaño considerable (~18-22 Mb) y pueden ser el resultado de varios cambios estructurales como deleción en sí, translocaciones no balanceadas o isocromosomas¹⁸⁵. La **del(17p) comprende de forma invariable al gen supresor de tumores TP53**¹⁵¹. Además, se han reportado mutaciones de TP53 en el alelo restante de un 80% de pacientes con del(17p), lo que indica que la pérdida bialélica de este gen es el mecanismo principalmente responsable de la patobiología y las implicaciones pronósticas de este subgrupo citogenético^{174,186-188}.

TP53 es un gen supresor de tumores que desempeña un papel clave en la intersección de múltiples vías de señalización como el **ciclo celular**, la **apoptosis** o la señalización por DDR¹⁸⁹. Particularmente, la desregulación de la apoptosis es el proceso causante de las malas respuestas de los pacientes con del(17p) a agentes quimioterapéuticos como los análogos de las purinas o los agentes alquilantes, dado que estos fármacos dependen de una proteína TP53 funcional para una correcta inducción de la apoptosis en las células tumorales^{73,190}. Además, el papel que ejerce TP53 en el DDR es clave para el mantenimiento de la integridad genómica, estando la presencia de del(17p) significativamente asociada con una alta inestabilidad genética y con una concurrencia de determinados CNAs como pérdidas de 4p, 9p, 18p y 20p, o alteraciones en el cromosoma 8 (tanto deleción de 8p como ganancia de 8q)^{145,148,187,191}. La presencia de esta gran complejidad genética parece ser una de las principales causas de la transformación de células de LLC con del(17p) a RS^{179,180,192}. Finalmente, debido al gran tamaño de las deleciones de 17p13 en LLC, es posible que este tipo de alteración involucre la desregulación de otros genes adicionales a TP53, aunque se necesitan realizar más estudios para determinar el impacto biológico de estas haploinsuficiencias asociadas a del(17p)¹⁸⁵.

2.2.1.4 Trisomía 12

La ganancia de una copia extra del cromosoma 12 es frecuente en la LLC, afectando a un 12-18% de los pacientes al diagnóstico^{63,134-136}. La trisomía 12 se considera como una alteración de **riesgo intermedio** en las LLCs de nuevo diagnóstico, sin embargo, el estudio exhaustivo de este subgrupo citogenético ha revelado que esta entidad es bastante **heterogénea a nivel clínico**^{63,193-196}. Las células de LLC con trisomía 12 se caracterizan por una alta expresión de CD38 y CD49d, y pérdida de expresión del antígeno CD5 en algunos casos^{197,198}.

Dado que existe una copia completa adicional del cromosoma 12 en este subgrupo de pacientes, resulta difícil determinar un candidato o grupo de genes responsable de la patobiología de la enfermedad. Sin embargo, se ha observado una sobreexpresión de varios genes localizados en el cromosoma 12 (ej. *MDM2*, *BAX*, *E2F1* o *CDK4*), sugiriendo una disregulación del ciclo celular, apoptosis o proliferación en este subtipo citogenético¹⁹⁹. Además, los pacientes con trisomía 12 presentan un **panorama citogenético característico** en comparación con el resto de subgrupos de LLC, definido por una alta concurrencia con trisomías adicionales (especialmente en los cromosomas 18 y 19), translocaciones de 14q32 y pérdida de 14q^{194,195,200-205}. Los pacientes de LLC con trisomía 12 también están enriquecidos en mutaciones que afectan genes implicados en la vía de Notch o MAPK-ERK, lo que podría indicar un papel clave de estas rutas en la progresión de los casos con trisomía 12^{193,196,206-209}.

2.2.1.5 Otras alteraciones citogenéticas

Además de las alteraciones cromosómicas mencionadas en los anteriores apartados, otros CNAs recurrentes han sido reportados en 1-5% de los casos de LLC. Concretamente, se han reportado de forma consistente tanto deleciones de 3p, 6p, 6q, 8p, 9p, 10q, 14q, 18p y 20p, como ganancias en 2p, 8q, trisomía 18 y trisomía 19^{145,151,153,191,210,211}. Las regiones mínimas delecionadas o amplificadas de estas lesiones incluyen genes implicados en vías de señalización importantes para la patogénesis de la LLC, por ejemplo, *CDKN2A/B* en la deleción de 9p^{153,210}, *TRAF3* en la deleción de 14q²¹², *XPO1*, *MYCN* y *REL* en la amplificación de 2p^{213,214} o *MYC* en la amplificación de 8q²¹¹. Sin embargo, el impacto biológico y clínico de muchas de estas alteraciones citogenéticas no ha sido estudiado hasta el momento.

Además de deleciones, amplificaciones o ganancias de cromosomas enteros, otros eventos citogenéticos como las translocaciones son recurrentes, en bajas frecuencias, en la LLC. Las principales translocaciones que se han observado en estos enfermos suelen involucrar a la región 14q32/*IGH*, normalmente de forma recíproca con los genes *BCL2* -t(14,18)- o *BCL3* -t(14,19)-, aunque también se han descrito otros genes acompañantes no recurrentes²¹⁵. Otras translocaciones que pueden encontrarse en células de LLC afectan a 8q24/*MYC* o 13q14^{215,216}, y el impacto pronóstico de algunas de estas alteraciones ha sido estudiado en varias investigaciones^{203,216-219}.

2.2.1.6 Cariotipo complejo

El cariotipo complejo (CK; complex karyotype) se define como la presencia de ≥ 3 alteraciones citogenéticas numéricas o estructurales en uno o más clones, aunque algunos estudios establecen el límite en 5 o más alteraciones^{64,215,220-222}. Recientemente, la presencia de complejidad genómica ha ganado gran relevancia en la comunidad de la LLC, dado que numerosos estudios han reportado que la presencia de CK, además de representar un marcador pronóstico independiente²²²⁻²²⁵, podría servir como marcador predictivo de refractariedad, no solo a los regímenes basados en quimioinmunoterapia^{226,227}, sino también a nuevos fármacos dirigidos, de manera independiente a las alteraciones en *TP53*²²⁸⁻²³². Una particular excepción al pronóstico adverso conferido por la presencia de CK está constituida por el subgrupo de pacientes con trisomía 12 que portan trisomías adicionales en los cromosomas 18 y 19. Estos pacientes muestran unas respuestas clínicas excelentes, que pueden llegar a ser incluso mejores que las de aquellos pacientes que no tienen CK^{64,194}.

A pesar de que la presencia de complejidad genética tiene un impacto en el pronóstico de la LLC, su evolución y la respuesta al tratamiento²³³, los mecanismos biológicos responsables de estos aspectos de la enfermedad no han sido dilucidados completamente. Se ha demostrado que la presencia de CK puede estar favorecida por defectos en la señalización de DDR y un incorrecto mantenimiento de la integridad genómica²³⁴. Estos datos están en consonancia con la mayor presencia de CK observada en casos de LLC con alteraciones en *del(11q)/ATM* y *del(17p)/TP53*^{64,153,191}.

2.2.2 Mutaciones somáticas

La aparición de las técnicas de NGS y la aplicación de la secuenciación del exoma completo (WES; whole-exome sequencing) y genoma completo (WGS; whole-genome sequencing) ha permitido el descubrimiento de mutaciones génicas recurrentes en una amplia variedad de genes *driver*, así como la refinación de algoritmos para la detección de CNAs a partir de datos de secuenciación, transformando nuestro conocimiento acerca de la heterogeneidad genética en la LLC^{65,66,83,235-240}. En general, estudios de WES y WGS en aproximadamente 1000 casos de LLC han revelado la presencia de 0,6-0,9 mutaciones por Mb y una media de 15,3-26,7 mutaciones somáticas por paciente, indicando una carga mutacional relativamente baja en comparación con otros tumores de origen linfóide o tumores sólidos^{65,66,241}. Específicamente, dos influyentes estudios llevados a cabo por Landau *et al.*⁶⁵ y Puente *et al.*⁶⁶ han proporcionando las series más grandes de pacientes de LLC secuenciados por WES/WGS hasta la fecha, revelando una **marcada heterogeneidad**

genética, con muy pocos genes *driver* mutados en frecuencias mayores al 10%, y un enorme número de candidatos *driver* mutados en frecuencias inferiores al 10% de los casos (Figura 3). Estos estudios no sólo han aportado información acerca de la heterogeneidad inter-tumoral en la LLC, sino que también han profundizado en el conocimiento de la heterogeneidad intra-tumoral en muchos de estos pacientes.

Alguno de los genes *driver* recurrentemente mutados en la LLC tienen un impacto pronóstico y en la respuesta al tratamiento de la LLC. En las próximas secciones, se describirán las mutaciones más frecuentes observadas en la LLC así como sus implicaciones clínicas.

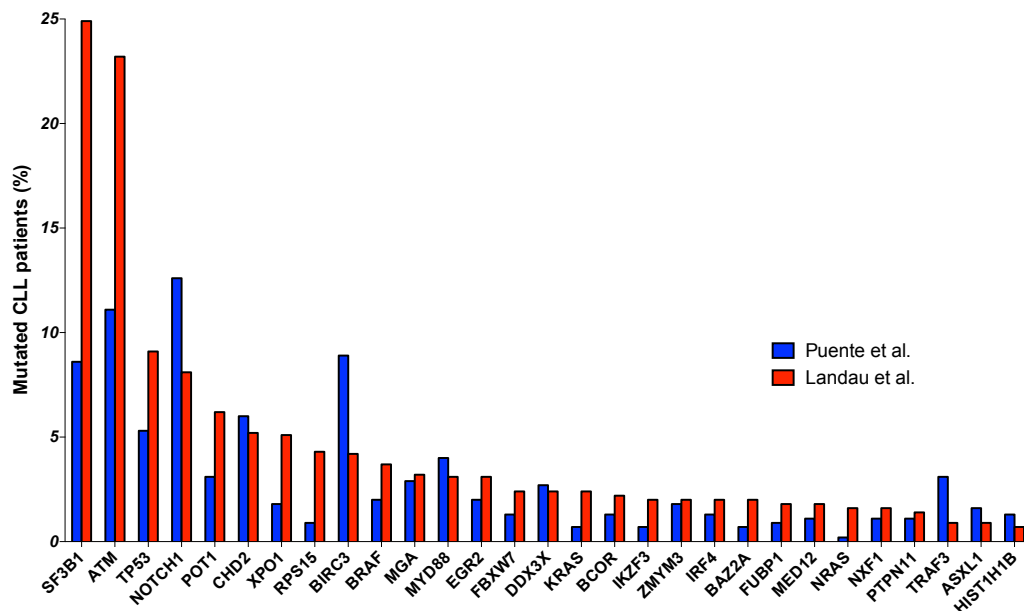


Figura 3. Genes *driver* recurrentemente mutados en la LLC, identificados en los estudios de Landau *et al.*⁶⁵ y Puente *et al.*⁶⁶ Adaptada de Rodríguez-Vicente AE *et al.* 2016²⁴¹

2.2.2.1 Mutaciones de ATM

Se han reportado mutaciones en el gen *ATM* en aproximadamente un 10-20% de los casos de LLC al diagnóstico o en el momento previo al inicio del tratamiento^{65,66,242,243}. Las mutaciones de *ATM* pueden ser sustituciones de tipo *missense*, inserciones o deleciones (indels) *in-frame* o *out-of-frame*, o mutaciones *nonsense*, *frameshift* o del sitio de *splicing* que dan como consecuencia una proteína *ATM* truncada o no funcional¹⁴⁷. Además, estas mutaciones pueden darse a lo largo de toda la región codificante de *ATM*, sin ningún *hotspot* claro identificado hasta la fecha¹⁴⁷. Como se indicó en la sección anterior (2.2.1 Alteraciones

cromosómicas), *ATM* se encuentra en la región cromosómica 11q22.3, y está incluido en la MDR de la práctica totalidad de los casos con del(11q), dando como resultado una pérdida monoalélica de *ATM*¹⁴⁷⁻¹⁴⁹. De hecho, **los casos con del(11q) están enriquecidos de mutaciones en *ATM*** – aproximadamente un tercio de los pacientes con del(11q) presentan mutaciones de *ATM* en el alelo restante-, teniendo como consecuencia una completa pérdida de función de *ATM*^{82,146,150}. A pesar de que una alta proporción de las mutaciones de *ATM* en la LLC son de carácter somático, se han reportado algunos casos de LLC con mutaciones heterocigóticas germinales de *ATM*, en los que se ha sugerido que la pérdida del alelo restante de *ATM* da lugar a una rápida progresión de la enfermedad^{242,244,245}.

En relación con la relevancia a nivel clínico, **las mutaciones de *ATM* tienen impacto pronóstica cuando dan lugar a una completa pérdida de función de *ATM***. Esto ha sido observado de manera significativa en los casos de LLC con del(11q), en los que la pérdida bialélica de *ATM* se relaciona con una PFS y OS más corta que en aquellos casos con del(11q) sin alteraciones adicionales en *ATM*^{82,146,150,246}. Por el contrario, las mutaciones monoalélicas en *ATM* no parecen conferir un pronóstico adverso en la LLC^{65,150,247}, aunque se han asociado con una reducción en el TTFT en algunas cohortes^{66,68}.

2.2.2.2 Mutaciones de *TP53*

Las mutaciones en *TP53* están presentes en un 5-10% de los pacientes con LLC al diagnóstico o en el momento previo al tratamiento, y su incidencia es bastante mayor los pacientes en recaída o con enfermedad refractaria (~40%)^{65,66,81,174,176,248}. Además, **la presencia de mutaciones en *TP53* se eleva hasta el 80% en los casos con del(17p)**, indicando un papel crucial de la disfunción de *TP53* en la patogénesis de la enfermedad^{174,186,187}. En menor frecuencia, las mutaciones de *TP53* también pueden estar acompañadas de una pérdida de heterocigosidad del segundo alelo de *TP53*, dando igualmente como consecuencia una disfunción bialélica de este gen^{65,66,151}. Las variantes somáticas en *TP53* incluyen tanto mutaciones de tipo *missense*, indels, mutaciones *nonsense* o mutaciones del sitio de *splicing*, dando lugar a un fenotipo de ganancia de función en el caso de las sustituciones *missense*, o a una pérdida de función de *TP53* para el resto de variantes^{188,249}. A pesar de que se han encontrado mutaciones a lo largo de toda la región codificante de *TP53*, la mayoría de ellas se agrupa entre los exones 4-8, correspondientes al dominio de unión al ADN de la proteína *TP53*¹⁸⁸.

Junto a la del(17p), **las mutaciones de TP53 son uno de los marcadores pronósticos y predictivos más robustos en la LLC**. Están asociadas con una marcada reducción en el TTFT y OS, así como una respuesta defectuosa a regímenes basados en quimioinmunoterapia^{65,66,81,174,176,248}. Tanto los defectos monoalélicos como bialélicos de TP53 están asociados con un pronóstico desfavorable, aunque algunos estudios han sugerido un mayor impacto de las alteraciones bialélicas en comparación con las monoalélicas^{81,150,186,187}. Las mutaciones de TP53 también parecen tener un impacto pronóstico sin importar su tamaño clonal en algunas cohortes^{68,250}, aunque se necesitan más estudios al respecto ya que otras investigaciones no han encontrado un impacto clínico de las mutaciones subclonales de TP53 (frecuencia variante alélica < 10-12%)^{156,187}. Cabe destacar que un estudio muy reciente ha mostrado que las mutaciones subclonales de TP53 solo tienen un impacto clínico en los pacientes UM-IGHV que no han recibido tratamiento con terapias dirigidas²⁵¹. Finalmente, investigaciones recientes sugieren que las lesiones en TP53 podrían tener también un impacto en el pronóstica de los pacientes tratados con fármacos dirigidos^{231,252,253}.

2.2.2.3 Mutaciones de BIRC3

BIRC3 aparece recurrentemente mutado en un 2.5-10% de casos de LLC al diagnóstico o en el momento previo al tratamiento^{65-67,85}. Las mutaciones en este gen son habitualmente de tipo *frameshift* o *nonsense* que afectan a los exones 6-9 y resultan en un truncamiento prematuro del dominio RING situado en el extremo C-terminal de la proteína BIRC3, teniendo como consecuencia una pérdida de función de la actividad E3-ubiquitina ligasa de este dominio^{85,155}. También se han reportado en menor medida mutaciones de tipo *frameshift* o *missense* en otros codones de BIRC3⁶⁶. Las mutaciones de BIRC3 aparecen frecuentemente en casos con del(11q) (~10%), y dado que BIRC3 está localizado en la región cromosómica 11q22 y está perdido de forma monoalélica en aproximadamente un 80% de los casos con del(11q), la presencia de mutaciones en el alelo restante da lugar a una pérdida bialélica de BIRC3 y una completa pérdida de función proteica^{66,85,146,154,156}.

Estudios recientes han demostrado que la inactivación bialélica de BIRC3 es un marcador pronóstico independiente de TTFT y OS en la LLC^{66,154,156}. Sin embargo, el significado pronóstico de las mutaciones monoalélicas en este gen es incierto, dado que algunos estudios han mostrado que las mutaciones de BIRC3 tienen un impacto clínico^{66,85,155,254}, mientras que otros no lo han validado^{65,68,156,247}. Además, las mutaciones de BIRC3 están enriquecidas en pacientes R/R a quimioinmunoterapia, confiriendo una PFS y OS reducidas en algunas

cohortes de pacientes tratados con fludarabina^{85,155}, aunque el mecanismo biológico por el cual las mutaciones de *BIRC3* podrían contribuir a la resistencia a fludarabina no ha sido descrito hasta el momento.

2.2.2.4 Mutaciones de *SF3B1*

SF3B1 es un gen que codifica la subunidad 3b del factor de *splicing*, componente de un complejo multi-proteico que se encarga de este proceso celular. *SF3B1* es uno de los genes más frecuentemente mutados en la LLC, con una incidencia que oscila entre el 10% de los casos de nuevo diagnóstico, hasta el 20% de los casos con necesidad de tratamiento^{65,66,236,238,255}. Las mutaciones en este gen son exclusivamente de tipo *missense*, agrupándose en un *hotspot* mutacional en los dominios proteicos HEAT, y dando lugar a un fenotipo de ganancia de función^{236,238,256,257}. De hecho, más del 50% de las mutaciones de *SF3B1* en la LLC corresponden a una sustitución exclusiva de un aminoácido, denominada como mutación K700E^{236,238,258}. Las mutaciones de *SF3B1* se asocian normalmente a del(11q) y UM-IGHV, y han mostrado tener impacto pronóstico a nivel de TTFT y OS en múltiples cohortes de LLC^{65,67,238,256,258-260}.

2.2.2.5 Mutaciones de *NOTCH1*

Se han reportado mutaciones de *NOTCH1* en un 8-12% de los casos de LLC al diagnóstico o previos al inicio del tratamiento^{65-67,83,235,258,259,261}, siendo esta incidencia mayor en aquellos casos R/R a quimioinmunoterapia así como en pacientes con RS^{84,153,180,235,261}. Este gen codifica para una proteína que juega un papel clave como activador de la vía de señalización de Notch²⁶². Las mutaciones de *NOTCH1* son predominantemente de tipo *frameshift* o *nonsense* y afectan al exón 34, que corresponde al dominio PEST en el extremo C-terminal proteico^{83,84,235,258,261}. Estudios recientes también han revelado la presencia de mutaciones no codificantes en la región 3'UTR de *NOTCH1*, dando lugar a la misma consecuencia funcional que las mutaciones "canónicas" de *NOTCH1*⁶⁶. Estas alteraciones son altamente concurrentes con trisomía 12 y UM-IGHV, y su presencia ha sido relacionada con un reducido TTFT y OS en algunas cohortes^{84,206,207,235,258,260,261,263,264}. Además, los pacientes de LLC con mutaciones de *NOTCH1* no se benefician del tratamiento con anticuerpos monoclonales anti-CD20 en el ámbito de la quimioinmunoterapia^{176,265}.

2.2.2.6 Otras mutaciones somáticas recurrentes con impacto pronóstico

Numerosos estudios de NGS en múltiples cohortes de LLC alrededor del mundo han investigado el impacto clínico de otros genes frecuentemente mutados en la enfermedad (**Figura 3**). De todos ellos, las mutaciones en *EGR2*, *RPS15*, *NFKBIE*, *SETD2*, *POT1* y genes pertenecientes a la vía de señalización MAPK-ERK (ie. *BRAF*, *KRAS*, *NRAS*) están particularmente asociadas a casos UM-IGHV y han sido relacionados con un posible pronóstico desfavorable^{86,117,126,156,196,208,227,239,266,267}, aunque se necesitan mayores esfuerzos a nivel colectivo y de armonización de datos de múltiples cohortes independientes para validar realmente estas mutaciones como marcadores pronósticos independientes en la LLC. Por el contrario, mutaciones *hotspot* en *MYD88* se asocian con marcadores biológicos de buen pronóstico como M-IGHV y del(13q) única, y podrían contribuir a una OS prolongada^{67,247,268,269}.

2.2.3 Expresión de microRNAs

Además de la presencia de alteraciones cromosómicas o mutaciones somáticas en regiones codificantes, la LLC también se caracteriza por una expresión aberrante de miRNAs, que son definidos como ARNs no codificantes que participan en la regulación post-transcripcional de la expresión génica a través de una unión directa a las regiones UTR^{270,271}. De hecho, la LLC fue la primera enfermedad en la que se observó una desregulación de los miRNAs, destacando el papel de miR-15a/16-1 en la MDR de los pacientes con del(13q)¹⁶⁰. A partir de ahí, se ha investigado el papel de numerosos miRNAs en la biología de la LLC, con especial atención en aquellos diferencialmente expresados por subgrupos de pacientes con características clínicas y biológicas distintivas^{272,273}. Por ejemplo, el miR-34a se encuentra infraexpresado en los casos con del(17p)/*TP53* mutado y está involucrado en la señalización de DDR, arresto del ciclo celular apoptosis^{89,274,275}, mientras que el miR-155 está sobreexpresado en casos con del(11q) y actúa como un amplificador de la señalización del BCR^{87,274}. Además, se ha demostrado que la expresión diferencial de ciertos miRNAs como miR-155, miR-150, miR-29c o miR-34a tiene un impacto pronóstico en los pacientes de LLC^{87,89,90,275,276}.

2.2.4 Epigenética

La epigenética describe cambios fenotípicos y hereditables en un cromosoma o sus histonas asociadas, que afectan a la actividad transcripcional pero no suponen un cambio en la secuencia del ADN. Esta desregulación en el control transcripcional puede estar causada

por metilación aberrante del ADN y/o modificaciones post-traduccionales de histonas, suponiendo una de las marcas distintivas de las células tumorales²⁷⁷. Estudios de metilación de ADN han revelado que la LLC muestra hipometilación a nivel global en genes y *enhancers*, en combinación con hipermetilación local en promotores de algunos genes^{71,277}. Además, el epigenoma de la LLC permanece estable desde el estadio de LBM a lo largo del resto del curso de la enfermedad, reflejando el de la célula de origen de la enfermedad^{71,278,279}. De hecho, diferentes firmas de metilación han permitido clasificar a los pacientes de LLC en tres subgrupos que se correlacionan con el estado mutacional de IGHV y el pronóstico de la enfermedad. Estos grupos son “memory-like CLL” (principalmente M-IGHV, buen pronóstico), “intermediate-like CLL” (casos tanto M-IGHV o UM-IGHV con un pronóstico intermedio) o “naïve-like CLL” (principalmente UM-IGHV, mal pronóstico)^{71,72}. Además, altos niveles de heterogeneidad intra-clonal a nivel de metilación se han observado en algunos casos de LLC y se correlaciona con alteraciones genéticas de alto riesgo, evolución clonal y pronóstico desfavorable^{280,281}.

Investigaciones recientes también han abordado el estudio de otros aspectos del epigenoma de la LLC mediante integración del análisis del metiloma del ADN, mapas de modificación de histonas, accesibilidad de la cromatina y arquitectura tridimensional de la cromatina, en correlación con datos del transcriptoma y el genoma completo, revelando que aunque la mayoría de las alteraciones genéticas no están asociadas de forma consistente con un perfil epigenético concreto, los pacientes con trisomía 12 o mutaciones en *MYD88* muestran configuraciones distintivas a nivel de la cromatina²⁸².

2.3 Evolución clonal y cinética de crecimiento de la LLC

La evolución clonal se caracteriza por la adquisición de alteraciones genéticas durante el tiempo de vida de una célula tumoral, y fue documentada por primera vez en la LLC gracias a estudios de cariotipo convencional y FISH en los años 2000. Sin embargo, no se ha obtenido un panorama completo de la evolución clonal a lo largo de la enfermedad hasta el desarrollo e implementación de las técnicas de WES y WGS en el estudio de la LLC^{65,237,283-286}.

El análisis de muestras pareadas de sangre periférica a lo largo de diferentes tiempos en el transcurso de la enfermedad ha permitido describir los patrones de dinámicas clonales en la LLC. Estos patrones incluyen: **evolución lineal**, definida como la persistencia de un clon fundador con la adquisición de nuevas alteraciones, **evolución ramificada**, definida como la

evolución en paralelo de diferentes clones que compiten entre ellos, o **evolución convergente**, que se da cuando se adquiere más de una mutación o alteración en el mismo gen. Además, algunos pacientes no muestran evolución clonal a lo largo del curso de la enfermedad²⁸⁷⁻²⁸⁹. Se han observado grandes fluctuaciones clonales entre muestras previas al tratamiento y en el momento de la recaída, mientras que una composición subclonal estática es más frecuente en aquellos casos que no requieren tratamiento y tienen una enfermedad estable^{65,237,290}. Por otro lado, la evolución de enfermedad estable a enfermedad activa está caracterizada por la adquisición de nuevas lesiones genéticas²⁹¹. En cuanto a alteraciones específicas, los datos de WGS y WES indican que la del(13q), la trisomía 12 y las mutaciones en *MYD88* son eventos clonales que ocurren temprano durante el curso de la enfermedad, mientras que las mutaciones de *ATM*, *TP53* o *BIRC3* son principalmente subclonales^{65,237}.

Las dinámicas del crecimiento de la LLC también son heterogéneas, algunos pacientes muestran un **crecimiento logístico** en el que el tamaño clonal se estabiliza a lo largo del tiempo, mientras que otros pacientes muestran un patrón de **crecimiento exponencial**²⁹². Estos últimos casos están caracterizados por un mayor número de mutaciones en genes *driver* y muestran una mayor proporción de evolución clonal tras el tratamiento²⁹². Por otro lado, se conoce que las alteraciones *driver* normalmente coexisten en el mismo clon tumoral, y además, la coexistencia de estas alteraciones no es aleatoria, dado que el análisis de datos genómicos a gran escala ha permitido identificar patrones específicos de concurrencia y mutual exclusividad entre lesiones características de la LLC (ej. concurrencia de del(11q) y mutación en *SF3B1* o mutua exclusividad entre del(13q) y trisomía 12)^{65,66}. De hecho, un estudio reciente ha demostrado que la combinación de delección de *ATM* y mutación en *SF3B1* en un modelo murino da lugar al desarrollo de LLC, mientras que las mismas alteraciones por separado no son capaces de generar este fenotipo²⁹³. Sin embargo, aún se necesita realizar un trabajo de investigación exhaustivo en este campo para poder determinar las causas biológicas por las que la cooperación de alteraciones específicas da lugar a un crecimiento exponencial de la LLC y progresión de la enfermedad.

3. BIOLOGÍA DE LA LLC – RUTAS DE SEÑALIZACIÓN COMO DIANAS TERAPÉUTICAS

3.1 Vías moleculares en la LLC

Las lesiones genéticas recurrentes observadas en la LLC se suelen agrupar en genes que pertenecen a rutas moleculares específicas, que tienen un papel crucial en la patogénesis y evolución de la enfermedad^{65,66}. Por ejemplo, tanto las alteraciones de *ATM* como las de *TP53* comparten una función común en la señalización de DDR y en los *checkpoints* del ciclo celular, mientras que las vías MAPK-ERK y NF-κB, activadas como resultado de la señalización por BCR, pueden estar afectadas por múltiples alteraciones que potencialmente tienen la misma consecuencia a nivel funcional^{196,208,294-298}. Además, la vía de Notch no sólo está afectada por mutaciones en regiones codificantes y no codificantes del gen *NOTCH1*, sino también por alteraciones en genes codificantes de reguladores positivos (ej. *MED12*) o negativos (ej. *FBXW7*, *SPEN*, *RBPJ*, *SNW1*) de la actividad de *NOTCH1*^{66,153,299,300}. Otras rutas moleculares relevantes en la LLC que están frecuentemente afectadas a cause de lesiones genéticas son el procesamiento del ARN (ej. *SF3B1*, *U1*, *XPO1*) o el procesamiento ribosómico (ej. *RPS15*)^{257,301-303}, así como la modificación de la cromatina (ej. *CHD2*, *STED2*, *HIST1H1B*, *HISTH1E*)^{65,66,267,304,305}. La **Tabla 2** resume las alteraciones de genes *driver* más frecuentemente identificadas en la LLC, agrupadas en base a la ruta biológica en la que están involucradas. Comprender la biología resultante de la heterogeneidad genética en la LLC es esencial a la hora de desarrollar nuevos fármacos dirigidos para el tratamiento personalizado de la enfermedad. Además, se ha reportado recientemente que el número de vías moleculares afectadas por mutaciones *driver* tiene un impacto pronóstico en la LLC y podría ser utilizado como biomarcador en los modelos pronósticos de la LLC²⁵⁴.

Tabla 2. Procesos biológicos afectados por alteraciones genéticas recurrentes en genes *driver* de la LLC.

Ruta biológica	Genes alterados en LLC*
Respuesta a daño en el ADN y control del ciclo celular	<i>ATM</i> , <i>TP53</i> , <i>POT1</i> , <i>MIR-15A/16-1</i> , <i>SAMHD1</i> , <i>CHK1</i> , <i>CHK2</i> , <i>ATRX</i> , <i>CCND2</i> , <i>CDKN1B</i> , <i>CDKN2A/B</i> , <i>BRCC3</i> , <i>ELF4</i>
Apoptosis	<i>TP53</i> , <i>MIR-15A/16-1</i> , <i>BCL2</i>
Señalización de BCR	<i>EGR2</i> , <i>IKZF3</i> , <i>BCOR</i> , <i>IGLL5</i> , <i>KLHL6</i> , <i>PAX5</i> , <i>IRF4</i> , <i>ITPKB</i> , <i>CARD11</i>
Señalización de MAPK-ERK	<i>HRAS</i> , <i>NRAS</i> , <i>BRAF</i> , <i>PTPN11</i> , <i>MAP2K1</i>
Señalización de TLR	<i>MYD88</i> , <i>TLR2</i> , <i>TLR6</i> , <i>IRAK1</i> , <i>IRAK2</i> , <i>IRAK4</i>
Señalización de NF-κB	<i>BIRC3</i> , <i>BIRC2</i> , <i>NFKBIE</i> , <i>TRAF3</i> , <i>TRAF2</i> , <i>NFKB2</i> , <i>REL</i> , <i>TNFAIP3</i>
Señalización de Notch	<i>NOTCH1</i> , <i>FBXW7</i> , <i>MED12</i> , <i>SPEN</i> , <i>RBPJ</i> , <i>SNW1</i>
Procesamiento de ARN y ribosoma	<i>SF3B1</i> , <i>XPO1</i> , <i>U1</i> , <i>RPS15</i> , <i>DDX3X</i> , <i>NXF1</i> , <i>XPO4</i> , <i>FUBP1</i> , <i>EWSR1</i>

Modificación de cromatina	<i>CHD2, ZMYM3, SETD2, HIST1H1B, HIST1H1E, ASXL1, ARD1A, BAZ2A, SETD1A, CREBBP</i>
Señalización de Wnt	<i>MED12, FAT1, BCL9, BRD7, FZD5</i>
Señalización de Hedgehog	<i>SMO, GLI1, GLI2, BCOR, MED12, CREBBP, EP300</i>
Señalización de MYC	<i>FBXW7, MGA, MYC, FUBP1, PTPN11</i>

*Se han incluido en la tabla los genes afectados tanto por CNAs recurrentes y/o mutaciones somáticas. Los genes marcados en negrita son aquellos afectados por alteraciones genéticas en más de un 5% de los casos de LLC al diagnóstico o previos al tratamiento; el resto de genes indicados presentan alteraciones ocurren en una frecuencia menor al 5% (estas frecuencias pueden variar entre las LLCs de estadio temprano, no tratadas de estadio tardío o cohortes de pacientes R/R). Algunos genes pueden estar involucrados en más de una vía de señalización^{65,66,307,83,153,203,236,237,268,301,306}.

3.1.1 Respuesta a daño en el ADN y control del ciclo celular

Las roturas de doble cadena (DSBs; double-strand breaks) o de cadena sencilla (SSBs; single-strand breaks) en el ADN representan una de los tipos de lesiones más perjudiciales en el ADN, y si no son reparadas pueden dar lugar a muerte celular o desencadenar inestabilidad genómica³⁰⁸. El proceso de señalización de DDR se inicia con el reconocimiento de estas lesiones y normalmente resulta en la activación de los *checkpoints* del ciclo celular para parar su progresión³⁰⁹. El mecanismo de activación de los *checkpoints* en respuesta a daño en el ADN está compuesto por sensores de daño, transductores de la señal y múltiples vías efectoras, y sus reguladores centrales son las proteínas quinasas ATM, ATR y DNA PK. Estas quinasas tienen numerosos sustratos, por ejemplo, CHK2 y TP53 son sustratos de ATM, mientras que CHK1 lo es de ATR, que en conjunto orquestan la parada del ciclo celular en las fases G1, S o G2, así como la iniciación de la reparación del daño y la muerte celular (**Figura 4**)³¹⁰.

Durante los *checkpoints* en fase G1 y G2 del ciclo celular, las DSBs pueden repararse principalmente por dos vías: **recombinación no homóloga (NHEJ;** non-homologous end joining) o **recombinación homóloga (HR;** homologous recombination). La NHEJ no depende de un molde de ADN intacto para la reparación, y se usa principalmente en la fase G1 del ciclo celular cuando no hay una cromátida hermana que pueda servir como molde de la reparación³¹¹. Brevemente, la NHEJ depende de la actividad catalítica de la proteína quinasas DNA PK, que es reclutada al sitio donde el DSB ha tenido lugar mediante la interacción con las subunidades no catalíticas Ku70 y Ku80 (**Figura 4**)^{308,312}. Tras esto, DNA PK, en coordinación con otras proteínas como XRCC4 y Lig4 es capaz de promover la ligación de los extremos del DSB en un proceso que es propenso a errores, ya que se pueden

producir pequeñas inserciones o deleciones de manera aleatoria^{308,312}. Por otro lado, la HR es un proceso de reparación de alta fiabilidad que requiere de un molde intacto de ADN para la reparación de la lesión, por lo que su uso está restringido a la fase S tardía o a la fase G2 del ciclo celular³¹¹. Durante la HR, inmediatamente después de la aparición de un DSB, el complejo MRN (consistente en las proteínas MRE11, RAD50 y NBS1) es reclutado al lugar de la lesión. En paralelo, ATM es activado y reclutado también al lugar de la lesión mediante interacción con NBS1, fosforilando subsecuentemente a la histona H2AX en el aminoácido Ser-139 (γ H2AX), lo que sirve como una plataforma de ensamblaje para el propio complejo MRN y otros complejos de reparación de ADN^{147,313,314}. ATM y el complejo MRN, en coordinación con el complejo BRCA1, regulan el proceso de resección del ADN, creando una hebra saliente de cadena sencilla 3', a la que se une y cubre la proteína RPA. Posteriormente, RPA es reemplazado por RAD51 en un proceso multi-proteico regulado por ATM, BRCA1 and BRCA2 y otras proteínas. Finalmente, RAD51 desempeña una función crucial en la búsqueda por homología e invasión de la cromátida hermana, dando lugar finalmente a la reparación de la lesión (**Figura 4**)^{308,315}.

El eje de señalización ATR/CHK1 se activa en respuesta a varios tipos de **SSBs**. Estas lesiones son principalmente reparadas por el **mecanismo de reparación por excisión de bases (BER; base excision repair)**, que precisa de la acción de las proteínas PARP1, LIG3 y XRCC1 (**Figura 4**)^{315,316}. A pesar de que los componentes del BER no están afectados por lesiones genéticas en la LLC, y raramente en otros tipos de cáncer, este mecanismo representa una diana terapéutica atractiva, que se basa en el concepto de **letalidad sintética**. Esta noción está definida como la situación en la que la pérdida de cualquiera de uno de dos genes no tiene un impacto en la célula, mientras que la combinación de ambos defectos tiene como resultado la muerte celular^{317,318}. En este contexto, los inhibidores de PARP1 inhiben el mecanismo de BER, lo que da lugar a la acumulación de lesiones en el ADN que en ausencia de esta vía de reparación deben ser reparadas mediante HR. Si la HR tampoco está disponible, el daño en el ADN inducido por la inhibición de PARP1 se acumula hasta que resulta tóxico para la célula y desencadena un proceso de muerte celular. Este paradigma fue inicialmente observado en tumores sólidos con mutaciones en *BRCA1* y *BRCA2*, y ha dado lugar al desarrollo clínico y aprobación de inhibidores de PARP en varios tipos de tumores con lesiones en genes implicados en HR³¹⁹⁻³²¹.

En la LLC, la **señalización de DDR** y el **control del ciclo celular** están desregulados principalmente por lesiones en **del(11q)/ATM** o **del(17p)/TP53**. La función alterada de cualquiera de estos dos genes resulta en una pérdida de los *checkpoints* en fase G1 o G2 así como una deficiencia en la reparación por HR, permitiendo a las células que entren en fase de mitosis con lesiones que no han sido reparadas, lo que favorece la aparición de inestabilidad genética²⁹⁴⁻²⁹⁶. En menor medida, también se han descrito mutaciones en los genes *ATRX*, *CHK1* o *CHK2* en casos de LLC, y es posible que produzcan un resultado similar en la señalización de DDR y el control del ciclo celular^{65,66}. Además, las mutaciones de pérdida de función en el protector de telómeros *POT1*, que aparecen en un 5% de casos de LLC aproximadamente, también favorecen la aparición de alteraciones cromosómicas estructurales³²². Finalmente, se han reportado alteraciones en genes codificantes de ciclinas cruciales para la progresión del ciclo celular, como *CCND2* y *CDKN2A/B*, estando la pérdida de este último relacionada con la transformación a RS (**Figura 4**)^{66,153,179}.

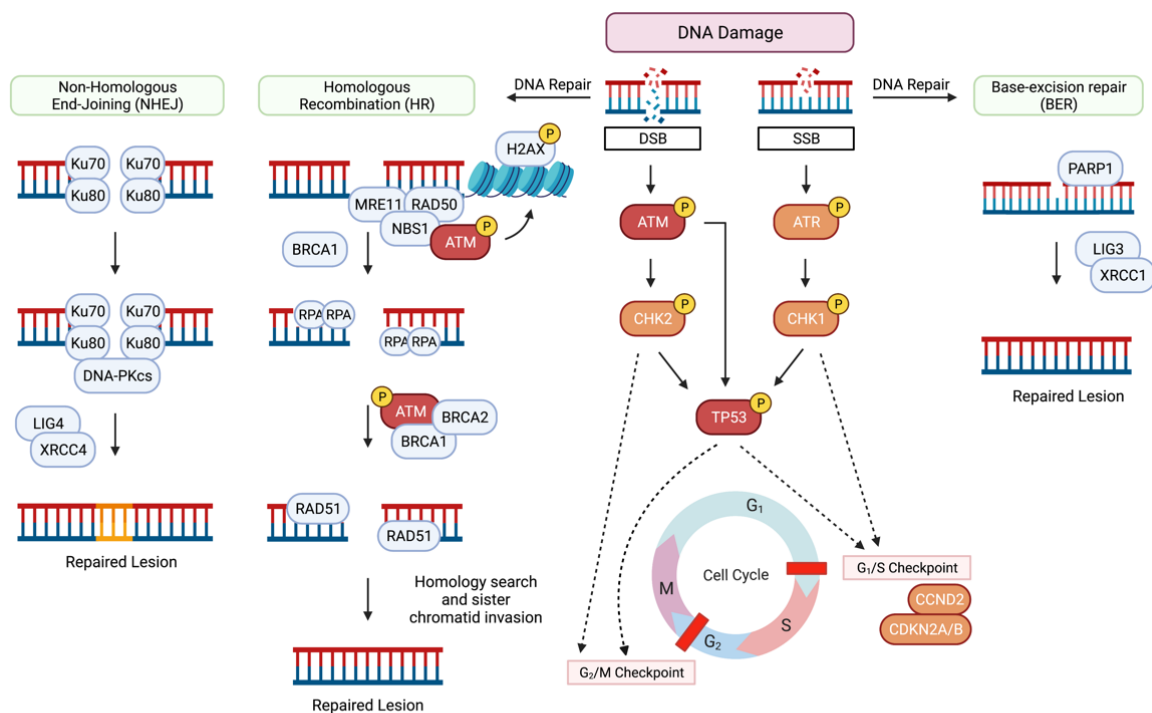


Figura 4. Señalización de DDR y ciclo celular en la LLC. Representación esquemática de las proteínas involucradas en la activación de los *checkpoints* del ciclo celular, señalización de DDR y vías de reparación del ADN en respuesta a la formación de DSBs o SSBs. Las proteínas codificadas por genes recurrentemente alterados en la LLC (bien por mutación somática o bien por ganancia o pérdida cromosómica) están señaladas en rojo (presentes en > 5% de los pacientes) o naranja (presentes en < 5% de los pacientes). Las proteínas señaladas en azul no están afectadas por lesiones genéticas recurrentes en la LLC.

3.1.2 Apoptosis

La evasión de la apoptosis, o muerte celular programada, es una de las marcas distintivas de las células tumorales³²³. La apoptosis se puede desencadenar por dos vías principales que se activan por estímulos extracelulares o intracelulares. La **vía extrínseca de la apoptosis** se inicia tras la unión de ligandos de la familia TNF α a receptores TNF en la superficie celular, lo que desencadena la formación de un complejo inductor de muerte celular y la activación de la caspasa-8. La **vía intrínseca** se inicia a partir de daño en el ADN o estrés celular, alterando el balance de proteínas pro- y anti-apoptóticas que da lugar a una pérdida del potencial de membrana mitocondrial (MMP, mitochondrial membrane potential), liberación de citocromo c, ensamblaje del complejo apoptosoma y activación de la caspasa-9 iniciadora, finalizando en muerte celular³²⁴. Los cambios en el MMP están altamente regulados por miembros de la **familia de proteínas BCL2**, consistente en un grupo de proteínas que comparten dominios de homología BCL2 (BH). Estas proteínas se subdividen en tres grupos en base a su función: anti-apoptóticas (ej. BCL2, BCL-xL, MCL1, BCL-w, BCL2A1, BCL-B), pro-apoptóticas multi-dominio (BAK y BAX) o pro-apoptóticas solo BH3 (ej. BIM, NOXA, PUMA, HRK)³²⁵. La apoptosis se desencadena cuando las proteínas pro-apoptóticas multi-dominio BAX and BAK se activan y oligomerizan, lo que facilita la formación de poros en la membrana mitocondrial y una pérdida del MMP. BAX y BAK son activados por proteínas pro-apoptóticas solo BH3, mientras que la función de las proteínas anti-apoptóticas es la de secuestrar las proteínas solo BH3 así como las pro-apoptóticas multi-dominio para mantener a BAX y BAK inactivos y prevenir su oligomerización³²⁶.

La apoptosis está ampliamente desregulada en la LLC y en otras neoplasias hematológicas, favoreciendo la supervivencia, la evolución clonal y la resistencia al tratamiento³²⁷. Por ejemplo, como se indicó anteriormente, la pérdida de miR-15a/16-1 a través de la del(13q) da lugar a sobreexpresión de BCL2, lo que evita la muerte de las células de LLC^{170,171}. Además, TP53 también está involucrado de forma directa en la inducción de apoptosis en respuesta a daño en el ADN a través de la sobreexpresión de proteínas pro-apoptóticas PUMA, NOXA y BAX³²⁸, lo que hace que los pacientes con del(17p) y/o mutación de TP53 sean altamente resistentes a regímenes basados en quimioinmunoterapia^{65,190}. Finalmente, se han descrito mutaciones en el propio gen BCL2 en un pequeño porcentaje de pacientes con LLC previa al tratamiento, y es posible que contribuyan también a una desregulación de la apoptosis^{66,203}.

3.1.3 Señalización de BCR y TLR

El BCR es un complejo multimérico compuesto por una molécula de IG de superficie específica de antígeno y un heterodímero formado por Ig- α (CD79A) y Ig- β (CD79B). La unión del antígeno a la IG de superficie induce la activación de las quinasas proximales SYK y LYN, que fosforilan los motivos de activación basados en tirosina (ITAMs) en CD79A y CD79B, desencadenando la **señalización de BCR** por fosforilación de otras quinasas proximales como BTK o PI3K, así como la activación del citoesqueleto mediada por HS1 (**Figura 5**)³²⁹⁻³³¹. La fosforilación de BTK supone la posterior fosforilación de otras quinasas como PLC γ 2, lo que activa diversas vías moleculares como liberación de calcio, NF- κ B, MAPK-ERK, o la vía de señalización de la proteína quinasa C (PKC), mientras que la fosforilación de PI3K activa el eje de señalización mediado por PI3K/AKT/mTOR. Esta convergencia de activación de rutas biológicas da lugar a una alta actividad transcripcional en el núcleo celular que finalmente desencadena procesos de **migración, proliferación y supervivencia (Figura 5)**^{2,329,331}. Además, la señalización de BCR está altamente regulada por la activación de las fosfatasa SHP1, SHIP1 y SHIP2, así como los receptores CD5 y CD22, que actúan como reguladores negativos de la respuesta a la señalización por BCR (**Figura 5**)³²⁹.

La presencia de un BCR funcional es esencial para la supervivencia de los linfocitos B maduros, lo que se mantiene en la mayoría de neoplasias linfoides, incluyendo la LLC². A pesar de que los componentes de esta ruta no suelen aparecer recurrentemente mutados en la LLC, muchos genes involucrados en la actividad transcripcional o en las rutas biológicas resultantes de la activación de esta vía sí son afectados por lesiones genéticas en esta enfermedad. En particular, las mutaciones en genes pertenecientes a la vía de señalización de **MAPK-ERK** (ej. *BRAF*, *KRAS*, *NRAS*) son frecuentes en la LLC, y dan lugar a una desregulación del ciclo celular y una proliferación descontrolada^{196,208}. Además, se ha reportado recientemente que las mutaciones en el factor de transcripción *IZKF3* incrementan la señalización de BCR y favorecen el desarrollo de la LLC³³². Otros genes relacionados de manera indirecta con esta vía y que aparecen mutados de forma recurrente en la LLC son *EGR2*, *BCOR*, *KLHL6*, *PAX5*, *IRF4* y aquellos pertenecientes a la **vía de señalización de NF- κ B** (ver siguiente apartado)^{65,66}.

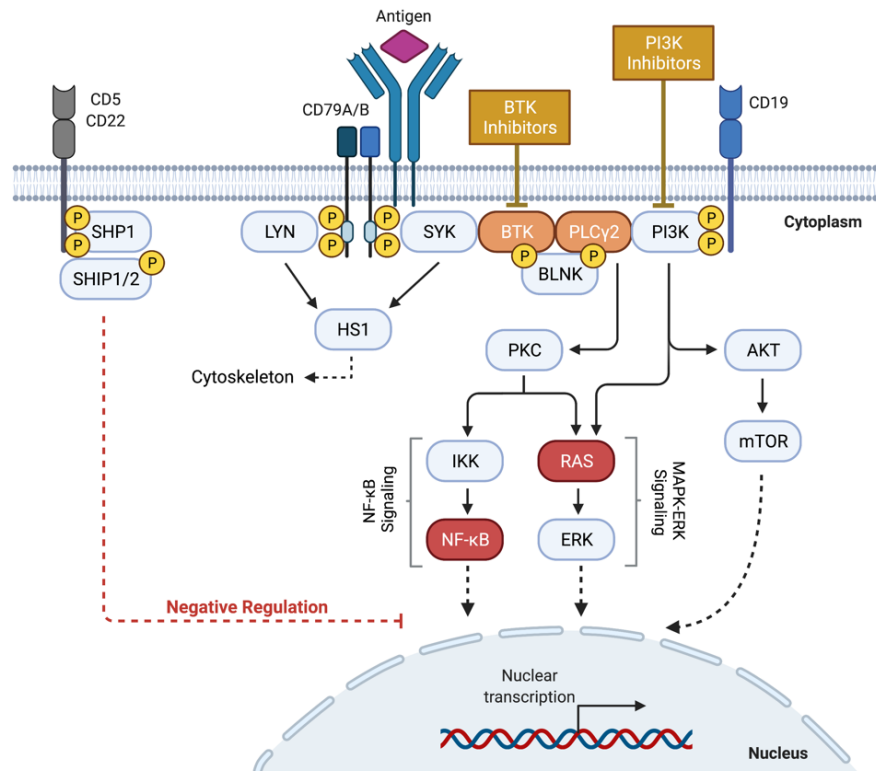


Figura 5. Señalización de BCR en la LLC. Representación de los eventos que ocurren tras el reconocimiento antigénico del BCR. Los inhibidores de BTK y PI3K son capaces de suprimir esta vía de señalización y representan un novedoso subgrupo de terapias dirigidas de gran eficacia para el tratamiento de la LLC (*ver sección 3.3.1: Inhibidores de la señalización de BCR*). Las proteínas codificadas por genes recurrentemente alterados en la LLC (bien por mutación somática o bien por ganancia o pérdida cromosómica) están señaladas en rojo (presentes en > 5% de los pacientes) o naranja (presentes en < 5% de los pacientes). Nota 1: múltiples genes pertenecientes a las vías de señalización de MAPK-ERK y NF- κ B están recurrentemente alterados en una frecuencia global > 5%. Una visión en detalle de la vía de NF- κ B se puede encontrar también en la Figura 6. Nota 2: las mutaciones en *BTK* y *PLCG2* solo aparecen en aquellos pacientes tratados con inhibidores de BTK, y no están presentes en ningún caso de LLC al diagnóstico³³³. Las proteínas señaladas en azul no están afectadas por lesiones genéticas recurrentes en la LLC.

Además, la señalización por otros receptores, como los que pertenecen a la familia Toll-like (**receptores TLR**), pueden inducir la proliferación y supervivencia de las células de LLC mediante la activación de vías como NF- κ B y STAT3^{298,334}. Algunos genes pertenecientes a la señalización de TLR aparecen recurrentemente mutados en la LLC, siendo el ejemplo más característico *MYD88*, un adaptador que actúa como transductor de la señal procedente de los TLR para activar la vía canónica de NF- κ B²⁶⁸. Las mutaciones en otros genes de esta vía son menos frecuentes en la LLC (< 1%), e incluyen aquellas en *TLR2*, *TLR6*, *IRAK1*, *IRAK2* e *IRAK4*^{65,66,83,268}.

3.1.4 Señalización de NF- κ B

La vía de NF- κ B desempeña un papel importante en la patogénesis, mantenimiento y evolución de la LLC, y está compuesta por dos rutas principales, la vía canónica y la vía no canónica²⁹⁸.

La **vía canónica de NF- κ B** es, con diferencia, la más estudiada de las dos en la LLC, y se desencadena principalmente por la activación de receptores de membrana como el BCR, TLRs, receptores TNF (TNFR) o receptor de interleucina-1 (IL-1R)³³⁵. La interacción entre el ligando y el receptor activa la el complejo quinasa I κ B (IKK), dando lugar a la fosforilación y posterior degradación mediada por el proteasoma de los inhibidores de las proteínas de NF- κ B, conocidos como I κ Bs, que son una familia de proteínas que secuestran a los factores de transcripción de NF- κ B y los mantienen inactivos en el citoplasma. Tras la degradación de los I κ Bs, los factores de transcripción de NF- κ B son liberados y se translocan al núcleo celular para activar la transcripción de sus genes diana (**Figura 6**)²⁹⁸. Los factores de transcripción de NF- κ B que están involucrados en la vía canónica son p65 (RelA), p105/p50 (NF κ B1) y c-Rel (Rel), y se translocan al núcleo celular formando varias combinaciones de homodímeros y heterodímeros con distintos patrones de actividad transcripcional³³⁶.

La **vía no canónica de NF- κ B** se inicia cuando diversos estímulos de TNF se unen a otros receptores de membrana de la célula B como el receptor del factor de activación B (BAFFR), CD40, el receptor de linfotóxina β -73 (LT β R) o el receptor activador de NF- κ B (RANK)³³⁵. En la ausencia de estímulo, esta vía se encuentra inactiva gracias a la acción de un complejo regulador multi-proteico que está compuesto por TRAF2, TRAF3, BIRC2 y BIRC3, que ubiquitina de forma continua a la quinasa inducible de NF- κ B (NIK), produciendo su degradación por el proteasoma³³⁷. Cuando se produce un estímulo del receptor, este complejo regulador es reclutado por el receptor activado y NIK se estabiliza en el citoplasma, promoviendo la activación de IKK α que fosforila a la forma inactiva del factor de transcripción NF κ B2 (p100), lo que produce una degradación de su extremo C-terminal y la translocación de p52 al núcleo celular en forma de homo- o heterodímero con RelB para iniciar la transcripción dependiente de NF- κ B (**Figura 6**)³³⁸.

De manera general, la señalización de NF- κ B está aumentada en las células de LLC en comparación con células B normales. Este incremento de actividad es el resultado de la activación constitutiva de la señalización de BCR, TLR o Notch, resultado de la presencia de alteraciones genéticas en alguno de los componentes de estas vías, o bien por interacciones con células del microambiente tumoral en el nicho del ganglio linfático²⁹⁸. Además, las

alteraciones genéticas en genes que codifican para componentes de la vía de NF- κ B son frecuentes en LLC. En relación con la vía canónica, se han reportado mutaciones truncadoras de *NFKBIE*, que codifica para la proteína inhibidora I κ B ϵ , en pacientes con LLC de estadio avanzado²⁶⁶. Otras alteraciones en genes pertenecientes a esta ruta son las pérdidas de 6q23/*TNFAIP3* o las ganancias de 2p16/*REL*^{213,339}. De manera interesante, a pesar de estar menos estudiada en la LLC, las alteraciones genéticas recurrentes son más frecuentes en genes implicados en la vía no canónica. Las mutaciones truncadoras de *BIRC3* dan lugar a la estabilización citoplasmática de NIK y activación constitutiva de la ruta^{85,155}, aunque no está claro cómo la pérdida monoalélica de *BIRC3* a través de la del(11q) contribuye a la biología de la LLC y si la activación constitutiva de la ruta no canónica de NF- κ B contribuye en la progresión de la LLC. Otros *drivers* recurrentemente mutados que pertenecen a la vía no canónica son *TRAF2* y *TRAF3*^{65,66}, mientras que *BIRC2* está frecuentemente delecionado en los casos con del(11q)³⁴⁰. Además, *TRAF3* también se pierde por deleción cromosómica de 14q32²¹² y *NFKB2* puede estar afectado por truncamientos en pacientes con pérdida de 10q24⁶⁶.

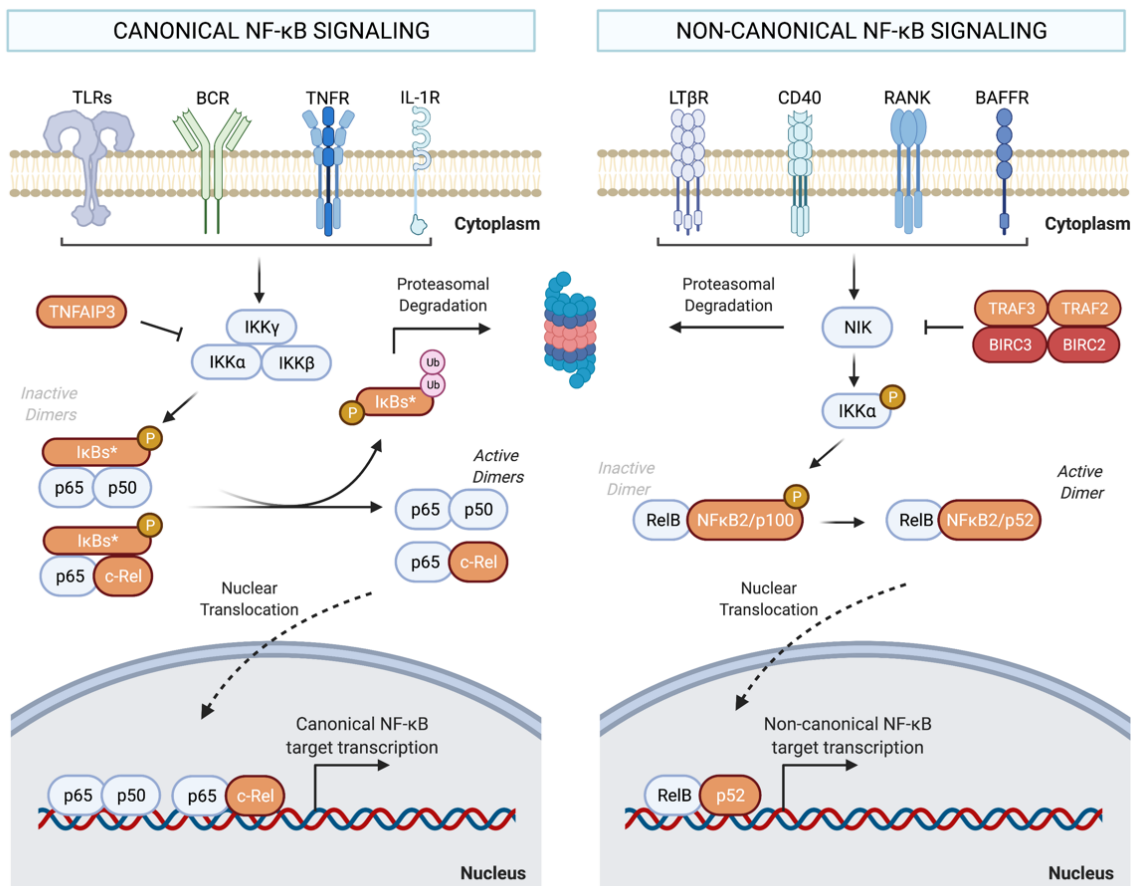


Figura 6. Señalización de NF- κ B en la LLC. Representación esquemática de la vía canónica y no canónica de NF- κ B en LLC. Las proteínas codificadas por genes recurrentemente alterados en la LLC (bien por mutación somática o bien por ganancia o pérdida cromosómica) están señaladas en rojo (presentes en > 5% de los pacientes) o naranja (presentes en < 5% de los pacientes). *Nota: la familia de proteínas I κ B está compuesta por varios miembros (ej. I κ B α , I κ B β , I κ B ϵ) y solamente I κ B ϵ , codificado por el gen *NFKBIE*, está afectado por alteraciones recurrentes en la LLC. Las proteínas señaladas en azul no están afectadas por lesiones genéticas recurrentes en la LLC.

3.2 El microambiente de la LLC

Las células de LLC son altamente dependientes de las señales proporcionadas por el microambiente para promover su proliferación y supervivencia. Los linfocitos de LLC son dirigidos a los ganglios linfáticos a través de gradientes de quimiocinas. Una vez allí, las células forman “centros de proliferación”, lugares donde las células leucémicas entran en contacto con células no tumorales del estroma, células “nurse-like” (NLCs), células T y células endoteliales entre otros grupos (**Figura 7**)². Las interacciones entre las células de LLC y este microambiente complejo son mediadas por una red de señalización que incluye ligandos de superficie, moléculas de adhesión, quimiocinas, citoquinas, y sus respectivos receptores.

Las NLCs son células de origen monocítico y desempeñan un papel clave en el microambiente de la LLC. Son capaces de inducir quimiotaxis y promover la supervivencia de la LLC a través de la secreción de las quimiocinas CXCL12 y CXCL13 (que son los ligandos de CXCR4 y CXCR5, respectivamente, en las células de LLC), y expresión de ligandos de la familia de TNF como BAFF o APRIL, promoviendo la señalización por BCR y NF- κ B en las células de LLC³⁴¹⁻³⁴⁴. Además, también secretan WNT5A, el ligando del receptor transmembrana ROR1, activando la señalización no canónica de Wnt, que induce la proliferación y migración de las células de LLC (**Figura 7**)^{345,346}. Las NLCs también expresan CD31, el ligando del receptor CD38 que se expresa habitualmente en los casos de LLC de alto riesgo³⁴⁷.

Las células T promueven la supervivencia de las células leucémicas principalmente por las interacciones mediadas por el eje CD40L/CD40, lo que activa la señalización de NF- κ B en las células de LLC^{329,348}. Adicionalmente, las células T secretan citoquinas como IL-4, favoreciendo la sobreexpresión de la IG de superficie en las células de LLC, y facilitando la interacción del BCR con (auto)antígenos³⁴⁹. Las **células estromales** están formadas por una capa de progenitores hematopoyéticos sanos que protegen a las células de LLC de la

de la genética y la biología de la enfermedad para el progreso hacia el desarrollo de terapias más eficaces en un contexto de medicina personalizada.

3.3.1 Inhibidores de la señalización de BCR

El amplio conocimiento adquirido durante años acerca del papel clave del receptor de BCR en la supervivencia de la célula de LLC resultó finalmente en el desarrollo de inhibidores de específicos de quinasas de la ruta del BCR en la última década, en concreto los inhibidores de BTK y PI3K³⁵³⁻³⁵⁵. Ensayos clínicos posteriores demostraron que los pacientes tratados con estos fármacos mostraban una respuesta biológica característica, definida por una rápida reducción del tamaño de los ganglios linfáticos acompañada por una egresión de las células de LLC a la sangre periférica y linfocitosis transitoria, lo que se traduce en buenas respuestas y remisiones duraderas a nivel clínico^{356,357}.

El primer inhibidor de BTK que se ha introducido en el esquema de tratamiento de la LLC es **ibrutinib**, un **inhibidor de primera generación, oral e irreversible de BTK**, que fue inicialmente aprobado para el tratamiento de la LLC R/R en el año 2014, y a día de hoy se usa ampliamente tanto en primera línea de tratamiento como en pacientes R/R^{356,358-360}. Su mecanismo de acción se basa en la unión covalente a un residuo conservado de cisteína (Cys481) en el sitio activo de BTK, inhibiendo por la tanto la señalización del BCR y su efecto en la supervivencia, proliferación, migración e interacciones con el microambiente tumoral de la LLC (**Figura 5**)^{354,361,362}. Además de sus efectos *on-target*, se ha demostrado que ibrutinib ejerce otros efectos en vías moleculares adicionales o incluso una acción inmunomoduladora de las células T mediante la inhibición de la quinasa ITK, que es un regulador central de la señalización del receptor de célula T (TCR)^{363,364}. Desde la aprobación de ibrutinib, han surgido nuevos **inhibidores de BTK de segunda generación**, y en particular, acalabrutinib ha sido aprobado por la FDA y la EMA para el tratamiento de la LLC en primera línea o R/R^{365,366}. **Acalabrutinib** también es un inhibidor de irreversible de BTK en el residuo Cys481, aunque es más selectivo que ibrutinib, lo que resulta en un mejor perfil de seguridad y la aparición de menos efectos adversos³⁶⁷. Otros inhibidores de BTK de segunda generación que se encuentran en fases avanzadas de ensayos clínicos son zanubrutinib y tirabrutinib, que también se unen de forma irreversible y altamente selectiva al residuo Cys481 de BTK^{368,369}. Además, se han desarrollado nuevos **inhibidores reversibles de BTK de tercera generación** como pirtobrutinib (LOXO-305) y ARQ-531, y se encuentran en la actualidad en

fases tempranas de investigación clínica para aquellos pacientes de LLC R/R resistentes a ibrutinib o acalabrutinib³⁷⁰⁻³⁷².

Los **inhibidores de PI3K** también representan una opción prometedora para la inhibición de la señalización mediada por BCR en la LLC. **Idelalisib** es un inhibidor oral y reversible de la subunidad catalítica de la isoforma δ de PI3K y bloquea la señalización mediada por esta quinasa, resultando en una inhibición de la fosforilación de AKT y reducción de la actividad de mTOR (**Figura 5**), alterando las interacciones entre las células de LLC y el microambiente tumoral^{355,373}. Idelalisib se encuentra aprobado a día de hoy para el tratamiento de la LLC R/R, aunque su uso es limitado debido a que ibrutinib o acalabrutinib tienen un mejor perfil de seguridad^{357,366}. Otros inhibidores de PI3K de nueva generación en fases de investigación clínica son duvelisib (un inhibidor dual de PI3K γ/δ) y umbralisib (inhibidor dual de PI3K δ /CK1 ϵ). En particular, duvelisib ha sido recientemente aprobado por la FDA para pacientes con LLC R/R que han recibido al menos dos líneas previas de tratamiento³⁷⁴⁻³⁷⁶.

Aunque el uso de inhibidores de la señalización de BCR ha permitido conseguir respuestas profundas y duraderas en muchos pacientes de LLC, el desarrollo de nuevos **mecanismos de resistencia** a estas terapias se reporta cada vez de forma más frecuente y se ha convertido en un reto a nivel terapéutico en la LLC, precisando del uso de nuevos tratamientos o regímenes de combinación. La resistencia a ibrutinib y acalabrutinib está principalmente asociada a la aparición de **mutaciones en BTK y PLCG2**, que han sido reportadas en aproximadamente un 80% de los pacientes con resistencia adquirida a estos inhibidores^{333,377,378}. Las mutaciones de *BTK* normalmente aparecen en el sitio de unión de ibrutinib, siendo la más común la sustitución C481S, que impide la unión de ibrutinib al sitio activo de BTK, resultando en una pérdida de la inhibición de la actividad mediada por esta enzima^{333,379}. Por otro lado, las mutaciones en *PLCG2* (R665W, L845F and S707Y) son una potencial ganancia de función y promueven la señalización de BCR de forma independiente a la inhibición de BTK^{333,380,381}. También se han propuesto otros mecanismos de resistencia como la evolución clonal, la del(8p) o las mutaciones en reguladores de BTK como *ITPKB* o *CDIPT*^{288,377,382}. Además, la presencia de CK o alteraciones en del(17p)/*TP53* también se han postulado como marcadores predictivos de mal pronóstico al tratamiento con ibrutinib^{228,231,383}. Por el contrario, varios estudios han sugerido que la del(11q) podría ser un marcador predictivo de respuesta favorable en pacientes tratados en primera línea, pero se

asocia con una reducción en la PFS en pacientes R/R^{231,384-386}, aunque se desconocen las causas biológicas de esta respuesta diferencial entre ambos subgrupos de pacientes. Los mecanismos de resistencia a inhibidores de PI3K han sido menos estudiados, aunque una investigación reciente apunta a la presencia de mutaciones activadoras de los genes de la vía MAPK-ERK³⁸⁷.

3.3.2 Inhibidores de BCL2

Los miméticos BH3 son pequeñas moléculas antagonistas de proteínas anti-apoptóticas de la familia BCL2 (ej. BCL2, BCL-xL o MCL1). Concretamente, los miméticos BH3 se unen a las proteínas anti-apoptóticas gracias a su similitud estructural a los dominios BH3 de las proteínas pro-apoptóticas solo BH3 como BIM y NOXA, reemplazando a estas e induciendo la apoptosis mediada por la oligomerización de BAX y BAK³⁸⁸. El único mimético BH3 aprobado actualmente para el tratamiento de la LLC es **venetoclax**, un **inhibidor oral altamente selectivo de BCL2**. A nivel de mecanismo, venetoclax se une a BCL2, desplazando a BIM y provocando una potente inducción de la apoptosis en un mecanismo independiente de TP53³⁸⁹⁻³⁹¹. Venetoclax fue inicialmente aprobado para los pacientes de LLC R/R, en los que mostró respuestas muy eficaces tanto a nivel de PFS como OS en todos los subgrupos de LLC³⁹¹⁻³⁹³, y actualmente su uso está aprobado en combinación con anticuerpos anti-CD20 también para los pacientes de LLC en primera línea^{394,395}.

La resistencia adquirida a venetoclax también puede surgir en algunos pacientes tratados con este fármaco y supone un reto a nivel clínico. De forma similar a lo que se observa con los inhibidores de BTK, el primer **mecanismo de resistencia** descubierto, y el más común, es la **adquisición de una mutación puntual en BCL2 (G101V)**, lo que reduce drásticamente la afinidad de unión de venetoclax a BCL2^{396,397}. Desde el descubrimiento de esta mutación, se han reportado otras sustituciones de tipo *missense* en la misma región, y todas ellas dan como resultado una reducción de la afinidad de unión de venetoclax³⁹⁸⁻⁴⁰⁰. Además, también se ha descrito la sobreexpresión de proteínas anti-apoptóticas alternativas como posibles mecanismos de resistencia. Concretamente, se ha observado amplificación de MCL1 o sobreexpresión de BCL-xL en algunos pacientes resistentes a venetoclax^{396,401}. Otros mecanismos de resistencia que han sido propuestos son las deleciones *CKNA2A/B*, las mutaciones en *BTG1* o niveles altos de fosforilación oxidativa mediada por amplificación de *PRKAB2*^{401,402}. Finalmente, aunque todavía no se sabe mucho sobre el valor predictivo de las alteraciones genéticas recurrentes de la LLC en respuesta a venetoclax, dos ensayos clínicos

recientes sugieren que las alteraciones en del(17p)/TP53 se mantienen como un marcador de pronóstico adverso al tratamiento con estos regímenes^{253,403}.

4. MODELOS *IN VITRO*, *IN VIVO* y *EX VIVO* PARA EL ESTUDIO DE LA BIOLOGÍA DE LA LLC

La elevada heterogeneidad genética y la diversa desregulación de vías de señalización en la LLC, así como los efectos de estas alteraciones en la respuesta clínica de estos enfermos, hace necesario el estudio de los efectos individuales o combinados de las lesiones genéticas de la LLC en la biología de la enfermedad con el fin de tomar decisiones terapéuticas personalizadas. Tradicionalmente, la significancia biológica de las alteraciones *driver* de la LLC se ha estudiado a través de la combinación de aproximaciones *in vitro*, *in vivo* o *ex vivo*, cada una de ellas con unas ventajas y desventajas.

4.1 Modelos *in vitro*

El cultivo de líneas celulares linfoblastoides (LCLs) derivadas de pacientes de LLC ha sido la punta de lanza del estudio biológico y molecular de la LLC a nivel *in vitro*. Estos modelos son útiles para la determinación de funciones génicas, regulación de vías de señalización o interacciones proteicas, así como para evaluar la respuesta a diversos tratamientos. Al contrario que las células primarias de LLC, las líneas celulares presentan gran capacidad proliferativa en ausencia del microambiente tumoral y no sufren procesos de apoptosis espontánea, lo que hace que sean fáciles de mantener en cultivo, transfectar con vectores de expresión o injertar en ratones inmunodeficientes^{404,405}.

Sin embargo, el **número de líneas celulares de LLC que reflejan la heterogeneidad inherente a la enfermedad es muy limitado**⁴⁰⁴. Hasta la fecha, solo unas pocas líneas celulares inmortalizadas derivadas de pacientes de LLC están disponibles para la investigación en laboratorio, y este conjunto de líneas celulares no cubre todos los subgrupos citogenéticos de la enfermedad. Por ejemplo, existen líneas celulares con del(13q), trisomía 12 o del(17p), pero **no existen modelos celulares con del(11q)**, impidiendo el estudio del impacto biológico de esta alteración citogenética o las consecuencias de la haploinsuficiencia de determinados genes localizados en esta región⁴⁰⁴. Además, algunas de estas líneas presentan un cariotipo triploide o tetraploide, algo que no es representativo del panorama citogenético habitual de los pacientes con LLC⁴⁰⁴. A nivel de mutaciones somáticas, algunas de estas líneas celulares han sido estudiadas mediante técnicas de WES, y solo se han

identificado mutaciones en algunos genes *driver* de la enfermedad, lo que dificulta al estudio de las consecuencias funcionales de la mayoría de mutaciones *driver* observadas en los pacientes. De hecho, en ninguna de estas líneas celulares se han identificado mutaciones somáticas en muchos de los genes más frecuentemente mutados en la LLC como *ATM*, *SF3B1* o *NOTCH1*. La **Tabla 3** resume las principales características a nivel de inmunofenotipo, estado mutacional de IGHV, cariotipo, FISH y NGS de las líneas celulares de LLC disponibles para investigación en la actualidad.

La resistencia de las células de LLC a la transformación viral mediada por el virus de Epstein-Barr (EBV) ha sido citada como el principal motivo de ausencia de variedad de líneas celulares inmortalizadas de LLC^{405,406}. Además, la utilidad de líneas celulares como modelos ha sido cuestionada debido a los efectos producidos por la transformación mediada por EBV, ya que las líneas celulares no recapitulan las interacciones pro-supervivencia del microambiente y además la propia inmortalización en sí podría desregular vías de señalización importantes en la patogénesis de la LLC^{404,407}. Sin embargo, estudios del perfil de expresión génica han demostrado que la mayoría de cambios transcripcionales entre las LCLs y las células B primarias son de pequeña magnitud, y las LCLs normalmente recapitulan la variación en la expresión génica que se observa en las células B primarias⁴⁰⁷.

Tabla 3. Características de las líneas celulares derivadas de pacientes de LLC y verificadas, disponibles para investigación (Adaptada de Lanemo-Myhrinder *et al.*⁴⁰⁴).

Línea celular	Edad/sexo/Binet/Rai del paciente	Immuno-fenotipo ¹	IGHV	Cariotipo/FISH ²	Mutación <i>drivers</i> ³	Disponi ble en	Ref.
MEC1	62/Hombre/Rai II	IgM, κ CD5-/CD19+	M	Diploide/ Del(17p), -12	TP53 ^{MUT} BIRC3 ^{DEL}	DSMZ	408
MEC2	62/Hombre/Rai II	IgM, κ CD5-/CD19+	M	Triploide/ Del(17p), -12	TP53 ^{MUT}	DSMZ	408
HG3	70/Hombre/Rai II	IgM, λ CD5+/CD19+	UM	Diploide/ Del(13q)	Ninguna	DSMZ	409
PGA1	Hombre	IgG, λ CD5 ^{dim} /CD19+	M	Diploide/ +12, del(13q)	KRAS ^{MUT}	DSMZ	410
OSU-CLL	Hombre	IgM, κ CD5+/CD19+	M	Diploid/ +12, +19	Ninguna	OSU	405
I83-E95	75/Hombre/Binet A	IgM, λ CD5+/CD19+	M	Tetraploide/ +12, del(13q), del(17p)	ND	DSMZ	404
WaC3CD5+	Hombre/Rai I	IgM, κ CD5+/CD19+	UM	Diploide/ Del(13q), del(17p)	ND	DSMZ	404

Wa-ose1	Hombre/Rai I	IgM, κ CD5-/CD19 ⁺	UM	Tetraploide	ND	DSMZ	404
232B4	Hombre/Rai 0	IgG, κ CD5-/CD19 ⁺	M	Tetraploide -17	ND	Li.U	404

¹Más información acerca de marcadores inmunofenotípicos adicionales en www.dsmz.de o las referencias indicadas en la tabla. ²Solo los CNAs recurrentes están indicados en la tabla, para más información del cariotipo completo consultar www.dsmz.de o las referencias indicadas en la tabla. ³Los datos de NGS para las líneas celulares MEC1, HG3 y PGA1 han sido obtenidos en nuestro laboratorio mediante el estudio de un conjunto de 54 genes *driver* de la LLC⁴¹¹. También hay disponibles datos de WES para las líneas MEC1, HG3 y PGA1⁴¹². En el caso de la línea celular MEC2, solo se conoce el estado mutacional de *TP53*. En la línea celular OSU-CLL solo se han analizado mutaciones en las regiones *hotspot* de los genes *NOTCH1*, *TP53*, *MYD88*, *KLHL6*, *XPO1*, *SF3B1*, *BRAF* y *BTK*⁴⁰⁵. ⁴Las líneas celulares MEC1 y MEC2 presentan un cariotipo casi diploide o triploide, respectivamente, con un 10% de poliploidía (www.dsmz.de). M: mutato; UM: no mutato; ND: no disponible; DSMZ: German Collection of Microorganisms and Cell Cultures; OSU: Ohio State University; Li.U: Linköping University.

4.2 Modelos *in vivo* de LLC

Los modelos de ratón que mimetizan las neoplasias hematológicas humanas son útiles para determinar los mecanismos implicados en la biología de la enfermedad y su progresión, así como para la evaluación de respuesta a fármacos en estado pre-clínico. En la LLC, existen principalmente dos tipos de abordaje para el estudio *in vivo* de la enfermedad: los modelos de xenotrasplante murino o los modelos de ratón generados mediante técnicas de ingeniería genética^{413,414}.

Los **modelos de xenotrasplante murino** se han llevado a cabo utilizando o bien líneas celulares de LLC o bien células primarias de pacientes. La mayoría de las líneas celulares son capaces de injertar de forma subcutánea o intravenosa en ratones con gran inmunodeficiencia como los de las cepas NOD-scid IL2R $\gamma^{-/-}$ (NSG) o Rag2 $^{-/-}$ $\gamma_c^{-/-}$, que se caracterizan por la falta de células B, T y NK^{405,413,415-417}. El xenotrasplante de líneas celulares de LLC a estos modelos es fácilmente reproducible, y las células se diseminan de forma rápida y sistémica en el ratón, emulando el comportamiento de la LLC humana de alto riesgo. Sin embargo, una de las limitaciones que tienen estos modelos es que la proliferación celular es inducida por la transformación mediada por EBV y no por las interacciones con el microambiente tumoral, lo que impide el estudio de este aspecto crítico en la LLC^{413,415}. Por otro lado, en la última década se han llevado a cabo numerosos esfuerzos para el desarrollo de **modelos xenograft derivados de pacientes de LLC**. Estos modelos también emplean ratones con alto grado de inmunodeficiencia como los NSG y se basan en la infusión intravenosa de células mononucleadas de sangre periférica de pacientes de LLC,

normalmente en presencia de células T autólogas previamente activadas *in vitro* o *in vivo*^{413,418-421}. Los modelos xenograft derivados de pacientes de LLC son herramientas útiles para evaluar la respuesta a fármacos así como las interacciones con el microambiente tumoral, supliendo las limitaciones de los modelos xenograft de líneas celulares. Sin embargo, las diferencias metodológicas que han sido reportadas entre distintos grupos de investigación han de ser estandarizadas para que se pueda realizar un uso generalizado de este tipo de modelos en la investigación de la LLC⁴¹⁸⁻⁴²⁴. Cabe destacar que recientemente se han desarrollado también modelos xenograft derivados de pacientes con RS, demostrando que son útiles para la evaluación de nuevas aproximaciones terapéuticas en este subgrupo de alto riesgo⁴²⁵⁻⁴²⁷.

Los **modelos de ratón generados mediante técnicas de ingeniería genética** se basan en dos aproximaciones: emulación de la desregulación de la expresión génica o emulación de lesiones genéticas específicas de la LLC. El modelo más empleado con diferencia es el ratón transgénico *TCL1*, que sobreexpresa el gen humano *TCL1* y emula el desarrollo de una forma agresiva de LLC⁴²⁸. Otros modelos de este tipo para el estudio de la LLC incluyen el modelo doble transgénico *BCL2* x *Traf2dn*, el ratón transgénico *APRIL* o el ratón transgénico *ROR1*^{414,429-431}. Todos estos modelos son bastante útiles para el estudio de respuesta a fármacos en fase pre-clínica y para determinar diversos aspectos de la patogénesis de la enfermedad, aunque también conllevan desventajas como un largo tiempo de manifestación de la enfermedad (normalmente de más de un año) y ausencia de células del microambiente tumoral. Además, tampoco recapitulan la heterogeneidad genética de la LLC^{414,420}. Con respecto a modelos de ratón que emulan las lesiones genéticas de la LLC, se ha investigado que la delección restringida al linfocito B del locus del *mir-15a/16-1* o del las regiones comunes o mínimas delecionadas del cromosoma 14qC3 del genoma del ratón, todas ellas análogas a la del(13q) humana, es capaz de generar una neoplasia linfoide con fenotipo de LLC^{171,172}. Además, gracias al empleo de novedosas y prometedoras aproximaciones se han conseguido establecer recientemente modelos de ratón que desarrollan una enfermedad de fenotipo de LLC mediante la combinación restringida al linfocito B de delección de *Atm* y mutación de *Sf3b1*²⁹³ o mediante la mutación de *Ikzf3*³³². Sin embargo, se necesitarían numerosos estudios futuros para poder generar modelos murinos que sean capaces de cubrir las principales lesiones del heterogéneo panorama genético de la LLC. Además, los modelos murinos de CNAs de gran tamaño suponen un gran reto, no solo por razones técnicas, sino por las notorias diferencias en la distribución génica entre los cromosomas humanos y murinos⁴³².

4.3 Modelos *ex vivo* de LLC

Como se mencionaba en las secciones anteriores, las células de LLC tienen una alta dependencia del microambiente para su supervivencia, por este motivo, las células primarias presentan apoptosis espontánea cuando son cultivadas *in vitro*. De esta forma, los cultivos *ex vivo* de LLC se han enfocado tradicionalmente en emular las interacciones con el microambiente mediante la implementación de sistemas de co-cultivo con células accesorias o medio condicionado que sea capaz de replicar la señalización inducida por el microambiente⁴²⁰.

Los sistemas más relevantes de co-cultivo hasta el momento se basan en el uso de células del estroma de la médula ósea (BMSCs; bone marrow stromal cells) o NLCs. En los **co-cultivos de LLC y BMSCs** se pueden emplear BMSCs derivadas de pacientes, líneas celulares de estroma murino (ej. M210B4, SUM4, KUSA-H1) o líneas celulares de estroma humano (HS5 o StromaNKTert)^{433,434}. Este tipo de co-cultivo ha mostrado una alta eficacia en el mantenimiento de las células de LLC en cultivos durante semanas, previniendo tanto la apoptosis espontánea como la inducida por fármacos, mediante la sobreexpresión de proteínas anti-apoptóticas o activación de vías de señalización pro-supervivencia como PI3K o NF- κ B^{420,433-435}. Adicionalmente, los **co-cultivos de LLC y NLCs** se establecen a partir de NLCs derivadas de pacientes que son capaces de inducir activación de la señalización por BCR y NF- κ B, resultando en sobreexpresión de proteínas anti-apoptóticas y proporcionando supervivencia a largo plazo e inducción de la proliferación de las células de LLC^{341,343,344}.

La señalización inducida por el microambiente tumoral también se puede reproducir *ex vivo* mediante el empleo de **factores solubles** que funcionen como ligandos de los receptores de superficie de las células de LLC, desencadenando la señalización de diversas vías pro-supervivencia. Concretamente, la ligación del BCR mediante anti-IgM induce la señalización de BCR y activación de NF- κ B, lo que resulta en una disminución de la apoptosis espontánea y un incremento de la proliferación, especialmente en los casos UM-IGHV⁴³⁶⁻⁴³⁸. Además, la estimulación de la señalización del TLR mediante CpG-ODN se usa de manera generalizada en los cultivos *ex vivo* y también da lugar a activación de NF- κ B y producción de citoquinas pro-supervivencia^{439,440}. La estimulación de CD40 por medio de su ligando, CD40L, es también otro método ampliamente utilizado en cultivos *ex vivo* y emula las interacciones entre las células T y los linfocitos B de LLC^{348,420}.

Los sistemas de co-cultivo y factores solubles también se pueden usar de forma combinada para los cultivos *ex vivo* de células primarias de LLC. Algunas de las mejores aproximaciones para inducir proliferación de la LLC y alta reducción de la apoptosis espontánea incluyen co-cultivo con células estromales HS5 en presencia de CpG-ODN e IL-2 o IL-15, así como co-cultivo con fibroblastos que expresan de forma constitutiva CD40L suplementados con IL-4 o IL-21⁴⁴¹⁻⁴⁴⁴. En resumen, los cultivos *ex vivo* de células primarias de LLC representan una opción adecuada para el estudio de las interacciones de las células leucémicas con los componentes del microambiente, así como la respuesta a fármacos en el contexto de estas interacciones. Sin embargo, la heterogeneidad genética que existe entre diferentes pacientes en la LLC es difícil de recapitular en este tipo de modelos a no ser que se empleen cohortes de un elevado número de casos. Además, los estudios a nivel genético y de mecanismos biológicos en estas células son muy limitados debido a la gran dificultad de transfección o transducción de las células primarias de LLC^{445,446}.

4.4 Técnicas de edición genética para la generación de nuevos modelos de LLC

Como se ha ido indicando a lo largo de esta sección de introducción, el dinámico desarrollo de técnicas genómicas de alta resolución ha revelado la presencia de un enorme número de alteraciones genéticas en la LLC tanto a nivel de cromosoma, como a nivel de genes individuales o la expresión de estos, así como incluso en regiones no codificantes del genoma^{65,66}. Las funciones biológicas de algunas de estas lesiones están empezando a ser entendidas parcialmente gracias a la mejora de los modelos *in vitro*, *in vivo* y *ex vivo* de la enfermedad^{404,413,414,420}. Sin embargo, la LLC, así como la mayoría de los tipos de cáncer, se presenta y progresa gracias a la compleja interacción entre múltiples *drivers* de la enfermedad, por lo que se requieren nuevos modelos capaces de evaluar la contribución individual o conjunta de estas lesiones genéticas en la capacidad proliferativa y de supervivencia de la célula, sus mecanismos de concurrencia o mutual exclusividad preferentes y cuál es el resultado de la desregulación de las vías biológicas en la evolución clonal o la respuesta al tratamiento.

Avances recientes en el campo de la ingeniería genética han abierto un amplio abanico de posibilidades para generar nuevos modelos de diferentes enfermedades, tanto a nivel *in vitro* como *in vivo*. En particular, los **sistemas de edición genómica** proporcionan una excelente herramienta para modificar el genoma de una forma precisa, y, de esa forma,

evaluar el impacto de alteraciones *driver* específicas en la función celular. Las primeras técnicas de edición genética implementadas para la generación de modelos celulares en cáncer fueron las nucleasas ZNFs (zinc-finger nucleases) y TALENs (transcription activator-like effector nucleases), aunque su uso generalizado fue limitado por su complejidad técnica y altos costes^{447,448}. Sin embargo, la reciente introducción de la tecnología denominada en inglés como **Clustered Regularly Interspaced Short Palindromic Repeats (CRISPR)/Cas9** ha supuesto un cambio sustancial en el panorama de la ingeniería genética, resolviendo las limitaciones aportadas por los métodos anteriores. Así, este sistema de edición genética ha sido capaz de transformar nuestra capacidad de evaluar el impacto de las mutaciones somáticas y alteraciones cromosómicas a nivel *in vitro*, *in vivo* y *ex vivo* ⁴⁴⁹⁻⁴⁵².

La tecnología CRISPR/Cas9 deriva del sistema inmune adaptativo de organismos procariontes y está formado principalmente por dos componentes biológicos: una endonucleasa de ADN guiada por ARN y denominada **Cas9** y un ARN guía quimérico denominado **sgRNA** (single-guide RNA). La molécula de sgRNA se compone a su vez de una secuencia de ARN CRISPR (crRNA), complementaria a la región diana de interés, y un crRNA transactivador (tracrRNA), que se une a la nucleasa Cas9 y la dirige a la región genómica de interés mediante complementariedad de bases (**Figura 8**). El único requerimiento de la región diana es que debe ser adyacente a un motivo PAM (protospacer adjacent motif), que consiste en una secuencia de tres nucleótidos NGG, en el caso de utilizar una proteína Cas9 derivada de *S. pyogenes*, que es una de las nucleasas más comunes para la edición genética mediante CRISPR^{449,453}. De esta forma, con solo combinar la expresión de la proteína Cas9 y un sgRNA de 20 pares de bases complementario a la región de ADN de interés, se puede conseguir una ruptura de alta eficiencia en la región genética diana, dando lugar a la aparición de un DSB que será reparado por los mecanismos de NHEJ o HR (**Figura 8**)⁴⁵³ (Ver sección 3.1.1 *Respuesta a daño en el ADN y control del ciclo celular*). La reparación mediada por NHEJ da lugar a la introducción de pequeñas indels que resultan en la aparición de mutaciones *frameshift* y la generación de codones de parada prematuros, lo que es útil para emular mutaciones de pérdida de función. Por otro lado, en presencia de un molde de ADN donador, los DSBs se pueden reparar mediante el mecanismo de HR, lo que se puede usar para hacer modificaciones precisas de la secuencia del ADN como sustituciones de tipo *missense* que dan lugar a un fenotipo de ganancia de función, así como la corrección de mutaciones existentes (**Figura 8**)^{449,453}.

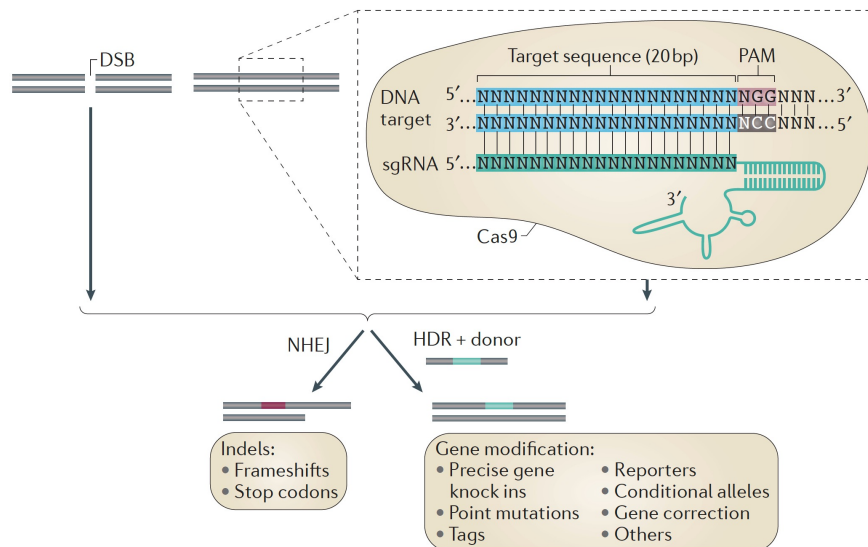


Figura 8. Componentes del sistema CRISPR/Cas9 y sus aplicaciones. Esquema representativo de los componentes requeridos para el sistema de edición genética CRISPR/Cas9. La nucleasa Cas9 es dirigida a la región genómica de interés (azul), adyacente a la secuencia de tres nucleótidos PAM (rojo) esencial para el reconocimiento del lugar de acción, por complementariedad de bases de la molécula de sgRNA (verde). La actividad nucleasa de la proteína Cas9 resulta en la formación de un DSB entre los nucleótidos 17 y 18 de la secuencia diana, que será posteriormente reparado por NHEJ, dando lugar a la formación de indels, o mediante modificación precisa de la secuencia mediante reparación dirigida por homología (HDR; homology-directed repair) en la presencia de un molde de ADN donador (Tomada de Sánchez-Rivera FJ & Jacks T. 2015)⁴⁵³.

La simplicidad y versatilidad de este sistema de edición genética ha supuesto el desarrollo un **amplio rango de aplicaciones para la generación de modelos de estudio de la biología del cáncer**, muchas de las cuales han sido implementadas de manera exitosa en cultivos celulares y modelos animales⁴⁵³. Además de poder reproducir mutaciones de pérdida o ganancia de función en un contexto isogénico y de manera rápida y sencilla, así como la corrección de mutaciones puntuales, el sistema CRISPR/Cas9 se puede utilizar para generar **reordenamientos cromosómicos**. Esto se puede conseguir introduciendo dos DSBs de forma simultánea en diferentes cromosomas, lo que puede dar lugar a translocaciones, o introduciendo dos DSBs en dos sitios distantes de un mismo cromosoma, produciendo inversiones o deleciones cromosómicas⁴⁵⁴⁻⁴⁵⁷. Otras aplicaciones del sistema CRISPR/Cas9 útiles para el estudio del cáncer son la generación de alelos condicionales para el desarrollo de modelos animales o el marcaje de alelos con reporteros fluorescentes o etiquetas sintéticas^{453,458}. Además, este sistema se puede emplear para determinar la función de elementos no codificantes del ADN como promotores y enhancers^{459,460}. La facilidad de **multiplexar** el sistema CRISPR/Cas9 también ofrece numerosas oportunidades para investigar

interacciones entre genes que dan lugar a letalidad sintética o también para realizar *screenings* genéticos a gran escala para identificar nuevos genes implicados en diversos procesos celulares, o para descubrir genes implicados en resistencia o vulnerabilidad a fármacos^{453,461}. Adicionalmente, se pueden usar variaciones del sistema CRISPR/Cas9 para reprimir o activar la expresión génica, inducir modificaciones a nivel de cromatina o editar secuencias de ARN⁴⁶²⁻⁴⁶⁴. Por último, este sistema puede ser potencialmente aplicable a nivel clínico y, de hecho, existen numerosos ensayos clínicos en curso explorando la posibilidad de corregir mutaciones o inhibir la función de genes relacionados con procesos tumorales⁴⁶⁵.

En paralelo al desarrollo de esta tesis doctoral, algunos estudios han empleado el sistema CRISPR/Cas9 para dilucidar la función de algunas mutaciones en genes *driver* de la LLC como *NOTCH1*, *TP53*, *FBXW7* o *RPS15* a nivel *in vitro* en líneas celulares de LLC^{299,303,416,466}. Otros estudios también han aplicado esta metodología para estudiar la contribución de proteínas específicas como 14-3-3ζ o ADAR en la señalización de Wnt o en procesos de edición de ARN, respectivamente^{467,468}. Además, se han empleado *screens* de CRISPR a gran escala para investigar mecanismos desconocidos implicados en la resistencia a venetoclax⁴⁰¹ y recientemente se ha descrito la edición de genes *driver* de LLC de forma combinada para la generación de nuevos modelos murinos⁴⁶⁹. Sin embargo, la versatilidad del sistema CRISPR/Cas9 ofrece muchísimas oportunidades, hasta el momento inexploradas, para el progreso de nuestro conocimiento en la LLC. Esta tecnología se puede aprovechar no solo para reproducir mutaciones génicas de significado biológico desconocido, sino también para reproducir alteraciones cromosómicas que juegan un papel clave en la patogénesis de la enfermedad. Además, esta metodología nos permite profundizar en el conocimiento del proceso de evolución clonal, así como saber de qué forma cooperan las alteraciones cromosómicas y mutaciones génicas para influir en la progresión de la enfermedad y en la respuesta al tratamiento. Finalmente, el sistema CRISPR/Cas9 puede ser empleado para el descubrimiento de nuevas vulnerabilidades terapéuticas basadas en letalidad sintética, aportando valiosa información para la implementación de novedosas estrategias terapéuticas y para el progreso de la medicina personalizada en la LLC.

HIPÓTESIS

Los recientes avances perpetrados en el estudio del genoma de la leucemia linfática crónica (LLC) han desvelado la amplia heterogeneidad a nivel genético que define a esta entidad, caracterizada por la presencia de un gran número de alteraciones cromosómicas y mutaciones génicas recurrentes que reflejan en gran medida el variable curso clínico entre diferentes pacientes. Los avances realizados también en el campo de la secuenciación masiva de ADN han revelado la presencia de una gran heterogeneidad intra-clonal en la LLC, definiendo patrones específicos de concurrencia y mutua exclusividad entre algunas alteraciones genéticas. Es importante comprender cuál es el momento de la aparición de estas lesiones así como la contribución de cada una de ellas en la biología de la enfermedad, con el fin de determinar cómo la interacción entre múltiples *drivers* da lugar a evolución clonal y progresión de la LLC, así como su influencia en la respuesta al tratamiento.

Ciertas evidencias sugieren que la expansión de clones malignos de LLC se origina a partir de células que han transitado, o no, a través de los centros germinales, dependiendo del estado mutacional de la región variable del gen de la cadena pesada de las inmunoglobulinas. Sin embargo, el momento específico de la hematopoyesis en el que ocurre el primer evento oncogénico relacionado con la LLC es un asunto controvertido que no está claro a día de hoy. Varios estudios han sugerido que algunas mutaciones *driver* de la LLC podrían aparecer en un estadio de maduración previo, o incluso en los propios progenitores hematopoyéticos CD34⁺. Sin embargo, se necesitan nuevas investigaciones para determinar si existen alteraciones genéticas específicas que aparecen de forma preferente en este estadio de la maduración y por lo tanto son candidatas a participar en el origen de la LLC, o bien si existen lesiones determinadas que aparecen en momentos más tardíos, lo que sugeriría un papel en el mantenimiento y expansión de la enfermedad más que en el origen en sí. Además, de todo el conjunto de alteraciones genéticas identificadas en la LLC, solo se ha investigado la presencia de mutaciones génicas específicas en los progenitores hematopoyéticos de estos pacientes, mientras que la existencia de algunas alteraciones citogenéticas como del(11q) no ha sido estudiada, lo que genera interrogantes acerca del papel de este tipo de alteraciones en la iniciación de la enfermedad.

La deleción monoalélica del brazo largo del cromosoma 11, del(11q), define un subgrupo de pacientes de LLC de alto riesgo que se caracterizan por la presencia de linfadenopatías evidentes, rápida progresión de la enfermedad y supervivencia reducida. El tamaño de esta deleción es variable, y puede llegar a abarcar cientos de genes, de entre los cuales se ha

sugerido que específicamente *ATM* y *BIRC3* podrían tener un papel en la patogénesis de la enfermedad, ya que se dan mutaciones de pérdida de función en *ATM* o *BIRC3* de forma preferente en casos con del(11q). Se ha demostrado que la disfunción completa de las proteínas *ATM* o *BIRC3* empeora el pronóstico de los pacientes de LLC con del(11q). Sin embargo, los determinantes biológicos por los que la concurrencia de estas alteraciones orquestan la progresión, evolución clonal y respuesta al tratamiento de la LLC son ampliamente desconocidos. Además, se han descrito otras alteraciones genéticas concomitantes en pacientes con del(11q), pero su papel en el pronóstico de este subgrupo específico de enfermos no ha sido dilucidado.

El estudio de las implicaciones biológicas de la del(11q), así como las mutaciones asociadas en *ATM* o *BIRC3* ha sido muy limitado debido a la falta de líneas celulares que porten estas lesiones cromosómicas específicas y a la falta de modelos murinos que reproduzcan la biología de la del(11q), sumado a la dificultad de manipulación de células primarias de LLC *ex vivo*. Comprender el papel que desempeñan estas alteraciones en la biología de la enfermedad es más relevante que nunca debido a la introducción de nuevos fármacos dirigidos en el algoritmo de tratamiento de la LLC, no solo para determinar qué subgrupos específicos de pacientes podrían beneficiarse de estas terapias, sino también para explorar nuevas aproximaciones terapéuticas basadas en letalidad sintética. La reciente introducción del sistema de edición genética CRISPR/Cas9 ha transformado nuestra capacidad de dilucidar la función de mutaciones *driver* y alteraciones cromosómicas, tanto a nivel *in vitro* como *in vivo*, y su aplicación en la LLC abre prometedores horizontes para determinar cómo interaccionan las diferentes lesiones genéticas en la patogénesis y evolución de la enfermedad.

Creemos que el sistema CRISPR/Cas9 puede ser empleado para generar nuevos modelos *in vitro* e *in vivo* de LLC que reproduzcan de forma precisa la biología de la del(11q) y las mutaciones concurrentes en *ATM*, *BIRC3* y otros genes. Estos modelos, en combinación con cultivos *ex vivo* de células primarias de pacientes con las mismas alteraciones genéticas, nos permitirán entender la contribución específica de cada una de estas lesiones en aspectos cruciales de la biología y respuesta al tratamiento de la LLC. Además, la implementación en paralelo de técnicas de secuenciación masiva de ADN para el estudio del perfil mutacional de los pacientes con del(11q) y sus progenitores hematopoyéticos, podría descifrar otras alteraciones genéticas con relevancia pronóstica en este subgrupo de pacientes de alto riesgo,

así como la contribución de la del(11q) y otras lesiones *driver* en el origen de la enfermedad. Por lo tanto, la integración del análisis genómico y de los modelos celulares generados mediante CRISPR/Cas9 podría ser útil para entender el papel de la del(11q) y sus alteraciones concurrentes en numerosos aspectos de la enfermedad: desde la iniciación a la progresión y evolución clonal, mejorando el tratamiento personalizado de este subgrupo de pacientes en base a su perfil genético.

OBJETIVOS

Objetivo general

Profundizar en los determinantes biológicos causantes de la iniciación, progresión y evolución clonal de la LLC con del(11q), así como explorar nuevas vulnerabilidades terapéuticas en este subgrupo de pacientes, mediante la combinación de técnicas de secuenciación masiva, modelos *in vitro* isogénicos editados mediante CRISPR/Cas9, modelos de xenotrasplante murino *in vivo* y cultivos *ex vivo* de células primarias de LLC.

Objetivos específicos

1. Analizar la presencia de mutaciones génicas y alteraciones cromosómicas en progenitores hematopoyéticos CD34⁺ de pacientes de LLC para determinar el estadio de maduración donde estos eventos ocurren así como la contribución de estas lesiones al origen de la LLC.
2. Determinar el perfil mutacional de los enfermos de LLC con del(11q) para identificar patrones preferentes de concurrencia o mutual exclusividad con relevancia clínica.
3. Generar modelos isogénicos de LLC que reproduzcan la biología de la del(11q) y/o mutaciones de pérdida de función asociadas en los genes *ATM*, *TP53* o *BIRC3* mediante el sistema de edición genómica CRISPR/Cas9.
4. Evaluar el impacto funcional de la pérdida monoalélica y bialélica de *ATM* en la LLC con del(11q) a nivel de señalización en respuesta a daño en el ADN e identificar potenciales vulnerabilidades terapéuticas de este subgrupo de pacientes basadas en letalidad sintética.
5. Caracterizar el impacto biológico de la concurrencia de alteraciones monoalélicas y bialélicas en los genes *ATM* y *TP53* en la LLC con del(11q) a nivel *in vitro* e *in vivo*. Determinar la implicación de la combinación de estas lesiones genéticas en la respuesta al tratamiento.
6. Dilucidar el efecto biológico de la pérdida de *BIRC3* mediada por del(11q) y/o mutaciones de pérdida de función de *BIRC3* en la señalización de NF-κB y en la desregulación de la apoptosis, así como su contribución en la progresión, respuesta al tratamiento y evolución clonal de la LLC.

RESULTADOS - Resúmenes

CAPÍTULO 1 - RESUMEN

Next-generation sequencing and FISH studies reveal the appearance of gene mutations and chromosomal abnormalities in hematopoietic progenitors in chronic lymphocytic leukemia

Miguel Quijada-Álamo, María Hernández-Sánchez, Cristina Robledo, Jesús María Hernández-Sánchez, Rocío Benito, Adrián Montaña, Ana E Rodríguez-Vicente, Dalia Quwaider, Ana-África Martín, María García-Álvarez, María Jesús Vidal Manceñido, Gonzalo Ferrer-Garrido, María-Pilar Delgado-Beltrán, Josefina Galende, Juan-Nicolás Rodríguez, Guillermo Martín-Núñez, José-María Alonso, Alfonso García de Coca, José A. Queizán, Magdalena Sierra, Carlos Aguilar, Alexander Kohlmann, José-Ángel Hernández, Marcos González, Jesús-María Hernández Rivas

Journal of Hematology & Oncology. 2017 Apr 11;10(1):83. doi: 10.1186/s13045-017-0450-y. PMID: 28399885

INTRODUCCIÓN Y OBJETIVOS

La leucemia linfática crónica (LLC) es una neoplasia de células B maduras que presenta una elevada heterogeneidad a nivel genético. Tradicionalmente, se ha considerado que las alteraciones genéticas de la LLC aparecen en el propio linfocito B maduro, sin embargo, varios estudios independientes han sugerido que algunas de estas alteraciones podrían aparecer en estadios más tempranos de la maduración, afectando a progenitores hematopoyéticos CD34⁺. Estos estudios se han centrado principalmente en el análisis de mutaciones de genes *driver* en células CD34⁺ de pacientes de LLC, pero se desconoce si las alteraciones citogenéticas típicas de la LLC aparecen también en estadios tempranos de la maduración, y la presencia combinada de alteraciones citogenéticas y mutaciones génicas en las células CD34⁺ de un mismo paciente no ha sido estudiada hasta la fecha. De esta forma, nos propusimos analizar la presencia tanto de mutaciones somáticas como de alteraciones citogenéticas en células progenitoras CD34⁺ de la médula ósea de pacientes con LLC, con el fin de determinar cuáles de estos eventos ocurren en una etapa inicial de la diferenciación de células B.

PACIENTES Y MÉTODOS

Se analizaron muestras obtenidas de médula ósea de un total de 56 pacientes de LLC. De cada una de estas muestras, se realizó un aislamiento de la población de progenitores hematopoyéticos CD34⁺ (que incluye tanto células madre hematopoyéticas (HSCs) CD34⁺CD19⁻ como células pro-B CD34⁺CD19⁺) y de la población de linfocitos B maduros CD19⁺ mediante separación inmunomagnética (MACS) empleando MicroBeads CD34 y CD19, respectivamente (Miltenyi Biotec). Se determinó la pureza de cada una de estas fracciones celulares mediante citometría de flujo, siendo mayor del 90% y del 98% para las poblaciones CD34⁺ y CD19⁺, respectivamente. La fracción CD19⁺ de todos los pacientes de la serie fue analizada mediante hibridación fluorescente *in situ* (FISH) y secuenciación masiva (NGS) de amplicones con el sistema GS-Junior (454-Roche) para el estudio de alteraciones citogenéticas recurrentes y el estado mutacional de *TP53* (exones 4-11), *NOTCH1* (exones 33-34), *SF3B1* (exones 10-16), *FBXW7* (exones 8-12), *MYD88* (exones 4-5), y *XPO1* (exones 14-15). Todas las mutaciones reportadas en este análisis fueron posteriormente investigadas en la fracción CD34⁺ mediante la misma metodología. Además, la fracción CD34⁺ de 9/56 pacientes fue analizada mediante FISH para determinar la presencia de alteraciones citogenéticas en este subtipo celular.

Por otro lado, se realizó separación por citometría de flujo de la subpoblación específica de HSCs CD34⁺CD19⁻ de 7/56 pacientes, así como de poblaciones pertenecientes a otros linajes celulares maduros como linfocitos T (CD3⁺) y monocitos (CD14⁺), obteniendo purezas mayores del 98% para todos los tipos celulares. Estas subpoblaciones fueron analizadas por NGS de alta profundidad en el sistema MiSeq (Illumina), obteniendo una cobertura media 4399 lecturas por amplicón.

RESULTADOS

Los estudios de NGS de amplicones revelaron la presencia de un total de 28 mutaciones en 24 de los 56 (42,9%) pacientes de la serie. El gen más frecuentemente mutado fue *NOTCH1* (23,2%), seguido de *XPO1* (8,9%), *SF3B1* (7,1%), *FBXW7* (5,4%), *TP53* (3,6%) y *MYD88* (1,8%). 15 de estos 24 pacientes (62,5%) presentaron las mismas mutaciones en su correspondiente fracción CD34⁺. Comparando la frecuencia alélica de estas variantes entre cada una de las poblaciones, se pudieron distinguir principalmente dos patrones. Por un lado, la mayoría de las mutaciones en *NOTCH1* (7/9), *XPO1* (4/4) y *MYD88* (1/1) mostraron una carga mutacional similar entre las fracciones CD19⁺ y CD34⁺. Por otro lado, las mutaciones en *TP53* (2/2), *FBXW7* (2/2) y *SF3B1* (3/4) mostraron una frecuencia variante alélica considerablemente inferior, o incluso ausencia de mutación, en la población CD34⁺ en comparación con la fracción CD19⁺. El estudio de NGS de alta profundidad en 7 pacientes confirmó la presencia de las mutaciones de *NOTCH1*, *XPO1*, *MYD88* y *FBXW7* en la subpoblación CD34⁺CD19⁻ de progenitores hematopoyéticos tempranos (6/7). Además, se detectó la presencia de alguna de estas mutaciones concretas (*MYD88* y *FBXW7*) en las fracciones CD3⁺ y CD14⁺, mientras que las mutaciones en *NOTCH1* (2/2) solo se observaron en la población CD34⁺CD19⁻ y en los linfocitos B maduros CD19⁺. Finalmente, el análisis de FISH en 9 pacientes de la serie reveló la presencia de del(11q) (2/2) y del(13q) (3/5) en la fracción CD34⁺, mientras que las alteraciones de *IGH* no fueron detectadas en esta subpoblación celular en ninguno de los pacientes analizados (0/2).

En base a los resultados obtenidos mediante los estudios de NGS y FISH, las diferentes cargas alélicas en cada una de las alteraciones observadas en las diferentes fracciones celulares, así como el análisis de pacientes con alteraciones concurrentes, sugerimos un modelo de aparición y expansión de estas lesiones a lo largo de la diferenciación B de los pacientes con LLC. De esta forma, gran parte de los eventos *driver* de la LLC aparecerían inicialmente en los progenitores hematopoyéticos de estos pacientes, sin embargo, cada una

de estas alteraciones podría participar en el inicio de la expansión tumoral en diferentes estadios de la maduración.

CONCLUSIONES

Este estudio demuestra la presencia tanto de mutaciones genéticas como alteraciones cromosómicas en los progenitores hematopoyéticos CD34⁺ de los pacientes de LLC. En concreto, las mutaciones en *NOTCH1* y *MYD88*, así como la del(11q) y del(13q) podrían considerarse eventos tempranos de la enfermedad, mientras que la expansión de las mutaciones de *XPO1* tendría lugar en un estadio intermedio de la maduración B. Por otro lado, el origen y expansión de las mutaciones en *TP53*, *SF3B1* y *FBXW7*, así como las alteraciones de *IGH*, aparecería en los linfocitos B maduros de la LLC.

CAPÍTULO 2 - RESUMEN

CRISPR/Cas9-generated models uncover therapeutic vulnerabilities of del(11q) CLL cells to dual BCR and PARP inhibition

Miguel Quijada-Álamo, María Hernández-Sánchez, Verónica Alonso Pérez, Ana E Rodríguez-Vicente, Ignacio García-Tuñón, Marta Martín Izquierdo, Jesús María Hernández-Sánchez, Ana B Herrero, José María Bastida, Laura San Segundo, Michaela Gruber, Juan Luis García, Shanye Yin, Elisa ten Hacken, Rocío Benito, José Luis Ordóñez, Catherine J Wu, Jesús María Hernández-Rivas

Leukemia. 2020 Jun;34(6):1599-1612. doi: 10.1038/s41375-020-0714-3.

PMID: 31974435

INTRODUCCIÓN Y OBJETIVOS

La del(11q) es una alteración citogenética frecuente que puede afectar a alrededor de un 20% de los pacientes de LLC al diagnóstico, asociándose con una rápida progresión de la enfermedad y un pronóstico adverso. Aunque el tamaño de esta deleción es altamente variable, en la práctica totalidad casos la región mínima común delecionada incluye al gen supresor de tumores *ATM*, que además, puede estar afectado por mutaciones de pérdida de función en el alelo restante de un tercio de los pacientes con del(11q). Esta inactivación bialélica de *ATM* confiere un pronóstico aún más desfavorable que el de la del(11q) única, y también se relaciona con resistencia a regímenes de tratamiento basados en quimioterapia. En el contexto de los nuevos fármacos dirigidos como los inhibidores de la señalización del BCR o de BCL2, se desconoce la implicación pronóstica de la pérdida monoalélica o bialélica de *ATM*, sin embargo, las resistencias a estas terapias se han convertido en un reto a nivel clínico, lo que hace necesaria la exploración de nuevas aproximaciones terapéuticas para el tratamiento de la LLC de alto riesgo.

Uno de los mayores impedimentos para el estudio de la biología de la LLC, y en especial de las consecuencias funcionales que tienen las distintas alteraciones en genes *driver* de la enfermedad, ha sido la falta de modelos celulares que reproduzcan de forma fidedigna estas lesiones. Por ejemplo, en el caso de la del(11q), no existen líneas celulares portadoras de esta alteración, y tampoco existen líneas celulares derivadas de LLC con mutaciones en *ATM*. Sin embargo, la reciente irrupción del sistema de edición genómica CRISPR/Cas9 ha abierto nuevas posibilidades para la generación rápida y eficiente de modelos isogénicos que reproducen mutaciones génicas y alteraciones cromosómicas diversas, entre otros tipos de lesiones. Por este motivo, nos propusimos emplear el sistema CRISPR/Cas9 para la generación de modelos celulares isogénicos derivados de LLC y portadores de del(11q) y/o mutaciones en *ATM*, con el fin de dilucidar el impacto funcional de la pérdida mono- y bialélica de este gen en la patogénesis de la LLC, así como de encontrar nuevas vulnerabilidades terapéuticas que puedan ser aprovechadas para el tratamiento de este subgrupo de pacientes de alto riesgo.

PACIENTES Y MÉTODOS

Para la generación de modelos celulares portadores de del(11q) y/o mutaciones de pérdida de función en *ATM* se emplearon las líneas celulares derivadas de LLC HG3 (que presenta del(13q)) y MEC1 (que presenta del(17p)). Estas líneas celulares fueron

transducidas de forma estable con la nucleasa Cas9. Para la generación de del(11q) se diseñaron dos sgRNA dirigidos a las regiones 11q22.1 y 11q22.3, separadas entre sí por aproximadamente 17 Mb, y se introdujeron de forma simultánea en las líneas celulares con expresión constitutiva de Cas9 mediante nucleofección. Se realizó una separación de célula única por citometría de flujo de las células positivas para ambos sgRNAs, y los clones resultantes se validaron por PCR y secuenciación Sanger para detectar la fusión entre ambas regiones cromosómicas. Además, la presencia de la del(11q) en el 100% de las células de la línea celular seleccionada se confirmó por FISH. Por otro lado, las mutaciones de pérdida de función de *ATM* se introdujeron en líneas celulares con o sin del(11q) mediante el diseño de un sgRNA frente al exón 10 de la secuencia codificante de *ATM*. La selección y validación de clones con mutaciones truncadoras de *ATM* en estos tipos celulares se realizó con las mismas metodologías que las empleadas en la generación de la del(11q), y se confirmó la ausencia de proteína mediante western blot. Por último, el impacto biológico y en la respuesta al tratamiento de estas líneas celulares se evaluó mediante diversas técnicas entre las que se incluyen inmunofluorescencia, ensayos de cometa, citometría de flujo, western blot, ensayos de viabilidad y apoptosis, migración en *transwell*, ensayos de recombinación homóloga y modelos *in vivo* de xenotrasplante murino.

Para el modelo *ex vivo* se aislaron células mononucleadas de sangre periférica de 38 pacientes de LLC mediante gradiente por Ficoll-Paque Plus (GE Healthcare), que fueron criopreservadas de forma viable hasta el momento de su análisis. Todas las muestras mostraron una pureza CD19⁺CD5⁺ mayor del 85% por citometría de flujo, y se analizó la presencia de del(11q) y otras alteraciones cromosómicas mediante FISH. Para la determinación del estado mutacional de *ATM* y otros 54 genes driver de la LLC se emplearon técnicas de NGS de captura (Agilent SureSelect) en la plataforma NextSeq (Illumina). Los experimentos de viabilidad *ex vivo* se realizaron en un sistema de co-cultivo con células estromales HS5 en suplementación de CpG-ODN e IL-2, y el análisis de viabilidad se realizó por medición de ATP mediante Cell-Titer Glo (Promega).

RESULTADOS

Mediante el empleo del sistema CRISPR/Cas9 se generaron de forma eficiente líneas celulares HG3 con del(11q) y/o mutaciones truncadoras de *ATM* (tres clones diferentes por condición), así como líneas celulares MEC1 con mutaciones truncadoras de *ATM* (tres clones independientes). A nivel biológico, las células con del(11q), y en mayor medida aquellas con

pérdida bialélica de *ATM*, tanto en los modelos *in vitro* generados por CRISPR/Cas9, como en el modelo *ex vivo* con células primarias, mostraban deficiencias en la señalización de daño en el ADN en forma de roturas de doble cadena, así como defectos en la reparación de estas lesiones y acumulación de daño en el ADN. Además, observamos que las células con pérdida bialélica de *ATM* eran hipersensibles al tratamiento con el inhibidor de PARP olaparib *in vitro*, *in vivo* y *ex vivo*.

En base a estos resultados, evaluamos la actividad farmacológica de olaparib en combinación con el inhibidor de BCR ibrutinib, demostrando sinergismo en la reducción de la viabilidad de las líneas celulares con del(11q). Asimismo, estudiamos el efecto *ex vivo* de esta combinación en presencia del microambiente tumoral en una cohorte de 38 LLCs, revelando que las células primarias de aquellos pacientes con pérdida bialélica de *ATM* eran especialmente sensibles a este tratamiento combinado. Además, al profundizar en el posible mecanismo de sinergia de esta combinación, mostramos que la acción de ibrutinib tiene un efecto *off-target* en la reparación por recombinación homóloga debido a defectos en la formación de focos de reparación de RAD51 en un proceso dependiente de la señalización de PI3K, lo que se traduce en una acción inhibitoria de esta vía de reparación y mayores niveles de daño en el ADN que acaban siendo letales para la célula, especialmente en presencia de inductores de daño en el ADN como la bendamustina.

CONCLUSIONES

Este estudio demuestra que la técnica de edición genética CRISPR/Cas9 es una herramienta eficaz para la generación de modelos celulares que reproducen las alteraciones genéticas características de la LLC. Específicamente, este sistema puede ser empleado para la generación de mutaciones génicas de pérdida de función como grandes deleciones cromosómicas, de forma individual o combinada. Gracias a ello, hemos podido generar modelos celulares de del(11q) y/o mutaciones en *ATM* únicos hasta el momento para el estudio en profundidad de la biología de la LLC.

Mediante el empleo de estos modelos celulares, así como de modelos *in vivo* de xenotrasplante murino y modelos *ex vivo* con células primarias, hemos demostrado que a nivel biológico, la pérdida monoalélica y bialélica de *ATM* da lugar a defectos en la señalización en respuesta a daño en el ADN y aumento de la inestabilidad genética, así como una hipersensibilidad específica a inhibidores de PARP en los casos con inactivación bialélica de *ATM* con del(11q) y mutación. Además, las células de pacientes pertenecientes a este

subgrupo de alto riesgo son especialmente sensibles a la combinación de olaparib e ibrutinib, que tiene un efecto sinérgico y anti-proliferativo en las células de LLC causado por la desregulación de RAD51 mediada por ibrutinib a través de la vía de PI3K. De esta forma, nuestros resultados aportan evidencia pre-clínica para el empleo de esta combinación en pacientes de LLC con del(11q) e inactivación bialélica de *ATM*.

CAPÍTULO 3 - RESUMEN

Dissecting the role of *TP53* alterations in del(11q) chronic lymphocytic leukemia

Miguel Quijada-Álamo, Claudia Pérez-Carretero, María Hernández-Sánchez, Ana-Eugenia Rodríguez-Vicente, Ana-Belén Herrero, Jesús-María Hernández-Sánchez, Marta Martín-Izquierdo, Sandra Santos-Mínguez, Mónica del Rey, Teresa González, Araceli Rubio-Martínez, Alfonso García de Coca, Julio Dávila-Valls, José-Ángel Hernández-Rivas, Helen Parker, Jonathan C. Strefford, Rocío Benito, José-Luis Ordóñez, Jesús-María Hernández-Rivas

**Clinical and Translational Medicine. 2021 Feb;11(2):e304. doi: 10.1002/ctm2.304.
PMID: 33634999**

INTRODUCCIÓN Y OBJETIVOS

Estudios de secuenciación del exoma y del genoma completo de la LLC han identificado la presencia de un gran número de alteraciones genéticas *driver* implicadas en la patogénesis y evolución de esta enfermedad. Además, estos análisis han revelado que muchas de estas lesiones suelen coexistir en un mismo clon tumoral, pero se desconoce cómo la cooperación entre múltiples alteraciones genéticas en un mismo clon contribuye a la progresión de la enfermedad. Asimismo, también se han revelado patrones de mutua exclusividad entre algunas de estas alteraciones, aunque las causas biológicas por las que estos eventos nunca tienen lugar en un mismo clon también son desconocidos.

En el caso concreto de la LLC de alto riesgo, conformada por los subgrupos citogenéticos con alteraciones en del(11q)/*ATM* o del(17p)/*TP53*, apenas se ha estudiado el impacto de la concurrencia de estos dos tipos de alteraciones a nivel clínico. Asimismo, se desconoce cuál podría ser el impacto biológico de la combinación de estas alteraciones a nivel de evolución clonal y respuesta al tratamiento. Por todas estas razones, este trabajo se planteó como objetivo la determinación del impacto clínico de las alteraciones concurrentes en del(11q)/*ATM* y del(17p)/*TP53* en la LLC, así como la evaluación funcional *in vitro* e *in vivo* de la concurrencia de estas lesiones en modelos celulares generados mediante CRISPR/Cas9.

PACIENTES Y MÉTODOS

Para este estudio, se empleó una cohorte de 271 pacientes de LLC de las que se disponían datos clínicos completos y datos de FISH, de los cuales 47/271 (17,3%) presentaban del(11q). Se analizó el estado mutacional de 54 genes *driver* de la LLC, incluyendo *ATM* y *TP53*, en la cohorte completa mediante NGS de captura (Agilent, SureSelect) en la plataforma NextSeq (Illumina). El análisis estadístico de supervivencia, así como las asociaciones entre parámetros clínicos y biológicos se llevaron a cabo en el software SPSS v23.0 (IBM Corp.).

Para el estudio biológico de la concurrencia de alteraciones en *ATM* y *TP53*, se generaron modelos celulares mediante la metodología de edición genética CRISPR/Cas9 de la misma forma que la mencionada en el capítulo anterior, empleando los mismos sgrNAs para la generación de la del(11q) y las mutaciones (mut) de *ATM*, y diseñando sgrNAs específicos dirigidos al exón 4 de *TP53*. Específicamente, se generaron líneas celulares HG3 con las siguientes alteraciones: HG3-del(11q), HG3 *TP53*^{MUT}, HG3-del(11q) *TP53*^{MUT} y HG3-del(11q) *ATM*^{MUT}*TP53*^{MUT}. Para la caracterización *in vitro* del efecto biológico de estas alteraciones se

realizaron ensayos de crecimiento celular, tinción Giemsa, ciclo celular en respuesta a roturas de doble cadena en el ADN, western blot y ensayos de viabilidad en respuesta a fármacos. Para el estudio *in vivo* de xenotrasplante murino, se emplearon ratones inmunodeficientes de la cepa NOD-scid IL2R γ ^{-/-} (NSG) y se realizaron análisis de competición clonal mediante inyección intravenosa simultánea de varios clones en un mismo animal, haciendo un seguimiento de los clones por citometría de flujo en bazo y médula ósea 7 y 14 días después de la inyección. Además, se realizó un experimento de supervivencia global en animales inyectados de forma individual con cada una de las condiciones del estudio.

RESULTADOS

El análisis de NGS reveló en primer lugar que la gran mayoría (93,6%) de pacientes de LLC con del(11q) presentaba alguna alteración en los genes *driver* analizados. Con respecto al perfil mutacional específico de este subgrupo de pacientes, validamos que presentaban una alta concurrencia de mutaciones en *ATM* y *BIRC3*. Por otro lado, el análisis de la presencia conjunta de alteraciones en del(11q)/*ATM* y del(17p)/*TP53* reveló que las alteraciones bialélicas en *ATM* y *TP53* eran mutuamente excluyentes, ya que de hecho ningún paciente de la serie presentaba esta combinación de eventos. Sin embargo, detectamos un subgrupo de pacientes que presentaban del(11q) monoalélica (sin mutación de *ATM* en el alelo restante), y alteraciones en del(17p)/*TP53*. Este subgrupo presentaba una supervivencia global significativamente inferior a los pacientes que portaban estas alteraciones de forma individual.

La caracterización funcional de líneas celulares de LLC portadoras de estas alteraciones reveló que los clones HG3-del(11q) *TP53*^{MUT} presentaban mayores tasas de crecimiento *in vitro* en comparación con las células HG3-del(11q), mientras que los clones HG3-del(11q) *ATM*^{MUT}*TP53*^{MUT} mostraban una morfología atípica, defectos en la mitosis y el ciclo celular y marcada disminución de la capacidad de crecimiento, en concordancia con la mutua exclusividad de estos eventos observada en los pacientes. Por otro lado, el estudio de competición clonal *in vivo* reveló que los clones HG3-del(11q) *TP53*^{MUT} tenían una mayor ventaja clonal tanto en médula ósea y en bazo, lo que se traducía en una reducción de la supervivencia global en comparación con los ratones trasplantados con clones HG3-del(11q). Además, las células HG3-del(11q) *ATM*^{MUT}*TP53*^{MUT} presentaban ausencia de capacidad de competición *in vivo*. Finalmente, el estudio de respuesta a fármacos reveló que las líneas celulares portadoras de del(11q) y mutaciones en *TP53* presentaban solo respuestas parciales

al tratamiento con inhibidores de BTK (ibrutinib) y PI3K (idelalisib), mientras que obtenían un beneficio del tratamiento con el inhibidor de ATR AZD6738 similar al observado en las células sin estas alteraciones.

CONCLUSIONES

Este estudio muestra que la del(17p) y/o mutaciones en *TP53* pueden aparecer en un subgrupo de pacientes de LLC con del(11q), confiriendo una ventaja clonal *in vivo*, lo que se traduce en una reducción de la supervivencia global para los pacientes portadores de estas alteraciones. Además, nuestro empleo combinado de NGS y modelos celulares editados mediante CRISPR/Cas9 indica que las alteraciones bialélicas en *ATM* y *TP53* dan lugar a defectos en la mitosis y limitaciones en la capacidad de competición clonal *in vitro* e *in vivo*, descifrando por primera vez las bases biológicas de la exclusividad mutua entre dos alteraciones en la LLC. Finalmente, nuestros resultados sugieren que el subgrupo de pacientes con alteraciones simultáneas en del(11q) y *TP53* podrían presentar peores respuestas al tratamiento con inhibidores de BTK o PI3K que aquellos pacientes sin estas alteraciones, mientras que se podrían beneficiar del tratamiento con inhibidores de ATR.

CAPÍTULO 4 - RESUMEN

Biological significance of monoallelic and biallelic *BIRC3* loss in del(11q) chronic lymphocytic leukemia progression

Miguel Quijada-Álamo, María Hernández-Sánchez, Ana-Eugenia Rodríguez-Vicente, Claudia Pérez-Carretero, Alberto Rodríguez-Sánchez, Marta Martín-Izquierdo, Verónica Alonso-Pérez, Ignacio García-Tuñón, José María Bastida, María Jesús Vidal-Manceñido, Josefina Galende, Carlos Aguilar, José Antonio Queizán, Isabel González-Gascón y Marín, José-Ángel Hernández-Rivas, Rocío Benito, José Luis Ordóñez and Jesús-María Hernández-Rivas

Blood Cancer Journal. 2021. In press

INTRODUCCIÓN Y OBJETIVOS

El gen *BIRC3* aparece mutado de forma recurrente en un 2,5-10% de los casos de LLC al diagnóstico o en el momento previo al tratamiento. Este gen se localiza en la región cromosómica 11q22.2 y se encuentra deletado en aproximadamente un 80% de los casos de LLC con del(11q). Además, el 10% de estos pacientes presenta mutaciones de pérdida de función en el otro alelo del gen, confiriendo un pronóstico desfavorable. Además, algunos estudios han reportado que los pacientes refractarios o en recaída tras el tratamiento con fludarabina u otros regímenes basados en quimioterapia están enriquecidos en mutaciones de este gen, aunque se desconocen las causas biológicas por las cuales este tipo de mutaciones podrían conferir resistencia a estos fármacos.

A nivel biológico, *BIRC3* es un regulador negativo de la ruta no canónica de NF- κ B, y las mutaciones de pérdida de función en este gen producen una activación constitutiva de esta vía de señalización. Sin embargo, se desconoce el impacto biológico de la pérdida monoalélica de este gen a través de la del(11q), así como las causas por las cuales la pérdida bialélica de *BIRC3* por del(11q) y mutación puede dar lugar a una progresión de la enfermedad. Además tampoco existen modelos celulares de LLC que reproduzcan este tipo de alteraciones, lo que dificulta el estudio de estos aspectos de la biología de este gen *driver* de la LLC. De esta forma, nos propusimos generar modelos celulares isogénicos portadores de del(11q) y/o mutaciones en *BIRC3* mediante CRISPR/Cas9, con el fin de dilucidar el impacto funcional de la pérdida mono- y bialélica de este gen en la ruta de NF- κ B y en la apoptosis, así como su implicación en los procesos de evolución clonal, respuesta al tratamiento y progresión de la LLC mediante un estudio integrativo a nivel *in vitro*, *in vivo* y *ex vivo*.

PACIENTES Y MÉTODOS

Para la generación de líneas celulares con del(11q) y/o mutaciones de pérdida de función en *BIRC3* se empleó la herramienta de edición genética CRISPR/Cas9 partiendo de las líneas celulares HG3-Cas9 con o sin del(11q) y MEC1-Cas9 generadas en nuestros estudios previos. Se diseñaron sgRNAs frente a los exones 2 y 7 de *BIRC3* para reproducir mutaciones observadas en pacientes que afectan a diferentes dominios de la proteína, y la selección y validación de las mutaciones se realizó por secuenciación Sanger y western blot como en los estudios anteriores. Para el estudio del impacto biológico de estas mutaciones en la ruta de NF- κ B y en la apoptosis, se realizaron ensayos de actividad nuclear de los factores de

transcripción de NF- κ B mediante ELISA y western blot. Para la evaluación de la respuesta a fármacos de estas líneas se realizaron estudios de viabilidad mediante MTT, medición de apoptosis por citometría de flujo mediante marcaje con anexina V y yoduro de propidio, y ciclo celular. La capacidad de crecimiento y evolución clonal se estudió mediante ensayos de viabilidad, ciclo celular y competición clonal *in vitro*, así como en un modelo *in vivo* de xenotrasplante murino en el que se estudió la diseminación de cada uno de los clones con diferentes alteraciones en el bazo mediante citometría de flujo e inmunohistoquímica.

El estudio *ex vivo* se realizó en células mononucleadas de sangre periférica de una cohorte de 22 pacientes de LLC con datos de la presencia de del(11q) y el estado mutacional de *BIRC3* obtenidos mediante FISH y NGS (Agilent SureSelect), de los cuales 11/22 presentaban alteraciones en *BIRC3*. Las células fueron cultivadas en un sistema de co-cultivo con células estromales HS5 en suplementación con CpG ODN e IL-2. Se evaluó la actividad de los factores de transcripción de la ruta no canónica de NF- κ B p52 y RelB mediante ELISA, así como los niveles de proteínas implicadas en esta ruta y en la apoptosis en 7 pacientes con del(11q), de los cuales 4 incluían *BIRC3* en la región delecionada y 3 no incluían *BIRC3* dentro de la del(11q).

RESULTADOS

El análisis de la actividad nuclear de todos los factores de transcripción de la familia de NF- κ B reveló que la pérdida monoalélica de *BIRC3* mediante del(11q) producía un incremento en la actividad de los factores RelB y p52, implicados en la vía no canónica. Además, mostramos que este efecto es dependiente de la dosis alélica de *BIRC3*, ya que las células con pérdida bialélica de este gen (por del(11q) y mutación truncadora en el otro alelo) tienen aun mayor actividad de la ruta no canónica de NF- κ B. A nivel del resto de los componentes de la ruta, observamos que la pérdida bialélica de *BIRC3* favorece la estabilización citoplasmática de NIK y los eventos de fosforilación y translocación nuclear subsecuentes, lo que finalmente resulta en un incremento de los niveles de proteínas anti-apoptóticas BCL2 y BCL-xL. Además, el tratamiento con el inhibidor de NIK, NIK SMI1, era capaz de inhibir esta sobreexpresión de proteínas anti-apoptóticas en las células con pérdida bialélica de *BIRC3*.

A nivel *ex vivo*, validamos que los pacientes con alteraciones en *BIRC3* presentaban mayor actividad transcripcional de p52 y RelB, incremento de los niveles proteicos de NIK en incremento de los niveles de BCL2. Además, cabe destacar que detectamos una

correlación directa entre el porcentaje de alteración de *BIRC3*, los niveles de p52 y la expresión proteica de BCL2. En base a estos resultados, testamos la sensibilidad de los modelos celulares previamente generados mediante CRISPR/Cas9, observando que las células con pérdida bialélica de *BIRC3* eran más sensibles a venetoclax (inhibidor de BCL2) y A-1331852 (inhibidor de BCL-xL). Por otra parte, estudios de respuesta a fludarabina no mostraron diferencias en la respuesta al tratamiento de los clones con alteraciones de *BIRC3*, cosa que sí observamos en controles de resistencia con mutaciones en *TP53*, lo que indica que las alteraciones de *BIRC3* no son capaces de conferir resistencias por sí solas al tratamiento con este fármaco.

Por último, estudiamos el impacto de las alteraciones de *BIRC3* en el crecimiento de las células de LLC, demostrando que la pérdida bialélica del gen, por del(11q) y mutación, confería un incremento de la viabilidad, proliferación y competición clonal *in vitro*, lo que podía ser contrarrestado mediante inhibición farmacológica de NIK. Asimismo, el modelo *in vivo* de xenotrasplante murino reveló que las células con pérdida bialélica de *BIRC3* tenían una ventaja significativa de invasión del bazo de los ratones 14 días después de la inyección intravenosa, en comparación con las células sin estas alteraciones.

CONCLUSIONES

En resumen, este trabajo demuestra que la pérdida bialélica de *BIRC3*, causada por la concurrencia entre la del(11q) y una mutación de pérdida de función de este gen en el otro alelo, desencadena la activación constitutiva de la ruta no canónica de NF- κ B, dando lugar a una sobreexpresión de BCL2 y confiriendo una ventaja clonal de las células portadoras de estas alteraciones. Estos datos aportan un significado biológico al impacto pronóstico adverso observado en los pacientes con este tipo de alteraciones, que una reducción significativa en el tiempo hasta el primer tratamiento. Por lo tanto, los pacientes pertenecientes a este subgrupo deberían considerarse como individuos con un alto riesgo de progresión, que a su vez podrían beneficiarse del tratamiento con regímenes basados en venetoclax.

CONCLUSIONES

1. Las alteraciones cromosómicas y mutaciones en genes *driver* no están presentes exclusivamente en los linfocitos B maduros, sino también en los progenitores hematopoyéticos CD34⁺ de los pacientes de LLC. Específicamente, la del(11q) y la del(13q), así como las mutaciones *NOTCH1* y *MYD88* son eventos tempranos en la hematopoyesis de la LLC, mientras que las alteraciones de IGH y las mutaciones de *TP53*, *SF3B1* y *FBXW7* emergen en estadios posteriores de la maduración de la célula B.
2. La mayoría de los pacientes de LLC con del(11q) presenta mutaciones adicionales en genes *driver* de la LLC. El perfil mutacional de estos pacientes se caracteriza por una alta concurrencia de mutaciones en *ATM*, *TP53* y *BIRC3*.
3. Los modelos isogénicos generados mediante CRISPR/Cas9 representan una herramienta novedosa y eficaz para determinar la implicación individual o combinada de alteraciones *driver* en diversos procesos celulares y evolución clonal. Además, estos modelos proporcionan una plataforma innovadora para el estudio pre-clínico de la respuestas terapéuticas en base a un genotipo específico en la LLC.
4. La pérdida monoalélica de *ATM* a través de la del(11q) produce defectos en la señalización y reparación de roturas de doble cadena, dando lugar a acumulación de daño en el ADN. Estos defectos se incrementan en la presencia de mutaciones de pérdida de función en el alelo restante de *ATM*. Las células de LLC con inactivación bialélica de *ATM* muestran hipersensibilidad a la inhibición de PARP *in vitro*, *in vivo* y *ex vivo*.
5. La inhibición simultánea de BCR y PARP a través de la combinación de ibrutinib y olaparib es sinérgica en líneas celulares y células primarias de pacientes de LLC con alteraciones en del(11q)/*ATM*, superando la inducción de proliferación mediada por el microambiente del estroma. El mecanismo de sinergia de esta combinación se basa en un efecto *off-target* de ibrutinib en la reparación por recombinación homóloga a través de defectos en la formación de focos de RAD51 en las roturas de doble cadena, lo que da lugar a una acumulación letal de daño en el ADN en las células de LLC con del(11q).
6. Las lesiones bialélicas en *ATM* y *TP53* son mutuamente excluyentes en la LLC. A nivel de mecanismo, la combinación de ambos eventos da lugar a defectos en la

- mitosis y disminución de la capacidad proliferativa *in vitro*, sumado a una adaptabilidad clonal deficiente a nivel *in vivo*.
7. La combinación de del(11q) monoalélica y alteraciones en *TP53* define a un subgrupo de LLC de riesgo extremo con una supervivencia global inferior a los pacientes que presentan estas alteraciones de forma individual. La del(11q) coopera con la pérdida de *TP53* para inducir ventaja clonal *in vitro* e *in vivo*, así como para alterar la respuesta *in vitro* a inhibidores de BCR o BTK.
 8. La mutación y/o deleción de *BIRC3* a través de la del(11q) activa la vía no canónica de NF- κ B mediante la estabilización citoplasmática de NIK y la translocación nuclear y activación del heterodímero RelB-p52, lo que resulta en sobreexpresión de BCL2 y define una vulnerabilidad específica de este genotipo al tratamiento con venetoclax. Además, la activación de la vía no canónica de NF- κ B dependiente de *BIRC3* puede ser suprimida mediante inhibición farmacológica de NIK con NIK SMI1.
 9. La mutación de *BIRC3* en el alelo restante de las células de LLC con del(11q) produce un incremento aún mayor de la actividad de la vía no canónica de NF- κ B, confiriendo ventaja clonal *in vitro* y acelerando la progresión leucémica en un modelo de xenotrasplante murino *in vivo*. Estos resultados aportan una explicación biológica del impacto pronóstico negativo de la inactivación bialélica de *BIRC3* en los pacientes de LLC.

REFERENCES

1. Swerdlow SH, Campo E, Pileri SA, et al. The 2016 revision of the World Health Organization classification of lymphoid neoplasms. *Blood*. 2016;127.
2. Kipps TJ, Stevenson FK, Wu CJ, et al. Chronic lymphocytic leukaemia. *Nat Rev Dis Prim*. 2017;3.
3. Chiorazzi N, Rai KR, Ferrarini M. Chronic lymphocytic leukemia. *N Engl J Med*. 2005;352.
4. Hallek M. Chronic lymphocytic leukemia: 2020 update on diagnosis, risk stratification and treatment. *Am J Hematol*. 2019;94.
5. Nabhan C, Aschebrook-Kilfoy B, Chiu BCH, et al. The impact of race, ethnicity, age and sex on clinical outcome in chronic lymphocytic leukemia: A comprehensive Surveillance, Epidemiology, and End Results analysis in the modern era. *Leuk Lymphoma*. 2014;55.
6. Li Y, Wang Y, Wang Z, Yi D, Ma S. Racial differences in three major NHL subtypes: Descriptive epidemiology. *Cancer Epidemiol*. 2015;39.
7. Mauro FR, Foa R, Giannarelli D, et al. Clinical characteristics and outcome of young chronic lymphocytic leukemia patients: A single institution study of 204 cases. *Blood*. 1999;94.
8. Yang SM, Li JY, Gale RP, Huang XJ. The mystery of chronic lymphocytic leukemia (CLL): Why is it absent in Asians and what does this tell us about etiology, pathogenesis and biology? *Blood Rev*. 2015;29.
9. Speedy HE, Sava G, Houlston RS. Inherited susceptibility to CLL. *Adv Exp Med Biol*. 2013;792.
10. Cerhan JR, Slager SL. Familial predisposition and genetic risk factors for lymphoma. *Blood*. 2015;126.
11. Lichtenstein P, Holm N V., Verkasalo PK, et al. Environmental and Heritable Factors in the Causation of Cancer — Analyses of Cohorts of Twins from Sweden, Denmark, and Finland. *N Engl J Med*. 2000;343.
12. Berndt SI, Skibola CF, Joseph V, et al. Genome-wide association study identifies multiple risk loci for chronic lymphocytic leukemia. *Nat Genet*. 2013;45.
13. Di Bernardo MC, Crowther-Swanepoel D, Broderick P, et al. A genome-wide association study identifies six susceptibility loci for chronic lymphocytic leukemia. *Nat Genet*. 2008;40.
14. Crowther-Swanepoel D, Broderick P, Di Bernardo MC, et al. Common variants at 2q37.3, 8q24.21, 15q21.3 and 16q24.1 influence chronic lymphocytic leukemia risk. *Nat Genet*. 2010;42.
15. Speedy HE, Di Bernardo MC, Sava GP, et al. A genome-wide association study identifies multiple susceptibility loci for chronic lymphocytic leukemia. *Nat Genet*. 2014;46.
16. Slager SL, Skibola CF, Di Bernardo MC, et al. Common variation at 6p21.31 (BAK1) influences the risk of chronic lymphocytic leukemia. *Blood*. 2012;120.
17. Slager SL, Rabe KG, Achenbach SJ, et al. Genome-wide association study identifies a novel susceptibility locus at 6p21.3 among familial CLL. *Blood*. 2011;117.
18. Sava GP, Speedy HE, Di Bernardo MC, et al. Common variation at 12q24.13 (OAS3) influences chronic lymphocytic leukemia risk. *Leukemia*. 2015;29.
19. Berndt SI, Camp NJ, Skibola CF, et al. Meta-analysis of genome-wide association studies discovers multiple loci for chronic lymphocytic leukemia. *Nat Commun*. 2016;7.
20. Law PJ, Berndt SI, Speedy HE, et al. Genome-wide association analysis implicates dysregulation of immunity genes in chronic lymphocytic leukaemia. *Nat Commun*. 2017;8.
21. Baumann Kreuziger LM, Tarchand G, Morrison VA. The impact of Agent Orange exposure on presentation and prognosis of patients with chronic lymphocytic leukemia. *Leuk Lymphoma*. 2014;55.
22. Schinasi LH, De Roos AJ, Ray RM, et al. Insecticide exposure and farm history in relation to risk of lymphomas and leukemias in the Women's Health Initiative observational study cohort. *Ann Epidemiol*. 2015;25.
23. Kesminiene A, Evrard AS, Ivanov VK, et al. Risk of hematological malignancies among chernobyl liquidators. *Radiat Res*.

- 2008;170.
24. Radivoyevitch T, Sachs RK, Gale RP, Smith MR, Hill BT. Ionizing radiation exposures in treatments of solid neoplasms are not associated with subsequent increased risks of chronic lymphocytic leukemia. *Leuk Res.* 2016;43.
25. Hjalgrim H, Rostgaard K, Vasani SK, et al. No evidence of transmission of chronic lymphocytic leukemia through blood transfusion. *Blood.* 2015;126.
26. Hallek M, Cheson BD, Catovsky D, et al. iwCLL guidelines for diagnosis, indications for treatment, response assessment, and supportive management of CLL. *Blood.* 2018;131.
27. Matutes E, Owusu-Ankomah K, Morilla R, et al. The immunological profile of B-cell disorders and proposal of a scoring system for the diagnosis of CLL. *Leukemia.* 1994;8.
28. Moreau EJ, Matutes E, A'Hern RP, et al. Improvement of the chronic lymphocytic leukemia scoring system with the monoclonal antibody SN8 (CD79b). *Am J Clin Pathol.* 1997;108.
29. Ginaldi L, De Martinis M, Matutes E, Farahat N, Morilla R, Catovsky D. Levels of expression of CD19 and CD20 in chronic B cell leukaemias. *J Clin Pathol.* 1998;51.
30. Rawstron AC, Kreuzer KA, Soosapilla A, et al. Reproducible diagnosis of chronic lymphocytic leukemia by flow cytometry: An European Research Initiative on CLL (ERIC) & European Society for Clinical Cell Analysis (ESCCA) Harmonisation project. *Cytom Part B - Clin Cytom.* 2018;94.
31. Landgren O, Albitar M, Ma W, et al. B-Cell Clones as Early Markers for Chronic Lymphocytic Leukemia. *N Engl J Med.* 2009;360.
32. Rawstron AC, Bennett FL, O'Connor SJM, et al. Monoclonal B-Cell Lymphocytosis and Chronic Lymphocytic Leukemia. *N Engl J Med.* 2008;359.
33. Nieto WG, Almeida J, Romero A, et al. Increased frequency (12%) of circulating chronic lymphocytic leukemia-like B-cell clones in healthy subjects using a highly sensitive multicolor flow cytometry approach. *Blood.* 2009;114.
34. Almeida J, Nieto WG, Teodosio C, et al. CLL-like B-lymphocytes are systematically present at very low numbers in peripheral blood of healthy adults. *Leukemia.* 2011;25.
35. Criado I, Rodríguez-Caballero A, Gutiérrez ML, et al. Low-count monoclonal B-cell lymphocytosis persists after seven years of follow up and is associated with a poorer outcome. *Haematologica.* 2018;103.
36. Vardi A, Dagklis A, Scarfo L, et al. Immunogenetics shows that not all MBL are equal: The larger the clone, the more similar to CLL. *Blood.* 2013;121.
37. Morabito F, Mosca L, Cutrona G, et al. Clinical monoclonal B lymphocytosis versus Rai 0 chronic lymphocytic leukemia: A comparison of cellular, cytogenetic, molecular, and clinical features. *Clin Cancer Res.* 2013;19.
38. Rossi D, Gaidano G. Richter syndrome: Pathogenesis and management. *Semin Oncol.* 2016;43.
39. Hallek M, Cheson BD, Catovsky D, et al. Guidelines for the diagnosis and treatment of chronic lymphocytic leukemia: A report from the International Workshop on Chronic Lymphocytic Leukemia updating the National Cancer Institute-Working Group 1996 guidelines. *Blood.* 2008;111.
40. Mao Z, Quintanilla-Martinez L, Raffeld M, et al. IgVH mutational status and clonality analysis of Richter's transformation: Diffuse large B-cell lymphoma and Hodgkin lymphoma in association with B-cell chronic lymphocytic leukemia (B-CLL) represent 2 different pathways of disease evolution. *Am J Surg Pathol.* 2007;31.
41. Rossi D, Spina V, Deambrogi C, et al. The genetics of Richter syndrome reveals disease heterogeneity and predicts survival after transformation. *Blood.* 2011;117.
42. Tsimberidou AM, O'Brien S, Kantarjian HM, et al. Hodgkin transformation of chronic lymphocytic leukemia: The M. D. Anderson Cancer Center experience. *Cancer.* 2006;107.
43. Bockorny B, Codreanu I, Dasanu CA. Hodgkin lymphoma as Richter transformation in chronic lymphocytic leukaemia: A retrospective analysis of

- world literature. *Br J Haematol.* 2012;156.
44. Parikh SA, Rabe KG, Call TG, et al. Diffuse large B-cell lymphoma (Richter syndrome) in patients with chronic lymphocytic leukaemia (CLL): A cohort study of newly diagnosed patients. *Br J Haematol.* 2013;162.
 45. Parikh SA, Habermann TM, Chaffee KG, et al. Hodgkin transformation of chronic lymphocytic leukemia: Incidence, outcomes, and comparison to de novo Hodgkin lymphoma. *Am J Hematol.* 2015;90.
 46. Dighiero G, Hamblin T. Chronic lymphocytic leukaemia. *Lancet.* 2008;371.
 47. Rai KR, Sawitsky A, Cronkite EP, Chanana AD, Levy RN, Pasternack BS. Clinical staging of chronic lymphocytic leukemia. *Blood.* 1975;46.
 48. Binet JL, Auquier A, Dighiero G, et al. A new prognostic classification of chronic lymphocytic leukemia derived from a multivariate survival analysis. *Cancer.* 1981;48.
 49. Vinolas N, Reverter JC, Urbano-Ispizua A, Montserrat E, Rozman C. Lymphocyte doubling time in chronic lymphocytic leukemia: An update of its prognostic significance. *Blood Cells.* 1987;12.
 50. Rozman C, Hernandez-Nieto L, Montserrat E, Bruges R. Prognostic Significance of Bone-Marrow Patterns in Chronic Lymphocytic Leukaemia. *Br J Haematol.* 1981;47.
 51. Cramer P, Hallek M. Prognostic factors in chronic lymphocytic leukemia-what do we need to know? *Nat Rev Clin Oncol.* 2011;8.
 52. Pérez-Carretero C, González-Gascón-y-Marín I, Rodríguez-Vicente AE, et al. The Evolving Landscape of Chronic Lymphocytic Leukemia on Diagnosis, Prognosis and Treatment. *Diagnostics.* 2021;11.
 53. Hallek M, Wanders L, Ostwald M, et al. Serum β 2-microglobulin and serum thymidine kinase are independent predictors of progression-free survival in chronic lymphocytic leukemia and immunocytoma. *Leuk Lymphoma.* 1996;22.
 54. Wierda WG, O'Brien S, Wang X, et al. Prognostic nomogram and index for overall survival in previously untreated patients with chronic lymphocytic leukemia. *Blood.* 2007;109.
 55. Gentile M, Cutrona G, Neri A, Molica S, Ferrarini M, Morabito F. Predictive value of β 2-microglobulin (β 2-m) levels in chronic lymphocytic leukemia since Binet A stages. *Haematologica.* 2009;94.
 56. Magnac C, Porcher R, Davi F, et al. Predictive value of serum thymidine kinase level for Ig-V mutational status in B-CLL. *Leukemia.* 2003;17.
 57. Callea V, Morabito F, Luise F, et al. Clinical significance of sIL2R, sCD23, sICAM-1, IL6 and sCD14 serum levels in B-cell chronic lymphocytic leukemia. *Haematologica.* 1996;81.
 58. Knauf WU, Langenmayer I, Ehlers B, et al. Serum levels of soluble CD23, but not soluble CD25, predict disease progression in early stage B-cell chronic lymphocytic leukemia. *Leuk Lymphoma.* 1997;27.
 59. Damle RN, Wasil T, Fais F, et al. Ig V Gene Mutation Status and CD38 Expression As Novel Prognostic Indicators in Chronic Lymphocytic Leukemia. *Blood.* 1999;94.
 60. Hamblin TJ, Davis Z, Gardiner A, Oscier DG, Stevenson FK. Unmutated Ig V(H) genes are associated with a more aggressive form of chronic lymphocytic leukemia. *Blood.* 1999;94.
 61. Jaramillo S, Agathangelidis A, Schneider C, et al. Prognostic impact of prevalent chronic lymphocytic leukemia stereotyped subsets: Analysis within prospective clinical trials of the German CLL Study Group. *Haematologica.* 2020;105.
 62. Rosenquist R, Ghia P, Hadzidimitriou A, et al. Immunoglobulin gene sequence analysis in chronic lymphocytic leukemia: Updated ERIC recommendations. *Leukemia.* 2017;31.
 63. Döhner H, Stilgenbauer S, Benner A, et al. Genomic Aberrations and Survival in Chronic Lymphocytic Leukemia. *N Engl J Med.* 2000;343.
 64. Baliakas P, Jeromin S, Iskas M, et al. Cytogenetic complexity in chronic lymphocytic leukemia: Definitions, associations, and clinical impact. *Blood.* 2019;133.
 65. Landau DA, Tausch E, Taylor-Weiner AN,

- et al. Mutations driving CLL and their evolution in progression and relapse. *Nature*. 2015;526.
66. Puente XS, Beà S, Valdés-Mas R, et al. Non-coding recurrent mutations in chronic lymphocytic leukaemia. *Nature*. 2015;526.
67. Baliakas P, Hadzidimitriou A, Sutton LA, et al. Recurrent mutations refine prognosis in chronic lymphocytic leukemia. *Leukemia*. 2015;29.
68. Nadeu F, Delgado J, Royo C, et al. Clinical impact of clonal and subclonal TP53, SF3B1, BIRC3, NOTCH1, and ATM mutations in chronic lymphocytic leukemia. *Blood*. 2016;127.
69. Larrayoz M, Rose-Zerilli MJ, Kadalayil L, et al. Non-coding NOTCH1 mutations in chronic lymphocytic leukemia; their clinical impact in the UK CLL4 trial. *Leukemia*. 2017;31.
70. Calin GA, Ferracin M, Cimmino A, et al. A MicroRNA Signature Associated with Prognosis and Progression in Chronic Lymphocytic Leukemia. *N Engl J Med*. 2005;353.
71. Kulis M, Heath S, Bibikova M, et al. Epigenomic analysis detects widespread gene-body DNA hypomethylation in chronic lymphocytic leukemia. *Nat Genet*. 2012;44.
72. Queirós AC, Villamor N, Clot G, et al. A B-cell epigenetic signature defines three biologic subgroups of chronic lymphocytic leukemia with clinical impact. *Leukemia*. 2015;29.
73. Orchard JA, Ibbotson RE, Davis Z, et al. ZAP-70 expression and prognosis in chronic lymphocytic leukaemia. *Lancet*. 2004;363.
74. Rassenti LZ, Huynh L, Toy TL, et al. ZAP-70 Compared with Immunoglobulin Heavy-Chain Gene Mutation Status as a Predictor of Disease Progression in Chronic Lymphocytic Leukemia. *N Engl J Med*. 2004;351.
75. Gattei V, Bulian P, Del Principe MI, et al. Relevance of CD49d protein expression as overall survival and progressive disease prognosticator in chronic lymphocytic leukemia. *Blood*. 2008;111.
76. Rossi D, Zucchetto A, Rossi FM, et al. CD49d expression is an independent risk factor of progressive disease in early stage chronic lymphocytic leukemia. *Haematologica*. 2008;93.
77. Pflug N, Bahlo J, Shanafelt TD, et al. Development of a comprehensive prognostic index for patients with chronic lymphocytic leukemia. *Blood*. 2014;124.
78. An international prognostic index for patients with chronic lymphocytic leukaemia (CLL-IPi): a meta-analysis of individual patient data. *Lancet Oncol*. 2016;17.
79. González-Gascón-y-marín I, Muñoz-Novas C, Rodríguez-Vicente AE, et al. From biomarkers to models in the changing landscape of chronic lymphocytic leukemia: Evolve or become extinct. *Cancers (Basel)*. 2021;13.
80. Baliakas P, Hadzidimitriou A, Sutton LA, et al. Clinical effect of stereotyped B-cell receptor immunoglobulins in chronic lymphocytic leukaemia: A retrospective multicentre study. *Lancet Haematol*. 2014;1.
81. Zenz T, Kröber A, Scherer K, et al. Monoallelic TP53 inactivation is associated with poor prognosis in chronic lymphocytic leukemia: Results from a detailed genetic characterization with long-term follow-up. *Blood*. 2008;112.
82. Austen B, Skowronska A, Baker C, et al. Mutation status of the residual ATM allele is an important determinant of the cellular response to chemotherapy and survival in patients with chronic lymphocytic leukemia containing an 11q deletion. *J Clin Oncol*. 2007;25.
83. Puente XS, Pinyol M, Quesada V, et al. Whole-genome sequencing identifies recurrent mutations in chronic lymphocytic leukaemia. *Nature*. 2011;475.
84. Villamor N, Conde L, Martínez-Trillos A, et al. NOTCH1 mutations identify a genetic subgroup of chronic lymphocytic leukemia patients with high risk of transformation and poor outcome. *Leukemia*. 2013;27.
85. Rossi D, Fangazio M, Rasi S, et al. Disruption of BIRC3 associates with fludarabine chemorefractoriness in TP53 wild-type chronic lymphocytic leukemia. *Blood*. 2012;119.
86. Young E, Noerenberg D, Mansouri L, et al.

- EGR2 mutations define a new clinically aggressive subgroup of chronic lymphocytic leukemia. *Leukemia*. 2017;31.
87. Cui B, Chen L, Zhang S, et al. Micro RNA-155 influences B-cell receptor signaling and associates with aggressive disease in chronic lymphocytic leukemia. *Blood*. 2014;124.
88. Mraz M, Chen L, Rassenti LZ, et al. MiR-150 influences B-cell receptor signaling in chronic lymphocytic leukemia by regulating expression of GAB1 and FOXP1. *Blood*. 2014;124.
89. Mraz M, Malinova K, Kotaskova J, et al. miR-34a, miR-29c and miR-17-5p are downregulated in CLL patients with TP53 abnormalities. *Leukemia*. 2009;23.
90. Stamatopoulos B, Meuleman N, Haibe-Kains B, et al. microRNA-29c and microRNA-223 down-regulation has in vivo significance in chronic lymphocytic leukemia and improves disease risk stratification. *Blood*. 2009;113.
91. Thompson PA, Wierda WG. Eliminating minimal residual disease as a therapeutic end point: Working toward cure for patients with CLL. *Blood*. 2016;127.
92. Rawstron AC, Fazi C, Agathangelidis A, et al. A complementary role of multiparameter flow cytometry and high-throughput sequencing for minimal residual disease detection in chronic lymphocytic leukemia: An European Research Initiative on CLL study. *Leukemia*. 2016;30.
93. Böttcher S, Ritgen M, Fischer K, et al. Minimal residual disease quantification is an independent predictor of progression-free and overall survival in chronic lymphocytic leukemia: A Multivariate analysis from the randomized GCLLSG CLL8 trial. *J Clin Oncol*. 2012;30.
94. Kovacs G, Robrecht S, Fink AM, et al. Minimal residual disease assessment improves prediction of outcome in patients with chronic lymphocytic Leukemia (CLL) who achieve partial response: Comprehensive analysis of two phase III Studies of the German CLL Study Group. *J Clin Oncol*. 2016;34.
95. Kwok M, Rawstron AC, Varghese A, et al. Minimal residual disease is an independent predictor for 10-year survival in CLL. *Blood*. 2016;128.
96. Burger JA, O'Brien S. Evolution of CLL treatment – from chemoimmunotherapy to targeted and individualized therapy. *Nat Rev Clin Oncol*. 2018;15.
97. Roeker LE, Dreger P, Brown JR, et al. Allogeneic stem cell transplantation for chronic lymphocytic leukemia in the era of novel agents. *Blood Adv*. 2020;4.
98. Kharfan-Dabaja MA, Kumar A, Hamadani M, et al. Clinical Practice Recommendations for Use of Allogeneic Hematopoietic Cell Transplantation in Chronic Lymphocytic Leukemia on Behalf of the Guidelines Committee of the American Society for Blood and Marrow Transplantation. *Biol Blood Marrow Transplant*. 2016;22.
99. Porter DL, Hwang WT, Frey N V., et al. Chimeric antigen receptor T cells persist and induce sustained remissions in relapsed refractory chronic lymphocytic leukemia. *Sci Transl Med*. 2015;7.
100. Gauthier J, Hirayama A V., Purushe J, et al. Feasibility and efficacy of CD19-targeted CAR T cells with concurrent ibrutinib for CLL after ibrutinib failure. In: *Blood*. Vol 135. American Society of Hematology; 2020:1650-1660.
101. Liu E, Marin D, Banerjee P, et al. Use of CAR-Transduced Natural Killer Cells in CD19-Positive Lymphoid Tumors. *N Engl J Med*. 2020;382.
102. Bosch F, Dalla-Favera R. Chronic lymphocytic leukaemia: from genetics to treatment. *Nat Rev Clin Oncol*. 2019;16.
103. Sutton LA, Hadzidimitriou A, Baliakas P, et al. Immunoglobulin genes in chronic lymphocytic leukemia: Key to understanding the disease and improving risk stratification. *Haematologica*. 2017;102.
104. Fais F, Ghiotto F, Hashimoto S, et al. Chronic lymphocytic leukemia B cells express restricted sets of mutated and unmutated antigen receptors. *J Clin Invest*. 1998;102.
105. Chiorazzi N, Ferrarini M. B cell chronic lymphocytic leukemia: Lessons learned from studies of the B cell antigen receptor. *Annu Rev Immunol*. 2003;21.
106. Ghiotto F, Fais F, Valetto A, et al. Remarkably similar antigen receptors

- among a subset of patients with chronic lymphocytic leukemia. *J Clin Invest.* 2004;113.
107. Messmer BT, Albesiano E, Efremov DG, et al. Multiple distinct sets of stereotyped antigen receptors indicate a role for antigen in promoting chronic lymphocytic leukemia. *J Exp Med.* 2004;200.
108. Tobin G, Thunberg U, Johnson A, et al. Chronic lymphocytic leukemias utilizing the VH3-21 gene display highly restricted Vλ2-14 gene use and homologous CDR3s: Implicating recognition of a common antigen epitope. *Blood.* 2003;101.
109. Widhopf GF, Rassenti LZ, Toy TL, Gribben JG, Wierda WG, Kipps TJ. Chronic lymphocytic leukemia B cells of more than 1% of patients express virtually identical immunoglobulins. *Blood.* 2004;104.
110. Caligaris-Cappio F, Gobbi M, Bofill M, Janossy G. Infrequent normal B lymphocytes express features of B-chronic lymphocytic leukemia. *J Exp Med.* 1982;155.
111. Stall AM, Farinas MC, Tarlinton DM, et al. Ly-1 B-cell clones similar to human chronic lymphocytic leukemias routinely develop in older normal mice and young autoimmune (New Zealand Black-related) animals. *Proc Natl Acad Sci U S A.* 1988;85.
112. Oscier DG, Thompson A, Zhu D, Stevenson FK. Differential rates of somatic hypermutation in V(H) genes among subsets of chronic lymphocytic leukemia defined by chromosomal abnormalities. *Blood.* 1997;89.
113. Klein U, Tu Y, Stolovitzky GA, et al. Gene expression profiling of B cell chronic lymphocytic leukemia reveals a homogeneous phenotype related to memory B cells. *J Exp Med.* 2001;194.
114. Rosenwald A, Alizadeh AA, Widhopf G, et al. Relation of gene expression phenotype to immunoglobulin mutation genotype in B cell chronic lymphocytic leukemia. *J Exp Med.* 2001;194.
115. Stamatopoulos K, Belessi C, Moreno C, et al. Over 20% of patients with chronic lymphocytic leukemia carry stereotyped receptors: Pathogenetic implications and clinical correlations. *Blood.* 2007;109.
116. Murray F, Darzentas N, Hadzidimitriou A, et al. Stereotyped patterns of somatic hypermutation in subsets of patients with chronic lymphocytic leukemia: Implications for the role of antigen selection in leukemogenesis. *Blood.* 2008;111.
117. Agathangelidis A, Chatzidimitriou A, Gemenetzi K, et al. Higher-order connections between stereotyped subsets: implications for improved patient classification in CLL. *Blood.* 2021;137.
118. Jeromin S, Haferlach C, Dicker F, Alpermann T, Haferlach T, Kern W. Differences in prognosis of stereotyped IGHV3-21 chronic lymphocytic leukaemia according to additional molecular and cytogenetic aberrations. *Leukemia.* 2016;30.
119. Xochelli A, Baliakas P, Kavakiotis I, et al. Chronic lymphocytic leukemia with mutated IGHV4-34 receptors: Shared and distinct immunogenetic features and clinical outcomes. *Clin Cancer Res.* 2017;23.
120. Gounari M, Ntoufa S, Apollonio B, et al. Excessive antigen reactivity may underlie the clinical aggressiveness of chronic lymphocytic leukemia stereotyped subset #8. *Blood.* 2015;125.
121. Seifert M, Sellmann L, Bloehdorn J, et al. Cellular origin and pathophysiology of chronic lymphocytic leukemia. *J Exp Med.* 2012;209.
122. Husby S, Grønbaek K. Mature lymphoid malignancies: Origin, stem cells, and chronicity. *Blood Adv.* 2017;1.
123. Kikushige Y, Ishikawa F, Miyamoto T, et al. Self-Renewing Hematopoietic Stem Cell Is the Primary Target in Pathogenesis of Human Chronic Lymphocytic Leukemia. *Cancer Cell.* 2011;20.
124. Sala-Torra O, Hanna C, Loken MR, et al. Evidence of Donor-Derived Hematologic Malignancies after Hematopoietic Stem Cell Transplantation. *Biol Blood Marrow Transplant.* 2006;12.
125. Gahn B, Schäfer C, Neef J, et al. Detection of trisomy 12 and Rb-deletion in CD34+ cells of patients with B-cell chronic lymphocytic leukemia. *Blood.* 1997;89.
126. Damm F, Mylonas E, Cosson A, et al. Acquired initiating mutations in early hematopoietic cells of CLL patients.

- Cancer Discov. 2014;4.
127. Marsilio S, Khiabani H, Fabbri G, et al. Somatic CLL mutations occur at multiple distinct hematopoietic maturation stages: Documentation and cautionary note regarding cell fraction purity. *Leukemia*. 2018;32.
128. Jaiswal S, Fontanillas P, Flannick J, et al. Age-Related Clonal Hematopoiesis Associated with Adverse Outcomes. *N Engl J Med*. 2014;371.
129. Genovese G, Köhler AK, Handsaker RE, et al. Clonal Hematopoiesis and Blood-Cancer Risk Inferred from Blood DNA Sequence. *N Engl J Med*. 2014;371.
130. Agathangelidis A, Ljungström V, Scarfò L, et al. Highly similar genomic landscapes in monoclonal b-cell lymphocytosis and ultra-stable chronic lymphocytic leukemia with low frequency of driver mutations. *Haematologica*. 2018;103.
131. Loh PR, Genovese G, Handsaker RE, et al. Insights into clonal haematopoiesis from 8,342 mosaic chromosomal alterations. *Nature*. 2018;559.
132. Terao C, Suzuki A, Momozawa Y, et al. Chromosomal alterations among age-related haematopoietic clones in Japan. *Nature*. 2020;584.
133. Puiggros A, Blanco G, Espinet B. Genetic abnormalities in chronic lymphocytic leukemia: Where we are and where we go. *Biomed Res Int*. 2014;2014.
134. Van Dyke DL, Werner L, Rassenti LZ, et al. The Döhner fluorescence in situ hybridization prognostic classification of chronic lymphocytic leukaemia (CLL): the CLL Research Consortium experience. *Br J Haematol*. 2016;173.
135. Dewald GW, Brockman SR, Paternoster SF, et al. Chromosome anomalies detected by interphase fluorescence in situ hybridization: Correlation with significant biological features of B-cell chronic lymphocytic leukaemia. *Br J Haematol*. 2003;121.
136. Geisler C, Jurlander J, Bullinger L, et al. Danish CLL2-Study revisited: FISH on a cohort with a 20-yr follow-up confirms the validity of the hierarchical model of genomic aberrations in chronic lymphocytic leukaemia. *Eur J Haematol*. 2009;83.
137. Döhner H, Stilgenbauer S, James MR, et al. 11q deletions identify a new subset of B-cell chronic lymphocytic leukemia characterized by extensive nodal involvement and inferior prognosis. *Blood*. 1997;89.
138. Fegan C, Robinson H, Thompson P, Whittaker JA, White D. Karyotypic evolution in CLL: Identification of a new sub-group of patients with deletions of 11q and advanced or progressive disease. *Leukemia*. 1995;9.
139. Neilson JR, Auer R, White D, et al. Deletions at 11q identify a subset of patients with typical CLL who show consistent disease progression and reduced survival. *Leukemia*. 1997;11.
140. Kern W, Dicker F, Schnittger S, Haferlach C, Haferlach T. Correlation of flow cytometrically determined expression of Zap-70 using the SBZAP antibody with IgVH mutation status and cytogenetics in 1,229 patients with chronic lymphocytic leukemia. *Cytom Part B - Clin Cytom*. 2009;76.
141. Wierda WG, O'Brien S, Wang X, et al. Multivariable model for time to first treatment in patients with chronic lymphocytic leukemia. *J Clin Oncol*. 2011;29.
142. Marasca R, Maffei R, Martinelli S, et al. Clinical heterogeneity of de novo 11q deletion chronic lymphocytic leukaemia: Prognostic relevance of extent of 11q deleted nuclei inside leukemic clone. *Hematol Oncol*. 2013;31.
143. Hernández JÁ, Hernández-Sánchez M, Rodríguez-Vicente AE, et al. A Low Frequency of Losses in 11q Chromosome Is Associated with Better Outcome and Lower Rate of Genomic Mutations in Patients with Chronic Lymphocytic Leukemia. Gibson SB, ed. *PLoS One*. 2015;10.
144. Stilgenbauer S, Liebisch P, James MR, et al. Molecular cytogenetic delineation of a novel critical genomic region in chromosome bands 11q22.3-923.1 in lymphoproliferative disorders. *Proc Natl Acad Sci U S A*. 1996;93.
145. Gunnarsson R, Mansouri L, Isaksson A, et al. Array-based genomic screening at diagnosis and during follow-up in chronic lymphocytic leukemia. *Haematologica*.

- 2011;96.
146. Rose-Zerilli MJJ, Forster J, Parker H, et al. ATM mutation rather than BIRC3 deletion and/or mutation predicts reduced survival in 11q-deleted chronic lymphocytic leukemia: data from the UK LRF CLL4 trial. *Haematologica*. 2014;99.
147. Stankovic T, Skowronska A. The role of ATM mutations and 11q deletions in disease progression in chronic lymphocytic leukemia. *Leuk Lymphoma*. 2014;55.
148. Edelmann J, Holzmann K, Miller F, et al. High-resolution genomic profiling of chronic lymphocytic leukemia reveals new recurrent genomic alterations. *Blood*. 2012;120.
149. Gardiner A, Parker H, Glide S, et al. A new minimal deleted region at 11q22.3 reveals the importance of interpretation of diminished FISH signals and the choice of probe for ATM deletion screening in chronic lymphocytic leukemia. *Leuk Res*. 2012;36.
150. Skowronska A, Parker A, Ahmed G, et al. Biallelic ATM inactivation significantly reduces survival in patients treated on the United Kingdom Leukemia Research Fund Chronic Lymphocytic Leukemia 4 trial. *J Clin Oncol*. 2012;30.
151. Ouillette P, Collins R, Shakhan S, et al. Acquired genomic copy number aberrations and survival in chronic lymphocytic leukemia. *Blood*. 2011;118.
152. Ouillette P, Fossum S, Parkin B, et al. Aggressive chronic lymphocytic leukemia with elevated genomic complexity is associated with multiple gene defects in the response to DNA double-strand breaks. *Clin Cancer Res*. 2010;16.
153. Edelmann J, Holzmann K, Tausch E, et al. Genomic alterations in high-risk chronic lymphocytic leukemia frequently affect cell cycle key regulators and NOTCH1-regulated transcription. *Haematologica*. 2020;105.
154. Raponi S, Del Giudice I, Ilari C, et al. Biallelic BIRC3 inactivation in chronic lymphocytic leukaemia patients with 11q deletion identifies a subgroup with very aggressive disease. *Br J Haematol*. Published online May 22, 2018.
155. Diop F, Moia R, Favini C, et al. Biological and clinical implications of BIRC3 mutations in chronic lymphocytic leukemia. *Haematologica*. 2020;105.
156. Blakemore SJ, Clifford R, Parker H, et al. Clinical significance of TP53, BIRC3, ATM and MAPK-ERK genes in chronic lymphocytic leukaemia: data from the randomised UK LRF CLL4 trial. *Leukemia*. Published online 2020.
157. Kalla C, Scheuermann MO, Kube I, et al. Analysis of 11q22-q23 deletion target genes in B-cell chronic lymphocytic leukaemia: Evidence for a pathogenic role of NPAT, CUL5, and PPP2R1B. *Eur J Cancer*. 2007;43.
158. Bullrich F, Veronese ML, Kitada S, et al. Minimal region of loss at 13q14 in B-cell chronic lymphocytic leukemia. *Blood*. 1996;88.
159. Van Dyke DL, Shanafelt TD, Call TG, et al. A comprehensive evaluation of the prognostic significance of 13q deletions in patients with B-chronic lymphocytic leukaemia. *Br J Haematol*. 2010;148.
160. Calin GA, Dumitru CD, Shimizu M, et al. Frequent deletions and down-regulation of micro-RNA genes miR15 and miR16 at 13q14 in chronic lymphocytic leukemia. *Proc Natl Acad Sci U S A*. 2002;99.
161. Palamarchuk A, Efanov A, Nazaryan N, et al. 13q14 deletions in CLL involve cooperating tumor suppressors. *Blood*. 2010;115.
162. Hammarsund M, Corcoran MM, Wilson W, et al. Characterization of a novel B-CLL candidate gene - DLEU7 - Located in the 13q14 tumor suppressor locus. *FEBS Lett*. 2004;556.
163. Mosca L, Fabris S, Lionetti M, et al. Integrative genomics analyses reveal molecularly distinct subgroups of B-cell chronic lymphocytic leukemia patients with 13q14 deletion. *Clin Cancer Res*. 2010;16.
164. Parker H, Rose-Zerilli MJJ, Parker A, et al. 13q deletion anatomy and disease progression in patients with chronic lymphocytic leukemia. *Leukemia*. 2011;25.
165. Liu Y, Szekeley L, Grandner D, et al. Chronic lymphocytic leukemia cells with allelic deletions at 13q14 commonly have one intact RB1 gene: Evidence for a role of an adjacent locus. *Proc Natl Acad Sci U S A*.

- 1993;90.
166. Ouillette P, Collins R, Shakhan S, et al. The prognostic significance of various 13q14 deletions in chronic lymphocytic leukemia. *Clin Cancer Res.* 2011;17.
 167. Dal Bo M, Rossi FM, Rossi D, et al. 13q14 Deletion size and number of deleted cells both influence prognosis in chronic lymphocytic leukemia. *Genes Chromosom Cancer.* 2011;50.
 168. Chena C, Avalos JS, Bezares RF, et al. Biallelic deletion 13q14.3 in patients with chronic lymphocytic leukemia: Cytogenetic, FISH and clinical studies. *Eur J Haematol.* 2008;81.
 169. Puiggros A, Delgado J, Rodriguez-Vicente A, et al. Biallelic losses of 13q do not confer a poorer outcome in chronic lymphocytic leukaemia: Analysis of 627 patients with isolated 13q deletion. *Br J Haematol.* 2013;163.
 170. Cimmino A, Calin GA, Fabbri M, et al. miR-15 and miR-16 induce apoptosis by targeting BCL2. *Proc Natl Acad Sci U S A.* 2005;102.
 171. Klein U, Lia M, Crespo M, et al. The DLEU2/miR-15a/16-1 Cluster Controls B Cell Proliferation and Its Deletion Leads to Chronic Lymphocytic Leukemia. *Cancer Cell.* 2010;17.
 172. Lia M, Carette A, Tang H, et al. Functional dissection of the chromosome 13q14 tumor-suppressor locus using transgenic mouse lines. *Blood.* 2012;119.
 173. Stilgenbauer S, Zenz T, Winkler D, et al. Subcutaneous alemtuzumab in fludarabine-refractory chronic lymphocytic leukemia: Clinical results and prognostic marker analyses from the CLL2H study of the German chronic lymphocytic leukemia study group. *J Clin Oncol.* 2009;27.
 174. Zenz T, Eichhorst B, Busch R, et al. TP53 mutation and survival in chronic lymphocytic leukemia. *J Clin Oncol.* 2010;28.
 175. Lazarian G, Tausch E, Eclache V, et al. TP53 mutations are early events in chronic lymphocytic leukemia disease progression and precede evolution to complex karyotypes. *Int J Cancer.* 2016;139.
 176. Stilgenbauer S, Schnaiter A, Paschka P, et al. Gene mutations and treatment outcome in chronic lymphocytic leukemia: results from the CLL8 trial. *Blood.* 2014;123.
 177. Döhner H, Fischer K, Bentz M, et al. p53 Gene deletion predicts for poor survival and non-response to therapy with purine analogs in chronic B-cell leukemias. *Blood.* 1995;85.
 178. Catovsky D, Richards S, Matutes E, et al. Assessment of fludarabine plus cyclophosphamide for patients with chronic lymphocytic leukaemia (the LRF CLL4 Trial): a randomised controlled trial. *Lancet.* 2007;370.
 179. Chigrinova E, Rinaldi A, Kwee I, et al. Two main genetic pathways lead to the transformation of chronic lymphocytic leukemia to Richter syndrome. *Blood.* 2013;122.
 180. Fabbri G, Khiabani H, Holmes AB, et al. Genetic lesions associated with chronic lymphocytic leukemia transformation to Richter syndrome. *J Exp Med.* 2013;210.
 181. Tam CS, Shanafelt TD, Wierda WG, et al. De novo deletion 17p13.1 chronic lymphocytic leukemia shows significant clinical heterogeneity: The M. D. Anderson and Mayo Clinic experience. *Blood.* 2009;114.
 182. Kröber A, Seiler T, Benner A, et al. VH mutation status, CD38 expression level, genomic aberrations, and survival in chronic lymphocytic leukemia. *Blood.* 2002;100.
 183. Best OG, Gardiner AC, Davis ZA, et al. A subset of Binet stage A CLL patients with TP53 abnormalities and mutated IGHV genes have stable disease. *Leukemia.* 2009;23.
 184. Delgado J, Salaverria I, Baumann T, et al. Genomic complexity and IGHV mutational status are key predictors of outcome of chronic lymphocytic leukemia patients with TP53 disruption. *Haematologica.* 2014;99.
 185. Malek SN. The biology and clinical significance of acquired genomic copy number aberrations and recurrent gene mutations in chronic lymphocytic leukemia. *Oncogene.* 2013;32.
 186. Malcikova J, Smardova J, Rocnova L, et al. Monoallelic and biallelic inactivation of TP53 gene in chronic lymphocytic leukemia: selection, impact on survival,

- and response to DNA damage. *Blood*. 2009;114.
187. Yu L, Kim HT, Kasar SN, et al. Survival of Del17p CLL depends on genomic complexity and somatic mutation. *Clin Cancer Res*. 2017;23.
188. Campo E, Cymbalista F, Ghia P, et al. TP53 aberrations in chronic lymphocytic leukemia: An overview of the clinical implications of improved diagnostics. *Haematologica*. 2018;103.
189. Hafner A, Bulyk ML, Jambhekar A, Lahav G. The multiple mechanisms that regulate p53 activity and cell fate. *Nat Rev Mol Cell Biol*. 2019;20.
190. Zenz T, Häbe S, Denzel T, et al. Detailed analysis of p53 pathway defects in fludarabine-refractory chronic lymphocytic leukemia (CLL): dissecting the contribution of 17p deletion, TP53 mutation, p53-p21 dysfunction, and miR34a in a prospective clinical trial. *Blood*. 2009;114.
191. Leeksa AC, Baliakas P, Moysiadis T, et al. Genomic arrays identify high-risk chronic lymphocytic leukemia with genomic complexity: A multi-center study. *Haematologica*. 2020;105.
192. Klintman J, Appleby N, Stamatopoulos B, et al. Genomic and transcriptomic correlates of Richter's transformation in Chronic Lymphocytic Leukemia. *Blood*. Published online November 18, 2020.
193. Balatti V, Lerner S, Rizzotto L, et al. Trisomy 12 CLLs progress through NOTCH1 mutations. *Leukemia*. 2013;27.
194. Baliakas P, Puiggros A, Xochelli A, et al. Additional trisomies amongst patients with chronic lymphocytic leukemia carrying trisomy 12: The accompanying chromosome makes a difference. *Haematologica*. 2016;101.
195. Roos-Weil D, Nguyen-Khac F, Chevret S, et al. Mutational and cytogenetic analyses of 188 CLL patients with trisomy 12: A retrospective study from the French Innovative Leukemia Organization (FILO) working group. *Genes Chromosom Cancer*. 2018;57.
196. Vendramini E, Bomben R, Pozzo F, et al. KRAS, NRAS, and BRAF mutations are highly enriched in trisomy 12 chronic lymphocytic leukemia and are associated with shorter treatment-free survival. *Leukemia*. 2019;33.
197. Criel A, Wlodarska I, Meeus P, et al. Trisomy 12 is uncommon in typical chronic lymphocytic leukemias. *Br J Haematol*. 1994;87.
198. Autore F, Strati P, Laurenti L, Ferrajoli A. Morphological, immunophenotypic, and genetic features of chronic lymphocytic leukemia with trisomy 12: A comprehensive review. *Haematologica*. 2018;103.
199. Kienle DL, Korz C, Hosch B, et al. Evidence for distinct pathomechanisms in genetic subgroups of chronic lymphocytic leukemia revealed by quantitative expression analysis of cell cycle, activation, and apoptosis-associated genes. *J Clin Oncol*. 2005;23.
200. Sellmann L, Gesk S, Walter C, et al. Trisomy 19 is associated with trisomy 12 and mutated IGHV genes in B-chronic lymphocytic leukaemia. *Br J Haematol*. 2007;138.
201. Martín-Subero JI, Ibbotson R, Klapper W, et al. A comprehensive genetic and histopathologic analysis identifies two subgroups of B-cell malignancies carrying a t(14;19)(q32;q13) or variant BCL3-translocation. *Leukemia*. 2007;21.
202. Put N, Meeus P, Chatelain B, et al. Translocation t(14;18) is not associated with inferior outcome in chronic lymphocytic leukemia. *Leukemia*. 2009;23.
203. Pérez-Carretero C, Hernández-Sánchez M, González T, et al. Chronic lymphocytic leukemia patients with IGH translocations are characterized by a distinct genetic landscape with prognostic implications. *Int J Cancer*. 2020;147.
204. Reindl L, Bacher U, Dicker F, et al. Biological and clinical characterization of recurrent 14q deletions in CLL and other mature B-cell neoplasms. *Br J Haematol*. 2010;151.
205. Cosson A, Chapiro E, Belhouachi N, et al. 14q deletions are associated with trisomy 12, NOTCH1 mutations and unmutated IGHV genes in chronic lymphocytic leukemia and small lymphocytic lymphoma. *Genes Chromosom Cancer*. 2014;53.
206. Balatti V, Bottoni A, Palamarchuk A, et al.

- NOTCH1 mutations in CLL associated with trisomy 12. *Blood*. 2012;119.
207. Del Giudice I, Rossi D, Chiaretti S, et al. NOTCH1 mutations in +12 chronic lymphocytic leukemia (CLL) confer an unfavorable prognosis, induce a distinctive transcriptional profiling and refine the intermediate prognosis of +12 CLL. *Haematologica*. 2012;97.
208. Giménez N, Martínez-Trillos A, Monraveta A, et al. Mutations in the RAS-BRAF-MAPK-ERK pathway define a specific subgroup of patients with adverse clinical features and provide new therapeutic options in chronic lymphocytic leukemia. *Haematologica*. 2019;104.
209. Dietrich S, Oleś M, Lu J, et al. Drug-perturbation-based stratification of blood cancer. *J Clin Invest*. 2018;128.
210. Grubor V, Krasnitz A, Troge JE, et al. Novel genomic alterations and clonal evolution in chronic lymphocytic leukemia revealed by representational oligonucleotide microarray analysis (ROMA). *Blood*. 2009;113.
211. Brown JR, Hanna M, Tesar B, et al. Integrative genomic analysis implicates gain of PIK3CA at 3q26 and MYC at 8q24 in chronic lymphocytic leukemia. *Clin Cancer Res*. 2012;18.
212. Nagel I, Bug S, Tönnies H, et al. Biallelic inactivation of TRAF3 in a subset of B-cell lymphomas with interstitial del(14)(q24.1q32.33). *Leukemia*. 2009;23.
213. Cosson A, Chapiro E, Bougacha N, et al. Gain in the short arm of chromosome 2 (2p+) induces gene overexpression and drug resistance in chronic lymphocytic leukemia: Analysis of the central role of XPO1. *Leukemia*. 2017;31.
214. Deambrogi C, De Paoli L, Fangazio M, et al. Analysis of the REL, BCL11A, and MYCN proto-oncogenes belonging to the 2p amplicon in chronic lymphocytic leukemia. *Am J Hematol*. 2010;85.
215. Haferlach C, Dicker F, Schnittger S, Kern W, Haferlach T. Comprehensive genetic characterization of CLL: A study on 506 cases analysed with chromosome banding analysis, interphase FISH, IgVH status and immunophenotyping. *Leukemia*. 2007;21.
216. Huh YO, Lin KIC, Vega F, et al. MYC translocation in chronic lymphocytic leukaemia is associated with increased prolymphocytes and a poor prognosis. *Br J Haematol*. 2008;142.
217. Van Den Neste E, Robin V, Francart J, et al. Chromosomal translocations independently predict treatment failure, treatment-free survival and overall survival in B-cell chronic lymphocytic leukemia patients treated with cladribine. *Leukemia*. 2007;21.
218. Cavazzini F, Hernandez JA, Gozzetti A, et al. Chromosome 14q32 translocations involving the immunoglobulin heavy chain locus in chronic lymphocytic leukaemia identify a disease subset with poor prognosis. *Br J Haematol*. 2008;142.
219. Fang H, Reichard KK, Rabe KG, et al. IGH translocations in chronic lymphocytic leukemia: Clinicopathologic features and clinical outcomes. *Am J Hematol*. 2019;94.
220. Juliusson G, Oscier DG, Fitchett M, et al. Prognostic Subgroups in B-Cell Chronic Lymphocytic Leukemia Defined by Specific Chromosomal Abnormalities. *N Engl J Med*. 1990;323.
221. Mayr C, Speicher MR, Kofler DM, et al. Chromosomal translocations are associated with poor prognosis in chronic lymphocytic leukemia. *Blood*. 2006;107.
222. Baliakas P, Iskas M, Gardiner A, et al. Chromosomal translocations and karyotype complexity in chronic lymphocytic leukemia: A systematic reappraisal of classic cytogenetic data. *Am J Hematol*. 2014;89.
223. Dicker F, Schnittger S, Haferlach T, Kern W, Schoch C. Immunostimulatory oligonucleotide-induced metaphase cytogenetics detect chromosomal aberrations in 80% of CLL patients: A study of 132 CLL cases with correlation to FISH, IgVH status, and CD38 expression. *Blood*. 2006;108.
224. Rigolin GM, Cavallari M, Quaglia FM, et al. In CLL, comorbidities and the complex karyotype are associated with an inferior outcome independently of CLL-IPI. *Blood*. 2017;129.
225. Rigolin GM, Saccenti E, Guardalben E, et al. In chronic lymphocytic leukaemia with complex karyotype, major structural

- abnormalities identify a subset of patients with inferior outcome and distinct biological characteristics. *Br J Haematol.* 2018;181.
226. Badoux XC, Keating MJ, Wang X, et al. Fludarabine, cyclophosphamide, and rituximab chemoimmunotherapy is highly effective treatment for relapsed patients with CLL. *Blood.* 2011;117.
227. Herling CD, Klaumünzer M, Rocha CK, et al. Complex karyotypes and KRAS and POT1 mutations impact outcome in CLL after chlorambucil-based chemotherapy or chemoimmunotherapy. *Blood.* 2016;128.
228. Thompson PA, O'Brien SM, Wierda WG, et al. Complex karyotype is a stronger predictor than del(17p) for an inferior outcome in relapsed or refractory chronic lymphocytic leukemia patients treated with ibrutinib-based regimens. *Cancer.* 2015;121.
229. Mato AR, Hill BT, Lamanna N, et al. Optimal sequencing of ibrutinib, idelalisib, and venetoclax in chronic lymphocytic leukemia: results from a multicenter study of 683 patients. *Ann Oncol Off J Eur Soc Med Oncol.* 2017;28.
230. Anderson MA, Tam C, Lew TE, et al. Clinicopathological features and outcomes of progression of CLL on the BCL2 inhibitor venetoclax. *Blood.* 2017;129.
231. O'Brien S, Furman RR, Coutre S, et al. Single-agent ibrutinib in treatment-naïve and relapsed/refractory chronic lymphocytic leukemia: a 5-year experience. *Blood.* 2018;131.
232. Takahashi K, Hu B, Wang F, et al. Clinical implications of cancer gene mutations in patients with chronic lymphocytic leukemia treated with lenalidomide. *Blood.* 2018;131.
233. Jarošová M, Plevová K, Kotašková J, Doubek M, Pospíšilová Š. The importance of complex karyotype in prognostication and treatment of chronic lymphocytic leukemia (CLL): a comprehensive review of the literature. *Leuk Lymphoma.* 2019;60.
234. Ratnaparkhe M, Wong JKL, Wei PC, et al. Defective DNA damage repair leads to frequent catastrophic genomic events in murine and human tumors. *Nat Commun.* 2018;9.
235. Fabbri G, Rasi S, Rossi D, et al. Analysis of the chronic lymphocytic leukemia coding genome: Role of NOTCH1 mutational activation. *J Exp Med.* 2011;208.
236. Wang L, Lawrence MS, Wan Y, et al. SF3B1 and Other Novel Cancer Genes in Chronic Lymphocytic Leukemia. *N Engl J Med.* 2011;365.
237. Landau DA, Carter SL, Stojanov P, et al. Evolution and Impact of Subclonal Mutations in Chronic Lymphocytic Leukemia. *Cell.* 2013;152.
238. Quesada V, Conde L, Villamor N, et al. Exome sequencing identifies recurrent mutations of the splicing factor SF3B1 gene in chronic lymphocytic leukemia. *Nat Genet.* 2012;44.
239. Ljungström V, Cortese D, Young E, et al. Whole-exome sequencing in relapsing chronic lymphocytic leukemia: Clinical impact of recurrent RPS15 mutations. *Blood.* 2016;127.
240. Kasar S, Kim J, Improgo R, et al. Whole-genome sequencing reveals activation-induced cytidine deaminase signatures during indolent chronic lymphocytic leukaemia evolution. *Nat Commun.* 2015;6.
241. Rodríguez-Vicente AE, Bikos V, Hernández-Sánchez M, Malcikova J, Hernández-Rivas J-M, Pospisilova S. Next-generation sequencing in chronic lymphocytic leukemia: recent findings and new horizons. *Oncotarget.* 2017;8.
242. Stankovic T, Weber P, Stewart G, et al. Inactivation of ataxia telangiectasia mutated gene in B-cell chronic lymphocytic leukaemia. *Lancet.* 1999;353.
243. Austen B, Powell JE, Alvi A, et al. Mutations in the ATM gene lead to impaired overall and treatment-free survival that is independent of IGVH mutation status in patients with B-CLL. *Blood.* 2005;106.
244. Skowronska A, Austen B, Powell JE, et al. ATM germline heterozygosity does not play a role in chronic lymphocytic leukemia initiation but influences rapid disease progression through loss of the remaining ATM allele. *Haematologica.* 2012;97.
245. Tiao G, Improgo MR, Kasar S, et al. Rare

- germline variants in ATM are associated with chronic lymphocytic leukemia. *Leukemia*. 2017;31.
246. Lozano-Santos C, García-Vela JA, Pérez-Sanz N, et al. Biallelic ATM alterations detected at diagnosis identify a subset of treatment-naïve chronic lymphocytic leukemia patients with reduced overall survival similar to patients with p53 deletion. *Leuk Lymphoma*. 2017;58.
247. Tausch E, Beck P, Schlenk RF, et al. Prognostic and predictive role of gene mutations in chronic lymphocytic leukemia: results from the pivotal phase III study COMPLEMENT1. *Haematologica*. Published online January 9, 2020.
248. Guièze R, Robbe P, Clifford R, et al. Presence of multiple recurrent mutations confers poor trial outcome of relapsed/refractory CLL. *Blood*. 2015;126.
249. Leroy B, Ballinger ML, Baran-Marszak F, et al. Recommended guidelines for validation, quality control, and reporting of TP53 variants in clinical practice. *Cancer Res*. 2017;77.
250. Rossi D, Khiabani H, Spina V, et al. Clinical impact of small TP53 mutated subclones in chronic lymphocytic leukemia. *Blood*. 2014;123.
251. Malcikova J, Pavlova S, Kunt Vonkova B, et al. Low-burden TP53 mutations in CLL: Clinical impact and clonal evolution within the context of different treatment options. *Blood*. Published online May 4, 2021.
252. Ahn IE, Farooqui MZH, Tian X, et al. Depth and durability of response to ibrutinib in CLL: 5-year follow-up of a phase 2 study. *Blood*. 2018;131.
253. Tausch E, Schneider C, Robrecht S, et al. Prognostic and predictive impact of genetic markers in patients with CLL treated with obinutuzumab and venetoclax. *Blood*. Published online March 23, 2020.
254. Brieghel C, da Cunha-Bang C, Yde CW, et al. The number of signaling pathways altered by driver mutations in chronic lymphocytic leukemia impacts disease outcome. *Clin Cancer Res*. 2020;26.
255. Wan Y, Wu CJ. SF3B1 mutations in chronic lymphocytic leukemia. *Blood*. 2013;121.
256. Rossi D, Bruscatto A, Spina V, et al. Mutations of the SF3B1 splicing factor in chronic lymphocytic leukemia: Association with progression and fludarabine-refractoriness. *Blood*. 2011;118.
257. Wang L, Brooks AN, Fan J, et al. Transcriptomic Characterization of SF3B1 Mutation Reveals Its Pleiotropic Effects in Chronic Lymphocytic Leukemia. *Cancer Cell*. 2016;30.
258. Jeromin S, Weissmann S, Haferlach C, et al. SF3B1 mutations correlated to cytogenetics and mutations in NOTCH1, FBXW7, MYD88, XPO1 and TP53 in 1160 untreated CLL patients. *Leukemia*. 2014;28.
259. Oscier DG, Rose-Zerilli MJ, Winkelmann N, et al. The clinical significance of NOTCH1 and SF3B1 mutations in the UK LRF CLL4 trial. *Blood*. 2013;121.
260. Mansouri L, Cahill N, Gunnarsson R, et al. NOTCH1 and SF3B1 mutations can be added to the hierarchical prognostic classification in chronic lymphocytic leukemia. *Leukemia*. 2013;27.
261. Rossi D, Rasi S, Fabbri G, et al. Mutations of NOTCH1 are an independent predictor of survival in chronic lymphocytic leukemia. *Blood*. 2012;119.
262. Rosati E, Baldoni S, De Falco F, et al. NOTCH1 aberrations in Chronic lymphocytic leukemia. *Front Oncol*. 2018;8.
263. Weissmann S, Roller A, Jeromin S, et al. Prognostic impact and landscape of NOTCH1 mutations in chronic lymphocytic leukemia (CLL): A study on 852 patients. *Leukemia*. 2013;27.
264. Sportoletti P, Baldoni S, Del Papa B, et al. A revised NOTCH1 mutation frequency still impacts survival while the allele burden predicts early progression in chronic lymphocytic leukemia. *Leukemia*. 2014;28.
265. Pozzo F, Bittolo T, Arruga F, et al. NOTCH1 mutations associate with low CD20 level in chronic lymphocytic leukemia: Evidence for a NOTCH1 mutation-driven epigenetic dysregulation. *Leukemia*. 2016;30.
266. Mansouri L, Sutton LA, Ljungström V, et al. Functional loss of IκBε leads to NF-κB

- deregulation in aggressive chronic lymphocytic leukemia. *J Exp Med.* 2015;212.
267. Parker H, Rose-Zerilli MJ, Larrayoz M, et al. Genomic disruption of the histone methyltransferase SETD2 in chronic lymphocytic leukaemia. *Leukemia.* 2016;30.
268. Martínez-Trillos A, Pinyol M, Navarro A, et al. Mutations in TLR/MYD88 pathway identify a subset of young chronic lymphocytic leukemia patients with favorable outcome. *Blood.* 2014;123.
269. Martínez-Trillos A, Navarro A, Aymerich M, et al. Clinical impact of MYD88 mutations in chronic lymphocytic leukemia. *Blood.* 2016;127.
270. Bartel DP. MicroRNAs: Genomics, Biogenesis, Mechanism, and Function. *Cell.* 2004;116.
271. Croce CM. Causes and consequences of microRNA dysregulation in cancer. *Nat Rev Genet.* 2009;10.
272. Mraz M, Kipps TJ. MicroRNAs and B cell receptor signaling in chronic lymphocytic leukemia. In: *Leukemia and Lymphoma.* Vol 54. *Leuk Lymphoma;* 2013:1836-1839.
273. Musilova K, Mraz M. MicroRNAs in B-cell lymphomas: how a complex biology gets more complex. *Leukemia.* 2015;29.
274. Visone R, Rassenti LZ, Veronese A, et al. Karyotype-specific microRNA signature in chronic lymphocytic leukemia. *Blood.* 2009;114.
275. Zenz T, Mohr J, Eldering E, et al. miR-34a as part of the resistance network in chronic lymphocytic leukemia. *Blood.* 2009;113.
276. Asslaber D, Piñón JD, Seyfried I, et al. microRNA-34a expression correlates with MDM2 SNP309 polymorphism and treatment-free survival in chronic lymphocytic leukemia. *Blood.* 2010;115.
277. Mansouri L, Wierzbinska JA, Plass C, Rosenquist R. Epigenetic deregulation in chronic lymphocytic leukemia: Clinical and biological impact. *Semin Cancer Biol.* 2018;51.
278. Cahill N, Bergh AC, Kanduri M, et al. 450K-array analysis of chronic lymphocytic leukemia cells reveals global DNA methylation to be relatively stable over time and similar in resting and proliferative compartments. *Leukemia.* 2013;27.
279. Kretzmer H, Biran A, Purroy N, et al. Preneoplastic Alterations Define CLL DNA Methylome and Persist through Disease Progression and Therapy. *Blood Cancer Discov.* 2021;2.
280. Landau DA, Clement K, Ziller MJ, et al. Locally Disordered Methylation Forms the Basis of Intratumor Methylome Variation in Chronic Lymphocytic Leukemia. *Cancer Cell.* 2014;26.
281. Oakes CC, Claus R, Gu L, et al. Evolution of DNA methylation is linked to genetic aberrations in chronic lymphocytic leukemia. *Cancer Discov.* 2014;4.
282. Beekman R, Chapaprieta V, Russiñol N, et al. The reference epigenome and regulatory chromatin landscape of chronic lymphocytic leukemia. *Nat Med.* 2018;24.
283. Shanafelt TD, Witzig TE, Fink SR, et al. Prospective evaluation of clonal evolution during long-term follow-up of patients with untreated early-stage chronic lymphocytic leukemia. *J Clin Oncol.* 2006;24.
284. Schuh A, Becq J, Humphray S, et al. Monitoring chronic lymphocytic leukemia progression by whole genome sequencing reveals heterogeneous clonal evolution patterns. *Blood.* 2012;120.
285. Amin NA, Seymour E, Saiya-Cork K, Parkin B, Shedden K, Malek SN. A quantitative analysis of subclonal and clonal gene mutations before and after therapy in chronic lymphocytic leukemia. *Clin Cancer Res.* 2016;22.
286. Leeksa AC, Taylor J, Wu B, et al. Clonal diversity predicts adverse outcome in chronic lymphocytic leukemia. *Leukemia.* 2019;33.
287. Ojha J, Ayres J, Secreto C, et al. Deep sequencing identifies genetic heterogeneity and recurrent convergent evolution in chronic lymphocytic leukemia. *Blood.* 2015;125.
288. Landau DA, Sun C, Rosebrock D, et al. The evolutionary landscape of chronic lymphocytic leukemia treated with ibrutinib targeted therapy. *Nat Commun.* 2017;8.
289. Condoluci A, Rossi D. Genomic instability and clonal evolution in chronic

- lymphocytic leukemia: Clinical relevance. *JNCCN J Natl Compr Cancer Netw.* 2021;19.
290. Smith EN, Ghia EM, DeBoever CM, et al. Genetic and epigenetic profiling of CLL disease progression reveals limited somatic evolution and suggests a relationship to memory-cell development. *Blood Cancer J.* 2015;5.
291. Hernández-Sánchez M, Kotaskova J, Rodríguez AE, et al. CLL cells cumulate genetic aberrations prior to the first therapy even in outwardly inactive disease phase. *Leukemia.* 2019;33.
292. Gruber M, Bozic I, Leshchiner I, et al. Growth dynamics in naturally progressing chronic lymphocytic leukaemia. *Nature.* 2019;570.
293. Yin S, Gambe RG, Sun J, et al. A Murine Model of Chronic Lymphocytic Leukemia Based on B Cell-Restricted Expression of Sf3b1 Mutation and Atm Deletion. *Cancer Cell.* 2019;35.
294. Pettitt AR, Sherrington PD, Stewart G, Cawley JC, Malcolm R Taylor A, Stankovic T. p53 dysfunction in B-cell chronic lymphocytic leukemia: Inactivation of ATM as an alternative to TP53 mutation. *Blood.* 2001;98.
295. Stankovic T, Stewart GS, Fegan C, et al. Ataxia telangiectasia mutated-deficient B-cell chronic lymphocytic leukemia occurs in pregerminal center cells and results in defective damage response and unrepaired chromosome damage. *Blood.* 2002;99.
296. Stankovic T, Hubank M, Cronin D, et al. Microarray analysis reveals that TP53- and ATM-mutant B-CLLs share a defect in activating proapoptotic responses after DNA damage but are distinguished by major differences in activating prosurvival responses. *Blood.* 2004;103.
297. Te Raa GD, Moerland PD, Leeksma AC, et al. Assessment of p53 and ATM functionality in chronic lymphocytic leukemia by multiplex ligation-dependent probe amplification. *Cell Death Dis.* 2015;6.
298. Mansouri L, Papakonstantinou N, Ntoufa S, Stamatopoulos K, Rosenquist R. NF- κ B activation in chronic lymphocytic leukemia: A point of convergence of external triggers and intrinsic lesions. *Semin Cancer Biol.* 2016;39.
299. Close V, Close W, Kugler SJ, et al. FBXW7 mutations reduce binding of NOTCH1, leading to cleaved NOTCH1 accumulation and target gene activation in CLL. *Blood.* 2019;133.
300. Wu B, Słabicki M, Sellner L, et al. MED12 mutations and NOTCH signalling in chronic lymphocytic leukaemia. *Br J Haematol.* 2017;179.
301. Shuai S, Suzuki H, Diaz-Navarro A, et al. The U1 spliceosomal RNA is recurrently mutated in multiple cancers. *Nature.* 2019;574.
302. Taylor J, Sendino M, Gorelick AN, et al. Altered nuclear export signal recognition as a driver of oncogenesis. *Cancer Discov.* 2019;9.
303. Bretones G, Álvarez MG, Arango JR, et al. Altered patterns of global protein synthesis and translational fidelity in RPS15-mutated chronic lymphocytic leukemia. *Blood.* 2018;132.
304. Yusufova N, Kloetgen A, Teater M, et al. Histone H1 loss drives lymphoma by disrupting 3D chromatin architecture. *Nature.* 2021;589.
305. Rodríguez D, Bretones G, Quesada V, et al. Mutations in CHD2 cause defective association with active chromatin in chronic lymphocytic leukemia. *Blood.* 2015;126.
306. Wang L, Shalek AK, Lawrence M, et al. Somatic mutation as a mechanism of Wnt/ β -catenin pathway activation in CLL. *Blood.* 2014;124.
307. Ghia EM, Rassenti LZ, Neuberg DS, et al. Activation of hedgehog signaling associates with early disease progression in chronic lymphocytic leukemia. *Blood.* 2019;133.
308. Ciccia A, Elledge SJ. The DNA Damage Response: Making It Safe to Play with Knives. *Mol Cell.* 2010;40.
309. Warmerdam DO, Kanaar R. Dealing with DNA damage: Relationships between checkpoint and repair pathways. *Mutat Res - Rev Mutat Res.* 2010;704.
310. Bartek J, Lukas J. DNA damage checkpoints: from initiation to recovery or adaptation. *Curr Opin Cell Biol.* 2007;19.

311. Chapman JR, Taylor MRG, Boulton SJ. Playing the End Game: DNA Double-Strand Break Repair Pathway Choice. *Mol Cell*. 2012;47.
312. Mahaney BL, Meek K, Lees-Miller SP. Repair of ionizing radiation-induced DNA double-strand breaks by non-homologous end-joining. *Biochem J*. 2009;417.
313. Lee JH, Paull TT. ATM activation by DNA double-strand breaks through the Mre11-Rad50-Nbs1 complex. *Science* (80-). 2005;308.
314. Lavin MF. Ataxia-telangiectasia: from a rare disorder to a paradigm for cell signalling and cancer. *Nat Rev Mol Cell Biol*. 2008;9.
315. Knittel G, Liedgens P, Reinhardt HC. Targeting ATM-deficient CLL through interference with DNA repair pathways. *Front Genet*. 2015;6.
316. Jackson SP, Bartek J. The DNA-damage response in human biology and disease. *Nature*. 2009;461.
317. Ashworth A, Lord CJ, Reis-Filho JS. Genetic interactions in cancer progression and treatment. *Cell*. 2011;145.
318. O'Neil NJ, Bailey ML, Hieter P. Synthetic lethality and cancer. *Nat Rev Genet*. 2017;18.
319. Bryant HE, Schultz N, Thomas HD, et al. Specific killing of BRCA2-deficient tumours with inhibitors of poly(ADP-ribose) polymerase. *Nature*. 2005;434.
320. Farmer H, McCabe H, Lord CJ, et al. Targeting the DNA repair defect in BRCA mutant cells as a therapeutic strategy. *Nature*. 2005;434.
321. Curtin NJ, Szabo C. Poly(ADP-ribose) polymerase inhibition: past, present and future. *Nat Rev Drug Discov*. 2020;19.
322. Ramsay AJ, Quesada V, Foronda M, et al. POT1 mutations cause telomere dysfunction in chronic lymphocytic leukemia. *Nat Genet*. 2013;45.
323. Hanahan D, Weinberg RA. Hallmarks of cancer: The next generation. *Cell*. 2011;144.
324. Green DR, Llambi F. Cell death signaling. *Cold Spring Harb Perspect Biol*. 2015;7.
325. Kale J, Osterlund EJ, Andrews DW. BCL-2 family proteins: Changing partners in the dance towards death. *Cell Death Differ*. 2018;25.
326. Shamas-Din A, Kale J, Leber B, Andrews DW. Mechanisms of action of Bcl-2 family proteins. *Cold Spring Harb Perspect Biol*. 2013;5.
327. Vogler M, Walter HS, Dyer MJS. Targeting anti-apoptotic BCL2 family proteins in haematological malignancies – from pathogenesis to treatment. *Br J Haematol*. 2017;178.
328. Vousden KH, Lu X. Live or let die: The cell's response to p53. *Nat Rev Cancer*. 2002;2.
329. ten Hacken E, Burger JA. Microenvironment interactions and B-cell receptor signaling in Chronic Lymphocytic Leukemia: Implications for disease pathogenesis and treatment. *Biochim Biophys Acta - Mol Cell Res*. 2016;1863.
330. Burger JA, Chiorazzi N. B cell receptor signaling in chronic lymphocytic leukemia. *Trends Immunol*. 2013;34.
331. Stevenson FK, Krysov S, Davies AJ, Steele AJ, Packham G. B-cell receptor signaling in chronic lymphocytic leukemia. *Blood*. 2011;118.
332. Lazarian G, Yin S, ten Hacken E, et al. A hotspot mutation in transcription factor IKZF3 drives B cell neoplasia via transcriptional dysregulation. *Cancer Cell*. 2021;39.
333. Woyach JA, Furman RR, Liu T-M, et al. Resistance Mechanisms for the Bruton's Tyrosine Kinase Inhibitor Ibrutinib. *N Engl J Med*. 2014;370.
334. Yu H, Lee H, Herrmann A, Buettner R, Jove R. Revisiting STAT3 signalling in cancer: New and unexpected biological functions. *Nat Rev Cancer*. 2014;14.
335. Oeckinghaus A, Hayden MS, Ghosh S. Crosstalk in NF- κ B signaling pathways. *Nat Immunol*. 2011;12.
336. Oeckinghaus A, Ghosh S. The NF-kappaB family of transcription factors and its regulation. *Cold Spring Harb Perspect Biol*. 2009;1.
337. Zarnegar BJ, Wang Y, Mahoney DJ, et al. Noncanonical NF-kappaB activation requires coordinated assembly of a regulatory complex of the adaptors cIAP1, cIAP2, TRAF2 and TRAF3 and the kinase

- NIK. *Nat Immunol.* 2008;9.
338. Sun S-C. The non-canonical NF- κ B pathway in immunity and inflammation. *Nat Rev Immunol.* 2017;17.
339. Philipp C, Edelmann J, Bühler A, Winkler D, Stilgenbauer S, Küppers R. Mutation analysis of the TNFAIP3 (A20) tumor suppressor gene in CLL. *Int J Cancer.* 2011;128.
340. Asslaber D, Wacht N, Leisch M, et al. BIRC3 expression predicts CLL progression and defines treatment sensitivity via enhanced NF- κ B nuclear translocation. *Clin Cancer Res.* 2019;25.
341. Burger JA, Tsukada N, Burger M, Zvaifler NJ, Dell'Aquila M, Kipps TJ. Blood-derived nurse-like cells protect chronic lymphocytic leukemia B cells from spontaneous apoptosis through stromal cell-derived factor-1. *Blood.* 2000;96.
342. Bürkle A, Niedermeier M, Schmitt-Gräff A, Wierda WG, Keating MJ, Burger JA. Overexpression of the CXCR5 chemokine receptor, and its ligand, CXCL13 in B-cell chronic lymphocytic leukemia. *Blood.* 2007;110.
343. Nishio M, Endo T, Tsukada N, et al. Nurselike cells express BAFF and APRIL, which can promote survival of chronic lymphocytic leukemia cells via a paracrine pathway distinct from that of SDF-1 α . *Blood.* 2005;106.
344. Burger JA, Quiroga MP, Hartmann E, et al. High-level expression of the T-cell chemokines CCL3 and CCL4 by chronic lymphocytic leukemia B cells in nurselike cell cocultures and after BCR stimulation. *Blood.* 2009;113.
345. Yu J, Chen L, Cui B, et al. Wnt5a induces ROR1/ROR2 heterooligomerization to enhance leukemia chemotaxis and proliferation. *J Clin Invest.* 2016;126.
346. Chen Y, Chen L, Yu J, et al. Cirmtuzumab blocks Wnt5a/ROR1 stimulation of NF- κ B to repress autocrine STAT3 activation in chronic lymphocytic leukemia. *Blood.* 2019;134.
347. Deaglio S, Vaisitti T, Bergui L, et al. CD38 and CD100 lead a network of surface receptors relaying positive signals for B-CLL growth and survival. *Blood.* 2005;105.
348. Kitada S, Zapata JM, Andreff M, Reed JC. Bryostatins and CD40-ligand enhance apoptosis resistance and induce expression of cell survival genes in B-cell chronic lymphocytic leukaemia. *Br J Haematol.* 1999;106.
349. Aguilar-Hernandez MM, Blunt MD, Dobson R, et al. IL-4 enhances expression and function of surface IgM in CLL cells. *Blood.* 2016;127.
350. Burger JA, Burger M, Kipps TJ. Chronic Lymphocytic Leukemia B Cells Express Functional CXCR4 Chemokine Receptors That Mediate Spontaneous Migration Beneath Bone Marrow Stromal Cells. *Blood.* 1999;94.
351. Burger JA, Zvaifler NJ, Tsukada N, Firestein GS, Kipps TJ. Fibroblast-like synoviocytes support B-cell pseudoemperipolesis via a stromal cell-derived factor-1- and CD106 (VCAM-1)-dependent mechanism. *J Clin Invest.* 2001;107.
352. Till KJ, Lin K, Zuzel M, Cawley JC. The chemokine receptor CCR7 and α 4 integrin are important for migration of chronic lymphocytic leukemia cells into lymph nodes. *Blood.* 2002;99.
353. Herishanu Y, Pérez-Galán P, Liu D, et al. The lymph node microenvironment promotes B-cell receptor signaling, NF- κ B activation, and tumor proliferation in chronic lymphocytic leukemia. *Blood.* 2011;117.
354. Herman SEM, Gordon AL, Hertlein E, et al. Bruton tyrosine kinase represents a promising therapeutic target for treatment of chronic lymphocytic leukemia and is effectively targeted by PCI-32765. *Blood.* 2011;117.
355. Hoellenriegel J, Meadows SA, Sivina M, et al. The phosphoinositide 3'-kinase delta inhibitor, CAL-101, inhibits B-cell receptor signaling and chemokine networks in chronic lymphocytic leukemia. *Blood.* 2011;118.
356. Byrd JC, Furman RR, Coutre SE, et al. Targeting BTK with Ibrutinib in Relapsed Chronic Lymphocytic Leukemia. *N Engl J Med.* 2013;369.
357. Furman RR, Sharman JP, Coutre SE, et al. Idelalisib and Rituximab in Relapsed Chronic Lymphocytic Leukemia. *N Engl J Med.* 2014;370.
358. Burger JA, Tedeschi A, Barr PM, et al.

- Ibrutinib as Initial Therapy for Patients with Chronic Lymphocytic Leukemia. *N Engl J Med.* 2015;373.
359. Moreno C, Greil R, Demirkan F, et al. Ibrutinib plus obinutuzumab versus chlorambucil plus obinutuzumab in first-line treatment of chronic lymphocytic leukaemia (iLLUMINATE): a multicentre, randomised, open-label, phase 3 trial. *Lancet Oncol.* 2019;20.
360. Woyach JA, Ruppert AS, Heerema NA, et al. Ibrutinib Regimens versus Chemoimmunotherapy in Older Patients with Untreated CLL. *N Engl J Med.* 2018;379.
361. Ponader S, Chen SS, Buggy JJ, et al. The Bruton tyrosine kinase inhibitor PCI-32765 thwarts chronic lymphocytic leukemia cell survival and tissue homing in vitro and in vivo. *Blood.* 2012;119.
362. De Rooij MFM, Kuil A, Geest CR, et al. The clinically active BTK inhibitor PCI-32765 targets B-cell receptor- and chemokine-controlled adhesion and migration in chronic lymphocytic leukemia. *Blood.* 2012;119.
363. Maharaj K, Sahakian E, Pinilla-Ibarz J. Emerging role of BCR signaling inhibitors in immunomodulation of chronic lymphocytic leukemia. *Blood Adv.* 2017;1.
364. Dubovsky JA, Beckwith KA, Natarajan G, et al. Ibrutinib is an irreversible molecular inhibitor of ITK driving a Th1-selective pressure in T lymphocytes. *Blood.* 2013;122.
365. Sharman JP, Egyed M, Jurczak W, et al. Acalabrutinib with or without obinutuzumab versus chlorambucil and obinutuzumab for treatment-naive chronic lymphocytic leukaemia (ELEVATE TN): a randomised, controlled, phase 3 trial. *Lancet.* 2020;395.
366. Ghia P, Pluta A, Wach M, et al. Ascend: Phase III, randomized trial of acalabrutinib versus idelalisib plus rituximab or bendamustine plus rituximab in relapsed or refractory chronic lymphocytic leukemia. In: *Journal of Clinical Oncology.* Vol 38. American Society of Clinical Oncology; 2020:2849-2861.
367. Byrd JC, Harrington B, O'Brien S, et al. Acalabrutinib (ACP-196) in Relapsed Chronic Lymphocytic Leukemia. *N Engl J Med.* 2016;374.
368. Tam CS, Trotman J, Opat S, et al. Phase 1 study of the selective BTK inhibitor zanubrutinib in B-cell malignancies and safety and efficacy evaluation in CLL. *Blood.* 2019;134.
369. Danilov A V., Herbaux C, Walter HS, et al. Phase Ib study of tirabrutinib in combination with idelalisib or entospletinib in previously treated chronic lymphocytic leukemia. *Clin Cancer Res.* 2020;26.
370. Mato AR, Shah NN, Jurczak W, et al. Pirtobrutinib in relapsed or refractory B-cell malignancies (BRUIN): a phase 1/2 study. *Lancet.* 2021;397.
371. Reiff SD, Mantel R, Smith LL, et al. The BTK Inhibitor ARQ 531 Targets Ibrutinib-Resistant CLL and Richter Transformation. *Cancer Discov.* 2018;8.
372. Woyach J, Stephens DM, Flinn IW, et al. Final Results of Phase 1, Dose Escalation Study Evaluating ARQ 531 in Patients with Relapsed or Refractory B-Cell Lymphoid Malignancies. *Blood.* 2019;134.
373. Lannutti BJ, Meadows SA, Herman SEM, et al. CAL-101, a p110 δ selective phosphatidylinositol-3-kinase inhibitor for the treatment of B-cell malignancies, inhibits PI3K signaling and cellular viability. *Blood.* 2011;117.
374. Flinn IW, Hillmen P, Montillo M, et al. The phase 3 DUO trial: Duvelisib vs ofatumumab in relapsed and refractory CLL/SLL. *Blood.* 2018;132.
375. Lunning M, Vose J, Nastoupil L, et al. Ublituximab and umbralisib in relapsed/refractory B-cell non-Hodgkin lymphoma and chronic lymphocytic leukemia. *Blood.* 2019;134.
376. Mato AR, Ghosh N, Schuster SJ, et al. Phase 2 Study of the Safety and Efficacy of Umbralisib in Patients with CLL Who Are Intolerant to BTK or PI3K δ Inhibitor Therapy. *Blood.* Published online December 1, 2020.
377. Burger JA, Landau DA, Taylor-Weiner A, et al. Clonal evolution in patients with chronic lymphocytic leukaemia developing resistance to BTK inhibition. *Nat Commun.* 2016;7.
378. Woyach JA, Ruppert AS, Guinn D, et al. BTKC481S-Mediated resistance to

- ibrutinib in chronic lymphocytic leukemia. *J Clin Oncol*. 2017;35.
379. Furman RR, Cheng S, Lu P, et al. Ibrutinib Resistance in Chronic Lymphocytic Leukemia. *N Engl J Med*. 2014;370.
380. Liu TM, Woyach JA, Zhong Y, et al. Hypermorphic mutation of phospholipase C, $\gamma 2$ acquired in ibrutinib-resistant CLL confers BTK independency upon B-cell receptor activation. *Blood*. 2015;126.
381. Wist M, Meier L, Gutman O, et al. Noncatalytic Bruton's tyrosine kinase activates PLC $\gamma 2$ variants mediating ibrutinib resistance in human chronic lymphocytic leukemia cells. *J Biol Chem*. 2020;295.
382. Ahn IE, Underbayev C, Albitar A, et al. Clonal evolution leading to ibrutinib resistance in chronic lymphocytic leukemia. *Blood*. 2017;129.
383. Brown JR, Hillmen P, O'Brien S, et al. Extended follow-up and impact of high-risk prognostic factors from the phase 3 RESONATE study in patients with previously treated CLL/SLL. *Leukemia*. 2018;32.
384. Barr PM, Robak T, Owen C, et al. Sustained efficacy and detailed clinical follow-up of first-line ibrutinib treatment in older patients with chronic lymphocytic leukemia: extended phase 3 results from RESONATE-2. *Haematologica*. 2018;103.
385. Kipps TJ, Fraser G, Coutre SE, et al. Long-Term Studies Assessing Outcomes of Ibrutinib Therapy in Patients With Del(11q) Chronic Lymphocytic Leukemia. *Clin Lymphoma Myeloma Leuk*. Published online July 15, 2019.
386. Byrd JC, Furman RR, Coutre SE, et al. Ibrutinib Treatment for First-Line and Relapsed/Refractory Chronic Lymphocytic Leukemia: Final Analysis of the Pivotal Phase Ib/II PCYC-1102 Study. *Clin Cancer Res*. 2020;26.
387. Murali I, Kasar S, Naeem A, et al. Activation of the MAPK pathway mediates resistance to PI3K inhibitors in chronic lymphocytic leukemia (cll). *Blood*. Published online March 8, 2021.
388. Lin VS, Xu ZF, Huang DCS, Thijssen R. Bh3 mimetics for the treatment of b-cell malignancies—insights and lessons from the clinic. *Cancers (Basel)*. 2020;12.
389. Souers AJ, Levenson JD, Boghaert ER, et al. ABT-199, a potent and selective BCL-2 inhibitor, achieves antitumor activity while sparing platelets. *Nat Med*. 2013;19.
390. Anderson MA, Deng J, Seymour JF, et al. The BCL2 selective inhibitor venetoclax induces rapid onset apoptosis of CLL cells in patients via a TP53-independent mechanism. *Blood*. 2016;127.
391. Roberts AW, Davids MS, Pagel JM, et al. Targeting BCL2 with Venetoclax in Relapsed Chronic Lymphocytic Leukemia. *N Engl J Med*. 2016;374.
392. Seymour JF, Kipps TJ, Eichhorst B, et al. Venetoclax–Rituximab in Relapsed or Refractory Chronic Lymphocytic Leukemia. *N Engl J Med*. 2018;378.
393. Kater AP, Seymour JF, Hillmen P, et al. Fixed duration of venetoclax-rituximab in relapsed/refractory chronic lymphocytic leukemia eradicates minimal residual disease and prolongs survival: Post-treatment follow-up of the Murano phase III study. *J Clin Oncol*. 2019;37.
394. Al-Sawaf O, Zhang C, Tandon M, et al. Venetoclax plus obinutuzumab versus chlorambucil plus obinutuzumab for previously untreated chronic lymphocytic leukaemia (CLL14): follow-up results from a multicentre, open-label, randomised, phase 3 trial. *Lancet Oncol*. 2020;21.
395. Fischer K, Al-Sawaf O, Bahlo J, et al. Venetoclax and Obinutuzumab in Patients with CLL and Coexisting Conditions. *N Engl J Med*. 2019;380.
396. Blombery P, Anderson MA, Gong JN, et al. Acquisition of the recurrent Gly101Val mutation in BCL2 confers resistance to venetoclax in patients with progressive chronic lymphocytic leukemia. *Cancer Discov*. 2019;9.
397. Birkinshaw RW, Gong J nan, Luo CS, et al. Structures of BCL-2 in complex with venetoclax reveal the molecular basis of resistance mutations. *Nat Commun*. 2019;10.
398. Tausch E, Close W, Dolnik A, et al. Venetoclax resistance and acquired BCL2 mutations in chronic lymphocytic leukemia. *Haematologica*. 2019;104.
399. Lucas F, Larkin K, Thomas Gregory C, et al. Novel BCL2 mutations in venetoclax-

- resistant, ibrutinib-resistant CLL patients with BTK/PLCG2 mutations. *Blood*. 2020;135.
400. Blombery P, Thompson ER, Nguyen T, et al. Multiple BCL2 mutations cooccurring with Gly101Val emerge in chronic lymphocytic leukemia progression on venetoclax. *Blood*. 2020;135.
401. Guièze R, Liu VM, Rosebrock D, et al. Mitochondrial Reprogramming Underlies Resistance to BCL-2 Inhibition in Lymphoid Malignancies. *Cancer Cell*. 2019;36.
402. Herling CD, Abedpour N, Weiss J, et al. Clonal dynamics towards the development of venetoclax resistance in chronic lymphocytic leukemia. *Nat Commun*. 2018;9.
403. Kater AP, Wu JQ, Kipps T, et al. Venetoclax plus rituximab in relapsed chronic lymphocytic leukemia: 4-year results and evaluation of impact of genomic complexity and gene mutations from the MURANO phase III study. In: *Journal of Clinical Oncology*. Vol 38. American Society of Clinical Oncology; 2020:4042-4054.
404. Lanemo Myhrinder A, Hellqvist E, Bergh A-C, et al. Molecular characterization of neoplastic and normal "sister" lymphoblastoid B-cell lines from chronic lymphocytic leukemia. *Leuk Lymphoma*. 2013;54.
405. Hertlein E, Beckwith KA, Lozanski G, et al. Characterization of a New Chronic Lymphocytic Leukemia Cell Line for Mechanistic In Vitro and In Vivo Studies Relevant to Disease. *PLoS One*. 2013;8.
406. Walls E V., Doyle MG, Patel KK, Allday MJ, Catovsky D, Crawford DH. Activation and immortalization of leukaemic B cells by epstein-barr virus. *Int J Cancer*. 1989;44.
407. Çalişkan M, Cusanovich DA, Ober C, Gilad Y. The effects of EBV transformation on gene expression levels and methylation profiles. *Hum Mol Genet*. 2011;20.
408. Stacchini A, Aragno M, Vallario A, et al. MEC1 and MEC2: Two new cell lines derived from B-chronic lymphocytic leukaemia in prolymphocytoid transformation. *Leuk Res*. 1999;23.
409. Rosén A, Bergh AC, Gogolák P, et al. Lymphoblastoid cell line with B1 cell characteristics established from a chronic lymphocytic leukemia clone by in vitro EBV infection. *Oncoimmunology*. 2012;1.
410. Lewin N, Åman P, Mellstedt H, Zech L, Klein G. Direct outgrowth of in vivo epstein-barr virus (EBV)-infected chronic lymphocytic leukemia (CLL) cells into permanent lines. *Int J Cancer*. 1988;41.
411. Hernández-Sánchez M, Rodríguez-Vicente AE, González-Gascón Y, Marín I, et al. DNA damage response-related alterations define the genetic background of patients with chronic lymphocytic leukemia and chromosomal gains. *Exp Hematol*. 2019;72.
412. Quentmeier H, Pommerenke C, Dirks WG, et al. The LL-100 panel: 100 cell lines for blood cancer studies. *Sci Rep*. 2019;9.
413. Bertilaccio MTS, Scielzo C, Simonetti G, et al. Xenograft models of chronic lymphocytic leukemia: Problems, pitfalls and future directions. *Leukemia*. 2013;27.
414. Simonetti G, Bertilaccio MTS, Ghia P, Klein U. Mouse models in the study of chronic lymphocytic leukemia pathogenesis and therapy. *Blood*. 2014;124.
415. Bertilaccio MTS, Scielzo C, Simonetti G, et al. A novel Rag2-/- γ c-/- xenograft model of human CLL. *Blood*. 2010;115.
416. Arruga F, Gizdic B, Bologna C, et al. Mutations in NOTCH1 PEST domain orchestrate CCL19-driven homing of chronic lymphocytic leukemia cells by modulating the tumor suppressor gene DUSP22. *Leukemia*. 2017;31.
417. Mancikova V, Peschelova H, Kozlova V, et al. Performance of anti-CD19 chimeric antigen receptor T cells in genetically defined classes of chronic lymphocytic leukemia. *J Immunother Cancer*. 2020;8.
418. Bagnara D, Kaufman MS, Calissano C, et al. A novel adoptive transfer model of chronic lymphocytic leukemia suggests a key role for T lymphocytes in the disease. *Blood*. 2011;117.
419. Herman SEM, Sun X, McAuley EM, et al. Modeling tumor-host interactions of chronic lymphocytic leukemia in xenografted mice to study tumor biology and evaluate targeted therapy. *Leukemia*. 2013;27.
420. Herman SEM, Wiestner A. Preclinical

- modeling of novel therapeutics in chronic lymphocytic leukemia: The tools of the trade. *Semin Oncol.* 2016;43.
421. Chen SS. Method for Generating a Patient-Derived Xenograft Model of CLL. In: *Methods in Molecular Biology.* Vol 1881. Humana Press Inc.; 2019:165-171.
422. Os A, Bürgler S, Ribes AP, et al. Chronic lymphocytic leukemia cells are activated and proliferate in response to specific T helper cells. *Cell Rep.* 2013;4.
423. Davies NJ, Kwok M, Gould C, et al. Dynamic changes in clonal cytogenetic architecture during progression of chronic lymphocytic leukemia in patients and patient-derived murine xenografts. *Oncotarget.* 2017;8.
424. Decker S, Zwick A, Saleem SK, et al. Optimized xenograft protocol for chronic lymphocytic leukemia results in high engraftment efficiency for all CLL subgroups. *Int J Mol Sci.* 2019;20.
425. Vaisitti T, Braggio E, Allan JN, et al. Novel richter syndrome xenograft models to study genetic architecture, biology, and therapy responses. *Cancer Res.* 2018;78.
426. Vaisitti T, Arruga F, Vitale N, et al. ROR1 targeting with the antibody drug-conjugate VLS-101 is effective in Richter syndrome patient-derived xenograft mouse models. *Blood.* Published online January 14, 2021.
427. Iannello A, Vitale N, Coma S, et al. Synergistic efficacy of dual PI3K-d/g inhibitor Duvelisib with Bcl2 inhibitor Venetoclax in Richter's Syndrome PDX models. *Blood.* Published online March 30, 2021.
428. Bichi R, Shinton SA, Martin ES, et al. Human chronic lymphocytic leukemia modeled in mouse by targeted TCL1 expression. *Proc Natl Acad Sci U S A.* 2002;99.
429. Zapata JM, Krajewska M, Morse HC, Choi Y, Reed JC. TNF receptor-associated factor (TRAF) domain and Bcl-2 cooperate to induce small B cell lymphoma/chronic lymphocytic leukemia in transgenic mice. *Proc Natl Acad Sci U S A.* 2004;101.
430. Stein J V., López-Fraga M, Elustondo FA, et al. APRIL modulates B and T cell immunity. *J Clin Invest.* 2002;109.
431. Widhopf GF, Cui B, Ghia EM, et al. ROR1 can interact with TCL1 and enhance leukemogenesis in Eli-TCL1 transgenic mice. *Proc Natl Acad Sci U S A.* 2014;111.
432. Waterston RH, Lindblad-Toh K, Birney E, et al. Initial sequencing and comparative analysis of the mouse genome. *Nature.* 2002;420.
433. Panayiotidis P, Jones D, Ganeshaguru K, Foroni L, Hoffbrand A V. Human bone marrow stromal cells prevent apoptosis and support the survival of chronic lymphocytic leukaemia cells in vitro. *Br J Haematol.* 1996;92.
434. Kurtova A V., Balakrishnan K, Chen R, et al. Diverse marrow stromal cells protect CLL cells from spontaneous and drug-induced apoptosis: Development of a reliable and reproducible system to assess stromal cell adhesion-mediated drug resistance. *Blood.* 2009;114.
435. Edelmann J, Klein-Hitpass L, Carpinteiro A, et al. Bone marrow fibroblasts induce expression of PI3K/NF- κ B pathway genes and a pro-angiogenic phenotype in CLL cells. *Leuk Res.* 2008;32.
436. Bernal A, Pastore RD, Asgary Z, et al. Survival of leukemic B cells promoted by engagement of the antigen receptor. *Blood.* 2001;98.
437. Longo PG, Laurenti L, Gobessi S, Sica S, Leone G, Efremov DG. The Akt/Mcl-1 pathway plays a prominent role in mediating antiapoptotic signals downstream of the B-cell receptor in chronic lymphocytic leukemia B cells. *Blood.* 2008;111.
438. Guarini A, Chiaretti S, Tavolaro S, et al. BCR ligation induced by IgM stimulation results in gene expression and functional changes only in IgVH unmutated chronic lymphocytic leukemia (CLL) cells. *Blood.* 2008;112.
439. Jahrsdorfer B, Blackwell S, Weiner G. The effects of CpG ODN on CLL proliferation, apoptosis or phenotype could have an impact on its clinical utility [1]. *Leukemia.* 2007;21.
440. Decker T, Schneller F, Sparwasser T, et al. Immunostimulatory CpG-oligonucleotides cause proliferation, cytokine production, and an immunogenic phenotype in chronic lymphocytic leukemia B cells. *Blood.*

- 2000;95.
441. Purroy N, Abrisqueta P, Carabia J, et al. Co-culture of primary CLL cells with bone marrow mesenchymal cells, CD40 ligand and CpG ODN promotes proliferation of chemoresistant CLL cells phenotypically comparable to those proliferating in vivo. *Oncotarget*. 2015;6.
442. Primo D, Scarfò L, Xochelli A, et al. A novel ex vivo high-throughput assay reveals antiproliferative effects of idelalisib and ibrutinib in chronic lymphocytic leukemia. *Oncotarget*. 2018;9.
443. Mongini PKA, Gupta R, Boyle E, et al. TLR-9 and IL-15 Synergy Promotes the In Vitro Clonal Expansion of Chronic Lymphocytic Leukemia B Cells. *J Immunol*. 2015;195.
444. Pascutti MF, Jak M, Tromp JM, et al. IL-21 and CD40L signals from autologous T cells can induce antigen-independent proliferation of CLL cells. *Blood*. 2013;122.
445. Seiffert M, Stilgenbauer S, Döhner H, Lichter P. Efficient nucleofection of primary human B cells and B-CLL cells induces apoptosis, which depends on the microenvironment and on the structure of transfected nucleic acids. *Leukemia*. 2007;21.
446. Cantwell MJ, Sharma S, Friedmann T, Kipps TJ. Adenovirus vector infection of chronic lymphocytic leukemia B cells. *Blood*. 1996;88.
447. Urnov FD, Rebar EJ, Holmes MC, Zhang HS, Gregory PD. Genome editing with engineered zinc finger nucleases. *Nat Rev Genet*. 2010;11.
448. Joung JK, Sander JD. TALENs: A widely applicable technology for targeted genome editing. *Nat Rev Mol Cell Biol*. 2013;14.
449. Hsu PD, Lander ES, Zhang F. Development and Applications of CRISPR-Cas9 for Genome Engineering. *Cell*. 2014;157.
450. Komor AC, Badran AH, Liu DR. CRISPR-Based Technologies for the Manipulation of Eukaryotic Genomes. *Cell*. 2017;168.
451. Tothova Z, Krill-Burger JM, Popova KD, et al. Multiplex CRISPR/Cas9-Based Genome Editing in Human Hematopoietic Stem Cells Models Clonal Hematopoiesis and Myeloid Neoplasia. *Cell Stem Cell*. 2017;21.
452. Heckl D, Kowalczyk MS, Yudovich D, et al. Generation of mouse models of myeloid malignancy with combinatorial genetic lesions using CRISPR-Cas9 genome editing. *Nat Biotechnol*. 2014;32.
453. Sánchez-Rivera FJ, Jacks T. Applications of the CRISPR-Cas9 system in cancer biology. *Nat Rev Cancer*. 2015;15.
454. Choi PS, Meyerson M. Targeted genomic rearrangements using CRISPR/Cas technology. *Nat Commun*. 2014;5.
455. Torres R, Martin MC, Garcia A, Cigudosa JC, Ramirez JC, Rodriguez-Perales S. Engineering human tumour-associated chromosomal translocations with the RNA-guided CRISPR-Cas9 system. *Nat Commun*. 2014;5.
456. Xiao A, Wang Z, Hu Y, et al. Chromosomal deletions and inversions mediated by TALENs and CRISPR/Cas in zebrafish. *Nucleic Acids Res*. 2013;41.
457. Essletzbichler P, Konopka T, Santoro F, et al. Megabase-scale deletion using CRISPR/Cas9 to generate a fully haploid human cell line. *Genome Res*. 2014;24.
458. Yang H, Wang H, Shivalila CS, Cheng AW, Shi L, Jaenisch R. One-step generation of mice carrying reporter and conditional alleles by CRISPR/cas-mediated genome engineering. *Cell*. 2013;154.
459. Mansour MR, Abraham BJ, Anders L, et al. An oncogenic super-enhancer formed through somatic mutation of a noncoding intergenic element. *Science (80-)*. 2014;346.
460. Ho TT, Zhou N, Huang J, et al. Targeting non-coding RNAs with the CRISPR/Cas9 system in human cell lines. *Nucleic Acids Res*. 2015;43.
461. Shalem O, Sanjana NE, Hartenian E, et al. Genome-scale CRISPR-Cas9 knockout screening in human cells. *Science (80-)*. 2014;343.
462. Gilbert LA, Larson MH, Morsut L, et al. CRISPR-mediated modular RNA-guided regulation of transcription in eukaryotes. *Cell*. 2013;154.
463. Gilbert LA, Horlbeck MA, Adamson B, et al. Genome-Scale CRISPR-Mediated Control of Gene Repression and Activation. *Cell*. 2014;159.

464. Cox DBT, Gootenberg JS, Abudayyeh OO, et al. RNA editing with CRISPR-Cas13. *Science* (80-). 2017;358.
465. Tian X, Gu T, Patel S, Bode AM, Lee M-H, Dong Z. CRISPR/Cas9 – An evolving biological tool kit for cancer biology and oncology. *npj Precis Oncol*. 2019;3.
466. Amin NA, Balasubramanian S, Saiya-Cork K, Shedden K, Hu N, Malek SN. Cell-intrinsic determinants of ibrutinib-induced apoptosis in chronic lymphocytic leukemia. *Clin Cancer Res*. 2017;23.
467. Yu J, Chen L, Chen Y, et al. Wnt5a induces ROR1 to associate with 14-3-3 ζ for enhanced chemotaxis and proliferation of chronic lymphocytic leukemia cells. *Leukemia*. 2017;31.
468. Gassner FJ, Zaborsky N, Buchumenski I, et al. RNA editing contributes to epitranscriptome diversity in chronic lymphocytic leukemia. *Leukemia*. 2021;35.
469. ten Hacken E, Clement K, Li S, et al. High throughput single-cell detection of multiplex CRISPR-edited gene modifications. *Genome Biol*. 2020;21.
470. Di Ianni M, Baldoni S, Del Papa B, et al. NOTCH1 is aberrantly activated in chronic lymphocytic leukemia hematopoietic stem cells. *Front Oncol*. 2018;8.
471. Wang L, Fan J, Francis JM, et al. Integrated single-cell genetic and transcriptional analysis suggests novel drivers of chronic lymphocytic leukemia. *Genome Res*. 2017;27.
472. Rodriguez-Meira A, Buck G, Clark SA, et al. Unravelling Intratumoral Heterogeneity through High-Sensitivity Single-Cell Mutational Analysis and Parallel RNA Sequencing. *Mol Cell*. 2019;73.
473. Rodriguez-Meira A, O'Sullivan J, Rahman H, Mead AJ. TARGET-Seq: A Protocol for High-Sensitivity Single-Cell Mutational Analysis and Parallel RNA Sequencing. *STAR Protoc*. 2020;1.
474. Ramassone A, D'Argenio A, Veronese A, et al. Genetic dynamics in untreated CLL patients with either stable or progressive disease: A longitudinal study. *J Hematol Oncol*. 2019;12.
475. Kostopoulou F, Gabillaud C, Chapiro E, et al. Gain of the short arm of chromosome 2 (2p gain) has a significant role in drug-resistant chronic lymphocytic leukemia. *Cancer Med*. 2019;8.
476. Chapiro E, Leporrier N, Radford-Weiss I, et al. Gain of the short arm of chromosome 2 (2p) is a frequent recurring chromosome aberration in untreated chronic lymphocytic leukemia (CLL) at advanced stages. *Leuk Res*. 2010;34.
477. Kandath C, McLellan MD, Vandin F, et al. Mutational landscape and significance across 12 major cancer types. *Nature*. 2013;502.
478. Cisowski J, Bergo MO. What makes oncogenes mutually exclusive? *Small GTPases*. 2017;8.
479. Yeang C-H, McCormick F, Levine A. Combinatorial patterns of somatic gene mutations in cancer. *FASEB J*. 2008;22.
480. Saarinen S, Aavikko M, Aittomäki K, et al. Exome sequencing reveals germline NPAT mutation as a candidate risk factor for Hodgkin lymphoma. *Blood*. 2011;118.
481. Zhao G, Gong L, Su D, et al. Cullin5 deficiency promotes small-cell lung cancer metastasis by stabilizing integrin β 1. *J Clin Invest*. 2019;129.
482. Wang SS, Esplin ED, Li JL, et al. Alterations of the PPP2R1B gene in human lung and colon cancer. *Science* (80-). 1998;282.
483. Wlodarchak N, Xing Y. PP2A as a master regulator of the cell cycle. *Crit Rev Biochem Mol Biol*. 2016;51.
484. Tibaldi E, Pagano MA, Frezzato F, et al. Targeted activation of the SHP-1/PP2A signaling axis elicits apoptosis of chronic lymphocytic leukemia cells. *Haematologica*. 2017;102.
485. Close V, Close W, Kugler SJ, et al. NOTCH1 Signaling Is Activated in CLL By Mutations of FBXW7 and Low Expression of USP28 at 11q23. *Blood*. 2018;132.
486. Weston VJ, Oldreive CE, Skowronska A, et al. The PARP inhibitor olaparib induces significant killing of ATM-deficient lymphoid tumor cells in vitro and in vivo. *Blood*. 2010;116.
487. Knittel G, Rehkämper T, Korovkina D, et al. Two mouse models reveal an actionable PARP1 dependence in aggressive chronic lymphocytic leukemia. *Nat Commun*.

- 2017;8.
488. Montraveta A, Lee-Vergés E, Roldán J, et al. CD69 expression potentially predicts response to bendamustine and its modulation by ibrutinib or idelalisib enhances cytotoxic effect in chronic lymphocytic leukemia. *Oncotarget*. 2016;7.
489. Modi P, Balakrishnan K, Yang Q, Wierda WG, Keating MJ, Gandhi V. Idelalisib and bendamustine combination is synergistic and increases DNA damage response in chronic lymphocytic leukemia cells. *Oncotarget*. 2017;8.
490. Kost SEF, Saleh A, Mejia EM, et al. Transcriptional modulation by idelalisib synergizes with bendamustine in chronic lymphocytic leukemia. *Cancers (Basel)*. 2019;11.
491. Davids MS, Brander DM, Kim HT, et al. Ibrutinib plus fludarabine, cyclophosphamide, and rituximab as initial treatment for younger patients with chronic lymphocytic leukaemia: a single-arm, multicentre, phase 2 trial. *Lancet Haematol*. 2019;6.
492. von Tresckow J, Cramer P, Bahlo J, et al. CLL2-BIG: sequential treatment with bendamustine, ibrutinib and obinutuzumab (GA101) in chronic lymphocytic leukemia. *Leukemia*. 2019;33.
493. Davids MS, Fisher DC, Tyekucheva S, et al. A phase 1b/2 study of duvelisib in combination with FCR (DFCR) for frontline therapy for younger CLL patients. *Leukemia*. 2021;35.
494. Kwok M, Davies N, Agathangelou A, et al. ATR inhibition induces synthetic lethality and overcomes chemoresistance in TP53- or ATM-defective chronic lymphocytic leukemia cells. *Blood*. 2016;127.
495. Riabinska A, Daheim M, Herter-Sprie GS, et al. Therapeutic targeting of a robust non-oncogene addiction to PRKDC in ATM-defective tumors. *Sci Transl Med*. 2013;5.
496. Thijssen R, Ter Burg J, Garrick B, et al. Dual TORC/DNA-PK inhibition blocks critical signaling pathways in chronic lymphocytic leukemia. *Blood*. 2016;128.
497. Boudny M, Zemanova J, Khirsariya P, et al. Novel CHK1 inhibitor MU380 exhibits significant single-agent activity in TP53-mutated chronic lymphocytic leukemia cells. *Haematologica*. 2019;104.
498. Agathangelou A, Smith E, Davies NJ, et al. USP7 inhibition alters homologous recombination repair and targets CLL cells independently of ATM/p53 functional status. *Blood*. 2017;130.
499. Haselager M, Thijssen R, West C, et al. Regulation of Bcl-XL by non-canonical NF- κ B in the context of CD40-induced drug resistance in CLL. *Cell Death Differ*. Published online 2021.
500. Annunziata CM, Davis RE, Demchenko Y, et al. Frequent Engagement of the Classical and Alternative NF- κ B Pathways by Diverse Genetic Abnormalities in Multiple Myeloma. *Cancer Cell*. 2007;12.
501. Demchenko YN, Glebov OK, Zingone A, Keats JJ, Leif Bergsagel P, Michael Kuehl W. Classical and/or alternative NF- κ B pathway activation in multiple myeloma. *Blood*. 2010;115.
502. Demchenko YN, Brents LA, Li Z, Bergsagel LP, McGee LR, Kuehl MW. Novel inhibitors are cytotoxic for myeloma cells with NF κ B inducing kinase-dependent activation of NF κ B. *Oncotarget*. 2014;5.
503. Döhner H, Stilgenbauer S, Benner A, et al. Genomic aberrations and survival in chronic lymphocytic leukemia. *N Engl J Med*. 2000;343.
504. Zimmermann M, Murina O, Reijns MAM, et al. CRISPR screens identify genomic ribonucleotides as a source of PARP-trapping lesions. *Nature*. 2018;559.
505. Mangolini M, Maiques-Diaz A, Charalampopoulou S, et al. NOTCH1 drives immune-escape mechanisms in B cell malignancies. *bioRxiv*. Published online April 11, 2021.
506. Caesar R, Di Re M, Krupka JA, et al. Genetic modification of primary human B cells to model high-grade lymphoma. *Nat Commun*. 2019;10.
507. Caesar R, Gao J, Di Re M, Gong C, Hodson DJ. Genetic manipulation and immortalized culture of ex vivo primary human germinal center B cells. *Nat Protoc*. 2021;16.
508. Mandal PK, Ferreira LMR, Collins R, et al. Efficient ablation of genes in human hematopoietic stem and effector cells

- using CRISPR/Cas9. *Cell Stem Cell*. 2014;15.
509. Vakulskas CA, Dever DP, Rettig GR, et al. A high-fidelity Cas9 mutant delivered as a ribonucleoprotein complex enables efficient gene editing in human hematopoietic stem and progenitor cells. *Nat Med*. 2018;24.

SUPPLEMENTARY APPENDIX

SUPPLEMENTARY APPENDIX – CHAPTER 1

Quijada-Álamo et al. *Journal of Hematology & Oncology* (2017) 10:83
DOI 10.1186/s13045-017-0450-y

Journal of
Hematology & Oncology

RESEARCH

Open Access



Next-generation sequencing and FISH studies reveal the appearance of gene mutations and chromosomal abnormalities in hematopoietic progenitors in chronic lymphocytic leukemia

Miguel Quijada-Álamo^{1†}, María Hernández-Sánchez^{1†}, Cristina Robledo¹, Jesús-María Hernández-Sánchez¹, Rocío Benito¹, Adrián Montaña¹, Ana E. Rodríguez-Vicente^{1,2}, Dalia Quwaider¹, Ana-África Martín¹, María García-Álvarez¹, María Jesús Vidal-Manceño³, Gonzalo Ferrer-Garrido⁴, María-Pilar Delgado-Beltrán⁴, Josefina Galende⁵, Juan-Nicolás Rodríguez⁶, Guillermo Martín-Núñez⁷, José-María Alonso⁸, Alfonso García de Coca⁹, José A. Queizán¹⁰, Magdalena Sierra¹¹, Carlos Aguilar¹², Alexander Kohlmann^{13,14}, José-Ángel Hernández¹⁵, Marcos González¹ and Jesús-María Hernández-Rivas^{1,16*}

ADDITIONAL TABLES – CHAPTER 1

Additional Table 1. Clinico-biological characteristics from CLL patients.

Characteristic	Category	
Age (years)		61 [25-91]
Gender	Male	55.4%
Binet Clinical Stage	A	70.3%
	B	27%
	C	2.7%
Lymphadenopathies	Yes	51.4%
Splenomegaly	Yes	15.8%
Hepatomegaly	Yes	7.9%
Leukocyte count (x10 ⁹ /L)		16.7 [5.1-369]
Lymphocyte count (x10 ⁹ /L)		10.3 [1.5-355]
Platelet count (x10 ⁹ /L)		173 [83-337]
Hemoglobin (g/dL)		14.1 [7.2-16.6]
Serum LDH	High	3%
Serum β_2 microglobulin	High	29.2%
<i>IGHV</i> mutational status	Unmutated	53.6%
CD38 expression	Positive	10.6%
FISH	Normal	30.4%
	11q-	11.3%
	+12	17%
	13q-	46.3%
	<i>IGH</i> alterations	9.3%
	17p-	1.9%
First Therapy*	Yes	84.2%
Median TFT** (months)		35
Died during follow-up	Yes	11.4%
Median OS*** (months)		76

*13 BM samples were collected after treatment.

TFT: Time to first therapy; *OS: Overall Survival.

Additional Table 2. Illumina Primer Design.

Gene	Exon	Forward Primer (5'-3')	Reverse Primer (5'-3')	Amplicon Product Length (bp)
<i>FBXW7</i>	9	GIGTTTTCCAGTGTCTGAGAACAT	AGAAGTCCCAACCATGACAAGA	227
<i>MYD88</i>	4	TCCCAGGGGATATGCTGAAC	ATTCTCTTGCCAGAGCAGGG	183
<i>NOTCH1</i>	34	TGACCGCAGCCCAGTTC	ACTTGAAGGCCTCCGGAATG	240
<i>SF3B1</i>	14	TACCAACTCATGACTGTCCTTTC	CAGTGTGTCTCGCTTGCCA	224
<i>XPO1</i>	15	AGTAGGTCAATACCCACGTTTT	TCACAAGCCATATCCTGGACTC	243

Additional Table 3. Validation of mutations detected at low frequency by ultra-deep NGS in flow-sorted cell fractions using 454 sequencing.

Patient ID	Mutated Gene	%mut CD34+CD19-	%mut CD3+	%mut CD14+
13	<i>MYD88</i>	7.1	1.3	3.7
31	<i>NOTCH1</i>	2.7	0	-
37	<i>XPO1</i>	-	2.3	-
42	<i>NOTCH1</i>	5.1	0	-
50	<i>SF3B1</i>	1.6	-	-
57	<i>FBXW7</i>	4.4	0.9	-

Additional Table 4. Patients characteristics regarding the presence of mutations in CD34+ progenitors

Characteristic	Category	Patients with mutated CD34+ cells (n=15) (%)	Patients with unmutated CD34+ cells (n=41) (%)	P
Age (years)		61 [50-83]	61 [25-91]	0.749
Leukocytes, range / μ L		26200 [5090-369000]	15900 [7200-279000]	0.226
Lymphocytes, range / μ L		20300 [1520-355000]	9100 [3400-270000]	0.226
Platelet count, range / μ L		137000 [83000-213000]	176000 [95000-337000]	0.416
Hemoglobin, range g/dL		12.8 [7.2-16.2]	14.5 [8.0-16.6]	0.08
<i>IGHV</i>	Unmutated	86.7	42.5	0.003
CD38	Positive	7.1	12.1	0.613
FISH	11q-	14.3	10.3	0.683
	+12	7.1	20.5	0.253
	13q-	53.3	43.6	0.520
	<i>IGH alt</i>	7.1	10.0	0.751
	17p-	0	2.6	0.545
Sex	Male	40.0	61.0	0.162
B ₂ microglobulin	High	62.5	12.5	0.011
Binet Stage	B and C	44.4	25.0	0.267
Lymphadenopathy	Yes	50.0	52.0	0.915
Hepatomegaly	Yes	20.0	3.6	0.098
Splenomegaly	Yes	30.0	10.7	0.151
Died during follow-up	Yes	23.1	0	0.007
Therapy during follow-up	Yes	90.9	80.8	0.444

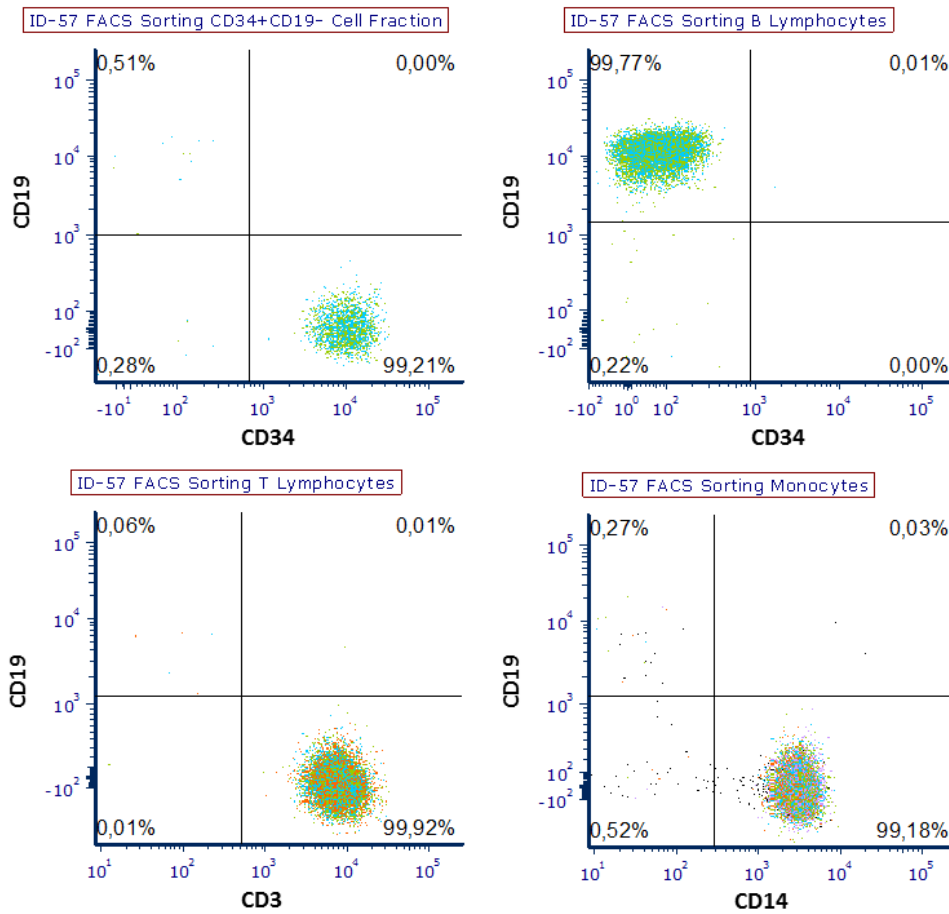
Additional Table 5. Patients characteristics regarding the mutational burden maintenance or decrease in CD34+ progenitors.

Characteristic	Category	Mutations maintained on CD34+ progenitors (n=12) (%)	Mutations decreased on CD34+ progenitors (n=8) (%)	P
Age (years)		60 [50-83]	67 [60-82]	0.302
Leukocytes, range / μ L		18000 [5090-369000]	26400 [11900-87300]	1.0
Lymphocytes, range / μ L		13900 [1520-355000]	21100 [7200-74900]	1.0
Platelet count, range / μ L		150000 [100000-226000]	116000 [83000-262000]	1.0
Hemoglobin, range g/dL		12.6 [7.2-16.2]	14.6 [8.0-15.3]	1.0
<i>IGHV</i>	Unmutated	92.3	57.1	0.061
CD38	Positive	0	14.3	0.179
FISH	11q-	15.4	0	0.310
	+12	0	33.3	0.028
	13q-	46.2	42.9	0.888
	<i>IGH alt</i>	15.4	0	0.310
	17p-	0	0	-
Sex	Male	30.8	71.4	0.081
B ₂ microglobulin	High	50.0	100	0.197
Binet Stage	B and C	33.3	50.0	0.569
Lymphadenopathy	Yes	44.4	25.0	0.506
Hepatomegaly	Yes	22.2	0	0.255
Splenomegaly	Yes	22.2	20.0	0.923
Died during follow-up	Yes	27.3	33.3	0.793
Therapy during follow-up	Yes	90.0	100.0	0.464

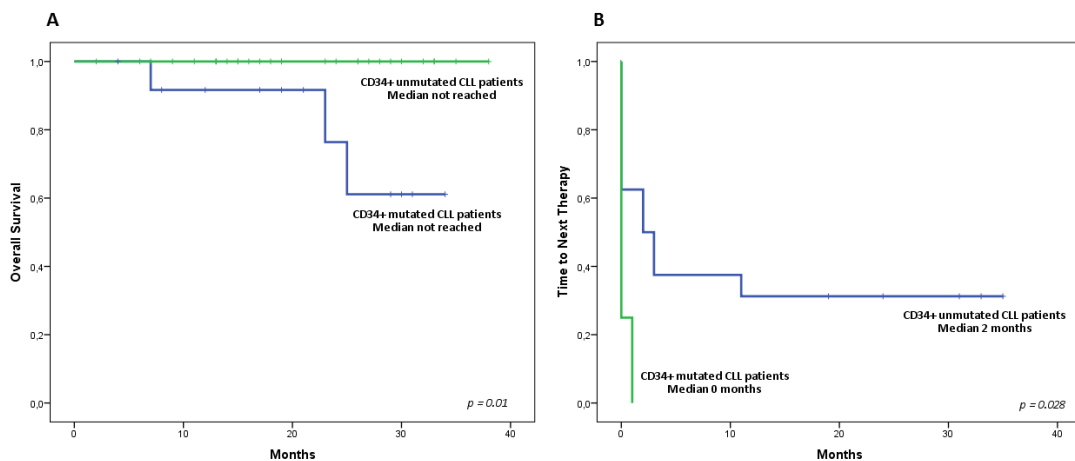
Additional Table 6. Treatments prior bone marrow extraction of 4 CLL patients who relapsed and correlation with the CD19+ and CD34+ mutational status.

Patient ID	Last treatment before BM extraction	Time between last dose and BM extraction (months)	Mutated Gene	%CD19	%CD34
8	Lenalidomide + Rituximab	18	<i>NOTCH1</i>	97.5	79.5
33	Fludarabine + Rituximab	36	<i>NOTCH1</i>	41.0	40.5
34	Bendamustine	27	<i>NOTCH1</i>	50.0	51.5
			<i>XPO1</i>	24.5	24.5
43	Chlorambucil + Obinutuzumab	31	<i>SF3B1</i>	47.5	45.0

ADDITIONAL FIGURES – CHAPTER 1



Additional Figure 1. Representation of the purity analysis of FACS sorted cell populations. CD34⁺CD19⁻hematopoietic stem cells; CD19⁺ B lymphocytes; CD3⁺ T lymphocytes; CD14⁺ monocytes.



Additional Figure 2. Kaplan-Meier analysis of overall survival (A) and time to first therapy (B) in patients with mutations in their CD34⁺ progenitors.

SUPPLEMENTARY APPENDIX – CHAPTER 2

Leukemia
<https://doi.org/10.1038/s41375-020-0714-3>

ARTICLE



Chronic lymphocytic leukemia

CRISPR/Cas9-generated models uncover therapeutic vulnerabilities of del(11q) CLL cells to dual BCR and PARP inhibition

Miguel Quijada-Álamo^{1,2} · María Hernández-Sánchez^{1,2,3,4} · Verónica Alonso-Pérez^{1,2} · Ana E. Rodríguez-Vicente^{1,2} · Ignacio García-Tuñón^{1,2} · Marta Martín-Izquierdo^{1,2} · Jesús María Hernández-Sánchez^{1,2} · Ana B. Herrero^{1,2} · José María Bastida² · Laura San Segundo^{1,2} · Michaela Gruber^{3,4,5,6} · Juan Luis García^{1,2} · Shanye Yin^{3,4} · Elisa ten Hacken^{3,4} · Rocío Benito^{1,2} · José Luis Ordóñez^{1,2} · Catherine J. Wu^{3,4} · Jesús María Hernández-Rivas^{1,2,7}

SUPPLEMENTAL METHODS

Cell lines and culture conditions

The human CLL-derived cell lines HG3 and MEC1 were purchased from DMSZ (Deutsche Sammlung von Mikroorganismen and Zellkulturen). HG3 cells were cultured in RPMI 1640 medium (Life Technologies) supplemented with 15% Fetal Bovine Serum (FBS), 1% glutaMAX and 1% penicillin/streptomycin (Life Technologies). MEC1 cells were cultured in Iscove'sMDM medium (Lonza) supplemented with 10% FBS, 1% glutaMAX and 1% penicillin/streptomycin. HEK 293T cells and HS-5 bone marrow stromal cells were obtained from DMSZ and ATCC (American Type Culture Collection), respectively, and used for lentiviral production and primary CLL co-cultures, respectively. They were maintained in DMEM (Life Technologies) supplemented with 10% FBS, 1% glutaMAX and 1% penicillin/streptomycin. All cell lines were incubated at 37°C in a 5% CO₂ atmosphere. The presence of mycoplasma was tested frequently in all cell lines with MycoAlert kit (Lonza), only using mycoplasma-free cells in all the experiments carried out.

Drugs and Reagents

Olaparib and ibrutinib, were obtained from LC Laboratories, bendamustine and copanlisib were from Selleckchem and B02 was from Sigma. For the *in vitro* experiments, all drugs were resuspended in DMSO (Sigma). In the *in vivo* model, olaparib was prepared in

2-hydroxyl-propyl- β cyclodextrin 10% (Sigma) in phosphate-buffered saline (PBS) plus 10% DMSO.

Next-Generation Sequencing

A targeted-capture next-generation sequencing (NGS) strategy was used to analyze the mutational status of *ATM*, *BIRC3*, *NOTCH1*, *TP53*, *SE3B1*, *XPO1*, *MYD88* and *FBXW7*. These genes were included in a custom-panel of 57 genes previously reported as mutated in CLL or involved in the disease pathogenesis^{1,2} following the approach of Agilent SureDesign. Sequence data generated by Illumina NextSeq 500 was analyzed by an in-house bioinformatic pipeline mapping reads to the Reference Human Genome (hg19). Burrows-Wheeler-Aligner (BWA) and Genome Analysis Tool Kit (GATK) were used for variant-calling of single nucleotide variants (SNVs) and short insertions/deletions (InDels)³. Supplementary Table S2 shows the regions analyzed for this study and the coverage data for each gene. Filters were set to display sequence variants occurring in more than 2% of reads. Variants were then filtered according to the severity of the consequence, to accept variants leading to an amino acid change in the protein sequence (missense, nonsense, frameshift) and those in the splice site. Minor allelic frequencies (MAFs) were consulted in the Exome Variant Server, 1000 Genomes Browser and exome aggregation consortium (ExAC) databases; removing those with a MAF of >1%. Several in silico tools such as Sorting Intolerant From Tolerant (SIFT) and Polymorphism Phenotyping v2 (PolyPhen-2) (HDIV and HVAR scores) were used to predict the functional effects and pathogenicity of the novel variants. All accepted mutations were reviewed individually by Integrative Genomics Viewer (IGV) (Broad Institute, Cambridge, MA, USA) software. Supplementary Table S3 shows the list of mutations in CLL patients.

Lentiviral production and cell transduction

The lentiviral constructions were co-transfected in addition to pMD2.G (Addgene #12259) and psPAX2 (Addgene #12260) into HEK 293T using Lipofectamine 2000[®] (Life Technologies). Supernatant containing the lentiviral particles was collected 48 and 72 hours after transfection and subsequently concentrated using Lenti-X concentrator[®] (Clontech). For transduction, fresh lentiviruses were used to infect 5×10^5 cells cultured in medium supplemented with 8 $\mu\text{g}/\text{mL}$ polybrene and seeded in a 24-well plate.

Lentiviral particles containing plasmids for expression of Cas9 and blasticidine were transduced into each cell line and selected by blasticidine (20 µg/ml) for two weeks⁴. Cas9 activity was tested using a previously reported system⁵.

pLKO5 vectors carrying the desired sgRNAs were packed into lentiviral particles and transduced in Cas9-expressing HG3 and MEC1 cell lines. 72 hours after transduction, GFP+ and/or RFP+ cells were flow-sorted and single-cell seeded in 96-well plates. Clones were analyzed by Sanger sequencing to investigate the presence of mutations at the cut sites.

sgRNAs nucleofection

To generate del(11q) in HG3 cells, pLKO5 vectors targeting both 11q22.1 and 11q23.3 were nucleofected simultaneously using the Cell Line V Nucleofector Kit (Lonza). Clones were analyzed by Sanger sequencing to investigate the presence of the fusion region between 11q22.1 and 11q23.3 and the positive clones were validated by fluorescence *in situ* hybridization (FISH).

PCR and sequencing of sgRNA target sites

Genomic DNA (gDNA) was extracted using the QIAampDNA Micro Kit (Qiagen) following the manufacturer's instructions. PCR was performed using primers flanking the target sites for the sgRNAs (Table S4). For screening the loss-of-function mutations, PCR products were purified using High Pure PCR Product Purification Kit (Roche) and resulting indels at the expected locations were confirmed by Sanger sequencing. The efficiency of the sgRNAs was assessed by Tracking of Indels by Decomposition (TIDE) software (<https://tide-calculator.nki.nl>; Netherlands Cancer Institute)⁶. For del(11q), the resultant product was screened by a pair of primers flanking upstream and downstream of the 2 sgRNA cleavage sites for each deletion. In the absence of deletion, this product is too large to be efficiently amplified. Two additional pair of primers flanking each sgRNA target site being one of the primers internal to the sequence to be deleted were used to characterize the non-deleted allele in monoallelic deletion clones.

Fluorescence in situ hybridization

Interphase FISH was carried out in primary CLL samples as well as CRISPR/Cas9 generated cell lines using the commercially available probes: 11q22/*ATM*, 12p11.1-q11 (alpha satellite), 13q14 and 17p13/*TP53* (Vysis/Abbott Co, Abbott Park, IL, USA). Dual-color FISH using differently labeled control and test probes was implemented following the methods previously described⁷.

Flow cytometry

Virally transduced cell lines were single-cell sorted by fluorescence-activated cell sorting (FACS) in a FACS Aria cytometer (BD Biosciences) using two strategies: 1) for 11q deletion, GFP and RFP double positive cells were sorted; 2) for loss-of-function mutated cells, either RFP and/or GFP cells were selected.

In addition, Cas9 activity of HG3-Cas9 and MEC1-Cas9 cell lines transduced with pXPR-011 plasmid was assessed by flow cytometry. Cells were washed twice in PBS and the samples and the data were acquired in an Accuri C6 Flow Cytometer and analyzed using Flowjo software.

Western blot analysis

For whole cell-lysates, cells were washed with PBS and lysed in ice-cold lysis buffer (140 mmol/l NaCl, 50 mmol/l EDTA, 10% glycerol, 1% Nonidet P-40, 20 mmol/l TrisHCl pH 7) containing protease inhibitors (cOmplete™) (Roche). Protein concentration was measured using the Bradford assay (BioRad). Protein samples were subjected to SDS-PAGE and transferred to a nitrocellulose membrane (GE Healthcare). After blocking, membranes were incubated with anti-human antibodies. The following primary antibodies purchased from Cell Signaling Technologies were used: anti-ATM (#2873, Rabbit), anti-PARP1 (#9542, Rabbit), anti-p-BTK (#5082, Rabbit), anti-BTK (#8547, Rabbit), anti-p-AKT (#9271, Rabbit), anti-AKT (#9272, Rabbit), anti-HMGB1 (#3935, Rabbit), anti- β -actin (#4967, Rabbit), anti-Vinculin (#4650, Rabbit), anti α/β tubulin (#2148, Rabbit) and anti-GAPDH (#5174, Rabbit). Horseradish peroxidase-linked anti-rabbit antibody (#7074, Cell Signaling Technologies) was used as secondary antibody at 1:5,000 dilution. Antibody signal was detected using ECL™ Western Blotting Detection Reagents (RPN2209, GE Healthcare).

Viability assay

Cell proliferation was assessed using 3-(4,5-dimethylthiazol-2-yl)-2,5-diphenyltetrazolium bromide (MTT) colorimetric assay (Sigma-Aldrich). After drug treatment, cells were incubated for 2h with a 1:10 MTT solution and subsequently added 1:2 SDS-HCl in agitation for 6 hours. Absorbance was read on an Infinite® F500 Tecan plate reader (Tecan) at 570nm. To define drug-drug interactions (in terms of synergism, additivity, or antagonism), the combination index (CI) was calculated according to the Chou-Talalay method^{8,9}, using CalcuSyn software Version 2.0 (Biosoft). Synergy levels were divided into:

< 0.1 very strong synergism; 0.1-0.90, synergism (ranging from strong synergism to slight synergism), and 0.90-1.10, nearly additive to additive.

γ H2AX and RAD51 immunofluorescence

Cells were irradiated at a dose of 2 Gy during the exponential phase of cell growth with γ -rays using a Gammacell 1000 Elite irradiator (Cesium137). After 1 hour (γ H2AX) or 6 hour (RAD51) incubation at 37°C, 5×10^4 cells were fixed and permeabilized onto poly-L lysine-coated slides as previously described¹⁰. After blockade, slides were incubated with anti- γ H2AX (Millipore) or anti-RAD51 (Calbiochem) antibodies at 1:1,000 dilution for 2 hours. CyTM5 Goat Anti-Mouse or CyTM3 Goat Anti-Rabbit (Jackson ImmunoResearch) were used as secondary antibodies (1:1,000; 1 hour). Nuclei were stained with DAPI (4',6'-diamidino-2-phenylindol), diluted in PBS and incubated for 3 min in agitation at room temperature. Cells were washed twice in PBS and slides were mounted with Vectashield reagent (Vector Laboratories). Images were acquired using a Leica TCS SP5DMI-6000B confocal microscope (Leica) and analyzed with Leica LAS AF (Leica) and ImageJ software (<https://imagej.nih.gov/ij/>).

Comet assay

Cells were irradiated at a dose of 40 Gy during the exponential phase of cell growth with γ -rays using a Gammacell 1000 Elite irradiator (Cesium137). After irradiation, samples were incubated for 3h at 37°C and processed for neutral comet assay as previously described¹¹. In the experiments of drug-induced analysis of DSBs, cells were pre-incubated with olaparib (5 μ M), ibrutinib (5 μ M) and/or bendamustine (50 μ M) for 16 hours and subsequently processed for neutral comet assay. In brief, 2×10^5 cells/ml were adjusted in ice-cold PBS and mixed with LMAgarose (Trevigen), at 37°C, at a ratio of 1:10 (v/v). Right after, 25 μ L of this mixture were transferred onto CometSlide slides (Trevigen) and placed at 4°C for 10-20 minutes. Slides were incubated in N1 lysis solution¹¹ overnight at 37°C in the dark. After rinsing twice in N2 buffer¹¹, slides were subjected to electrophoresis in N2 solution for 25 min at 1V/cm at 4°C. Samples were stained with ethidium bromide and analyzed with a fluorescence microscope (Zeiss Axioplan 2) equipped with a Hamamatsu Orca-EC camera. Images were obtained using Openlab software. CometScoreTM software was used for tail moment quantification of at least 50 cells per condition.

Apoptosis analysis

Apoptosis in response to drug treatment was measured by flow cytometry with annexin V-Dy634 (Immunostep) according to the manufacturer's instructions. In brief, 3×10^5 cells were seeded in 24-well plates and treated 48 hours with the drug concentration of interest, then they were labeled with annexin V and propidium iodide (PI). Since RFP⁺ signal was detected on the same channel as PI in our flow-cytometer, only GFP⁺ clones could be included in these studies.

Transwell migration assays

The migration studies were carried out in TranswellTM plates with permeable polycarbonate membrane inserts (Corning) with 6.5 mm diameter and 5 μ m pore size. Briefly, 3×10^5 cells were serum starved and incubated with olaparib, ibrutinib or the combination of both drugs at 1.25 μ M concentration. After 12 hours, cells were placed on the top of the TranswellTM membrane and migration towards 200 ng/ml CCL19 (300-29B; Peprotech) was performed. The number of migrated cells was subsequently quantified in an Accuri C6 Flow Cytometer.

Homologous recombination (HR) activity assay

The HR activity of HG3 cells after ibrutinib treatment was measured using an HR-reporter plasmid previously described¹². The plasmid was digested with the restriction enzyme I-SceI and purified. HG3 cells were pretreated with ibrutinib for 12 hours and subsequently transfected with the HR digested construct (2 μ g) together with the plasmid pDsRed-N1 (2 μ g) as a control of positive-transfected cells, using the Cell Line V Nucleofector Kit (Lonza). After transfection, cells were incubated with ibrutinib for another 24 hours. Live cells were selected by FSC/SSC gating, and live GFP⁺ and DsRed⁺ cells were quantified by flow cytometry. HR efficiency was calculated as the ratio of GFP⁺ to DsRed⁺ cells. One million events per sample were analyzed. Efficiency of HR was calculated by dividing the number of GFP⁺ cells of the totality of positive-transfected DsRed⁺ cells.

Xenograft experiments

To test the olaparib efficacy in an intravenous xenograft model 20 four-to-five-week-old female NSG mice were used. 3×10^6 cells were resuspended in 100 μ L of cellular medium and injected into the tail vein of the mice. Mice were injected either with HG3^{WT} cells ($n = 10$) or HG3-del(11q) *ATM*^{KO} cells ($n = 10$). Seven days after cell injection, mice were randomized and received either 100 mg/kg olaparib, or vehicle, 2-hydroxyl-propyl- β cyclodextrin 10% in PBS plus 10% DMSO, via intraperitoneal injection, twice daily during five days a week. Mice

were monitored daily during the survival experiment and sacrificed by anesthesia overdose when they presented symptoms of severe disease (lethargy and >20% loss of body weight).

For the analysis of the engraftment in NSG mice, 40 μ L of peripheral blood samples were collected from the tail vein. Red blood cells were lysed with erythrocyte lysis buffer, and the remaining cells were then washed twice in PBS. Samples were stained with fluorophore-conjugated antibodies against mouse-CD45 (PerCP-Cy5.5, BD Biosciences), human-CD45 (hCD45) (CF Blue, Immunostep), CD19 (PE-Cy7, Immunostep) and CD5 (APC, BD Biosciences). Data were obtained on a FACS Aria flow cytometer and analyzed with FlowJo software.

SUPPLEMENTAL REFERENCES

1. Landau DA, Tausch E, Taylor-Weiner AN, et al. Mutations driving CLL and their evolution in progression and relapse. *Nature*. 2015;526.
2. Puente XS, Beà S, Valdés-Mas R, Villamor N, et al. Non-coding recurrent mutations in chronic lymphocytic leukaemia. *Nature*. 2015;526.
3. DePristo MA, Banks E, Poplin R, et al. A framework for variation discovery and genotyping using next-generation DNA sequencing data. *Nat Genet*. 2011;43.
4. Sanjana NE, Shalem O, Zhang F. Improved vectors and genome-wide libraries for CRISPR screening. *Nat Methods*. 2014;11.
5. Doench JG, Hartenian E, Graham DB, et al. Rational design of highly active sgRNAs for CRISPR-Cas9-mediated gene inactivation. *Nat Biotechnol*. 2014;32.
6. Brinkman EK, Chen T, Amendola M, van Steensel B. Easy quantitative assessment of genome editing by sequence trace decomposition. *Nucleic Acids Res*. 2014;42.
7. González MB, Hernández JM, García JL, et al. The value of fluorescence in situ hybridization for the detection of 11q in multiple myeloma. *Haematologica*. 2004;89.
8. Chou TC, Talalay P. Quantitative analysis of dose-effect relationships: the combined effects of multiple drugs or enzyme inhibitors. *Adv Enzyme Regul*. 1984;22.
9. Chou TC, Motzer RJ, Tong Y, Bosl GJ. Computerized quantitation of synergism and antagonism of taxol, topotecan, and cisplatin against human teratocarcinoma cell growth: a rational approach to clinical protocol design. *J Natl Cancer Inst*. 1994;86.
10. Herrero AB, San Miguel J, Gutierrez NC. Deregulation of DNA double-strand break repair in multiple myeloma: implications for genome stability. *PLoS One*. 2015;10.
11. Olive PL, Banáth JP. The comet assay: a method to measure DNA damage in individual cells. *Nat Protoc*. 2006;1.
12. Mao Z, Bozzella M, Seluanov A, Gorbunova V. Comparison of nonhomologous end joining and homologous recombination in human cells. *DNA Repair (Amst)*. 2008;7.

SUPPLEMENTAL TABLES – CHAPTER 2

Supplemental Table 1. Clinical and biological characteristics of CLL patients.

Sample ID	Sex	Treatment	IGHV status	Cytogenetics (FISH)	% del(11q)	ATM mutations	ATM status	Other mutated CLL drivers	Sample used in
ID-01	F	No	NA	del(13q)			WT		Fig.2b, 4
ID-02	M	No	UM	del(11q)	59%		Monoallelic inactivation		Fig.2b, 4
ID-03	M	No	UM	del(11q), del(13q), +12	65%	p.R2993X (85%)	Biallelic inactivation	NOTCH1	Fig.2b, 4
ID-04	F	No	M	del(11q), del(13q)	27%		Monoallelic inactivation		Fig.2b, 4
ID-05	M	No	UM	del(11q)	75%	p.C2159X (67%)	Biallelic inactivation		Fig.2b, 4
ID-06	M	No	UM	del(11q), del(13q)	95%		Monoallelic inactivation	XPO1	Fig.2b, 4
ID-07	M	Yes	UM	del(11q), del(13q)	60%	p.G2023R (86%)	Biallelic inactivation	SF3B1	Fig.2b, 4
ID-08	F	No	NA	Normal			WT		Fig.2b, 4
ID-09	M	No	NA	del(11q), del(13q)	80%	p.R337C (95%)	Biallelic inactivation	SF3B1	Fig.2b, 4
ID-10	F	No	UM	del(13q)			WT	SF3B1, NOTCH1	Fig.2b, 4
ID-11	F	Yes	NA	del(11q), del(13q)	90%		Monoallelic inactivation		Fig.2b, 4
ID-12	M	Yes	M	del(11q)	95%		Monoallelic inactivation	SF3B1	Fig.2b, 4
ID-13	M	No	UM	del(13q)			WT	NOTCH1, XPO1	Fig.2b, 4
ID-14	M	No	M	del(13q)			WT	MYD88	Fig.2b, 4
ID-15	M	No	M	+12			WT	FBXW7	Fig.2b, 4
ID-16	F	No	M	Normal			WT		Fig.2b, 4
ID-17	M	No	M	del(13q)			WT		Fig.2b, 4
ID-18	M	No	UM	Normal		p.I2260fs (6%); p.Y2019C (8%)	Monoallelic inactivation	SF3B1	Fig.2b, 4
ID-19	F	Yes	M	del(13q)			WT		Fig.4, 5b
ID-20	M	NA	UM	del(11q), del(13q)	80%	p.C532Y (18%); p.L1162fs (13%); p.Q2433fs (44%)	Biallelic inactivation		Fig.4, 5b, 6b
ID-21	M	NA	UM	del(11q), del(13q), +12	70%		Monoallelic inactivation	BIRC3, XPO1, NOTCH1	Fig.4, 5b, 6b
ID-22	F	No	NA	del(11q), del(13q), +12	NA	p.1281_1282del (13%)	Biallelic inactivation	XPO1	Fig.4, 5b
ID-23	M	NA	UM	trisomy 12			WT	NOTCH1	Fig.4, 5b
ID-24	F	Yes	UM	del(13q), del(17p)			WT	TP53, NOTCH1	Fig.4, 5b
ID-25	F	No	M	trisomy 12			WT	BIRC3, FBXW7	Fig.4, 5b
ID-26	F	No	UM	Normal			WT	NOTCH1	Fig.4, 5b
ID-27	F	No	M	del(13q)			WT		Fig.4, 5b
ID-28	F	No	UM	del(13q), del(17p), +12			WT	TP53, FBXW7, NOTCH1	Fig.4, 5b
ID-29	F	Yes	UM	Normal		p.F1463C (45%)	Monoallelic inactivation	NOTCH1	Fig.4, 5b
ID-30	M	No	M	del(17p)			WT	TP53	Fig.4, 5b
ID-31	M	No	M	del(13q)		p.F1463C (39%)	Monoallelic inactivation		Fig.4, 5b
ID-32	F	Yes	UM	Normal			WT	TP53, NOTCH1	Fig.4, 5b
ID-33	M	NA	UM	del(11q), del(13q)	97%		Monoallelic inactivation		Fig.4, 5b, 6b
ID-34	M	No	UM	del(13q)			WT	XPO1	Fig.4, 5b, 6b
ID-35	M	NA	NA	del(13q)			WT		Fig.4, 5b, 6b
ID-36	M	No	UM	del(11q), del(13q)	45%		Monoallelic inactivation	TP53	Fig.4, 5b, 6b
ID-37	M	No	NA	del(11q), del(13q)	85%	p.H2125R (79%)	Biallelic inactivation	SF3B1	Fig.4, 5b, 6b
ID-38	F	No	M	del(13q)			WT		Fig.4, 5b, 6b

Supplemental Table 2. List of genes and regions analyzed in primary CLL samples and the mean read depth obtained by NGS-approach per gene.

Gen	Transcript	Regions	Mean of reads
<i>ATM</i>	ENST00000278616	Exons 2-63	489
<i>BIRC3</i>	ENST00000263464	Exons 2-9	463
<i>FBXW7</i>	ENST00000281708	Exons 7-12	1198
<i>MYD88</i>	ENST00000396334	Exons 2-5	2051
<i>NOTCH1</i>	ENST00000277541	Exon 34 and 3'UTR	2341
<i>SF3B1</i>	ENST00000335508	Exons 14-16, 18	669
<i>TP53</i>	ENST00000269305	Exons 4-11	1402
<i>XPO1</i>	ENST00000401558	Exons 15-16	540

Supplemental Table 3. List of mutations detected by NGS in primary CLL samples included in this study.

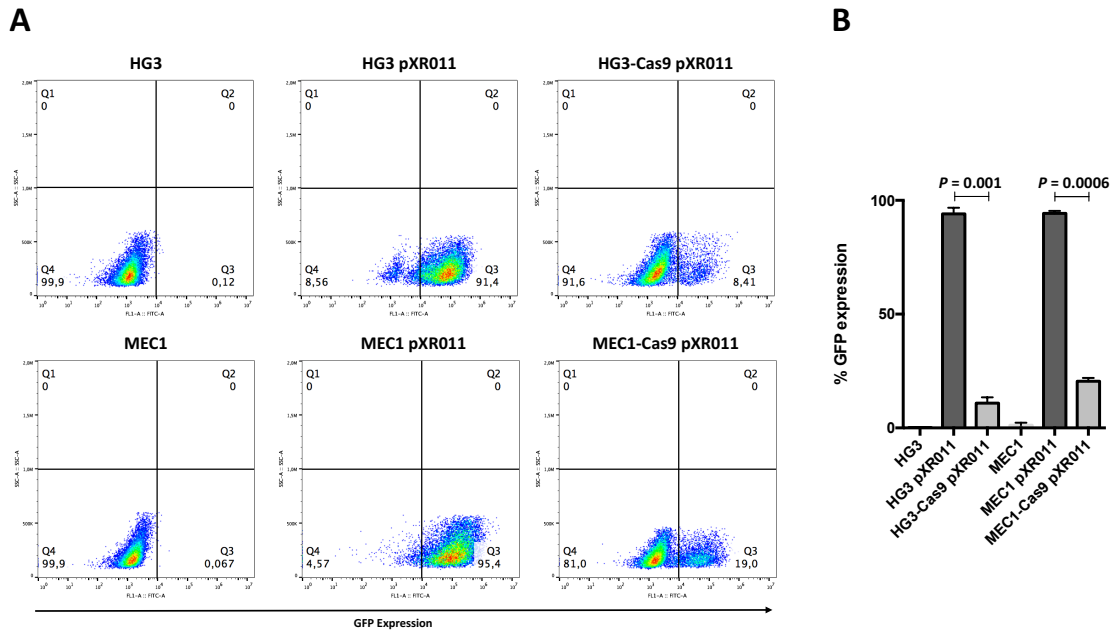
Group	ID Patient	Gene	Chromosome	Start	End	Reference	Altered	Depth (> Q30)	Reference depth	Altered depth	Frequency	Function	Exonic consequence	Transcript: cDNA change: AA change	SIFT (T=Tolerated; D=Deleterious)	Polyphen2_HDIV (B=Benign; P=Possibly damaging; D=Damaging)	Polyphen2_HVAR (B=Benign; P=Possibly damaging; D=Damaging)
del(11q)	ID-03	ATM	chr11	108235935	108235935	C	T	247	38	209	84,62	exonic	stopgain	NM_000051:c.C8977T;p.R2993X	-	-	-
del(11q)	ID-03	NOTCH1	chr9	139390734	139390734	G	T	704	412	292	41,48	exonic	stopgain	NM_017617:c.C7457A;p.S2486X	-	-	-
del(11q)	ID-05	ATM	chr11	108192052	108192052	T	A	242	81	161	66,53	exonic	stopgain	NM_000051:c.T6477A;p.C2159X	-	-	-
del(11q)	ID-06	XPO1	chr2	61719472	61719472	C	T	377	179	196	51,99	exonic	nonsynonymous SNV	NM_003400:c.G1711A;p.E571K	D	D	D
del(11q)	ID-07	ATM	chr11	108186610	108186610	G	A	261	36	224	85,82	exonic	nonsynonymous SNV	NM_000051:c.G6067A;p.G2023R	D	D	D
del(11q)	ID-07	SF3B1	chr2	198267371	198267371	G	C	365	212	153	41,92	exonic	nonsynonymous SNV	NM_012433:c.C1986G;p.H662Q	D	D	D
del(11q)	ID-09	ATM	chr11	108117798	108117798	C	T	167	9	158	94,61	exonic	nonsynonymous SNV	NM_000051:c.C1009T;p.R337C	D	D	D
del(11q)	ID-09	SF3B1	chr2	198266834	198266834	T	C	364	284	80	21,98	exonic	nonsynonymous SNV	NM_012433:c.A2098G;p.K700E	D	D	D
del(11q)	ID-12	SF3B1	chr2	198266834	198266834	T	C	340	186	154	45,29	exonic	nonsynonymous SNV	NM_012433:c.A2098G;p.K700E	D	D	D
non del(11q)	ID-10	SF3B1	chr2	198267361	198267361	T	C	357	298	59	16,53	exonic	nonsynonymous SNV	NM_012433:c.A1996G;p.K666E	D	D	D
non del(11q)	ID-13	NOTCH1	chr9	139390649	139390650	AG	-	1020	959	60	5,88	exonic	frameshift deletion	NM_017617:c.7541_7542del;p.P2514fs	-	-	-
non del(11q)	ID-13	XPO1	chr2	61719472	61719472	C	T	309	118	191	61,81	exonic	nonsynonymous SNV	NM_003400:c.G1711A;p.E571K	D	D	D
non del(11q)	ID-14	MYD88	chr3	38182641	38182641	T	C	652	375	277	42,48	exonic	stoploss	NM_001172566:c.T478C;p.X160R	D	D	D
non del(11q)	ID-15	BIRC3	chr11	102201946	102201947	AA	-	121	111	10	8,26	exonic	frameshift deletion	NM_001165:c.1298_1299del;p.E433fs	-	-	-
non del(11q)	ID-15	BIRC3	chr11	102207657	102207657	C	-	274	256	17	6,2	exonic	frameshift deletion	NM_001165:c.1639delC;p.Q547fs	-	-	-
non del(11q)	ID-15	FBXW7	chr4	153249384	153249384	C	T	485	473	11	2,27	exonic	nonsynonymous SNV	NM_001013415:c.G1040A;p.R347H	D	D	D
non del(11q)	ID-18	ATM	chr11	108186599	108186599	A	G	397	366	30	7,56	exonic	nonsynonymous SNV	NM_000051:c.A6056G;p.Y2019C	D	D	D
non del(11q)	ID-18	ATM	chr11	108196242	108196242	-	T	114	107	7	6,14	exonic	frameshift insertion	NM_000051:c.6779dupT;p.I2260fs	-	-	-
non del(11q)	ID-18	SF3B1	chr2	198266834	198266834	T	C	259	153	106	40,93	exonic	nonsynonymous SNV	NM_012433:c.A2098G;p.K700E	D	D	D
del(11q)	ID-20	ATM	chr11	108121787	108121787	G	A	196	160	36	18,37	exonic	nonsynonymous SNV	NM_000051:c.G1595A;p.C532Y	D	D	D
del(11q)	ID-20	ATM	chr11	108151804	108151805	TA	-	138	120	18	13,04	exonic	frameshift deletion	NM_000051:c.3485_3486del;p.L1162fs	-	-	-
del(11q)	ID-20	ATM	chr11	108199955	108199958	CAGA	-	34	19	15	44,12	exonic	frameshift deletion	NM_000051:c.7297_7300del;p.Q2433fs	-	-	-
del(11q)	ID-21	BIRC3	chr11	102207759	102207759	T	G	106	40	66	62,26	exonic	nonsynonymous SNV	NM_001165:c.T1741G;p.C581G	D	D	D
del(11q)	ID-21	XPO1	chr2	61719472	61719472	C	T	183	101	82	44,81	exonic	nonsynonymous SNV	NM_003400:c.G1711A;p.E571K	D	D	D
del(11q)	ID-21	NOTCH1	chr9	139390649	139390650	AG	-	624	400	225	36	exonic	frameshift deletion	NM_017617:c.7541_7542del;p.P2514fs	-	-	-
del(11q)	ID-22	ATM	chr11	108155050	108155052	TCT	-	181	158	23	12,71	exonic	nonframeshift deletion	NM_000051:c.3843_3845del;p.I281_128	-	-	-
del(11q)	ID-22	XPO1	chr2	61719471	61719471	T	C	193	166	27	13,99	exonic	nonsynonymous SNV	NM_003400:c.A1712G;p.E571G	D	D	D
non del(11q)	ID-23	NOTCH1	chr9	139390649	139390650	AG	-	609	485	124	20,36	exonic	frameshift deletion	NM_017617:c.7541_7542del;p.P2514fs	-	-	-
non del(11q)	ID-24	TP53	chr17	7578542	7578542	G	C	231	36	195	84,42	exonic	nonsynonymous SNV	NM_001126118:c.C271G;p.L91V	T	D	D
non del(11q)	ID-24	NOTCH1	chr9	139390690	139390690	G	A	630	359	271	43,02	exonic	stopgain	NM_017617:c.C7501T;p.Q2501X	-	-	-
non del(11q)	ID-25	BIRC3	chr11	102207688	102207688	-	TAAA	188	145	46	23,96	exonic	frameshift insertion	NM_001165:c.1670_1671insTAAA;p.C557	-	-	-
non del(11q)	ID-25	FBXW7	chr4	153249510	153249510	C	A	366	224	142	38,8	exonic	nonsynonymous SNV	NM_001013415:c.G914T;p.G305V	D	D	D
non del(11q)	ID-26	NOTCH1	chr9	139390649	139390650	AG	-	697	672	25	3,59	exonic	frameshift deletion	NM_017617:c.7541_7542del;p.P2514fs	-	-	-
non del(11q)	ID-28	TP53	chr17	7577579	7577579	G	T	314	295	19	6,05	exonic	stopgain	NM_001126115:c.C306A;p.Y102X	-	-	-
non del(11q)	ID-28	FBXW7	chr4	153249384	153249384	C	T	307	287	20	6,51	exonic	nonsynonymous SNV	NM_001013415:c.G1040A;p.R347H	D	D	D
non del(11q)	ID-28	NOTCH1	chr9	139390649	139390650	AG	-	641	607	34	5,3	exonic	frameshift deletion	NM_017617:c.7541_7542del;p.P2514fs	-	-	-
non del(11q)	ID-29	ATM	chr11	108160480	108160480	T	G	99	54	45	45,45	exonic	nonsynonymous SNV	NM_000051:c.T4388G;p.F1463C	D	D	D
non del(11q)	ID-29	NOTCH1	chr9	139390649	139390650	AG	-	554	360	196	35,25	exonic	frameshift deletion	NM_017617:c.7541_7542del;p.P2514fs	-	-	-
non del(11q)	ID-30	TP53	chr17	7577610	7577610	T	A	260	225	34	13,08	splicing	-	-	-	-	-
non del(11q)	ID-31	ATM	chr11	108160480	108160480	T	G	94	57	37	39,36	exonic	nonsynonymous SNV	NM_000051:c.T4388G;p.F1463C	D	D	D
non del(11q)	ID-32	TP53	chr17	7578271	7578271	T	C	399	372	27	6,77	exonic	nonsynonymous SNV	NM_001126115:c.A182G;p.H61R	D	D	D
non del(11q)	ID-32	NOTCH1	chr9	139390649	139390650	AG	-	649	390	259	39,91	exonic	frameshift deletion	NM_017617:c.7541_7542del;p.P2514fs	-	-	-
non del(11q)	ID-32	NOTCH1	chr9	139391824	139391824	G	A	704	399	304	43,18	exonic	stopgain	NM_017617:c.C6367T;p.Q2123X	-	-	-
non del(11q)	ID-34	XPO1	chr2	61719472	61719472	C	T	212	118	94	44,34	exonic	nonsynonymous SNV	NM_003400:c.G1711A;p.E571K	D	D	D
del(11q)	ID-36	TP53	chr17	7578402	7578402	G	C	626	587	38	6,07	exonic	nonsynonymous SNV	NM_001126115:c.C132G;p.C44W	D	D	D
del(11q)	ID-37	ATM	chr11	108190707	108190707	A	G	74	22	51	68,92	exonic	nonsynonymous SNV	NM_000051:c.A6374G;p.H2125R	D	D	D
del(11q)	ID-37	SF3B1	chr2	198266611	198266611	C	T	186	109	77	41,4	exonic	nonsynonymous SNV	NM_012433:c.G2225A;p.G742D	T	D	P

Supplemental Table 4. Oligos designed for each sgRNA and PCR primers of sgRNA target sites.

Target	Forward (5'-3')	Reverse (5'-3')
<i>ATM</i> exon 10 sgRNA1	CACCGGTAAGGCATCGTAACACATA	AAACTATGTGTTACGATGCCTTACC
<i>ATM</i> exon 10 sgRNA2	CACCGGACACAATGCAACTTCCGTA	AAACTACGGAAGTTGCATTGTGTCC
11q22.1 sgRNA-A	CACCGAGATGACTTCCTGAACAGTG	AAACCACTGTTCAGGAAGTCATCTC
11q23.3 sgRNA-B	CACCGTGGCACC GGACTCAGATCCC	AAACGGGATCTGAGTCCGGTCGCAC
Control sgRNA1	CACCGACGGAGGCTAAGCGTCGAA	AAACTTGCGACGCTTAGCCTCCGTC
<i>ATM</i> exon 10	TCCTGCCAATTTAGGAAGTAGGAC	CTGCAGGCTGACCCAGTAAA
11q22.1 sgRNA cut site	GCTGCCAGCTTCAATTAGGA	ACAATACCTTATGAGACCTGGTGA
11q23.3 sgRNA cut site	CGTTACGCGTTGAGGCATT	GAGGCTCGAGATGTAAGCGG

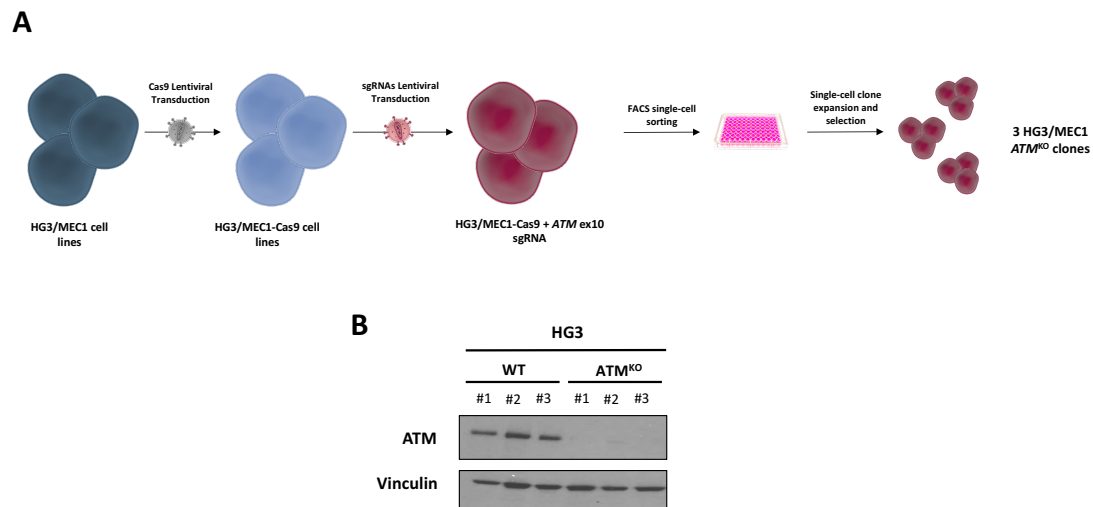
SUPPLEMENTAL FIGURES – CHAPTER 2

Supplemental Figure 1



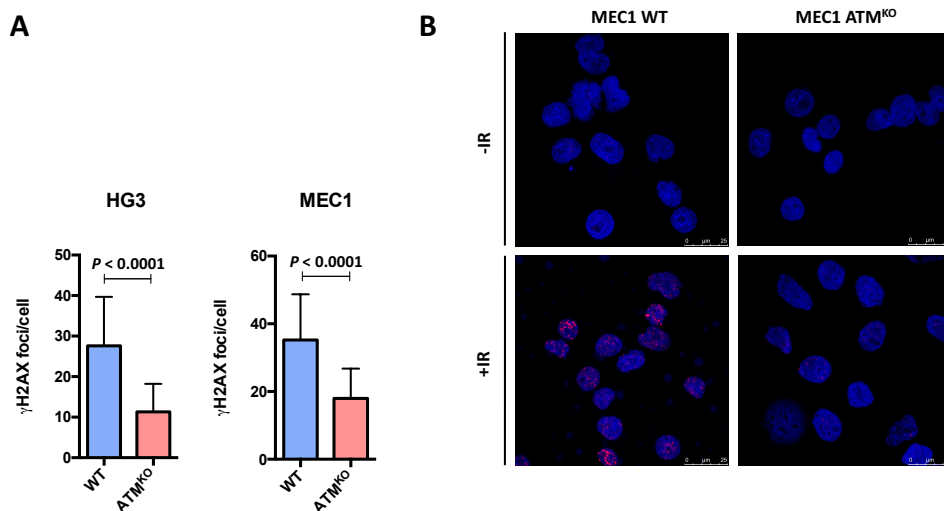
Determination of Cas9 activity in HG3-Cas9 and MEC1-Cas9 cell lines. (A) Representative plots of isogenic CLL cell lines stably expressing Cas9 protein and transduced with pXR011 plasmid, which delivers GFP and the RNA guide (sgRNA) targeting GFP. HG3 and MEC1 parental cell lines transduced with pXR011 highly expressed GFP whereas HG3-Cas9 and MEC1-Cas9 cells showed lower levels of GFP expression, indicating the activity of the Cas9 protein in these cell lines. **(B)** GFP expression quantification of HG3 and MEC1 cell lines transduced with pXR011. Data is shown as mean \pm SD of two independent experiments.

Supplemental Figure 2



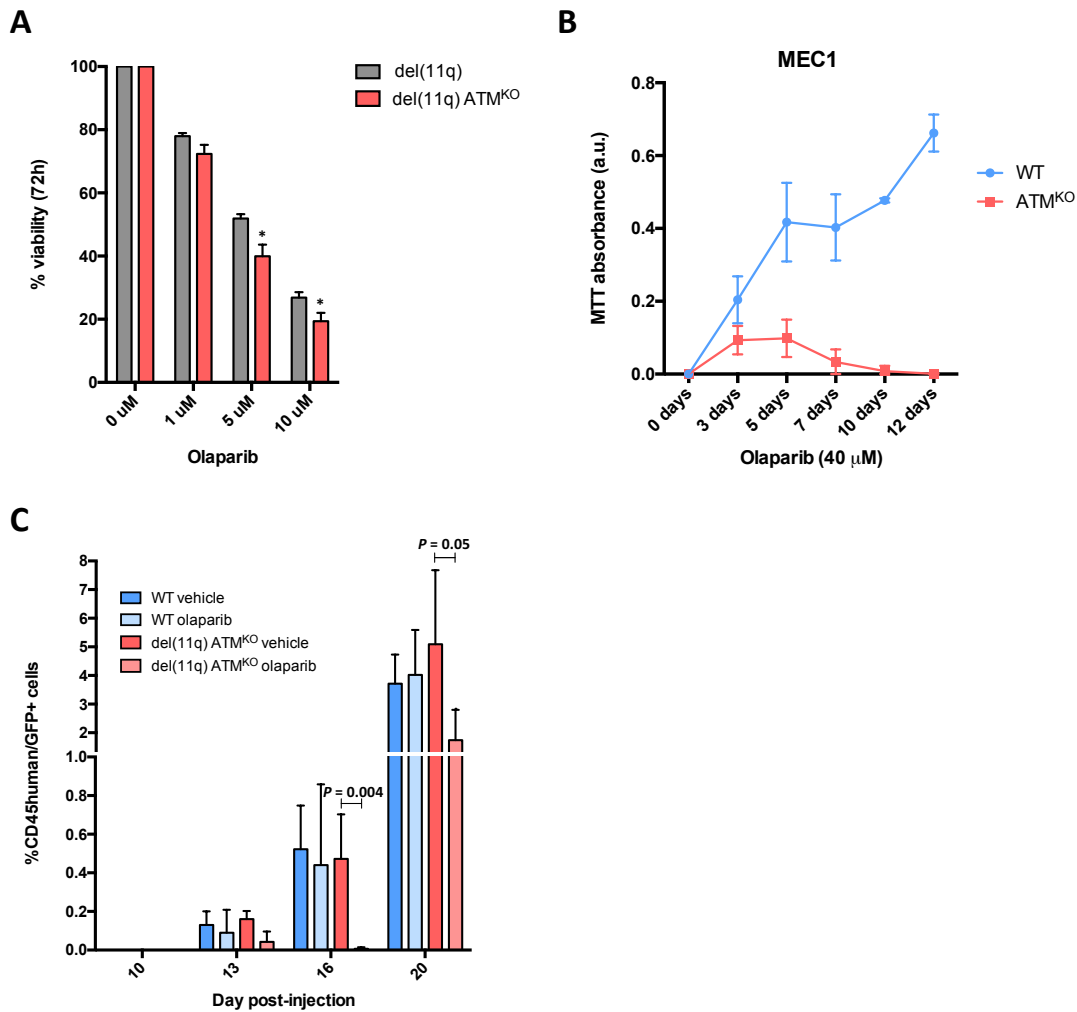
Generation of isogenic CLL cell lines with *ATM* mutations using the CRISPR/Cas9 system. (A) Diagram showing the steps for the generation of HG3/MEC1 *ATM*^{KO} clones. Three clones of each cell line were generated and used in the functional studies. **(B)** Western blot analysis of HG3-edited clones showing *ATM* protein expression.

Supplemental Figure 3



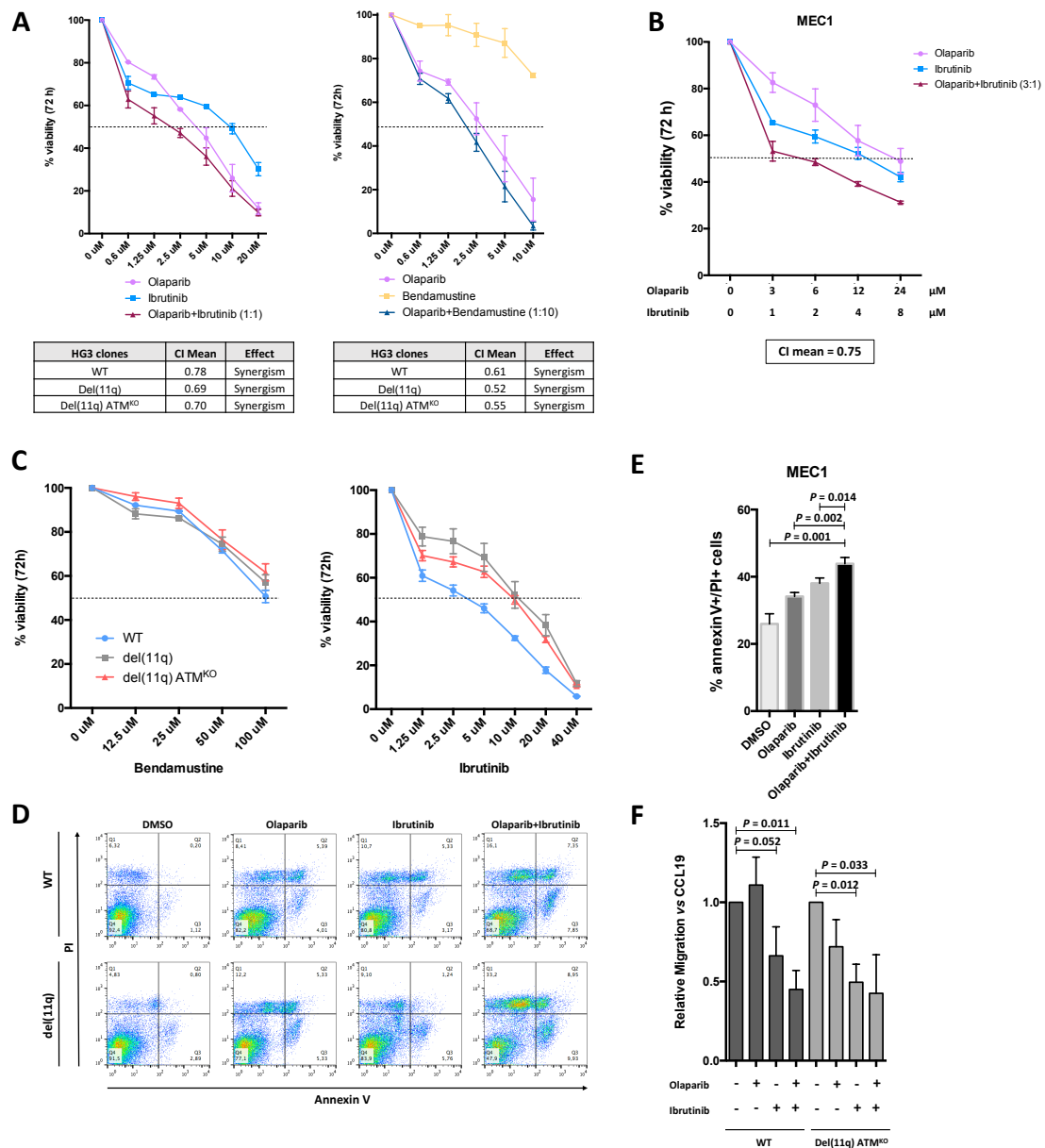
Evaluation of double strand breaks signaling in HG3 and MEC1-edited clones. (A) Quantification of the number of γ H2AX foci per cell 1 hour after irradiation (2 Gy) in HG3 (left panel) and MEC1 (right panel) WT and *ATM*^{KO} clones. Data are represented as the mean values \pm SD of 2 independent experiments. At least 75 cells per experiment and clone were counted. **(B)** Representative images of γ H2AX foci formation (red) in MEC1 clones. Upper panel shows non-irradiated MEC1 cells and lower panel represents MEC1 clones 1 hour post-irradiation (2 Gy).

Supplemental Figure 4



Olaparib response of CRISPR/Cas9-edited CLL cell lines *in vitro* and *in vivo*. (A) HG3-del(11q) and HG3-del(11q) *ATM*^{KO} clones were treated with increasing doses of olaparib and cell viability was assessed by MTT after 72 hours. Surviving fraction is expressed relative to untreated (DMSO) controls. Data is summarized as the mean \pm SD of three independent experiments. $P < 0.05$ (*) (B) MEC1-edited clones were treated with olaparib (40 μ M) and cell viability was assessed by MTT at different time points up to 12 days. Proliferation rates are presented as MTT absorbance units, and data are represented as mean \pm SD. (C) Quantification of hCD45⁺/GFP⁺ cell populations in the peripheral blood of HG3^{WT} and HG3-del(11q) *ATM*^{KO} xenografted mice at different time points after engraftment. Data is shown as mean \pm SD.

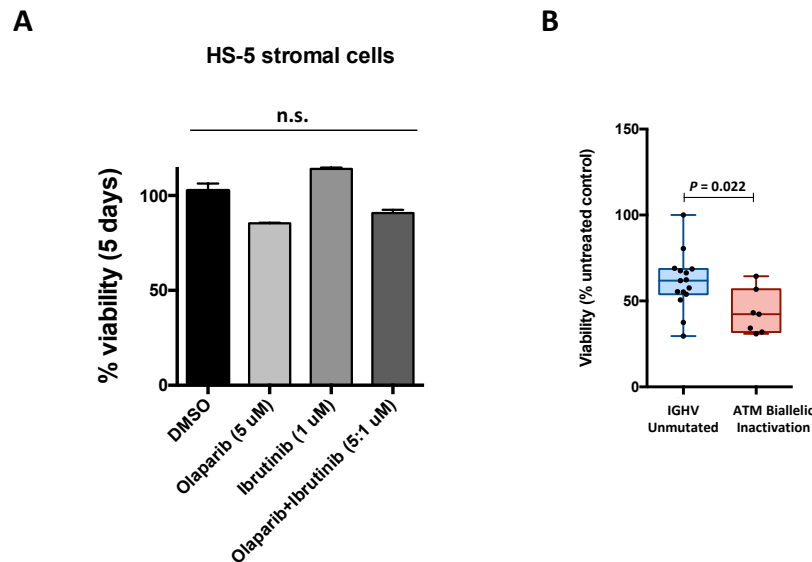
Supplemental Figure 5



Cell viability analysis of the effects of olaparib in combination with ibrutinib in MEC1 cells. (A) HG3-edited clones were treated with olaparib in combination with ibrutinib or bendamustine and cell viability was assessed by MTT assay 72 hours later. Upper graphs are representative of HG3-del(11q) ATM^{KO} clones. Surviving fraction is expressed relative to untreated controls and data is presented as the mean \pm SD of three independent experiments. Combination indexes (CI) for all the clones are detailed in the lower tables (CI values $<$ 0.9 indicate synergism). (B) MEC1 cells were treated with olaparib in combination with ibrutinib at the indicated doses and cell viability was assessed by MTT assay 72 hours later. Surviving fraction is expressed relative to untreated controls and data is presented as the mean \pm SD of three independent experiments. The mean combination index is displayed in the lower box (CI values $<$ 0.9 indicate synergism). (C) CRISPR/Cas9-generated HG3 clones were treated

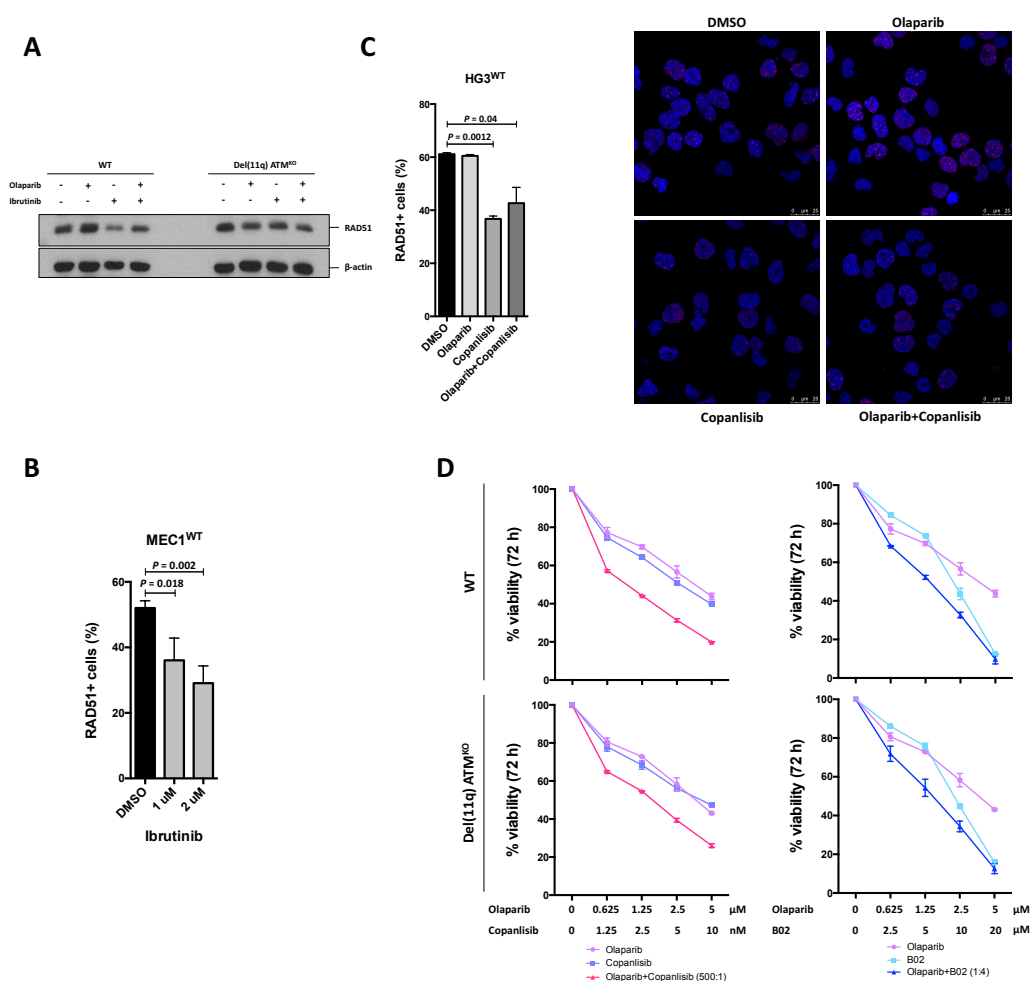
with increasing concentrations of bendamustine or ibrutinib and cell viability was measured after 72 hour- treatment. Surviving fraction is expressed relative to untreated controls and data is presented as the mean \pm SD of three independent experiments. **(D)** Representative plots from Fig. 3c of annexin V/PI stained HG3^{WT} and HG3-del(11q) cell lines 48 hours after 5 μ M olaparib and ibrutinib treatment. Necrotic cells are allocated on the PI+/annexin V-quadrant. **(E)** Cytotoxicity studies by annexin V/PI staining of MEC^{WT} cells treated with 12 μ M olaparib and 4 μ M ibrutinib for 48 hours. Cytotoxicity is measured as the percentage of PI+ and annexin V+ cells. Data is summarized as the mean \pm SD of three independent experiments. **(F)** Cells were treated with 1.25 μ M olaparib, ibrutinib or the combination of both for 12 hours. Migration values are normalized with respect to the control (DMSO) condition. Data is shown as the mean \pm SD of three independent experiments.

Supplemental Figure 6



Effects of the combination of olaparib and ibrutinib in HS-5 bone marrow stromal cells and IGHV unmutated primary CLL cells. **(A)** HS-5 cells were treated with olaparib (5 μ M), ibrutinib (1 μ M) or the combination of both and cell viability was assessed by MTT assay 5 days later. The drug combination did not affect HS-5 cell viability. Surviving fraction is expressed relative to an untreated control and data is presented as the mean \pm SD. **(B)** Response to the combination of olaparib and ibrutinib in IGHV unmutated/*ATM*^{WT} primary cells and *ATM* biallelic inactivated primary CLL cells.

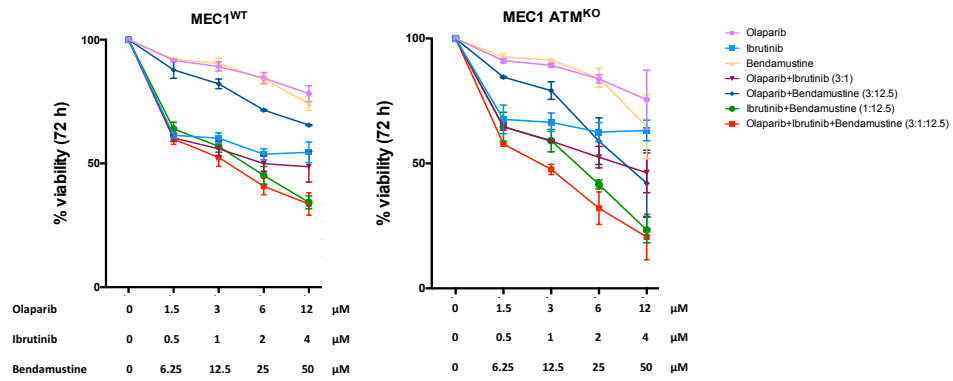
Supplemental Figure 7



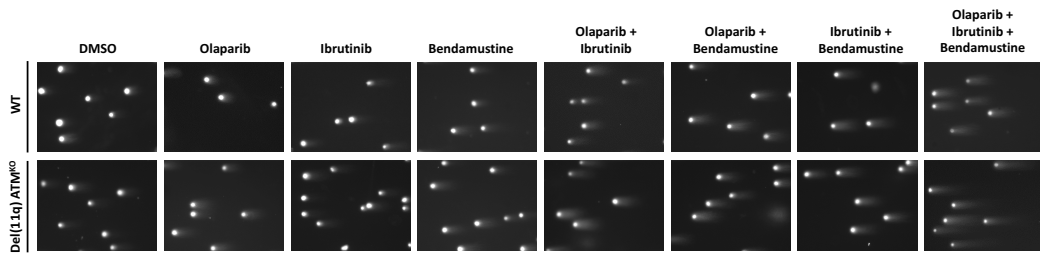
Evaluation of RAD51 levels after ibrutinib treatment in HG3 and MEC1 cells. (A) HG3^{WT} and HG3-del(11q) ATM^{KO} cells were pretreated for 24 hours with 5 μM olaparib and/or ibrutinib and subsequently irradiated (2 Gy). After 6 hours of incubation, cells were lysed for immunoblot analysis. **(B)** MEC1^{WT} cells were pretreated for 24 hours with increasing doses of ibrutinib and subsequently irradiated (2 Gy) and analyzed for foci formation 6 hours later. Data are represented as the mean values \pm SD. Cells were scored RAD51+ when 5 or more foci were formed. At least 100 cells per experiment were counted **(C)** HG3^{WT} cells were pretreated for 12 hours with the PI3K inhibitor copanlisib (10 nM) and/or 5 μM olaparib and subsequently irradiated (2 Gy). After 6 hours of incubation, cells were analyzed for RAD51 foci formation. Data are represented as the mean values for each treatment condition \pm SD. Cells were scored RAD51+ when 5 or more foci were formed. At least 100 cells per experiment were scored for quantification. **(D)** HG3^{WT} and HG3-del(11q) ATM^{KO} cells were treated with olaparib in combination with the PI3K inhibitor copanlisib (left) or the RAD51 inhibitor B02 (right) and cell viability was assessed by MTT assay 72 hours later. RAD51 and PI3K inhibition potentiated the effects of olaparib treatment in both cell lines. Surviving fraction is expressed relative to untreated controls and data is presented as the mean \pm SD of three independent experiments.

Supplemental Figure 8

A

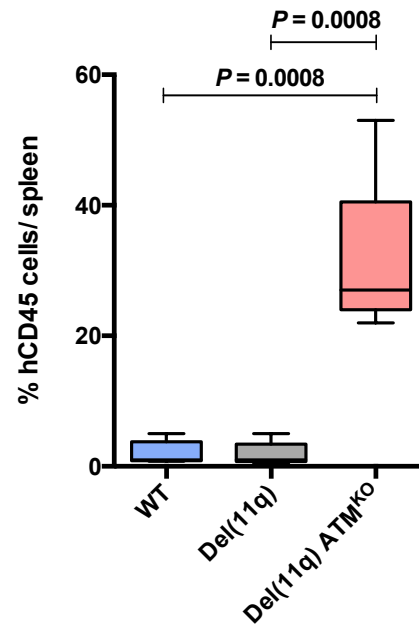


B



Effects of the combination of olaparib, ibrutinib and bendamustine in cell viability and DSB accumulation of CRISPR/Cas9-edited clones. (A) MEC1-edited clones were treated with olaparib, ibrutinib and/or bendamustine and cell viability was assessed by MTT assay 72 hours later. Surviving fraction is expressed relative to untreated controls and data is presented as the mean \pm SD of two independent experiments. **(B)** Representative images of comet assays from Fig. 6c.

APPENDIX 2



***In vivo* analysis of leukemic progression of del(11q)/ATM^{KO} CRISPR/Cas9-edited clones.** Spleen infiltration of xenotransplanted HG3^{WT}, HG3-del(11q) and HG3-del(11q) ATM^{KO} cell lines (n = 5/per group) into NSG mice. Mice spleens were analyzed by FACS 14 days after cell injection and hCD45⁺ cells were monitored to evaluate the leukemic infiltration in each condition.

SUPPLEMENTARY APPENDIX – CHAPTER 3

Received: 5 August 2020 | Revised: 13 January 2021 | Accepted: 18 January 2021 | Published online: 4 February 2021

DOI: 10.1002/ctm2.304



WILEY

RESEARCH ARTICLE

Dissecting the role of *TP53* alterations in del(11q) chronic lymphocytic leukemia

Miguel Quijada-Álamo^{1,2,#} | Claudia Pérez-Carretero^{1,2,#} |
María Hernández-Sánchez^{1,2,3,4} | Ana-Eugenia Rodríguez-Vicente^{1,2} |
Ana-Belén Herrero^{1,2} | Jesús-María Hernández-Sánchez^{1,2} |
Marta Martín-Izquierdo^{1,2} | Sandra Santos-Mínguez^{1,2} | Mónica del Rey^{1,2} |
Teresa González² | Araceli Rubio-Martínez⁵ | Alfonso García de Coca⁶ |
Julio Dávila-Valls⁷ | José-Ángel Hernández-Rivas⁸ | Helen Parker⁹ |
Jonathan C. Strefford⁹ | Rocío Benito^{1,2} | José-Luis Ordóñez^{1,2,#} |
Jesús-María Hernández-Rivas^{1,2,10,#} 

SUPPLEMENTARY METHODS

Cell lines, culture conditions, drugs and reagents

The human CLL-derived cell line HG3 was purchased from DMSZ (Deutsche Sammlung von Mikroorganismen and Zellkulturen) and was cultured in RPMI 1640 medium (Life Technologies) supplemented with 15% Fetal Bovine Serum (FBS), 1% glutaMAX and 1% penicillin/streptomycin (Life Technologies). HEK 293T cells for lentiviral production were obtained from DMSZ and maintained in DMEM (Life Technologies) supplemented with 10% FBS, 1% glutaMAX and 1% penicillin/streptomycin. All cell lines were incubated at 37°C in a 5% CO₂ atmosphere. The presence of mycoplasma was tested frequently with MycoAlert kit (Lonza), only using mycoplasma-free cells in all the experiments carried out.

Idelalisib and AZD6738 were obtained from Selleckchem, ibrutinib was from LC Laboratories and fludarabine was from Sigma. All drugs were resuspended in DMSO (Sigma).

Fluorescence in situ hybridization (FISH)

Interphase FISH was performed on peripheral blood or bone marrow samples using commercially available probes for the 13q14, CEP12, 11q22/*ATM*, 17p13/*P53* and 14q32 regions (Vysis, Abbott Laboratories, IL, USA). The methods used for FISH analysis have been described elsewhere¹. Signal screening was carried out in at least 200 cells with well-delineated fluorescent spots. In all cases, a score of $\geq 10\%$ was considered positive, based on the cut-off value used by our laboratory.

NGS data analysis and variant calling

After the enrichment of interest regions, paired-end sequencing (151-bp reads) was run on the Illumina NextSeq instrument (Illumina). At the end of the process, this platform collects all the information in demultiplexed and paired FASTQ files to continue with bioinformatic analysis. SureSelect^{QXT} adaptor sequences were trimmed using SureCall (Agilent's NGS data analysis software) and sequenced reads were aligned to the hg19 human reference genome (GRCh37/hg19). Coverage along the targeted regions was analyzed using BAM files generated by SAMtools² from the FASTQ files.

We used GATK (Genome Analysis Toolkit),³ to generate the variant calling files (VCFs), and thereby to identify somatic substitutions or variant calling. The VCFs were annotated using Annovar⁴ and filtered by depth and variant allele frequency (VAF), position, and function of the variant in the coding sequence (hg19 refGene), in common polymorphism databases (dbSNP, 1000 genomes), in the cancer-specific database Catalogue of Somatic Mutations in Cancer (COSMIC) or in the Exome Aggregation Consortium (ExAC). Aligned reads were manually reviewed with the Integrative Genomics Viewer (IGV) to confirm and interpret variant calls and reduce the risk of false positives⁵. For a deeper analysis we manually screened variants in VarSome, which integrates a wide range of population databases and pathogenicity predictors (gnomAD, ICGC, SIFT, Polyphen2, ClinVar, MutationAssesor, MutPred and FATHMM among others). Functional impact of *TP53* mutations described in this work was checked in IARC TP53 database. All mutations were annotated as non-functional with the exception of variant p.R290H, previously described as 'supertrans' or with high transcriptional activity.

sgRNA cloning, lentiviral generation and transduction

sgRNA cloning was carried out as previously described⁶. The pLKO5 plasmids carrying the sgRNAs of interest were co-transfected in addition to pMD2.G (Addgene #12259) and

psPAX2 (Addgene #12260) into HEK 293T using Lipofectamine 2000[®] (Life Technologies). Supernatant containing the lentiviral particles was collected 48 and 72 hours after transfection and concentrated using Lenti-X concentrator[®] (Clontech). HG3 cell transduction was carried out in the presence of polybrene (8 μ g/mL) as previously described⁷. pLKO5 vectors carrying the desired sgRNAs packed into lentiviral particles were then transduced into Cas9-expressing HG3 cells and single-cell flow-sorted clones were expanded and screened. Three to five different clones harboring loss-of-function mutations were chosen for each CRISPR-generated cell line to perform further functional studies.

PCR and sequencing of sgRNA target sites

Genomic DNA (gDNA) was extracted using the QIAampDNA Micro Kit (Qiagen) following the manufacturer's instructions. PCR was performed using primers flanking the target sites for the sgRNAs (Supplemental Table S2) or the sgRNA off-target sites (Supplementary Table S3). For screening the loss-of-function mutations, PCR products were purified using High Pure PCR Product Purification Kit (Roche) and resulting indels at the expected locations were confirmed by Sanger sequencing. The efficiency of the sgRNAs was assessed by Tracking of Indels by Decomposition (TIDE) software (<https://tide-calculator.nki.nl>; Netherlands Cancer Institute)⁸.

Western blot analysis

Cells were washed twice in PBS and lysed in ice-cold lysis buffer (50 nM TrisHCl pH 7.4, 150 mM NaCl, 1 mM EDTA, 1% Triton X-100) containing protease inhibitors (cOmplete[®], Roche) and phosphatase inhibitors (PhosSTOP[™], Roche). Protein concentration was measured using the Bradford assay (BioRad). Protein samples were subjected to SDS-PAGE and transferred to a nitrocellulose membrane (GE Healthcare). After blockade, membranes were incubated with the following primary antibodies purchased from Cell Signaling Technologies: anti-ATM (#2873, Rabbit), anti-TP53 (#9282, Rabbit), anti- β -actin (#4967, Rabbit), anti-GAPDH (#5174, Rabbit), anti-PARP1 (#9542, Rabbit) and anti-caspase 3 (#9662, Rabbit). Horseradish peroxidase-linked anti-rabbit antibody (#7074, Cell Signaling Technologies) was used as secondary antibody at 1:5,000 dilution. Antibody signal was detected using ECL[™] Western Blotting Detection Reagents (RPN2209, GE Healthcare).

Cell cycle analysis

Cell distribution in the cell cycle phase was analyzed measuring the DNA content by propidium iodide (PI) labeling after cell permeabilization. In brief, cells were irradiated at a dose of 2 Gy during the exponential phase of cell growth with γ -rays using a Gammacell 1000 Elite irradiator (Cesium137). After irradiation, 3×10^5 cells were seeded in 24-well plates and ethanol permeabilization and PI labeling were performed at different time points. DNA content was measured by flow cytometry.

Viability and growth assays

Cell viability was assessed using 3-(4,5-dimethylthiazol-2-yl)-2,5-diphenyltetrazolium bromide (MTT) colorimetric assay (Sigma-Aldrich). After drug treatment, cells were incubated for 2h with a 1:10 MTT solution and subsequently added 1:2 SDS-HCl in agitation for 6 hours. Absorbance was read on an Infinite® F500 Tecan plate reader (Tecan) at 570nm.

For the determination of the growth exponential curves of HG3 CRISPR/Cas9-edited clones, cells were seeded at a concentration of 3×10^4 cells/mL and cell counts were assessed every 24 hours for a total of 5 days by Trypan Blue exclusion.

SUPPLEMENTARY REFERENCES

1. González MB, Hernández JM, García JL, et al. The value of fluorescence in situ hybridization for the detection of 11q in multiple myeloma. *Haematologica*. 2004;89.
2. Li H, Handsaker B, Wysoker A, et al. The Sequence Alignment/Map format and SAMtools. *Bioinformatics*. 2009;25.
3. McKenna A, Hanna M, Banks E, et al. The genome analysis toolkit: A MapReduce framework for analyzing next-generation DNA sequencing data. *Genome Res*. 2010;20.
4. Wang K, Li M, Hakonarson H. ANNOVAR: Functional annotation of genetic variants from high-throughput sequencing data. *Nucleic Acids Res*. 2010;38.
5. Robinson JT, Thorvaldsdóttir H, Wenger AM, Zehir A, Mesirov JP. Variant Review with the Integrative Genomics Viewer. *Cancer Res*. 2017;77.
6. García-Tuñón I, Hernández-Sánchez M, Ordoñez JL, et al. The CRISPR/Cas9 system efficiently reverts the tumorigenic ability of BCR/ABL in vitro and in a xenograft model of chronic myeloid leukemia. *Oncotarget*. 2017;8.
7. Quijada-Álamo M, Hernández-Sánchez M, Alonso-Pérez V, et al. CRISPR/Cas9-generated models uncover therapeutic vulnerabilities of del(11q) CLL cells to dual BCR and PARP inhibition. *Leukemia*. 2020;34.
8. Brinkman EK, Chen T, Amendola M, van Steensel B. Easy quantitative assessment of genome editing by sequence trace decomposition. *Nucleic Acids Res*. 2014;42.

SUPPLEMENTARY TABLES – CHAPTER 3

Supplementary Table S1. List of regions and mean coverage of genes included in the custom-designed panel of NGS.

Gene	Transcript	Regions	Mean coverage (reads/base)
ARID1A	ENST00000324856	Exons 1-20	814
ASXL1	ENST00000375687	Exons 1-13	701
ATM	ENST00000278616	Exons 2-63	456
ATRX	ENST00000373344	Exons 1-35	243
BAX	ENST00000345358	Exon 2-6	826
BAZ2A	ENST00000551812	Exons 2-28	819
BCL2	ENST00000333681	Exons 2-3 and 5'UTR	536
BCOR	ENST00000378444	Exons 2-15	398
BIRC3	ENST00000263464	Exons 2-9	483
BRAF	ENST00000288602	Exons 11-16	499
BTK	ENST00000308731	Exons 2-19	456
CARD11	ENST00000396946	Exons 3-17	795
CCND2	ENST00000261254	Exons 1-5	827
CD19	ENST00000324662	Exons 1-6	845
CDC73	ENST00000367435	Exons 1-16	436
CHD2	ENST00000394196	Exons 2-39	463
DDX3X	ENST00000399959	Exons 1-16	376
EGR2	ENST00000242480	Exons 1-2	1021
FAM50A	ENST00000393600	Exons 2-12	478
FAT1	ENST00000441802	Exons 2-27	754
FBXW7	ENST00000281708	Exons 7-12	721
FUBP1	ENST00000370768	Exons 1-19	451
HIST1H1B	ENST00000331442	Exon 1	954
HIST1H1E	ENST00000304218	Exon 1	668
IGLL5	ENST00000526893	Exons 1-3, 5'UTR	555
IKZF3	ENST00000346872	Exon 5	696
IRF4	ENST00000380956	Exons 2-9	698
KLHL6	ENST00000341319	Exons 1-7	693
KRAS	ENST00000311936	Exons 2-5	543
MAP2K1	ENST00000307102	Exons 1-11	561
MED12	ENST00000374080	Exons 1-4	389
MGA	ENST00000570161	Exons 2-23	572
MYD88	ENST00000396334	Exons 2-5	781
NFKBIE	ENST00000275015	Exons 1-2	969
NOTCH1	ENST00000277541	Exon 34 and 3'UTR	1208
NRAS	ENST00000369535	Exons 2-3	587
NXF1	ENST00000294172	Exons 3-21	653
PAX5	ENST00000358127	enhancer	791
PCDH10	ENST00000264360	Exons 1-5	562
PIK3CD	ENST00000377346	Exons 3-24	848
PLCG2	ENST00000564138	Exons 2-33	618
POT1	ENST00000357628	Exons 5-19	405
PTPN11	ENST00000351677	Exons 2-15	645
RPS15	ENST00000593052	Exons 2-4	679
SAMHD1	ENST00000262878	Exons 1-16	465
SETD2	ENST00000409792	Exons 1-21	476
SF3B1	ENST00000335508	Exons 14-16	524
SORCS2	ENST00000507866	Exons 1-27	876
TP53	ENST00000269305	Exons 4-10	634
TRAF3	ENST00000392745	Exons 1-12	641
XPO1	ENST00000401558	Exons 15-16	556
ZC3H18	ENST00000301011	Exons 2-18	780
ZMYM3	ENST00000373998	Exons 2-25	507
ZNF292	ENST00000339907	Exons 1-8	401

Supplementary Table S2. Oligos designed for each sgRNA and PCR primers of sgRNA target sites.

Target	Forward (5'-3')	Reverse (5'-3')
<i>ATM</i> exon 10 sgRNA1	CACCGGTAAGGCATCGTAACACATA	AAACTATGTGTTACGATGCCTTACC
<i>ATM</i> exon 10 sgRNA2	CACCGGACACAATGCAACTTCCGTA	AAACTACGGAAGTTGCATTGTGTCC
<i>TP53</i> exon 4 sgRNA1	CACCGCCATTGTTCAATATCGTCCG	AAACCGGACGATATTGAACAATGGC
<i>TP53</i> exon 4 sgRNA2	CACCGCCCCGGACGATATTGAACAA	AAACTTGTTCATATCGTCCGGGGC
Control sgRNA1	CACCGACGGAGGCTAAGCGTCGCAA	AAACTTGCACGCTTAGCCTCCGTC
<i>ATM</i> exon 10 (PCR)	TCCTGCCAATTTAGGAAGTAGGAC	CTGCAGGCTGACCCAGTAAA
<i>TP53</i> exon 4 (PCR)	AGACCTGTGGGAAGCGAAAA	GACAGGAAGCCAAAGGGTGA

Supplementary Table S3. Predicted off-target regions and oligos designed for PCR and Sanger sequencing.

sgRNA sequence	Off-target sequence	Gene name	Ensembl ID	# mismatches	Chromosome	Exon/Intron	Forward Primer (5'-3')	Reverse Primer (5'-3')
ATM ex10 sgRNA1 GTAAGGCATCGTAACACATA	tTAAGGtATgGTAAaACATA-AGG	NRXN1	ENSG00000179915	4	2	Intron 15-16	TGCAAGATCTATGTTGAGGCCA	CTGAGAATCGAGCGGTGTCA
	aTAAGGCtaCGTAtCACATA-GGG	BICDL1	ENSG00000135127	4	12	Intron 2-3	TAGCTCCACTTGCTGTGTGTT	TTGACGCAAGGGCATTTC
	fTAAGGCcTfTAAACACATA-GGG	NRAP	ENSG00000197893	4	10	Intron 22-23	CCAGGTGGACTAGAGAGGCT	AAGACGCAGCTCAAACCCTT
ATM ex10 sgRNA2 GACACAATGCAACTTCCGTA	GAgtaAAA GCAACTTCCGTA-GGG	NBPF3	ENSG00000142794	4	1	Exon 13	CAGAGAGCTGCCGGAGGTAG	GAATCAGAGTGCCACAGGCAT
	cAgAgAAGGCAgCTTCCGTA-AGG	ZNF407	ENSG00000215421	5	18	Intron 7-8	AATCAGCCCCTGAAAACGG	AACGAAATCAGAGCCCTGCC
	aAgACAAgGCACtGcCCGTA-TGG	ZNF704	ENSG00000164684	5	8	Intron 2-3	TGTAGTGCATGCCTGAGGGG	TTGTGCAGGTGGTAACTGCG
TP53 ex4 sgRNA1 CCATTGTTCAATATCGTCCG	aaATcaTTCcATATCGTCCG-CGG	PTPN3	ENSG00000070159	5	9	5' upstream seq	CTCCTGAAATGAGAGCCACGA	CTCGGCTTTCAAAGATGGCA
	gCAaTGTTcAgcAgCGTCCG-TGG	TMEM132C	ENSG00000181234	5	12	Intron 1-2	AGACAGCAGGGGATGAAAACC	TTCAAGTGCCTCATTCCACA
	CCAgGaaCAATAgCGTCCG-CGG	THSD7A	ENSG00000005108	5	7	5' UTR	TGAGGACAGTGCCTCCG	TCTTCCACAGATAGAGGGTGGG
TP53 ex4 sgRNA2 CCCCGGACGATATTGAACAA	aCCCaGAgGATAttAACAA-GGG	SUN3	ENSG00000164744	4	7	Intron 10-11	CAGTTCAGTATGGCGACGCA	TGTTTGAACGGTGGTTCCTGT
	CCctGGAgctTATTGAACAA-TGG	NAV2	ENSG00000166833	4	11	5' upstream seq	CACTGGACATCCCTATGCCG	CCTTGGCACATCCAGAGAGC
	CCCAGGACctaATTGAACAA-GGG	EXOC3	ENSG00000180104	4	5	Exon 4	GCATGCAGGCAGCCTTTTAT	GCCAGTTGCTTTTCCGGT

Supplementary Table S4. Overall survival (OS) of del(11q) CLL cases according to the presence of additional genetic alterations ($n = 47$).

	Yes (median OS, months)	No (median OS, months)	P^a
N° of mutated genes >2	67	66	0.729
<i>ATM</i> ^{MUT}	67	33	0.286
<i>NOTCH1</i> ^{MUT}	27	67	0.547
<i>SF3B1</i> ^{MUT}	66	65	0.352
<i>BIRC3</i> ^{MUT}	33	67	0.268
<i>DDX3X</i> ^{MUT}	24	66	0.301
<i>TP53</i> ^{MUT}	15	88	0.0001
Del(17p)	19	88	0.01
<i>TP53</i> alteration (deletion/mut)	17	88	0.0004
Monoallelic <i>TP53</i> loss	17	88	0.01
Biallelic <i>TP53</i> loss	11	88	0.001

^a Log-rank Test**Supplementary Table S5.** List of CRISPR/Cas9-generated indels in *ATM*, *TP53* and off-target regions.

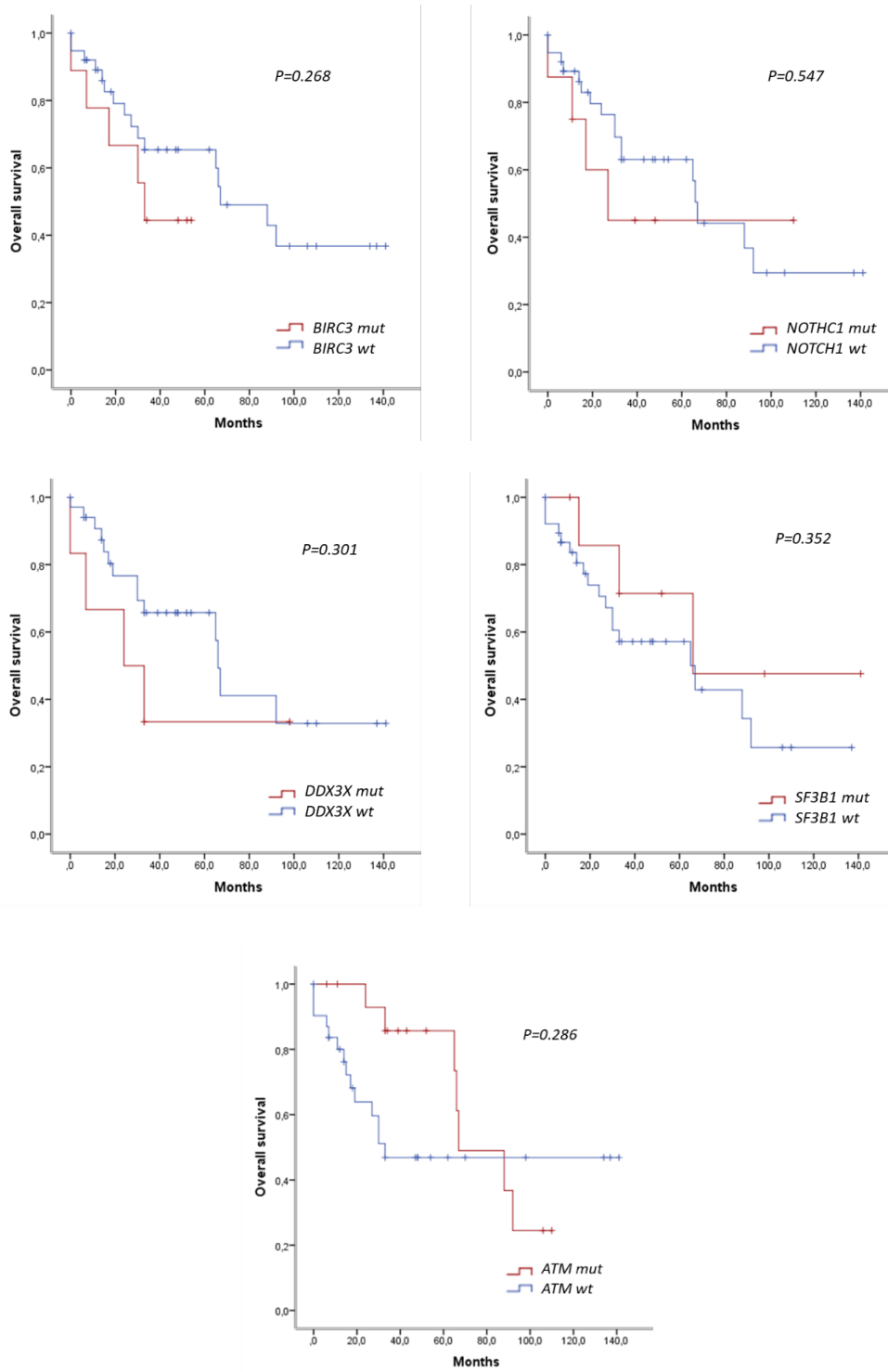
HG3 Clone	sgRNA	Indels in <i>TP53</i>	Indels in <i>ATM</i>	Off-target indels
WT Clone #1	Control sgRNA1	WT/WT	WT/WT	None
WT Clone #2	Control sgRNA1	WT/WT	WT/WT	None
WT Clone #3	Control sgRNA1	WT/WT	WT/WT	None
<i>TP53</i> ^{MUT} Clone #1	<i>TP53</i> ex4 sgRNA1	+1/+1	WT/WT	None
<i>TP53</i> ^{MUT} Clone #2	<i>TP53</i> ex4 sgRNA2	+1/+1	WT/WT	None
<i>TP53</i> ^{MUT} Clone #3	<i>TP53</i> ex4 sgRNA2	+1/+1	WT/WT	None
Del(11q) Clone #1	Control sgRNA1	WT/WT	Del(11q)/WT	None
Del(11q) Clone #2	Control sgRNA1	WT/WT	Del(11q)/WT	None
Del(11q) Clone #3	Control sgRNA1	WT/WT	Del(11q)/WT	None
Del(11q) <i>TP53</i> ^{MUT} Clone #1	<i>TP53</i> ex4 sgRNA2	-7/+1	Del(11q)/WT	None
Del(11q) <i>TP53</i> ^{MUT} Clone #2	<i>TP53</i> ex4 sgRNA2	-8/+1	Del(11q)/WT	None
Del(11q) <i>TP53</i> ^{MUT} Clone #3	<i>TP53</i> ex4 sgRNA2	+1/+1	Del(11q)/WT	None
Del(11q) <i>TP53</i> ^{MUT} Clone #4	<i>TP53</i> ex4 sgRNA2	-7/-7	Del(11q)/WT	None
Del(11q) <i>TP53</i> ^{MUT} Clone #5	<i>TP53</i> ex4 sgRNA2	-4/-4	Del(11q)/WT	None
Del(11q) <i>ATM</i> ^{MUT} <i>TP53</i> ^{MUT} Clone #1	<i>TP53</i> ex4 sgRNA2; <i>ATM</i> ex10 sgRNA2	+1/+1	Del(11q)/+1	None
Del(11q) <i>ATM</i> ^{MUT} <i>TP53</i> ^{MUT} Clone #2	<i>TP53</i> ex4 sgRNA2; <i>ATM</i> ex10 sgRNA2	-302/-302	Del(11q)/+1	None
Del(11q) <i>ATM</i> ^{MUT} <i>TP53</i> ^{MUT} Clone #3	<i>TP53</i> ex4 sgRNA2; <i>ATM</i> ex10 sgRNA2	+1/-7	Del(11q)/-14	None
Del(11q) <i>ATM</i> ^{MUT} <i>TP53</i> ^{MUT} Clone #4	<i>TP53</i> ex4 sgRNA2; <i>ATM</i> ex10 sgRNA2	-7/-7	Del(11q)/+1	None
Del(11q) <i>ATM</i> ^{MUT} <i>TP53</i> ^{MUT} Clone #5	<i>TP53</i> ex4 sgRNA2; <i>ATM</i> ex10 sgRNA2	+1/-11	Del(11q)/-22	None

Supplementary Table S6. Phenotypical characteristics of Giemsa-stained CRISPR/Cas9-generated CLL cell lines.

	Presence of pleomorphic cells (%)	Mitotic index (per 40X field)	Presence of degenerative vacuoles
HG3 ^{WT}	No	4-5	No
HG3 <i>TP53</i> ^{MUT}	< 1 %	4-5	No
HG3 del(11q)	No	3-4	No
HG3 del(11q) <i>TP53</i> ^{MUT}	< 1%	5-6	No
HG3 del(11q) <i>ATM</i> ^{MUT} <i>TP53</i> ^{MUT}	> 5%	1-2	Yes

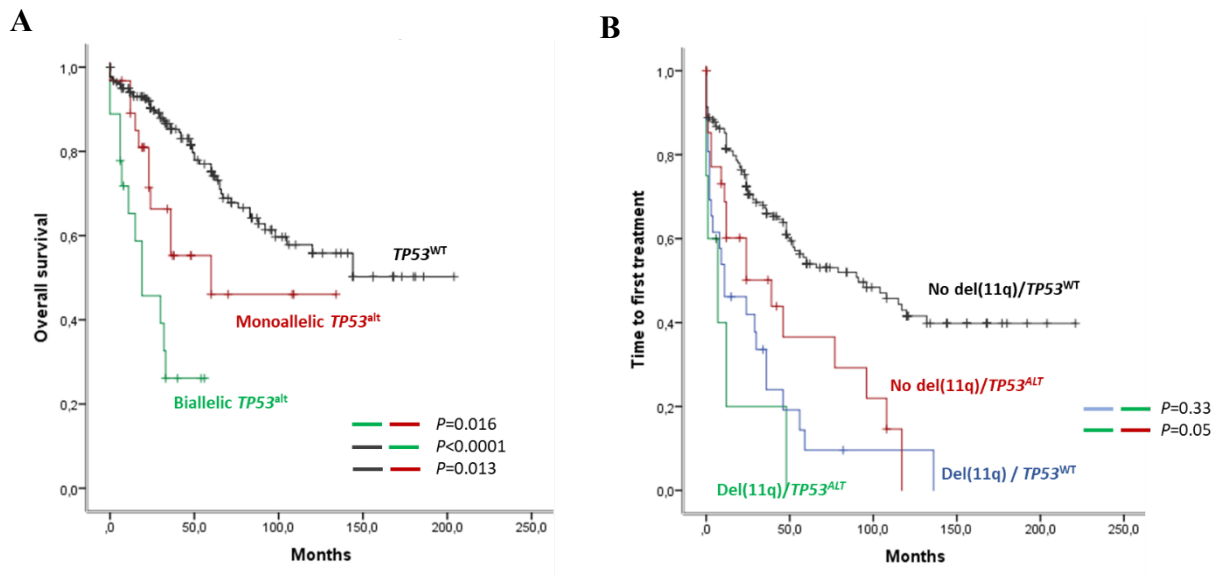
SUPPLEMENTARY FIGURES – CHAPTER 3

Supplementary Figure S1



Impact of *ATM*, *BIRC3*, *NOTCH1*, *DDX3X* and *SF3B1* mutations in the survival of del(11q) CLL patients. Median overall survival (months) and *p*-values are shown in Supplementary Table S4.

Supplementary Figure S2



Impact of *TP53* alterations on (A) overall survival of CLL patients and on (B) time to first treatment according to the presence of additional del(11q) ($n = 271$).

SUPPLEMENTARY APPENDIX – CHAPTER 4

Biological significance of monoallelic and biallelic *BIRC3* loss in del(11q) chronic lymphocytic leukemia progression

Miguel Quijada-Álamo, María Hernández-Sánchez, Ana-Eugenia Rodríguez-Vicente, Claudia Pérez-Carretero, Alberto Rodríguez-Sánchez, Marta Martín-Izquierdo, Verónica Alonso-Pérez, Ignacio García-Tuñón, José María Bastida, María Jesús Vidal-Manceñido, Josefina Galende, Carlos Aguilar, José Antonio Queizán, Isabel González-Gascón y Marín, José-Ángel Hernández-Rivas, Rocío Benito, José-Luis Ordóñez and Jesús-María Hernández-Rivas

Blood Cancer Journal. 2021, *In press*

SUPPLEMENTARY METHODS

Cell lines, culture conditions, drugs and reagents

The human CLL-derived cell lines HG3 and MEC1 were purchased from DMSZ (Deutsche Sammlung von Mikroorganismen and Zellkulturen). HG3 cells were cultured in RPMI 1640 medium (Life Technologies) supplemented with 15% Fetal Bovine Serum (FBS), 1% glutaMAX and 1% penicillin/streptomycin (Life Technologies). MEC1 cells were cultured in Iscove'sMDM medium (Lonza) supplemented with 10% FBS, 1% glutaMAX and 1% penicillin/streptomycin. HS-5 bone marrow stromal cells for *ex vivo* co-cultures were purchased from ATCC and HEK 293T cells for lentiviral production were obtained from DMSZ. Both cell lines were maintained in DMEM (Life Technologies) supplemented with 10% FBS, 1% glutaMAX and 1% penicillin/streptomycin. All cell lines were incubated at 37°C in a 5% CO₂ atmosphere. The presence of mycoplasma was tested frequently with MycoAlert kit (Lonza), only using mycoplasma-free cells in all the experiments carried out.

Venetoclax (ABT-199) and birinapant were obtained from LC Laboratories, A-1331852 (BCL-xL inhibitor), S63845 (MCL1 inhibitor) and SMI1 (NIK inhibitor) were purchased from Selleckchem and fludarabine was from Sigma. All drugs were resuspended in DMSO (Sigma).

Next-generation sequencing

A targeted-capture next-generation sequencing (NGS) strategy was used to analyze the mutational status of *BIRC3* in CLL patients, as well as other 57 genes previously reported as mutated in CLL or involved in the disease pathogenesis^{1,2} following the approach of Agilent SureDesign. Sequence data generated by Illumina NextSeq 500 was analyzed by an in-house bioinformatic pipeline as previously reported³. Supplementary Table S2 shows the list of mutations of each CLL patient.

In addition, targeted-capture NGS data was also used to assess whether or not the deleted region on del(11q) detected by FISH included *BIRC3* gene in CLL patients. The mean coverage depth of each individual exon target was first normalized in a set of samples without deletion on 11q by FISH using the total read number of each sample. The mean coverage of all these samples was used as the reference. To detect del(11q) and assess which genes were involved, the normalized coverage of exons of genes located in 11q (*NXF1*, *BIRC3* and *ATM*) from each study sample was compared to the mean coverage of the same target in the reference file generated above. Copy number variations (CNVs) were called using fixed thresholds representing the log₂ ratio of mean coverage of testing to that of reference. A log₂ ratio <-0.5 suggested a heterozygous deletion of 11q. Therefore, these analyses allowed us to determine whether *BIRC3* was deleted or not in CLL samples with del(11q). HG3-del(11q) cell line, in which *ATM* and *BIRC3* is monoallelic deleted, was analyzed as a control positive since the deletion size was known (Supplementary Fig. S1). This method was based on a previously published analysis to detect deletions from targeted-capture NGS data⁴ and has been also used to determine CNVs in inherited platelet disorders⁵.

Fluorescence *in situ* hybridization (FISH)

Interphase FISH was performed in primary CLL PBMCs or CRISPR/Cas9-engineered cell lines using commercially available probes for the 13q14, CEP12, 11q22/*ATM* and 17p13/*P53* (Vysis, Abbott Laboratories, IL, USA) as previously described⁶. Signal screening was carried out in at least 200 and the cut-off for positive cases was set at >10% events.

Subcellular fractionation and western blot

Subcellular fractionation was performed using the Subcellular Protein Fractionation Kit (ThermoFisher Scientific) according to the manufacturer's instructions. For whole cell-lysates, cells were washed with PBS and lysed in ice-cold lysis buffer (140 mmol/l NaCl, 50 mmol/l EDTA, 10% glycerol, 1% Nonidet P-40, 20 mmol/l TrisHCl pH 7) containing protease inhibitors (cOmplete™, Roche) and phosphatase inhibitors (PhosSTOP™, Roche). The following primary antibodies purchased from Cell Signaling Technologies were used in the

western blot experiments: anti-BIRC3 (#3130, Rabbit), anti-NF- κ B2 (#4882, Rabbit), anti-p-NF- κ B2 (#4810, Rabbit) anti-NIK (#4994, Rabbit), anti-RelB (#10544, Rabbit), anti-p-IKK α / β (#2697, Rabbit), anti- NF- κ B1 (#13586, Rabbit), anti-BCL2 (#2872, Rabbit), anti-BCL-xL (#2762, Rabbit), anti-MCL1 (#94296, Rabbit), anti-BIM (#2933, Rabbit), anti-BAK (#12105, Rabbit), anti-BAX (#5023, Rabbit) anti-NOXA (#14766, Rabbit), anti- β -actin (#4967, Rabbit), anti-H3 (#4499, Rabbit) and anti-GAPDH (#5174, Rabbit). Horseradish peroxidase-linked anti-rabbit antibody (#7074, Cell Signaling Technologies) was used as secondary antibody at 1:5,000 dilution. Antibody signal was detected using ECLTM Western Blotting Detection Reagents (RPN2209, GE Healthcare). Protein expression level was calculated by testing the ratios of each protein in relation to the loading control (β -actin, GAPDH or H3) using ImageJ software.

MTT viability and growth assays

Cell viability and proliferation was assessed using 3-(4,5-dimethylthiazol-2-yl)-2,5-diphenyltetrazolium bromide (MTT) colorimetric assay (Sigma-Aldrich). Cells were counted and seeded at a density of 1×10^4 cells/well (for 72h experiments) or 2×10^4 (for 48h experiments) in 96-well plates and treated with or without different drug treatments. At the time of analysis, cells were incubated for 2h with a 1:10 MTT solution and subsequently added 1:2 SDS-HCl in agitation for 6 hours. Absorbance was read on an Infinite® F500 Tecan plate reader (Tecan) at 570nm.

For the determination of the growth exponential curves of CRISPR/Cas9-edited clones, cells were seeded at a concentration of 4×10^4 cells/mL and cell counts were assessed every 24 hours by Trypan Blue exclusion.

Apoptosis and cell cycle analysis

Apoptosis in response to drug treatment was measured by flow cytometry with annexin V-Dy634 (Immunostep) according to the manufacturer's instructions. In brief, 3×10^5 cells were seeded in 24-well plates and treated 48 hours with the drug concentration of interest, then they were labeled with annexin V and propidium iodide (PI). In parallel, cell distribution in the cell cycle phase was also analyzed measuring the DNA content by PI labeling after cell permeabilization.

***In vitro* clonal competition assays**

GFP- or RFP-tagged CRISPR/Cas9-generated clones were mixed at a 1:1 ratio and seeded at a density of 5×10^5 cells/mL in 75 cm³ flasks. *In vitro* clonal evolution was assessed every

3-4 days by quantification of GFP+ and RFP+ population using a FACS Aria flow cytometer (BD Biosciences). Data was analyzed using FlowJo software.

Subcutaneous xenograft experiments

20 four-to-five-week-old female NOD/SCID/IL2 receptor gamma chain null (NSG) mice were used in a subcutaneous xenograft model to compare tumor volumes between HG3-edited clones. Tumor xenografts were induced by subcutaneous injection of cell suspensions containing 5×10^6 cells in 0.2 ml of cellular medium into the mouse flank. Two groups of mice (n=10) were injected in the right flank with either HG3 WT clones or HG3 *BIRC3* mutated clones. Tumor volumes were measured with a caliper every 2-3 days. Volumes were calculated using the formula: $a^2b\pi/2$, where a and b are the 2 maximum diameters. Mice were sacrificed by anesthesia overdose 18 days after cell injection, when tumors were weighted and collected for histopathological analysis.

Immunohistochemistry

Tumor processing and immunohistochemistry (IHC) were performed as previously described⁷ using an anti-NF- κ B2 antibody (#3017, Cell Signaling Technologies). An experienced pathologist from the Molecular Pathology Unit of the Cancer Research Center of Salamanca supervised the analysis of the samples under a Leica microscope for the evaluation of p52 expression in the subcutaneous and intravenous xenografts.

SUPPLEMENTARY REFERENCES

1. Landau DA, Tausch E, Taylor-Weiner AN, et al. Mutations driving CLL and their evolution in progression and relapse. *Nature*. 2015;526.
2. Puente XS, Beà S, Valdés-Mas R, et al. Non-coding recurrent mutations in chronic lymphocytic leukaemia. *Nature*. 2015;526.
3. Quijada-Álamo M, Hernández-Sánchez M, Alonso-Pérez V, et al. CRISPR/Cas9-generated models uncover therapeutic vulnerabilities of del(11q) CLL cells to dual BCR and PARP inhibition. *Leukemia*. 2020;34.
4. Feng Y, Chen D, Wang G-L, Zhang VW, Wong L-JC. Improved molecular diagnosis by the detection of exonic deletions with target gene capture and deep sequencing. *Genet Med*. 2015;17.
5. Bastida JM, Lozano ML, Benito R, et al. Introducing high-throughput sequencing into mainstream genetic diagnosis practice in inherited platelet disorders. *Haematologica*. 2018;103.
6. González MB, Hernández JM, García JL, et al. The value of fluorescence in situ hybridization for the detection of 11q in multiple myeloma. *Haematologica*. 2004;89.
7. Ordóñez JL, Amaral AT, Carcaboso AM, et al. The PARP inhibitor olaparib enhances the sensitivity of Ewing sarcoma to trabectedin. *Oncotarget*. 2015;6.

SUPPLEMENTARY TABLES – CHAPTER 4

Supplementary Table S1. sgRNA sequences and PCR primers of sgRNA target sites.

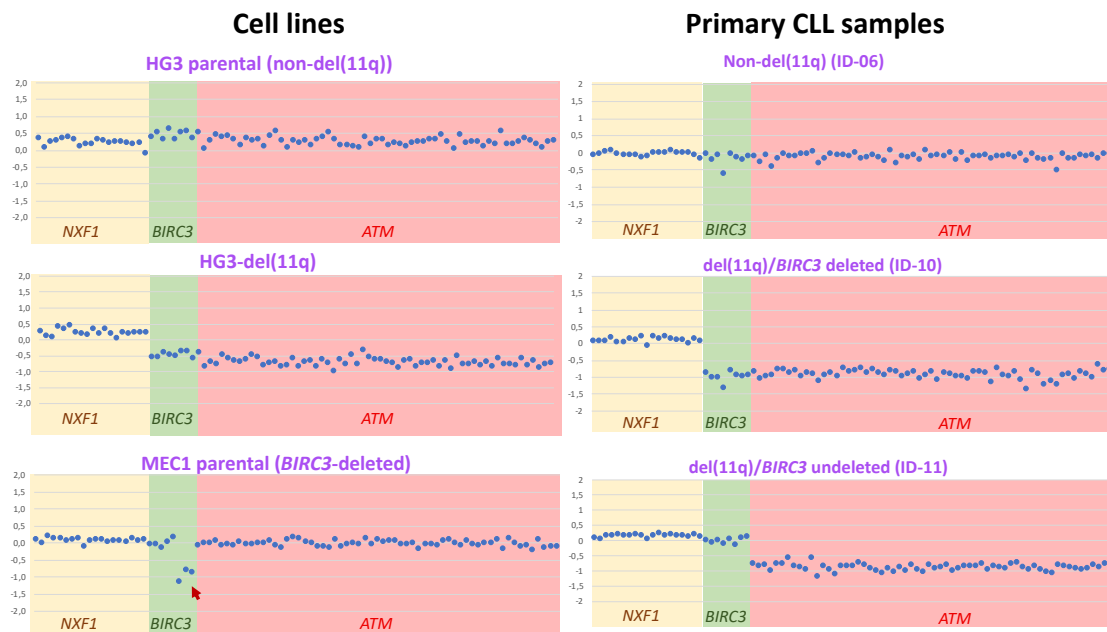
Target	Forward (5'-3')	Reverse (5'-3')
<i>BIRC3</i> exon 2 sgRNA1	CACCGATTGAGCAATTGGGAACCGA	AAACTCGGTTCCCAATTGCTCAATC
<i>BIRC3</i> exon 2 sgRNA2	CACCGGAGAGTTTGAATAAGAGCCA	AAACTGGCTCTTATTCAAACCTCTCC
<i>BIRC3</i> exon 7 sgRNA3	CACCGATTAATCCGGAAGAATAGAA	AAACTTCTATTCTTCCGGATTAATC
Control sgRNA1	CACCGACGGAGGCTAAGCGTCGCAA	AAACTTGCGACGCTTAGCCTCCGTC
<i>BIRC3</i> exon 2 (PCR)	ACGACTTGTCATGTGAACTGTACC	GCAGATTCAGTTTCTTACCCACATA
<i>BIRC3</i> exon 7 (PCR)	GAGACACCCCTAAACCTAGCA	GCCAAATACTCATTTC AAGGCAAC

Supplementary Table S2. Biological characteristics of CLL patients.

Sample ID	Sex	IGHV status	Cytogenetics (FISH)	% del(11q)	BIRC3 deleted	BIRC3 mutations	Other known mutations	Sample used in
ID-01	M	UM	del(11q), del(13q), trisomy 12	65%	Yes		NOTCH1, ATM, ZNF292	Fig. 3a, b
ID-02	F	M	del(11q), del(13q)	27%	Yes		POT1	Fig. 3a
ID-03	M	UM	del(11q)	75%	Yes		ATM, ARID1B	Fig. 3a
ID-04	M	UM	del(11q), del(13q)	95%	Yes		XPO1, FUBP1	Fig. 3a, b
ID-05	M	UM	del(11q), del(13q)	60%	Yes		SF3B1, ATM, DDX3X	Fig. 3a
ID-06	F	NA	Normal				ZNF292	Fig. 3a
ID-07	M	NA	del(11q), del(13q)	80%	No		SF3B1, ATM, ARID1A, ZC3H18	Fig. 3a, b
ID-08	F	UM	del(13q)				SF3B1, NOTCH1, MED12, RPS15	Fig. 3a
ID-09	F	UM	trisomy 12				ATM, TRAF3	Fig. 3a
ID-10	F	NA	del(11q), del(13q)	90%	Yes		MAP2K1, BRAF, DDX3X	Fig. 3a, b
ID-11	M	M	del(11q)	95%	No		SF3B1, EGR2	Fig. 3a, b
ID-12	M	UM	del(13q)				NOTCH1, XPO1, MGA	Fig. 3a
ID-13	M	M	del(13q)				MYD88	Fig. 3a
ID-14	M	M	trisomy 12			p.E433fs (8%); p.Q547fs (6%)	FBXW7, IGLL5, ARID1B	Fig. 3a
ID-15	F	M	Normal					Fig. 3a
ID-16	M	M	del(13q)					Fig. 3a
ID-17	M	UM	Normal				SF3B1, ATM, POT1	Fig. 3a
ID-18	M	UM	del(11q), del(13q)	80%	Yes		ATM	Fig. 3a
ID-19	M	UM	del(11q), del(13q), trisomy 12	70%	Yes	p.C581G (62%)	XPO1, NOTCH1, CHD2, SETD2, ZMYM3, ZNF292	Fig. 3a, b
ID-20	F	M	trisomy 12			p.C557fs (24%)	FBXW7, KRAS, KLHL6	Fig. 3a
ID-21	M	UM	del(11q), del(13q)	97%	No		TRAF3	Fig. 3a, b
ID-22	M	NA	del(11q), del(13q)	85%	Yes		SF3B1, ATM, CHD2, ASXL1, ENTPD4	Fig. 3a

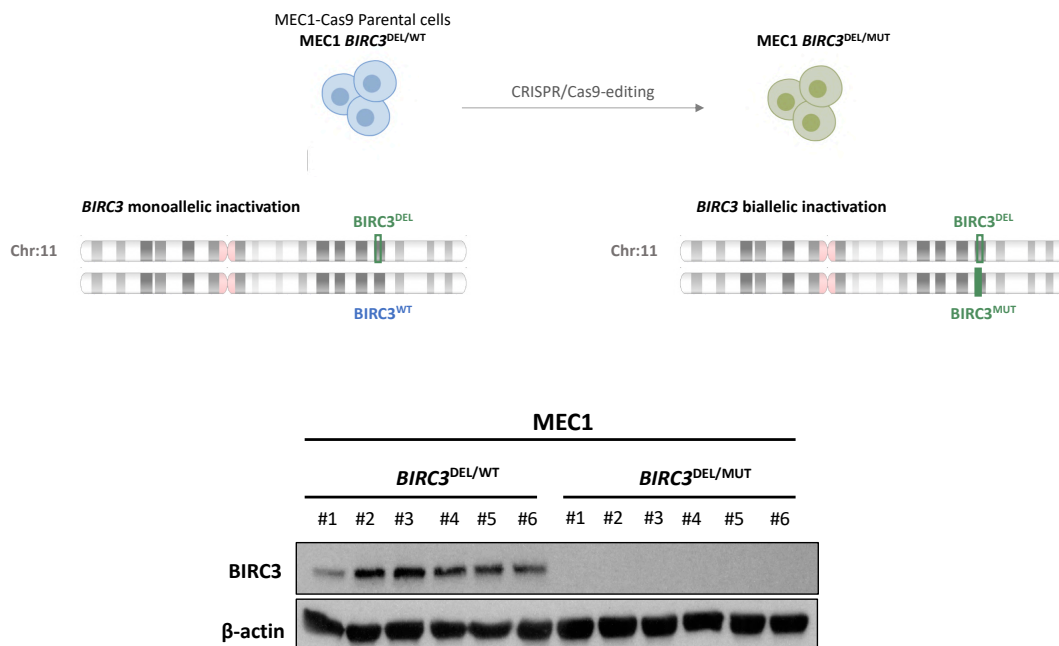
SUPPLEMENTARY FIGURES – CHAPTER 4

Supplementary Figure S1



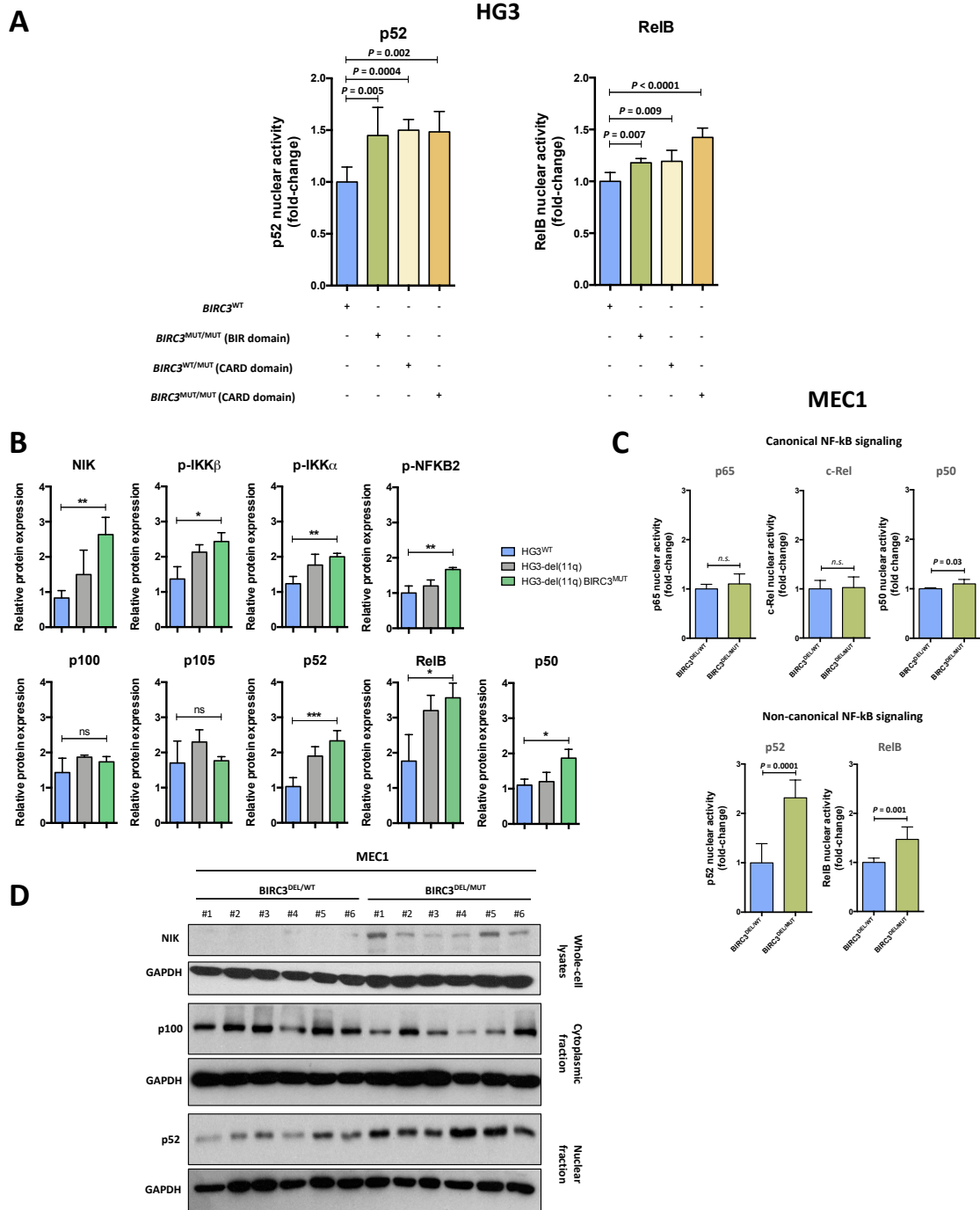
Detection of 11q deletion in cell lines and primary CLL samples using targeted-capture NGS data. Profile of log₂ ratios of normalized mean coverage of individual exon target of genes located in 11q (*NFX1*, *BIRC3* and *ATM*) to that of the reference, was plotted against the target. The x-axis shows the targets in the panel plotted by relative genome order. The y-axis corresponds to the log₂ ratio of the mean coverage of testing to that of reference. A log₂ normalized coverage ratio <-0.05 indicates a heterozygous deletion of chr11 (11q region). This analysis allowed us to determine whether *BIRC3* is deleted or not in CLL samples with del(11q). Left panel shows graphs from HG3 parental cell line (therefore, without del(11q)), HG3-del(11q) generated by CRISPR/Cas9, confirming the presence of del(11q) encompassing *ATM* and *BIRC3*, and MEC1 parental cell line harboring a monoallelic deletion of *BIRC3* (exons 7-9). Right panel shows three representative graphs from primary CLL samples: ID-06 without del(11q); ID-10 with del(11q) including loss of *ATM* and *BIRC3*; ID-11 with del(11q) including only loss of *ATM* (*BIRC3* undeleted). The presence of del(11q) was validated by FISH in cell lines as well as primary CLL samples.

Supplementary Figure S2



Generation of isogenic MEC1 CLL derived cell lines harboring *BIRC3* mutations using the CRISPR/Cas9 system. Upper panel: scheme of CRISPR/Cas9 induction of *BIRC3* mutations in MEC1 cells. sgRNA targeting *BIRC3* was transduced in MEC1 parental cells (which harbor a *BIRC3* monoallelic deletion; *BIRC3*^{DEL/WT}), generating MEC1-edited clones with *BIRC3* biallelic inactivation (*BIRC3*^{DEL/MUT}). Lower panel: western blot analysis of MEC1-edited cell lines harboring *BIRC3* loss-of-function mutations. β -actin was used as loading control.

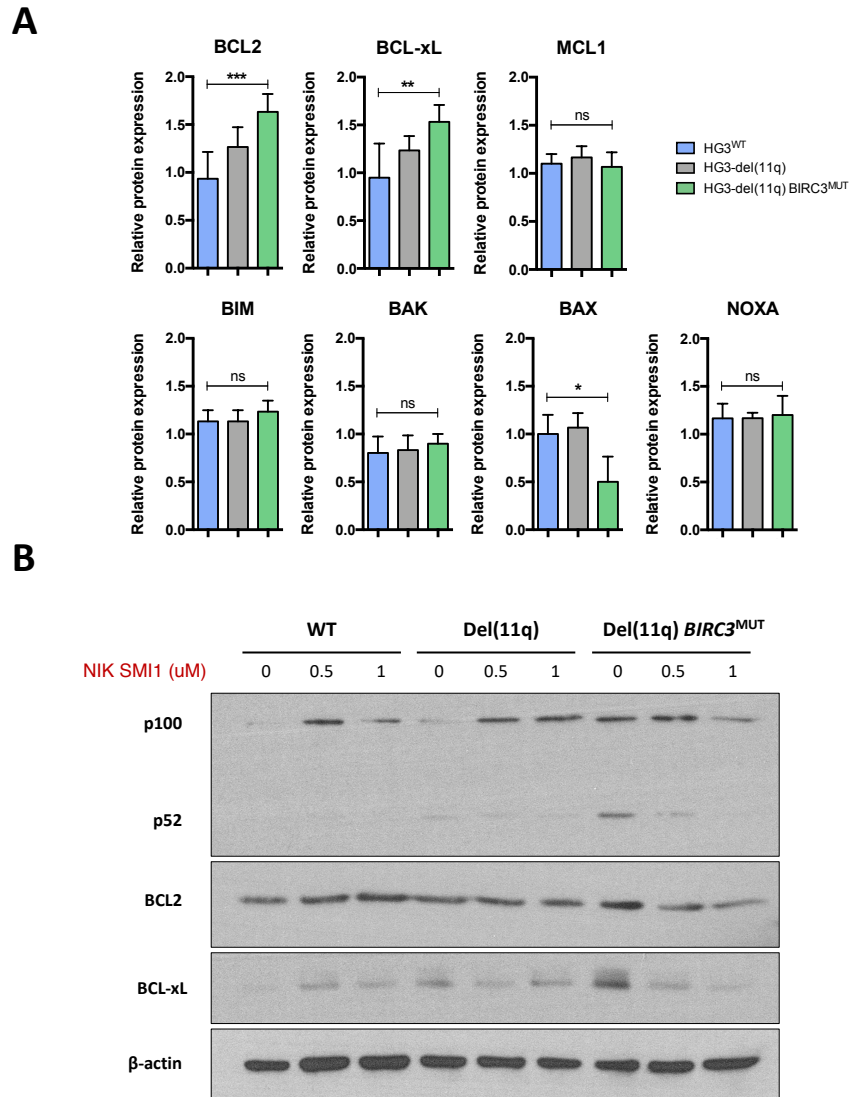
Supplementary Figure S3



NF-κB-related effects of *BIRC3* deletion and/or mutation in CRISPR/Cas9-edited HG3 and MEC1 CLL cell lines. (A) ELISA measurement of relative NF-κB2 p52 and RelB DNA-binding activity in nuclear extracts from HG3^{WT} and HG3 *BIRC3*^{MUT} clones. Bars represent the mean ± SD. (B) Quantification of proteins analyzed by western blot in Fig. 2b relative to loading control. Data is summarized as the mean ± SD of three independent clones. (C) ELISA measurement of relative NF-κB family transcription factor DNA-binding activity in nuclear extracts from MEC1-edited clones. Left panel shows DNA-binding activity of NF-κB

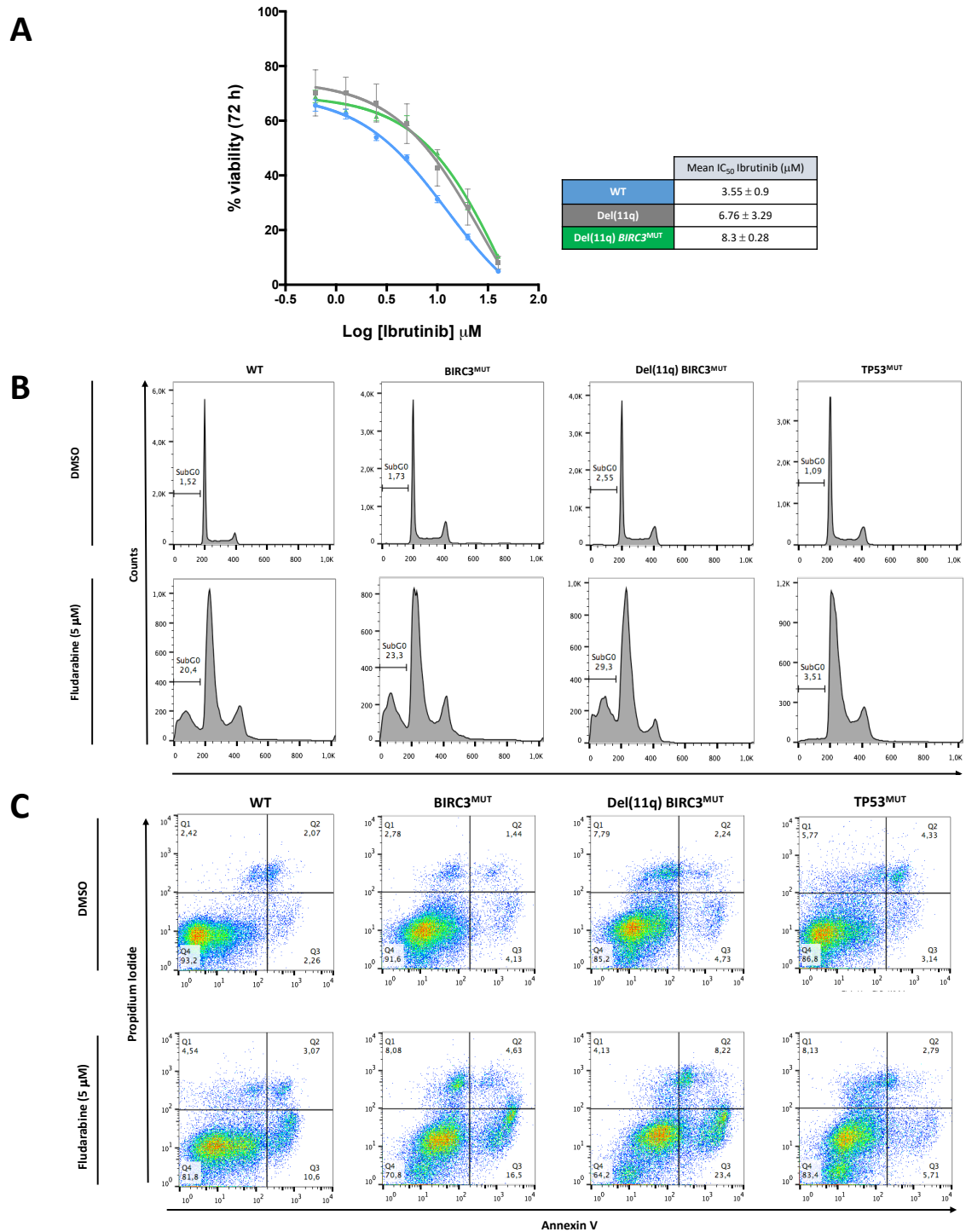
transcription factors involved in the canonical signaling (p65, c-Rel and p50). Right panel displays the DNA-binding activity of non-canonical NF- κ B transcription factors (p52 and RelB). Data are represented as the mean \pm SD. (D) Whole-cell, cytoplasmic and nuclear lysates of CRISPR/Cas9-edited MEC1 clones analyzed by immunoblotting for NIK and NF- κ B2 (p100/p52) protein. GAPDH was used as loading control.

Supplementary Figure S4



Impact of BIRC3-mediated non-canonical NF- κ B signaling activation in BCL2-family members. (A) Quantification of proteins analyzed by western blot in Fig. 2c relative to loading control. Data is summarized as the mean \pm SD of three independent clones. (B) Western blot analysis of HG3^{WT}, HG3-del(11q) and HG3-del(11q) BIRC3^{MUT} cells treated with the indicated doses of NIK SMI1. Whole-cell lysates were extracted 24 hours after treatment and probed for NF- κ B2 (p100/p52), BCL2 and BCL-xL proteins. β -actin was used as loading control.

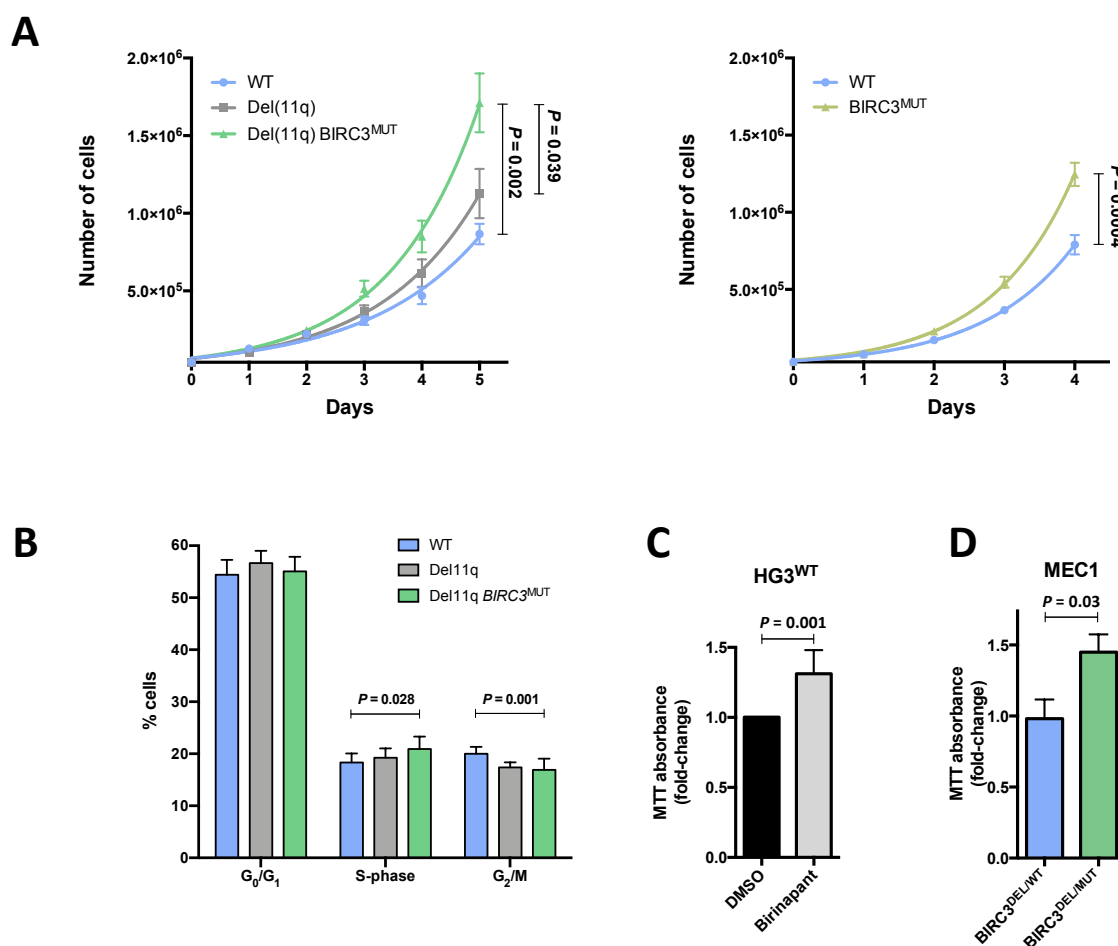
Supplementary Figure S5



Response to ibrutinib and fludarabine of HG3 CRISPR/Cas9-generated clones. (A) Dose-response curves of HG3^{WT}, HG3-del(11q) and HG3-del(11q) *BIRC3*^{MUT} clones treated with ibrutinib. Cell viability was assessed by MTT assay after 72 hours and surviving fraction is expressed relative to DMSO control. Data is summarized as mean ± SEM. **(B)** Cell cycle analysis of CRISPR/Cas9-edited clones after 48 hours 5 μM fludarabine exposure. SubG₀ peak is indicative of the presence of apoptotic cells. **(C)** Representative plots of annexin V/PI

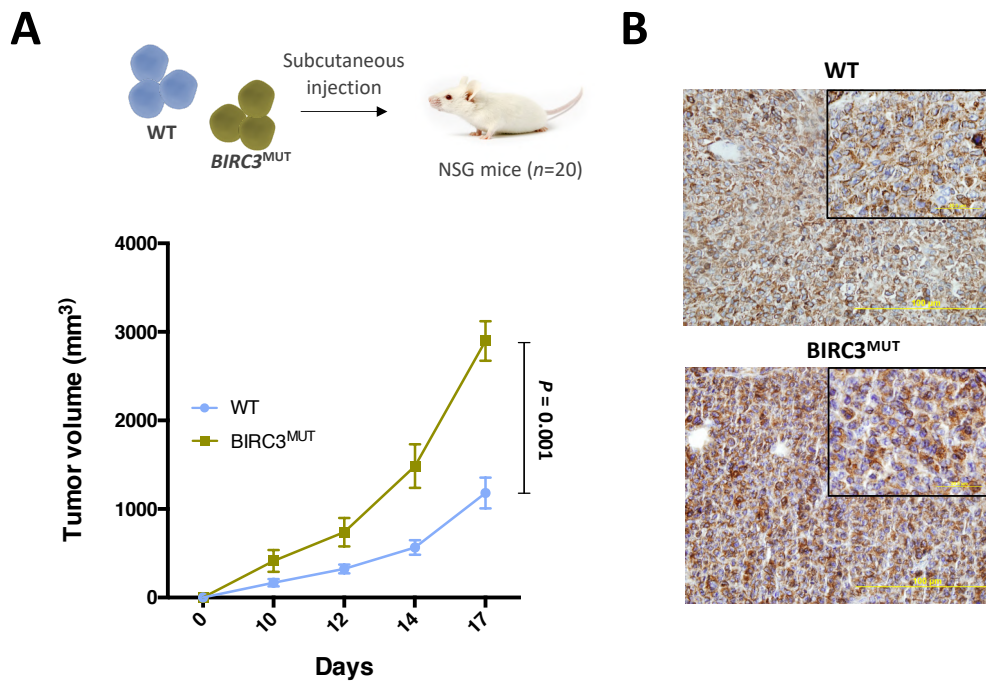
stained HG3^{WT}, HG3 *BIRC3*^{MUT}, HG3-del(11q) *BIRC3*^{MUT} and HG3 *TP53*^{MUT} cell lines 48 hours after 5 μ M fludarabine exposure. Fludarabine induced apoptosis is shown by the presence of annexin V⁺ cells.

Supplementary Figure S6



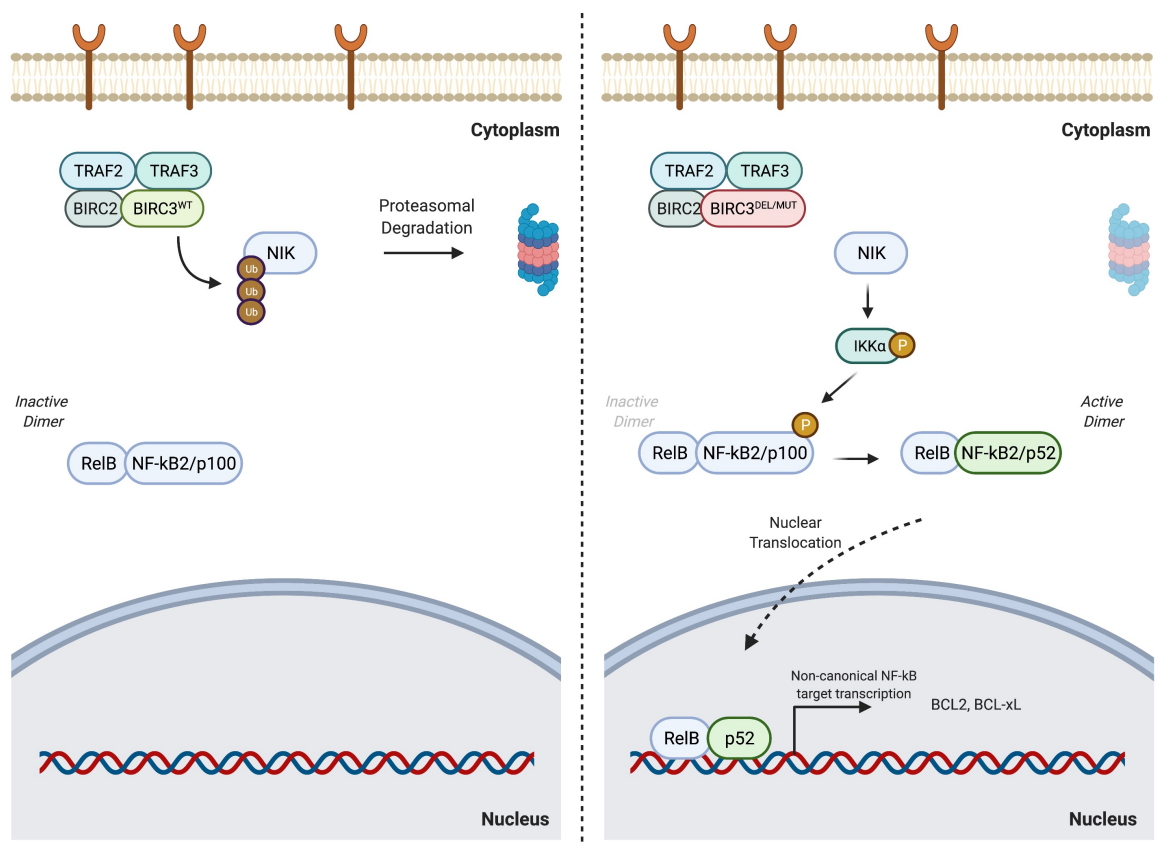
Effects of BIRC3 deletion, mutation or inhibition in growth, viability and cell cycle of HG3 and MEC1 CLL cell lines. (A) Growth rate assessment of HG3^{WT}, HG3-del(11q) and HG3-del(11q) *BIRC3*^{MUT} cells (left panel), or HG3^{WT} and HG3 *BIRC3*^{MUT} cells (right panel), by trypan blue exclusion. Data were fitted in an exponential growth equation, and time point values are presented as the mean \pm SEM. (B) Cell cycle phase distribution of HG3-edited cell clones. Data represent the mean values \pm SD of three independent experiments. (C) HG3^{WT} cells were treated with the BIRC2/BIRC3 inhibitor bircinapant (2.5 μ M) and viability was assessed at 6 days by MTT. Absorbance values are represented normalized with the control (DMSO) condition. Data are summarized as mean \pm SD. (D) Effect of *BIRC3* mutation in the proliferation of MEC1 cells after 72 hours. MTT absorbance values are represented normalized with the MEC1^{DEL/WT} clones. Data are represented as the mean \pm SD.

Supplementary Figure S7



Implications of *BIRC3* mutations in tumor growth of *in vivo* subcutaneous xenografts. (A) Tumor growth evolution (mm³) following subcutaneous cell injection of HG3^{WT} and HG3 *BIRC3*^{MUT} cells ($n = 10$ mice/group). The plot displays mean \pm SD values over 17 days. **(B)** Immunohistochemical analysis of NF- κ B2 (p52) expression of tumor xenografts.

Supplementary Figure S8



Impact of *BIRC3* deletion and/or mutation in the non-canonical NF- κ B signaling. Left panel: Functional *BIRC3*^{WT} protein targets NIK for proteasomal degradation in the cytoplasm of CLL cells, keeping the non-canonical NF- κ B signaling inactive. Right panel: when *BIRC3* is deleted through del(11q) or truncated through loss-of-function mutations, NIK is stabilized in the cytoplasm activating downstream signaling and ultimately leading to RelB-p52 nuclear translocation and overexpression of anti-apoptotic BCL2 family members.

List of Tables and Figures

INTRODUCTION

Table 1. Main prognostic biomarkers identified in CLL.....	16
Table 2. Biological processes affected by recurrent genetic lesions in CLL drivers.....	35
Table 3. Characteristics of currently available, authenticated patient-derived CLL cell lines for research.....	48
Figure 1. Treatment algorithm for treatment-naïve and relapsed/refractory CLL patients.....	18
Figure 2. Cellular origin of CLL.....	22
Figure 3. Recurrently mutated CLL driver genes identified in Landau <i>et al</i> and Puente <i>et al</i>	28
Figure 4. DDR signaling and cell cycle in CLL.....	37
Figure 5. The BCR signaling pathway in CLL.....	39
Figure 6. The NF-κB signaling pathway in CLL.....	42
Figure 7. The CLL microenvironment.....	43
Figure 8. CRISPR/Cas9 system components and applications.....	53

RESULTS – CHAPTER 1

Table 1. Mutations in CD19 ⁺ and CD34 ⁺ cell populations identified in 56 CLL patients.....	74
Table 2. Mutations in CD19 ⁺ , CD34 ⁺ CD19 ⁻ , CD3 ⁺ and CD14 ⁺ PB cell populations identified by ultra-deep NGS.....	76
Table 3. FISH analysis in CD34 ⁺ cell populations of nine CLL patients.....	76
Figure 1. Cytogenetics and molecular characteristics of CD19 ⁺ and CD34 ⁺ cells.....	75

Figure 2. Mutational burden in CD19⁺ and CD34⁺ cells from CLL patients.....75

Figure 3. Schematic model of events occurring in CLL hematopoiesis.....78

RESULTS – CHAPTER 2

Figure 1. Generation of 11q deletion and *ATM* mutations in CLL cell lines using the CRISPR/Cas9 system.....87

Figure 2. Evaluation of double-strand breaks signaling and repair in del(11q)/*ATM*-deficient CLL cells.....88

Figure 3. Olaparib effects in CRISPR/Cas9-edited del(11q) cells *in vitro*, *in vivo* and in combination with ibrutinib.....89

Figure 4. Response to dual BCR and PARP inhibition of 38 CLL primary samples in the presence of stromal stimulation.....91

Figure 5. Effects of ibrutinib in RAD51-mediated HR repair in CLL.....92

Figure 6. Implications of BCR inhibition in HR-mediated DSBs repair in CRISPR/Cas9-edited clones and primary CLLs.....94

RESULTS – CHAPTER 3

Table 1. Clinical and biological characteristics of CLL patients.....104

Table 2. *TP53* alterations identified in del(11q) CLL patients.....107

Figure 1. Mutational analysis and overall survival of del(11q) patients.....106

Figure 2. Generation of CRISPR/Cas9-edited CLL cell lines harboring del(11q), *TP53* and/or *ATM* mutations and phenotypical analysis of edited cells.....108

Figure 3. Effects of biallelic loss of *TP53* and *ATM* on viability, cell growth, apoptosis, and cell cycle control of CRISPR/Cas9-edited cell lines.....110

Figure 4. *In vivo* clonal competition analysis of xenotransplanted NSG mice.....111

Figure 5. Cell viability studies of HG3-edited clones in response to different drug treatments.....113

RESULTS – CHAPTER 4

Figure 1. Generation of isogenic CRISPR/Cas9-edited CLL cell lines harboring del(11q) and/or <i>BIRC3</i> mutations.....	125
Figure 2. Evaluation of canonical and non-canonical NF- κ B activity in del(11q)/ <i>BIRC3</i> -deficient CRISPR/Cas9-engineered CLL cells.....	127
Figure 3. Effects of <i>BIRC3</i> loss in NF- κ B activity and BCL2 levels of del(11q) primary CLL cells.....	129
Figure 4. Cell viability studies of del(11q)/ <i>BIRC3</i> -mutated cell lines in response to BCL2, BCL-xL, MCL1 inhibition or fludarabine treatment.....	130
Figure 5. Effects of del(11q) and/or <i>BIRC3</i> mutations in CLL cell lines proliferation and clonal evolution.....	132
Figure 6. <i>In vivo</i> analysis of leukemic progression of del(11q)/ <i>BIRC3</i> -mutated CRISPR/Cas9-edited clones.....	133

